Sorbonne Université

Ecole doctorale 129 : Sciences de l'environnement d'Ile de France

Centre Scientifique de Monaco / Equipe d'écophysiologie corallienne

Impacts des vagues de chaleur marine sur le microbiome de *Corallium rubrum* et d'autres octocoralliaires méditerranéens

Impacts of marine heatwaves on the microbiome of Corallium rubrum and other Mediterranean octocorals

Par Camille Prioux

Thèse de doctorat de Sciences de l'environnement

Dirigée par Dr. Christine Ferrier-Pagès et co-encadrée par Dr. Romie Tignat-Perrier

Présentée et soutenue publiquement le 11 décembre 2025 à Monaco

Devant un jury composé de :

Pr. Rodolphe Lemée	Professeur	Président du jury
Pr. Jillian Petersen	Professeure	Rapportrice
Pr. Sébastien Duperron	Professeur	Rapporteur
Dr. Jean-Baptiste Raina	Maitre de conférences	Examinateur
Pr. Javier del Campo	Professeur	Examinateur
Dr. Christine Ferrier-Pagès	Directrice de recherche	Directrice de thèse
Dr. Romie Tignat-Perrier	Chargée de recherche	Co-encadrante de thèse

Except where otherwise noted, this work is licensed under
http://creativecommons.org/licenses/by-nc-nd/3.0/

A mes parents et leur amour inconditionnel,

A l'Ile de Houat où j'ai compris ce que je voulais faire de ma vie.

Remerciements | Acknowledgements

Après 3 ans et demi passés au CSM, voilà enfin venu le temps d'écrire ces fameux remerciements. Je ne sais pas combien de fois je me suis imaginée écrire ces lignes, l'aboutissement de toutes ces années de travail !

First of all, I would like to thank the jury of my thesis, in particular Prof. Sébastien Duperron and Prof. Jillian Petersen for agreeing to be « rapporteurs », but also Dr. Jean-Baptiste Raina, Prof. Rodolphe Lemée, and Prof. Javier del Campo for agreeing to review my thesis. I'm truly honored that you will bring your considerable expertise to the evaluation of this work.

I would also like to thank the members of my thesis committee, including Prof. Javier Del Campo, Dr. Lorenzo Bramanti, and Prof. Cristina Varese for their unfailing support and valuable advice throughout these three years. I would like to express my particular gratitude to Dr. Javier Del Campo, as well as Dr. Laure Guillou, for their valuable expertise and the enthusiasm with which they accompanied me in the development of our special red coral "UnNonMet" primers to explore the fascinating world of microeukaryotes.

Prof.ssa Cristina Varese, grazie mille per la calorosa accoglienza che mi avete riservato in occasione di ciascuna delle mie missioni nella vostra magnifica università di Torino, e alla dott.ssa Valeria Prigione e alla dott.ssa Marina Carrasco Acosta per la loro guida, disponibilità e sostegno in ciascuna delle fasi dell'isolamento dei miei ceppi fungini.

Je tiens à remercier chaleureusement le Président, Pr. Jean-Jacques Risso, ainsi que son prédécesseur, Pr. Patrick Rampal, pour m'avoir accueillie au sein de leur institution. J'adresse également toute ma reconnaissance à la direction du Centre Scientifique de Monaco, Dr. Sylvie Tambutté et son prédécesseur, le Pr. Denis Allemand, ainsi qu'à Mme Flora Ginocchio et sa prédécesseuse, Mme Delphine Frappier, qui ont rendu possible la réalisation de ce projet doctoral au sein du CSM. Enfin, je remercie le Musée Océanographique de Monaco de m'avoir ouverte les portes de cette magnifique salle de conférence, me permettant de clôturer ce chapitre dans les plus belles conditions.

Je voudrais également remercier tout le personnel administratif, Karine, et sa prédécesseuse Karen, Jennifer, Barbara et Muriel pour leur bonne humeur constante, leur bienveillance et surtout leur efficacité pour résoudre les moindres soucis administratifs. Un grand merci tout particulier à Giovanna, notre secrétaire scientifique pour ton sourire et ta bienveillance constante lorsque nous nous croisions dans le couloir, ta présence au CSM met vraiment du baume au cœur. Merci aussi à l'équipe informatique, Jorge, Tristan et Noureddine pour leur aide quand tout buggait sur nos ordis et au support technique, Robert (et ses blagues), Sébastien et Eric E., qui mettent tout en place pour que tout fonctionne correctement au labo. Merci à Dominique, notre aquariologiste expert, de prendre si soin de nos aquariums et pour ta solidarité entre bretonnisants.

Je remercie aussi de tout cœur l'équipe Ecophysio pour m'avoir si bien accueillie dès mon arrivée en stage de M2. Les permanents, Stéphanie, Eric, Renaud, Maria et Cécile, qui m'ont vu évoluer et grandir, de la petite stagiaire que j'étais à la future chercheuse que je deviens. Je voudrais aussi remercier les gens de passage dans notre équipe, Alice, Lucie, Katarina et Juan José pour votre gentillesse sans égal. Je remercie aussi l'équipe Chanel : Denis, Sylvie, Guillaume, Philippe de m'avoir écouté de nombreuses fois parler de l'importance du microbiote du corail rouge, j'espère que vous êtes convaincus ! Merci également aux autres membres de l'équipe de physiologie, Eric T., Benoit, Xavier, Alex, Didier, Natacha et Nathalie, pour votre accueil chaleureux au sein du CSM

et pour nos petits-déjeuners communs dont je garde de bons souvenirs (pas seulement de nourriture, promis).

Je souhaite exprimer toute ma reconnaissance au Dr. Jeroen Van De Water pour m'avoir encadrée lors de mon stage de M2, ainsi que pour son soutien constant et la qualité de ses conseils. Je le remercie tout particulièrement de m'avoir encouragée à approfondir l'étude des relations évolutives entre les coraux et leur microbiote au cours de ma thèse, ce qui a permis l'aboutissement d'un bel article scientifique.

Je voudrais également remercier Dr. Doria Filipponi, que j'ai introduit au monde fascinant des microeucaryotes et qui a toujours montré un enthousiame débordant face à notre publication commune. Merci de ta bienveillance et bonne humeur constante qui donne envie de se donner à fond !

Enfin, et pas des moindres, je réserve ce paragraphe pour exprimer mon immense gratitude envers Dr. Christine Ferrier-Pagès, ma directrice de thèse et Dr. Romie Tignat-Perrier ma co-encadrante. Je n'aurai pas pu rêver meilleur encadrement de votre part. Comme je te l'ai dit une fois Christine, nous avons une belle synergie de groupe toutes les trois et je réalise à quel point cela est précieux. Nous avons réussi à travailler en harmonie, notamment grâce à votre investissement et votre efficacité hors-norme, et ma thèse n'aurait jamais été aussi aboutie sans votre aide. Vos conseils avisés, vos relectures minutieuses et toujours pertinentes ont considérablement enrichi mon travail. Merci infiniment Christine, avec ton expérience extraordinaire, d'avoir été notre « commerciale » quand Romie et moi ne savions pas nous vendre aux éditeurs ou au COPIL. Merci aussi pour ton enthousiasme débordant à chaque fois que je venais te montrer un nouveau schéma bilan ! Ta force et ta résilience, y compris dans les moments les plus difficiles, forcent mon admiration. Je suis impressionnée par ta capacité à te relever et à aller de l'avant, quoi qu'il arrive. Je suis vraiment heureuse de te retrouver à mes côtés pour conclure ensemble ce dernier chapitre de ma thèse. Romie, je suis profondément reconnaissante d'avoir pu travailler avec toi. Ta patience, ta pédagogie et ta disponibilité lorsque je me posais mille questions m'ont permis de m'approprier le sujet et d'aborder la fin de cette thèse avec confiance. Tu me l'avais dit au tout début, la thèse c'est une aventure et je suis heureuse d'avoir choisi de la faire à tes côtés. J'ai aussi énormément apprécié tes qualités humaines : tu as toujours été à l'écoute, veillant à ce que je me sente bien au labo et nos conversations sur la vie vont me manquer. Les mots me manquent pour dire à quel point j'ai été chanceuse de faire cette thèse à vos côtés alors je vais simplement vous dire que travailler avec vous va énormément me manquer et que vous avez mis la barre très haute pour mes futurs collègues !

Vient maintenant le moment de remercier l'équipe de la tour de Pizz'a (merci Clem pour le super jeu de mot) qui ont égayé mon quotidien et rendu mon expérience au CSM infiniment plus agréable. Merci pour les midis à la digue, les fous rires partagés, les moments d'entraide pendant les journées difficiles, et pour toutes ces petites attentions qui ont fait la différence. Je suis profondément reconnaissante d'avoir eu la chance de partager cette aventure avec vous. Ophélie, qui a été ma co-bureau microbiogirl pendant 2 ans, merci d'avoir supporté mes accès de folies quand j'étais un peu trop fatiguée (ou que Gael m'avait donné du café) et pour nos razzias au Palais des thés parce que nous sommes des puristes du thé et qu'on ne boit pas n'importe quoi. Merci aussi de m'avoir laissé utiliser ta bouilloire sur laquelle on peut régler la température (très important) lorsque tu es partie du labo. Promis tu vas bientôt pouvoir la récupérer ! Clémence, nous avons traversé ces trois ans et demi ensemble, on voit le bout enfin !! Merci d'avoir été un petit rayon de soleil dans le bureau avec des blagues dont seule toi a le secret, le

bureau aurait été bien différent sans toi et ton rire communicatif. Je te souhaite de réussir tout ce que tu entreprendras après ta thèse, plein de liberté, d'aventures et d'épanouissement ! Kiara, merci d'avoir été notre grande sœur de thèse, pour tes conseils et ta bienveillance constante. La team polaire Gaelito et Téo, merci d'exister au CSM, quand ça n'allait pas je savais que pouvais venir boire le café (déso Ophélie) et refaire le monde dans votre grotte au fond du couloir. Merci aussi à Céline de m'avoir soutenue chaque midi où je disais qu'on allait tous crever de toute façon. A nos randos, à la globotutre (merci Gael de me l'avoir prêté de nombreuses fois) et surtout à nos pizzas aux Amoureux (à la burrata gratuite). Vous allez tous me manquer !! Je vous souhaite de belles aventures aux quatre coins du monde !

Je voudrais aussi remercier mes stagiaires, Joséphine et Rose, mais aussi Thibaud, super tech, pour leur engagement, leur curiosité et leur énergie pour m'aider à mener à bien mes projets de thèse. Je vous souhaite à tous une belle réussite pour la suite de votre parcours ! Merci aussi aux autres stagiaires et gens de passage au CSM qui ont apporté de l'énergie nouvelle au labo et qui nous permettait d'agrandir la bande de jeunes du CSM pour quelques mois : Lucie, Léna, Anna, Eva, Sacha, Frank, Lana, Margaux et surtout … Marie, merci d'être toi, je suis tellement heureuse que tu sois à Villefranche maintenant !! A nos soirées folles et moins folles (avec ou sans collage douteux).

Grazie a tutti i miei amici di Torino, Francesco (C3-spacer), Mateo, Federica, Davide e tutti gli altri che hanno reso piacevoli i miei soggiorni. Mi avete accolta nel vostro gruppo fin dal primo giorno e mi avete sempre fatto sentire a mio agio nel vostro laboratorio, grazie mille!

Je souhaite également remercier les autres membres du CSM en biologie marine et médicale. Même si je n'ai pas eu l'occasion de tous vous connaître de près, j'ai apprécié l'accueil et l'ambiance collective qui ont contribué à rendre mon passage ici agréable et enrichissant.

A mes amis qui m'ont toujours soutenue quelque soient mes projets plus ou moins fous (tu vas faire une thèse à MONACO ?) depuis l'enfance Anne et Andréa, lors de mes années folles au lycée Floriane, Charlène, Lucile, Eva, Claire, Jay, Toinou et Carla, à ceux qui m'ont toujours rappelé que je n'étais pas stupide en prépa et qui sont venus me voir aux quatres coins de la France, les M&As : Alexandre, Elsa, Eva et Allegra, vous êtes des petits soleils dans ma vie. A mes amis d'école d'ingé, les presk'archaiques, pour nos soirées mémorables mais surtout qui m'ont entendu tellement de fois répéter que ce que je voulais faire c'est de la biologie marine et pas savoir combien de fourrage il faut donner à un porc pour qu'il s'engraisse de X kilos par semaine. A Jeanne (RANITO <3), d'avoir toujours écouté mes podcasts de crise existentielle, à notre stage hors du temps à Mahahual, à Leïla et Gabi ma compitaya farava je vous aime depuis l'autre côté de l'Atlantique (mais j'arrive bientôt vous inquiétez pas). Aux chkrougnounes du 66, à Banyuls, là où j'ai enfin commencé à faire ce que je voulais de ma vie et où tout a pris sens.

A la team Villefranche, Solène, Louis, Paco, Zoé, Thomas, Lou, Théo, Alex, Marie Barbieux, Cécile, Fred, Loïc (nos embrassades du matin avant le train!), vous avez été mon cocon de bienveillance sur cette côte d'Azur si étrangère pour moi. Je ne sais pas comment j'aurai fait sans vous. Camille et Laurie les meilleurs, je ne saurais même pas quoi écrire tellement vous êtes importants. Vous êtes des personnes extraordinaires, je vous aime profondément et savoir que je vous quitte bientôt me déchire le cœur. Je suis tellement reconnaissante d'avoir croisé votre route. A nos interminables soirées à la trinquette, à Beuil, à votre petit bateau, à nos apéros plage, à la bugada, au beach volley (RIP le terrain), à nos sorties apnée, à nos nombreuses randos, soirées jeux, soirées musiques, aux bières du Picard et aux mozzas sticks qui nous ont toujours tenus compagnie.

Merci aux petits vieux de Villefranche qui me disaient toujours bonjour le matin en allant au train, et que j'étais en retard (souvent). Merci à Axel du marché pour tous les fruits gratuits que tu nous as donné dans le dos de ton père. Merci à Marcel, mon vélo, infatigable destrier de cette dernière année car j'en pouvais plus du TER ZOU blindé et en retard. Merci à mon copain de vélo dont je ne connais même pas le nom, pour nos discussions du matin sur la route du labo, ça rendait ce trajet si stressant un peu moins hostile.

Merci à tous les gens que j'ai rencontré grâce à l'impro, Saber, Charlie, Kacem, Romain (la team de Thonooooooon non ?) mais aussi les CountaBlabla, Aline, Souf, Loann, Quentin, Johan, Pierre et tous les autres. Vous avez été ma bouffée d'oxygène pour cette dernière année, à nos nombreux spectacles musicaux ou non, à votre bienveillance et bonne humeur constante.

A ma famille, mes parents et mes trois supers frères, je n'aurai pas pu rêver mieux comme famille. Vous avez été et vous resterez mon ancre dans ce monde si chaotique. Merci d'avoir toujours su m'accompagner et me soutenir dans tous mes projets, même quand vous n'approuviez pas totalement (au MEXIQUE ??). Thomas, Mathieu et Damien, vous êtes des frères géniaux. On m'a souvent demandé si ce n'était pas trop dur d'être la seule fille avec trois frères et je n'ai jamais compris cette question. Je n'aurai pas voulu d'autres frères que vous, même si on a cassé quelques chaises et carreaux (oups). A nos aventures dans la forêt et la rivière du fond du jardin, à nos expéditions « scientifiques » sur nos bateaux fait de tables, de chaises et de sacs IKEA, à notre musée du granit et nos caches-caches géants dans le jardin. Papa et Maman, votre amour inconditionnel et la bienveillance dans laquelle vous nous avez élevé ont façonné la personne que je suis devenue. Je suis fière d'être votre fille et je suis extrêmement reconnaissante de vous avoir comme parents. Merci de m'avoir transmis votre passion de la mer, de nous avoir mis les pied dans l'eau dès tous petits, de ne pas avoir eu peur de nous trimballer partout, y compris en voilier sur le Tocam puis le Tocamada, d'avoir traversé le Golfe de Gascogne avec quatres enfants, de leur mettre des paillettes dans les yeux lorsque l'on croise des dauphins (ou des MOLA MOLA), de ne pas avoir eu peur de les laisser pour traverser l'Atlantique (je vais faire pareil maintenant, bravo l'exemple). Vous êtes des personnes incroyables et je vous aime de tout mon cœur.

Erwan, merci à la vie d'avoir fait que nos chemins se croisent de nouveau, merci d'être toi et d'avoir toujours accompagné ma folie avec la tienne. Je nous souhaite à tous les deux des choses magnifiques dans notre vie.

Elsa, comment écrire ici tout ce que nous avons vécu ensemble ? Tu es bien plus qu'une coloc pour moi. Nous avons vécu ces trois années ensemble, parfois tellement en phase que ça faisait peur. A notre vie commune, aux arancinis de trois heure du mat, à la danse dans la cuisine, aux déter peinture, couture, aux soirées mémorables qu'on a organisé dans l'appart, à nos larvages Netflix quand ça faisait trop, aux kilos de pesto (rosso mais aussi verde rucola j'oublie pas) engloutis, je pense qu'on fait le chiffre d'affaires de Barilla. A ton lavage intempestif du sol, à mes déter de vaisselle, à nos magnifiques toilettes pleines de post it, à notre projet voyage parce qu'on pouvait quand même pas se quitter comme ça ! A nos squatteurs de l'appart Utami et Oliver, les meilleurs amis pour la chasse aux croquettes, merci de nous avoir soutenues quand on craquait, surtout en cette fin de thèse.

J'aurai pu écrire encore des pages sur chacun d'entre vous mais apparemment il faut que je laisse de la place pour l'impact des vagues de chaleurs sur le microbiote du corail rouge alors je vais simplement terminer cette déclaration par ma phrase favorite :

JADOR LA MAIR

Table des matières | Table of contents

Remerciements | Acknowledgements 1

Avant-propos | Foreword 9

Liste des publications | List of publications 9

Liste des communications orales | List of oral communications 10

Liste des principales abréviations | List of the main abbreviations 11

Table des illustrations | Table of illustrations 12

Liste des tableaux | List of tables 17

Résumé en français 18

Abstract in English 19

Introduction 20

I. Ecological and economic importance of Mediterranean marine animal forests 21

A. What are the Marine Animal Forests (MAFs)? 21

1. General definition 21

2. Ecosystem services 22

3. Specificities of Mediterranean MAFs 22

B. Octocorals: the main builders of Mediterranean MAFs 23

1. General taxonomy and anatomy of corals 24

2. *Paramuricea clavata* and other notable gorgonians of the Mediterranean Sea 26

3. The red coral *Corallium rubrum*: an ecological and cultural keystone species 28

II. Corals are holobionts 33

A. Bacterial communities of coral holobionts 34

1. *Endozoicomonas* is a widespread coral-associated bacterium 34

2. Spirochaetales are other major coral symbionts present notably in *C. rubrum* 35

3. Other key bacterial families in coral microbiomes 37

4. Shared evolutionary history between corals and their bacterial communities 39

B. Microeukaryotic communities in coral holobionts 40

1. Dinoflagellates and other photosynthetic microeukaryotes 41

2. Fungi 43

3. Protists 44

C. Other microbial communities associated with corals 47

1. Archaea 47

2. Viruses 48

D. Methods for studying microbial communities 50
1. Culture-based methods 51
2. Metabarcoding 52
3. Quantification by qPCR 54
4. Functional and metabolic studies of microbiomes 54
III. Anthropogenic disturbances in the Mediterranean Sea and their consequences on octocoral species 56
A. Anthropogenic disturbances 56
1. Global warming intensifies the severity and frequency of marine heatwaves in the Mediterranean Sea 57
2. Other local stressors for Mediterranean octocorals 59
3. The unique status of the economically valuable red coral 59
B. The consequences of seawater warming on octocoral populations 61
1. Massive mortality episodes (MMEs) 61
2. Physiological impairments 63
3. Microbiome dysbiosis 66
a. Response of Symbiodiniaceae and the other members of the eukaryome 67
b. Response of the bacterial communities 68
Aims of the Thesis 73
Axis 1: Diversity of the microbiome of Mediterranean octocorals
Chapter 1: Evolutionary relationships between octocorals and their bacterial microbiome 81
I. Overview of the chapter 81
II. Publication 83
Chapter 2: Unveiling the composition and spatiotemporal stability of the eukaryome of *Corallium rubrum* 113
I. Overview of the chapter 113
II. Publication 115
Chapter 3: Characterization of the cultivable fungal community of *Corallium rubrum* 135
I. Overview of the chapter 135
II. Publication 136

Axis 2: Response of the microbiome of *C. rubrum* and *P. clavata* to thermal stress

Chapter 4: Response of the bacterial microbiome of *Corallium rubrum* and *Paramuricea clavata* to the 2022 marine heatwaves 155

I. Overview of the chapter 155

II. Publication 157

Chapter 5: Response of the eurakyome of *Corallium rubrum* to the 2022 marine heatwaves 189

I. Overview of the chapter 189

II. Publication 191

Chapter 6: Assessing the short-term resilience of *Corallium rubrum* holobiont to thermal stress 221

I. Overview of the chapter 221

II. Publication 223

Discussion 256

I. General discussion 256

A. Summary of the key results 257

B. Integrative approach of experimental results 261

C. Limitations of this PhD 272

1. *In-situ* experiments/sampling: Limited consideration of environmental parameters beyond temperature 272

2. *In-situ* experiments/sampling: Inability to sample colonies before MHWs 272

3. Laboratory experiments: Technical limitations 273

4. Differences between laboratory and natural microeukaryotic communities 273

5. Limited use of taxon-specific qPCR for tracking key microbes 274

II. Future directions in microbial ecology research on octocorals 275

1. Investigating all microbial compartments 275

2. Elucidating the role of *Vibrio* spp. (and other microbes) in coral mortality 275

3. Expanding and optimizing qPCR assays for broader microbial coverage 276

4. Shifting toward functional and multi-omics approaches 276

5. In an ideal scenario: implement long-term holistic monitoring programs 277

III. Conclusion: insights into understanding the role of the microbiome in the health and resilience of Mediterranean octocorals in a changing world 279

Résumé général de la thèse en français 282

Appendix 1 – Introduction 326

Appendix 2 – Chapter 1 330
Appendix 3 – Chapter 2 336
Appendix 4 – Chapter 3 352
Appendix 5 – Chapter 4 366
Appendix 6 – Chapter 5 386
Appendix 7 – Chapter 6 417
References 430

Avant-propos | Foreword

Note sur la traduction française | Note on the French translation

Ce manuscrit est essentiellement écrit en anglais. Toutefois, un résumé détaillé en français est fourni à la fin du manuscrit.

This manuscript is written primarily in English. However, a detailed summary in French is provided at the end of the manuscript.

Contenu | Content

Cette thèse se présente sous la forme de six articles, dont quatre publiés (Chapitres 1, 4, 5 et 6), ainsi qu'un article sous le deuxième tour de révision (Chapitre 2) et un article soumis (Chapitre 3).

This thesis is presented in the form of six articles, four of which have been published (Chapters 1, 4, 5, and 6), one of which is undergoing a second round of revision (Chapter 2), and one of which has been submitted for publication (Chapter 3).

Financement | Funding

Cette thèse a été réalisée dans le cadre d'un projet financé par la Maison CHANEL, en partenariat avec le Centre Scientifique de Monaco, à l'occasion de la création de l'unité de Recherche sur la Biologie des Coraux Précieux CSM–CHANEL.

This thesis was completed as part of a project funded by CHANEL, in partnership with the Scientific Center of Monaco, on the occasion of the creation of the CSM–CHANEL Precious Coral Biology Research Unit.

Liste des publications | List of publications

2023

Prioux, Camille, Romie Tignat-Perrier, Ophélie Gervais, et al. 2023. "Unveiling Microbiome Changes in Mediterranean Octocorals during the 2022 Marine Heatwaves: Quantifying Key Bacterial Symbionts and Potential Pathogens." Microbiome 11 (1): 271. https://doi.org/10.1186/s40168-023-01711-x.

2024

Prioux, Camille, C. Ferrier-Pages, J. Deter, et al. 2024. "Insights into the Occurrence of Phylosymbiosis and Co-Phylogeny in the Holobionts of Octocorals from the Mediterranean Sea and Red Sea." Animal Microbiome 6 (1): 62. https://doi.org/10.1186/s42523-024-00351-2.

2025

Prioux, Camille, Christine Ferrier-Pagès, Javier Del Campo, et al. 2025. "Unraveling the Impact of Marine Heatwaves on the Eukaryome of the Emblematic Mediterranean Red Coral *Corallium Rubrum*." ISME Communications, February 21, ycaf035. https://doi.org/10.1093/ismeco/ycaf035.

Prioux, Camille, Christine Ferrier-Pagès, Thibaut Lamarca, Denis Allemand, and Romie Tignat-Perrier. 2025. "Heatwave-Driven Persistent Microbes Threaten the Resilience of Mediterranean

Coral Holobionts." Environmental Microbiome 20 (1): 107. https://doi.org/10.1186/s40793-025-00765-8.

En preparation | In preparation

Prioux Camille and Filipponi Doria, Christine Ferrier-Pagès, Denis Allemand, Romie Tignat-Perrier. "Unveiling the microeukaryotic landscape of the red coral *Corallium rubrum* across the Northwestern Mediterranean Sea". Environmental Microbiology Reports, *Under 2nd review*.

Prioux Camille, Marina Carrasco-Acosta, Valeria Prigione, Francesco Venice, Romie Tignat-Perrier, Denis Allemand, Christine Ferrier-Pages and Giovanna Cristina Varese. "Hidden fungal diversity of the precious Mediterranean red coral *Corallium rubrum*: Culture-based discoveries and challenges of metabarcoding". Environmental Microbiology Reports, *Under 1st review*.

Liste des communications orales | List of oral communications

Congrès de l'Association francophone d'écologie microbienne (AFEM), Carqueiranne (Var, France). 17-20 Octobre 2023: Unveiling Microbiome Changes in Mediterranean Octocorals During the 2022 Marine Heatwaves: Quantifying Key Bacterial Symbionts and Potential Pathogens. Prioux C, Tignat Perrier R, Gervais O, Estaque T, Schull Q, Reynaud S, Beraud E, Merigot B, Beauvieux A, Marcus MI, Richaume J, Bianchimani O, Cheminee A, Allemand D., Ferrier-Pagès C. Poster.

2nd congress on Marine Evolution. rEvolutionary routes in the Sea, Virtual congress, 14-17 Novembre 2023: Evolutionary patterns in octocoral-microbiota associations. Prioux C, Tignat-Perrier R, Ferrier-Pagès C, Guilbert A, Reynaud S, Rottier C, Deter J, Ballesta L, Allemand A, Van De Water J. Présentation orale.

European Culture Collections Organisation (ECCO), Bari (Italy), 18-20 Sept. 2024 : Fungal diversity in the precious Mediterranean red coral Corallium rubrum. Camille Prioux, Marina Carrasco-Acosta, Valeria Prigione, Romie Tignat-Perrier, Denis Allemand, Christine Ferrier-Pagès, Giovanna Cristina Varese. Poster.

Federation of European Microbiological Societies (FEMS), Milan (Italy), 14-17 Juillet 2025. The microbiome of octocorals in a warming Mediterranean Sea: role in thermotolerance and resilience. Camille Prioux, Romie Tignat-Perrier, Denis Allemand, Christine Ferrier-Pagès. Présentation orale.

Liste des principales abréviations | List of the main abbreviations

A. coralloides: *Alcyonium coralloides*

ASV: Amplicon Sequence Variant (variante de séquence d'amplicon)

C. rubrum: *Corallium rubrum*

C. verticillata: *Callogorgia verticillata*

E. cavolini: *Eunicella cavolini*

E. verrucosa: *Eunicella verrucosa*

K. utinomii: *Klyxum utinomii*

MAF: Marine Animal Forest (Forêt animale marine)

MME : Mass Mortality Event (événement de mortalité massive)

MHW: Marine Heatwave (vague de chaleur marine)

MPA: Marine Protected Area (Aire marine protégée)

OTU: Operational Taxonomic Unit (Unité Taxonomique Opérationnelle)

P. clavata: *Paramuricea clavata*

P. thyrsoides: *Paralemnalia thyrsoides*

S. eilatense: *Sclerophytum eilatense*

S. glaucum: *Sarcophyton glaucum*

S. loyai: *Sclerophytum loyai*

S. polydactylum: *Sclerophytum polydactylum*

S. vrijmoethi: *Sclerophytum vrijmoethi*

V. coralliilyticus: *Vibrio coralliilyticus*

Table des illustrations | Table of illustrations

Introduction

Figure 1: Organisms with three-dimensional structures. (A) Tropical rainforest and (B) arborescent octocorals in Indonesia, ©IStock (A) and ©Reinhard Dirscherl/Prisma (B).....21

Figure 2: Schematic representation of the ecological and societal benefits provided by marine animal forests, ©Personal illustration.....22

Figure 3: A Mediterranean Marine Animal Forest, featuring octocorals species, sponges, bryozoans, and diverse fish species, ©Laurent Ballesta.....23

Figure 4: Simplified phylogenetic tree of Cnidaria, with the subclass Octocorallia. Only families that include species referenced at least once in this thesis are represented, ©Personal illustration adapted from McFadden et al. (2022).....24

Figure 5: Schematic representation of a polyp of Hexacorallia (A) and an autozooid polyp of Octocorallia (B). The Octocorallia here is a gorgonian, with an internal axis. Modified from Integrated Principles of Zoology Fifteenth edition, by Hickman et al. (2010).....26

Figure 6: Most common gorgonian species of the Mediterranean Sea. (A) *Eunicella cavolini* ©Eric Béraud, (B) *Eunicella singularis* ©Eric Béraud, (C) *Paramuricea clavata*, ©Eric Béraud, (D) *Paramuricea macrospina* ©Egidio Trainito, (E) *Callogorgia verticillata* ©INPN.....28

Figure 7: *Coralliidae* species classified as precious corals and commercially harvested for their skeletons. (A) White skeleton of *Corallium konojoi*, (B) Pink skeleton of *Corallium elatius,* (C) Red skeleton of *Paracorallium japonicum*, (D) Red skeleton of *Corallium rubrum*. Pictures of coral skeletons are personal illustrations.....29

Figure 8: (A) Branching structure of *Corallium rubrum* © Eric Tambutté, **(B) A cave with colonies of *C. rubrum* in Villefranche-sur-Mer (France)** © Paco Stil, **(C) Known geographical distribution of *Corallium rubrum*.** This species occurs along the central and western basin of the Mediterranean and the neighboring eastern Atlantic along the coast of Africa and the Canary Islands, southern Portugal and Cape Verde, from Bruckner 2016.....30

Figure 9: The red coral *Corallium rubrum* throughout history, highlighting its cultural, commercial, and spiritual significance (A) Harvested Mediterranean red coral collected by a licensed coral fisher, one of the few remaining with a permit to operate in the region ©Jean-Philippe Giordano, (B) Crafting of a jewelry from a Mediterranean red coral skeleton ©Jean-Philippe Giordano, (C) Painting illustrating a merchant showcasing red coral in his store, Petrus Christius (1473) St. Elgio and Godeberta, Lehman collection, New-York, (D) The Madonna of Victory, Andrea Mantegna (1431-1506), The Louvre, Paris, (E) Coral talisman with silver bells made by an English jeweller, XVII-XVIIIth century, Basilio Liverno Museum of Coral, (F) Turkish pectoral in silver and Mediterranean red coral, XVIIth, Basilio Liverino Museum of Coral, (G) Madonna and Child, Piero della Francesca, XVth century, Palazzo Ducale, Urbino, (H) One of the earliest examples of sculpture in red coral. British Museum, Jove-Sarapis, Greaco-Roman art.....32

Figure 10: Average relative abundance of bacterial taxa classified as *Spirochaetales* across microbial metabarcoding studies of hexacorals and octocorals. Additional details, including references and sample-specific information, are provided in Supplementary Table S1.....36

Figure 11: Known composition and potential roles (to our knowledge) of the different microbial compartments of the octocoral holobiont. © Personal illustration based on the results of the studies presented in this chapter.....50

Figure 12: Overview of the most common methods used to study microbial communities, highlighting their key strengths and limitations. The figure emphasizes the complementarity of these approaches and the benefits of combining different techniques for a more comprehensive understanding of microbial dynamics. The methods employed in this thesis are represented by solid arrows, while other methods are shown with dashed arrows.....51

Figure 13: Time series of monthly mean (blue line) and 24-month filtered (red line) sea surface temperature anomalies in the Mediterranean Sea from 1993 to 2022. Anomalies are calculated relative to the climatological period 1993–2014 and are based on satellite observations from the Copernicus Marine Environment Monitoring Service (CMEMS) dataset. The sea surface temperature trend, along with its 95% confidence interval (shown in the box), is estimated using the X-11 seasonal adjustment procedure, a statistical method for analyzing time series data (Pezzulli et al., 2005; Pisano et al., 2020), and Sen's method, a technique for detecting trends in climate data (Sen, 1968). © Copernicus Marine Service.....56

Figure 14: Average daily surface water temperature in the Mediterranean Sea, showing the annual evolution in recent years. The year 2003 is also highlighted due to a major heatwave that affected the entire basin. The black line represents the median of historical temperature records from 1982 to 2019, while the gray bands indicate the range within which 90% of historical records fall. Water temperatures exceeding this range are considered exceptionally high. © Icatmar.....57

Figure 15: Number of marine heatwaves in the Mediterranean Sea between May and August 2022. The Western basin experienced a higher frequency of events compared to the Eastern basin, with some areas recording up to seven marine heatwave episodes, an unprecedented maximum for the region. © Mercator Ocean International.....58

Figure 16: Red List status of anthozoans in the Mediterranean region. *Corallium rubrum* is classified as "Endangered" and *Paramuricea clavata* is listed as "Vulnerable**"**, from the IUCN conservation status of Mediterranean anthozoans (Otero Del Mar et al. 2017).....60

Figure 17: Number of mass mortality events reported in the Mediterranean Sea. Geographic distribution and taxa affected over the period from 1979 to 2017. From Garrabou et al. (2019)..62

Figure 18: Summary diagram of the results of studies on the impact of thermal stress on Mediterranean octocorals. The results were separated between *in-situ* studies and laboratory-based controlled aquarium experiments, as well as between the presence or absence of lost tissue. At present, no results have been observed on necrotic corals in the natural environment.70

Chapter 1

Figure 1: Locations of the different sampling sites. The corresponding sampling missions are indicated for each site.....88

Figure 2 : (A) NMDS on Bray-Curtis distance matrix showing ordination of coral samples ; (B) Bacterial community composition for each species per location (taxa less abundant than 2% are grouped together under Others ; Lowercase letters correspond to taxonomic levels, p : Phylum, c : Class, f : Family, g : Genus ; Uppercase letters correspond to sampling locations, A : Eilat, B : Tombants des Américains, C : Saint Martin, D : Nord 1 Site 1, E : Massif du Raventurier, F : Capense, G : Cap Corse 8A, H : Scalo, I : Anneaux Site A).....95

Figure 3: Phylosymbiosis in octocorals. Juxtaposition of the coral host phylogenetic tree and the microbiota dendrogram for **(A)** all the coral samples and **(B)** a subset of the Mediterranean coral species only.....98

Figure 4: Relative abundance of the OTUs involved in host-symbiont associations contributing significantly to cophylogenetic congruence (positive residual frequencies values) for all Mediterranean and Red Sea coral species (the stars correspond to the contributing associations between a host and an OTU) along with their respective phylogeny. Taxonomic annotation: p – phylum; o – order; f – family; g – genus.....101

Chapter 2

Figure 1: Geographic distribution of the sampling sites. Map of the Northwestern Mediterranean Sea showing the sampling locations: Cap de Creus, Spain (42.3°N, 3.3°E); Cassis, France (43.2°N, 5.5°E); Porticcio, Corsica, France (41.8°N, 8.8°E); Villefranche-sur-Mer, France (43.7°N, 7.3°E) and Portofino, Italy (44.3°N, 9.2°E). Samples were collected from visually healthy colonies at 30–40 m depth.....118

Figure 2: Alpha diversity metrics across sampling sites. Observed richness (ASV level) **(A)**, Shannon index **(B)**, Simpson index **(C)** and Inverse Simpson index **(D)**. Graphs are showing value distributions, their median and interquartile range per sampling site. Groups assigned with same letters are not statistically different.....124

Figure 3: Structure of the red coral eukaryome depending on the sampling site and year. Hierarchical cluster analysis on the Aitchison distance matrix based on the eukaryome structure (CLR-transformed ASV data) **(A) and** beta dispersion (within-site variability) of the samples based on the community composition at the ASV level. Boxplots display value medians and interquartile ranges for each site **(B)**.....126

Figure 4: Composition of the eukaryome of *C. rubrum* across the sampling sites. Composition of the whole microeukaryotic community of the red coral across the samples (Family level). In each sample, families with a relative abundance lower than 3% were grouped **(A)**. Relative abundance of core families and their top five ASVs across all samples **(B)**.....128

Figure 5: ASVs differentially abundant (ANCOM-BC results) between the sampling years (A) and sites (B). Differences in relative abundance are calculated as a log2 fold change (base 2). In **(A)**, positive values indicate taxa significantly more abundant in samples from autumn 2023 than spring 2013 and negative values taxa less abundant in these samples. In **(B)**, statistically significant values are framed in black.....130

Chapter 3

Figure 1: Composition of the culturable fungal communities isolated from soft tissue and skeleton of *Corallium rubrum*, at the different taxonomic ranks.....144

Figure 2: Influence of the isolation techniques on the number of culturable fungal species isolated from *Corallium rubrum*. Influence of growth media (A) and incubation temperature (B).

Details on the number of exclusive and common species found in the two coral tissues (soft tissue and skeleton) at different incubation temperatures (15 and 25 °C) (C).....145

Figure 3: Composition of the mycobiome of *Corallium rubrum*. Colony-forming unit (CFU) per gram of skeleton or soft tissue dry-weight across isolation temperatures and growth media...148

Chapter 4

Figure 1: Species and number of samples collected at the different geographical locations. Collection depths (in brackets) and the number of samples per condition (blue for 0% tissue loss and red for 90% tissue loss) are indicated next to the names of the sites.....163

Figure 2: Temperature regime in 2022 and in the past twenty years at one of the collection sites (*Riou Sud*, Calanques National Park, Marseille, France). Seawater temperature at 15 m and 30 m depth from January to September 2022 (**A**), and number of exposure days at temperatures between 23°C and 27°C at 15 m (**B**) and 30 m depth (**C**) over the past twenty years.....165

Figure 3: Impact of the 2022 heatwaves on coralligenous reefs of the Calanques National Park (Marseille, France). (**A**) Average percentage of *P. clavata* and *C. rubrum* colonies affected by tissue loss at the different sampling sites. (**B**) Colonies of *C. rubrum* (**a**) and *P. clavata* (**b**) exhibiting tissue loss (August 2022); Coralligenous assemblage before (**c**) and during (**d**) the heatwaves. Credit: *Septentrion Environnement*.....167

Figure 4: Estimation of the bacterial species richness in *C. rubrum* (left) and *P. clavata* (right) depending on the collection site and the colony health status (0% and 90% tissue loss). Statistical significance levels of differences between octocorals experiencing tissue loss or not are indicated by stars (*** for $p < 0.001$).....172

Figure 5: Relative abundance of the ASVs associated with *C. rubrum* (A) and *P. clavata* (B) depending on the collection site and the percentage of tissue loss (0% and 90%)......173

Figure 6: Bacterial ASVs differentially abundant between *C. rubrum* colonies with 0% and 90% tissue loss. (**A**) Difference in relative abundance calculated as log fold change (natural log) in the 90% tissue loss condition compared to the 0% tissue loss condition, all sites combined. (**B**) Venn diagram of the bacterial ASVs differentially abundant between tissue loss percentages and common between sites ('+' in red and '-' in blue indicating a significant increase or decrease of the ASV in the 90% tissue loss condition, respectively).....176

Figure 7: Bacterial ASVs differentially abundant in colonies of *P. clavata* with 0% and 90% tissue loss, all sites combined. The difference in relative abundance is calculated as log fold change (natural log) in the 90% compared to 0% tissue loss condition.....177

Figure 8: Relative expression ratio (fold change) between the 90% and 0% tissue loss conditions of the different targeted genes. Concentration per host cell of the total bacteria (A), *Vibrio* bacteria (B), *Spirochaetaceae* (C) and *Endozoicomonas* bacteria (D) per site. Graphs are presented in logarithmic scale. Statistical significance levels of differences between octocorals experiencing tissue loss or not are indicated by stars (* for $p < 0.05$ and ** for $p < 0.01$).....179

Figure 9: Differential responses of the octocoral microbiota to the marine heatwaves of 2022. By providing complimentary qPCR-based data to amplicon sequencing information, our study brings valuable insight on the microbiota changes occurring in two octocoral species

experiencing the marine heatwaves of 2022. Biological and environmental factors were also identified as putative drivers of the differential responses.....184

Chapter 5

Figure 1: Locations of the different sampling sites. Colony health condition (with or without tissue loss) and intensity of the MHWs are indicated for each site.....196

Figure 2: Number of days for which temperatures reached 23°C in the different sampling sites and depths, in 2022 (Marseille, Portofino) or 2023 (Villefranche-sur-Mer). Values of seawater temperature were extracted from the T-MEDNet database (www.t-mednet.org) at Riou Sud (Calanques National Park, France, 2022) and Portofino (MPA, Italy, 2022) and from Somlit (www.somlit.fr) at Villefranche-sur-Mer (Point B, France, 2022 and 2023).....197

Figure 3: Relative abundance of the microeukaryotic families associated with *C. rubrum* colonies depending on the colony health condition (0% or 90% tissue loss) and collection site. Microeukaryotic taxa are ordered by taxonomic division for those with an average relative abundance above 1%.....205

Figure 4: Composition of the microeukaryote communities associated with *C. rubrum* colonies (ASV level). Relative abundance and taxonomy of the most abundant microeukaryote ASVs associated with *C. rubrum* colonies of different health conditions and collected at different sites. Microeukaryotic taxa with an average relative abundance below 3% are aggregated.....206

Figure 5: Microeukaryote species richness associated with *C. rubrum* colonies depending on the collection site and the colony health condition. Colonies collected at the control sites are represented in blue. Heat-stressed colonies without tissue loss but collected in MHWs-impacted sites are represented in yellow, while those with tissue loss are represented in red. Significant statistical differences (p-value < 0.05) between groups are indicated by letters.....208

Figure 6: **Microeukaryote ASVs differentially abundant (ANCOM-BC results) between the *C. rubrum* colonies collected at the control sites (*Villefranche-sur-Mer* and *Bigo*) and the *C. rubrum* colonies collected at the other sampling sites.** Differences in relative abundance calculated as log fold change (natural log).....209

Figure 7: Schematic representation of the composition of the microeukaryote communities associated with *C. rubrum* colonies according to the sampling site and coral health condition. Only the most prevalent microeukaryote groups are represented.....210

Figure 8: **Structure of the microeukaryote communities associated with *C. rubrum* colonies with 0% and 90% tissue loss in the Calanques National Park (Marseille). (A)** Principal component analysis of the Aitchison distance matrix based on the composition of the microeukaryote communities (ASV level), showing the distribution and dispersion of the *C. rubrum* samples collected at the different sites. **(B)** Beta-dispersion assessment using the distance to centroids of samples with and without tissue loss.....211

Figure 9: Conceptual diagram illustrating potential interrelationships and feeding dynamics among the most prevalent microeukaryote groups associated with *C. rubrum* colonies...219

Chapter 6

Figure 1: Schematic representation of the experimental design. (**A)** Experimental temperature regimes applied to the corals, with the three sample collection time points. **(B)** Nine colonies were cut in nine nubbins randomly allocated into groups of three in the aquaria. One nubbin per colony and thermal treatment was removed at each sampling time point.....228

Figure 2: Relative abundance of the bacterial and microeukaryotic families associated with *C. rubrum* colonies depending on the sampling time and thermal treatment. Taxa with an average relative abundance below 3% are grouped.....237

Figure 3: Bacteria and microeukaryote ASVs differentially abundant (ANCOM-BC results) between the sampling times and thermal treatments. Differences in relative abundance are calculated as log fold change (natural log).....239

Figure 4: Network representation of significant microbial associations inferred from *16S* (prokaryotic) and *18S* (microeukaryotic) *rRNA* genes metabarcoding datasets. Nodes represent ASVs, with colors distinguishing bacterial (blue) and microeukaryotic (green) taxa. Edges indicate associations: red edges denote positive correlations, and blue edges denote negative correlations. Edge thickness corresponds to the strength of the association. Families of the ASVs of the 6 higher positive correlations for each group (intra-kingdom and inter-kingdom) as well as the first 3 higher negative correlations are labeled next to the nodes.....243

Figure 5: Relative expression ratio of stress response genes in fold change (TNFR1 and HSP70) between control and thermally treated colonies (C+4 and C+8) at the different sampling times. Graphs are presented in logarithmic scale. Statistical significance levels of differences compared to the controls are indicated by stars (* for $p < 0.05$ and ** for $p < 0.01$)..244

Figure 6: Relative expression ratio (fold change) between control and thermally treated colonies (C+4 and C+8) at the different sampling times of the different targeted genes. Concentration per host cell of the total bacteria, *Vibrio* and Spirochaetaceae bacteria. Graphs are presented in logarithmic scale. Statistical significance levels of differences compared to the controls are indicated by stars (* for $p < 0.05$, ** for $p < 0.01$ and *** for $p < 0.001$).....246

Figure 7: Microbiome dynamics of the red coral observed in this study during and after the heat stress. Under control conditions, the coral microbiome remained stable and was primarily composed of Spirochaetaceae bacteria and Labyrinthulaceae microeukaryotes. Exposure to elevated temperatures induced compositional changes in the microbiome: first in the eukaryome then in the bacterial communities. We observed an increase in opportunistic taxa and a decline in the relative abundance of microbial taxa consistently associated with healthy corals. As conditions normalize post-stress (2-weeks recovery period), the abundance of most original community members returned to baseline levels while the relative abundance of most opportunistic taxa declined. However, the coral microbiome did not fully recovered as some heat stress-associated microorganisms persisted at elevated relative abundances.....247

Discussion

Figure 1: Schematic overview of the key results presented in this thesis.....260

Liste des tableaux | List of tables

Table 1: Characteristics of the primer sets used for Sanger sequencing.....91

Résumé en français

Les gorgones méditerranéennes, telles que *Corallium rubrum* et *Paramuricea clavata*, jouent un rôle écologique clé en tant qu'espèces ingénieures, structurant des habitats riches en biodiversité. Toutefois, leur survie est menacée par les vagues de chaleur marines, responsables de mortalités massives. Dans ce contexte, une approche holistique centrée sur le concept d'holobionte, considérant l'hôte et son microbiote comme une unité biologique fonctionnelle, peut apporter un éclairage nouveau sur la vulnérabilité et la résilience de ces coraux face aux stress climatiques.

Cette thèse a permis de caractériser le microbiote associé aux octocoralliaires méditerranéens, d'explorer les liens coévolutifs entre les hôtes et leurs symbiotes bactériens ainsi que l'effet du stress thermique sur les holobiontes de *C. rubrum* et *P. clavata* en utilisant une approche combinant observations *in situ* et expérimentations en laboratoire. Des analyses ciblant à la fois l'hôte et son microbiote (PCR quantitative, séquençage haut débit, cultures microbiennes) ont permis cette caractérisation et notamment la documentation de la réponse des holobiontes aux anomalies thermiques.

Les résultats montrent que ces octocoralliaires abritent un microbiote bactérien spécifique, souvent dominé par un taxon unique, comme les *Spirochaetaceae* ou les *Endozoicomonadaceae*. Les analyses de phylosymbiose et de cophylogénie révèlent une congruence évolutive entre les hôtes et certains symbiotes, suggérant une histoire commune ancienne, notamment entre *C. rubrum* et les *Spirochaetaceae*. Le microbiote de ce dernier apparaît particulièrement stable dans l'espace et dans le temps. En revanche, les communautés microeucaryotes (eucaryome) sont plus sensibles aux conditions environnementales. Le jeu de données de métabarcoding basé sur l'*ARNr 18S* produit durant cette thèse constitue l'un des premiers inventaires de l'eucaryome corallien. Il révèle une diversité élevée, incluant des ciliés (Licnophoridae), straménopiles (Labyrinthulomycètes) et dinoflagellés (Syndiniales). Par ailleurs, la culture fongique à partir de tissus et de squelettes de corail a permis d'isoler de nombreuses espèces cultivables.

Nos études sur l'impact du stress thermique ont mis en évidence une dysbiose marquée du microbiote sous température élevée, avec une augmentation notable de bactéries opportunistes et potentiellement pathogènes, telles que les *Vibrionaceae* et *Rhodobacteraceae*. Néanmoins, l'abondance des symbiotes majeurs comme *Spirochaetaceae* et *Endozoicomonaceae* est restés stable. L'eucaryome de *C. rubrum* a montré une réponse plus rapide et plus sensible au stress thermique que la communauté bactérienne. De plus, après retour à des conditions normales, le microbiote n'a pas complètement retrouvé son état initial, bien que l'expression génique de l'hôte soit revenue à la normale. Les *Vibrio*, notamment, sont restés abondants, suggérant qu'un stress sublétal peut laisser une empreinte microbienne durable, susceptible d'affecter la résistance future du corail.

Ces travaux mettent en lumière le rôle déterminant du microbiote dans la santé des coraux, en révélant les profondes altérations que peut induire un stress thermique. Les changements observés au sein des communautés microbiennes, notamment l'émergence de bactéries opportunistes et la persistance de certaines signatures dysbiotiques après le stress, suggèrent que le microbiote constitue un indicateur sensible de l'état de santé des coraux et de leur exposition aux perturbations environnementales, en particulier celles liées au changement climatique.

Abstract in English

Mediterranean gorgonians such as *Corallium rubrum* and *Paramuricea clavata* play a crucial ecological role as habitat-forming species that support a rich biodiversity. However, their survival is increasingly threatened by recurrent marine heatwaves, that trigger widespread mass mortalities. Recent research suggested that a holobiont perspective, in which the host and its associated microbiome are considered as a functional biological unit, could provide new insights into the vulnerability and resilience of these corals in the face of climate stressors. In this thesis, we first characterized the Mediterranean octocoral microbiome and investigated the evolutionary congruence between hosts and their bacterial symbionts. Combining *in situ* approaches with controlled laboratory experiments, we then investigated the impact of thermal stress on the holobionts of *C. rubrum* and *P. clavata*. Approaches targeting both the host and its microbiome, including host and microbe-based quantitative PCR analyses, metabarcoding sequencing (*16S* and *18S rRNA* genes to target bacterial and microeukaryotic symbionts) and microbial cultures, were used to characterize the holobiont response to thermal anomalies.

Our results show that Mediterranean octocorals harbor a specific bacterial microbiome, often dominated by one bacterial taxon, such as Spirochaetaceae and Endozoicomonadaceae. Phylosymbiosis and cophylogeny analyses assessing the evolutionary congruence between the hosts and their microbiome provided arguments for a co-evolutionary history between Mediterranean coral hosts and some bacterial symbionts. For example, the red coral *C. rubrum* and Spirochaetaceae bacteria probably have had a long-term association and speciated together. More generally, the bacterial community associated with *C. rubrum* is characterized by a highly stable microbiome, both spatially and temporally. Our results revealed that it is not the case for the microeukaryotic communities (eukaryome), whose diversity and structure vary depending on the environmental conditions. Our *18S rRNA* gene-based metabarcoding dataset is among the first to be reported in the literature on the coral eukaryome to date. Sequencing and fungal cultures-based data showed that the red coral eukaryome was composed of microeukaryotes as diverse as Licnophoridae ciliates, Labyrinthulomycetes stramenopiles, Syndiniales dinoflagellates and a myriad of fungal species differing depending on the host tissue (red tissue versus skeleton).

Our studies investigating the impact of thermal stress on octocoral holobionts showed that abnormally high temperatures result in large changes in the microbiome, leading to a dysbiosis. These changes are likely due to the proliferation of bacterial opportunists and putative pathogens such as Vibrionaceae and Rhodobacteraceae. However, the abundance of the main symbionts Spirochaetaceae and Endozoicomonaceae remained stable. Investigations of the red coral eukaryome showed that structural changes in the microeukaryotic community occur more rapidly and are observed under lower temperatures compared to the bacterial community. After the stress has passed, the microbiome did not fully return to its original state after two weeks under the control temperature. While the expression of host stress-related genes returned to normal based on qPCR analyses, opportunistic microbes such as *Vibrio* bacteria remained in high abundances in the microbiome. These results suggest that sublethal thermal stress can leave a microbial footprint that may affect the coral's ability to withstand future stress. Taken together, our results suggest that the resistance and resilience of Mediterranean octocorals to thermal stress might be compromised by the overgrowth of opportunistic microbes. This work highlights the essential role of the microbiome in coral health and stress response, and it has important implications for understanding octocoral' vulnerability to climate change.

General introduction



Introduction

I. Ecological and economic importance of Mediterranean marine animal forests

A. What are the Marine Animal Forests (MAFs)?

1. General definition

Tropical coral reefs and temperate coralligenous assemblages are part of Marine Animal Forests (MAFs), a concept originally introduced by Alfred Wallace in 1869 and later refined by Rossi et al. (2017a). This term describes a benthic ecosystem dominated by large, sessile suspension-feeding invertebrates greater than 1 cm in size, including corals, gorgonians, sponges, bryozoans, sea pens, ascidians, hydrozoans, tubeworms, and bivalves. These species act as ecosystem engineers by forming intricate three-dimensional structures that resemble tree canopies (Figure 1 and Rossi et al. 2017a). Although they are composed of animals and not plants, MAFs fulfill ecological functions similar to terrestrial forests. Their complex structures provide shelter for a wide variety of marine species (Piazzi et al., 2021), and promote biodiversity by influencing key ecological processes such as recruitment, recovery, predation, and competition (Paoli et al. 2017). As some of the most diverse and productive ecosystems in the world (Bianchi and Morri 2000; Ballesteros 2006; Wilkinson 2008; Gori et al. 2011), MAFs also play a crucial role in regulating water flow. By reducing flow velocity, they minimize the resuspension of sediment (Eckman et al. 1989) and extend the residence time of food particles, thereby significantly influencing the ecosystem dynamics (Gili et al. 1998).

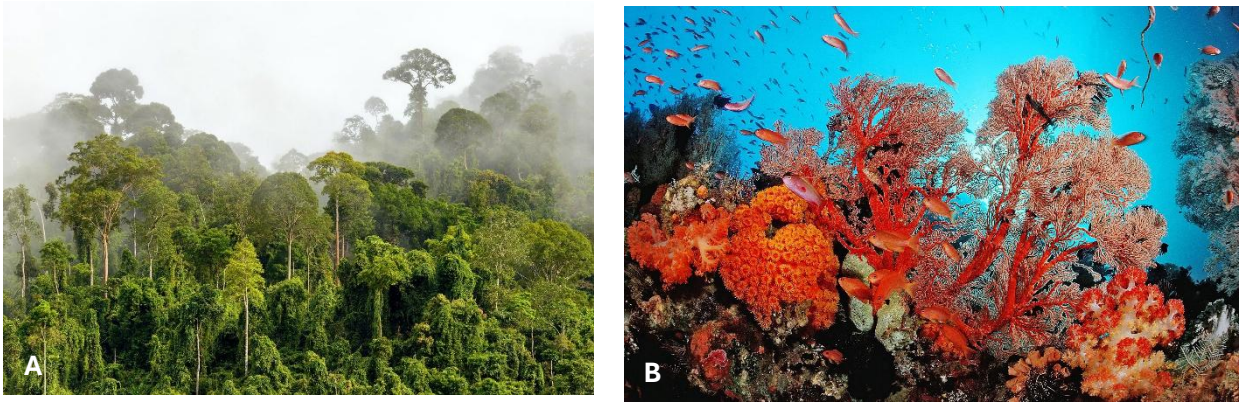

Figure 1: Organisms with three-dimensional structures. (A) Tropical rainforest and (B) arborescent octocorals in Indonesia, ©IStock (A) and ©Reinhard Dirscherl/Prisma (B).

2. Ecosystem services

Mediterranean coralligenous assemblages and tropical coral reefs are critical for marine biodiversity and offer a wide range of social and economic benefits (Bianchi et al. 2000; Ballesteros 2006; Tonin 2018; Buonocore et al. 2020; Figure 2) that enhance human well-being, both directly and indirectly (Paoli et al. 2017). These ecosystems are vital sources of commercially valuable seafood for the surrounding regions (Peterson et al. 2003; White et al. 2000). They also attract millions of tourists, generating significant revenue(Paoli et al. 2017). In tropical regions for example, their total value is estimated at nearly US$36 billion (Spalding et al. 2017). Additionally, they stabilize the seabed and prevent erosion and damage from storms and currents (Ferrario et al. 2014). They are also a valuable source of bioactive molecules with potential pharmaceutical applications (Häder 2021). The total value of the ecosystem services these coral ecosystems provide could reach several trillion dollars annually (Costanza et al. 2014).

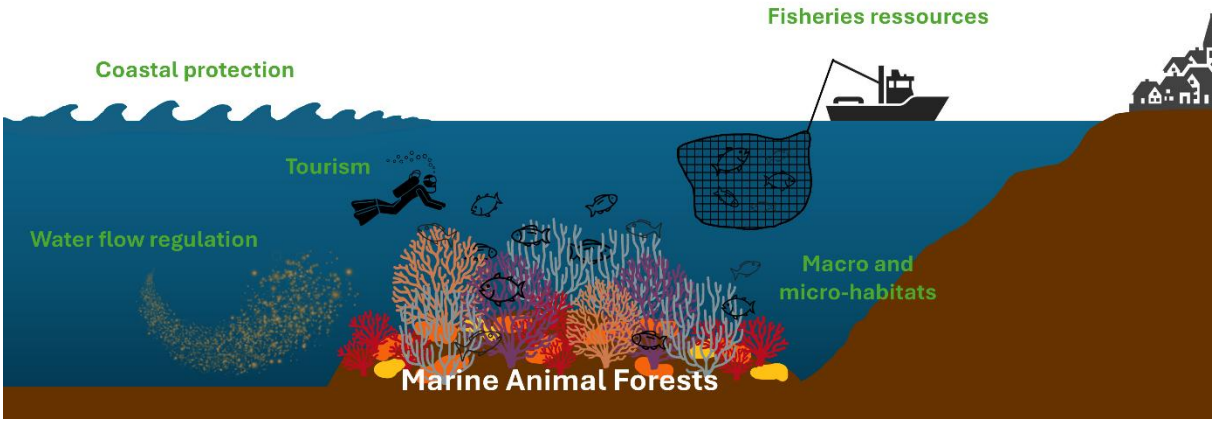

Figure 2: Schematic representation of the ecological and societal benefits provided by marine animal forests, ©Personal illustration.

3. Specificities of Mediterranean MAFs

In contrast to the most well-known tropical coral reefs which are built by hexacorals (scleractinian corals) that form calcareous structures of calcium carbonate in warm, sunlit waters (Allemand et al. 2004), the Mediterranean marine animal forests (or coralligenous assemblages) consist of biogenic calcareous structures formed by sessile organisms such as octocoral gorgonians, sponges, and bryozoans, with the accumulation of encrusting algae (Gibson et al. 2006; Figure 3).

Mediterranean marine animal forests exhibit diversity across various depths and habitats, ranging from deep coastal areas (40-80 m) to the continental shelf (50-80 m), as well as shelf edges and offshore seamounts (110-200 m; Gori et al. 2017). Gorgonians of the subclass Octocorallia such as *Eunicella singularis* and *Paramuricea clavata* dominate in deep nearshore rocky bottoms alongside black corals (*Antipathella subpinnata*), soft corals, and sponges, creating structurally complex habitats (Bo et al. 2012; 2014; Gori et al. 2011; 2017). On the continental shelf, coralligenous reefs harbour dense assemblages of *Corallium rubrum*, *Eunicella cavolini*, and sea pens, with large sponges and bryozoans increasing species diversity (Ballesteros 2006; Grinyó et al. 2016; Priori et al. 2013). With increasing depth towards the shelf edge and offshore seamounts, gorgonian diversity increases with species such as *Callogorgia verticillata*, while black corals (*Leiopathes glaberrima*, *Parantipathes larix*) become more abundant, especially on seamounts such as Carloforte Shoal (Bo et al. 2014; Cau et al. 2015). These habitats provide refuge and feeding grounds for numerous fishes, crustaceans and mollusks (Santín et al. 2021; Cartes et al. 2022; Deidun et al. 2014; D'Onghia et al. 2012). Various species, including crabs, ophiuroids, and predatory gastropods, inhabit or feed on corals (Bo et al. 2014; Cau et al. 2015). Coral canopies also serve as egg-laying sites (Bo et al. 2015).

B. Octocorals: the main builders of Mediterranean MAFs



Figure 3: A Mediterranean Marine Animal Forest, featuring octocorals species, sponges, bryozoans, and diverse fish species, ©Laurent Ballesta

1. General taxonomy and anatomy of corals

Corals are assigned to the phylum Cnidaria and the subphylum Anthozoa (Figure 4). Their presence in the geological record dates to the time between the Cryogenian and the Tonian (648-894 Ma; (McFadden et al. 2022)), which emphasizes their evolutionary importance and adaptability. Today, cnidarians exhibit remarkable diversity, with approximately 11,000 known species, including 7,500 within Anthozoa (Daly et al. 2007).

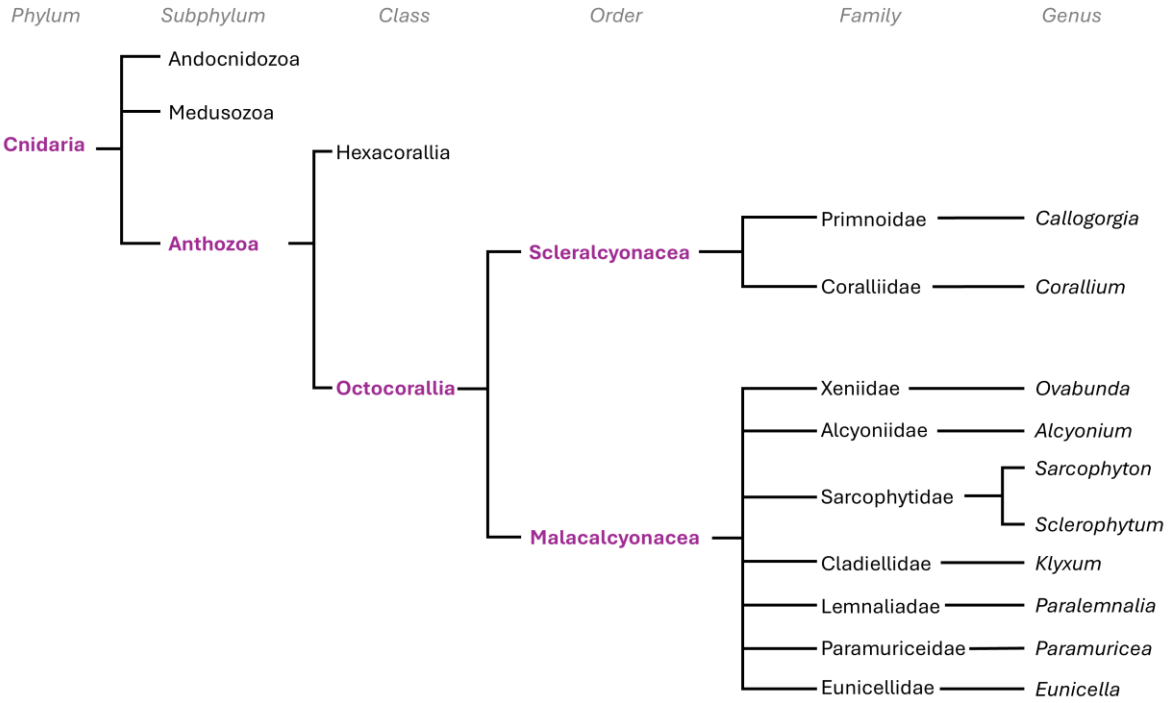

Figure 4: Simplified phylogenetic tree of Cnidaria, with the subclass Octocorallia. Only families that include species referenced at least once in this thesis are represented, ©Personal illustration adapted from McFadden et al. (2022).

Organisms of the Cnidarian phylum are diploblastic, with a simple organization characterized by two cell layers: ectoderm (epidermis) and endoderm (gastrodermis), separated by the mesoglea. They have radial symmetry and lack specialized respiratory, circulatory, or excretory systems (Berzins et al. 2021). Instead, their mouth is connected to the gastrovascular cavity by a pharynx (Figure 5A). Unlike other cnidarians which alternate between motile medusa and sessile polyp forms, corals, that are in the Anthozoa subphylum, remain in the polyp form throughout their life. Coral polyps are small, cylindrical organisms, usually a few millimeters to centimeters in diameter. They possess tentacles to capture prey, and their structure includes a gastrovascular cavity for

digestion. The ectoderm contains sensory cells, mucus-secreting cells, and cnidocytes. Asexual reproduction occurs through fission, fragmentation, or budding, leading to the formation of coral colonies. Sexual reproduction also produces planktonic larvae (planulae; Berzins et al. 2021).

The subphylum Anthozoa is divided into two classes: Hexacorallia and Octocorallia, each distinguished by unique anatomical and ecological traits ((McFadden et al. 2022; WoRMS, Anthozoa, 2024; Figure 4). Hexacorallia corals (or hexacorals) exhibit sixfold radial symmetry, reflected in their tentacles and mesenteries (Figure 5A). Their pharynx, known as the stomodeum, is connected to the gastrovascular cavity, while the mesoglea (coenosarc) connects the polyps and helps in nutrient transport within the colony. The Scleractinia order is composed of "hard corals," which produce a calcareous skeleton primarily composed of aragonite, a crystalline form of calcium carbonate.

Octocorallia corals (or octocorals) have an eightfold radial symmetry, with tentacles and mesenteries arranged in multiples of eight (Figure 5B). Their tentacles are lined with pinnules, which enhance surface area for feeding. Octocorals can be monomorphic (with only one polyp type: autozooid) or dimorphic (with two polyp types: autozooid and siphonozooid; Fabricius et al. 2001). The autozooids are responsible for feeding and reproduction and consist of the anthocodia (mouth and tentacles) and the anthostele (gastrovascular cavity and pharynx). Siphonozooids, smaller polyps with underdeveloped tentacles, facilitate seawater circulation within the colony via a prominent siphonoglyph (Fabricius et al. 2001). The mesoglea (coenenchyme), containing fibers, amoeboid cells, and scleroblasts, connects polyps through solenia, a network of canals linking their gastrovascular cavities.

Octocorals don’t have a hard skeleton of calcium carbonate. However, they have sclerites, small calcite structures (<0.3 mm) formed by scleroblasts in the coenenchyma. They create a support for the colony by cementing themselves together. Some species also develop internal skeletal axes, made of gorgonin (in gorgonians) or calcite (in *Corallium rubrum*). Sclerite morphology and skeletal structure are key traits for octocoral classification, contributing to their diverse colony shapes (Fabricius et al. 2001).

Octocorals are now classified into two monophyletic orders, Malacalcyonacea and Scleralcyonacea, based on the revised classification by McFadden et al. (2022; Figure 4). This update replaces the previous system, which divided octocorals into three orders: Helioporacea (blue corals), Pennatulacea (sea pens), and Alcyonacea, the latter encompassing most octocoral species, including gorgonians, soft corals, sea fans, sea whips, and sea rods.

The order Malacalcyonacea (from Greek malacos, meaning "soft") includes taxa with either a proteinaceous skeletal axis or no skeletal axis, covering soft corals and some gorgonians. In contrast, Scleralcyonacea (from Greek scler, meaning "hard") comprises species with solid calcium carbonate axes or sclerites fused with calcite, incorporating the remaining gorgonians as well as the former Helioporacea and Pennatulacea orders.

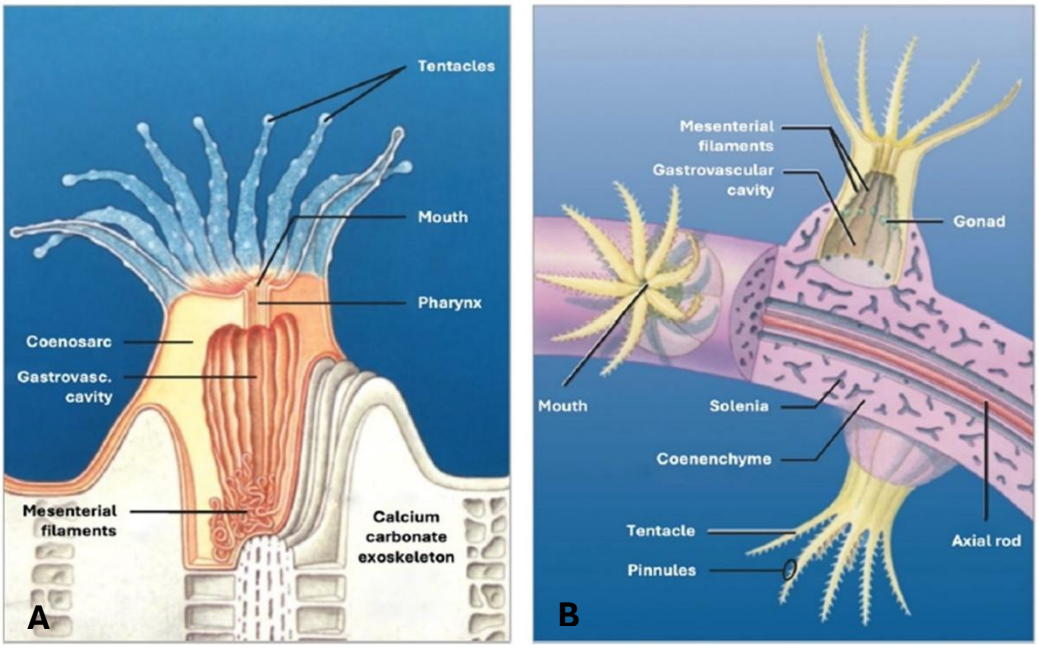

Figure 5: Schematic representation of a polyp of Hexacorallia (A) and an autozooid polyp of Octocorallia (B). The Octocorallia here is a gorgonian, with an internal axis. Modified from Integrated Principles of Zoology Fifteenth edition, by Hickman et al. (2010).

2. *Paramuricea clavata* and other notable gorgonians of the Mediterranean Sea

The term gorgonian refers to a group that was historically classified as Gorgonacea, later incorporated into the order Alcyonacea, and is now distributed between the orders Malacalcyonacea and Scleralcyonacea, making it a paraphyletic group. It can be defined

as a sessile colonial cnidarian with a branched, tree-like, or fan-shaped morphology, supported by a flexible, proteinaceous axial skeleton primarily composed of gorgonin (protein) and calcified spicules.

Gorgonians are widespread in the Mediterranean. They usually inhabit hard seabeds but also adapt to soft substrates and high sedimentation rates (Angiolillo et al. 2018). They form dense assemblages at different depths and environments, with species composition mainly influenced by depth (Bo et al. 2012; 2014; Cau et al. 2018; Fabri et al. 2014; Angiolillo and Canese 2018; Gibson et al. 2006; Gori et al. 2017; Ponti et al. 2019).

Among the most common Mediterranean gorgonians, the red gorgonian *Paramuricea clavata* (Risso, 1826; Figure 6A) plays a crucial role in coralligenous assemblages. It used to be considered endemic (Carpine et al. 1975), but its distribution area has expanded to the neighboring Atlantic (Boavida et al. 2016; Pilczynska et al. 2019). It thrives in rocky substrates from 5 to over 200 m (Mokhtar-Jamaï et al. 2011), and forms dense aggregations of 7-20 colonies/m^2 (Gori et al. 2011; Ponti et al. 2019; Linares et al. 2008), especially in areas with strong currents. The colonies grow up to 1.5 m in size, with an average vertical growth rate of 0.8 cm/year, and suggesting a lifespan of 50-100 years (Linares et al. 2008).

Paramuricea macrospina (Koch, 1882), is another important species, endemic to the Mediterranean, and coexisting with *P. clavata* (Pica et al. 2018; Figure 6B). It inhabits rocky bottoms at 40-100 m and is particularly abundant on the continental shelf (65-90 m) and shelf-edge (110-160 m) in the Menorca Channel (Paletta et al. 2019; Grinyó et al. 2018). High morphological plasticity may lead to misidentification with *P. clavata* (Pica et al. 2018).

Among the *Eunicella* species, *Eunicella singularis* (Esper, 1791) is a symbiotic white gorgonian in the western Mediterranean (Figure 6C), that occurs at depths of 5-50 m, with the highest density at 15-30 m (Forcioli et al. 2011). It thrives in rocky substrates with strong currents (Gori et al. 2012) but is sensitive to temperatures above 24-26°C. There are two morphotypes: a shallow, candelabra-like form with Symbiodiniaceae algal symbionts (20-30 m) and a deeper, more branched form without symbionts (40-60 m; Gori et al. 2012). Their lifespan is 25-30 years, with annual reproduction taking place at the end

of May-June (Ghanem et al. 2021). *Eunicella cavolini* (Koch, 1887), the yellow gorgonian (Figure 6D), lives at depths of 50-290 m, with the highest densities occurring at 120-160 m (Carugati et al. 2021). It prefers rocky substrates under high hydrodynamic conditions with moderate eutrophication and often coexists with *Corallium rubrum* (Carugati et al. 2021). *Callogorgia verticillata* (Pallas, 1766; Figure 6E) is found in deeper waters (200-500 m), both in Mediterranean and western Atlantic deep-sea coral forests, although little is known about its biology and ecology (Cau et al. 2018; Bo et al. 2012; 2014; Fabri et al. 2014).

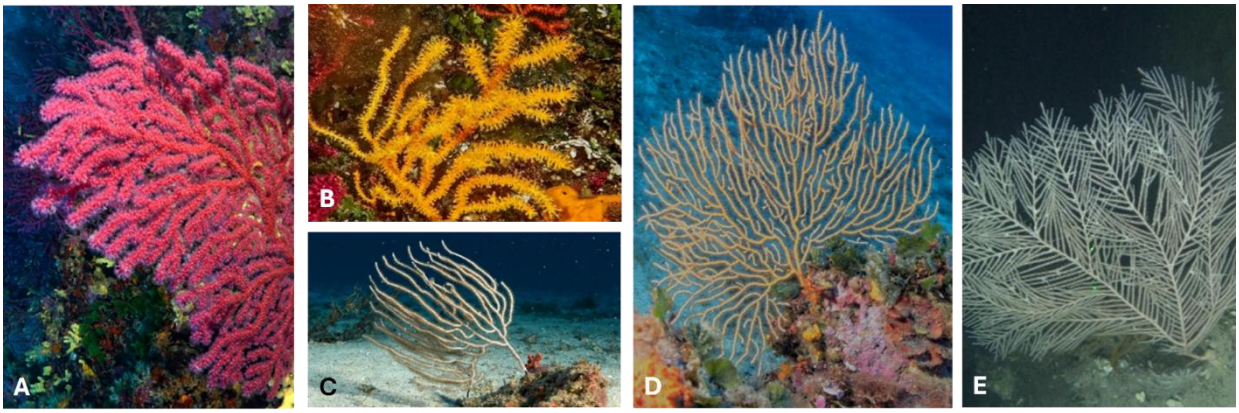

Figure 6: Most common gorgonian species of the Mediterranean Sea. (A) *Eunicella cavolini* ©Eric Béraud, (B) *Eunicella singularis* ©Eric Béraud, (C) *Paramuricea clavata*, ©Eric Béraud, (D) *Paramuricea macrospina* ©Egidio Trainito, (E) *Callogorgia verticillata* ©INPN.

3. The red coral *Corallium rubrum*: an ecological and cultural keystone species

The family *Coralliidae* comprises 36 species and was originally believed to consist of a single genus, *Corallium*. However, extensive debate over the accuracy of the taxonomic classification and phylogeny of the *Coralliidae* indicated that *Coralliidae* should be divided into three distinct genera (Ardila et al., 2012; Figueroa & Baco, 2014), supporting the three-genus classification originally proposed by Gray (1867). According to this revised system, the family *Coralliidae* is now categorized into *Corallium* (7 species), *Hemicorallium* (16 species), and *Pleurocorallium* (14 species) (Tu et al., 2015).

This family is characterized by a rigid, calcareous axis composed mainly of calcite (Carpine & Grasshoff, 1975), whose coloration depends on the species (Figure 7A-D). Several *Coralliidae* species are classified as precious corals and are commercially harvested due to the high value of their skeletons. Their biological characteristics, such

as slow growth rates, exceptional longevity, and size-dependent fecundity, make them highly susceptible to overexploitation (Grigg 1984; Torrents et al. 2005; Luan et al. 2013). In Japanese waters, three species are commercially collected at depths of 90-300 m: *Paracorallium japonicum*, *Corallium elatius*, and *Corallium konojoi*. The long-term exploitation of these species has led to significant population decline (Santangelo et al. 2001,2010; Grigg 2002; Chen et al. 2012). As a result, concern over the conservation of precious corals and other deep-sea coral species has increased in recent years (CITES, 2007; CITES, 2010).

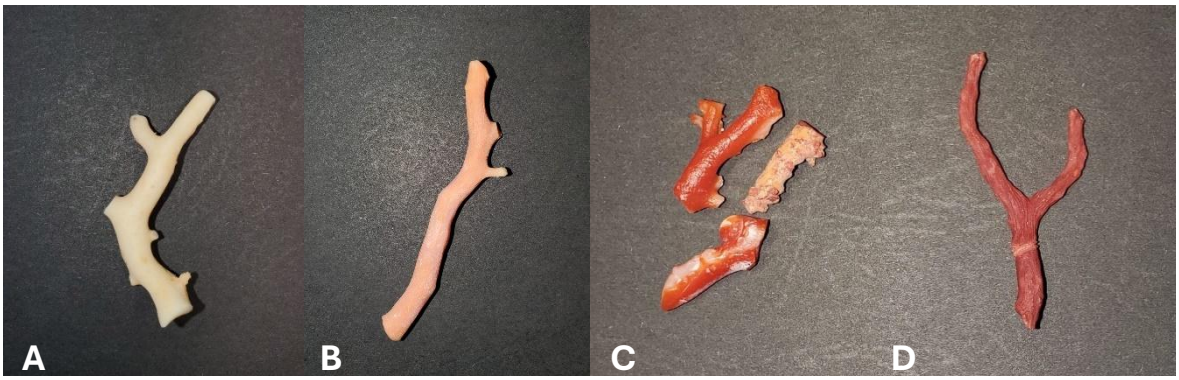

Figure 7: *Coralliidae* species classified as precious corals and commercially harvested for their skeletons. (A) White skeleton of *Corallium konojoi*, (B) Pink skeleton of *Corallium elatius,* (C) Red skeleton of *Paracorallium japonicum*, (D) Red skeleton of *Corallium rubrum*. Pictures of coral skeletons are personal illustrations.

Corallium rubrum (Linnaeus, 1758) is an iconic branching coral species of the Mediterranean Sea (Figure 8A), notable for its red calcareous skeleton, although the origin of its pigmentation remains unknown. The skeleton is completely covered by a thin red tissue which is never of uniform thickness even on the same branch, ranging from 0.2 to 0.3 mm (Liverino, 1989). The eight tentacles of the polyps protrude through the tissue, leaving tiny holes on withdrawals. Being sciaphilous, it thrives in environments such as cave entrances, overhangs, and crevices, often coexisting with encrusting sponges (Ballesteros 2006; Figure 8B). *C. rubrum* primarily inhabits the western Mediterranean basin (Cattaneo-Vietti et al. 2016) but is also found in the eastern Mediterranean (Chintiroglou et al. 1989) and along the Atlantic coasts near the Strait of Gibraltar (Zibrowius et al. 1984; Figure 8C). Its depth range extends from shallow waters at 10 m to the deep sea at 1,000 m (Costantini et al. 2010; Knittweis et al. 2016; Pratlong et al. 2021). This species is characterized by a slow growth rate, long population turnover time, and

high post-settlement mortality, increasing its vulnerability to natural and human-induced pressures (Gallmetzer et al. 2010).

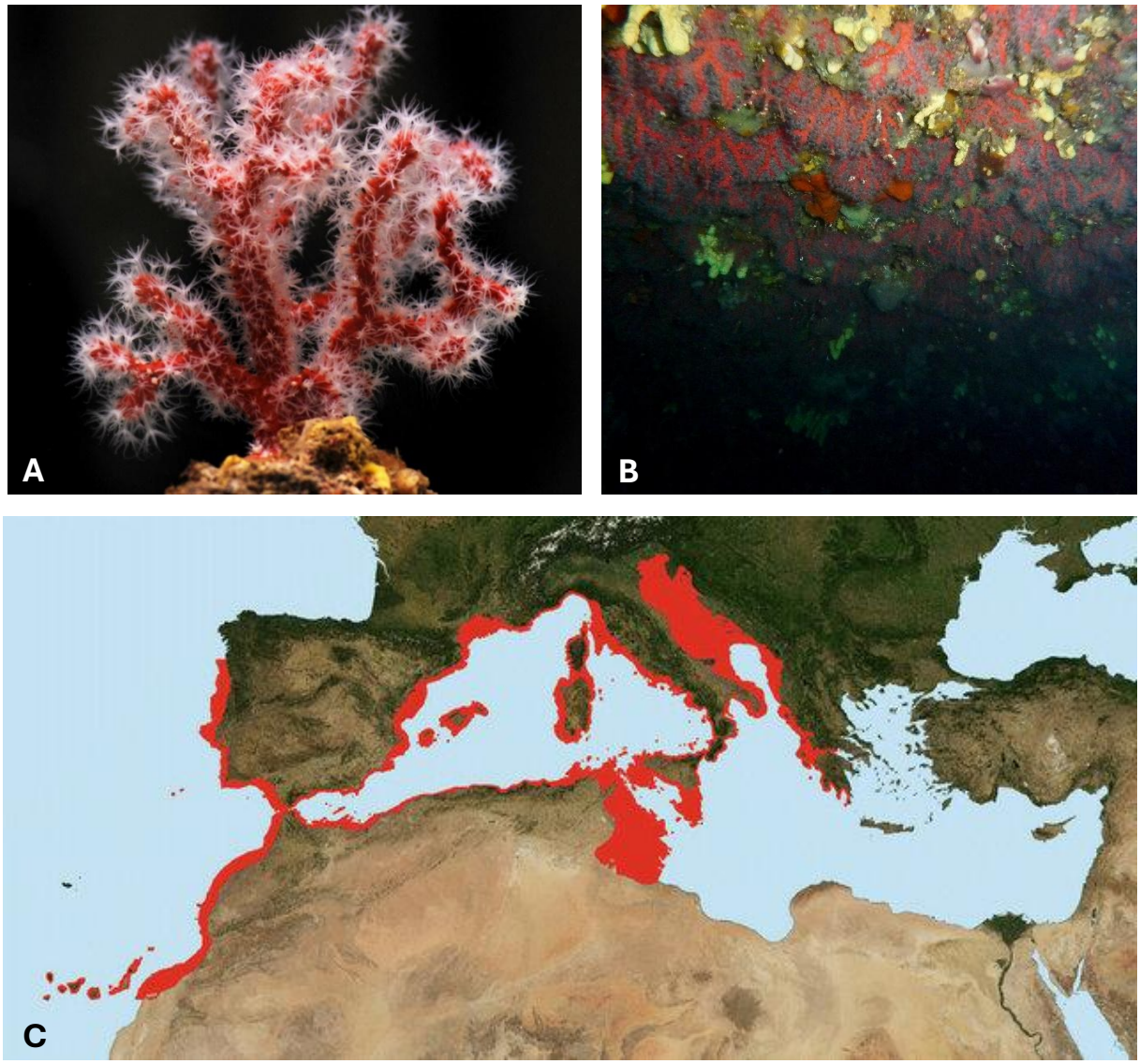

Figure 8: (A) Branching structure of *Corallium rubrum* © Eric Tambutté, **(B) A cave with colonies of *C. rubrum* in Villefranche-sur-Mer (France)** © Paco Stil, **(C) Known geographical distribution of *Corallium rubrum*.** This species occurs along the central and western basin of the Mediterranean and the neighboring eastern Atlantic along the coast of Africa and the Canary Islands, southern Portugal and Cape Verde, from Bruckner 2016.

Due to its high commercial value, *C. rubrum* has been extensively harvested, making it one of the most economically significant marine resources in the Mediterranean (Figure 9A-C; Santangelo et al. 2001; Tsounis et al. 2010). The red coral has been used in various decorative (ornaments, statues, sculptures), spiritual (amulets, talismans) and jewelry items (Figure 9D-H; (Tsounis et al. 2006; 2010; 2013; Cattaneo-Vietti et al. 2016). We have no precise information about the origins of coral workmanship, neither about the period nor the people who initiated it. However, the discovery of small objects in red coral or other material decorated with red coral seems to suggest that it began to be worked by man as long ago as the prehistoric age (Liverino, 1989). Many creations of the past can be seen in museums, including one the earliest examples of sculpture in Mediterranean coral depicting a Graeco-Roman Jove Sarapis (British museum; Figure 9H). Paintings featuring red coral frequently highlight its symbolic meanings, often linked to themes of protection, vitality, and mystical power (Figure 9D and G).



Figure 9: The red coral *Corallium rubrum* throughout history, highlighting its cultural, commercial, and spiritual significance (A) Harvested Mediterranean red coral collected by a licensed coral fisher, one of the few remaining with a permit to operate in the region ©Jean-Philippe Giordano, (B) Crafting of a jewelry from a Mediterranean red coral skeleton ©Jean-Philippe Giordano, (C) Painting illustrating a merchant showcasing red coral in his store, Petrus Christius (1473) St. Elgio and Godeberta, Lehman collection, New-York, (D) The Madonna of Victory, Andrea Mantegna (1431-1506), The Louvre, Paris, (E) Coral talisman with silver bells made by an English jeweller, XVII-XVIIIth century, Basilio Liverno Museum of Coral, (F) Turkish pectoral in silver and Mediterranean red coral, XVIIth, Basilio Liverino Museum of Coral, (G) Madonna and Child, Piero della Francesca, XVth century, Palazzo Ducale, Urbino, (H) One of the earliest examples of sculpture in red coral. British Museum, Jove-Sarapis, Greaco-Roman art.

II. Corals are holobionts

The concept of the holobiont has fundamentally transformed our understanding of biological systems, by conceptualizing the host organism and its associated microbiome as a single functional unit (Margulis and Fester 1991; Baedke et al. 2020; Simon et al. 2019a). This integrative perspective underscores the importance of microbial symbiosis in the evolution, ecology, and physiological functioning of the host, emphasizing that no organism exists in isolation but rather as part of a complex, interdependent community. In the case of corals, both Hexacorallia and Octocorallia form intricate symbiotic associations with a diverse array of microorganisms, including bacteria, archaea, viruses, and microeukaryotes, which together constitute the coral holobiont (van de Water et al. 2018; Stévenne et al. 2021; Voolstra et al. 2024). Among these microbial partners, the dinoflagellate symbionts of the family Symbiodiniaceae are the most well-characterized, playing a central role in providing the host with essential nutrients through photosynthesis. However, the microbial consortium as a whole contributes to a wide range of ecological and physiological processes, including nutrient cycling, organic matter degradation, production of antimicrobial compounds that regulate pathogenic microorganisms, and the enhancement of stress tolerance, particularly to temperature fluctuations and other environmental perturbations (Voolstra et al. 2024a).

While coral-associated bacterial communities have been the most intensively studied component of the holobiont, providing valuable insights into host-microbe interactions and ecosystem function, the roles of other microbial groups, particularly microeukaryotes beyond the Symbiodiniaceae and viral elements, remain largely unexplored. These under-researched components may play crucial yet unrecognized roles in maintaining the stability and resilience of the holobiont, especially in the context of ongoing environmental change. Therefore, a more comprehensive and integrative investigation of the entire coral microbiome is essential to advance our understanding of coral biology and to inform conservation strategies for reef ecosystems. Given the greater availability of information on Hexacorallia holobionts compared to Octocorallia holobionts, this chapter will provide an overview of the microbial diversity and composition of both coral classes. However, particular emphasis will be placed on Octocorallia, which constitutes the primary focus of this thesis.

A. Bacterial communities of coral holobionts

The taxonomic diversity of coral-associated bacteria is significant, with at least 39 phyla (Huggett et al. 2019) and tens to thousands of species-level taxa identified depending on the sequencing approach and the methodology used to do the taxonomic classification (Hernandez-Agreda et al. 2017). Among the most common phyla are Pseudomonadota (formerly Proteobacteria), Bacteroidota, Bacillota, and Cyanobacteriota (Bourne et al. 2016).

1. *Endozoicomonas* is a widespread coral-associated bacterium

The most well-known bacterial partners in corals belong to the family Endozoicomonadaceae, particularly the genus *Endozoicomonas* (Neave et al. 2016), which has been the focal point in lots of studies (Neave et al. 2017). These bacteria are frequently dominant in healthy corals but can decline under environmental stress, such as thermal stress (Bourne et al. 2016). Some *Endozoicomonas* genotypes are site-specific, whereas others, such as those found in *Pocillopora* corals, display a global distribution (Neave et al. 2016).

In Mediterranean octocorals, such as soft gorgonians from the genera *Paramuricea*, *Leptogorgia*, and *Eunicella*, *Endozoicomonas* can constitute over 96% of an individual's bacterial community (van de Water et al. 2018; Ransome et al. 2014; La Rivière et al. 2013; Bayer et al. 2013; Correa et al. 2013; Pike et al. 2013). These bacteria form dense microbial aggregates within coral tissues and contribute to amino acid synthesis, organosulfur compound processing, and B vitamin production (Tandon et al. 2022). Additionally, they are involved in the digestion of complex molecules (Alex et al. 2019; Speck et al. 2012) such as dimethylsulfoniopropionate (DMSP; Raina et al. 2009; 2010) and chitin (Da Silva et al. 2023). They can also play a role in sulfur cycling (Tandon et al. 2022), immune defense, and microbiome stability (Morrow et al. 2012; Bourne et al. 2016). However, the precise role of *Endozoicomonas* in coral health remains a subject of debate. While its broad distribution across coral species suggests a beneficial symbiotic relationship, researchers are questioning its role in coral holobionts due to emerging evidence of its potential pathogenicity, the complexity of its interactions with other microorganisms, and the need for more functional studies to clarify its diverse lifestyle

possibilities beyond a purely mutualistic relationship (Ziegler et al. 2019; Pogoreutz and Ziegler 2024).

2. Spirochaetales are other major coral symbionts present notably in *C. rubrum*

The microbiome of the red coral Corallium rubrum is characterized by a strong dominance of Spirochaetales, which can account for up to 70% of the bacterial community (van de Water et al. 2016a). This composition contrasts with the *Endozoicomonas*-dominated microbiomes typically observed in other Mediterranean octocorals (van de Water et al. 2016a) and *has sparked interest in this previously overlooked bacterial family in corals*. Spirochaetales have also been detected in both healthy and diseased tropical and cold-water hexacorals and octocorals (Figure 10), although they are more frequently associated with visually healthy individuals. This pattern suggests a possible commensal or symbiotic relationship between Spirochaetales and their coral hosts. The relative abundance of Spirochaetales, primarily assessed through metabarcoding approaches, varies considerably across coral species, from as low as 0.01% in the tropical hexacoral Montastrea cavernosa to as high as 90% in *Heliofungia actiniformis (Frias-Lopez et al. 2002; Boote 2021)*. Within-species variability is also substantial. For instance, in hexacorals such as *Acropora cervicornis*, *Acropora granulosa*, *Lophelia pertusa*, and *Savalia lucifica*, as well as in octocorals like *Anthothela grandiflora*, *Muricea californica*, and *Sinularia* spp., Spirochaetales relative abundance ranges from 0% to 85% depending on the sample (Figure 10; Supp. Table X). In *Corallium rubrum*, the dominance of Spirochaetales appears to be geographically and temporally stable (van de Water et al. 2016a). These bacteria are primarily located in the coenenchyme and polyps, rather than the skeleton, representing approximately 80%, 50%, and 5% of the total bacterial community in these respective compartments *(van de Water et al. 2024)*.

Spirochaetales are not restricted to corals, as they are also common symbionts of various invertebrates, including arthropods, mollusks, and oligochaete worms (Ruehland et al. 2008; Brune 2014; Mayasich et al. 1987). In termite guts, they contribute to lignocellulose breakdown (Brune 2014) and nitrogen fixation (Lilburn et al. 2001). However, their role in corals remain unknown. It has been suggested that they can play a

potential role in host physiology, possibly contributing to nitrogen (Lilburn et al. 2001) and carbon fixation (Leadbetter et al. 1999), similar to Symbiodinium and nitrogen-fixing bacteria. Their stable association with *Corallium rubrum* and relatively high abundance in their microbiome suggests that they might play an important role in the holobiont metabolism and health but that remains to be investigated.

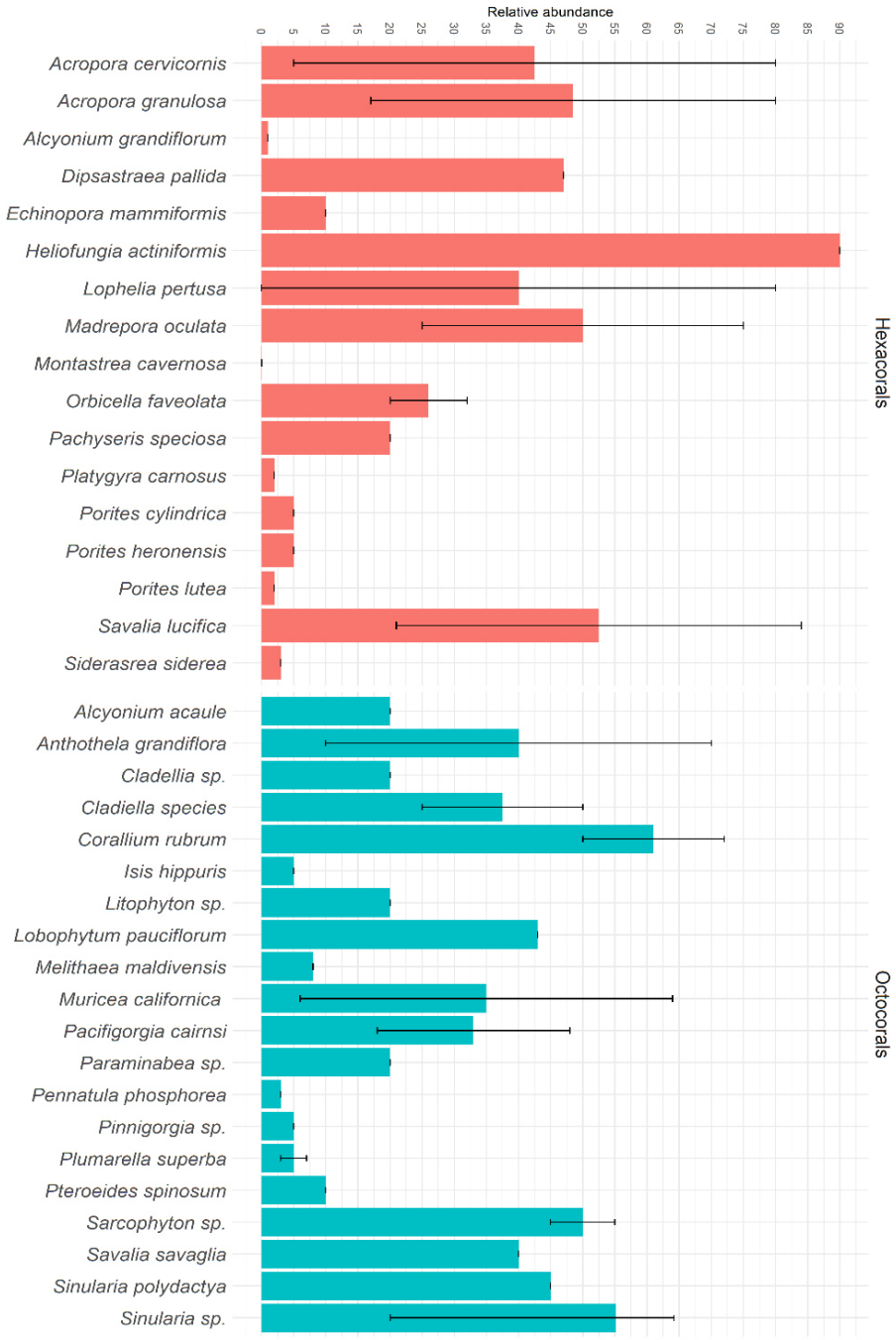

Figure 10: Average relative abundance of bacterial taxa classified as *Spirochaetales* across microbial metabarcoding studies of hexacorals and octocorals. Additional details, including references and sample-specific information, are provided in Supplementary Table S1.

3. Other key bacterial families in coral microbiomes

In addition to the Endozoicomonadaceae and Spirochaetaceae, coral microbiomes harbor other important bacterial families, including Vibrionaceae, Rhodobacteraceae, and the Alteromonadales order (Hernandez-Agreda et al. 2017; van Oppen et al. 2019; Bourne et al. 2016).

The Vibrionaceae family, particularly *Vibrio* spp., is widely distributed in marine environments and frequently associated with corals, where members of this group may function as both pathogens and symbionts (Rubio-Portillo et al. 2018; Sharon et al. 2010). These bacteria are strongly thermodependent, proliferating in warm waters and becoming more abundant during summer or in response to climate change, particularly in temperate zones like the Mediterranean (Baker-Austin et al. 2013; Vezzulli et al. 2010; 2012; 2013). Although many studies have focused on the role of *Vibrio* spp. as tropical coral pathogens, implicated in diseases such as white syndrome, yellow band disease, and white spot disease, as reviewed in Munn (2015), their virulence is often temperature-dependent (Billaud et al. 2022; Boyett et al. 2007; Kimes et al. 2012). For example, species like *V. coralliilyticus* and *V. mediterranei* have been shown to trigger tissue necrosis under thermal stress in tropical corals (Tout et al. 2015; Ben-Haim et al. 2003; 2003) but especially in Mediterranean gorgonians (Martin et al. 2002; Tignat-Perrier et al. 2023; Rubio-Portillo et al. 2014; Vezzulli et al. 2010).

However, *Vibrio* spp. are also natural members of the coral microbiome, representing over 40% of cultured isolates from healthy corals (Ritchie 2006; Sharon et al. 2010). Certain *Vibrio* strains isolated from corals were show to form a mutualistic relationship with the host by fixing nitrogen in the coral holobiont (Chimetto et al. 2008) while others may help defend their coral hosts from pathogens (Ritchie 2006), indicating that their roles extend beyond pathogenesis. Their metabolic plasticity and genomic adaptability enable them to occupy diverse niches and respond to environmental fluctuations (Le Roux et al. 2018; Lin et al. 2018; Zhang et al. 2018; Ceccarelli et al. 2014), although some species are also subject to predation by protozoa and bacteriophages (Fu et al. 2022; Pfeifer et al. 2019). While pathogenic vibrios are a concern during mass mortality events and disease outbreaks, the full ecological significance of *Vibrio* spp. in

coral reef ecosystems remains incompletely understood, underscoring the need for further research into their dual roles in coral health and disease.

Members of the Rhodobacteraceae family are widespread in coral ecosystems and have been found in association with a variety of coral species, often increasing in abundance under environmental stress such as elevated seawater temperatures (Ziegler et al. 2019; Pootakham et al. 2019a; Tignat-Perrier et al. 2023; Rosales et al. 2020; 2023; Clark et al. 2021). Traditionally considered opportunistic or potentially pathogenic, especially during disease outbreaks and thermal stress (Clark et al. 2021; Rosales et al. 2020; 2023), Rhodobacteraceae are now being reconsidered for their potential beneficial roles. Recent studies suggest that Rhodobacteraceae, that consistently increases under stress, positively interact with coral symbionts and microbial communities (Y.-H. Chen et al. 2012; Dang et al. 2008; Buchan et al. 2014). Notably, *Ruegeria* spp., a genus within Rhodobacteraceae, may enhance coral health through antimicrobial activity, quorum sensing interference, microbial network stabilization, and mitigation of pathogenic infections such as *Vibrio coralliilyticus* (Kitamura et al. 2021; Xu et al. 2024). This family also contributes to nutrient cycling and stress response mechanisms within the coral holobiont, supporting coral resilience (Pootakham et al. 2019a). Genetic and functional diversity among Rhodobacteraceae, particularly across different coral microhabitats (e.g., mucus, tissue, skeleton), reveals specialized adaptations like osmolyte utilization and survival in low-energy environments (Luo et al. 2021; Cardénas et al. 2021). While their proliferation under stress underscores a potentially protective role, it also raises concerns about shifts in microbiome balance and the long-term implications for coral resilience in a changing climate (Rosales et al. 2020; 2023; Gajigan et al. 2017).

The order Alteromonadales, particularly the families Alteromonadaceae and Pseudoalteromonadaceae, is commonly found in association with corals, especially within the mucus of tropical species (Huggett et al. 2019; Sunagawa et al. 2009; Ziegler et al. 2017; Allers et al. 2008; Weatherup et al. 2024). These families of bacteria were shown to exhibit a range of potentially beneficial traits, including antimicrobial activity, nutrient provision, nitrogen fixation, and antioxidant properties (Ng et al. 2015; Dungan et al. 2021; Ceh et al. 2013). Some strains are also involved in dimethylsulfoniopropionate (DMSP) metabolism, contributing to the production of compounds which may aid in

osmoregulation and stress mitigation (Raina et al. 2009a; Gardner et al. 2016; Hopkins et al. 2016; Sunda et al. 2002). These functions may enhance coral resilience to environmental stressors such as high salinity and thermal anomalies, particularly in regions like the northern Red Sea (Osman et al. 2020; Gegner et al. 2017; 2019). Evidence also suggests that *Alteromonas* may play a role in coral disease resistance, as its abundance increases in colonies of the tropical coral *Acropora millepora* that were resistant to *Vibrio* infection (Wright et al. 2017). However, the role of Alteromonadales remains controversial. While some studies emphasize the probiotic potential of these bacteria, considering that their abundance tends to rise with increasing temperatures (Von Scheibner et al. 2017; Ziegler et al. 2019), others associate them with coral pathogenesis (Gignoux-Wolfsohn et al. 2017; Liang et al. 2017; Sunagawa et al. 2009). In Mediterranean octocorals, members of the Alteromonadaceae and Pseudoalteromonadaceae families have been found in both visually healthy individuals (van de Water et al. 2016a; 2017b) and in gorgonians exposed to heat stress (Tignat-Perrier et al. 2022; 2023), highlighting the ambiguity of their functional role within these holobionts.

4. Shared evolutionary history between corals and their bacterial communities

Corals exhibit stable and complex associations with some bacteria such as *Endozoicomonas*, suggesting an evolutionary connection. This has led to discussions of parallel evolution between corals and their microbial symbionts, suggesting coevolution in which reciprocal evolutionary changes occur between interacting species. Concepts such as phylosymbiosis and cophylogeny have emerged to explore these relationships.

Phylosymbiosis is a pattern where microbial community structures reflect their host's phylogeny (Lim and Bordenstein 2020). It has been observed across diverse taxa, including plants (Van Bel et al. 2021), mammals (Bornbusch et al. 2023), insects (Li et al. 2022), sponges (O'Brien et al. 2020), and corals (Pollock et al. 2018; O'Brien et al. 2020). In Mediterranean gorgonian corals, microbial communities remain highly conserved over time and across environmental gradients, suggesting that phylosymbiosis may be significant in these octocorals as well (van de Water et al. 2017b; 2016a; van de Water, Voolstra, et al. 2018a). Supporting this, cophylogeny identifies specific bacterial lineages

that may share an evolutionary history with their coral hosts (Page 2003; Blasco-Costa et al. 2021), shaped by mechanisms such as coevolution, vicariance, and vertical transmission (Hafner et al. 1988; Weckstein 2004). Evidence of host-microbe cophylogeny has been particularly noted in scleractinian corals, especially with *Endozoicomonas* (Pollock et al. 2018; O'Brien et al. 2021). However, cophylogenetic studies do not fully clarify the underlying mechanisms, which could involve coevolutionary selection (Godsoe et al. 2009; Smith et al. 2008) or biogeographic factors. These interactions are crucial for understanding how microbial symbionts influence coral health, resilience, and adaptation to environmental changes.

Conclusion

The intricate relationships between corals and their bacterial communities underscore the fundamental role of prokaryotic symbionts in shaping holobiont health, metabolism, and resilience. From nitrogen fixation and sulfur cycling to immune modulation and microbiome stabilization, bacteria are thought to play a central role in maintaining coral homeostasis. However, further functional studies are needed to clarify their specific contributions. Key taxa such as *Endozoicomonas* and *Spirochaetales* are consistently found in association with corals, suggesting a long-term symbiotic relationship and making them valuable candidates for further research. Furthermore, while much research has focused on bacterial communities, they represent only one component of the broader coral microbiome. Other microbial partners, including archaea, fungi, and protists, also contribute to coral functioning. These non-bacterial symbionts also likely participate in essential processes such as nutrient processing and disease resistance. Understanding their contributions is crucial to gaining a holistic perspective on coral symbiosis.

B. Microeukaryotic communities in coral holobionts

Corals engage in complex symbiotic relationships with various microeukaryotes, of which photosynthetic dinoflagellates from the family Symbiodiniaceae are the most extensively studied. These symbionts supply their coral hosts with energy-rich photosynthates derived from photosynthesis. However, this association is not common in all coral species, especially not in octocorals. Globally, ca. 38% of octocorals do not

harbour Symbiodiniaceae (Schubert et al. 2016). In the Mediterranean Sea, where our octocoral species of interest are located, only one of 43 documented octocoral species (*Eunicella singularis*) maintains such a symbiosis (Schubert et al. 2016). But the coral microbiome also includes other microeukaryotes, such as protists and fungi, whose diversity, functions, and ecological role are still largely unexplored (Bonacolta et al. 2023; Ainsworth et al. 2017). These other microeukaryotes remain a major knowledge gap due to technical issues described in the chapter below (II. D). The investigation of microeukaryotic communities associated with animals has historically been limited to cultures, visual identification or molecular studies of selected groups, in contrast to the more comprehensive approaches used for bacterial microbiomes. Only a handful of studies have applied high-throughput barcoding techniques to explore animal-associated microeukaryotes in a systematic, microbiome-like manner (del Campo et al. 2020). Searching on the Sequence Read Archive from NCBI (https://www.ncbi.nlm.nih.gov/sra) for the current number of tag sequencing studies using the *16S rRNA* gene for bacteria and comparing this number to those using *18S rRNA* gene for eukaryotes, reveals this bias, with approximately 95% focusing on bacteria and only 5% on eukaryotes (SRA-NCBI; Keeling et al. 2017). In coral holobionts, for instance, only two studies to date have focused on the eukaryotic component using metabarcoding methods (Clerissi et al. 2018; Bonacolta et al. 2023). When combined with conventional methods such as culturing and microscopy, these efforts have uncovered a rich diversity of microeukaryotic associates, including microalgae, fungi and protists (Bonacolta et al. 2023). Nevertheless, a more comprehensive view of these communities is necessary to fully understand their taxonomic and functional variability across different coral species. This could help identify symbionts that are consistently associated with corals, similar to *Endozoicomonas* or Spirochaetaceae among bacteria, and allow for an analysis of how community composition and dynamics shift over time and space, especially in response to human-induced environmental changes.

1. Dinoflagellates and other photosynthetic microeukaryotes

Many tropical corals have long been known for their close relationship with photosynthetic dinoflagellates from the family Symbiodiniaceae, a partnership central to coral reef ecosystems and the subject of extensive research (Muscatine and Porter 1977;

Baker 2003). These dinoflagellates reside in host-derived vacuolar structures called symbiosomes (Muscatine et al. 1998), where they supply the coral with up to 95% of their photosynthetic products, mainly sugars and lipids (Muscatine et al. 1981; Treignier et al. 2008; Burriesci et al. 2012). In return, they receive essential nutrients like nitrogen and phosphorus from coral heterotrophic feeding and metabolic byproducts (Rahav et al. 1989; Tremblay et al. 2014; Grover et al. 2002).

Dinoflagellates in general play a complex and often dual role in coral reef ecosystems, functioning both as potential symbionts and as parasites. The order Syndiniales, for example, is commonly found in coral reef environments, including plankton, sediments, and coral tissues (Clerissi et al. 2018; Qiu et al. 2021). Many of these species are parasitic, capable of killing hosts such as metazoans, radiolarians, and ciliates through the release of infectious dinospores (Guillou et al. 2008), which has raised concerns about their potential negative impact on corals (Harada et al. 2007). However, a specific subgroup, Dino-Group I, has been identified in healthy corals such as *Pocillopora damicornis* and the Mediterranean octocoral *Paramuricea clavata*, particularly in heat-resistant colonies, suggesting it may have a commensal or neutral role (Clerissi et al. 2018; Bonacolta et al. 2024). Other dinoflagellates are implicated in coral disease processes, either through toxin production or interactions with bacterial pathogens, as seen in black band disease and stony coral tissue loss disease (Hold et al. 2001a; Green et al. 2004; Sala et al. 2005; Sekar et al. 2008; Kim 1999; López-Cortés et al. 2019), while some may offer protective benefits such as UV resistance through the production of mycosporine-like amino acids (Klisch et al. 2001).

In addition to dinoflagellates, corals host other photosynthetic microeukaryotes. A notable example is *Ostreobium*, an endolithic green alga found in coral skeletons (Tandon et al. 2022). Highly adapted to low-light conditions and pH and oxygen fluctuations, *Ostreobium* contributes to the nitrogen and carbon cycles in the coral holobiont (Massé et al. 2018). It is thought to feed on organic matter in the skeleton and may rely on bacterial symbionts for B12 vitamin synthesis (Iha et al. 2021). Other green algal genera, including *Phaeophila* (a microborer possibly contributing to reef erosion), *Ochlochaete* (likely an opportunistic species), and *Ulvella* (sometimes

associated with pathogenesis), are also found in coral tissues (Marcelino and Verbruggen 2016).

2. Fungi

Most metagenomic and metabarcoding studies on microeukaryotes focused on fungi, known as the mycobiome (Cui et al. 2013). Corals host a diverse fungal community, including beneficial symbionts and potential pathogens, which are either epibiotic or endolithic species (Yarden 2014; Wegley et al. 2007; Amend et al. 2012). Many fungi found in corals, such as *Aspergillus*, *Penicillium*, and *Fusarium*, have terrestrial origins but have been consistently detected in marine environments (Soler-Hurtado et al. 2016; Ravindran et al. 2001; Golubic et al. 2005; Gleason et al. 2017).

Among them, some are pathogens such as *Aspergillus sydowii*, affecting gorgonians such as *Leptogorgia* spp. in the Ecuadorian Pacific (Soler-Hurtado et al. 2016) as well as Caribbean fans of the *Gorgonia* genus (Alker et al. 2001; Kim and Rypien 2015). It is responsible for the coral disease "aspergillosis" which causes severe tissue lesions and leads to mass mortality (Nagelkerken et al. 1997; Smith et al. 1996; Toledo-Hernández et al. 2008). Other species from the *Cladosporium* and *Fusarium* genera are associated with gray patch disease and dark spot syndrome, although their pathogenicity remains unclear (Sweet et al. 2019). But fungi in corals are not exclusively pathogens and some other species may play a beneficial role within the coral holobiont. For example, some endolithic fungi, colonizing the coral skeletons, participate in nutrient cycling (Kohlmeyer 1969; Golubic et al. 2005). Furthermore, although their specific functions in corals remain unproven, some halophilic black yeasts can produce mycosporine-like amino acids, which help reduce UV-induced damage (Kogej et al. 2006). Additionally, fungi found in the tropical coral *Porites astreoides*, such as members of *Sordariomycetes*, possess genes involved in nitrogen and carbon cycling (Wegley et al. 2007). Finally, certain fungi isolated from scleractinian corals in the South China Sea, belonging to the genera *Aspergillus, Penicillium, Fusarium,* and *Cladosporium*, exhibit strong inhibitory activity against pathogenic bacteria, suggesting a role in microbiome regulation (Xu et al. 2018). Beyond their ecological functions, marine fungi produce bioactive compounds with antifungal, antiviral, and anticancer properties, underscoring their potential for biotechnological applications (El-Gendy et al. 2018; Bovio et al. 2019; Kamat et al. 2020).

Despite their importance, fungal communities in corals remain understudied, particularly in octocorals (Roik et al. 2022). Research has revealed consistent fungal associations with octocorals worldwide, including *Aspergillus* and *Penicillium* in *Gorgonia ventalina* (Caribbean), *Leptogorgia* (Eastern Pacific), and octocorals from Singapore and the South China Sea (Roik et al. 2022). Other common fungal associates include *Cladosporium*, *Tritirachium*, *Nigrospora*, and *Fusarium*, with local environmental conditions influencing their abundance (Soler-Hurtado et al. 2016; Gleason et al. 2017). However, these studies remain limited in scope and often focus on a narrow range of species. There is a pressing need to extend fungal surveys to a broader diversity of octocoral species and geographic regions to build a more comprehensive understanding of these associations. Furthermore, the ecological and physiological roles of these fungi, whether mutualistic, pathogenic, or commensal, remain largely unknown and warrant detailed investigation to elucidate their potential impacts on coral health and resilience.

3. Protists

Ciliates are an important component of coral-associated protist communities and play a crucial role in the health and pathology of reef-building organisms (Sweet and Séré 2016). In corals, they are particularly notable for their role in pathogenesis. They are rarely found in healthy coral colonies but are frequently observed in diseased individuals, often accumulating at the forefront of advancing lesions (Sweet et al. 2016; Ravindran et al. 2022). Ciliates have been associated with a range of tropical coral diseases including white band disease (Sweet et al. 2014), white plague disease (Randall et al. 2015), white syndrome (Sweet et al. 2012; 2015), skeletal eroding band disease (Antonius 1999; Anthony et al. 2008; Montano et al. 2020), brown band disease (Bourne et al. 2008; Katz et al. 2014; Randall et al. 2015), and brown jelly syndrome (Sweet et al. 2012; Randall et al. 2015). As opportunistic feeders, these ciliates exploit weakened coral tissue and exacerbate the progression of the disease (Sniezek et al. 1995; Poynton et al. 2001; Song et al. 2009). Among the most concerning disease-associated ciliates are folliculinids and scuticociliates. *Halofolliculina corallasia* was the first protist pathogen identified in corals and is responsible for skeletal eroding band syndrome (Antonius et al. 2000). Scuticociliates, particularly members of the *Philaster* genus, have been documented across multiple coral reef systems and exhibit a global distribution comparable to

Halofolliculina (Sweet et al. 2012; 2014; 2015; 2016). Further research using metabarcoding and phylogenetic tools is essential to resolve taxonomic uncertainties and deepen our understanding of ciliate diversity and their role in coral disease dynamics. Among Mediterranean octocorals, the only metabarcoding assessment to date has identified three genera (*Licnophora*, *Holosticha*, and *Ephelota*) in the eukaryome of the gorgonian *P. clavata*, with their relative abundances varying across samples (Bonacolta et al. 2024). However, no direct link has been established between their presence and any impact on coral health.

Apicomplexans, a diverse group of alveolate protists, are best known as human parasites, responsible for diseases such as malaria or toxoplasmosis (Seeber et al. 2016). However, they are widespread among corals (70% of screened coral genera) and can be detected both in shallow and deep-sea corals (up to 1400 m; Vohsen et al. 2020), sometimes at high abundances (Bonacolta et al. 2023; Kwong et al. 2019; 2021) suggesting an important relationship with their hosts, including possible commensal or symbiotic roles (Vohsen et al. 2020). Corallicolids are the most widely studied coral-associated Apicomplexa (Bonacolta et al. 2023). They possess genes for chlorophyll biosynthesis but lack ones for photosynthetic function, suggesting an evolutionary transition from photoautrophy to heterotrophy, but their role in the coral holobiont remains unclear. A recent study by Bonacolta et al. (2024) found a higher abundance of corallicolids in thermally susceptible *Paramuricea clavata* compared to heat-resistant individuals, suggesting a potential role of this apicomplexan in modulating host vulnerability to thermal stress. Other apicomplexan lineages may also play significant roles in their coral hosts. *Gemmocystis cylindrus*, for example, contributes to diseases such as the white plague in corals from the southern Great Barrier Reef (Šlapeta et al. 2013). Overall, the complex nature between Apicomplexa and corals emphasizes the need for further research, especially to understand their functional roles under different environmental conditions.

Labyrinthulomycetes are a group of ubiquitous and diverse unicellular stramenopiles characterized by the production of an ectoplasmic network, a branched membrane network secreted through a unique organelle called the bothrosome (sagenogenetosome), which is involved in saprotrophic nutrient uptake (Bennett et al.

2017). They are found in diverse marine habitats, including coral-associated environments, where they potentially play a role as symbionts (Raghukumar and Damare 2011). Labyrinthulomycetes have been observed in association with a variety of coral species, including *P. clavata* (Kramarsky-Winter et al. 2006; Ben-Dov et al. 2009; Harel et al. 2008; Siboni et al. 2010; Burge et al. 2012; Bonacolta et al. 2024). They have been found in coral mucus, where they could contribute to primary defenses by engaging in bacterivory and niche occupation, helping to regulate microbial communities (Thompson et al. 2015). It is also assumed that these microorganisms contribute to the resilience of corals, possibly through nutrient transfer. Indeed, some Labyrinthulomycetes species from seawater can produce polyunsaturated fatty acids, including docosahexaenoic acid and eicosapentaenoic acid (Carmona et al. 2003; Lee Chang et al. 2012). However, there is currently no direct evidence that the Labyrinthulomycetes associated with corals produce these compounds, and their potential role in lipid transfer remains speculative. While primarily considered beneficial symbionts, Labyrinthulomycetes can also shift their behavior under environmental stress conditions. Their presence has been noted in corals exhibiting tissue loss, where they may act as opportunistic scavengers, feeding on decaying organic matter following bacterial proliferation (Raghukumar et al. 2011; 1991; Ravindran et al. 2001). In some cases, they have been linked to multifocal purple spot disease (MFPS) affecting Caribbean sea fans, although their exact role remains uncertain due to their presence in both healthy and diseased tissues (Burge et al. 2012; Dennis et al. 2020).

Conclusion

The coral holobiont is a dynamic and complex system in which microeukaryotes play diverse roles, ranging from essential symbiotic functions to opportunistic pathogenesis. Photosynthetic microeukaryotes such as members of the Syndiniales order and *Ostreobium* genus can contribute to coral resilience by providing an alternative energy source, while fungi and protists can act as both symbionts and potential pathogens. Despite these emerging insights, microeukaryotic communities remain largely underexplored in the coral holobiont compared to their bacterial counterparts, except for the photosymbiotic Symbiodiniaceae.

C. Other microbial communities associated with corals

Beyond bacteria and microeukaryotes, the coral holobiont harbors a diverse and dynamic ensemble of other microorganisms, including archaea and viruses, which probably play crucial roles in coral health and functioning. However, much of our knowledge about these microbial partners, especially in octocorals, remains preliminary and highlights significant gaps for future exploration.

1. Archaea

Reef-building corals are associated with a diverse array of archaeal species, primarily belonging to the phyla Thermoproteota and Euryarchaeota, with representatives such as Marine Group II and *Thermoplasmata* (Kellogg 2004; Siboni et al. 2008; Mohamed et al. 2023). These archaea can constitute up to half of the prokaryotic community in the surface mucus layer (SML) of some corals, where they are often implicated in nitrogen cycling, particularly in nitrogen recycling and ammonia oxidation (Siboni et al. 2008; 2012). Functional roles are suggested by recent metagenomic studies, including the identification of two Nitrososphaerota genomes from *Porites lutea*, which possess metabolic pathways potentially beneficial to the host, such as a reductive tricarboxylic acid cycle and cobalamin biosynthesis, indicative of roles in vitamin and carbon supply (Robbins et al. 2019). In this context, archaea likely contribute to autotrophic and heterotrophic processes within the coral holobiont, including nitrification, denitrification, and carbon fixation, though their functions are not yet fully experimentally validated (Voolstra et al. 2024b; Mohamed et al. 2023).

In contrast, archaeal populations in octocorals appear to be less diverse and abundant compared to bacteria, and their roles remain largely unexplored. In the gorgonian *Eunicella labiata*, for instance, archaea represented only about 0.6% of the prokaryotic community, predominantly from the order Thermoplasmatales, including the ammonia-oxidizing genus *Nitrosopumilus* (Keller-Costa et al. 2017). Similar low archaeal abundances were observed in *Eunicella gazella* and *Leptogorgia sarmentosa* (Couceiro et al. 2021), suggesting a potential, though limited, involvement in nitrification and nitrogen cycling within certain gorgonian species.

2. Viruses

Research into the viral communities (viromes) associated with corals is still in its early stages, with much of our knowledge stemming from studies on reef-building (Scleractinia) corals (Thurber et al. 2017; van de Water et al. 2018; Cárdenas et al. 2020; Wood-Charlson et al. 2015; Voolstra et al. 2024; Davy and Patten 2007; Wallace et al. 2025). Over 60 different viral families have been detected in coral holobionts, spanning a wide range of morphologies and hosts, including viruses infecting coral cells, Symbiodiniaceae, bacteria, archaea, and even fungi (Davy and Patten 2007; Cárdenas et al. 2020; Wallace et al. 2025; Thurber et al. 2017; Voolstra et al. 2024). Among these, double-stranded DNA (dsDNA) viruses are the most abundant and well described, with bacteriophages dominating the viromes (viral communities) and playing important roles in shaping coral bacterial communities (Correa et al. 2016; Cárdenas et al. 2020). Nucleocytoplasmic large DNA viruses (NCLDVs), such as the Phycodnaviridae and Mimiviridae, are also universally observed in corals and inferred to infect the coral host and Symbiodiniaceae, sometimes increasing in abundance during bleaching events, which implicates them in the destruction of the symbiotic algae under stress (Correa et al. 2013; 2016; Marhaver et al. 2008; Howe-Kerr et al. 2023; Levin et al. 2017). Other common viruses include Parvoviridae, Totiviridae, and Circoviridae, although their specific roles within the coral holobiont remain unclear (Gudenkauf and Hewson 2016; van de Water et al. 2018; Wallace et al. 2025). Single-stranded DNA viruses like Circoviridae and retro-transcribing viruses (e.g., Retroviridae, Caulimoviridae) are present but less well understood (Wallace et al. 2025).

Despite the progress made with reef-building corals, our understanding of viromes in octocorals remains very limited, with only a handful of studies available (Hewson et al. 2012; Gudenkauf and Hewson 2016; van de Water et al. 2018). Most viruses detected in octocorals appear to be bacteriophages of heterotrophic bacteria and cyanobacteria (Cárdenas et al. 2020; Hewson et al. 2012; Gudenkauf and Hewson 2016; van de Water et al. 2018). Notably, increased viral loads and distinct viral community structures have been found in diseased specimens of *Gorgonia ventalina* compared to healthy ones, suggesting that host health influences the virome composition in these corals (Gudenkauf and Hewson 2016; van de Water et al. 2018). Certain viruses may even play

roles in disease processes, such as Totiviridae infecting fungi and potentially impacting the virulence of fungal pathogens causing disease in octocorals (Gudenkauf and Hewson 2016; van de Water et al. 2018). Intriguingly, some viral sequences, such as those resembling Mimivirus and genetic elements like the mitochondrial mtMutS gene, suggest potential evolutionary impacts of viruses, possibly through mechanisms like horizontal gene transfer (Claverie et al. 2009; Bilewitch and Degnan 2011; Keller-Costa et al. 2016). However, the ecological roles and functional relevance of viruses in octocorals remain almost entirely speculative due to insufficient experimental evidence (van de Water et al. 2018). The field faces technical challenges such as the low concentration of viral genetic material in samples, which can introduce biases in sequencing protocols (Weynberg et al. 2014; van de Water, Allemand, et al. 2018). As such, while the importance of viruses, particularly phages, in regulating microbial communities and coral health is becoming increasingly recognized (Barr et al. 2013; Thompson et al. 2015; Mohamed et al. 2023), the specific contributions of the octocoral virome to holobiont functioning, disease resistance or susceptibility, and holobiont evolution are major knowledge gaps and prime areas for future research (van de Water et al. 2018; Voolstra et al. 2024; Mohamed et al. 2023).

Conclusion

In summary, both archaea and viruses represent pivotal yet comparatively understudied components of the coral holobiont, with evidence pointing to their involvement in essential nutrient cycles, microbial regulation, and disease dynamics. Archaea are particularly notable for their potential involvement in nitrogen cycling and carbon fixation, though their abundance and functional significance vary considerably between reef-building and octocoral hosts. Viruses are emerging as key regulators of microbial populations and potential contributors to both coral resilience and disease. Although recent metagenomic advances have uncovered remarkable diversity and hinted at important ecological roles for these microorganisms, especially in reef-building corals, the functional contributions of archaea and viruses, particularly in octocorals, remain largely speculative. Continued research is needed to better understand these microbial communities and their interactions, which may hold critical

insights for coral health, adaptation, and reef ecosystem resilience to environmental change.

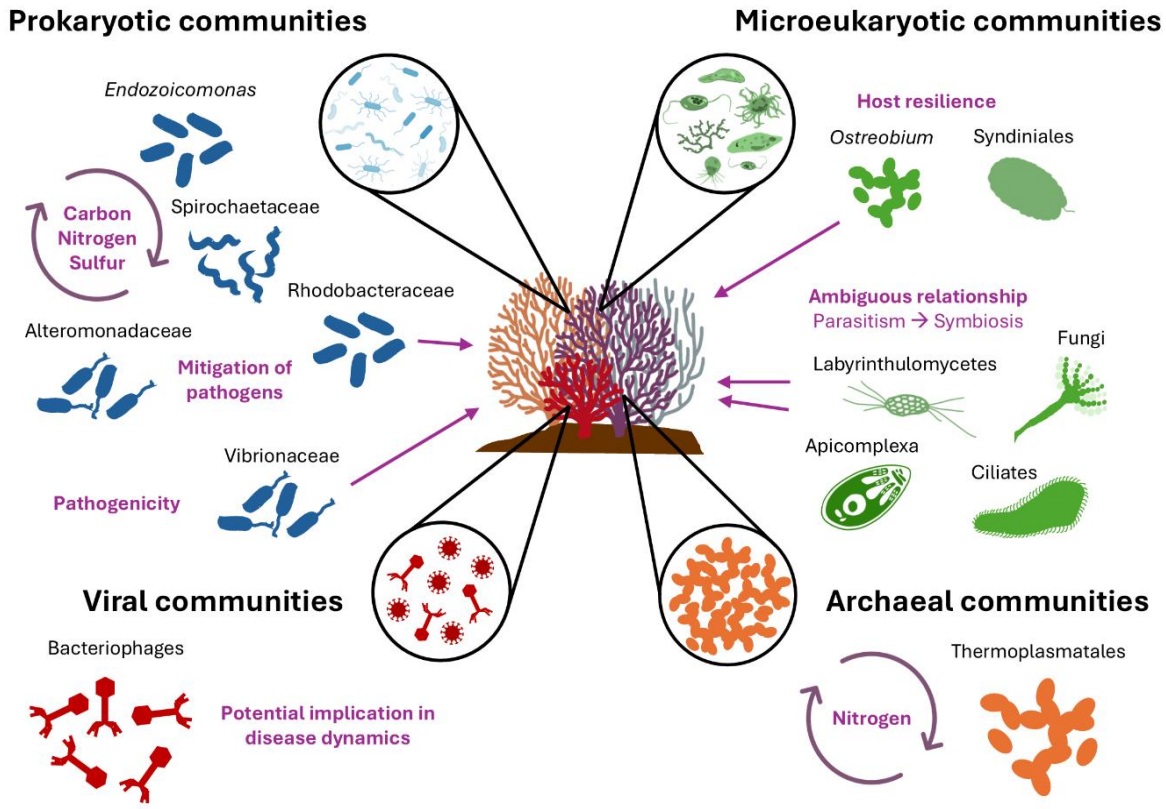

Figure 11: Known composition and potential roles (to our knowledge) of the different microbial compartments of the octocoral holobiont. © Personal illustration based on the results of the studies presented in this chapter.

D. Methods for studying microbial communities

The holobiont concept redefines the way we look at the biology and physiology of organisms, by viewing the host and its microbiome as an integrated unit and emphasizing microbial interactions in evolution and ecology. The growing awareness of these relationships, combined with advances in "omics" technologies, has greatly propelled research in this field. The classic method for studying microbial diversity primarily rely on culturing techniques, which however present several limitations (see below). Therefore, to overcome these limitations, and characterize complex microbial communities or compare multiple samples, microbiologists have turned to "culture-independent" techniques based on nucleic acid analyses (DNA or RNA), commonly referred to as “omics” technologies (Caron 2005; Nocker et al. 2007). These methods not only provide

taxonomic insights but also enable the assessment of genetic and functional diversity within communities. However, molecular approaches have their own limitations, so combining culture-based and culture-independent techniques provides a more comprehensive understanding of microbial diversity (Caron 2005). The strengths and limitations of the most commonly used methods for studying microbial communities are illustrated in Figure 12 and described below.

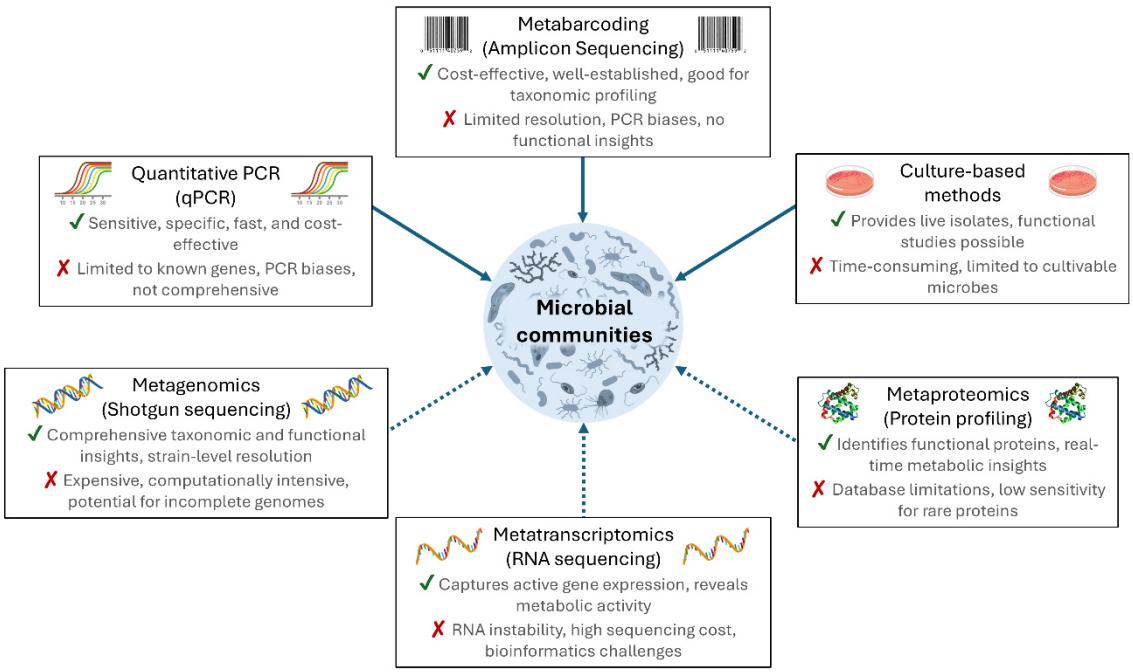

Figure 12: Overview of the most common methods used to study microbial communities, highlighting their key strengths and limitations. The figure emphasizes the complementarity of these approaches and the benefits of combining different techniques for a more comprehensive understanding of microbial dynamics. The methods employed in this thesis are represented by solid arrows, while other methods are shown with dashed arrows.

1. Culture-based methods

Despite their limitations compared to culture-independent techniques, culture-based approaches offer several key advantages, such as the isolation and maintenance of viable microbes on specific culture media and their identification at the strain level (Palleroni 1997). Once in culture, the phenotypic characteristics of the microbes, as well as their enzymatic and biochemical properties, or metabolic pathways, can be studied under different environmental conditions. Moreover, co-cultivation methods help to study symbiotic or competitive interactions between different species and many

antibiotics and bioactive compounds have been discovered by culturing microbes (Cabanillas-Bojórquez et al. 2023; Peng et al. 2021).

However, culture methods only capture a small fraction of the microbial diversity, due to the difficulty of replicating natural environmental conditions in artificial media (Rappé et al. 2003). This limitation is even more pronounced in marine environments, where less than 0.1% of species are cultivable (Schleifer 2004). Many microbes also rely on complex metabolic interactions between different species that are difficult to reproduce in vitro, limiting the complete characterization of microbial communities.

2. Metabarcoding

Metabarcoding is an amplicon-based sequencing technique that enables the simultaneous identification of multiple taxa within a sample by amplifying specific genetic markers, such as *16S rRNA* for bacteria and archaea, *18S rRNA* for eukaryotes, and *ITS2* for dinoflagellates such as Symbiodiniaceae photosymbionts, green algae or fungi (Creer et al. 2016; Taberlet et al. 2012; Santoferrara et al. 2020; LaJeunesse 2001; Mai et al.1997). It is a cost-effective tool for large-scale comparisons of microbial communities, and for the study of unculturable microorganisms. It thus provides a comprehensive view of microbial diversity. However, the reliance on PCR amplification introduces biases in community composition, and taxonomic resolution is often limited to the genus or family level, preventing accurate identification of species or strains. Additionally, it does not provide direct information on microbial functions. Another major limitation is that metabarcoding only indicates the proportion of each species within a community (relative abundance), making it difficult to determine the absolute number of different taxa. As a result, changes in the abundance of one species may give the impression that other species have changed, even if their actual population size remains unchanged. For example, if a particular microbial species increases greatly, or vice versa, the relative abundance of other species may decrease (or increase) even if their absolute numbers remain the same (Damhorst et al. 2021; Galazzo et al. 2020).

Among metabarcoding techniques, *16S rRNA* gene sequencing remains the most widely applied method for analyzing bacterial communities as the *16S rRNA* gene contains conserved and variable regions that facilitate differentiation between taxa

(Weisburg et al. 1991). In contrast, the Internal Transcribed Spacer 2 (ITS2) region is the most commonly used marker in studies of Symbiodiniaceae. To improve taxonomic resolution and confirm species-level identifications, the non-coding region of the plastid mini-circle psbA gene ($psbA^{ncr}$) can be used alongside ITS2. This region contains hypervariable nucleotide sequences well suited for distinguishing Symbiodiniaceae species (LaJeunesse and Thornhill 2011; Moore et al. 2003) and can help validate ITS2 type profiles (Smith et al. 2017). ITS2 has also been successfully applied to the identification of fungi (Schoch et al. 2012).

In contrast, *18S rRNA* metabarcoding, widely used to study microeukaryotic communities, faces significant challenges when microeukaryotes are associated with a host such as corals, as the overwhelming presence of host DNA contamination obscures the detection of microeukaryotic taxa. Indeed, universal *18S rRNA* primers preferentially amplify host sequences rather than those of the associated microeukaryotic communities (Parfrey et al. 2014; Wilcox et al. 2018), and this problem also relates to coral associated microeukaryotes (Clerissi et al. 2018; Bonacolta et al. 2023; Del Campo et al. 2019). Several strategies have been developed to solve the problem of host DNA amplification in *18S rRNA* gene metabarcoding. One solution is the design of specific primers, such as UNonMet-PCR primers (Bower et al. 2004; Del Campo et al. 2019), which minimize host DNA amplification while ensuring broad coverage of microeukaryotic sequences. However, the application of these primers to some corals such as *Corallium rubrum* failed to prevent host DNA amplification, necessitating the development of species-specific primers. An alternative method is to use blocking primers, which are chemically modified oligonucleotides (e.g., with a C3 spacer) designed to bind to host *18S rRNA* sequences without elongating, thus preventing their amplification during PCR (Boessenkool et al. 2012; Hino et al. 2016; Wilcox et al. 2014). However, blocking primers must be customized for each host species, which makes them un-usable for large-scale microbiome studies on different metazoans. Another approach is the nested PCR, a two-step amplification process in which a first round of PCR using universal 18S primers is followed by a second PCR with more specific primers targeting microeukaryotic sequences. This method, commonly used in studies of free-living protists (e.g., marine

water and sediment samples), increases taxonomic resolution, but also raises the risk of amplifying biases and sequencing errors.

An ideal approach would involve the development of universal primers that effectively exclude host sequences while maintaining broad taxonomic coverage for microeukaryotic lineages. By integrating improved primer design with computational filtering and complementary sequencing approaches, metabarcoding can be a powerful tool for microbial ecology, enabling deeper insights into host-associated eukaryotic microbiomes.

3. Quantification by qPCR

Quantitative PCR (qPCR) addresses the limitation of the metabarcoding method concerning the lack of microbe accurate quantification. It measures the absolute abundance of target organisms, allowing researchers to distinguish true biological changes from artifacts created by relative measurements. It is useful for validating sequencing results and monitoring microbial dynamics over time (Galazzo et al. 2020). However, qPCR is limited to known target genes and cannot provide comprehensive insights of the whole community, due to the challenge of designing taxa-specific primers caused by the lack of knowledge regarding the genomes of most symbionts. Therefore, a limited number of studies have investigated the microbiome by coupling relative and absolute quantification of microbiome members (Shiu et al. 2020; Pogoreutz et al. 2022).

4. Functional and metabolic studies of microbiomes

While qPCR and metabarcoding provide insights into the composition and dynamics of the microbiome, a deeper understanding of the microbiome functions requires techniques such as metagenomics, metatranscriptomics, and metaproteomics. Each of these methods has distinct strengths and limitations, and no single approach can fully capture the complexity of microbial communities. Shotgun metagenomics allows for both taxonomic and functional profiling of entire microbial communities (including viruses if the DNA extraction method is appropriate) by sequencing all genetic material in a sample. Although this method is expensive and computationally demanding, it remains the most powerful approach for broadly profiling microbes. It might be especially useful for the detection of viruses, due to its ability to capture all genetic material present in a

sample, because, unlike other microbial groups, viruses do not have a universally conserved gene like *16S rRNA* or *18S rRNA*. Metatranscriptomics captures actively expressed genes, providing real-time insights into microbial activity, although RNA instability and bias from dominant taxa present some challenges. In turn, metaproteomics identifies proteins and thus directly assesses functional activity, but assigning proteins to specific microbes remains difficult. Proteogenomics, which is a combination of metagenomics and metaproteomics, is based on protein identification and provides a more comprehensive view of microbial metabolism. These advanced techniques help decipher microbial interactions, metabolic pathways, and functional roles in ecosystems such as the coral microbiome.

To achieve a robust and accurate understanding of microbial diversity, functions, and ecological roles, researchers often employ a combination of these techniques (Jovel et al. 2022; Busing et al. 2021). However, despite their potential, only a dozen studies have combined these approaches to study coral microbiomes (Voolstra et al. 2024). This is largely due to the technical and financial challenges associated with these high-resolution methods, including the need for deep sequencing, advanced computational analysis, and specialized expertise. In addition, the complexity of coral holobionts and the difficulty of working in marine environments further limit large-scale functional studies.

Conclusion

The study of microbial diversity, functional dynamics, and microbial responses to environmental conditions is becoming essential in ecology research. The holobiont concept, which integrates the host and its associated microorganisms as a functional unit, has transformed our understanding of organism biology and ecological processes. Technological advances in "omics" methodologies have significantly expanded the capacity to explore complex microbial assemblages. In the field of microbial ecology, a wide range of techniques is currently used to characterize microbial communities. Culture-based approaches enable detailed phenotypic and functional analyses of isolates, while advanced omics techniques generate high-throughput taxonomic data and offer insights into functional and metabolic processes.

In the context of global climate change, elucidating the factors that influence the resilience or vulnerability of organisms is of critical importance. The microbial component, considered within the framework of the holobiont concept, should be integrated into ecological and physiological research. In marine ecosystems, particularly within coral holobionts, shifts in microbial community composition in response to environmental stressors such as elevated sea temperatures and ocean acidification can have contrasting effects, either enhancing or undermining host resilience. Consequently, the development and application of a comprehensive, integrative research framework is essential for characterizing the functional roles of microbial communities. Such approach will not only advance our understanding of host-microbe interactions but also support the formulation of evidence-based conservation strategies in an increasingly variable and stressed marine environment.

III. Anthropogenic disturbances in the Mediterranean Sea and their consequences on octocoral species

A. Anthropogenic disturbances

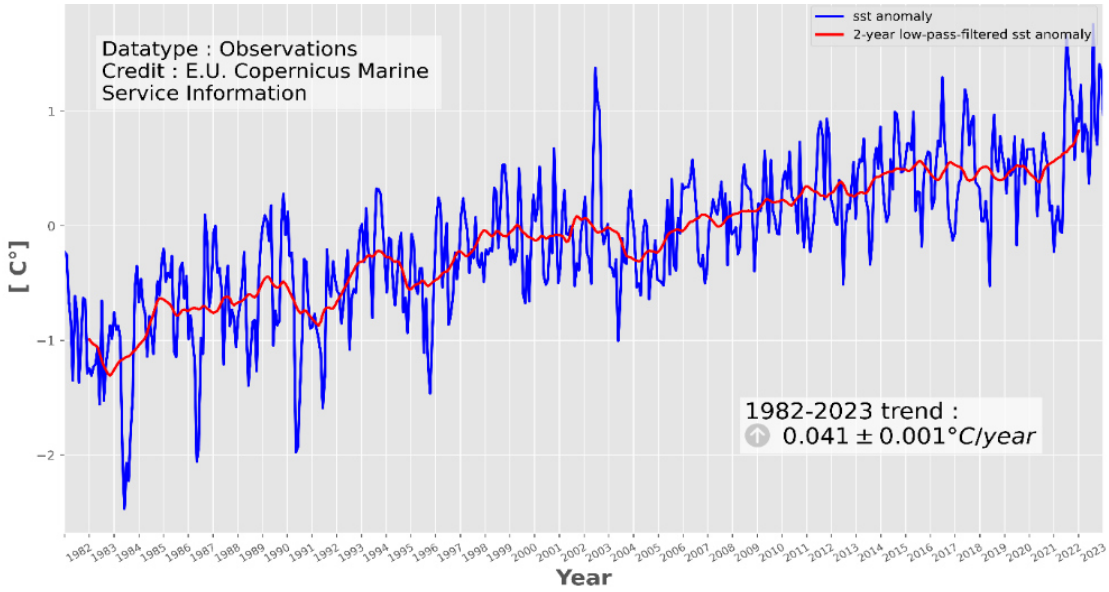

Figure 13: Time series of monthly mean (blue line) and 24-month filtered (red line) sea surface temperature anomalies in the Mediterranean Sea from 1982 to 2022. Anomalies are calculated relative to the climatological period 1993–2014 and are based on satellite observations from the Copernicus Marine Environment Monitoring Service (CMEMS) dataset. The sea surface temperature trend, along with its 95% confidence interval (shown in the box), is estimated using the X-11 seasonal adjustment procedure, a statistical method for analyzing time series data (Pezzulli et al., 2005; Pisano et al., 2020), and Sen's method, a technique for detecting trends in climate data (Sen, 1968). © Copernicus Marine Service

1. Global warming intensifies the severity and frequency of marine heatwaves in the Mediterranean Sea

Anthropogenic activities, particularly the burning of fossil fuels and large-scale deforestation, are driving global warming by releasing massive greenhouse gas emissions into the atmosphere (Wigley et al. 1981; Houghton et al. 1990; Hawkins et al. 2012). Current projections estimate that air temperatures will rise by at least 2°C by 2050 (Yerlikaya et al. 2020).

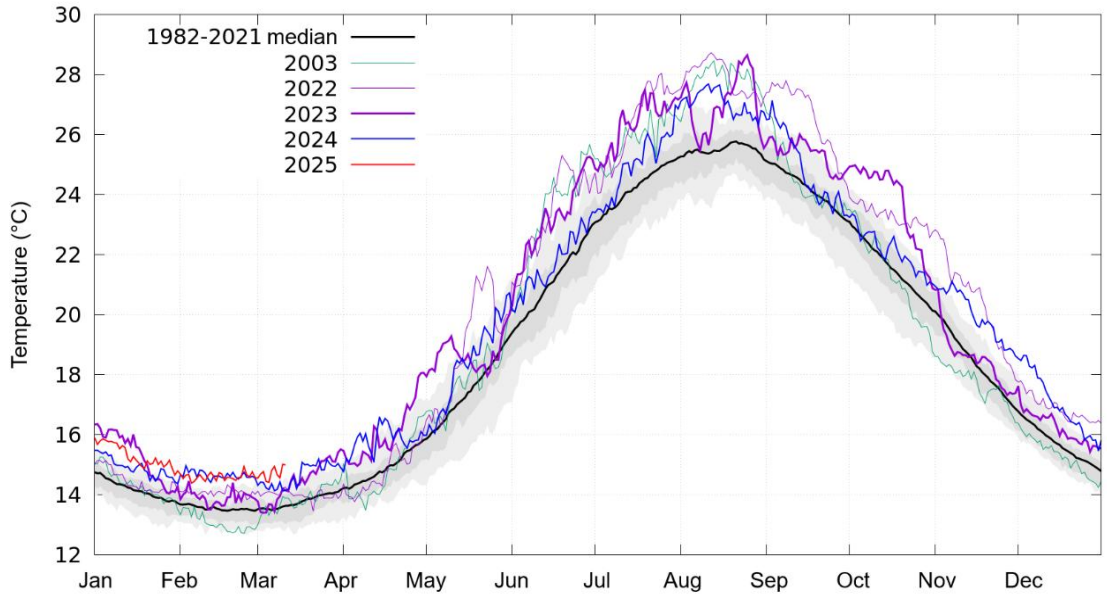

Figure 14: Average daily surface water temperature in the Mediterranean Sea, showing the annual evolution in recent years. The year 2003 is also highlighted due to a major heatwave that affected the entire basin. The black line represents the median of historical temperature records from 1982 to 2019, while the gray bands indicate the range within which 90% of historical records fall. Water temperatures exceeding this range are considered exceptionally high. © Icatmar

Regions classified as climate change hotspots are particularly sensitive to global warming, and the Mediterranean basin is one such hotspot (Tuel et al. 2020). As a result, the Mediterranean region is one of the fastest-warming marine regions, with temperatures increasing 20% faster than the global average (MedECC 2020; Pastor et al. 2020; Cos et al. 2022). Long-term observations show an increase of ca. 0.041°C per year in sea surface temperatures (SST; Figure 13) and of 0.0005°C per year in deeper layers since 1900 (Pastor et al. 2020; Pisano et al. 2020; Vargas-Yáñez et al. 2010). Moreover, Argo float data indicates that the Western Mediterranean is warming faster than the Eastern Mediterranean (Kubin et al. 2022). Projections under the Representative Concentration

Pathways 85 (RCP85) scenario indicate that the entire Mediterranean basin will continue to experience temperature increases, with significant SST warming of up to 2.6°C per century (Shaltout et al. 2014).

Due to this continuous global warming, the Mediterranean Sea is experiencing a rising number of marine heatwaves (MHWs), defined as prolonged periods of anomalously high sea surface temperatures during summer. Their frequency, intensity, and duration have increased significantly in the Mediterranean Sea (Darmaraki 2019; Juza et al. 2022; Omneya et al. 2021; Pastor et al. 2024) and, more generally, worldwide (Frölicher et al. 2018; Oliver et al. 2018) since the past two decades. In the Mediterranean Sea, the estimated rise is equal to 1.3 ± 0.25 events per decade (Hamdeno et al. 2023), with higher anomalies in the upper layers of the water column (Lionello et al. 2018; Sakalli 2017; Juza et al. 2021; Figure 14). Observations indicate that in 2022, between three and seven record-breaking MHWs occurred in the Mediterranean, with SST anomalies locally reaching +4.6°C above the summer average, far exceeding the +2 to +3°C anomalies recorded during the 2003 MHWs (T-MEDNet 2023; Quade 2022; Guinaldo et al. 2023; Copernicus Marine Service 2023; Figure 15).

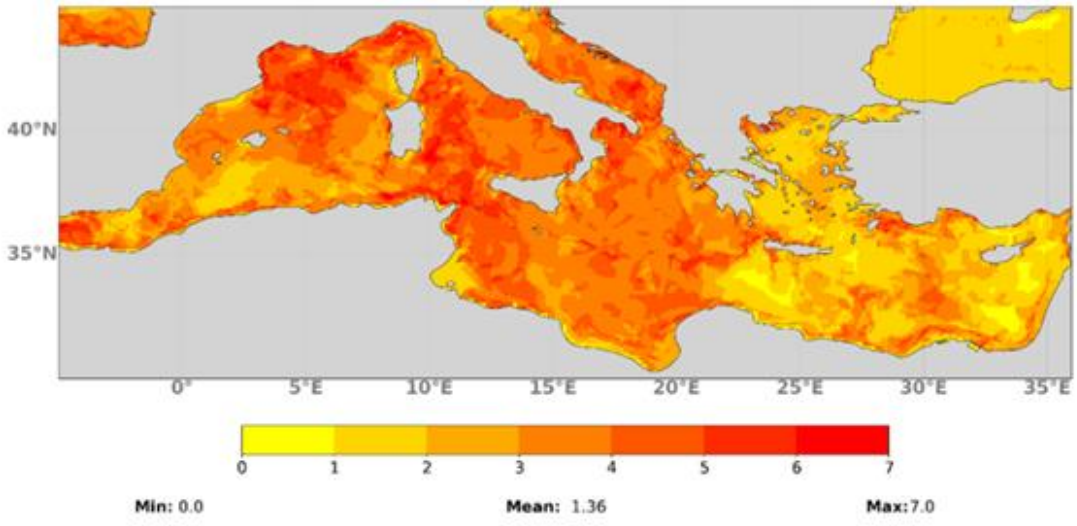

Figure 15: Number of marine heatwaves in the Mediterranean Sea between May and August 2022. The Western basin experienced a higher frequency of events compared to the Eastern basin, with some areas recording up to seven marine heatwave episodes, an unprecedented maximum for the region. © Mercator Ocean International

The intensification of these extreme events will have profound consequences on marine biodiversity, ecosystem resilience, and fisheries, necessitating urgent mitigation strategies and conservation efforts.

2. Other local stressors for Mediterranean octocorals

In addition to global warming, benthic organisms face multiple other anthropogenic threats. Ocean acidification, driven by increased atmospheric CO_2, is a major concern, as it reduces the biocalcification and growth rate of coral skeletons, increasing their vulnerability to environmental stressors. In *Corallium rubrum* for example, experimental studies showed that prolonged exposure to acidified conditions leads to reduced skeletal growth rates and abnormal spicule formation, which can weaken the coral structure (Bramanti et al. 2013; Cerrano et al. 2013). In addition to acidification, chemical pollution from heavy metals, pesticides, and other contaminants such as microplastics can accumulate in the organisms, negatively affecting health and reproduction (Corinaldesi et al. 2021; Bavestrello et al. 2014; Ricolleau et al. 2019). Furthermore, lost fishing gear, commonly referred to as ghost nets, significantly impacts Mediterranean octocoral populations. These nets entangle coral colonies, causing physical damage, tissue loss, and increased mortality rates (Canessa et al. 2024; Consoli et al. 2019).

These stressors, combined with heatwaves, contribute to species' decline. Therefore, some Mediterranean octocorals, such as the red coral *Corallium rubrum*, have been classified as "endangered" on the IUCN Red List (Figure 16) and are protected under various international and national regulations, such as the SPA/BD Protocol and the EU Habitats Directive (FAO-General Fisheries Commission for the Mediterranean; Cannas et al. 2019). Despite conservation measures, ongoing pressures continue to threaten the long-term survival of red coral populations.

3. The unique status of the economically valuable red coral

For centuries, *C. rubrum* has been highly valued for jewelry, leading to extensive harvesting that has severely reduced its population size and distribution (Torrents et al. 2005). Historical records show that populations were once much denser, but unsustainable fishing practices have led to a decline in both abundance and colony size

(Santangelo and Abbiati 2001a; Tsounis et al. 2010). Current harvesting regulations, including size and depth restrictions, aim to mitigate this impact, but illegal and unregulated fishing remains a significant challenge (Cannas et al. 2019). Passive restoration measures, such as the establishment of Marine Protected Areas (MPAs), have contributed to some recovery, particularly in shallow populations (Gazulla et al. 2021; Montero-Serra et al. 2019). However, restoration efforts must be further strengthened to ensure the long-term survival of the species.

IUCN Red List Categories	No. native species	No. endemic species
Critically Endangered (CR)	1	0
Endangered (EN)	9	2
Vulnerable (VU)	7	0
Near Threatened (NT)	10	0
Least Concern (LC)	40	3
Data Deficient (DD)	69	21
Not Applicable (NA)	2	0
Total number of species assessed	136	26

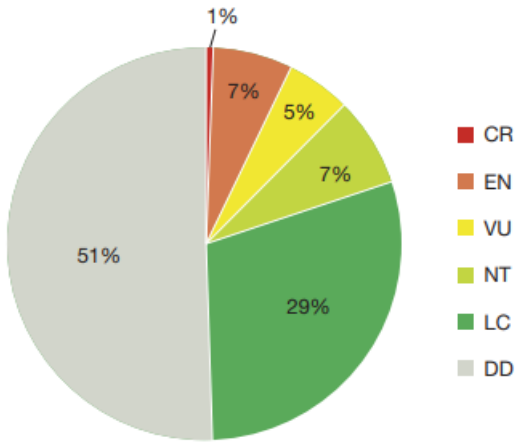

Figure 16: Red List status of anthozoans in the Mediterranean region. *Corallium rubrum* is classified as "Endangered" and *Paramuricea clavata* is listed as "Vulnerable**"**, from the IUCN conservation status of Mediterranean anthozoans (Otero Del Mar et al. 2017).

Conclusion

Anthropogenic disturbances have profoundly impacted the Mediterranean Sea, with global warming emerging as a primary driver of environmental degradation. The accelerated increase in sea surface temperatures and the intensification of marine heatwaves are already reshaping marine ecosystems, particularly affecting sensitive species like Mediterranean octocorals. These extreme thermal events, occurring at an unprecedented frequency and magnitude, threaten biodiversity and ecosystem services, with cascading effects on fisheries and coastal economies. In addition to climate change, local stressors such as ocean acidification, chemical pollution, and ghost fishing gear further exacerbate the vulnerability of marine organisms, including the economically and ecologically important red coral (*Corallium rubrum*). The cumulative effects of these

disturbances underscore the urgent need for robust mitigation and conservation strategies to protect marine biodiversity, ensure ecosystem resilience, and safeguard the long-term sustainability of Mediterranean marine resources. Without immediate and coordinated action, the survival of key species and the integrity of marine ecosystems in the region will remain at serious risk.

B. The consequences of seawater warming on octocoral populations

1. Massive mortality episodes (MMEs)

The Mediterranean Sea, with its unique geomorphological history and high biodiversity, harbors 7%-10% of all known marine species, including a high percentage of endemic species (Coll et al. 2010; Bianchi et al. 2000), and is a key model for studying the ecological impacts of climate change on marine ecosystems (Lejeusne et al. 2010). Octocorals, key structural species within MAFs, are particularly vulnerable to extreme temperature events, such as MHWs, which have triggered disease outbreaks and mass mortality events (MMEs), affecting up to 90% of colonies in some shallow populations (Cerrano et al. 2000; Huete-Stauffer et al. 2011; Piazzi et al. 2021b; Verdura et al. 2019; Garrabou et al. 2009; 2022; 2019); Figure 17). Over the past two decades, MHWs have repeatedly caused severe MMEs, particularly among gorgonians such as *Paramuricea clavata*, *Eunicella cavolini*, *Eunicella singularis*, and *Corallium rubrum* (Cerrano et al. 2000; Huete-Stauffer et al. 2011; Piazzi et al. 2021b; Verdura et al. 2019; Garrabou et al. 2009; 2022). These mortality episodes have led to significant shifts in community structure, favoring less diverse assemblages and compromising the ecosystem services provided by these coral-dominated habitats (Gómez-Gras et al. 2021).

Although mesophotic or deep-water ecosystems (50-200 m) are likely providing some refugia/protection from thermal stress due to greater water inertia, recent findings suggested that these mesophotic coralligenous assemblages are also increasingly at risk as global warming intensifies (Cerrano et al. 2019; Kahng et al. 2010; Soares et al. 2020). Some mesophotic areas have already experienced substantial impacts, with some colonies of *P. clavata* and *E. cavolini* from 70 m depth presenting tissue loss following thermal anomalies (Corinaldesi et al. 2022), raising concerns about the long-term persistence of octocoral populations in both shallow and deeper habitats.

Species once considered resilient, such as the white gorgonian *Eunicella singularis*, are exhibiting increased vulnerability, with recent MHWs causing significant declines in reproduction, recruitment, and survival (Sarda et al. 2024; Ramirez-Calero et al. 2024). Similarly, *P. clavata* and *C. rubrum* populations show high mortality and reduced resilience in response to successive MHWs, even within marine protected areas (Capdevila et al. 2023; Gómez-Gras et al. 2021). Projections indicate that *P. clavata* populations may collapse in shallow waters in about 40-50 years, due to limited adaptive capacity, a pattern observed across Mediterranean octocoral species (Capdevila et al. 2024; Orenes-Salazar et al. 2023).

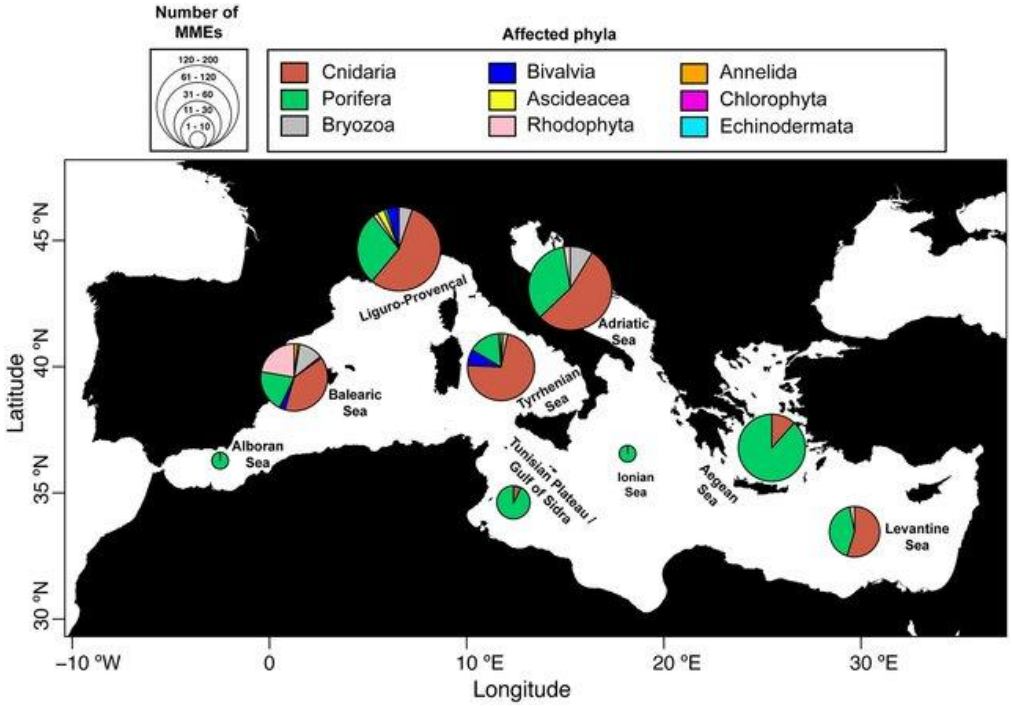

Figure 17: Number of mass mortality events (MMEs) reported in the Mediterranean Sea. Geographic distribution and taxa affected over the period from 1979 to 2017. From Garrabou et al. (2019).

Studies indicate that corals in shallow waters may possess greater thermotolerance and survival potential under stress conditions compared to their deeper-water counterparts. For example, in the species *C. rubrum*, shallow water samples exhibited significantly lower oxygen consumption and coenosarc necrosis when exposed to elevated temperatures (11-25°C), compared to deep water samples (Pratlong et al. 2021; Cau et al. 2018). Similarly, experimental investigations on *C. rubrum* and *E. cavolini* revealed that colonies in deeper waters exhibited lower tolerance to thermal anomalies, with necrosis risk rising more rapidly in deeper corals when exposed to

unusually high temperatures (Pivotto et al. 2015; Torrents et al. 2008; Ramirez-Calero et al. 2025).

The ongoing degradation of octocoral-dominated assemblages not only threatens biodiversity but also disrupts key ecological functions and services, such as habitat complexity and coastal resilience. Given the accelerating frequency and intensity of MHWs, urgent measures are needed to mitigate their effects on Mediterranean octocorals (Garrabou et al. 2021). To effectively address these challenges, research focused on uncovering the mechanisms driving octocoral mortality, including the factors that affect their vulnerability to marine heatwaves, is essential.

2. Physiological impairments

Most studies on the metabolic response of corals to heat stress have focused on scleractinian hexacorals. For instance, in *Heliopora fuscescens*, heat stress has been shown to lead to higher concentrations of macromolecules such as carbohydrates and lipids, increased anaerobic metabolism, and reduced ATP production (Pupier et al. 2024). Resilient stony corals (scleractinians) constitutively upregulate components of the coral cell death and immune pathways, as well as genes involved in stress response, such as heat-shock proteins (Barshis et al. 2013). Indeed, the heat shock protein (HSP) pathway, in which genes such as *HSP70* and *HSP90* are significantly upregulated to maintain protein stability and prevent denaturation, is a key component of the coral stress response (Desalvo et al. 2008; DeSalvo et al. 2010). Transcriptomic analyses have greatly advanced our understanding of the molecular mechanisms underlying coral responses to heat stress. In *Acropora hyacinthus*, heat stress triggers a dynamic and large-scale transcriptomic response characterized by early modulation of metabolic and cell cycle processes, as well as spliceosome activity, RNA and DNA-related metabolic processes, cell stress, and metabolism (Seneca and Palumbi 2015). A meta-analysis of the transcriptomic responses to various stressors in 10 *Acropora* species revealed a core "environmental stress response" toolkit comprising genes related to reactive oxygen species response, protein folding and degradation, NF-κB signaling, immune response, and cell death (Dixon et al. 2020), which are consistently modulated in corals exposed to environmental stress. Other studies on scleractinians have also shown an

upregulation of antioxidant defense genes such as *superoxide dismutase* (SOD) and *catalase* (CAT) to counteract the increased production of reactive oxygen species (ROS) under stress (Barshis et al. 2013). In some species, the disruption of calcium (Ca^{2+}) signaling and homeostasis has also been observed, indicating a breakdown in intracellular communication under thermal stress (Abrego et al. 2008). In *Porites astreoides*, the extracellular matrix (ECM) has been shown to undergo remodeling through the upregulation of ECM-related genes, as does the actin cytoskeleton, signaling cellular repair and adaptation mechanisms (Kenkel et al. 2013). In *Acropora* species, the pro-apoptotic pathways, including the upregulation of *caspase* and *NF-κB* genes, marked the onset of programmed cell death under extreme stress conditions (Abrego et al. 2008). Additionally, ribosomal and stress-responsive transcription factors may be either downregulated or upregulated, indicating a balance between conserving energy and activating genes to manage stress (Kenkel et al. 2013; Cziesielski et al. 2018).

While research on the physiological response of octocorals to heat stress remains limited, several mechanisms are similar to the ones observed in hexacorals (Cziesielski et al. 2019). For example, it has been observed that thermal stress leads to the overexpression of heat-shock proteins in species such as *Dendronephthya klunzingeri* (Wiens et al. 2000), *Sinularia cf. cruciata* (Shimpi et al. 2016), *Veretillum cynomorium* (Lopes et al. 2018) and the red coral *Corallium rubrum* (Tignat-Perrier et al. 2023). More particularly, recent studies on Mediterranean octocorals have revealed complex physiological and transcriptional responses, which vary depending on the species and the population.

For example, Tignat-Perrier et al. (2022) demonstrated different holobiont responses between *Paramuricea clavata* and *Eunicella cavolini* to prolonged heat stress (seven weeks at +6°C above controlled conditions). Colonies of *P. clavata* exhibited reduced feeding, leading to a severe depletion in energy reserve (a reduction of up to 55% in lipids and 58% in carbohydrates) and tissue loss (Figure 18). For the same thermal anomalies, colonies of *E. cavolini* displayed greater thermotolerance. Feeding activity was maintained, the total antioxidant capacity (ability to scavenge free radicals or reduce

metal complexes) remained high (~20 times higher compared to *P. clavata*) and no tissue loss was observed (Tignat-Perrier et al. 2022; Figure 18). In another study on *P. clavata*, it has been demonstrated that mucilage-induced oxidative stress leads to increased SOD and glutathione reductase enzymatic activity, as well as elevated lipid peroxidation levels, particularly in tissues adjacent to necrotic zones, indicating ongoing oxidative damage (Montalbetti et al. 2023). In the *in-situ* study by Corinaldesi et al. (2022), in which colonies were exposed to a less severe thermal stress (maximum +3°C), no tissue loss was observed neither in *P. clavata* nor *E. cavolini* (Figure 18). Experimental studies simulating thermal stress in aquarium-based systems shown that the red coral *Corallium rubrum* was quite tolerant to temperature anomalies, as no colony experienced signs of tissue loss, reduced feeding activity and reduced stress-induced gene expression at 21°C (+6°C compared to controlled conditions) during two weeks (Tignat-Perrier et al. 2023). Only after a two-week exposure at 24°C (+9°C) can we observe the overexpression of the tumor necrosis factor receptor 1 gene and colony mortality (~30% tissue loss).

At the gene level, heat stress was shown to induce a layered and dynamic transcriptional response in *Eunicella singularis*: a downregulation of multiple transcription factors such as those in the *zf-C2H2*, *AP-2*, and *HMG* families was observed, while other families like *IRF*, *RFX*, *P53*, and *NRF1* were upregulated (Belivermiş et al. 2025). In *P. clavata*, the observed decrease in DNA methylation under thermal stress suggests that octocorals may use phenotypic plasticity (the ability of the same genotype to produce different phenotypes, *i.e.*, observable physical or behavioral characteristics, in response to varying environmental conditions) as a way to cope with environmental changes (Belivermiş et al. 2025). This points to a possible role for epigenetic adaptation in enhancing octocoral resistance to heat stress (Belivermiş et al. 2025). Finally, recent research by Ramirez-Calero et al. (2025) has investigated the transcriptomic responses of *C. rubrum* populations from shallow (15 m) and mesophotic (48 m) depths to thermal stress. Their results have revealed 1,957 differentially expressed genes (DEGs) in response to heat stress, with the mesophotic population exhibiting a stronger and more extensive transcriptomic response (1,081 DEGs) compared to the shallow population (441 DEGs).

3. Microbiome dysbiosis

In corals, thermal stress can induce dysbiosis by altering the associated microbial communities, which is often associated with negative coral health outcomes such as reduced stress tolerance and increased disease susceptibility (Bourne et al. 2016; Mouchka et al. 2010). Dysbiosis refers to the disruption of the natural microbial community associated with an organism, often resulting in structural changes within the microbiome and likely affecting the holobiont functioning.

Under thermal stress, coral microbiome dysbiosis is most often characterized by a loss of the Symbiodiniaceae algae (for the zooxanthellate corals), an increased microbial species diversity and changes in the microbiome structure. The severity of the changes varies depending on the stress intensity but also on the coral species and among individuals (Voolstra et al. 2024b; Ashraf et al. 2023; van Oppen and Blackall 2019; Tignat-Perrier et al. 2022). In some species, major changes in the microbiome appeared colony-specific, preventing the identification of microbes that might contribute to coral health deterioration. The Anna Karenina Principle (AKP) was recently proposed for animal microbiomes. This principle states that stressed or dysbiotic organisms exhibit more variable microbiomes compared to healthy ones (Zaneveld et al. 2017). According to the AKP, healthy microbiomes tend to be similar and stable because all key factors for maintaining microbial balance are met. In contrast, dysbiotic state can occur when any one of these key factors fails, resulting in a wide range of possible disruptions and unpredictable changes in the microbial community. This principle, originally derived from Tolstoi's observation that "all happy families are alike; every unhappy family is unhappy in its own way," has been broadly applied to biological systems to explain why all essential conditions must be met for success (or health), while failure (or disease) can result from any single deficiency (Bornmann and Marx 2011). Thus, the variability observed in the compositional shifts of the coral microbiome under heat stress might reflect the AKP. Such shifts are likely associated with a weakened host immune response, allowing opportunistic or pathogenic bacteria to proliferate (Pinzón et al. 2015).

a. Response of Symbiodiniaceae and the other members of the eukaryome

As described in the first part of this introduction, many corals maintain a symbiotic relationship with photosynthetic Symbiodiniaceae, which supply the host with energy, UV protection, and other resources in exchange for nutrients and CO_2. When coral are stressed, the loss of these dinoflagellates or a reduction in their pigments leads to a phenomenon known as bleaching (Brown 1997). First described by Glynn in 1984 in the Pacific, coral bleaching and its mechanisms have been widely studied over the past decades (Van Woesik et al. 2022; Helgoe et al. 2024; Brown 1997). This phenomenon can be triggered by many stressors such as freshwater influx, disease, pollution, UV exposure and temperature anomalies (Glynn 1983; Goreau 1964). However, in recent decades, widespread bleaching has largely been attributed to climate change-induced warming (Hoegh-Guldberg 1999; Hughes et al. 2018; Sully et al. 2019). The initiation of bleaching is influenced by heating rates, cumulative thermal stress, and peak temperature levels (Middlebrook et al. 2010; Savary et al. 2021; Voolstra et al. 2020). Thermal stress negatively impacts cellular processes and nutrient dynamics in both partners (Rädecker et al. 2021; Roach et al. 2021). Symbiont identity plays a crucial role in thermal resilience. For example, *Pocillopora damicornis* corals with *Durusdinium* symbionts exhibited greater heat tolerance than those with *Cladocopium* (Wang et al. 2023).

Among octocorals, reports of bleaching in gorgonians are less common (Weil et al. 2016), with Caribbean gorgonians generally showing higher resistance to temperature-induced bleaching compared to other cnidarians (Lasker 2003). However, during extreme thermal events, many octocoral species have been observed to lose pigmentation (paling) or bleach completely (Weil et al. 2016). Notable tissue mortality was reported in species such as *Briaerum asbestinum*, *B. polyanthes*, and *Erythropodium caribaeorum* during major bleaching events (Harvell et al. 2001; Weil and Cróquer 2009). In 2005–2006, over 68% of octocoral species in La Parguera, Puerto Rico, showed bleaching (Prada et al. 2010; Weil et al. 2016). Climate change-driven increases in thermal anomalies and sea temperatures are expected to intensify bleaching events and disease outbreaks (Virgen-Urcelay and Donner 2023).

Very few studies have examined the response of other members of the microeukaryotic communities besides Symbiodiniaceae to thermal stress. Some studies, focusing on fungi associated with tropical hexacoral species, showed that high temperatures correlate with increased fungal diversity and abundance (Amend et al. 2012; Thurber et al. 2009), with Ascomycetes and Basidiomycetes being involved in coral skeleton bioerosion and diseases (Bentis et al. 2000; Gleason et al. 2017; Góes-Neto et al. 2020). Other studies focused on the endolithic algae *Ostreobium* spp., showing that during bleaching events, it may bloom near the coral surface, reducing light stress and aiding recovery (Galindo-Martínez et al. 2022), while also providing an alternative source of photosynthates when Symbiodiniaceae levels decline (Fine and Loya 2002; Iha et al. 2021). Regarding the response of the whole coral-associated microeukaryotic community during heat stress, research remains scarce. The only study that described the entire eukaryome to date, conducted by Bonacolta et al. (2024) on the Mediterranean octocoral *Paramuricea clavata*, suggests that high abundances of Dino-Group I and Corallicolidae may influence coral thermoresistance. However, further research is needed to better understand the dynamic and the role of microeukaryotic communities in octocoral responses to thermal stress.

b. Response of the bacterial communities

Many studies, mainly on tropical corals, have shown that thermal stress often leads to microbial shifts in bacterial communities, typically involving a reduction in the relative abundance of the dominant symbionts such as *Endozoicomonas* (Pootakham et al. 2019; McDevitt-Irwin et al. 2017; Marangon et al. 2025; Haydon et al. 2022; Voolstra et al. 2021; Woo 2021; Palacio-Castro et al. 2022; Ziegler et al. 2019; Weil et al. 2016). Furthermore, they also frequently observed an increase in the relative abundance of bacterial taxa such as Vibrionaceae and Rhodobacteraceae (Ben-Haim et al. 2003; Martin et al. 2002; Tout et al. 2015; Pootakham et al. 2019; McDevitt-Irwin et al. 2017; Marangon et al. 2025; Haydon et al. 2022; Voolstra et al. 2021; Woo 2021; Palacio-Castro et al. 2022; Ziegler et al. 2019; Chapron et al. 2021; Chemel et al. 2024). Several species within the Vibrionaceae family, including *Vibrio coralliilyticus*, are recognized as coral pathogens under elevated temperatures, capable of inducing tissue necrosis by the activation of virulence factors

(Billaud et al. 2022; Kimes et al. 2012; Ushijima et al. 2023; Weil et al. 2016). Similarly, Rhodobacteraceae have been shown to increase in relative abundance in the coral microbiome under heat stress (Pootakham et al. 2019a; Rosales et al. 2020; 2023; Marangon et al. 2025; McDevitt-Irwin et al. 2017; Palacio-Castro et al. 2022; Chapron et al. 2021; Chemel et al. 2024). These opportunistic bacteria were initially thought to be potentially pathogenic, however, recent research on *Acropora carduu* suggests that certain Rhodobacteraceae may confer protective benefits by mitigate infections caused by pathogens like *Vibrio coralliilyticus* (Xu et al. 2024).

Although the number of studies examining the effects of thermal stress on the microbiome of octocorals is limited (only a dozen to our knowledge, all cited here), similar patterns to those found for hexacorals have been observed: thermal stress tends to increase bacterial species richness and induce species-specific changes in the microbiome. Most of these studies have focused on Mediterranean octocorals. Following experimental heat stress or events of MHWs, microbiomes of *Eunicella cavolini, Paramuricea clavata, Leptogorgia sarmentosa* and *Corallium rubrum* have typically experienced a decrease in the relative abundance of the main symbionts *Endozoicomonas* (Tignat-Perrier et al. 2022; Corinaldesi et al. 2022; Rubio-Portillo et al. 2021) and *Spirochaetaceae* (Tignat-Perrier et al. 2023), and the proliferation of bacterial opportunists. The severity of dysbiosis varied depending on the coral species, with the microbiome of *P. clavata* experiencing larger changes in its structure than the microbiome of *E. cavolini* under +6°C laboratory-induced temperature anomalies for example (Tignat-Perrier et al. 2022; Figure 18). However, these results do not align with those of the study by Corinaldesi et al. (2022) conducted on site, in which the microbiome of *E. cavolini* was less affected than the microbiome of *P. clavata* during a moderate thermal stress (around +3°C). Indeed, they observed an increase in the bacterial species richness and a decrease in the relative abundance of *Endozoicomonas* only in *E. cavolini* colonies.

In the red coral *Corallium rubrum*, experimental studies simulating thermal stress in aquarium-based systems have also observed a reduction in the relative abundance of the main symbionts from the *Spirochaetaceae* family (Tignat-Perrier et al. 2023; Figure 18). In

this experiment, *C. rubrum* showed a high tolerance to 21°C (+6 °C, two weeks) without significant changes in its microbiome. A significant decrease in the relative abundance of *Spirochaetaceae* (from 66% to 8% of the microbiome) only appeared under an exposure at 24°C (+9°C). Interestingly, deep colonies of *C. rubrum* collected at 70 m depth during the 2011 marine heatwaves (positive thermal anomaly of more than 3°C at the sampling sites) also exhibited a significant decrease in *Spirochaetaceae*, dropping to 10% of the total community, even if these colonies did not suffer tissue loss (Corinaldesi et al. 2022; Figure 18). In shallower populations (30 m), however, the relative abundance of *Spirochaetaceae* remained stable, despite experiencing larger temperature increases during the heatwaves (Corinaldesi et al. 2022).

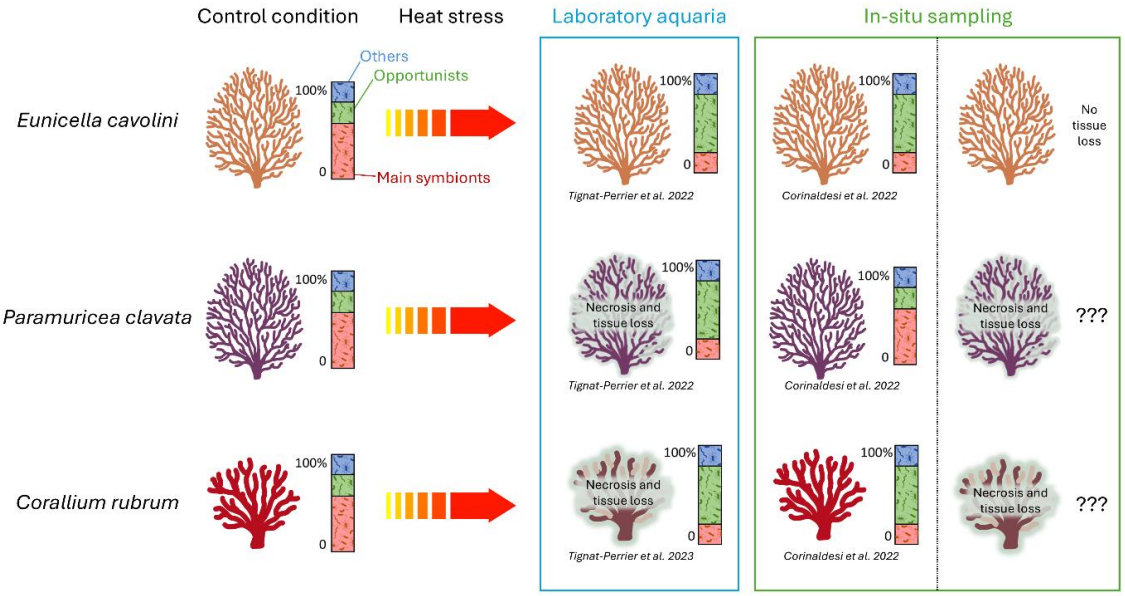

Figure 18: Summary diagram of the results of studies on the impact of thermal stress on Mediterranean octocorals. The results were separated between *in-situ* studies and laboratory-based controlled aquarium experiments, as well as between the presence or absence of lost tissue. At present, no results have been observed on necrotic corals in the natural environment.

Another trend often observed in these studies is the consistent increase in the relative abundance of opportunistic bacteria, especially from the families Rhodobacteraceae, Alteromonadaceae and Vibrionaceae (Figure 18). For instance, in the laboratory study by Tignat-Perrier et al. (2023) where red coral colonies were exposed two weeks to 24°C (+9°C compared to controlled conditions), a 3000-fold increase in the relative abundance of potentially pathogenic *Vibrio* species (ASV sequences close to *V. tubiashii*

sequences) was observed. As already described in the previous paragraph for hexacorals, *Vibrio* pathogens can be responsible of octocoral disease outbreaks and mass mortality events observed during heatwaves (Weil et al. 2016). They tend to proliferate at seawater temperatures exceeding 18-22 °C, with pathogenic strains producing extracellular enzymes (e.g., proteinase, gelatinase, DNase, lecithinase) that can contribute to tissue damage (Billaud et al. 2022; Kimes et al. 2012; Ushijima et al. 2023). Experimental infections confirmed that virulence increases with temperature, linking climate warming to disease outbreaks in *P. clavata* (Vezzulli et al. 2010a; Bally and Garrabou 2007a). However, whether these bacteria are the primary drivers of host decline or whether other bacteria simultaneously proliferating also play a role remains to be determined. Metagenomic analyses of unhealthy colonies of the temperate octocorals *Eunicella gazella*, *E. verrucosa* and *L. sarmentosa*, revealed that necrotic tissue was frequently colonized by *Flavobacteriaceae* and *Alphaproteobacteria* with enriched pathogenicity-related functions (e.g., type VI secretion system, virulence factors) and mechanisms to suppress the host immune system (e.g., arginase and nitric oxide reductase genes), suggesting microbial opportunistic colonization and evasion of immune defenses (Keller-Costa et al. 2021).

Despite these general trends, the microbiome response to thermal stress is not uniform across the board. For example, in the tropical Eastern Pacific, *Plexaura cairnsi* experiences a reduction in microbiome diversity during ENSO-induced thermal anomalies (e.g., El Niño and La Niña), which contrasts with the increased microbial diversity commonly observed (Montaño-Salazar et al. 2023a). Some octocorals, such as the soft coral *Lobophytum pauciflorum*, have shown a stable microbiome under short-term increases in temperature (+5°C compared to the controlled conditions) and decreases in pH (-0.2), which remains dominated by *Spirochaetes* and *Endozoicomonas* (Wessels et al. 2017). These findings suggest that the response of octocoral microbiomes to thermal stress include common patterns and species specificities and needs to be assessed on a case-by-case basis.

Despite growing research on Mediterranean corals and their microbiome, significant gaps remain in understanding microbial community dynamics during and after

heat stress. For example, changes in the microbial communities during MHWs, and their relationship with tissue loss and coral mortality remain misunderstood. Also, current knowledge on the resilience of the microbiome, i.e. the ability to recover from disturbance, is limited and only on tropical hexacorals, while it is likely a key factor in coral health and survival under thermal stress (Maher et al. 2020; Girija et al. 2024; Dunphy et al. 2021; Tracy et al. 2015). In Tracy et al. (2015), shifts in the microbiome of *Gorgonia ventalina* induced by thermal stress were shown to persist long after the 2010 Caribbean MHW events, with changes in the bacterial composition lasting more than a year.

Conclusion

Recurrent marine heatwaves are driving mass mortality events, especially in the Mediterranean Sea, with significant population losses reported in several octocoral species. Thermal stress significantly alters the physiology and microbiome composition of octocorals, with outcomes that vary depending on the species and environmental context. A consistent pattern observed in Mediterranean octocorals is microbial dysbiosis, marked by the apparent decline of key symbionts such as *Endozoicomonas* and *Spirochaetaceae*, alongside the proliferation of opportunistic bacteria, including *Vibrionaceae* and *Vibrio* species, which are associated with increased mortality at elevated temperatures. However, the causal relationship between these shifts in microbial communities and the observed tissue loss remains to be fully understood. All of these studies rely solely on metabarcoding sequencing, which has inherent biases. As discussed in the previous chapter, metabarcoding approaches reflect changes in relative abundances rather than absolute cell counts. This means that a decrease in the relative abundance of a microbe may result from the proliferation of other microbes rather than an actual decrease in its raw abundance. Therefore, it is worth determining whether the decrease in the relative abundance of the main symbionts (*Endozoicomonas* or *Spirochaetaceae*) commonly observed during stress corresponds to an actual loss of these symbionts. Other critical knowledge gaps remain in understanding the recovery of octocoral microbiomes, and the roles of both prokaryotic and microeukaryotic symbionts in coral resilience to thermal stress.

Aims of the Thesis

Understanding the interactions between corals and their microbiome has become a central topic in marine ecology, now that it has been accepted that microbial symbionts play essential roles in coral health, resistance, and adaptation to environmental stressors. Still, our knowledge of the microbial communities associated with Mediterranean octocorals remains limited, especially with respect to their diversity, functions, and response to climate change. This limited understanding is of concern given the increasing frequency of climate-induced mortalities in Mediterranean octocoral species, such as the precious red coral *Corallium rubrum* which has become an endangered species. The lack of information on their microbiome limits our ability to assess their adaptive potential and predict their resilience to ongoing environmental changes. A comprehensive investigation of these microbial assemblages is therefore essential to improve our understanding of host-microbe interactions in octocorals, and to inform conservation strategies aimed at mitigating the effects of climate change on coral ecosystems.

The overall aim of this thesis is to characterize the microbiome (both bacteria and microeukaryotes) of Mediterranean octocorals, and assess its response to global warming, with a special focus on the microbiome of the precious red coral *Corallium rubrum*.

We therefore investigated the microbial communities associated with two emblematic Mediterranean octocorals, the gorgonian *Paramuricea clavata* and the red coral *Corallium rubrum*, and we studied how marine heatwaves affect their microbiome. Our research aimed to offer insights into the functioning of octocoral symbiosis and the role of microbial symbionts in coral health and resilience. To achieve this, we used culture, amplicon sequencing and taxon-specific qPCR to characterize the microbiome and to evaluate the response of the holobiont (host and microbes) to thermal stress. The impact of heat stress was assessed through both *in-situ* observations and controlled laboratory experiments.

This research was structured into two axes as described below.

Axis 1: Diversity of the microbiome of Mediterranean octocorals

Sub-objectives pursued:

a. **Do the bacterial symbionts of *C. rubrum* and other octocorals, that have already been characterized, share a common evolutionary history with their host?**
b. **What is the composition of the eukaryome of *C. rubrum,* and does it remain stable across geography?**

a. Do the bacterial symbionts of *C. rubrum* and other octocorals, that have already been characterized, share a common evolutionary history with their host?

The high temporal and geographical stability of the bacterial communities associated with Mediterranean octocorals (van de Water et al. 2016; 2017; 2018) suggests a strong host-microbe association, which is potentially the result of a shared evolutionary history. Further exploration of this evolutionary perspective could provide new insights into the functional importance of certain microbial symbionts in coral health and functioning.

We explored putative evolutionary links between the octocoral species and their symbionts using analyses of phylosymbiosis and cophylogeny. Phylosymbiosis refers to microbial communities that mirror the host's phylogeny (Lim et al. 2020), while cophylogeny examines the evolutionary links between specific host species and microbes by comparing their phylogeny (Page 2003; Balbuena et al. 2013). Evolutionary patterns have been described in scleractinian corals (O'Brien et al. 2020; 2021; Pollock et al. 2018), but not in octocoral species. For this purpose, the prokaryotic communities of multiple octocoral species collected in the mesophotic zone (60-150 m depth) of the Mediterranean Sea and the tropical Red Sea were investigated. Mesophotic ecosystems are ideal for studying evolutionary links between corals and their microbiome, as they are less disturbed by physical and anthropogenic factors. The dataset, collected during the Gombessa V and VI expeditions (2019, 2021) and the ENCOR campaign (2019), included 14 octocoral species from 10 genera and 9 families across both orders of Octocorallia,

including *Corallium rubrum*, enabling to explore potential evolutionary links between octocorals and their microbiome.

b. What is the composition of the eukaryome of *C. rubrum*, and does it remain stable across geography?

In addition to bacterial communities, other microorganisms likely play essential roles in the holobiont functioning, for example in providing functional support to corals. Microeukaryotes, which include microscopic eukaryotes such as fungi and protists, are poorly studied in corals, and even less so in Mediterranean octocorals (Bonacolta et al. 2023; Ainsworth et al. 2017). Therefore, a substantial part of this thesis was devoted to characterizing the diversity of the microeukaryotic communities (or eukaryome) associated with *C. rubrum*. The identification of the associated microeukaryotes through *18S rRNA* gene-based sequencing was a major technical challenge, as commonly used primers for *18S rDNA* preferentially amplify host sequences. Thus, we designed primers targeting the V4 region of the *18S rRNA* gene and which reduced amplification of the red coral sequences while being universal enough for the amplification of microeukaryotes. This approach allowed a broad identification of the microeukaryotic partners of the red coral. This methodology was used in several investigations to characterize the composition of the microeukaryotic communities associated with *C. rubrum* under natural conditions along a geographic gradient but also the response of the eukaryome to thermal stress (please see in the next axis).

Common genetic markers, such as *18S rDNA* and *ITS* regions, often yield a low recovery of fungal sequences (Góes-Neto et al. 2020; Marcelino et al. 2016). This was also observed in our studies on *Corallium rubrum*. This motivated us to search for a complementary approach to look at the fungi associated with the red coral. We then performed fungal cultures in a specialized laboratory, using different culture media and conditions. Specifically, we investigated and compared the fungal diversity in the different coral compartments (tissue and skeleton), as there is evidence that these microhabitats support distinct fungal assemblages (Bonthond et al. 2018; Rabbani et al. 2021).

Axis 2: Response of the microbiome of *C. rubrum* and *P. clavata* to thermal stress

The second axis focused on the response of the octocoral holobiont (host + microbes) of *C. rubrum* and *P. clavata* to thermal stress, such as experienced during Mediterranean marine heatwaves (MHWs). MHWs caused by climate change have already led to severe mass mortality events in Mediterranean octocorals, yet the role of the microbiome in these events is still misunderstood. By analyzing shifts in bacterial and microeukaryotic communities under abnormally high temperatures, we gained insights into how thermal stress leads to microbial dysbiosis, and whether such changes contribute to coral mortality. Additionally, we investigated the resilience of the red coral microbiome to thermal stress, as the recovery capacity of the symbiosis might be a key factor in coral resilience and survival under repetitive disturbances such as observed during MHW episodes.

Sub-objectives pursued:

a. **How octocoral holobionts respond to marine heatwaves and is dysbiosis linked to tissue loss?**
b. **Can the host and its microbiome recover after thermal stress?**

a. How octocoral holobionts respond to marine heatwaves and is dysbiosis linked to tissue loss?

MHWs threaten Mediterranean octocorals by disrupting their symbiosis with microbes, which is essential for nutrient cycling, stress tolerance, and defense against pathogen. Previous studies have started to investigate the response of the microbiome to heat stress in different octocoral species but no clear correlation with tissue loss or coral mortality have been found (Tignat-Perrier et al. 2022; 2023). Laboratory experimental and field studies have sometimes provided inconsistent results on the response of the octocoral associated bacterial communities to thermal stress (Tignat-Perrier et al. 2022; 2023; Corinaldesi et al. 2022). These contradictory results emphasize the need for more comprehensive studies integrating several species, locations, thermal

stress intensities, and coral health conditions. As explained previously, not only sequencing-based relative abundances but also absolute abundances should be considered to understand the response of the microbial communities. Here, we first investigated the changes in the microbial community of *C. rubrum* (bacteria and microeukaryotes) and *P. clavata (bacteria) colonies*, with and without tissue loss, few weeks after the extreme 2022 MHWs. The samples were taken at different depths and locations in two protected marine areas. Amplicon sequencing of the *16S rRNA* gene and qPCR quantification of specific bacterial taxa were used to characterize the bacterial composition as a function of coral health, sampling depth and location.

So far, only one study investigated the eukaryome of a Mediterranean octocoral (*P. clavata* in Bonacolta et al. 2024) in the context of a thermal stress event. This study looked at the eukaryome composition before the stress but not during or after the stress. They showed that thermally resistant colonies were enriched with Dino-Group I Clade 1, while susceptible colonies harbored apicomplexan corallicolids. In this thesis work, we offered new insights into the heat-induced changes of the coral eukaryome. By studying simultaneously the host, bacterial and eukaryome response to abnormally high temperature conditions, our findings are important for getting a global picture of the consequences of MHWs on Mediterranean octocorals.

b. Can the host and its microbiome recover after thermal stress?

The extent of dysbiosis and the ability of the microbiome to recover, referred to as microbiome resilience, are likely crucial factors influencing coral health under disturbances. Our understanding of the ability of the coral microbiome to recover after stress, particularly in Mediterranean octocorals, is largely limited. This thesis was aimed at understanding the short-term resilience capacity of the red coral microbiome to heat stress, and its role in coral resilience. This research presents the initial comprehensive analysis of the short-term resilience of a Mediterranean octocoral to heat stress. A laboratory experiment was conducted to analyze the holobiont response to a moderate (19°C) and more severe (23°C) thermal stress. The physiological state of the host (stress response gene expression) and the composition of the bacterial microbiome and eukaryome using *16S* and *18S rRNA* gene sequencing and taxon-specific qPCR analyses

were assessed during and after the stress. Our findings offered valuable insights into the recovery capacity of octocoral holobionts following thermal anomalies and emphasized how MHWs may contribute to disease outbreaks and mass mortality in Mediterranean octocoral populations.

Conclusion

This research work enhances our understanding of the symbiosis between Mediterranean octocorals and the microbial communities, and the response of the coral holobiont to climate change. Our results provide new insights on the strong and rich association between octocorals and their microbes and contribute to a deeper understanding of the complex response of the holobiont to environmental stresses, such as those experienced during marine heatwaves. Our research findings help inform marine conservation efforts and mitigation strategies by providing knowledge on the MHW-induced mortality and resilience of octocoral populations in a rapidly changing Mediterranean Sea.

Axis 1: Diversity of the microbiome of Mediterranean octocorals

Chapter 1

Evolutionary relationships between octocorals and their bacterial microbiome



Chapter 1: Evolutionary relationships between octocorals and their bacterial microbiome

I. Overview of the chapter

Studies on Mediterranean octocorals have shown that their microbiome is highly conserved both temporally and geographically and over a wide range of temperatures (Tignat-Perrier et al., 2022, 2023; van de Water et al., 2016, 2017; 2018). Their remarkable stability suggests that microbial associations may be conserved among different Mediterranean octocoral species, possibly as a result of shared evolutionary trajectories. Exploring this evolutionary perspective could further emphasize the functional significance of these coral-bacteria relationships.

To investigate evolutionary links between corals and their microbiome, phylosymbiosis and cophylogeny analyses were used in this study. Phylosymbiosis refers to microbial communities that reflects the phylogeny of the host (Lim and Bordenstein 2020), and arises through processes such as codiversification, cospeciation, geographic shifts, diet, or ecological drift (Ley et al. 2008; Moeller et al. 2017; Yeoh et al. 2017; Erlandson et al. 2018; Grieneisen et al. 2019). Phylosymbiosis, which has been observed in plants, mammals, insects, sponges, and scleractinian corals (Van Bel et al. 2021; Pollock et al. 2018; O'Brien et al. 2020; Li et al. 2022; Bornbusch et al. 2023), may indicate profound host-microbe associations. Cophylogenetic analysis, comparing host and microbe phylogenies, detects congruence or similarities as evidence for a common evolutionary history, although the underlying mechanisms may involve both coevolution and biogeography (Hafner and Nadler 1988; Page 2003; Weckstein 2004; Smith et al. 2008; Godsoe et al. 2009; Balbuena et al. 2013). Notably, cophylogeny has been documented in tropical sponges, hexacorals and octocorals, especially with *Endozoicomonas* (Pollock et al. 2018; O'Brien et al. 2021).

This chapter explores these patterns between the prokaryotic communities and the octocorals from the mesophotic zones (60-150 m depth) of the Mediterranean Sea and the tropical Red Sea using *16S rRNA* gene amplicon sequencing. Mesophotic

ecosystems are ideal for studying evolutionary links between corals and their microbiome, as they are less disturbed by physical and anthropogenic factors. The dataset, collected during the Gombessa V and VI expeditions (2019, 2021) and the ENCOR campaign (2019), was composed of 14 octocoral species (including *Corallium rubrum*) from 10 genera and 9 families.

The microbiome composition differed significantly between the seas, which is probably due to long-term geographical isolation and different environmental conditions (Steininger and Rögl 1984; Tanhua et al. 2013; Manasrah et al. 2019). Mediterranean octocorals exhibited a species-specific microbiome, mainly characterized by the dominance of *Endozoicomonas* or Spirochaetaceae, which is consistent with previous studies (Bayer et al. 2013a; van de Water et al. 2016a; 2017b; van de Water, Voolstra, et al. 2018a). Shared phylotypes (Operational Taxonomic Units *i.e.*, OTUs), such as those observed between *P. clavata* and *Eunicella* spp., may reflect evolutionary convergence or similarities in life strategies (Groot and Weinberg 1982; McFadden 1999a; Quintanilla et al. 2013). In contrast, Red Sea octocorals, while also commonly harboring *Endozoicomonas* and Spirochaetaceae, displayed distinct microbiome clusters, influenced by additional taxa like Mollicutes and Rhodobacteraceae (O'Brien et al. 2020; Haydon et al. 2022; Alsharif et al. 2023). These associations align with findings reported in other tropical and Indo-Pacific octocorals (Morrow et al. 2012; Wessels et al. 2017).

Phylosymbiosis was present in Mediterranean species but not in the Red Sea species, suggesting that factors such as the environmental conditions or characteristics of the mucus layer may mask host-bacteria evolutionary patterns (Pollock et al. 2018; van de Water, Voolstra, et al. 2018a; Lim and Bordenstein 2020). Cophylogeny signals were found in 13 of the 14 octocoral species studied. Analyses showed that only certain bacteria, mainly *Endozoicomonas* and Spirochaetaceae, have a congruent evolutionary history with their hosts (Pollock et al. 2018; O'Brien et al. 2021). The genus *Endozoicomonas* displayed significant cophylogeny in corals from both seas, emphasizing its probable importance in the holobiont (Speck and Donachie 2012; Neave et al. 2017; Maire et al. 2023), although the nature of these relationships requires further clarification (Pogoreutz and Ziegler 2024). Some less dominant taxa, including Mollicutes and Spongiibacteraceae, also exhibited evidence of cophylogeny (Keller-Costa, Kozma,

Silva, Toscan, Gonçalves, Lago-Lestón, Kyrpides, Rocha, et al. 2022; Quintanilla et al. 2022; Rasmussen et al. 2023), suggesting that evolutionary links are not limited to the most common microbial partners.

Overall, our findings emphasize the importance of *Endozoicomonas* and Spirochaetaceae in coral symbiosis and the importance of studying host-microbiome evolutionary history for a comprehensive understanding of their interactions.

II. Publication

Insights into the occurrence of phylosymbiosis and co-phylogeny in the holobionts of octocorals from the Mediterranean Sea and Red Sea

Animal Microbiome | November 2024

DOI : https://doi.org/10.1186/s42523-024-00351-2

C. Prioux[1,2,5], C. Ferrier-Pages[2,5*], J. Deter[3,4], R. Tignat-Perrier[1,2,5], A. Guilbert[3], L. Ballesta[3], D. Allemand[5], J.A.J.M. van de Water[1,2,6*]

[1] Unité de Recherche sur la Biologie des Coraux Précieux CSM - CHANEL, Centre Scientifique de Monaco, 8 Quai Antoine 1er, MC 98000, Principality of Monaco

[2] Coral Ecophysiology Team, Centre Scientifique de Monaco, 8 Quai Antoine 1er, MC 98000, Principality of Monaco

[3] Andromède Océanologie, 7 place Cassan – Carnon plage, 34130 Mauguio, France

[4] MARBEC, Univ. Montpellier, CNRS, Ifremer, IRD, Place Eugène Bataillon, 34095 Montpellier, France

[5] Centre Scientifique de Monaco, 8 Quai Antoine 1er, MC 98000, Principality of Monaco

[6] Department of Estuarine & Delta Systems, Royal Netherlands Institute for Sea Research, Korringaweg 7, 4401 NT, Yerseke, The Netherlands

Abstract

Background: Corals are the foundational species of coral reefs and coralligenous ecosystems. Their success has been linked to symbioses with microorganisms, and a coral host and its symbionts are therefore considered a single entity, called the holobiont.

This suggests that there may be evolutionary links between corals and their microbiomes. While there is evidence of phylosymbiosis in scleractinian hexacorals, little is known about the holobionts of Alcyonacean octocorals.

Results: *16S rRNA* gene amplicon sequencing revealed differences in the diversity and composition of bacterial communities associated with octocorals collected from the mesophotic zones of the Mediterranean and Red Seas. The low diversity and consistent dominance of *Endozoicomonadaceae* and/or *Spirochaetaceae* in the bacterial communities of Mediterranean octocorals suggest that these corals may have a shared evolutionary history with their microbiota. Phylosymbiotic signals were indeed detected and cophylogeny in associations between several bacterial strains, particularly those belonging to *Endozoicomonadaceae* or *Spirochaetaceae*, and coral species were identified. Conversely, phylosymbiotic patterns were not evident in Red Sea octocorals, likely due to the high bacterial taxonomic diversity in their microbiota, but cophylogeny in associations between certain coral and bacterial species was observed. Noteworthy were the associations with *Endozoicomonadaceae*, suggesting a plausible evolutionary link that warrants further investigations to uncover potential underlying patterns.

Conclusions: Overall, our findings emphasize the importance of *Endozoicomonadaceae* and *Spirochaetaceae* in coral symbiosis and the significance of exploring host-microbiome interactions in mesophotic ecosystems for a comprehensive understanding of coral-microbiome evolutionary history.

Background

Octocorallia is a class of Anthozoans (Phylum Cnidaria) that diverged from the Hexacorallia during the Precambrian and includes over 3500 species that can be found around the world and at all depths, from the littoral zone to the deep sea, and from tropical to polar regions (McFadden et al., 2022). Corals engage in intricate and complex interactions with a range of microorganisms (e.g., protists, fungi, bacteria, archaea, and viruses). Together, a coral and its microbiota are considered a single entity, which is termed a “holobiont” (Knowlton et al., 2003). Symbionts play important roles in the health of their coral host (e.g., nutrient supply, protection against pathogens) and display an adaptive response to environmental changes (e.g., toxin degradation, thermal tolerance,

Peixoto et al., 2017). The bacterial communities associated with corals, particularly those of the reef-building Scleractinia (Class Hexacorallia), have been extensively studied. These are generally composed of a "core microbiome" of microbial phylotypes that are consistently associated with a host species (Ainsworth et al. 2015), and various transient microbes whose presence depends on local conditions (Hernandez-Agreda et al., 2016; van de Water et al., 2017; 2018). These stable associations between a coral species and members of its conserved core microbiome suggest that there may be an evolutionary connection. How coral-microbe symbioses have evolved is, however, still largely unknown.

Phylosymbiosis, defined as 'microbial community relationships that recapitulate the phylogeny of their host' (Lim et al., 2020), may arise from codiversification, cospeciation, coevolution or even short-term changes in the microbiota of a host, but also from shifts in geographical ranges, or the diet of the host and ecological drift in microbial communities (Moeller et al. 2017; Yeoh et al. 2017; Erlandson et al. 2018; Grieneisen et al. 2019; Ley et al. 2008). It has been observed in various systems, such as the roots of plants (Van Bel et al. 2021), the gut of mammals (Bornbusch et al. 2023), insects (Li et al. 2022), and sponges (O'Brien et al. 2020). In scleractinian corals, signals of phylosymbiosis have also been observed but at high bacterial taxonomic levels (family and genus; Pollock et al., 2018; O'Brien et al., 2020), and codiversification has been suggested to have played a role in the development of coral-microbiota interactions in Mediterranean octocorals (van de Water et al., 2018). While phylosymbiosis considers the whole microbial community associated with a host organism, more detailed analyses assess evolutionary links between host and specific microbial species, such as cophylogeny. Cophylogenetic assessments examine the concordance of phylogenies between two groups of species (Page 2003; Balbuena et al., 2013), with congruence suggesting shared evolutionary links (Hafner et al., 1988), although the underlying processes are not fully understood and can be attributed to coevolutionary (Smith et al. 2008; Godsoe et al. 2009) and biogeographic factors (e.g. co-vicariance; Weckstein 2004). Cophylogenetic patterns have also been observed in scleractinian corals, particularly with bacteria from the genus *Endozoicomonas* (Pollock et al. 2018; O'Brien et al. 2021).

In comparison with Scleractinia, the microbiota of octocorals is relatively understudied, and most studies have been conducted on octocoral populations in shallow waters (reviewed in van de Water et al., 2018). Studies on Mediterranean gorgonian corals have shown highly conserved microbiota on both temporal and geographical scales as well as over a wide range of temperatures (Tignat-Perrier et al., 2022, 2023; van de Water et al., 2016, 2017; 2018). This suggests that signals of phylosymbiosis and cophylogeny may be present in octocorals as well. Such patterns have indeed been described in octocorals from Australian reefs (O'Brien et al. 2021; 2020). It is, however, interesting from a coral holobiont evolutionary perspective to explore this hypothesis further in other regions and climatic zones.

In our study, we analyzed the prokaryotic communities of octocorals from the mesophotic zones (between 60 and 150 m depth) of the temperate Mediterranean Sea, characterized by its hot, dry summers and mild, wet winters (Lionello et al. 2006; Palutikof 2003), and the tropical Red Sea, known for its consistently high temperatures and high salinity (Elsawy et al., 2020; Manasrah et al., 2020; Mezger et al., 2016), emphasizing the different environmental conditions between these two seas. Mesophotic ecosystems are the ideal environment to study potential evolutionary links between corals and their microbiota as there is less disturbance by physical and anthropogenic factors at these depths, but access to these ecosystems is challenging. This dataset, collected during the *Gombessa V* and *VI* (technical diving; 2019, 2021) expeditions and the *ENCOR* campaign (Remotely Operated Vehicle; 2019), encompasses 14 species, belonging to 10 genera, 9 families and both orders of *Octocorallia*. This allowed us to explore whether an evolutionary link between octocorals and their microbiota may exist. The microbiota of several of these octocoral species have, to our knowledge, not been described before.

We show signals of phylosymbiosis in octocoral holobionts from the Mediterranean Sea, but not in those from the Red Sea. All species did, however, appear to have evolved with specific bacterial phylotypes, especially *Endozoicomonas* and *Spirochaetaceae*, as evidenced by cophylogenetic patterns in those coral-microbe associations. Overall, our results provide further insights into the link between the evolution of corals and their associated microbes, and the impact thereon of geographical separation.

Methods

Sample collection

Samples were collected during three scientific expeditions: the *Gombessa V* and *VI* expeditions took place in the temperate Mediterranean Sea, and the *ENCOR* expedition was in the tropical Red Sea (Figure 1). There is no overlap in coral species between these seas. A summary of the samples collected during these expeditions is provided in Suppl. File 1 as Table S1.

Gombessa expeditions V and VI – Corals were sampled along the Côte d'Azur (*Gombessa V*) in August 2019 and near Corsica (*Gombessa VI*) in July 2021 between 70 and 116 m depth. Samples were collected by divers using a combination of saturation diving and electronically controlled rebreather diving with the permission of the Direction Interrégionale de la Méditerranée (DIRM). At each site, fragments of approximately 20 cm were collected from 6 colonies per species. Fragments were placed individually in a plastic bag filled with ambient seawater and brought back to the surface.

ENCOR expedition – Corals were sampled between 65 and 120 m depths near Eilat (Israel) in October 2019, under the permits of the Israel Nature and Parks Authority. For each species, colony fragments of 25–30 cm^2 were collected with a ROV (ECA H800) equipped with an HD video camera (VS300 Eca Robotics) and a manipulative arm for sampling. The ROV was operated from a boat using a fiber-optics umbilical cable. Species were determined with the help of octocoral taxonomist Prof. Yehuda Benayahu (Tel Aviv University).

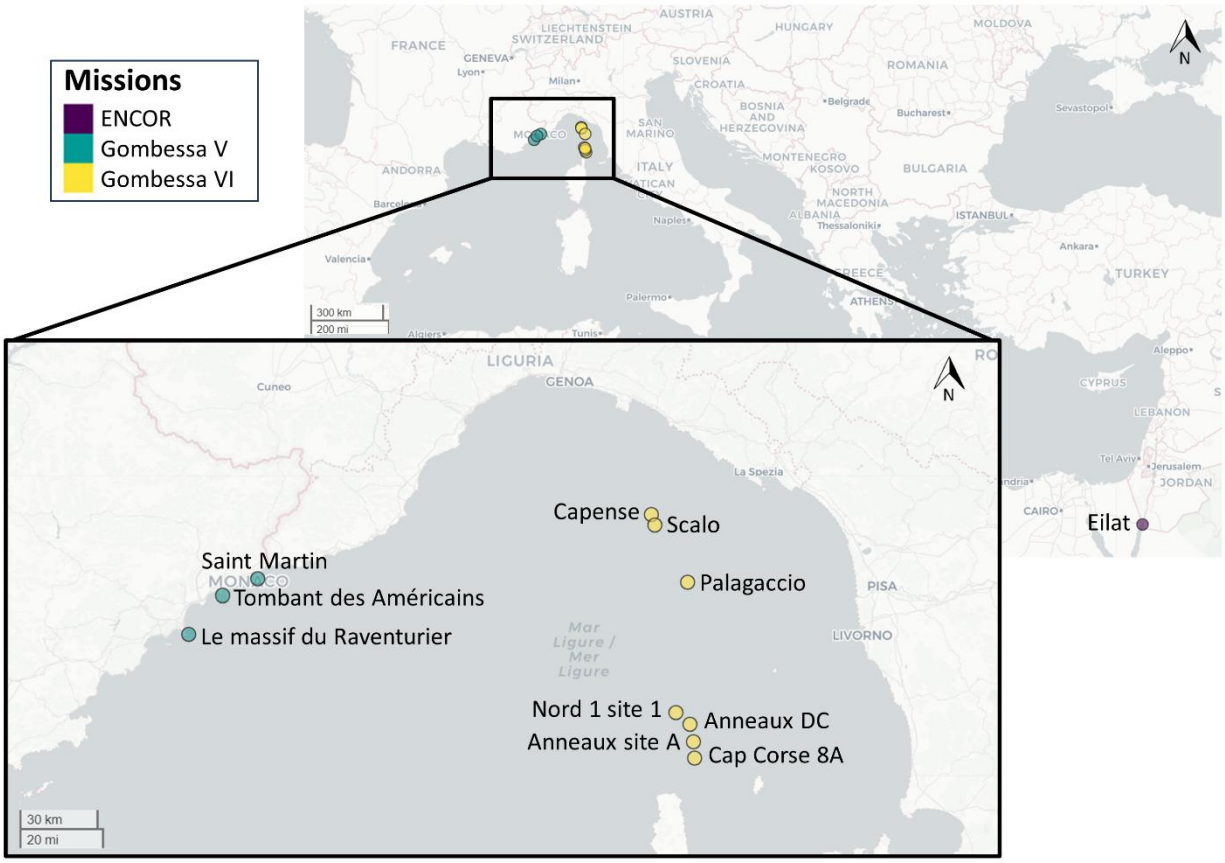

Figure 1: Locations of the different sampling sites. The corresponding sampling missions are indicated for each site.

All samples were rinsed twice with 0.2-µm filtered seawater to remove exogenous, loosely associated microorganisms and stored in RNAlater (ThermoFisher Scientific) at 4 °C. Additionally, we collected multiple replicates of 2 liters of seawater at most of the sampling sites, although logistical complications prevented us from collecting seawater at four sites. The water was filtered using 0.2 µm Whatman Nuclepore Track-Etched filters (Sigma-Aldrich), and the retentate was preserved in RNAlater and stored at 4 °C.

DNA extraction

DNA was extracted using the DNeasy PowerBiofilm kit (QIAGEN, Hilden, Germany) with the following modifications: during the cell lysis step, 2 µL of Proteinase K (600 U/ml) was added to the sample and incubated at 60 °C for 2 hours, followed by 2 min of bead beating using the CryoMill (Retch, Germany) at a frequency of 30 Hz. Negative extraction control samples (*i.e.,* extraction without sample material) were processed at the same time as the coral samples to account for contaminants. DNA concentration was measured using an Invitrogen™ Qubit™ 3 Fluorometer and DNA was stored at −20°C.

16S rRNA Gene amplicon library preparation

DNA was sent to STAB VIDA (Portugal) for amplicon library preparation using Illumina's standard "16S Metagenomic Sequencing Library Preparation" protocol (Illumina I. 2013) and sequencing. The V3-V4 region (~ 460 base pairs) of the *16S rRNA* gene was amplified using the forward primer 341F 5'-CCTACGGGNGGCWGCAG-3' and the reverse primer 785R 5'-GACTACHVGGGTATCTAATCC-3. PCR-amplified DNA was size-separated via gel electrophoresis and PCR products of the correct amplicon size were extracted using the Qiaquick Gel Extraction Kit (QIAGEN). Libraries were paired-end sequenced on the Illumina MiSeq platform (version 3 chemistry – 2 × 300 bp, 600 cycles). Raw sequence data has been deposited in the Sequence Read Archive (SRA) of the National Center for Biotechnology Information (NCBI) under accession number PRJNA1045964, PRJNA1047055 and PRJNA1047303.

16S rRNA gene amplicon data analysis

The *16S rRNA* gene amplicon data were processed using the USEARCH v11 software (64-bit version, https://drive5.com/usearch/). In total, 22,911,242 reads were obtained from all 214 samples (coral and seawater), ranging from 158 to 508,818 reads per sample. Negative controls contained 82 to 7,030 reads per sample. Reverse reads were truncated using -fastx_truncate function with a base quality threshold of >Q20 to ensure that high quality reverse read (R2) data was used for merging. Forward (R1) and reverse (R2) reads were merged using -fastq_mergepairs with the following settings: a minimum and maximum length of the merged sequence of 400 bp and 510 bp, and a minimum and maximum base-pair difference of 15 bp. The forward and reverse primer sequences (17 bp and 21 bp) were removed from the merged sequences using -fastq_truncate. The resulting sequences were quality filtered allowing a maximum of one expected error using -fastq_filter, obtaining a total of 15,862,422 sequences with a range of sequences per sample of 3,028 to 379,407 sequences. Unique sequences were identified using the -fastx_uniques command and then denoised using the UNOISE3 algorithm, obtaining 17,474 zero-radius operational taxonomic units' (zOTU, equivalent to an Amplicon Sequence Variant (ASV)). zOTUs were taxonomically annotated using the SINTAX algorithm and the SILVA reference database (version 138) with an assignment confidence cutoff of 0.8. An OTU table was generated by clustering sequences with an

identity similarity value of 0.99 using -otu_tab command. Considering the clustering into 99% OTUs, we refer to OTUs from hereon. The OTU table, the metadata as well as the sequences of each zOTU and their taxonomy annotation are available in Suppl. File 1 as Tables S2 and S3 and in Suppl. File 2 as File S1, respectively.

Bacterial community analysis

Analyses were run in the R environment (version 4.1.2, 2021-11-01). The R-package *decontam* (Davis et al. 2018) was used to identify contaminant OTUs in the samples based on the negative control samples (isContaminant function). A total of 2,386 of the 17,474 OTUs were identified as contaminants and were removed. Another 4,244 OTUs were removed from the dataset as these were annotated as unknown Kingdom, Mitochondria or Chloroplast and thus appeared to be of non-bacterial origin. Measures of the α-diversity, i.e. of the diversity of microbial phylotypes in a sample, were assessed using Chao1 estimations of the richness. This was calculated using the R-package *vegan* (Oksanen et al., Version 2.6-2, 2022) and analyses of variance (ANOVA) were used to test if the α-diversity of coral-associated bacterial communities was similar among coral species. To fit the assumption of homoscedasticity, a log transformation had been performed on the data prior to ANOVA. Tukey's Honestly Significant Difference (HSD) test was performed to identify potential differences between species. For β-diversity analyses, which compare the microbiota compositions between samples, all samples were rarefied to 9,000 reads using the R function *phyloseq_mult_raref_avg* from the *phyloseq* R-package (McMurdie et al., 2013). Non-metric multidimensional scaling (NMDS) analysis, as well as permutational multivariate analysis of variance (*adonis2*() function from the *vegan R*-package) based on the Bray-Curtis dissimilarity index (Bray et al., 1957) were used to assess differences in bacterial community β-diversity between the coral species using 9,999 permutations. A pairwise PERMANOVA test was performed to identify species having significantly different bacterial community compositions (*adonis_pairwise*() function from the *metagMisc* R-package; Mikryukov 2017). Hierarchical cluster analysis was used to create a dendrogram (*pvclust* R-package; Suzuki et al., 2006) using the unweighted pair group method with arithmetic mean (UPGMA) method on the Bray-Curtis distance matrix. *P*-values were computed for each of the clusters via multiscale bootstrap resampling. The core microbiome of each coral species was identified using the *core_members*() function (arguments: detection = 0,

prevalence = 99/100, include.lowest = FALSE) from the R-package *microbiome* (Lahti et al. 2017).

COI, *mtMutS* and *12S rRNA* Mitochondrial Genes Sequencing

The sequences of three mitochondrial genes (Cytochrome Oxidase Subunit 1 (*COI*), Mutator S (*MutS*), *12S rRNA*) were used to establish a phylogenetic tree of the different coral hosts (McFadden et al., 2011; Sánchez et al., 2003; France et al., 2002; Machida et al., 2012). PCR amplification of the genes of interest were done on three samples per species. Primers used to specifically target the three genes, and their respective annealing temperatures are given in table 1.

Table 1: Characteristics of the primer sets used for Sanger sequencing

Gene	Amplicon length	Primers	References
COI	~1080 bp	COII8068xF 5'-CCATAACAGGRCTWGCAGCATC-3' COIOCTR 5'-ATCATAGCATAGACCATA-3'	McFadden et al. 2011 France and Hoover 2002
mtMutS	~870 bp	ND42599F 5'-GCCATTATGGTTAACTATTAC-3' MUT3458R 5'-TSGAGCAAAAGCCACTC-3'	Sánchez et al. 2003 France and Hoover 2002
12S rRNA	~600 bp	12SF 5'-GTGCCAGCHNAHGCGGTYA-3' 12SR 5'-RAGDYGACGGGCRRTTTGT-3'	Machida et al. 2012

The Phusion High-Fidelity DNA Polymerase kit (ThermoFisher) was used following the manufacturer's recommendations. The three-step PCR protocol consisted of an initial denaturation step of 98 °C for 3 s followed by 30 amplification cycles (denaturation at 98 °C for 10 s, annealing at 46 °C for COI, 58 °C for MutS and 62 °C for 12S for 30 s and extension at 72 °C for 45 s) then a final extension at 72 °C for 10 min. The PCR products were size separated on an agarose gel and DNA fragments were excised from gel and purified using the GFX™ PCR DNA and Gel Band Purification kit (Illustra™). No PCR amplification was observed in the negative control samples. DNA amplicons were sent to Eurofins Genomics (Germany) for Sanger sequencing. Approximately 25 nucleotides were cut from each sequence on both sides to ensure a good quality and have sequences with identical lengths. Sequences were aligned using the ClustalW Multiple Alignment algorithm in the BioEdit software. For each gene and species, a consensus sequence was created, and the consensus sequences of *COI* (746 bp), *MutS* (779 bp) and *12S rRNA* (583 bp) were concatenated to create a single sequence per coral species. PhyML (Guindon et

al. 2010) was used to create the host phylogenetic tree based on the maximum-likelihood principle. The Gamma-distributed General Time-Reversible (GTR) model was selected based on the Akaike's Information Criteria (AIC) using the Smart Model Selection (SMS) software implemented in the PhyML environment (Lefort et al., 2017). To ensure statistical consistency, 1000 bootstrap replications of the test were performed.

Phylosymbiotic signal detection

Congruence between the topology of the coral host phylogenetic tree and the dendrogram of the bacterial microbiota was quantified using two topological comparison metrics: the Robinson–Foulds metric (Robinson et al., 1981) and the matching cluster metric (Bogdanowicz et al., 2013). The Robinson–Foulds (RF) metric quantifies the structural dissimilarity between trees by counting splits or bipartitions that are unique to each tree. The matching cluster metric evaluates the similarity between two sets of clusters by comparing how well the elements are grouped together or separately, providing a measure of agreement between different clustering outcomes. These two metrics were normalized by dividing the scores by the total possible congruence scores (or maximum congruence) between the two trees to reflect how different the actual trees are relative to that maximum similarity. These metrics were computed using a Python script adapted from Brooks et al. (2016) (Suppl. File 2 as File S2) and the TreeCmp program (Bogdanowicz et al., 2012), respectively, and then normalized by dividing the resulting scores by the total possible congruency scores for the two trees, giving distance values between 0 (complete congruence) and 1 (complete incongruence). Statistical significance of the phylosymbiotic patterns were assessed by comparing the host phylogenetic tree to 100,000 randomized dendrograms with equivalent topologies, and then estimating the *P*-value as the proportion of random trees giving an equivalent or more congruent result than the bacterial dendrogram. In addition, Mantel tests were performed to assess significance of the correlation between the bacterial composition distance matrix and the cophenetic distance matrix of the host tree using Pearson correlation with 9999 permutations, where a positive r-value indicates potential phylosymbiosis (mantel.rtest function from R-package ade4; Dray et al., 2007).

Cophylogenetic analyses

To identify bacterial phylotypes that may exhibit a concordant evolutionary history with their coral hosts along patterns of cophylogeny, we performed Random Tanglegram Partitions analyses (Balbuena et al., 2013; 2020) using the R-package RTapas (Llaberia-Robledillo et al. 2023). Given the complexity of the microbiome dataset, we applied a threshold for total relative abundance (> 0.0001), thereby reducing the dataset from 7793 phylotypes to 244 phylotypes. Next, three input files were generated: (1) the phylogenetic tree of the coral hosts (HH) based on the concatenated consensus sequences of the *COI*, *MutS* and *12S rRNA* genes (see above), (2) a phylogenetic tree of the 244 selected bacterial phylotypes (SS) based on the *16S rRNA* gene amplicon sequences aligned using the ClustalW Multiple Alignment (BioEdit software) and phylogenetic tree construction using PhyML (Guindon et al. 2010) with the Gamma-distributed General Time-Reversible (GTR) model and 100 bootstrap replications (Suppl. File 2 as File S3) ; and (3) a binary presence-absence matrix (A), containing rows and columns that correspond to the terminals in HH and SS, respectively, and where existing associations between each terminal are encoded as 1, and the absence of associations is represented as 0 (Suppl. File 2 as File S4). The Random Tanglegram Partitions algorithm (function max_incong()) was used on the dataset with N=10,000 iterations, and randomly selecting n=7 unique one-to-one associations between hosts (H) and symbionts (S) to maximize incongruence. Subsequently, the Procrustes Approach to Cophylogeny (PACo; Balbuena et al., 2013) was applied to the selected associations, and the residual frequencies of host-symbionts associations falling within the 1% percentile (res.fq = TRUE) were used to estimate the contribution of each host-symbiont association to the global cophylogenetic signal. Positive values denote host-symbiont associations contributing significantly to cophylogenetic congruence, whereas negative values identify associations leading to phylogenetic incongruence.

Results

Diversity and composition of the octocoral-associated bacterial community

Overall, significant differences in α-diversity (Chao1 index) of the octocoral microbiota were observed between coral species (Figure S1; Suppl. file 1 Table S4; $P = 6.29.10^{-8}$). Analyses of β-diversity showed that octocoral-associated bacterial communities were significantly different from the seawater bacterial communities ($P = 0.001$), and that the composition differed between coral species ($P = 1.10^{-4}$), particularly between those from the Red Sea and the Mediterranean Sea ($P = 1.10^{-4}$; Figure 2A, and Suppl. file 1 Table S5). However, the dispersion was also significantly greater among samples of corals from the Red Sea than of corals from the Mediterranean Sea ($P = 0.0003$; Suppl. file 1 Table S6). In addition, pairwise comparisons of the β-diversity of the microbiota showed differences between nearly all species from the Mediterranean Sea ($P < 0.05$; Suppl. file 1 Table S5), apart from the microbiota of *E. verrucosa* which did not differ from that of *E. cavolini* and *P. clavata* ($P = 0.1289$; Suppl. file 1 Table S5). And dispersion was not significantly different between species, except for *E. cavolini*, whose samples were significantly more dispersed than those of *A. coralloides* ($P = 0.012$) and *P. clavata* ($P = 0.0255$; Suppl. file 1 Table S6). Among the corals from the Red Sea, β-diversity of the microbiota was only different between *Ovabunda spp.* and *P. thyrsoides* ($P = 0.03$; Suppl. file 1 Table S5) and dispersion was statistically similar (Suppl. file 1 Table S6).

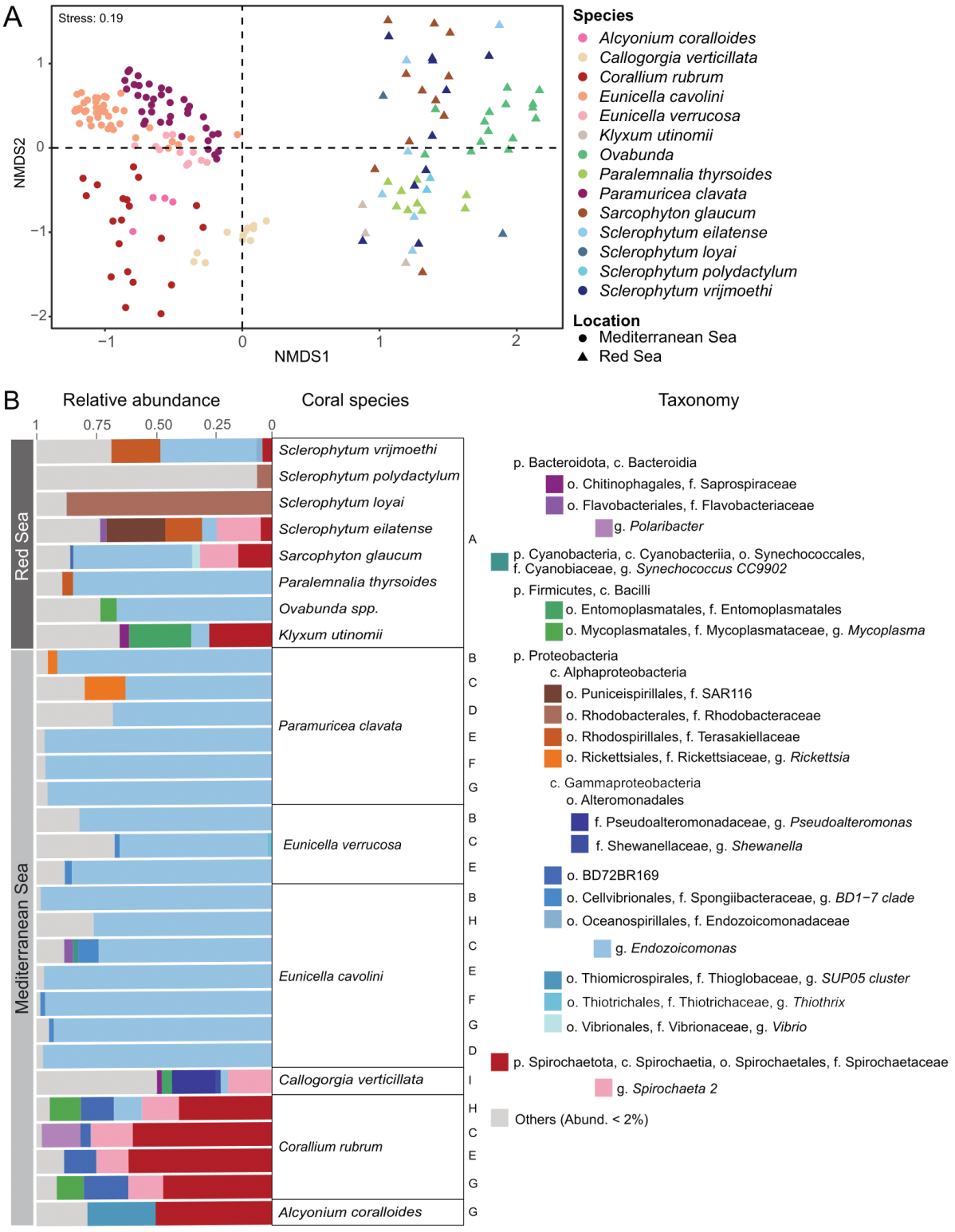

Figure 2 : (A) NMDS on Bray-Curtis distance matrix showing ordination of coral samples ; (B) Bacterial community composition for each species per location (taxa less abundant than 2% are grouped together under Others ; Lowercase letters correspond to taxonomic levels, p : Phylum, c : Class, f : Family, g : Genus ; Uppercase letters correspond to sampling locations, A : Eilat, B : Tombants des Américains, C : Saint Martin, D : Nord 1 Site 1, E : Massif du Raventurier, F : Capense, G : Cap Corse 8A, H : Scalo, I : Anneaux Site A)

The hierarchical cluster analysis also showed distinct patterns between the two seas. The octocoral species from the Red Sea, which all belong to the order Malacalcyonaceae, formed a separate cluster from the Mediterranean corals (Figure S2). Within the two geographic clusters, clustering generally followed the octocoral taxonomy. The Mediterranean cluster was divided into two main clusters corresponding to the orders Malacalcyonaceae (*E. cavolini*, *E. verrucosa*, *P. clavata*) and Scleralcyonaceae (*C. verticillata*, *C. rubrum;* Figure S2). Samples were mainly grouped along genus and species lineages, although a few exceptions were observed. For example, the Mediterranean *A. coralloides* clustered with the Scleralcyonaceae although it belonged to the Malacalcyonaceae order and among the Red Sea corals, *K. utinomi* was grouped with various *Sclerophytum* species (Figure S2).

The bacterial community compositions (Figure 2B) indeed showed differences between the species. Mediterranean gorgonians of the genera *Paramuricea* and *Eunicella* harbored a bacterial community dominated (52% to 98%) by *Endozoicomonas* (OTU1, OTU2, OTU3 and OTU5; Class *Gammaproteobacteria*; Order *Oceanospirillales*). The microbiota of *Ovabunda* spp. (65%)*, P. thyrsoides* (83%) and *S. glaucum* (48%) also largely consisted of *Endozoicomonas* but harbored different OTUs (e.g., OTU11, OTU6 and OTU7 respectively) than the Mediterranean gorgonians. The microbiota of all other octocoral species also contained *Endozoicomonas* but generally in very low (<1%) relative abundance. In contrast, the microbiota of both Scleralcyonaceae *C. rubrum* (48% to 67%, mainly OTU4 and OTU15) and *C. verticillata* (21%, mainly OTU24) consisted primarily of *Spirochaetota*, especially from the *Spirochaetaceae* family. *Spirochaetota* were also observed in some Malacalcyonaceae from the Mediterranean Sea (*A. coralloides* (15 %, mainly OTU4)) and the Red Sea (S. *glaucum* (35%, mainly OTU29), *S. eilatense* (22%, mainly OTU147 and OTU223) and *S. vrijmoethi* (4%, mainly OTU140)). Other bacterial taxa were also found to be relatively abundant in certain coral species. For instance, *Bacillota* were frequently found in association with *C. rubrum* (11%), *C. verticillata* (4%) and the Red Sea species *Ovabunda* spp. (7%) and *K. utinomii* (25%; Figure 2B). *C. rubrum* had a high percentage of *Gammaproteobacteria* of the order BD72BR169 (between 2% and 20% in average) as well, and the SUP05 cluster from the *Thioglobaceae* family accounted for about 30% of the total bacterial abundance of *A. coralloides*. Furthermore, *Pseudoalteromonas* represented about 20% of the bacterial abundance in *C. verticillata*,

and similar proportions of *Terasakiellaceae* were found in the microbiota of the Red Sea species *S. eilatense* and *S. vrijmoethi* (Figure 2B).

The analysis of the core microbiome highlighted the importance of certain symbionts, as only few OTUs composed the core microbiome of most coral species (between 0 and 33 OTUs; for *S. polydactylum* a core microbiome could not be accurately determined as there were only 2 samples present in the dataset; Suppl. file 1 Table S7). Notably, abundant OTUs annotated as *Endozoicomonas* (Suppl. file 1 Table S7), were part of the core microbiome of the Mediterranean gorgonians *E. cavolini* (OTU1, OTU3 and OTU5), *E. verrucosa* (OTU1, OTU3, OTU5 and OTU8) and *P. clavata* (OTU1, OTU2, OTU3 and OTU8). OTU1, OTU2 and OTU5 were also found in the core microbiome of *A. coralloides*. Contrastingly, *Spirochaetaceae* (OTU4 and OTU15) were the main members of the core microbiome of *C. rubrum*. *Spirochaetaceae* OTUs were also present in the core microbiome of *A. coralloides* (OTU4, OTU53, OTU135 and OTU1476) and *C. verticillata* (OTU24). Overall, the core microbiome of all species harboured OTUs belonging to the *Endozoicomonas* genus and/or the *Spirochaetaceae* family. However, OTUs belonging to other bacterial taxa were also part of the core microbiome of various coral species. For example, *Pseudoalteromonas* OTU397 and OTU458 are abundant in the microbiota of *C. verticillata* and are part of its core microbiome, while *Thioglobaceae* SUP05 cluster OTU73 was found in the core microbiome of *A. coralloides*. No core microbiome could be identified for *S. eilatense* (Suppl. file 1 Table S7).

Signals of Phylosymbiosis

Since the coral-associated bacterial communities were relatively well clustered according to host taxonomy, we assessed whether patterns of phylosymbiosis could be observed. When comparing the host phylogenetic tree to a simplified dendrogram representing bacterial community composition **(**Figure 3AB), the extent of congruence between the two structures is indicated by distance values close to 0 (complete congruence) and 1 (complete incongruence). Here, no signal of phylosymbiosis was observed when all coral species were considered given the high positive correlation values (Figure 3A and Suppl. file 1 Table S8; Robinson-Foulds distance of 0.68 (P = 0.00033); matching cluster distance of 0.85 (P=0.045); Mantel test r-value= 0.1 (P = 0.1)). However, patterns of phylosymbiosis were observed in the Mediterranean species (Figure 3B and Suppl. file 1 Table S8; Robinson-Foulds distance of 0.28 (P = 0.01); matching

cluster distance of 0.32 (*P* = 0.001); Mantel test r-value of 0.6 (*P* = 0.003)). It should be noted though that the position of *A. coralloides* and *C. verticillata* in the microbiome dendrogram was "reversed" in comparison with host phylogeny; and that the bacterial community compositions of *C. rubrum* and *A. coralloides* clustered despite their distant

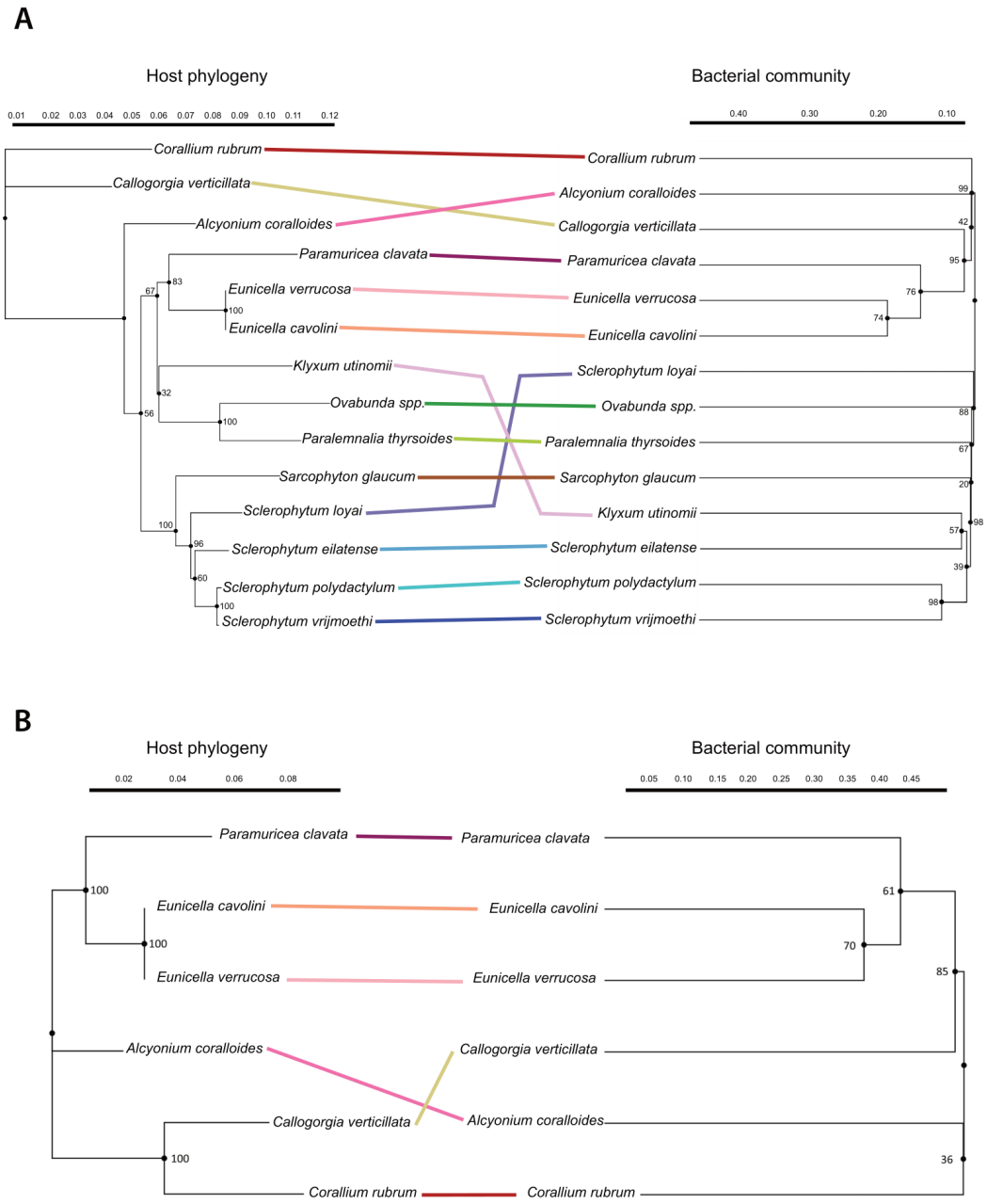

Figure 3: Phylosymbiosis in octocorals. Juxtaposition of the coral host phylogenetic tree and the microbiota dendrogram for **(A)** all the coral samples and **(B)** a subset of the Mediterranean coral species only

phylogenetic relationship (Figure 2B). In the Red Sea, phylosymbiosis patterns could not be discerned between the corals and their bacterial communities (Figure S3 and Suppl. file 1 Table S8; Robinson-Foulds distance of 1.08 (P = 0.99); matching cluster distance of 0.85 (P = 0.11); Mantel test r-value= 0.52 (P = 0.1)).

Cophylogeny between coral hosts and bacterial phylotypes

The Random TaPas algorithm was used to assess whether the evolutionary histories of both the octocoral species and certain bacterial phylotypes were correlated. A total of 120 host-symbiont associations, comprising 101 OTUs out of the 244 OTUs analyzed, contributed significantly to cophylogenetic congruence with the coral holobionts (Figure 4 and Suppl. file 1 Table S9). This was particularly true for associations with phylotypes belonging to the classes *Gammaproteobacteria*, *Alphaproteobacteria* and *Spirochaetia*. No signals of cophylogeny with bacterial phylotypes were observed in *K. utinomii*.

Associations with *Gammaproteobacteria* were the main contributors to cophylogenetic congruence (66% of all associations). This was particularly the case for *Endozoicomonas* phylotypes, which showed cophylogenetic links with 9 of the 13 octocoral species investigated. *Ovabunda* had the most associations with *Endozoicomonas* OTUs (n=23) contributing to cophylogeny, whereas most other Red Sea octocoral species (except *S. loyai* and *S. polydactylum*) had cophylogenetic associations with one to seven *Endozoicomonas* OTUs. Mediterranean octocorals had cophylogenetic associations with other *Endozoicomonas* OTUs (e.g. OTU1 and OTU3 in *E. cavolini*, OTU1 and OTU5 in *E. verrucosa* and OTU3 in *P. clavata*), which were also part of their respective core microbiomes (Figure 4 and Suppl. file 1 Table S9). Other Gammaproteobacterial taxa also presented cophylogenetic associations with several octocorals. Notably, the gorgonian *C. verticillata* had 8 cophylogenetic links with phylotypes from the order *Coxiellales,* the family *Shewanellaceae,* the *Spongiibacteraceae* clade *BD1-7* and the genus *Pseudoalteromonas*. Furthermore, 4 of these phylotypes were also found to be part of *C. verticillata* core microbiome (2 *Pseudoalteromonas* OTU397 and OTU458, OTU24 annotated as *Spirochaeta 2* and the *Spongiibacteraceae* clade *BD1-7* OTU103). Other cophylogenetic associations were observed between (1) *Vibrio* OTUs and Red Sea coral species (*S. vrijmoethi, S. eilatense, S. glaucum* and *P. thyrsoides*), (2) the

Spongiibacteraceae clade *BD1-7* (OTU103) and *E. verrucosa*, and (3) the order *BD72BR169* (OTU16) and *C. rubrum* (Figure 4 and Suppl. file 1 Table S9).

Associations with *Alphaproteobacteria* also contributed significantly to cophylogenetic congruence (15 OTUs, 13% of all associations) with octocorals. Cophylogenetic signals were found between *P. clavata* and 8 *Alphaproteobacteria* OTUs belonging to the families *Rhizobiaceae*, and *Terasakiellaceae*, the *Fokiniaceae* MD3-55, and the genera *Sneathiella* and *Candidatus Megaira*. Other octocoral species had only 1-3 cophylogenetic associations with *Alphaproteobacteria*, mainly between *Rhodobacteraceae* and *Sclerophytum* spp.

The class *Spirochaetia* accounted for 6% of the associations contributing to cophylogenetic congruence. *C. rubrum* showed cophylogeny with a *Spirochaetaceae* (OTU 15, Figure 4 and Suppl. file 1 Table S9), which was an abundant member of its core microbiome. Other *Spirochaetaceae* phylotypes also showed signals of cophylogeny in the Mediterranean coral species *A. coralloides* (OTU 135 and OTU 53) and *C. verticillata* (OTU 24), and these OTUs were also found in the core microbiomes of these corals. In octocorals from the Red Sea, two associations with *Spirochaetaceae* were found to contribute to cophylogenetic congruence, one in *S. eilatense* (OTU 43) and one in *S. loyai* (OTU 718; Suppl. file 1 Table S9).

Octocorals also showed cophylogenetic signals with phylotypes belonging to various other bacterial classes (14 out of the 120 contributing associations (11,6%); Suppl. file 1 Table S9). Notably, *C. rubrum* had associations with phylotypes belonging to different other classes, such as *Mollicutes* (OTU27 from the genus *Mycoplasma*), *Nitrospiria* (OTU360) and *Thermoanaaerobaculia* (OTU904) and two OTU from the phylum *Chloroflexi* (OTU416 and OTU534). The other *Scleralcyonaceae*, *C. verticillata*, showed cophylogeny with a *Mollicutes* phylotype (OTU101; order *Entomoplasmatales*) as well. *Verrucomicrobiae* phylotypes contributed to cophylogenetic congruence in *P. clavata* (OTU515; family *Puniceicoccaceae*) and *S. eilatense* (OTU239; genus *Lentimonas*). Cophylogeny between a phylotype from the *Helicobacteraceae* family (OTU645) and *S. glaucum* as well as between *Cyanobacteria* from the *Prochlorococcus* genus (OTU58) and *S. eilatense* were observed.

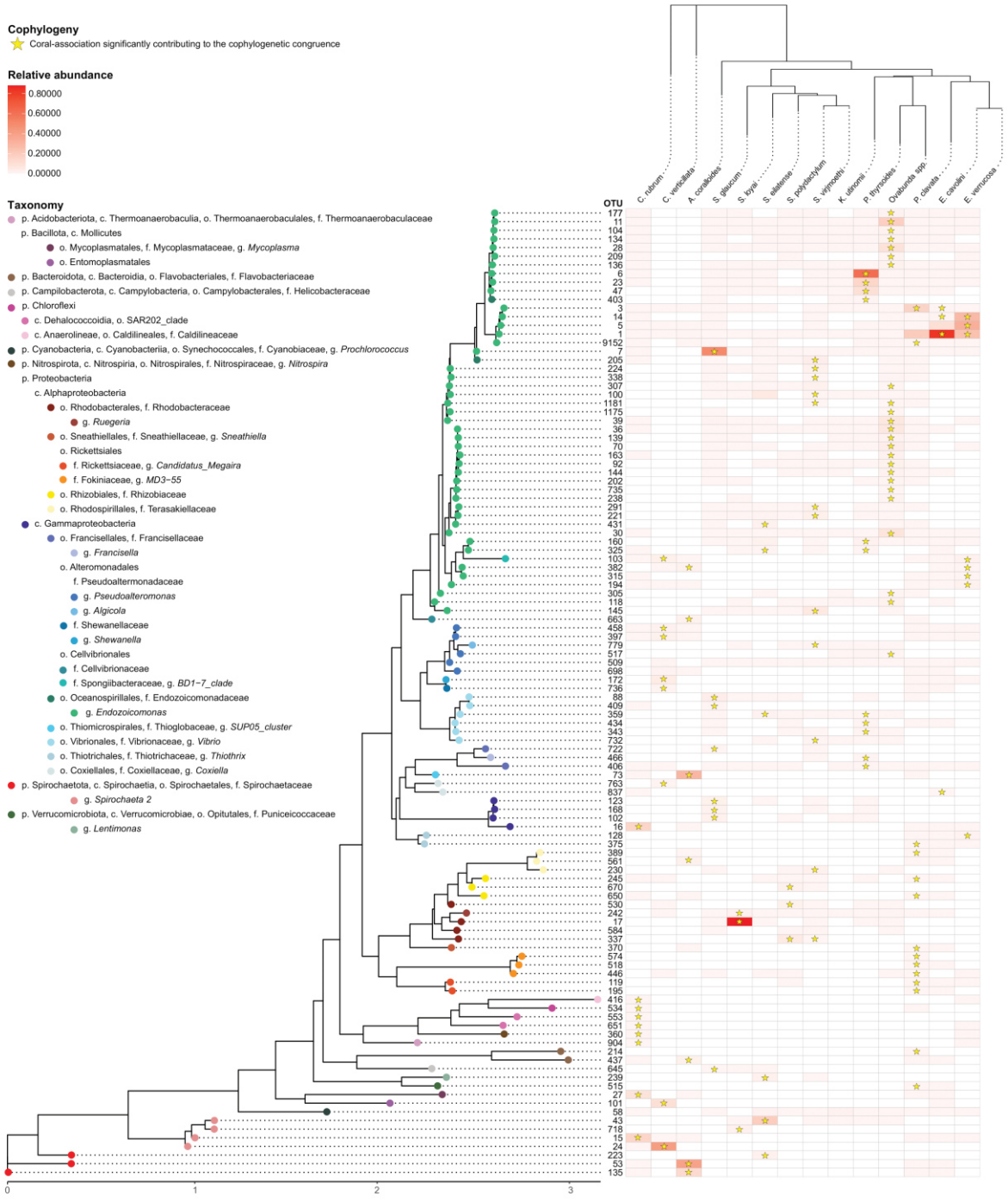

Figure 4: Relative abundance of the OTUs involved in host-symbiont associations contributing significantly to cophylogenetic congruence (positive residual frequencies values) for all Mediterranean and Red Sea coral species (the stars correspond to the contributing associations between a host and an OTU) along with their respective phylogeny. Taxonomic annotation: p – phylum; o – order; f – family; g – genus.

Discussion

We investigated the diversity and composition of bacterial communities associated with octocorals from the mesophotic zone of the Mediterranean Sea and Red Sea and assessed whether we can detect evolutionary patterns in these host-microbe associations. Our study revealed that Mediterranean and Red Sea octocoral holobionts harbor specific bacterial communities, but signals of phylosymbiosis were found only in octocorals from the Mediterranean Sea. However, indications of cophylogeny were detected in 13 of the 14 octocoral species investigated, suggesting that octocorals share a common evolutionary history with a few specific bacterial symbionts, primarily belonging to the *Endozoicomonadaceae* and *Spirochaetaceae*.

Octocorals are associated with specific bacterial communities.

The composition of the coral-associated bacterial communities differed significantly between corals from the Mediterranean Sea and those from the Red Sea. This difference may be related to the about 17 million-years separation of the Mediterranean Sea and the Red Sea before the opening of the Suez Canal in 1869 (Steininger et al., 1984). The different light, temperature, and salinity conditions in these two seas (Manasrah et al. 2019; Tanhua et al. 2013) may have contributed to the divergence observed in the microbiota of Mediterranean and Red Sea octocorals. Similarly, differences have been observed in the microbiota of coral species from different reefs or oceans (Lima et al., 2020; Roder et al., 2015; Pantos et al., 2015; Vohsen et al., 2023, van de Water et al., 2017).

Mediterranean octocorals from the mesophotic zone had species-specific microbiota, but two distinct 'clusters' could be observed – corals with a microbiota dominated by *Endozoicomonas* (*P. clavata* and *Eunicella* spp.) and corals with a *Spirochaetaceae*-dominated microbiota (*A. coralloides*, *C. rubrum*, *C. verticillata*). These patterns are consistent with reports on shallow populations (van de Water et al., 2016; 2017; 2018; Bayer et al., 2013; La Rivière et al., 2015; Ransome et al., 2014), suggesting that depth has little influence on the microbiota of these octocoral species. The latter 'cluster' was rather surprising as it was comprised of corals that belong to two different orders - the *Malacalcyonaceae* and *Scleralcyonaceae*, respectively. Each coral species did, however, harbor its own microbial phylotypes and taxa, explaining the overall

species-specific hierarchical clustering observed here, but some species also shared phylotypes. For example, the microbiota of *Eunicella* spp. and *P. clavata* had high abundances of *Endozoicomonas* OTU1 and OTU3, and the core microbiome of *A. coralloides* contained both phylotypes of *C. rubrum* (e.g., *Spirochaetaceae* OTU4) as well as gorgonians (e.g., *Endozoicomonas* OTU1, OTU2, OTU5). This overlap in the core microbiota is rather striking as *A. coralloides* is called the 'false red coral' in common language because of the similarities in appearance with *C. rubrum*, while it is in fact a 'parasite' or 'epibiont' that overgrows gorgonians, like *P. clavata* and *Eunicella* spp. (McFadden 1999; Groot et al., 1982; Quintanilla et al., 2013). This suggests that evolutionary patterns in host-microbiota associations may be masked by differences in species-specific life strategies and/or that associations with specific symbionts may have arisen multiple times during host evolution.

Other taxa found at relatively high abundances in the microbiota of Mediterranean octocorals here and in previous studies belonged to the genus *Rickettsia* in *P. clavata*, the *Spongiibacteraceae* BD1-7 clade in *C. rubrum* (Prioux et al. 2023; Tignat-Perrier et al. 2022), and the *Gammaproteobacteria* BD72BR169 in *E. cavolini* and *E. verrucosa* (van de Water et al., 2018). However, bacteria from these taxa are also present in the microbiota of various other Mediterranean gorgonians (Bayer et al., 2013; Tignat-Perrier et al., 2023; van de Water et al., 2018).

The microbiota of octocorals from the Red Sea were distinct from those from the Mediterranean, but *Endozoicomonas* and *Spirochaetaceae* were also frequent and abundant symbionts of several of these tropical soft coral species. Overall, they could be divided into three main groups based on their microbiota composition: (1) *Endozoicomonas*-*Spirochaetaceae*-dominated (*K. utinomi*, *S. glaucum*, *S. eilatensis*, *S. vrijmoethi*); (2) *Endozoicomonas*-dominated (*Ovabunda* spp., *P. thyrsoides*); and (3) others with relatively high abundances of *Rhodobacteraceae* (*S. polydactylum*, *S. loyai*). While matching relatively well with the hierarchical clustering analysis, these groups were not as clear-cut, as *Mollicutes* were abundant in *K. utinomi* (*Entoplasmatales*) and *Ovabunda* spp. (*Mycoplasmatales*), whereas *P. thyrsoides*, *S. eilatensis* and *S. vrijmoethi* contained a relatively high abundance of *Rhodospirillales* (family *Terasakiellaceae*) in their microbiota. The microbial taxa identified here as the main symbionts of octocorals from the Red Sea are consistent with reports on octocorals from other tropical locations.

For example, *Endozoicomonas* is a highly abundant symbiont of *Sclerophytum* and *Sarcophyton* species from the Indo-Pacific (Haydon et al., 2022; O'Brien et al., 2020; Park et al., 2022; Easson et al., 2024), but also, in many other octocorals from the Indo-Pacific (Wessels et al. 2017) and Caribbean (Morrow et al., 2012; Robertson et al., 2016; McCauley et al., 2016; Pike et al., 2013; Sunagawa et al., 2010). Spirochaetes have also been found relatively abundant in the microbiota of Indo-Pacific *Sarcophyton* spp. (Haydon et al. 2022; O'Brien et al. 2020), *Lobophytum* (Wessels et al. 2017) and in some *Sclerophytum* species (Park et al. 2022; O'Brien et al. 2020). But the holobionts of *Sclerophytum* species do not always harbor Spirochaetes in this region (Haydon et al. 2022). However, *Sclerophytum* spp. from both the Red Sea as the Indo-Pacific do associate with *Rhodospirillales* (Haydon et al. 2022) and *Rhodobacteraceae* (Lu et al., 2020; Chen et al., 2012; Alsharif et al., 2023).

Mollicutes, such as *Entoplasmatales* and *Mycoplasmatales*, were also highly abundant in the microbiota of *C. verticillata* and *K. utinomii*, and of *Ovabunda* spp. and *C. rubrum*, respectively. Members of these orders have previously been observed in association with deep-sea corals and gorgonians (*Entoplasmatales*: Gray et al., 2011; Chapron et al., 2020; Weiler et al., 2018; van de Water et al., 2018), and with other octocorals (*Mycoplasmatales*: Gray et al., 2011; Holm et al., 2016; Porporato et al., 2013; van de Water et al., 2017; 2018).

Overall, as for the hexacorals, octocorals are consistently found to have dominant associations with bacteria belonging to a few main taxa, particularly *Endozoicomonas* and *Spirochaetaceae*, but also harbor numerous other rare taxa. Of particular interest, are those phylotypes that belong to a coral species' core microbiome and those that are unique to a coral species. Such consistent associations of various microbial taxa with octocorals underscore their importance as symbionts and suggest that there may be an evolutionary link between these holobiont partners.

Unclear signals of phylosymbiosis in octocoral holobionts

Phylosymbiosis refers to a pattern in which the evolutionary relationships between hosts are reflected in the composition of their microbiomes, with closely related hosts harboring more similar microbial communities (Lim et al., 2020). This pattern suggests that host evolution has played a role in shaping the structure of their microbiomes, possibly through processes like co-diversification. However, phylosymbiosis does not

necessarily imply coevolution between hosts and microbes, as various ecological and environmental factors can also influence microbial community composition. Understanding phylosymbiosis provides important context for interpreting host-microbiome associations in an evolutionary framework.

A phylosymbiotic signal has been observed in scleractinian corals (Pollock et al. 2018) and octocorals from Australia (O'Brien et al. 2020). However, we did not observe phylosymbiotic signals between octocorals and their microbiota, when we considered all octocoral species studied here. This may be explained by a clear separation in bacterial community composition according to the two geographic locations, the Mediterranean Sea and the Red Sea. These seas have been isolated for at least 17 million years (Steininger et al., 1984), suggesting that the geographical separation of these coral populations (i.e., vicariance) influenced patterns in the structure of the microbiota more than host phylogeny.

However, when the coral populations from the two seas were assessed separately, signals of phylosymbiosis were observed in the temperate Mediterranean octocorals but not in corals from the tropical Red Sea. The Mediterranean octocorals *C. rubrum*, *P. clavata* and several *Eunicella* spp., have been extensively studied and possess a microbiota that is specific as well as temporally and spatially stable (van de Water et al., 2016; 2017; 2018). It was therefore previously hypothesized that the microbiota may have evolved closely with the host *via* co-diversification and/or *via* vertical transmission (maternal inheritance) of bacterial communities between coral generations in these larval-brooding species (van de Water et al., 2018). Here, we confirm that phylosymbiosis exists in Mediterranean coral holobionts, but the mechanisms explaining this pattern remain to be investigated.

On the contrary, the tropical octocorals from the Red Sea and their microbiota did not demonstrate phylosymbiotic relationships. This contrasts with the findings in octocorals from the Great Barrier Reef (O'Brien et al. 2020) and to the patterns observed in the temperate Mediterranean in this study. Particularly the positioning of *K. utinomi* and *S. loyai* in the bacterial community dendrogram did not match with the host phylogeny. O'Brien et al. (2020) also observed three such 'mismatches' but phylosymbiosis signals were still detected. However, their dataset contained a greater diversity of octocoral species representing a wider range of octocoral taxonomy, which may have contributed

to better detection of phylosymbiotic patterns (Lim et al., 2020). The relatively thick layer of mucus, which contains numerous environmental microbes, surrounding the tissues of these tropical octocorals is another factor that might have masked the phylosymbiosis signal in the Red Sea octocorals. In scleractinian corals, phylosymbiosis was in fact only found in bacterial communities associated with host animal tissues and skeleton, but not in the mucus (Pollock et al. 2018). To obtain a better understanding of the relationships between octocorals and their microbiome, it may be important to target different anatomical regions of the coral hosts to determine if this would result in different phylosymbiosis patterns. Besides, future studies into evolutionary links between tropical octocorals and their microbiota would likely benefit from expanding the dataset to include additional octocoral species representing higher diversity in octocoral taxonomy.

The observation that phylosymbiosis was only detected in octocoral holobionts from the Mediterranean Sea but not the Red Sea, and that these seas are geographically separated, suggest that vicariance may be a driver of the divergent evolutionary patterns between host phylogeny and microbiota composition. It further underscores the role of environmental conditions and evolutionary histories in shaping host-microbe interactions. In particular, the more extreme conditions in the Red Sea, such as higher temperatures and higher salinity could have significantly influenced how symbiosis between corals and their microbial associates established and evolved, as well as the nature of these interactions. As such, it may have affected the evolution of microbial communities in a way that differs from those in the Mediterranean. Comprehensive meta-analyses using standardized methods are necessary to further clarify these dynamics.

Cophylogenetic interactions are restricted to only a few host-symbiont associations.

While phylosymbiosis sheds light on how species that are closely related tend to have more similar microbiota, fine-scale tests of host-microbe cophylogeny help to identify specific microbial lineages, that may have a matching evolutionary history with their hosts. This could indicate shared events, such as cospeciation and codiversification, or other ecological or evolutionary relationships. Although studies of cophylogeny do not identify the processes by which host-symbiont associations arose,

studying these symbionts is particularly valuable as they could play key roles in shaping microbiota dynamics.

Of the 244 most abundant OTUs (with a relative abundance of > 0.1%) that were examined, 101 OTUs were found to have significant associations contributing to the cophylogenetic signal with one or more of the 14 octocoral species investigated (0-24 phylotypes per coral species). This finding supports the idea that a limited group of bacterial phylotypes might play a significant role in host fitness. Similar findings were observed in two previous studies on octocorals, scleractinian corals and marine sponges, where only a small number of bacterial genera, such as *Endozoicomonas*, displayed cophylogenetic patterns and contributed to a phylosymbiotic signal (Pollock et al. 2018; O'Brien et al. 2021). The cophylogenetic signals observed for the host-bacteria associations listed below suggest that codiversification (i.e., parallel evolutionary changes and speciation events in two or more host and symbiont lineages, leading to a shared evolutionary history) is likely significant between corals and certain bacterial lineages. It can result from different mechanisms such as coevolution but also vicariance (specificity of certain bacterial strains according to geographical and ecological factors) and vertical transmission.

In this study, nearly half of the 101 OTUs that showed a cophylogenetic signal with octocorals belonged to the genus *Endozoicomonas*, and such associations were present in 9 of the 14 octocoral species studied here. Interestingly, a cophylogenetic signal was observed between the abundant *Endozoicomonas* OTU3 and both *P. clavata* and *E. cavolini*, and between OTU1 and both *E. cavolini* and *E. verrucosa*. And in octocorals from the Red Sea, cophylogenetic associations with *Endozoicomonas* were particularly found in *Ovabunda* spp. (24), *S. vrijmoethi* (6) and *P. thyrsoides* (7). This shows the importance of the *Endozoicomonas*-coral associations in the evolutionary history of octocorals from both seas and highlights the possibly important contributions of these symbionts to their host's fitness, such as the digestion of complex molecules (Alex et al., 2019; Speck et al., 2012), the provision of amino acids (Neave et al. 2017), vitamins (Maire et al. 2023), and involvement in sulfur cycling (Tandon et al. 2022). However, others question the nature of the symbiosis between corals and *Endozoicomonas* (Pogoreutz et al., 2024).

Spirochaetaceae were another main microbial taxon identified as contributing to the cophylogenetic congruence in our study. This was the case in three temperate

octocorals (*C. rubrum*, *C. verticillata* and *A. coralloides*) and in two tropical octocorals (*S. loyai* and *S. eilatense*). The microbial associations showing a fit with cophylogeny were different for each coral species, and primarily involved the genus *Spirochaeta* as well as unclassified *Spirochaetaceae*. While some coral species may share a concordant evolutionary history with their most abundant *Spirochaetaceae* symbionts, others may have an evolutionary relationship with lower abundant or rare phylotypes, as previously observed in other coral species and sponges from the Great Barrier Reef (O'Brien et al. 2021). For example, the most abundant *Spirochaetaceae* in *C. rubrum* did not contribute to cophylogenetic congruence, whereas a member of the genus *Spirochaeta* did. This cophylogenetic link is interesting as the *Spirochaeta* of *C. rubrum* has been hypothesized to be involved in the characteristic color of this red coral (Van De Water et al., 2024). Surprisingly, however, most of the tropical octocorals assigned to the '*Endozoicomonas*-*Spirochaetaceae*'-dominated microbiota group did not show cophylogenetic relationships with their *Spirochaetes* symbionts. The role of *Spirochaetaceae* within the coral holobiont remains to be investigated, but other symbiotic Spirochaetes are known to fix nitrogen (Lilburn et al. 2001), metabolize carbon sources (Lim et al. 2019), and produce vitamin B6 and the antimicrobial compound pyrroloiminoquinone (Waterworth et al., 2021).

Rhodobacteraceae also showed cophylogeny with octocorals in which they were a main symbionts (*S. loyai*, *S. polydactylum*) as well as with *S. vrijmoethi*. O'Brien et al. (2021) also found cophylogenetic relationships between this taxon and corals from the Indo-Pacific. The function of these symbionts is yet unknown, but members of this taxon have been suspected to be opportunistic pathogens as they are often found in stress-impacted corals (Prioux et al. 2023; Alsharif et al. 2023; Rosales et al. 2023; Clark et al. 2021; Rosales et al. 2020). This also shows that it is difficult to interpret the results on evolutionary links between corals and microbes, as these analyses cannot distinguish between the nature of these host-microbe relationships, and thus the importance of these microbes in host health.

Besides members of the three taxa that dominated the bacterial communities of the octocorals studied here, phylotypes belonging to other taxa were also found to contribute to cophylogenetic congruence. For example, cophylogeny was observed between *A. coralloides* and *Thioglobaceae* SUP05 cluster OTU73. This microbe is part of

A. coralloides' core microbiome, and may be of importance for the health of this coral because of its amino acid and B vitamin biosynthesis capacities, as well as for its antiviral defense system and chemoautotrophic metabolism has been demonstrated (Keller-Costa et al., 2022). Cophylogenetic signals were also detected between *Mollicutes* and two corals from the Mediterranean Sea, particularly OTU101(*Entomoplasmatales*) and *C. verticillata*, and OTU27 (*Mycoplasma*) and *C. rubrum*. *Mycoplasma* has been proposed to feed commensally on remnants of prey captured by scleractinian cold-water corals (Kellogg et al., 2009; Neulinger et al., 2009), and may explain how this type of association evolved. It has also been shown that *Mycoplasma* have co-diversified with salmonids (Rasmussen et al. 2023). Moreover, associations between *Spongiibacteraceae* OTUs from clade BD 1-7 and the corals *C. verticillata* and *E. verrucosa* were detected to contribute to cophylogeny, which may not be surprising as these bacteria are commonly found at relatively high abundances in various gorgonian coral species (Quintanilla et al., 2022; van de Water et al., 2017; 2018). Characteristic for *P. clavata* were its cophylogenetic associations with various *Alphaproteobacteria* (*Rhizobiaceae*, *Terasakiellaceae*, *Fokiniaceae*, *Sneathiella* and *Candidatus Megaira*), which are not very abundant in its microbiome. These taxa have been observed, although in low abundance, within the microbiome of Mediterranean gorgonians (Prioux et al., 2023; Tignat-Perrier et al., 2022; 2023). *Terasakiellaceae* were also detected across multiple coral species (Parker et al., 2020; Quintanilla et al., 2022; Weiler et al., 2018). *Terasakiellaceae* as well as *Sneathiellaceae* may play a role in the cycling of nitrogenous compounds (Carareto Alves et al. 2014; Kurahashi et al. 2008) within the coral holobiont.

Interestingly, we also found cophylogenetic associations between the octocorals studied here from the Mediterranean Sea and Red Sea and several bacterial taxa that had previously been shown to have cophylogeny with octocorals from the tropical Indo-Pacific. Notably, O'Brien et al. (2021) found evolutionary links between *Sclerophytum* and *Sarcophyton* coral species and *Cyanobacteria*, *Chloroflexi*, *Verrucomicrobiae* and *Thermoanaerobaculaceae*. Compared with scleractinian corals, few similarities have been observed. While Pollock et al. (2018) found strong cophylogenetic signals between scleractinians and *Endozoicomonas*, they also revealed cophylogeny with *Clostridiaceae*, *Kiloniellales* and *Myxococcales*. Such relationships have, however, not been identified in octocorals so far.

The absence of cophylogenetic signals between certain high abundant phylotypes and their coral hosts raises intriguing questions about the dynamics of host-bacteria interactions. For example, neither OTU1 in *P. clavata* nor OTU4 in *C. rubrum* exhibited significant cophylogenetic associations with their respective hosts, despite their high abundance within the holobionts. This suggests a lack of specific evolutionary relationships between them. This finding challenges the conventional assumption that dominance within the microbiome implies a strong and persistent relationship with the host organism. Other factors could thus play important roles in shaping the nature and efficacy of these associations.

The observations by us and others highlight the potential importance of relatively few but taxonomically diverse microbial taxa in the evolutionary history of coral-bacteria associations. Corals throughout the world appear to engage in symbioses with several specific microbial taxa, particularly *Endozoicomonas*. Altogether, these observations also suggest that it is not necessarily the most abundant symbiont or all members of the consistently associated core microbiome that share similar evolution patterns with their host.

Limitations in cophylogeny studies into microbe-coral associations

Our investigation of cophylogenetic patterns in host-bacteria relationships may present some limitations. First, as with most cophylogenetic studies, our assessment of bacterial phylogeny is based on variations within the variable regions of the *16S rRNA* gene (Pollock et al. 2018; O'Brien et al. 2021; Youngblut et al. 2019). Although this approach is currently the most practical, it involves the use of amplicons, which are relatively short marker sequences with limited phylogenetic information and the results may have to be interpreted with some caution. For example, no overlap in *Endozoicomonas* symbionts was found between *P. clavata* and *Eunicella* spp. previously (van de Water et al. 2017b), whereas these corals share a dominant *Endozoicomonas* phylotype (OTU1) in this study. The main difference between these studies is the use of a different primer set (targeting V5-V6 and V3-V4, respectively) to generate the *16S rRNA* gene amplicons. Using full-length *16S rRNA* gene sequencing approaches may provide better resolution and insights into evolutionary aspects in coral-microbe symbiosis.

Second, as emphasized by O'Brien et al. (2021), cophylogenetic models do not provide insights into the nature of the symbiotic interaction between host and microbe

(i.e., whether it is mutualistic, parasitic, or commensal), nor into the underlying mechanisms responsible for these observed patterns. It is thus essential to recognize that associations showing cophylogenetic congruence may not always be beneficial. For instance, some *Vibrionaceae* and *Rhodobacteraceae* significantly contributed to the cophylogenetic signal in various coral species from both seas. Although their role in these coral holobionts is unclear, members of these families have been implicated in coral disease and mortality (Rosales et al., 2023; Clark et al., 2021; Gajigan et al., 2017; Martin et al., 2002; Sun et al., 2023), and their evolutionary relationship may thus also indicate a potentially harmful relationship. To understand the effect of symbiosis on host fitness, it is crucial to consider both parasitic and mutualistic symbiotic relationships as equally important factors.

Conclusion

While many bacteria associated with corals are host-specific, only a minority of bacterial phylotypes associated with corals display cophylogenetic patterns indicative of long-term host-microbe relationship, especially with *Endozoicomonas*. This result emphasizes the idea that, although host-microbe cophylogeny likely plays a role in phylosymbiosis, other factors, such as biogeographic influences, also play an important role in shaping this pattern. Furthermore, the different degrees of cophylogeny between coral microbes and their hosts underscore the fact that the microbiome is not a singular entity subject to uniform selection and that the abundance of the symbionts within the holobiont does not correlate with their common evolutionary history. Instead, it comprises a multitude of distinct participants with varying degrees of historical association with both the host and each other.

This study reveals important patterns between coral hosts and their microbiota, offering valuable insight into their potential evolutionary history. However, to better understand whether these patterns indicate coevolution or are driven by other factors, such as vicariance, further research is needed. Investigating whether these patterns remain consistent throughout the coral's life cycle and how environmental factors influence host-microbe interactions would add more clarity.

Chapter 2

Unveiling the composition and spatiotemporal stability of the eukaryome of *Corallium rubrum*

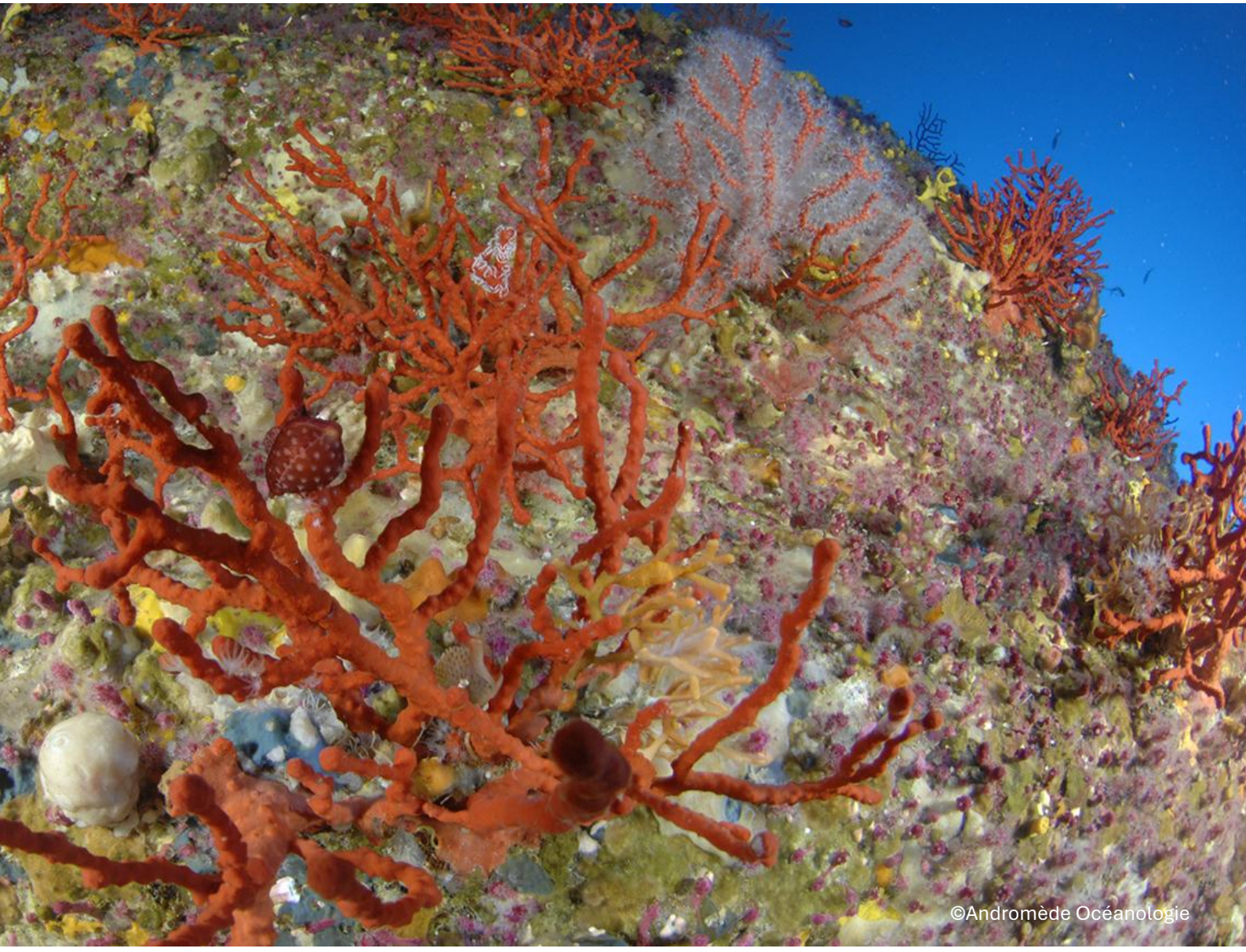

Chapter 2: Unveiling the composition and spatiotemporal stability of the eukaryome of *Corallium rubrum*

I. Overview of the chapter

Coral holobionts are complex meta-organisms composed of the coral animal host and a diverse consortium of microorganisms, including bacteria, archaea, viruses and microeukaryotes. While bacterial communities and photosynthetic dinoflagellates (Symbiodiniaceae) have been extensively studied, the other microeukaryotes, including protists, microalgae and fungi, remain poorly characterized (Ainsworth et al. 2017; del Campo et al. 2020; Bonacolta et al. 2023), especially in Mediterranean octocorals such as *C. rubrum*. Understanding the diversity, stability, and functional role of these microeukaryotic communities, termed the coral eukaryome, is crucial for elucidating the functioning and resilience of the coral holobiont under environmental stressors such as marine heatwaves and habitat degradation.

A major technical challenge in the study of coral-associated microeukaryotes is the dominant presence of host DNA in *18S rRNA* gene-based metabarcoding data, which obscures the detection of associated microeukaryotes (Parfrey et al. 2014; Del Campo et al. 2019). To address this issue, specific primers targeting a region of the *18S rRNA* gene were designed to minimize amplification of *C. rubrum* host sequences while capturing a broad diversity of microeukaryotes. This approach was applied to 46 *C. rubrum* colonies collected from five geographically diverse locations in the Northwestern Mediterranean Sea (*Porticcio, Cap de Creus, Cassis, Villefranche-sur-Mer* and *Portofino*), covering an area of approximately 44,670 km^2, to assess microeukaryotic diversity and spatial stability. Given that some samples were collected in spring 2013 and others in autumn 2023, we also examined whether the observed variability could be explained by this temporal difference.

Metabarcoding revealed a diverse microeukaryotic community with a small core defined by families consistently detected at all sites, in particular Licnophoridae ciliates

and Dino-Group I Clade 1 dinoflagellates. This consistent association suggests that these taxa, already observed in other coral species, such as the tropical hexacoral *Pocillopora damicornis* and the temperate gorgonian *Paramuricea clavata* (Clerissi et al. 2018; Bonacolta et al. 2024), likely play an important ecological role within the red coral holobiont. Licnophoridae species are known predators of other ciliates (Sweet and Séré 2016), a trait that may contribute to their functional role in maintaining the balance of the microbial community within the coral. Members of Dino-Group I Clade 1 were observed in high relative abundance in heat resistant P. *clavata* colonies suggesting a possible role in coral stress tolerance (Bonacolta et al. 2024) although this requires further investigation.

Still, the composition of the eukaryome showed significant spatial variability between sites, with a separation between samples collected in spring 2013 and autumun 2023. This contrasts with the more stable bacterial microbiome previously documented in *C. rubrum* (van de Water et al. 2016a; van de Water, Voolstra, et al. 2018a). For example, some microeukaryotes such as Corallicolidae apicomplexans were only prevalent at some sampling sites, suggesting that local environmental conditions strongly influence the structure of the microeukaryotic community.

Overall, this chapter demonstrates that the eukaryome of *C. rubrum* is defined by a stable core of key microeukaryotic taxa, mainly Licnophoridae ciliates and Dino-Group I Clade 1 dinoflagellates, which are consistently associated with the coral, alongside a variable fraction strongly shaped by local environmental factors. Core taxa likely provide essential functional support, such as nutritional support, microbial predation and defense against pathogens, while site-specific microeukaryotes may provide context-dependent benefits such as food supply or protection from local stressors. The spatiotemporal variability and sensitivity of the eukaryome to environmental conditions highlight the need for further research to clarify their ecological roles and their contribution to coral health and resilience. Understanding these dynamics is critical for predicting coral responses to climate change and for developing effective conservation strategies for endangered octocoral populations in the Mediterranean Sea.

II. Publication

Unveiling the microeukaryotic landscape of the red coral *Corallium rubrum* across the Northwestern Mediterranean Sea

Environmental Microbiology Reports | Reviewed October 2025

Camille Prioux[1,2,3*] and Doria Filipponi[1*], Christine Ferrier-Pagès[1], Denis Allemand[1], Romie Tignat-Perrier[1,2]

[1]Centre Scientifique de Monaco, 8 Quai Antoine 1er, MC 98000, Principality of Monaco

[2]Unité de Recherche sur la Biologie des Coraux Précieux CSM - CHANEL, Centre Scientifique de Monaco, 8 Quai Antoine 1er, MC 98000, Monaco, Principality of Monaco

[3]Sorbonne Université, Collège Doctoral, Paris, France

* These two authors contributed equally.

Abstract

Octocorals such as *Corallium rubrum* are key components of temperate Marine Animal Forests (MAFs), providing three-dimensional habitats that support diverse marine life. However, *C. rubrum* faces growing threats from overexploitation and climate stressors such as ocean warming. While the coral's bacterial microbiome is well-documented and stable across spatial and temporal scales, the associated microeukaryotes, collectively referred to as the coral eukaryome, remain poorly characterized. In this study, we used *18S rRNA* gene metabarcoding to explore the eukaryome of 46 *C. rubrum* colonies collected from five sites (~44,670 km^2) in the northwestern Mediterranean. We identified a limited set of core microeukaryotic families, including Licnophoridae and Dino-Group I Clade 1, which were present at all sampling locations. Despite shared core taxa, eukaryome composition showed high variability between sampling sites, seasons and years. This suggests the red coral eukaryome is strongly influenced by local environmental factors. Given the increasing frequency of marine heatwaves and habitat degradation, further research is needed to understand the

ecological roles of key eukaryotic taxa and their contribution to coral holobiont resilience. Clarifying the function of the eukaryome is essential for predicting how *C. rubrum* and other habitat-forming octocorals will respond to future climate scenarios.

Introduction

Marine Animal Forests (MAFs) are unique habitats and biodiversity hotspots (Casas-Güell et al. 2015; Roberts et al. 2002; Ponti et al. 2019), offering shelter to diverse marine species (Luigi Piazzi et al. 2021c) and providing valuable services such as fisheries support, coastal protection, and tourism (Paoli et al. 2017; Worm et al. 2006; Rossi et al. 2017a). Among these, the shallow and upper-mesophotic Marine Animal Forests (depths <60 m) of the Mediterranean Sea stand out as ecologically important ecosystems, primarily dominated by sponges and habitat-forming octocorals such as *Eunicella* spp., *Paramuricea clavata*, and the iconic red coral *Corallium rubrum* (Ballesteros 2006; Ponti et al. 2019; Gori et al. 2011). Like all meta-organisms, corals form complex holobionts with diverse microorganisms that collectively make up the microbiome, an essential component for maintaining health through nutrient cycling, resistance to stress and protection from pathogens (Voolstra et al. 2024; van de Water et al. 2018). In literature, the aforementioned functions are usually associated with the photosynthetic dinoflagellates from the family Symbiodiniaceae and the associated bacterial communities, which are the most studied symbionts of the coral microbiome. Still, the complex coral-associated microbial communities contain other microeukaryotic members (referred to as the “eukaryome”) that have been poorly investigated despite their likely relevance for the coral holobiont (del Campo et al. 2020; Bonacolta et al. 2023). This is mainly due to the large difficulty of culturing microeukaryotes, as well as the technical limitations of using *18S rRNA* gene-based sequencing to study coral-associated microeukaryotes (del Campo et al. 2019). Because both the microeukaryotes and their coral hosts are eukaryotes, the metabarcoding approach often results in data that is dominated by host DNA. To minimize this issue, specific methodological strategies have been developed, including optimized primer design and the use of host-specific blocking oligonucleotides (del Campo et al. 2019; Parfrey et al. 2014; Wilcox et al. 2014).

Recent DNA-based studies have emphasized the importance of coral-associated microeukaryotes in terms of species richness and abundance. Some microeukaryotes were frequently reported to be associated with corals and are suggested to be important players of the coral microbiome. For example, Corallicolidae apicomplexans were found in high prevalence across all major groups of corals (Kwong et al. 2019; 2021; Bonacolta et al. 2023; 2024). In Kwong et al. (2019), the apicomplexan *ARL-V 16S rRNA* gene was recovered in 83% of the 43 coral samples, covering 38 coral species. However, to date, only a few studies have examined the diversity of the eukaryome in Mediterranean octocorals (Bonacolta et al. 2024; Prioux et al. 2025a; 2025b), and these have focused exclusively on conditions of thermal stress. As a result, our understanding of octocoral-microeukaryotes associations under baseline, non-stressed conditions remains limited. They identified a large richness of microeukaryotes with up to 8,187 ASVs (Amplicon Sequence Variant) and 3,181 ASVs in association with colonies of *C. rubrum* and different populations of *P. clavata*, respectively (Prioux et al. 2025; Bonacolta et al. 2024). Some dominant microeukaryotes were found in the samples of both species such as the Syndiniales Dino-Group I, the Licnophoridae ciliates and the Corallicolidae apicomplexans (Prioux et al. 2025; Bonacolta et al. 2024). While these studies are pioneering and provide new insights on the large diversity of microeukaryotes associated with Mediterranean octocorals, further studies are necessary to get a better understanding of the dynamic of the octocoral-microeukaryotes association and identify key microeukaryotic members.

Previous studies have shown that *C. rubrum* maintains stable associations with specific bacterial symbionts (*i.e.*, Spirochaetaceae bacteria) across both temporal and geographical scales (van de Water et al. 2016; 2017). This knowledge has enabled following investigations to focus on these specific symbionts (Tignat-Perrier et al. 2023; 2025; Prioux et al. 2023; 2024), as they likely play a crucial role in the holobiont functioning. Although the stability and functional significance of bacterial symbionts in corals are well-documented, it is still unclear to what extent similar patterns hold true for the eukaryome. It is therefore essential to investigate whether these microeukaryotic associations exhibit stability and functional relevance, in order to fully comprehend their role in coral health, resilience, and the dynamics of the holobiont.

In this study, we analyzed samples of *C. rubrum* colonies collected at five different locations (*Porticcio*, *Cap de Creus*, *Cassis*, *Villefranche-sur-Mer*, *Portofino*) in the Northwestern Mediterranean Sea covering a total surface of 44,670 km^2. Here, we investigated the composition of the red coral eukaryome in different red coral populations using a *18S rRNA* gene metabarcoding approach with specific primers designed to minimize the red coral *18S rRNA* sequences signal, while covering a wide diversity of microeukaryotic taxa. We aimed to gain a better understanding of microeukaryotic diversity associated with the red coral, uncover the stability of the association between *C. rubrum* and its associated microeukaryotes, and assess how local environmental conditions may influence the composition of the red coral eukaryome.

Methods

Sample collection

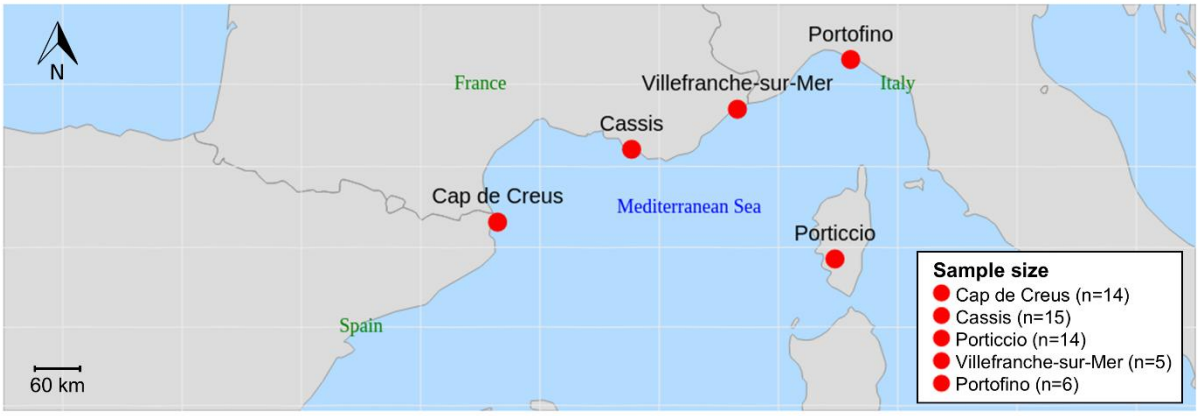

Figure 1: Geographic distribution of the sampling sites. Map of the Northwestern Mediterranean Sea showing the sampling locations: Cap de Creus, Spain (42.3°N, 3.3°E); Cassis, France (43.2°N, 5.5°E); Porticcio, Corsica, France (41.8°N, 8.8°E); Villefranche-sur-Mer, France (43.7°N, 7.3°E) and Portofino, Italy (44.3°N, 9.2°E). Samples were collected from visually healthy colonies at 30–40 m depth.

A total of 43 samples were collected from different colonies of *Corallium rubrum* in spring, between April and June 2013 at depths of 30-40 m from three sites: *Cap de Creus*, Spain (n=14; 42°18'N, 3°18'E); *Cassis*, France (n=15; 43°12'N, 5°28'E); and

Porticcio, Corsica Island, France (n=14; 41°50'N, 8°45'E) (Figure 1). At each site, visually healthy colonies were sampled, samples were rinsed with 0.2 µm-filtered seawater and subsequently preserved in ice-cold RNAlater® RNA Stabilization Solution (ThermoFisher Scientific) at 4°C. To broaden the geographic scope of the study and increase the sample size, data from Prioux et al., 2025, which included *C. rubrum* samples collected in autumn (November) 2023 from *Villefranche-sur-Mer*, France (n = 5; 43.7°N, 7.3°E) and *Portofino*, Italy (n = 6; 44°18'N, 9°12'E) were incorporated (Figure 1). These samples were processed following the same protocol described in this study, increasing the total number of samples in the dataset to 54.

DNA extraction

Approximately 1 cm^3 of coral (comprising the soft tissue and the skeleton) was used for DNA extraction using the DNeasy PowerBiofilm Kit (Qiagen), with the following modifications: samples were placed into pre-filled bead tubes containing 350 µL MLT buffer, 100 µL FB solution, and 2 µL Proteinase K solution (600 U/mL; Qiagen), and bead-beating was performed twice for 2 min at 30 Hz using a TissueLyser II (Qiagen). Two negative extraction control samples (*i.e.*, extraction without sample material) were included in each batch of extractions to monitor contamination. DNA concentrations were measured using an Invitrogen™ Qubit™ 4 Fluorometer (Fisher Scientific) and the Qubit® dsDNA BR (Broad-Range) Assay kit, and DNA samples were stored at -20°C.

Amplification of the *18S rRNA* gene

Design of primers targeting the eukaryotic V4 region and minimizing host signal

Previous studies on the coral microbiome (Clerissi et al. 2018; Bonacolta et al. 2024; del Campo et al. 2019) have shown that the different universal *18S rRNA* gene primer pairs amplify the coral host sequences over the microeukaryotic sequences which are in fewer numbers. We tested the universal *18S rRNA* gene primers TAReuk454FWD1 (5'-CCAGCASCYGCGGTAATTCC-3') and TAReukREV3 (5'-ACTTTCGTTCTTGATYRA-3'), which target the V4 region (Stoeck et al. 2010), and mainly obtained reads corresponding

to the red coral sequences (99,96% of reads were coral-derived; Supp. File 2 Table S1 and Figure S2).

To overcome this bias, we used customized primers derived from the UNonMet-PCR primers targeting the V4 region of the *18S rRNA* gene, initially described in Bower et al. (2004) and further validated for Illumina amplicon sequencing by del Campo et al. (2019). Originally, the UNonMet-PCR primers were designed to reduce the signal from metazoan hosts while amplifying that of microeukaryotes. Because these primers did not successfully reduce the signal from *C. rubrum* (Supp. File 2 Table S1), new primers, named 18S-NonMet_Cr-F (5'-AAGTCTGGTGCCAGCASCC-3') and 18S-NonMet_Cr-R (5'-TTTAAGTTTCAGCCTTGCGAT-3'). The NonMet_Cr-F primer was modified from the UNonMet-PCR forward primer, while the 18S-NonMet_Cr-R primer was fully designed. We used a manually curated database containing 544 *18S rRNA* gene sequences from a diverse array of eukaryotes, including *C. rubrum* and microeukaryotic lineages previously detected in coral microbiota and available from the nr (non-redundant) nucleotide database of NCBI. Each nucleotide in the designed primers was carefully screened to ensure maximum dissimilarity to *C. rubrum* sequences within the V4 region while simultaneously maintaining universality to target microeukaryote sequences, particularly paying attention to lineages yet described as being part of coral microbiome in previous literature. The alignment of the primers on the database is available as Supp. file 1.

In-silico PCRs were done against the sequences from the PR2 microeukaryotic database (https://app.pr2-primers.org/pr2-primers/; v. 2.0.0) using the newly designed primers 18S-NonMet_Cr to test their universality in targeting the different microeukaryotic taxonomic groups. A sequence was considered amplified by the primers set if each primer had ≤ two mismatches with the sequence, and the percentage of sequences amplified for each microeukaryotic taxonomic group was calculated. As a comparison, the same analysis was done using the universal primers TAReuk454FWD1 and TAReukREV3 known to amplify the *18S rRNA* gene V4 region of both microeukaryotes and eukaryotes (Stoeck et al. 2010).

Library preparation and sequencing

The composition of the eukaryome was assessed through the amplification and sequencing of the V4 region of the *18S rRNA* gene using the primers 18S-NonMet_Cr-F (5'-AAGTCTGGTGCCAGCASCC-3') and 18S-NonMet_Cr-R (5'-TTTAAGTTTCAGCCTTGCGAT-3'). These primers, adapted from Bower et al. (2004) and designed in Prioux et al. (2025), minimize the metazoan *18S rRNA* gene amplification and have previously been validated for assessing the composition of the eukaryome associated with *C. rubrum* (Prioux et al. 2025). Amplifications were performed in 25 µL reactions containing 5 µL of 5× Q5® buffer, 0.5 µL dNTPs, 1.25 µL of each primer (10 µM), 0.25 µL Q5® High-Fidelity DNA Polymerase, and 2 µL of template DNA (8 ng of DNA per sample). Cycling conditions were as follows: 98°C for 30 s; 35 cycles of 98°C for 10 s, 63°C for 30 s, 72°C for 30 s; and a final extension at 72°C for 2 min. Amplicon size was checked by agarose gel electrophoresis and purified with a GFX™ PCR and Gel Band Purification Kit (Illustra™). DNA concentrations were measured using a Qubit fluorometer, and quality was assessed on an Agilent Bioanalyzer. Libraries, following Illumina' standard "16S Metagenomic Sequencing Library Preparation" protocol (Illumina, 2013), were diluted to 4 nM and sequenced at STAB-VIDA (Portugal) on an Illumina MiSeq platform (2 × 300 bp). The fastq files containing the raw sequencing data have been deposited in the NCBI's Short Read Archive (SRA) under the BioProject accession number PRJNA1294578.

Bioinformatics data processing

Samples with fewer than 6,000 reads (maximum read count observed in negative controls) were excluded from downstream analysis. After this filtering step, a total of 46 out of 54 samples remained for downstream processing. Amplicon data were processed in the R environment (version 4.3.2) using the DADA2 pipeline (v1.16; Callahan et al. 2016) and the Cutadapt tool (v3.1; Martin 2011). Raw paired-end FASTQ files were filtered to remove reads containing ambiguous nucleotides (maxN=0). Primer sequences were identified using exact matching and removed with Cutadapt prior to further processing. Reads were truncated according to quality profiles (truncLen=c(298,200), maxEE=c(2,2), rm.phix=TRUE). Filtered reads were dereplicated, and sequencing error rates were learned separately for forward and reverse reads. Denoising was performed using the

DADA2 core algorithm with pool="pseudo" to increase sensitivity for rare variants. Due to the amplicon length (>600 bp), paired-end reads were concatenated instead of merged (mergePairs(..., justConcatenate=TRUE)) following data processing from Prioux et al. (2025). Chimeric ASVs were detected and removed using the consensus method (removeBimeraDenovo()). Taxonomic assignment was generated using assignTaxonomy() and the Protist Ribosomal Reference (PR2) database (v5.0.0; Guillou et al. 2012). Reads assigned to Metazoa and Embryophyceae were filtered out (subset_taxa()). The number of reads per sample passing through the different steps of the pipeline, the ASV table, the taxonomic annotation and metadata tables are available in Supp. File 1 as Table S1, S2, S3 and S4, respectively, and the sequences of the ASVs are available as Supp. File 2. The percentage of ASVs assigned by taxonomic rank as Figure S2.

Analysis of the *18S rRNA* gene sequencing data

Graphical and statistical analyses were conducted in the R environment, mainly using the R-package *phyloseq* (McMurdie and Holmes 2013). Alpha diversity metrics, including observed number of ASVs (*i.e.*, observed richness) and evenness (Shannon index, Simpson index and inverse Simpson index) were calculated using the R-package *vegan* (Oksanen et al. 2012). Rarefaction curves for each sample were generated using the rarecurve() function (*vegan*) to assess sequencing depth saturation and confirm that all 46 samples analyzed reached a plateau (Figure S1). Given the debate concerning the applicability of unrarefied versus rarefied data (McMurdie and Holmes 2014; Willis 2019), alpha diversity was also calculated on both rarefied and unrarefied ASV count tables (Supp. File 1 as Table S5). As no substantial differences in patterns or results were observed between the two approaches, the analyses presented in the manuscript were performed on the unrarefied ASV count table to maximize statistical power and retain the full dataset (McMurdie and Holmes 2014). Differences in alpha diversity among sites were assessed using non-parametric Kruskal-Wallis tests, followed by Wilcoxon rank-sum tests for post hoc pairwise comparisons, with multiple-testing correction applied. Pairwise Wilcoxon tests were performed with FDR correction (Supp. File 1 Table S5).

Compositional data analysis (CoDA) (Gloor et al. 2017; Quinn et al. 2018) was used to investigate the differences in the composition of the eukaryome (beta diversity and

dispersion) between sites. Zero counts in the ASV table were replaced using a Bayesian-multiplicative approach (cmultRepl() function from the R-package *zCompositions* (Palarea-Albaladejo and Martín-Fernández 2015), and ASV abundances were subsequently subjected to centered log-ratio (CLR) transformation (R-package *microbiome*; Lahti et al. 2017). An Aitchison distance matrix was then computed by calculating Euclidean distances between samples using the CLR-transformed data. Hierarchical clustering was performed using the pvclust() function from the R-package *pvclust* (Suzuki and Shimodaira 2006), using average linkage (UPGMA) and Euclidean distance. Statistical support for clustering was evaluated through multiscale bootstrap resampling with 1,000 iterations. Differences in the eukaryome composition among sites and sampling yars were further assessed using permutational multivariate analysis of variance (PERMANOVA), implemented with the adonis() function from the R-package *vegan* (Oksanen et al. 2012). Because the factors "Site" and "Year" were confounding in our sampling design, we assessed their effect in separate models, thereby enabling a comparison of the proportion of variance each factor explains. Results including p-values are reported in Supp. File 1 Table S6. Post hoc pairwise comparisons were conducted using the permanova_pairwise() function from the package *ecole* (Smith 2021), with p-values adjusted for false discovery rate correction (Supp. File 1 Table S6). Differential abundance analyses were conducted to identify differentially abundant ASVs between sites, using the R-package *ANCOM-BC* (Lin and Peddada 2020) and the ancombc2() function with the parameters prv_cut=0.1, alpha=0.05, p_adj_method="BH" and pairwise=TRUE (version 02–2023; Supp. File 1 Table S7). Core members of the eukaryome (ASV and family level) across the entire dataset were identified using the core_members() function (arguments: detection=0.001, prevalence=0.95, include.lowest=TRUE) of the R-package *microbiome* (Lahti et al. 2017; Supp. File 1 Table S8).

Results and Discussion

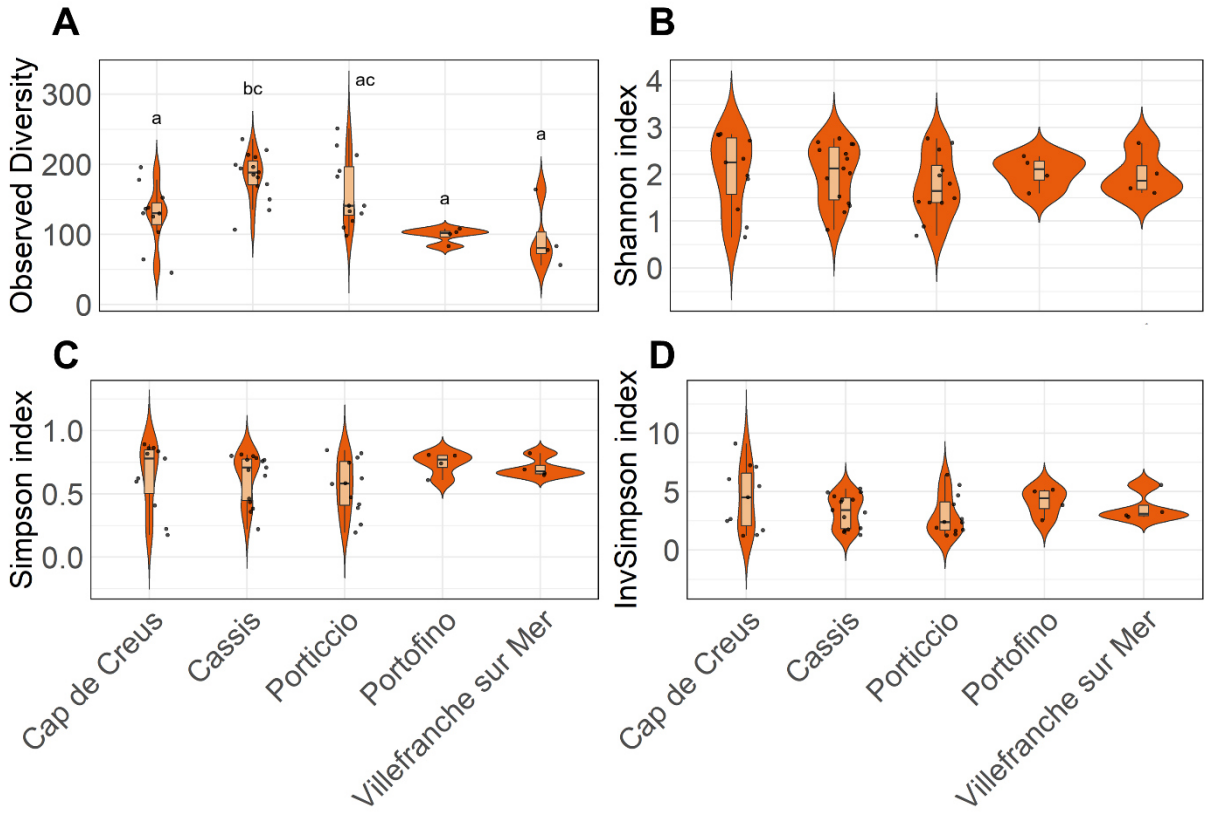

Figure 2: Alpha diversity metrics across sampling sites. Observed richness (ASV level) **(A)**, Shannon index **(B)**, Simpson index **(C)** and Inverse Simpson index **(D)**. Graphs are showing value distributions, their median and interquartile range per sampling site. Groups assigned with same letters are not statistically different.

After quality filtering, 46 samples were retained for downstream analysis. This process reduced the number of replicates for some sites, resulting in the following distribution: *Cap de Creus* (n = 11), *Cassis* (n = 15), *Porticcio* (n = 12), *Villefranche-sur-Mer* (n = 4), and *Portofino* (n = 4). Nevertheless, the remaining dataset comprised 2,404 ASVs and a total of 3,417,757 reads, with per-sample read counts ranging from 46,868 to 183,202, providing a comprehensive overview of eukaryome diversity across the five study sites (Supp. File 1, Table S1 and S2). Rarefaction analyses confirmed sequencing depth saturation for all samples, with curves reaching a plateau (Supplementary Figure S1), indicating that sequencing effort was sufficient to capture the majority of ASV diversity.

Observed number of ASVs varied significantly between sites (Kruskal-Wallis test; Statistic = 18.72, DF = 4, p = 0.00089; Supp. File 1 Table S5 and Figure 2A). Pairwise comparisons using Wilcoxon rank-sum tests with FDR correction showed that *Cassis* had the highest observed number of ASVs (mean = 183.7 ASVs; Supp. File 1 Table S5 and Figure 2A), which was significantly different from all other sites except *Porticcio*. The high level of diversity observed in *Cassis* is likely attributable to local factors, with geographical and/or temporal variables potentially driving this increased richness. Alpha diversity metrics calculated on rarefied datasets yielded comparable results (Supp. File 1 Table S5), supporting the robustness of these patterns and justifying the use of unrarefied data to maximize statistical power and retain the full dataset (McMurdie and Holmes 2014). In contrast, evenness, as measured by the Shannon index, did not differ significantly between sites (Supp. File 1 Table S5 and Figure 2B), suggesting that all coral eukaryomes are composed of a few dominant microeukaryotes alongside many low-abundance taxa. Similarly, no significant differences were observed for the Simpson and inverse Simpson indices (Supp. File 1 Table S5 and Figure 2CD), indicating that the overall community structure was relatively consistent despite variations in species richness. Altogether, these analyses show that the diversity of the *C. rubrum* eukaryome varies between sites, with site-specific differences primarily driven by observed richness.

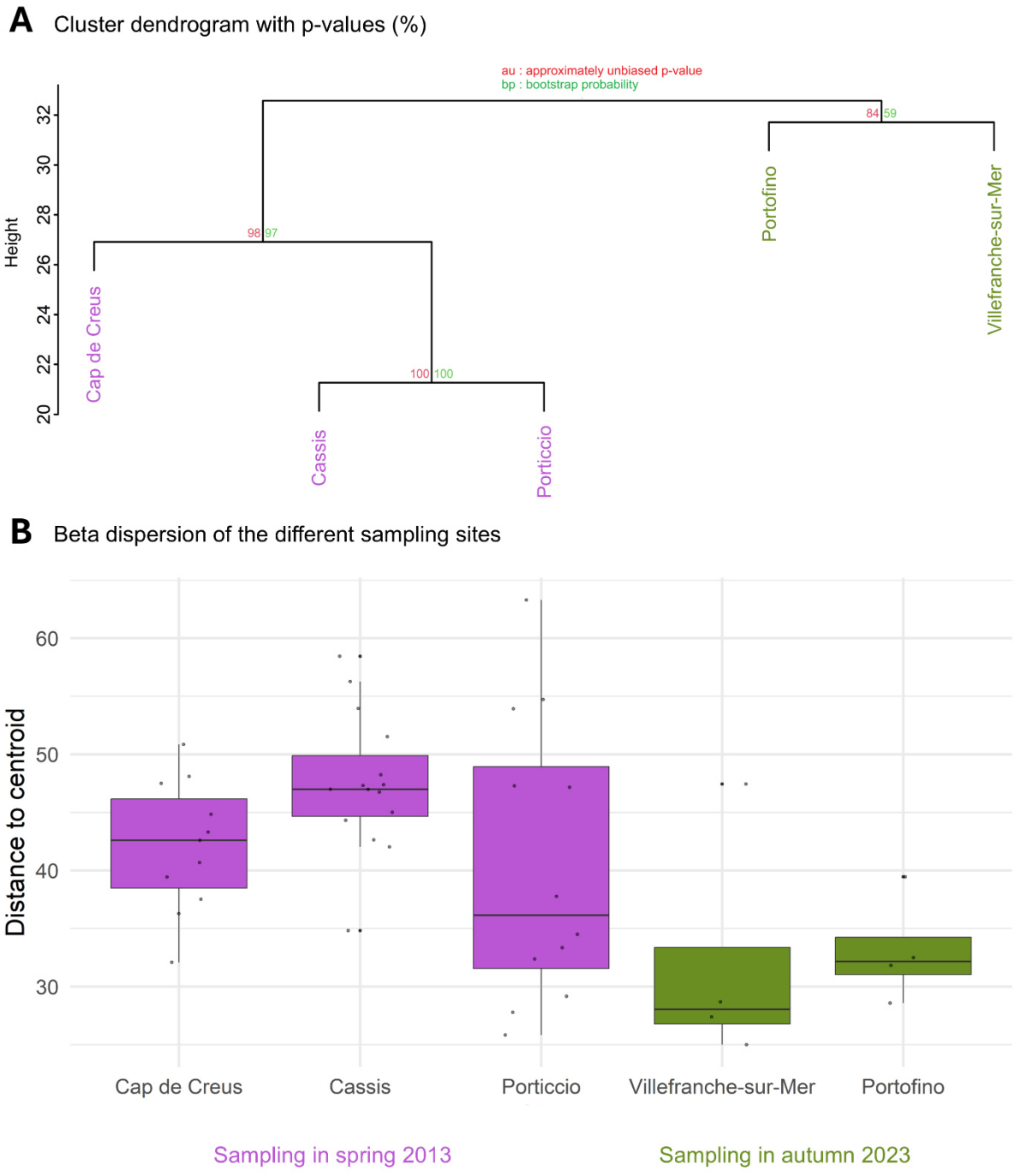

Figure 3: Structure of the red coral eukaryome depending on the sampling site and year. Hierarchical cluster analysis on the Aitchison distance matrix based on the eukaryome structure (CLR-transformed ASV data) **(A) and** beta dispersion (within-site variability) of the samples based on the community composition at the ASV level. Boxplots display value medians and interquartile ranges for each site **(B)**.

The hierarchical cluster analysis based on the eukaryome composition revealed two clusters of sites, with western sites sampled in spring 2013 (*Cap de Creus*, *Cassis*, *Porticcio*) clustering separately from eastern sites sampled in autumn 2023 (*Villefranche-sur-Mer*, *Portofino*) (Figure 3A). Moreover, the eukaryome structure was significantly different between sites (PERMANOVA; $R^2 = 0.14$, $F = 1.7$, $p = 1 \times 10^{-3}$; Supp. File 1 Table S6 and Figure 3A) and between sampling years (PERMANOVA; $R^2 = 0.04$, $F = 1.9$, $p = 1 \times 10^{-3}$; Supp. File 1 Table S6 and Figure 3A). Comparison of the resulting R^2 values revealed that the model with "Site" as factor explains 14% of the total variance in community composition, while "Year" accounts for 4%. This result suggests that variation in the structure of the microeukaryotic community between the samples is mainly explained by geography. Nevertheless, the percentage of variance explained remains modest, indicating that a substantial portion of community variation is likely attributable to unmeasured environmental factors. Furthermore, intra-site variability was significantly higher in samples from spring 2013 than autumn 2023 (Betadispersion; ANOVA; $p = 0.005$; Supp. File 1 Table S6 and Figure S2) and more precisely higher in *Cassis* than in *Villefranche-sur-Mer* and *Portofino* (Tukey test; $p = 0.017$ and $p = 0.030$; Supp. File 1 Table S6 and Figure 3B). Although physicochemical parameters were not measured, regional environmental differences, together with the temporal factor, likely underlie the observed structuring of red coral eukaryome. Previous studies indicate that hydrodynamics, nutrient availability, and local thermal regimes can modulate coral-associated microbiota (Sweet and Séré 2016; Martinez 1980; Mandal 2024; Maire et al. 2022), which could potentially explain these patterns.

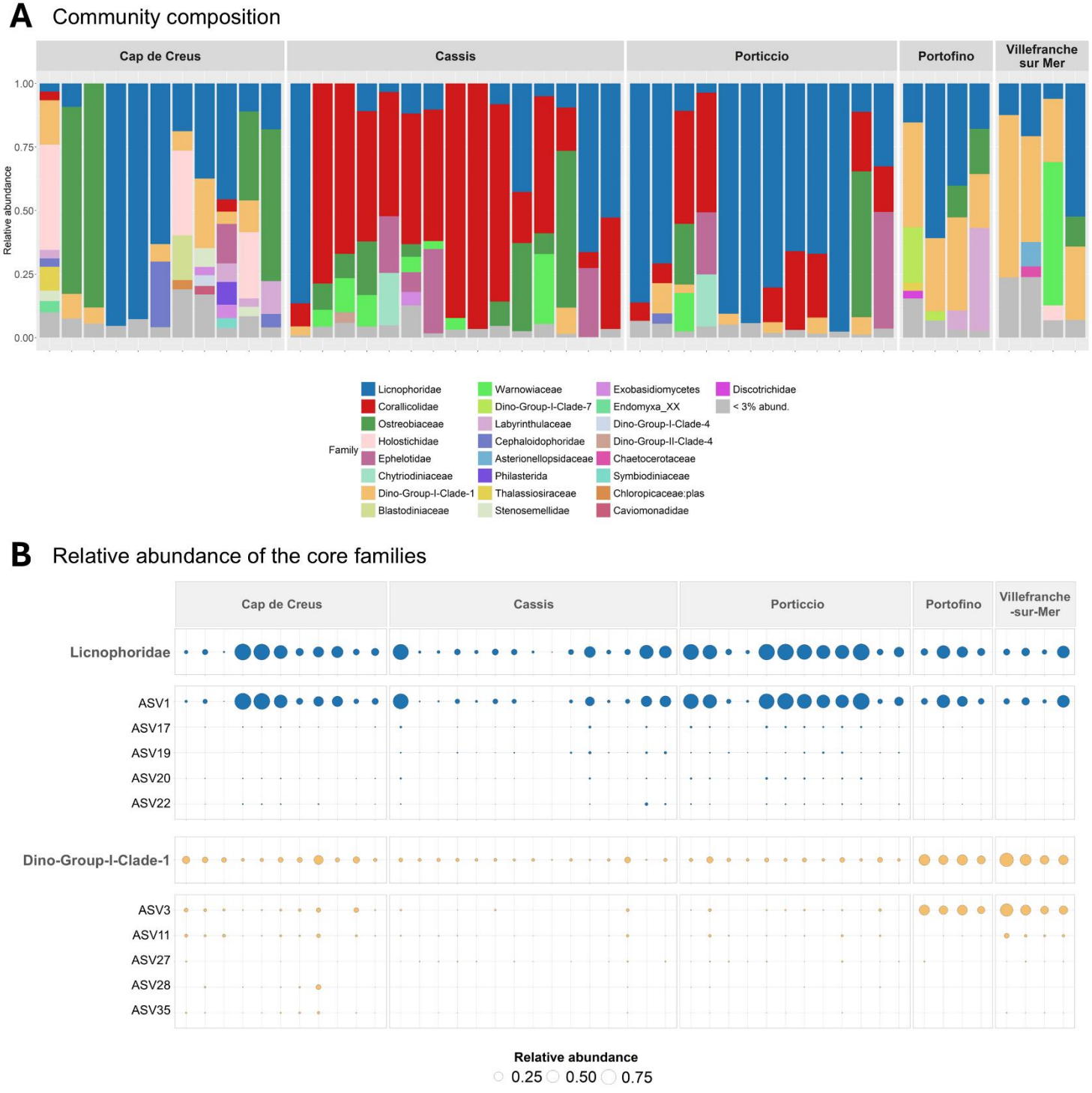

Figure 4: Composition of the eukaryome of *C. rubrum* across the sampling sites. Composition of the whole microeukaryotic community of the red coral across the samples (Family level). In each sample, families with a relative abundance lower than 3% were grouped **(A)**. Relative abundance of core families and their top five ASVs across all samples **(B)**.

Analysis of the core eukaryome revealed the consistent presence of one ASV, ASV1-Licnophoridae, representing a substantial proportion of the eukaryome at all sites (mean relative abundances per site: 59% in *Porticcio*, 51% in *Cap de Creus*, 36% in *Portofino*, 24% in *Villefranche-sur-Mer*, and 17% in *Cassis*; Supp. File 1 Table S7 and Figure 4AB). Despite high fluctuations in abundance, the constant association of these ciliates with *C. rubrum* suggests an important ecological role within the red coral holobiont. Licnophoridae have been previously reported in other corals, including the Mediterranean octocoral *Paramuricea clavata* (Bonacolta et al. 2024) and the tropical hexacoral *Pocillopora damicornis* (Clerissi et al. 2018), although their functional role remains uncharacterized. Species of Licnophoridae are known predators of other ciliates (Sweet and Séré 2016), potentially contributing to their ecological role within coral holobionts. Members of the Dino-Group I Clade 1 family were also detected in all red coral samples, generally at lower abundances, with relatively higher levels in *Portofino* and *Villefranche-sur-Mer* (Supp. File 1 Table S7; Figure 4AB). This family has also been identified in other corals, including *P. damicornis* and *P. clavata* (Clerissi et al., 2018; Bonacolta et al., 2024). The latter study showed that heat-resistant gorgonians harbored eukaryomes enriched with Dino-Group I Clade 1, suggesting a potential role in stress tolerance, although this remains to be investigated.

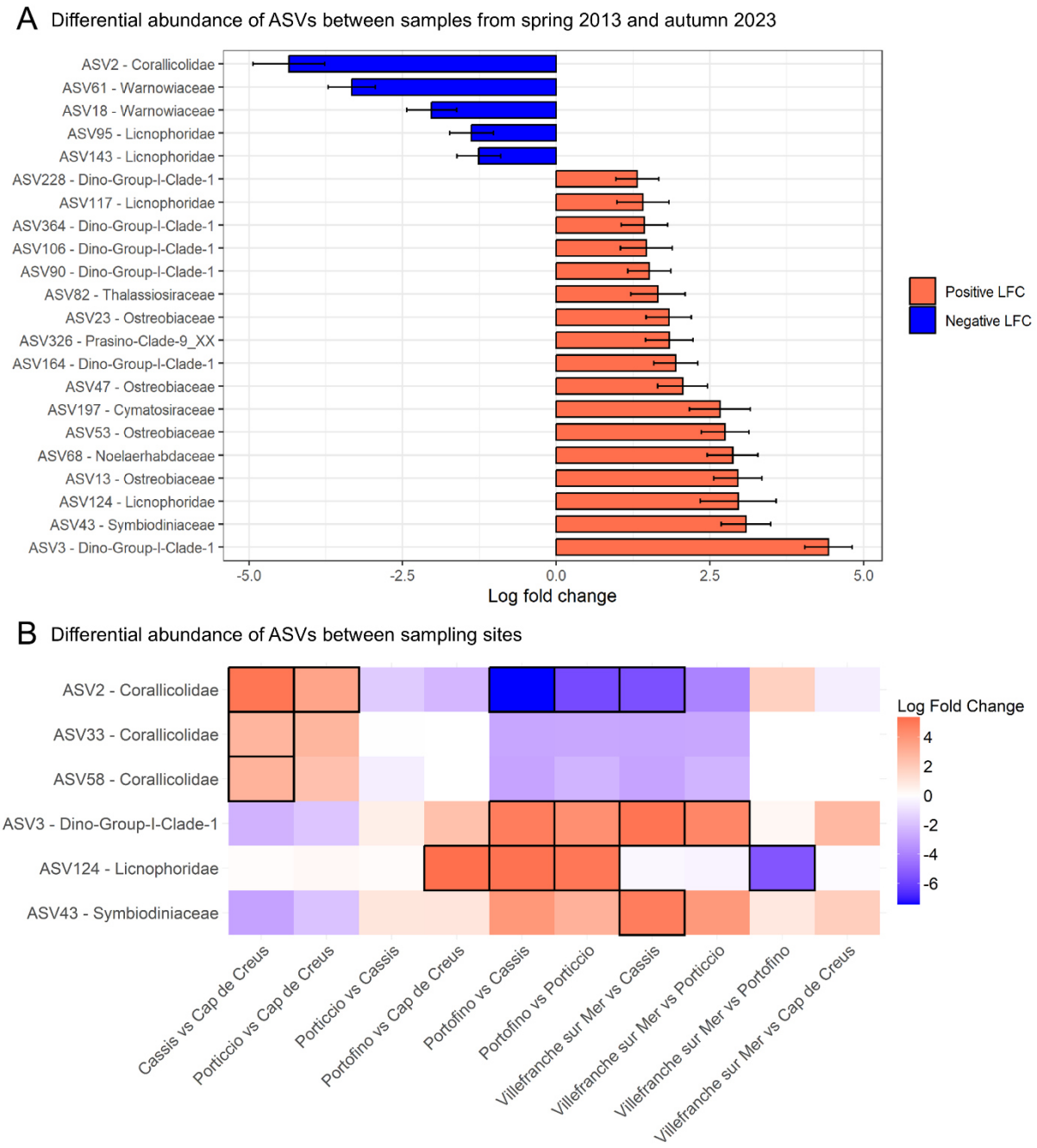

Figure 5: ASVs differentially abundant (ANCOM-BC results) between the sampling years (A) and sites (B). Differences in relative abundance are calculated as a log2 fold change (base 2). In **(A)**, positive values indicate taxa significantly more abundant in samples from autumn 2023 than spring 2013 and negative values taxa less abundant in these samples. In **(B)**, statistically significant values are framed in black.

Dino-Group I Clade 1, though ubiquitous, were significantly more abundant in samples from autumn 2023 (*Villefranche-sur-Mer* and *Portofino*), especially ASV3-Dino Group-I Clade-1 (mean of 37% and 33%, respectively; ANCOM-BC; Supp. File 1 Table S8 and S9; Figure 4A and 5AB). These relative differences may contribute to the observed clustering patterns, which are likely shaped by environmental fluctuations associated with site localization (western vs. eastern) and/or temporal factors (seasonal variation between spring and autumn, as well as differences between 2013 and 2023).

Additionally, some taxa were differentially abundant depending on the sampling site, contributing to the site-specific structure of the red coral eucaryome. For example, samples collected in *Cap de Creus* showed high relative abundances of ASV5-Ostreobiaceae (mean relative abundance of 15%; ANCOM-BC; Figure 4A and 5AB), a taxon that was already recovered in similar abundance in laboratory-maintained red coral colonies (Prioux et al. 2025b). In contrast, samples collected in *Cassis* and *Porticcio* showed high relative abundances of ASV2-Corallicolidae (ANCOM-BC; Supp. File 1 Table S7; Figure 3), which accounted for a mean of 55% and 18% of the community, respectively (Figure 4A and 5AB). Apicomplexan alveolates from the family Corallicolidae are widely distributed and were found in high prevalence across all major groups of corals (Kwong et al. 2019; 2021; Bonacolta et al. 2023; 2024). From a total of 43 samples representing 38 coral species, a large genomic survey recovered the apicomplexan *Type-N 18S rRNA* and *ARL-V 16S rRNA* genes in 62% and 83% of the coral samples, respectively (Kwong et al. 2019), highlighting is potential important role in coral holobionts. The sequence of ASV2 was identical (100% sequence identity) to the sequence of a Corallicolidae ASV associated with heat-stressed *C. rubrum* colonies (Prioux et al. 2025), and closely related to ASV sequences found in *P. clavata* colonies (99.21% sequence identity ; Bonacolta et al. 2024). This latter study hypothesized that this taxon may exhibit context-dependent functional roles within coral holobionts, potentially transitioning from a symbiotic or commensal lifestyle to an opportunistic/parasitic one in response to the host physiological state or environmental stressors.

Overall, our results showed that the composition of the eukaryome varied significantly depending on environmental parameters, including geographical and

temporal parameters. This contrasts with the bacterial community associated with the red coral, which has been shown to be relatively stable across geographical and temporal scales (van de Water et al. 2016a). Furthermore, our findings indicate that the eukaryome composition was relatively variable between the samples of the same sites. This high inter and intra-site variability suggests that local environmental conditions likely play a significant role in shaping the composition of the red coral eukaryome. The relative abundance of certain microeukaryotes might fluctuate in response to environmental factors such as temperature (Sweet and Séré 2016; Martinez 1980; Mandal 2024; Maire et al. 2022). Prioux et al. (2025b) also showed that the eukaryome of laboratory-maintained red coral colonies responded more rapidly to thermal stress than the bacterial microbiome. This heightened sensitivity suggests either a greater responsiveness to environmental fluctuations with a potential greater flexibility to adapt to local conditions or a more tenuous, less obligatory relationship between microeukaryotes and the coral host, in contrast to the more stable bacterial symbionts. In this study, the absence of environmental context prevented us from explaining this variability which could be attributed to factors such as temperature, site-specific resource availability, or interactions with surrounding microbial communities (Brannock et al. 2016; Pernice et al. 2013; W. Zhang et al. 2018). Future research exploring changes in the eukaryome composition over different seasons and under controlled environmental conditions will be critical to better understand how the eukaryome associated with *C. rubrum* is structured.

Conclusion

Our findings indicate that the composition of the eukaryome of the red coral *C. rubrum* is highly influenced by environmental conditions. Variations in species richness, community structure, and dominant microeukaryotes across geography and time highlight the high sensitivity of the eukaryome to the environmental context. While site-specific microeukaryotes may not be essential to the coral's core functioning, they could offer context-dependent benefits, such as assimilation of local ressources or protection

against local stressors. In contrast, certain families, such as Licnophoridae and Dino-Group I Clade 1, were consistently detected across all sites, suggesting that they may represent key symbiotic partners within the red coral holobiont. Future research should aim to elucidate the functional roles of these potentially critical taxa and investigate their responses to environmental variation, to enhance our understanding of holobiont stability and coral health in the face of global change. These results will be critical not only for understanding red coral resilience, but also for informing conservation strategies under accelerating climate stressors.

Chapter 3

Characterization of the cultivable fungal community of *Corallium rubrum*



©Personal illustration

Chapter 3: Characterization of the cultivable fungal community of *Corallium rubrum*

I. Overview of the chapter

Fungi are often overlooked while they are likely a critical component of the coral holobiont by contributing to nutrient cycling, defense against pathogens, and overall coral health (Golubic et al. 2005; Raghukumar 2017; Gladfelter et al. 2019; Masigol et al. 2019; Burgaud et al. 2022). Despite their importance, fungal communities associated with corals, particularly Mediterranean octocorals such as *Corallium rubrum*, remain poorly characterized (Bonthond et al. 2018; Rabbani et al. 2021). This study aimed to explore the fungal diversity associated with *C. rubrum* using culture-based approaches, with a focus on compartment-specific communities in soft tissue and skeleton.

Due to the limitations of the shotgun sequencing of common genetic markers (*18S rDNA* and *ITS* regions) in obtaining fungal sequences from corals (Marcelino and Verbruggen 2016; Góes-Neto et al. 2020), culture-based methods were employed in this chapter and compared with the metabarcoding approach to obtain a more comprehensive picture of the fungal community. Samples of soft tissue and skeleton of *C. rubrum* were analyzed separately to assess compartment-specific fungal assemblages and offer insights on the spatial structuring of coral-associated fungi.

Metabarcoding significantly underestimated fungal diversity compared to the culture-based approach. This result highlights the need for improved molecular protocols, such as optimized primer design, to better capture the coral mycobiome. Culture-based analyses revealed a rich fungal community dominated by Ascomycota genera such as *Penicillium*, *Cladosporium*, and *Aspergillus*, with 61% of the isolated species reported for the first time in association with corals. Different assemblages of fungi have been observed in the tissue versus skeleton, which are probably influenced by the local environment, such as light or the type and availability of nutrients. In particular, some isolated fungi, such as *Aspergillus sydowii*, are known to be potential pathogens, especially at elevated temperatures (>25°C), which can occur during Mediterranean

marine heatwaves, raising concerns about their impact on coral health (Alker et al. 2001; Kim and Rypien 2015; Soler-Hurtado et al. 2016). In addition, certain isolated fungi are known to produce bioactive compounds that exhibit a range of properties such as antibacterial activities.

The results of this chapter demonstrate that it is necessary to combine culture-based and molecular methods to gain a comprehensive understanding of coral-associated fungi. It shows that *C. rubrum* harbors a diverse and structured fungal community, with compartment-specific assemblages that may contribute to coral health and adaptation. The presence of potentially pathogenic fungi emphasizes the importance of monitoring fungal dynamics, especially during marine heatwaves and other climate-induced stressors. Furthermore, the discovery of fungal species that might produce bioactive compounds opens avenues for biotechnological applications and ecological studies.

II. Publication

Hidden fungal diversity of the precious Mediterranean red coral *Corallium rubrum*: Culture-based discoveries and challenges of metabarcoding

Environmental Microbiology Reports | Submitted October 2025

Camille Prioux[1,2,3], Marina Carrasco-Acosta[4,5], Valeria Prigione[5], Francesco Venice[5], Romie Tignat-Perrier[2,3], Denis Allemand[3], Christine Ferrier-Pages[3] and Giovanna Cristina Varese[5]

[1]Sorbonne Université, Collège Doctoral, Paris, France

[2]Unité de Recherche sur la Biologie des Coraux Précieux CSM - CHANEL, Centre Scientifique de Monaco, 8 Quai Antoine 1er, MC 98000, Monaco, Principality of Monaco

[3]Centre Scientifique de Monaco, 8 Quai Antoine 1er, MC 98000, Principality of Monaco

[4]Department of Biology, Instituto Universitario de Investigación en Estudios Ambientales y Recursos Naturales i-UNAT, University of Las Palmas de Gran Canaria, 35017 Las Palmas, Spain

[5]Mycotheca Universitatis Taurinensis, Department of Life Sciences and Systems Biology, University of Torino, Viale Mattioli 25, 10125 Turin, Italy

Abstract

Corals maintain complex symbiotic relationships with diverse microorganisms, including fungi, which are often overlooked but represent a critical component of the coral holobiont. This study explores the fungal diversity associated with the tissue and skeleton of the red coral *Corallium rubrum*, a key species in Mediterranean marine animal forests. Using complementary culture-based and metabarcoding approaches, we revealed that culture methods currently capture a broader spectrum of fungal diversity, dominated by Ascomycota such as *Penicillium*, *Cladosporium*, and *Aspergillus*. The discovery of numerous taxa with known bioactive properties underscores the potential ecological and biotechnological relevance of coral-associated fungi. At the same time, the presence of species such as *Aspergillus sydowii*, which is considered pathogenic under elevated temperatures, raises concerns about coral vulnerability during increasingly frequent Mediterranean marine heatwaves. These taxa should be further investigated to evaluate their pathogenic potential. Overall, our results expand current knowledge of coral–fungal associations, providing a foundation for future work on their ecological significance, role in coral resilience, and potential applications in biotechnology.

Introduction

Various microorganisms, including bacteria, archaea, viruses, protists and fungi, are of fundamental importance to marine ecosystems. They drive key processes such as nutrient cycling (Joye et al. 2022), and organic matter decomposition (Moran 2015; Vila-Costa et al. 2020; Underwood et al. 2022). In addition, they can also establish a symbiotic relationship with different hosts including corals, and together form an holobiont (Apprill 2017; Dittami et al. 2021; González-Pech et al. 2024). Among these microorganisms, marine fungi are still largely unexplored, despite their ecological importance, especially

regarding their roles in organic matter decomposition, host parasitism, and mutualism (Golubic et al. 2005; Raghukumar 2017; Gladfelter et al. 2019; Masigol et al. 2019; Burgaud et al. 2022). This knowledge gap is even more pronounced for fungi associated with corals (Roik et al. 2022), whereas bacteria communities have been extensively studied (van de Water, Allemand, et al. 2018; Voolstra et al. 2024a). Fungal diversity in coral holobionts includes both epibiotic and endolithic fungi (Wegley et al. 2007; Amend et al. 2012; Yarden 2014): the former are mainly found in coral tissue while the latter are able to colonize calcium carbonate skeletons (Kohlmeyer 1969; Kendrick et al. 1982; Golubic et al. 2005).

Coral-associated fungi fulfill various functions that go beyond pathogenicity (Raghukumar et al. 2012; Roik et al. 2022). While *Aspergillus sydowii* is a well-documented fungal pathogen associated with aspergillosis of Caribbean Sea fans (Alker et al. 2001; Kim and Rypien 2015; Soler-Hurtado et al. 2016), many fungi are opportunists rather than direct causative agents of disease (Roik et al. 2022). It has been hypothesized that fungi facilitate nutrient cycling and remineralization, that they produce antimicrobial and chemical compounds which promote coral health and regulate microbial balance, in addition to establishing symbiotic or probiotic relationships with corals, thereby enhancing their resilience to environmental stress (Raghukumar and Ravindran 2012; Roik et al. 2022). Some fungi can act as competitors of endolithic boring algae, potentially mitigating bioerosion under environmental stress (Tribollet et al. 2001; Golubic et al. 2005). Others have been shown to be involved in calcium carbonate biomineralization, through interactions with the organic matrix in different coral species (Le Campion-Alsumard et al. 1995; Domart-Coulon et al. 2004). Furthermore, coral-associated marine fungi have a high biotechnological potential as they produce a variety of bioactive molecules with antibacterial, antifungal, antiviral and anticancer properties (Chen et al. 2022a).

Despite these roles, there are significant gaps in our understanding of the diversity and ecological functions of coral-associated fungi. The study of fungal diversity in corals indeed poses a major challenge when using molecular methods such as metabarcoding, particularly due to host DNA contamination. Some studies report that commonly used genetic markers, like *18S rDNA* and *ITS* regions, result in low recovery of fungal sequences

in marine environments (Marcelino and Verbruggen 2016; Góes-Neto et al. 2020; Prioux, Ferrier-Pagès, Del Campo, et al. 2025), emphasizing the need for complementary approaches, such as culture-based methods. In addition, fungal communities within corals are often studied without distinguishing between specific compartments (tissue, mucus, and skeleton) despite the evidence that these microhabitats may support functionally distinct fungal assemblages (Bonthond et al. 2018; Rabbani et al. 2021). This compartmentalization could have important ecological implications that remain largely unexplored. Finally, most studies have focused on the fungal diversity of tropical corals (Roik et al. 2022), while the mycobiome of deep and temperate corals have been poorly studied (Galkiewicz et al. 2012; Marchese et al. 2021) despite their importance as ecosystem engineers, particularly in the Mediterranean Sea where they built MAFs (Rossi et al. 2017). The majority of these corals are octocoral gorgonians increasingly threatened by climate change and marine heat waves (Gómez-Gras et al. 2021; Garrabou et al. 2022; Estaque et al. 2023). One of them, the red coral *Corallium rubrum* not only has an ecological function in the MAFs, but also holds significant cultural and economic value, having been harvested for centuries for use in jewelry (Santangelo et al. 2001; Tsounis et al. 2010).

With this work, we aim to expand our knowledge of the fungal community associated with healthy-looking *C. rubrum* colonies and, more generally, our understanding of coral-fungi interactions in temperate zones by combining culture-dependent and culture-independent techniques. In addition to a comparison of the two applied methodologies, this study provides an essential baseline for monitoring changes in fungal communities due to climate change and for guiding future conservation efforts.

Material and Methods

Samples collection

Six multi-branched colonies of *Corallium rubrum* (7-8 cm in length) were collected at a depth of 40 meters in Villefranche-sur-Mer, France, under the authorization of the Direction Inter-Régionale de la Mer Méditerranée. Following collection, samples were

transported in seawater to the aquarium facilities of the Centre Scientifique de Monaco (10 km from Villefranche-sur-Mer), where they were maintained in two 20 L aquaria supplied with a continuous flow of Mediterranean seawater pumped at 40-50 m depth in front of the laboratory, filtered through a 5 µm charcoal filter and treated with UV light. Nubbins were then transported in aquarium seawater and processed at the laboratory facilities of the Mycotheca Universitatis Taurinensis (see section below). In addition, 2 L of seawater were also filtered from the aquaria through a 0.2 µm Nuclepore Track-Etch Membrane filter (Whatman, diameter of 47 mm) and then stored at -20°C for subsequent metabarcoding analysis.

Fungal isolation

Six coral nubbins were subjected to serial sonication (three times for 30 seconds each) in sterile seawater to remove debris and microorganisms not strictly associated with the red coral. For each nubbin, the soft tissue was separated from the skeleton using sterile scalpels and tweezers, and then homogenized in 5 mL of sterile seawater using a Sterilmixer II homogenizer (PBI International, Milan, Italy). For each nubbin, 1 mL of the homogenized mixture was stored at -20°C for subsequent metabarcoding analysis, while the remaining volume was diluted 1:50 (w/v) in sterile seawater. The remaining skeletons were sonicated five more times for 60 seconds to ensure complete removal of residual soft tissue. Each skeleton was crushed through a sterile mortar with 5 mL of sterile seawater, and 1 mL of the mixture obtained was stored at -20°C for metabarcoding analysis, with the rest was diluted 1:10 (w/v) in sterile seawater. The soft tissue and skeleton mixtures were used for culturomics, spreading 1 mL onto 15 cm diameter Petri dishes. Four different growth media were used to maximize fungal isolation: Corn Meal Agar Sea Water (CMA-SW, 2 g corn meal, 15 g agar in 1 L of seawater); Gelatin Agar Sea Water (GA-SW, 20 g gelatin, 15 g agar in 1 L of seawater) to mimic the composition of the organic material rich in collagen; Pimaricin Corn Meal Agar Sea Water (P-CMA-SW, consisting of CMA-SW supplemented with 5 mg/L pimaricin, 250 mg/L ampicillin, and 10 mg/L rifampicin), selective for Stramenopiles and other fungus-like organisms; Coral Agar Sea Water (CA-SW, containing homogenized 18 g coral soft tissue and skeleton, and 20 g agar in 1 L of seawater) a medium designed to mimic coral conditions. To prevent bacterial

growth, all media were supplemented with an antibiotic mix (Gentamicin sulfate, 40 mg/L; Piperacillin and Tazobactam, 11 mg/L).

Five replicates were prepared for each medium and tissue type (soft tissue and skeleton). Plates were incubated in the dark at 15°C for 6 weeks and at 25°C for an additional 6 weeks. During the incubation period, plates were constantly monitored for fungal growth. Fungal isolates that developed were transferred to axenic cultures and taxonomically identified.

Fungal identification

Fungi were identified using a polyphasic approach combining morpho-physiological observation with molecular analyses. DNA was extracted using the DNeasy PowerBiofilm kit (QIAGEN, Hilden, Germany), with modifications to enhance efficiency as described by Prioux and collaborators (2023). Specific primers were used to amplify DNA markers for each fungal genus identified during the morpho-physiological observations. When the initial amplification did not allow species-level identification on blastn (NCBI; https://blast.ncbi.nlm.nih.gov), a second round of amplification was performed with an alternative primer set, as detailed in Supplementary File 1. All sequences are available in Supplemenray file 1 and fungal strains are preserved at the Mycotheca Universitatis Taurinensis (MUT, http://www.mut.unito.it), University of Turin, Italy.

Statistical analyses

Statistical analyses were conducted in the R environment (version 4.2.1). Differences in abundance (CFU/g dry weight) were assessed using the Kruskal-Wallis test, considering tissue type, isolation temperature, and media as independent factors. To evaluate differences in mycobiome composition across culture media, tissue types, and isolation temperatures, we employed a permutational multivariate analysis of variance (PERMANOVA), with significance determined using a pseudo-F statistic and a p-value threshold of <0.05.

Comparison with Metabarcoding Approach

DNA was extracted from each coral sample (both soft tissue or skeleton) and seawater filter using the DNeasy PowerBiofilm kit (QIAGEN, Hilden, Germany), with

modifications to enhance efficiency as described in Prioux and collaborators (2023). To assess the specificity and biases of various primer sets in characterizing the fungal communities associated with red coral, multiple primers targeting different genomic regions were employed. These included the widely used *ITS2* region with a revised primer set from Taylor et al. (2016), universal *18S rRNA* gene primers targeting the V4 region (Stoeck et al. 2010), and a fungi-specific *18S rRNA* primer toolkit from Banos et al. (2018), which incorporates blocking primers to limit the amplification of non-fungal microeukaryotes (e.g., Stramenopiles, Alveolata, Rhizaria, and Telonema). Additionally, customized primers targeting the V4 region of the *18S rRNA* gene were used to minimize metazoan amplification; these were adapted from the UNonMet-PCR primers originally described by Bower et al. (2004) and later validated for Illumina amplicon sequencing by del Campo et al. (2019) and Prioux et al. (2025). PCR reactions were performed on coral and seawater samples, following the protocol outlined by Prioux and collaborators (2025). DNA concentration of the amplicons was verified using a Qubit fluorometer before being sent to STAB VIDA (Portugal) for paired-end sequencing (2 × 300 bp, 600 cycles) on an Illumina MiSeq platform using V3 chemistry. Raw sequencing data are available in the NCBI Short Read Archive (SRA) under BioProject accession number PRJNA1329203. The gene amplicon data were processed using the DADA2 pipeline (version 1.16; https://benjjneb.github.io/dada2/index.html). The R pipeline used was identical to the one detailed in Prioux et al. (2025) except for the *ITS2* primer sets that followed DADA2 ITS Pipeline Workflow (https://benjjneb.github.io/dada2/ITS_workflow.html). Taxonomic classification was performed using the assignTaxonomy() function in DADA2, with the PR2 reference database v5.0.0 for the primer sets targeting a region of the *18S rRNA* gene (Guillou et al. 2012) and the UNITE reference database v10.0 for the primer pair targeting the ITS region (Abarenkov et al. 2025). The proportion of sequences assigned to non-Metazoan and fungal ASVs relative to all sequences was calculated. Furthermore, *in-silico* PCRs were done against the PR2 microeukaryotic database (https://app.pr2-primers.org/pr2-primers/; v. 2.0.0) using the different primer sets targeting the *18S rRNA* gene to test their specificity in targeting the different fungal taxonomic groups. Details on primer pairs, Illumina MiSeq sequencing and sequences passing each step of the pipeline, *in-silico* PCRs and taxonomy annotations for the different primer sets are available as Supplementary File 2.

Results and discussion

Coral-associated fungi play pivotal roles within the coral holobiont, not only by supplying essential compounds and offering protection against pathogens, but also, in some cases, acting as pathogens themselves. However, fungal communities remain largely understudied compared to other coral-associated microorganisms (Roik et al. 2022). As corals face increasing anthropogenic stress, understanding the diversity and ecological functions of these fungi is crucial for advancing coral health research and guiding effective conservation efforts. Moreover, fungi isolated from corals are emerging as valuable sources of bioactive natural products, producing a diverse array of compounds with significant promise for drug discovery and biomedical applications (Said et al. 2018; Hou et al. 2019; Ma and Qi 2019; Chen et al. 2022a).

Overview of the mycobiome of *C. rubrum*

The polyphasic approach allowed the identification of almost all of the isolated fungi at species level, with the exception of a single strain (*Pleosporales* sp.; Supplementary File 1). The fungal communities associated with the soft tissue and skeleton of *C. rubrum* were predominantly composed of Ascomycota (87.2%), while Basidiomycota accounted for 12.8% (five taxa), a distribution pattern commonly observed in marine environments compared to terrestrial environments where Basidiomycota are generally more represented (Jones et al. 2015; Bärlocher et al. 2016). Ascomycota are known to dominate the fungal communities associated with corals, often exceeding 85% in relative abundance across various studies, with Sordariomycetes being the most frequently reported class (Roik et al. 2022). It can be hypothesized that marine Ascomycota may assume ecological functions in marine habitats that are often associated with Basidiomycota in terrestrial ecosystems, including the breakdown of lignocellulosic compounds (Panno et al. 2013; Raghukumar 2017; Balabanova et al. 2018) and hydrocarbons (Garzoli et al. 2015; Bovio et al. 2017). On the other hand, it cannot be excluded that the low presence of Basidiomycota observed derives from the intrinsic biases in the isolation techniques commonly applied in studies on marine fungi.

Among the identified genera, *Penicillium* (10 species), *Cladosporium* (7 species), and *Aspergillus* (5 species) were the most diverse (Figure 1). Despite the frequent associations of these genera with corals, the mycobiome of C. *rubrum* remains largely unexplored, as the majority of *Cladosporium* and *Penicillium* species identified had never been previously found in coral hosts. To our knowledge, among the species observed in *C. rubrum*, 60% of *Penicillium* species (*P. novae-zeelandiae*, *P. fundyense*, *P. charlesii*, *P. biforme*, *P. sanguifluum* and *P. brevicompactum*) and 43% of *Cladosporium* (*C. perangustum*, *C. asperulatum*, and *C. psychrotolerans*) were never reported in other coral species (Supplementary File 3). Some members of these genera, whose role in coral ecology is still obscure, are known to be producers of a wide range of bioactive metabolites, making them important targets for natural product discovery (Chen et al. 2022b). For instance, species like *C. halotolerans*, *C. cladosporioides*, and *A. versicolor*, isolated from corals, produce bioactive molecules such as polyketides, compounds that exhibit cytotoxic effects against certain types of cancer cells (Zhuang et al. 2011a; 2011b; Espinoza et al. 2021; Wang et al. 2021). Besides, a strain of *Aspergillus unguis* isolated from the tropical coral *Pocillopora damicornis* and recovered in the rec coral as well, was shown to produce anti-osteoclastogenic molecules (Zhang et al. 2022).

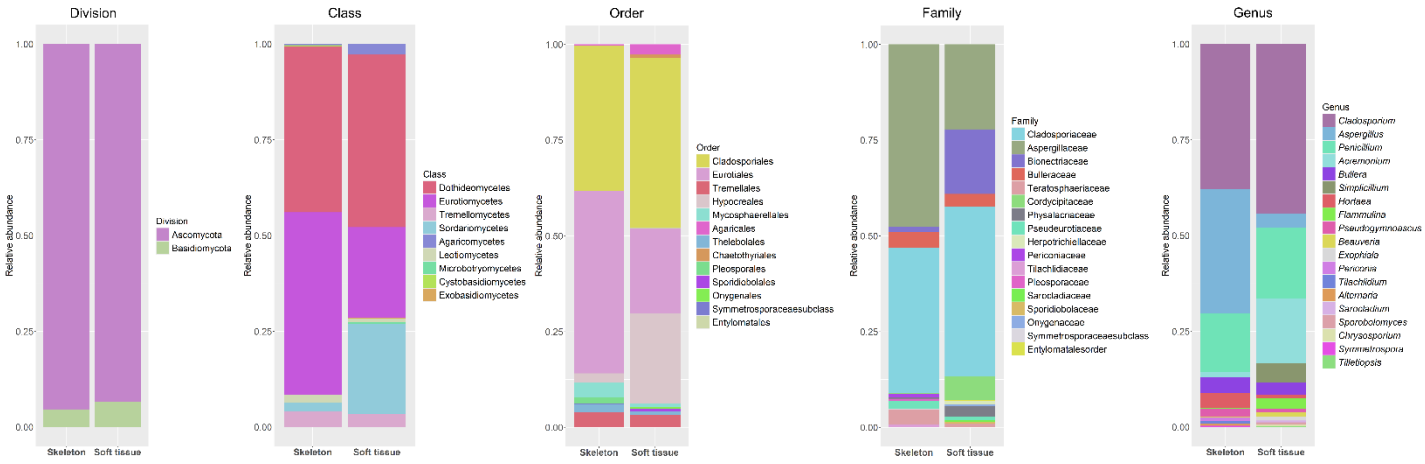

Figure 1: Composition of the culturable fungal communities isolated from soft tissue and skeleton of *Corallium rubrum*, at the different taxonomic ranks.

Several melanized fungal species identified in this study, including *H. werneckii*, *C. cladosporioides*, *C. sphaerospermum*, *A. fumigatus*, *A. versicolor* and *A. alternata*, have been shown to produce protective pigments and bioactive compounds, such as melanin, carotenoids and mycosporine-like amino acids, that may contribute to UV protection in

the coral holobiont (Volkmann et al. 2003; Kogej et al. 2006; Avalos and Carmen Limón 2015; Wong et al. 2019; Roik et al. 2022). However, as *C. rubrum* is a sciaphilous species, mainly observed in dark environments such as cave entrances, overhangs, and crevices (Ballesteros 2006), their role in the red coral remains to be fully elucidated.

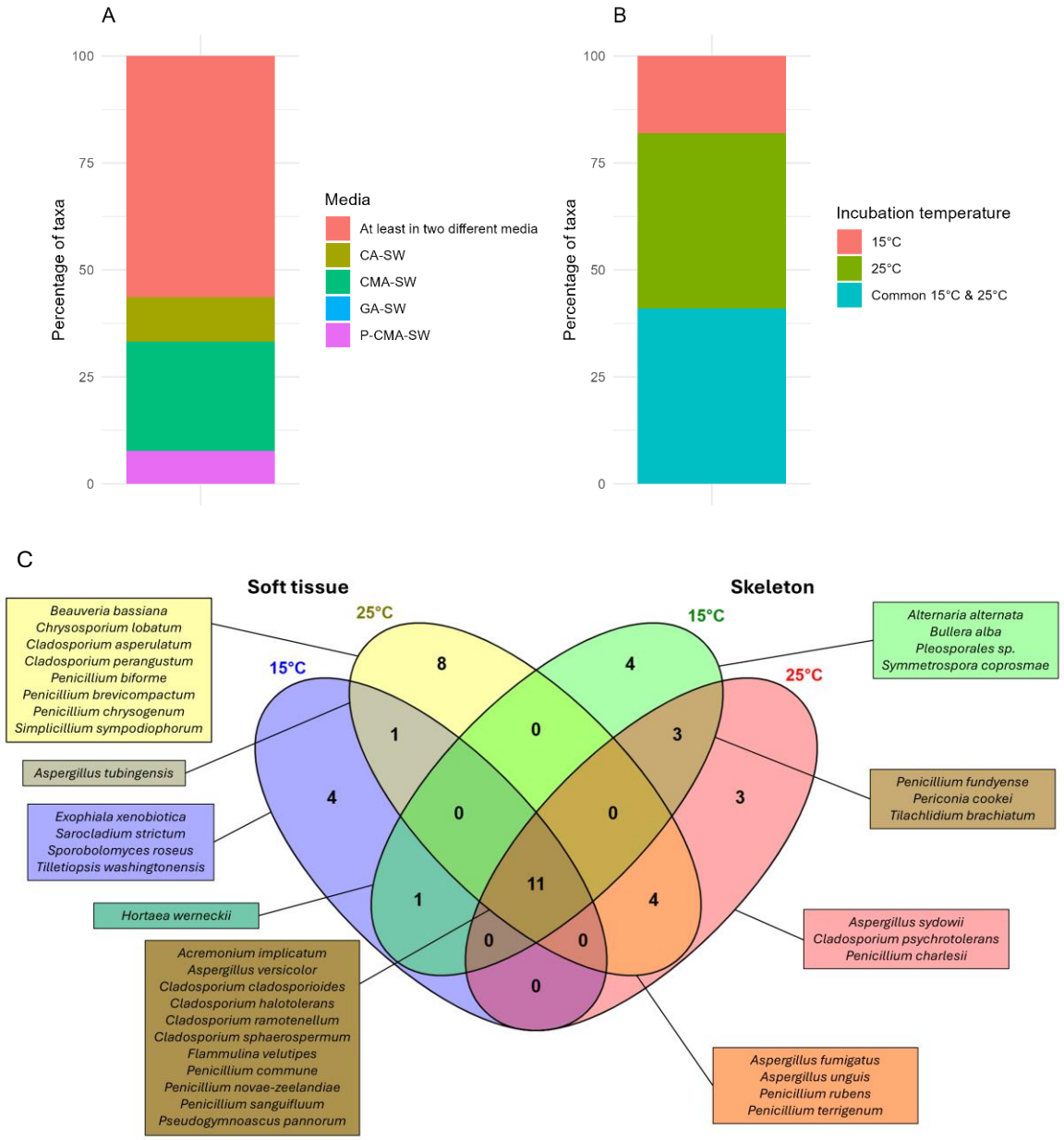

Figure 2: Influence of the isolation techniques on the number of culturable fungal species isolated from *Corallium rubrum*. Influence of growth media (A) and incubation temperature (B). Details on the number of exclusive and common species found in the two coral tissues (soft tissue and skeleton) at different incubation temperatures (15 and 25 °C) (C).

Number of fungal species isolated according to culture conditions

Overall, 39 taxa were isolated from the red coral *Corallium rubrum* (Supplementary File 1). The use of two different incubation temperatures and four growth media had a significant impact on the yield and diversity of cultivable fungi. More than half of the taxa (56.4%) were obtained from at least two different media (Figure 2A) but media-based patterns were also observed with 25.6% of taxa exclusive to CMA-SW, followed by 10.3% in CA-SW and 7.69% in P-CMA-SW, while no taxa were found exclusively in GA-SW. Nutrient-rich media such as CMA-SW and GA-SW may favor fast-growing and/or highly sporulating species, while media mimicking natural environmental conditions such as the unconventional CA-SW and the more selective P-CMA-SW may allow the recovery of less competitive but ecologically relevant taxa.

While 17.9% of taxa were exclusively isolated at 15°C (psychrotolerant), a larger portion (41%) grew only at 25°C (mesophilic) (Figure 2B), suggesting that many fungal strains display mesophilic/thermophilic tendencies, and could become prevalent under thermal stress conditions, such as those experienced by corals during marine heatwaves. Some of these fungi could be either opportunistic or pathogenic, which is particularly relevant in the context of increasingly frequent and intense marine heatwaves (MHWs), especially in the Mediterranean Sea, where sea surface temperatures are rising 20% faster than the global average and recurrent MHWs have caused record-breaking anomalies (Oliver et al. 2018; Darmaraki 2019) and widespread mortality in corals, including *C. rubrum* (Cerrano et al. 2000; Huete-Stauffer et al. 2011; Verdura et al. 2019b; Luigi Piazzi et al. 2021c; Garrabou et al. 2022).

Overall, 15 taxa were isolated from both tissue types, but 13 species were exclusively retrieved from soft tissue and can be defined as "soft tissue specialists" and 10 species were found exclusively in the skeleton, hence referred to as "skeleton specialists" (Figure 2C).

The composition of the mycobiome depends on tissue type and isolation temperature

The number of isolates (Colony forming unit per gram of dry-weight) was not significantly different between tissue types, isolation temperatures and media (Kruskal-Wallis; $p>0.05$; Figure 3; Supplementary File 4). However, the mycobiome composition was significantly different between the tissue types and isolation temperatures (PERMANOVA; $p=0.001$ and $p=0.052$ respectively; Figure 1; Supplementary File 4).

Interestingly, previous studies on other coral species have shown that some of the fungi isolated at 25° can exhibit antibacterial activity. This is the case of *A. versicolor* isolated from the coral *Hemicorallium imperiale*, a member of the same family (Coralliidae) as the red coral (Dong et al. 2023), *A. unguis* from the seagrass *Thalassia hemprichii* (Setyati et al. 2023), *A. fumigatus* from diverse Red Sea corals (Abd El-Rahman et al. 2020) and *P. rubens* from an unidentified coral species (Ying et al. 2023a; 2023b). In detail, they produce antibacterial compounds such as rubensteroids and polyketides, which exhibit inhibitory effects against *Vibrio harveyi*, *V. alginolyticus*, and *V. parahaemolyticus*. These *Vibrio* species are known for their pathogenicity in corals when seawater temperature exceed 22°C (Vezzulli et al. 2010b; Tout et al. 2015). They were observed to proliferate in the red coral during MHW events (Prioux et al. 2023; Tignat-Perrier et al. 2023). Therefore, it can be hypothesized that such fungi may play a protective role for corals by limiting the proliferation of pathogenic bacteria during MHWs. However, two *Cladosporium* species among tissue specialists isolated at 25°C (*C. perangustum*, *C. esperulatum*) are terrestrial plant pathogens (Jang et al. 2013; Liu et al. 2017; Temperini

et al. 2018; Hu 2023; Chen et al. 2024) often retrieved in marine environment, but their role in coral microbiome and health is still unknown.

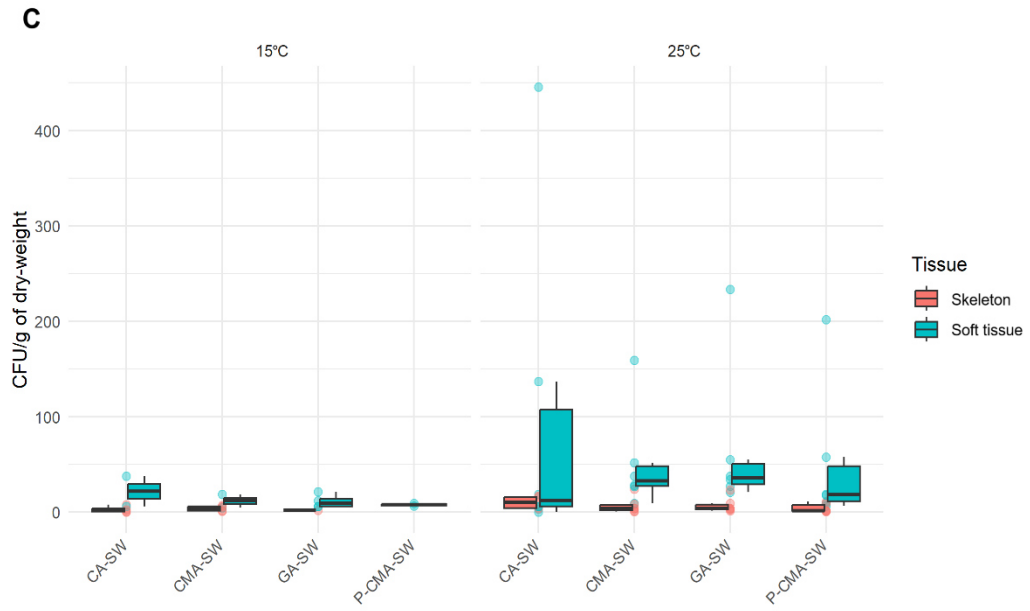

Figure 3: Composition of the mycobiome of *Corallium rubrum*. Colony-forming unit (CFU) per gram of skeleton or soft tissue dry-weight across isolation temperatures and growth media.

Skeleton specialists included three taxa isolated exclusively at 25 °C: *Aspergillus sydowii, Cladosporium psychrotolerans*, and *Penicillium charlesii*. While the two last have never been observed in corals before, *Aspergillus sydowii* is a well-known coral fungus, observed in at least 24 coral species including 9 octocoral species (Supplementary File 3). This fungus is a known pathogen of *Leptogorgia* spp. from the Ecuadorian Pacific (Soler-Hurtado et al. 2016) and of Caribbean fans of the *Gorgonia* genus (Alker et al. 2001; Kim et al. 2015), being responsible for the coral "aspergillosis", which causes severe tissue lesions and leads to mass mortality (Smith et al. 1996; Nagelkerken et al. 1997; Toledo-Hernández et al. 2008). Although its role in *C. rubrum* is still unclear, its presence in the skeleton-associated fungal community and its proliferation at 25 °C raise concern about its potential to develop under MHW conditions and its possible impact on coral health and resistance.

On the 15 species retrieved from both compartments, 11 species were consistently detected across all temperature conditions, suggesting a broad ecological plasticity (Figure 2C). The 4 *Cladosporium* species have been previously reported in

association with a wide range of coral hosts (24 species in total, including 10 octocoral species; Supplementary File 3) supporting their role as widespread generalists within coral fungal community. *C. halotolerans* in particular has been found to have beneficial effects on corals (Granit et al. 2025). Specifically, this fungus may help corals cope with heat stress by reducing tissue loss, lowering stress gene expression, and supporting higher photosynthetic efficiency in algal symbionts (Granit et al. 2025). *A. versicolor* and *P. commune* are also widely distributed among corals, especially *A. versicolor* (observed in 28 coral species, including 10 octocoral species; Supplementary File 3) and likely play a significant ecological role in coral holobiont. When isolated from corals, these species has been shown to exhibit a broad range of bioactivities, including antioxidant, radical-scavenging, antimicrobial and antifouling activity (Zhuang et al. 2011; Chen et al. 2012; Wang et al. 2012; Zhang et al. 2019).

On the other hand, the other consistently detected species were never reported in coral mycobiome to our knowledge (Supplementary File 3). One of them, *P. pannorum*, has already been isolated from marine animals thriving in Antarctica (Godinho et al. 2019; Ogaki et al. 2019) or from bivalves (Borzykh et al. 2015). Their repeated occurrence in all compartments and temperature conditions in this study could indicate potentially relevant specific associations with the red coral. Indeed, their potential to produce secondary metabolites (Fukushima-Sakuno 2020) and to exert antioxidant (Henríquez et al. 2014) and antimicrobial activities (Zhang et al. 2019; Zhang et al. 2021) could be of great importance for the holobiont. These findings raise questions about the functional roles of these fungi and whether their persistence under varying environmental conditions contributes to coral holobiont stability.

Finally, it is worth noting the isolation, from both soft tissue and skeleton, of *Hortaea werneckii*, a halophilic black yeast, causative agent of human skin infection “Tinea Nigra ” occurring in tropical and subtropical regions of the world and reported as a cause of occasional marine fish disease (Todaro et al. 1983; Bonifaz et al. 2008). *H. werneckii* was isolated for the first time from the Mediterranean Sea few years ago (De Leo et al. 2019). The presence in coral of this species with a pathogenic aptitude is, therefore, worthy of attention.

Comparison with the metabarcoding approach

Although the amplicon sequencing of the *18S rRNA* gene and the *ITS2* region yielded an acceptable number of reads per sample (ranging from 17,474 to 105,194 reads; Supplementary File 2), the DADA2 pipeline and subsequent taxonomic annotation resulted in a variable number of sequences associated with microeukaryotes (Supplementary File 2). In the coral samples, a substantial portion of the reads (ranging from 13% with the UnNonMet-Cr primer set to 100% with the ITS2 primer set) were assigned to Metazoa, likely reflecting host contamination, an issue explicitly highlighted by Prioux et al. (2025) in the context of studying microeukaryotes associated with *C. rubrum*. As for the number of fungal sequences in coral samples, it is even lower: 0 reads for the ITS2 and Fungi_18S primer sets, 41 reads for the Universal_18S primer set and 240 reads for the UnNonMet_18S_Cr primer set. Although the latter primer set appeared to allow recovering a higher number of fungal reads, the fungal ASVs represented only a small portion of the annotated microeukaryotic community, accounting for 5% of the total microeukaryotic ASVs (21 ASVs, including only 9 fungal ASVs from coral samples; Supplementary File 2). In this dataset, consistent with the community recorded through culturomics, the majority fungal ASVs belonged to Ascomycota (16 ASVs), mainly within the class Dothideomycetes (Supplementary File 2). Of the 9 ASVs from coral samples, only 3 were annotated at the genus level (*Cladosporium*) and one at the species level (*Malassezia restricta,* a basidiomycota yeast not retrieved by the culture dependent approach).

The consistently low proportion of sequences annotated as fungi across different primer sets highlights a key limitation of this method. This underrepresentation is likely attributable to a primer bias favoring the amplification of *C. rubrum* sequences, as previously reported by Prioux et al. (2025) when amplifying the *18S rRNA* gene. Such bias represents a major obstacle to the accurate characterization of *C. rubrum*-associated fungal communities using metabarcoding. In comparison, analysis of seawater samples, particularly those amplified using the Fungi_18S primer set, resulted in a substantially higher number of fungal reads (835 reads; Supplementary File 2), indicating that the primers perform effectively in the absence of host tissue. The high sequence similarity

between the *18S rRNA V4* and *ITS* regions of *C. rubrum* and those of fungi likely exacerbates non-target amplification.

Results from the in-silico PCRs indicated a very heterogenic amplification for all of the primer sets, with a very low percentage of recovered sequences from the Basidiomycota and Ascomycota phyla (0.7% and 19.3%, respectively; Supplementary File 2). Therefore, the primers used in this study likely exhibit strong biases against fungal groups, rendering them poorly suited for assessing fungal diversity in *C. rubrum*. Furthermore, amplification of the *ITS2* region, which is traditionally used for fungal community analysis, was similarly ineffective, likely due to host contamination. Querying of all *ITS2*-recovered sequences against blastn (NCBI; https://blast.ncbi.nlm.nih.gov) confirmed that the sequences matched closely to gorgonian DNA. Collectively, these limitations substantially hinder the effectiveness of the metabarcoding approach in capturing the true fungal diversity associated with *C. rubrum*. Therefore, the development and implementation of more specific primers, designed to limit host DNA amplification while reducing bias against fungal communities should be prioritized in future research. Thus, no single molecular technique is sufficient for a comprehensive detection and combining molecular and traditional culturing is recommended for accurate assessment. This evidence is supported by the results obtained in this study for metabarcoding and culture dependent community fungal characterization. In comparison with the culture-based approach, the low representation of fungal taxa suggests that metabarcoding, as applied here, significantly underestimate both the richness and the ecological composition of the mycobiome in this marine host. In contrast, the culture-based approach, while inherently limited, proved more successful in recovering fungal taxa. Although traditional culturing captures only a small fraction of microbial diversity (often estimated at around 1% for bacteria and even fewer archaea; Rappé and Giovannoni 2003), and less than 0.1% in marine environments (Schleifer 2004), it remains a valuable tool for detecting certain groups that are otherwise overlooked.

Conclusion

In conclusion, our findings support the idea that culture parameters, such as temperature and media selection, play crucial roles in uncovering the hidden diversity of cultivable fungi associated with corals. Overall, 61% of the isolated fungal species (24 species) were reported here for the first time in association with corals, underscoring the largely unexplored diversity of coral-associated fungi. The discovery of both generalist taxa, which may occur across multiple coral hosts or environmental contexts, and specialist taxa, which appear more tightly associated with *C. rubrum*, points to a complex and structured mycobiome. This structure is likely shaped by a combination of host-derived selection pressures, such as the distinct physicochemical characteristics of coral compartments (soft tissue and skeleton), and environmental conditions, including temperature, nutrient availability, and local microbial interactions. The fungal diversity observed in this study, along with findings reported in scientific literature, and the compartmentalization of the fungal community within the coral, may reflect ecological selection processes that potentially support coral function and enhance their ability to adapt to environmental stresses. On the other hand, the community structure characterized in this study through both metabarcoding and culture-based methods reveals a markedly low representation of fungal diversity in the metabarcoding data, indicating that this approach, as applied here, substantially underestimates the richness and ecological composition of the mycobiome associated with *C. rubrum*. In contrast, although inherently limited, the culture-based approach in this study proved more effective at recovering fungal diversity. Given these challenges, our findings highlight the importance of refining molecular protocols for fungal detection and emphasize the continued relevance of culturing as a complementary method in marine microbial ecology. Furthermore, the identification of certain fungal species, from which biomolecules of ecological and biotechnological interest have been described, creates opportunities for future studies focused on the valorization of marine fungi-derived biomolecules with potential applications in several industrial sectors.

Axis 2: Response of the microbiome of *C. rubrum* and *P. clavata* to thermal stress

Chapter 4

Response of the bacterial microbiome of *Corallium rubrum* and *Paramuricea clavata* to the 2022 marine heatwaves

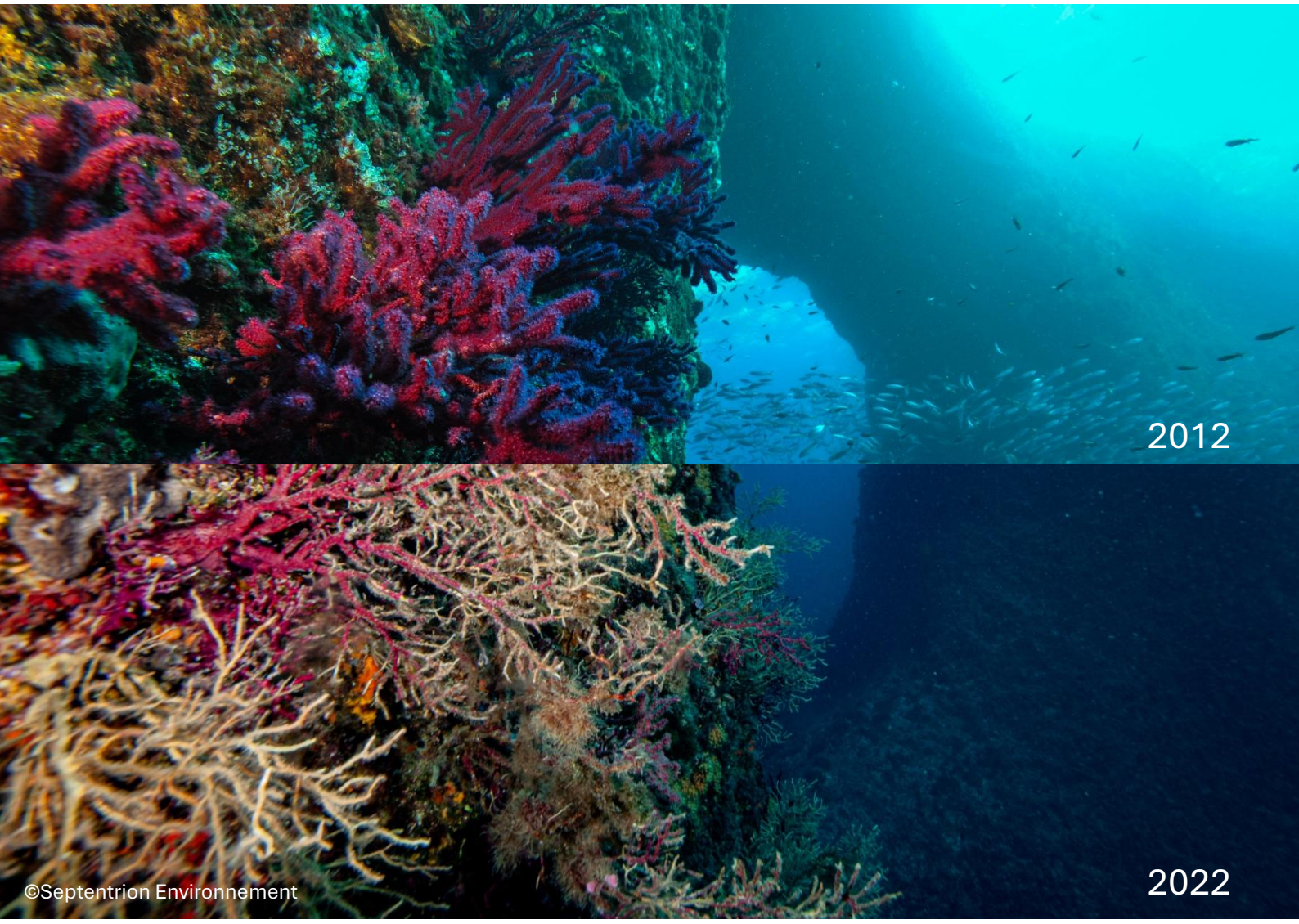

Chapter 4: Response of the bacterial microbiome of *C. rubrum* and *P. clavata* to the 2022 MHWs

I. Overview of the chapter

Marine heatwaves (MHWs) are emerging as one of the greatest threats to marine biodiversity, particularly in the Mediterranean Sea, where climate change has accelerated their frequency and intensity (Smale et al. 2019; Juza et al. 2022; Quade 2022; Grenier et al. 2023). Octocorals, including the red coral *C. rubrum* and the gorgonian *P. clavata*, form the foundation of marine animal forests (MAFs) and are particularly vulnerable to these extreme climatic events. Given that these corals likely depend on symbiotic relationships with microbial communities for nutrient cycling, stress tolerance, and pathogen resistance, MHW-induced dysbiosis could result in tissue loss and increased mortality (Voolstra et al. 2024c).

Several studies have explored the impact of thermal stress on the microbiome of octocorals. However, the correlation between microbial shifts, tissue loss and coral mortality is still unclear (Corinaldesi et al. 2022; Tignat-Perrier et al. 2022; 2023). This uncertainty stems largely from the widespread use of metabarcoding, which provides only relative and not absolute abundance estimates of bacterial taxa, and thus offers an incomplete representation of microbial community dynamics. In this study, we combined amplicon sequencing and taxon-specific qPCR to evaluate both the relative and absolute abundance of certain bacteria of interest in *C. rubrum* and *P. clavata* colonies after the 2022 Mediterranean MHWs. The aim was to decipher the role of microbial dysbiosis, in particular the proliferation of putative pathogens such as *Vibrio*, in the decline of octocoral health.

This chapter is based on field data collected in two marine protected areas (MPAs), the Calanques National Park (France) and the Portofino Marine Protected Area (Italy), in the Western Mediterranean Sea. A total of 96 octocoral colonies of *C. rubrum* and *P. clavata* were sampled at depths between 15 and 35 meters, with visual health status classified as either 0% or 90% tissue loss. During the MHWs of 2022, temperature

anomalies reached up to +4.3°C in the Western Mediterranean Sea, with temperature peaks of 27°C and 26°C at 15 m depth in the Calanques and Portofino, respectively (Crisci et al. 2011; Juza et al. 2022; Grenier et al. 2023). Bacterial communities were analyzed using amplicon sequencing of the *16S rRNA* gene to investigate the community structure, and taxon-specific qPCR to assess the absolute abundance of key taxa such as *Spirochaetaceae*, *Endozoicomonas* and *Vibrionaceae*.

The data revealed a significant decrease in the relative abundance of dominant symbionts (*Spirochaetaceae* and *Endozoicomonas*) in colonies with 90% tissue loss, with a 47% and 38% reduction observed in *C. rubrum* and *P. clavata*, respectively. However, most colonies that exhibited severe tissue loss did not show a significant decrease in the absolute abundance of their main symbionts. Instead, the observed decrease in relative abundance was attributed to the proliferation of opportunistic bacteria, in particular *Vibrio*, which increased up to 120 times in some *P. clavata* colonies from Portofino. Temperature stress was a primary driver in Marseille, where the most pronounced changes in microbial community composition were observed in the shallowest and warmest sampling sites. In contrast, the Portofino population showed more important shifts despite being at a cooler, deeper site. This suggests that additional stress factors, such as anthropogenic pollution and organic matter enrichment (Misic et al. 2011; Di Carro et al. 2018), may have contributed to the larger microbial dysbiosis in this region.

These results emphasize the importance of assessing the absolute abundance of bacteria to understand microbial dynamics under environmental stress. By considering both methods, this study provides evidence that the loss of the main symbionts is not the cause of tissue loss in heat-stressed octocorals. This chapter emphasizes the important role of microbial dysbiosis in the mortality of Mediterranean octocorals during MHWs. The heat-induced proliferation of putative pathogens, particularly *Vibrio* might be a key factor in the coral health degradation and loss of tissue. However, the observed variability between MPAs underscores the influence of local environmental and anthropogenic factors, suggesting that the impact of MHWs is not the same for all populations. As the frequency and intensity of MHW events continue to increase, such findings are crucial for the development of targeted conservation strategies to protect vulnerable marine habitats.

II. Publication

Unveiling Microbiome Changes in Mediterranean Octocorals During the 2022 Marine Heatwaves: Quantifying Key Bacterial Symbionts and Potential Pathogens

Microbiome | December 2023

DOI : https://doi.org/10.1186/s40168-023-01711-x

Camille Prioux[1,2,3], Romie Tignat-Perrier[2,3], Ophélie Gervais[2,3], Tristan Estaque[4], Quentin Schull[5], Stéphanie Reynaud[3], Eric Béraud[3], Bastien Mérigot[5], Anaïs Beauvieux[5], Maria-Isabelle Marcus[3], Justine Richaume[4], Olivier Bianchimani[4], Adrien Cheminée[4], Denis Allemand[3] and Christine Ferrier-Pagès[3]

[1]Sorbonne Université, Collège Doctoral, Paris, France

[2]Unité de Recherche sur la Biologie des Coraux Précieux CSM - CHANEL, Centre Scientifique de Monaco, 8 Quai Antoine 1er, MC 98000, Monaco, Principality of Monaco

[3]Centre Scientifique de Monaco, 8 Quai Antoine 1er, MC 98000, Principality of Monaco

[4]Septentrion Environnement, Campus Nature Provence, 13008, Marseille, France

[5]MARBEC, Univ. Montpellier, CNRS, IFREMER, IRD, Sète, France

Abstract

Background: Climate change has accelerated the occurrence and severity of heatwaves in the Mediterranean Sea and poses a significant threat to the octocoral species that form the foundation of marine animal forests (MAFs). As coral health intricately relies on the symbiotic relationships established between corals and microbial communities, our goal was to gain a deeper understanding of the role of bacteria in the observed tissue loss of key octocoral species following the unprecedented heatwaves in 2022.

Results: Using amplicon sequencing and taxon-specific qPCR analyses, we unexpectedly found that the absolute abundance of the major bacterial symbionts, *Spirochaetaceae* (*C. rubrum*) and *Endozoicomonas* (*P. clavata*), remained, in most cases,

unchanged between colonies with 0% and 90% tissue loss. These results suggest that the impairment of coral health was not due to the loss of the main bacterial symbionts. However, we observed a significant increase in the total abundance of bacterial opportunists, including putative pathogens such as *Vibrio*, which was not evident when only their relative abundance was considered. In addition, there was no clear relation between bacterial symbiont loss and the intensity of thermal stress, suggesting that factors other than temperature may have influenced the differential response of octocoral microbiomes at different sampling sites.

Conclusions: Our results indicate that tissue loss in octocorals is not directly caused by the decline of the main bacterial symbionts but by the proliferation of opportunistic and pathogenic bacteria. Our findings thus underscore the significance of considering both relative and absolute quantification approaches when evaluating the impact of stressors on coral microbiome as the relative quantification does not accurately depict the actual changes in the microbiome. Consequently, this research enhances our comprehension of the intricate interplay between host organisms, their microbiomes, and environmental stressors, while offering valuable insights into the ecological implications of heatwaves on marine animal forests.

Background

Marine heatwaves (MHWs), characterized by episodes of prolonged abnormally high sea surface temperatures (SST), have increased in frequency, intensity and length in the world's oceans in recent decades, fueled by global warming (Darmaraki et al. 2019; Oliver et al. 2018). In particular, the Mediterranean Sea is turning into one of the fastest-warming seas on Earth, with temperatures rising 20% faster than the global average (MedECC 2020; Cos et al. 2022; Pastor et al. 2020) and a high occurrence of MHWs over the past two decades (Darmaraki et al. 2019; Juza et al. 2022; Omneya et al. 2021). In 2022, between three and seven record-breaking MHWs hit the Mediterranean Sea between May and September, with SST anomalies locally reaching 4.3°C above the summer average, exceeding the previous maximum of +2-3°C during the 2003 MHWs (T-MEDNet 2023; Quade 2022; Guinaldo et al. 2023). Recurrent MHWs have had devastating effects on community structure and health of marine animal forests (MAFs) (Cerrano et al. 2000; Grenier et al. 2023), which are among the most biodiverse assemblages in the Mediterranean Sea (Paoli et al. 2017; Orejas et al. 2022; Rossi et al. 2017c).

MAFs are unique habitats and important hotspots of biodiversity (Casas-Güell et al. 2015; Roberts et al. 2002; Ponti et al. 2019), creating macro- and microhabitats that provide shelter for a wide variety of marine species (Piazzi et al., 2021). They also provide a range of valuable benefits to local populations, from fisheries to coastal protection and tourism (Paoli et al. 2017; Worm et al. 2006; Rossi et al. 2017c). Shallow and upper-mesophotic Mediterranean MAFs (<60 m deep) are mainly composed of sponges and octocoral species including the gorgonians *Eunicella cavolini* (Koch, 1887), *Eunicella singularis* (Esper, 1791) and *Paramuricea clavata* (Risso, 1826), as well as the red coral *Corallium rubrum* (Linnaeus, 1758). Particularly vulnerable to disturbances, octocorals are being highly affected by MHWs that have caused outbreaks of microbial diseases and mortality episodes, which can affect up to 90% of the colonies in certain shallow populations (Cerrano et al. 2000; Huete-Stauffer et al. 2011; Luigi Piazzi et al. 2021a; Verdura et al. 2019a; Garrabou et al. 2009b; 2022).

Octocoral mortality events following MHWs may result from a combination of the direct impacts of thermal stress on animal physiology and the disruption of the symbiosis

between the host and its microbial community, consequently affecting the functioning and overall health of the host (Bourne et al. 2016; Mouchka et al. 2010; Vezzulli et al. 2010). Corals indeed form a meta-organism called holobiont, which comprises the animal host and its associated microorganisms (*i.e.*, protists, fungi, bacteria, archaea, and viruses) that can provide a wide range of benefits. These latter include nutritional provisioning and recycling (Lema et al. 2012; Matthews et al. 2020; Raina et al. 2009), tolerance to environmental stress (Peixoto et al. 2017) and protection from pathogens by producing antibiotic compounds (Kvennefors et al. 2012; Nissimov et al. 2009; Ritchie 2006). Mediterranean octocorals harbor a specific microbiota that is stable across seasons, geographic locations, and depths. For gorgonians (*Paramuricea* and *Eunicella* genera), bacteria from the *Endozoicomonas* genus dominate the microbiota (representing up to 96% of the bacterial community; Bayer et al. 2013; van de Water et al. 2017), while bacteria from the *Spirochaetaceae* family are the main bacterial symbionts associated with the red coral *C. rubrum* (representing up to 70% of the bacterial community; van de Water et al. 2016; 2018).

Disturbances such as heat stress can induce changes in the octocoral microbiota by exerting a downward pressure on the survival of beneficial symbionts, thereby affecting the stress tolerance of the host, and promoting temperature-dependent bacterial diseases. However, there is currently limited research available on the response of the microbiome of Mediterranean octocorals to temperature anomalies representative of MHWs, and none of these studies can explain the extended mortality and tissue loss of octocorals observed during the 2022 MHWs (Tignat-Perrier et al. 2022; 2023; Corinaldesi et al. 2022). They reported different responses depending on the octocoral species, sampling depth and colony, with no clear relationship between tissue loss, thermal stress intensity, and microbiome changes. In the laboratory experiments of Tignat-Perrier et al. (2022, 2023), decreases in the relative abundance of the major symbionts (*Endozoicomonas* or *Spirochaetaceae*) following heat stress (24°C for several weeks) were associated with tissue loss in *Paramuricea clavata*, but not in *Eunicella cavolini* or *Corallium rubrum*. These findings were partially consistent with *in situ* data from gorgonian and red coral colonies during the 2011 MHWs (Corinaldesi et al. 2022), where it was observed that deep colonies of *C. rubrum* (70 m) exposed to heat stress also had a

lower relative abundance of the main symbiont *Spirochaetaceae*. However, such changes in the bacterial community were not observed in shallow *C. rubrum* populations (30 m), despite their exposure to greater increases in sea temperature (Corinaldesi et al., 2022). Altogether, these observations suggest that further studies are needed to explore changes in the microbiome of temperate octocorals following MHWs, with a broader investigation that includes multiple locations, species, and health states of octocorals. Because changes in the relative abundance of key symbionts cannot explain changes in holobiont health, other measurements, including absolute abundance of symbionts and putative pathogens, may help to better understand the symbiont/pathogen relationships.

To address the above gaps, we investigated how the microbiota associated with the gorgonian *P. clavata* and the red coral *C. rubrum* responded to the 2022 MHWs, some of the warmest heatwaves ever experienced by octocoral species in the Mediterranean Sea. To this end, we conducted an extensive sampling of ninety-six colonies of two key octocoral species, with different visual health states (0% and 90% of tissue loss) from 15 m to 35 m depth. Samples were collected in two marine protected areas in the Western Mediterranean Sea, the Calanques National Park (France) and the Portofino Marine Protected Area (Italy) where MAFs are protected from most commercial and recreational activities. These areas experienced different MHW intensities, with extreme temperatures reaching 27°C and 26°C at 15 m depth (Crisci et al. 2011), in the Calanques National Park and the Portofino Marine Protected Area, respectively. By assessing the composition of the bacterial communities associated with the octocorals using amplicon sequencing and taxon-specific qPCR analyses of the *16S rRNA* gene, we aimed to characterize actual changes in the octocoral microbiota in relation to the visual health status, collection site and depth of the colonies. This study provides important information on how octocoral-associated microbiota respond to thermal stress as well as how the bacterial symbionts contribute to the octocoral's health. The results obtained will enable better conservation and protection of Mediterranean MAFs.

Methods

Study areas, temperature regimes and impacts on octocorals

Octocoral samples were collected at different locations in two marine national parks of the Northern Mediterranean Sea during the 2022 MHWs (Fig. 1). The first sampling campaign was conducted in the core area of the Calanques National Park (Marseille, France; 43 500 ha surface area) between August 31 and September 3, 2022, with the consent of the Calanques National Park (France). Among the six sampling sites, two were located in a *no-taking zone* where commercial and recreational navigation is prohibited (total surface area of the *no-taking zones* in the park: 4 634 ha). The second sampling campaign was conducted on September 5, 2022, in the Portofino Marine Protected Area (Portofino MPA, Italy) where commercial and recreational activities are controlled. Only *P. clavata* was collected in the Portofino MPA. Considering the relatively small size of the latter (346 ha surface area), coral sampling was conducted at only one site (Fig. 1) with the consent of the Portofino MPA. The collection depth ranged from 15 m to 35 m depending on the collection site (Fig. 1).

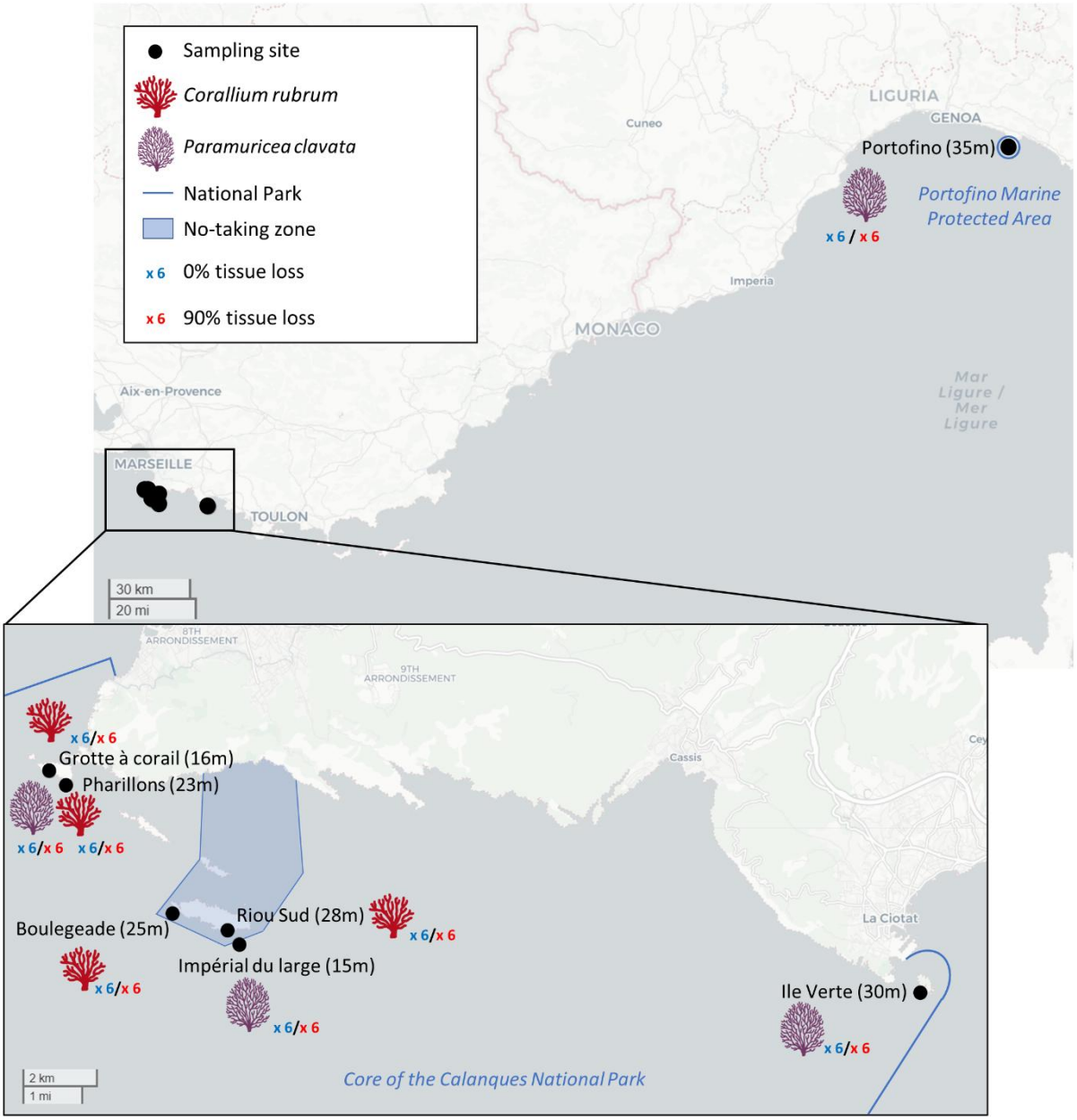

Figure 1: Species and number of samples collected at the different geographical locations. Collection depths (in brackets) and the number of samples per condition (blue for 0% tissue loss and red for 90% tissue loss) are indicated next to the names of the sites.

In 2022, the Mediterranean Sea experienced record sea surface temperatures from May to September, although temperature regimes varied by location during the MHWs. Hourly measurements of seawater temperature at *Riou Sud* (Calanques National Park, France) over the past two decades, and at *Portofino* (MPA, Italy) from 2019 to 2022 have been extracted from the T-MEDNet database (www.t-mednet.org) (Fig. 2 and Fig. S1). In the Northwestern Mediterranean Sea, thermal anomalies are either characterized by short periods (a few days) at temperatures reaching 27°C or by long periods (several days and weeks) at warm and stable temperatures of 23–24°C in shallow waters (Crisci et al. 2011; Estaque et al. 2023). We thus chose to graph temperatures ≥ 23°C on Fig. 2 and Fig. S1 as 23°C starts to be an abnormally warm temperature for the region if largely observed during the summer. During the 2022 MHWs, the seawater temperature at *Riou Sud* exhibited unprecedented records, with measurements reaching 27°C and 26°C at 15 m and 30 m depth, respectively (Fig. 2A). The temperature regime is characterized by upwelling events of dense and cold water coming from the deep, that occurred periodically during the MHWs (Fig. 2A). These events, that occur due to strong North-West winds, can lower seawater temperatures by up to 10°C within a few hours before rising again (Odic et al. 2022; Millot 1979) (Fig. 2A). In 2022, *Riou Sud* experienced an exceptional frequency of days with temperatures exceeding 24°C at both depths (17 and 3 days at 15 m and 30 m depth, respectively), surpassing any previous observations recorded in the past two decades (Fig. 2BC).

In *Portofino* (MPA, Italy), temperatures reached 26°C and 21°C at 15 m and 30 m depth, respectively (Fig. S1A), which correspond to 1°C and 5°C difference compared to those observed in *Riou Sud* (Calanques National Park, France) at the same depths (Fig. 1A). In *Portofino,* the number of days where abnormally warm temperatures (>24°C) were observed was not greater than the previous three years (Fig. 1B), suggesting that the 2022 MHWs did not exhibit unprecedented records at this location. Furthermore, at the sampling depth (35 m), the temperature only reached 19.8°C, which is comparable to what has been observed in the three previous years (Fig. S1).

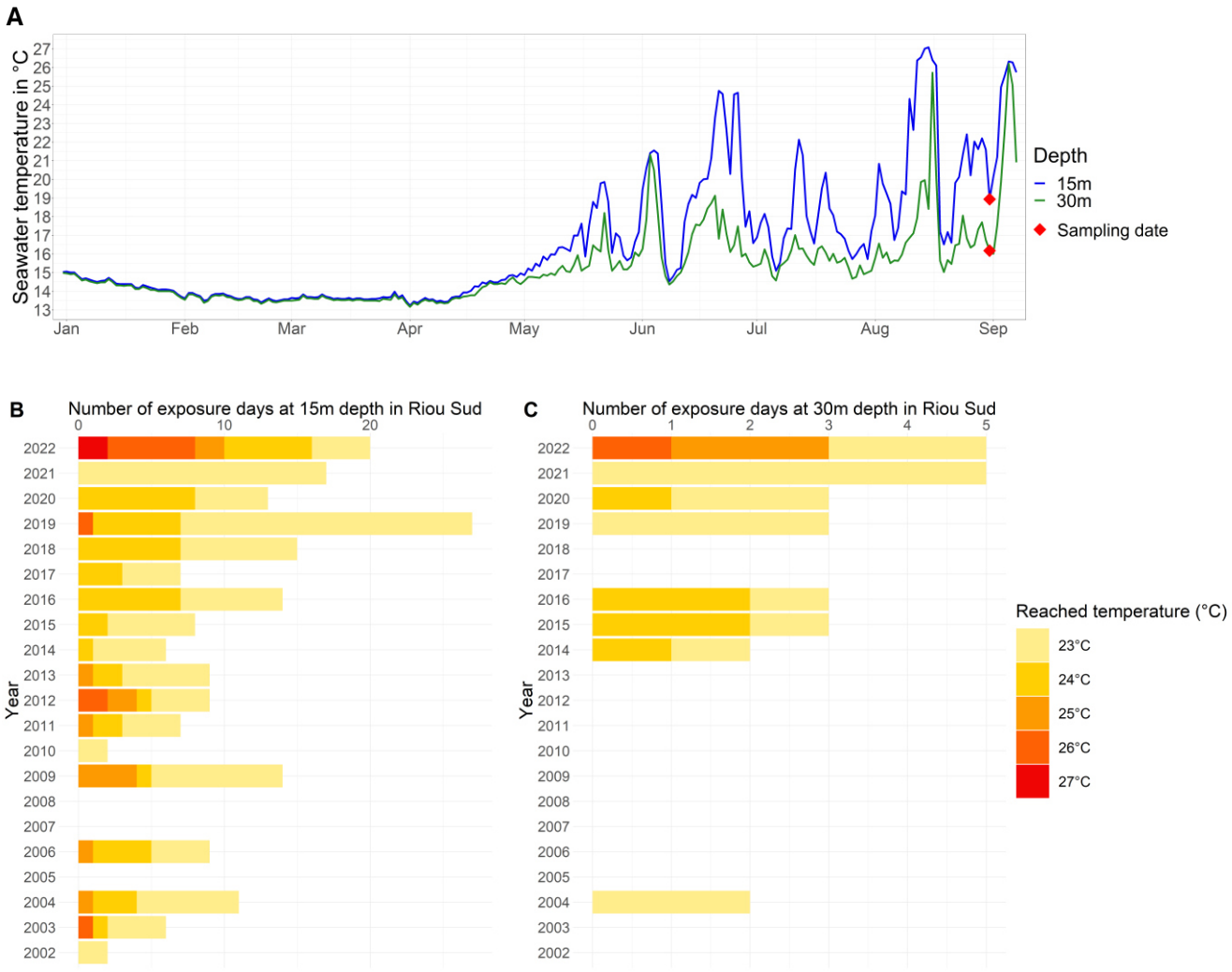

Figure 2: Temperature regime in 2022 and in the past twenty years at one of the collection sites (*Riou Sud*, Calanques National Park, Marseille, France). Seawater temperature at 15 m and 30 m depth from January to September 2022 (**A**), and number of exposure days at temperatures between 23°C and 27°C at 15 m (**B**) and 30 m depth (**C**) over the past twenty years.

A parallel survey of octocoral mortality was conducted to assess the percentage of colonies affected by the 2022 MHWs at the different sites in the Calanques National Park. The survey was performed according to a widely used method based on quantification of the proportion of affected colonies (Garrabou et al. 2009b; 2022) and described in detail in Estaque et al. (2023). A colony was considered affected if tissue loss represented at least 10% of the colony surface area. One or more dives were conducted at each site to enumerate the affected colonies among a hundred colonies (Table S1). Overall, *C. rubrum* suffered less from the 2022 MHWs than *P. clavata* (45% and 81% of colonies affected on average for *C. rubrum* and *P. clavata*, respectively), and octocoral populations were affected differently among sites (Fig. 3A and Table S1). Colonies of *C. rubrum* collected in *Grotte à corail* (83% of affected colonies) and *Pharillons* (51% of affected colonies) were the most affected, while *P. clavata* populations in *Pharillons* have suffered the most from the heatwaves with 100% of affected colonies (Fig. 3A).

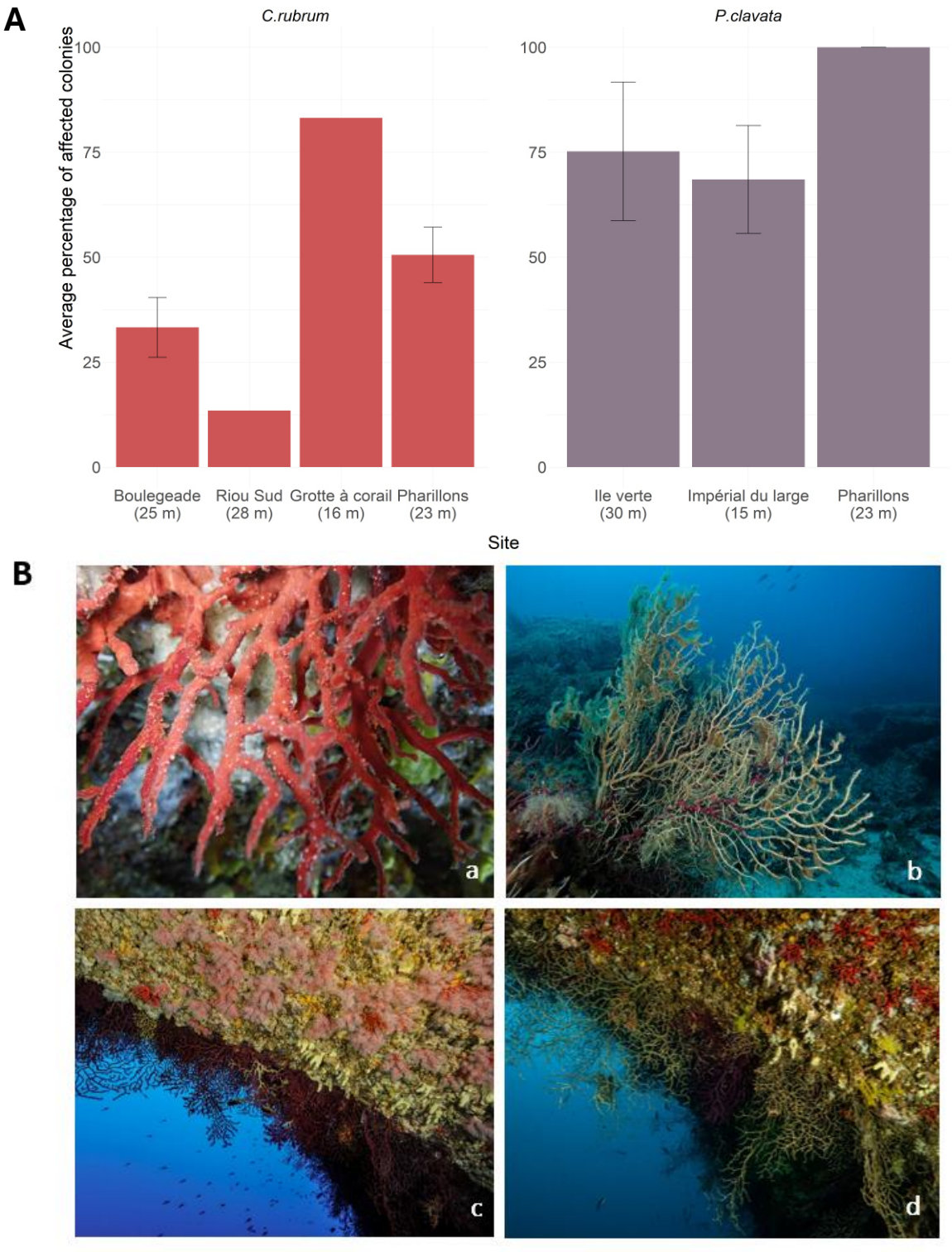

Figure 3: Impact of the 2022 heatwaves on coralligenous reefs of the Calanques National Park (Marseille, France). (**A**) Average percentage of *P. clavata* and *C. rubrum* colonies affected by tissue loss at the different sampling sites. (**B**) Colonies of *C. rubrum* (**a**) and *P. clavata* (**b**) exhibiting tissue loss (August 2022); Coralligenous assemblage before (**c**) and during (**d**) the heatwaves. Credit: *Septentrion Environnement*.

Sample collection

A total of ninety-six samples were collected from colonies of the red coral *C. rubrum* and the gorgonian *P. clavata* with different health status based on visible tissue loss (Fig. 1 and Fig. 3B). Samples of 3 cm were taken from colonies that showed no sign of tissue loss (0% of tissue loss) and from colonies showing 90% of tissue loss based on colony surface area. In the last case, the remaining tissue was sampled. While both *C. rubrum* (six samples per condition and site) and *P. clavata* (six samples per condition and site) colonies were sampled in the Calanques National Park, only *P. clavata* was collected in the Portofino MPA (six samples per condition; Fig. 1). Immediately after collection, samples were placed in separate Ziploc® plastic bags containing natural seawater. On board, they were transferred to Eppendorf tubes, fast-frozen in a dry shipper containing liquid nitrogen (~190°C, ©CX100 Worthington Industries) and then stored at −80°C in the lab until further processing.

DNA extraction

DNA was extracted using ~1.5 cm of octocoral sample and the DNeasy PowerBiofilm kit (QIAGEN, Hilden, Germany) with the following modifications: during the cell lysis step, 2 µL of Proteinase K (600 U/ml) was added to the sample and incubated at 60°C for 2 hours, followed by 2 min of bead beating using the CryoMill (Retch, Germany) at a frequency of 30 Hz and at room temperature. DNA concentration was measured using a Qubit fluorometer and DNA was stored at −20°C.

MiSeq amplicon sequencing of the 16S rRNA gene

Library preparation and sequencing. Extracted DNA samples were sent to STAB VIDA (Portugal) for a paired-end sequencing (2 × 300 bp, 600 cycles) with the V3 chemistry on Illumina MiSeq platform. Amplicon library preparation was conducted using Illumina's standard "16S Metagenomic Sequencing Library Preparation" protocol (Illumina 2013). The V3-V4 region (~ 550 bp) of the *16S rRNA* gene was amplified using the forward primer 341F 5'-CCTACGGGNGGCWGCAG-3' and the reverse primer 785R 5'-GACTACHVGGGTATCTAATCC-3'. The fastq files containing the raw sequencing data have

been deposited in the NCBI's Short Read Archive (SRA) under the BioProject accession number PRJNA991959.

Bioinformatics data processing. The *16S rRNA* gene amplicon data were processed using the DADA2 pipeline (version 1.16; https://benjjneb.github.io/dada2/index.html; Callahan et al. 2016). The sequencing of ten *P. clavata* samples and one *C. rubrum* sample was cancelled as no amplification was detected during the library preparation (amplicon PCR). On the 85 remaining samples, sequencing resulted in 14,363,708 reads ranging from 42,720 to 264,000 reads per sample (Table S2). Before any further analysis, read quality profiles were inspected and reads were filtered and trimmed with the following settings: truncLen = c(290, 250), maxN = 0, maxEE = c(2, 2). Primer sequences were also trimmed at the 5'-end of each read (17 bp and 21 bp on the reads R1 and R2, respectively). Error rates were computed and used for sequence inference. An amplicon sequence variant (ASV) table was constructed based on de-noised and merged R1 and R2 reads. Sequences smaller than 390 bp and longer than 450 bp were removed. Chimeras were detected and removed from the table using the removeBimeraDenovo function. The number of reads and sequences passing the different steps of the pipeline per sample is presented in Table S3. Taxonomy was assigned to the 12 509 ASVs using the assignTaxonomy function and the SILVA SSU reference database (version 138.1). The ASV table, the sequences of each ASV and the metadata are available as Table S4, S5 and S6, respectively.

Analysis of 16S rRNA gene sequencing data. All statistical analyses were conducted in the R environment (version 4.2.1) using the R-package *phyloseq* (McMurdie et al. 2013). Observed species richness and evenness (Shannon index) were calculated using the R-package *vegan* (Dixon 2003). Given the fact that rarefaction curves mostly reached the plateau (Fig. S2) and the current debate concerning the applicability of unrarefied versus rarefied data (Willis 2019; McMurdie et al. 2014), we conducted our alpha diversity analyses on the unrarefied ASV count table. Potential differences in observed richness were explained by constructing a generalized linear model (GLM) using a negative binomial distribution and considering site and tissue loss condition as fixed factors without taking into account the interaction as its effect was not significant (formula = Observed richness ~ Condition + Site; Table S7). Post-hoc tests were performed to identify

potential pairwise differences (R-package *emmeans* (Lenth 2023)). Compositional data analysis (CoDA) (Gloor et al. 2017; Quinn et al. 2018) was used to investigate the changes in the composition of the microbiota of *C. rubrum* and *P. clavata*. The raw ASV abundances were centered log-ratios (clr) transformed using the R-package *compositions* (van den Boogaart et al. 2008), after imputing zero counts based on Bayesian multiplicative replacement (Bayes-LaPlace BM method of the cmultRepl function in the R-package *zCompositions;* Palarea-Albaladejo et al. 2015). An Aitchison distance matrix was generated by computing Euclidean distance between samples using the clr-transformed data table. Principal component analyses (PCA), permutational multivariate analysis of variance (using functions adonis(); R-package *vegan*) were conducted to evaluate differences in the bacterial community structure between sites and conditions based on the percentage of tissue loss for each octocoral species (formula = Aitchison matrix ~ Condition + Site; Table S8). Potential pairwise differences were then considered (using the function permanova_pairwise(); R-package *ecole* (Smith 2021)) adjusting the p-values with the false discovery rate correction (p.adjust() function; R-package stats; Table S8). Differential abundance analyses were performed to identify ASVs that were differentially abundant between health conditions (0% versus 90% of tissue loss) and collection sites when the number of samples was sufficient using the R-package *ANCOM-BC* (Lin et al. 2020 ; ancombc2() function using prv_cut = 0.30 and alpha = 0.05; version 02-2023; Table S9).

Quantitative PCR (qPCR)

Comparative qPCR was used to track changes in the abundance of total bacteria as well as the abundance of bacteria belonging to the *Spirochaetaceae* family, *Vibrio* genus and *Endozoicomonas* genus in octocoral cells. Four primer pairs targeting the *16S rRNA* gene were used including universal primers (total bacteria; Fierer et al. 2005) and primers specific to the *Spirochaetaceae* group (Husmann et al. 2010), *Vibrio* genus (Thompson et al. 2004) and *Endozoicomonas* genus (modified from Shiu et al. 2020) (Table S10). To test the specificity of the taxon-specific primers on our octocoral samples, the amplification products obtained from four samples (two per octocoral species) were sequenced using the Sanger technology (Eurofins genomics, Germany) and aligned on the *nr* database using the *blastn* algorithm. For primer pairs targeting a sequence in the

V3-V4 region of the *16S rRNA* gene, primer sequences were aligned on all the ASV sequences annotated as the targeted taxon (58 ASV for *Endozoicomonas* and 190 ASV for *Vibrio*) using Clustal Omega (default parameters; Sievers et al. 2011) and sequence complementarity was verified (Table S11 and S12). Two pairs of primers targeting the *beta actin* gene of *C. rubrum* and *P. clavata* were designed using Primer3 (http://primer3.sourceforge.net/) and the host genomes, as internal controls (Table S10).

For all primer pairs, efficiency was evaluated using different primer concentrations and doing an amplification of a series of 10-fold dilutions of a mix of all DNA samples as template. The specificity of the product was assessed from a melting curve program. The amplification results were plotted as C_t vs. $\log_{10}$[DNA] and the amplification efficiencies were calculated using formula $E = 10^{(1/slope)}$ (Pfaffl et al, 2001). Primer concentrations and efficiencies for each targeted gene are given in Table S10.

qPCRs were carried out on all samples in duplicate on a QuantStudio3 qPCR machine (Applied Biosystems). Amplification reactions contained 0.4 µL of each primer (concentrations in Table S7), 10 µL of SensiFAST SYBR master mix (ThermoFisher) and 2 µL of diluted DNA (1/20) in a final volume of 20 µL. Amplification was done using standard cycling conditions, *i.e.,* 95°C for 10 min, followed by 40 cycles of 95°C for 15 s and 60°C for 1 min. The relative quantification of each selected gene was determined in comparison to the *beta* actin reference gene based on the Pfaffl method (Pfaffl, 2001). Fold changes (or relative expression ratio) of the different genes in the 90% tissue loss condition were calculated and expressed in comparison to the 0% tissue loss condition.

Two-way non-parametric Kruskal-Wallis analyses were performed to test differences in the total concentration of bacteria and the abundance of *Spirochaetaceae*, *Vibrio* and *Endozoicomonas* bacteria per host cell between the health conditions and the sampling sites for each octocoral species (Table S13).

Results

Bacterial richness associated with octocorals with different tissue loss conditions (0 and 90% tissue loss)

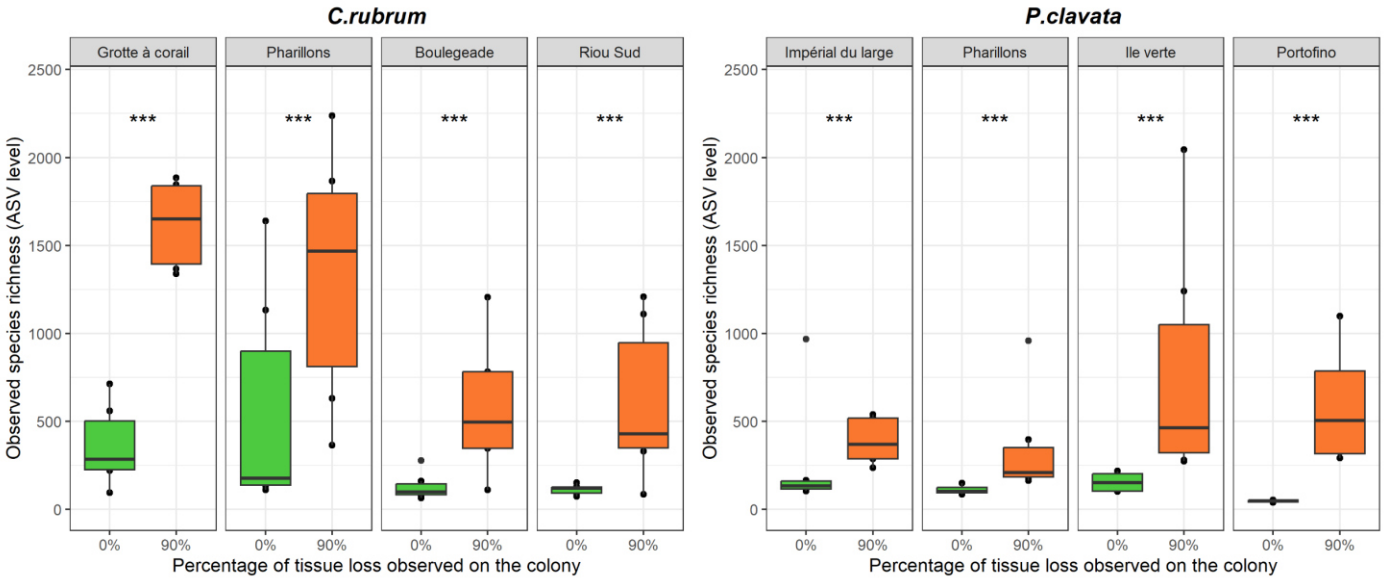

Figure 4: Estimation of the bacterial species richness in *C. rubrum* (left) and *P. clavata* (right) depending on the collection site and the colony health status (0% and 90% tissue loss). Statistical significance levels of differences between octocorals experiencing tissue loss or not are indicated by stars (*** for $p < 0.001$).

In colonies with 0% tissue loss, the bacterial species richness was site-specific in *C. rubrum*, with *Grotte à corail* and *Pharillons* showing higher richness values (average observed richness of 361 and 562 ASVs, respectively) compared to *Boulegeade* and *Riou Sud* (average observed richness of 129 ASVs and 113 ASVs, respectively; (post-hoc tests $0.0001 < p < 0.004$, Fig. 4 and Table S7)). No difference was observed between sites in *P. clavata* (post-hoc tests $0.46 < p < 1$, Fig. 4 and Table S7). Species richness increased by 4 and 3.3 times on average in colonies of *C. rubrum* and *P. clavata* with 90% tissue loss compared to colonies with no tissue loss (Estimate Std. = 1.4; Error = 0.19; z-value = 7.3; $p = 2.9 \times 10^{-13}$ and Estimate Std. = 1.3; Error = 0.23; z-value = 5.9; $p = 3.01 \times 10^{-9}$ for *C. rubrum* and *P. clavata*, respectively; Fig. 4 and Table S7). Consequently, colonies with 90% tissue loss showed higher species richness in *Grotte à corail* and *Pharillons* compared to *Boulegeade* and *Riou Sud* for *C. rubrum* (post-hoc tests $0.0001 < p < 0.004$), while no

difference between sites was observed for *P. clavata* (post-hoc tests 0.38 < p < 1, Fig. 4 and Table S7).

Changes in the structure of the bacterial communities associated with octocorals with 90% tissue loss

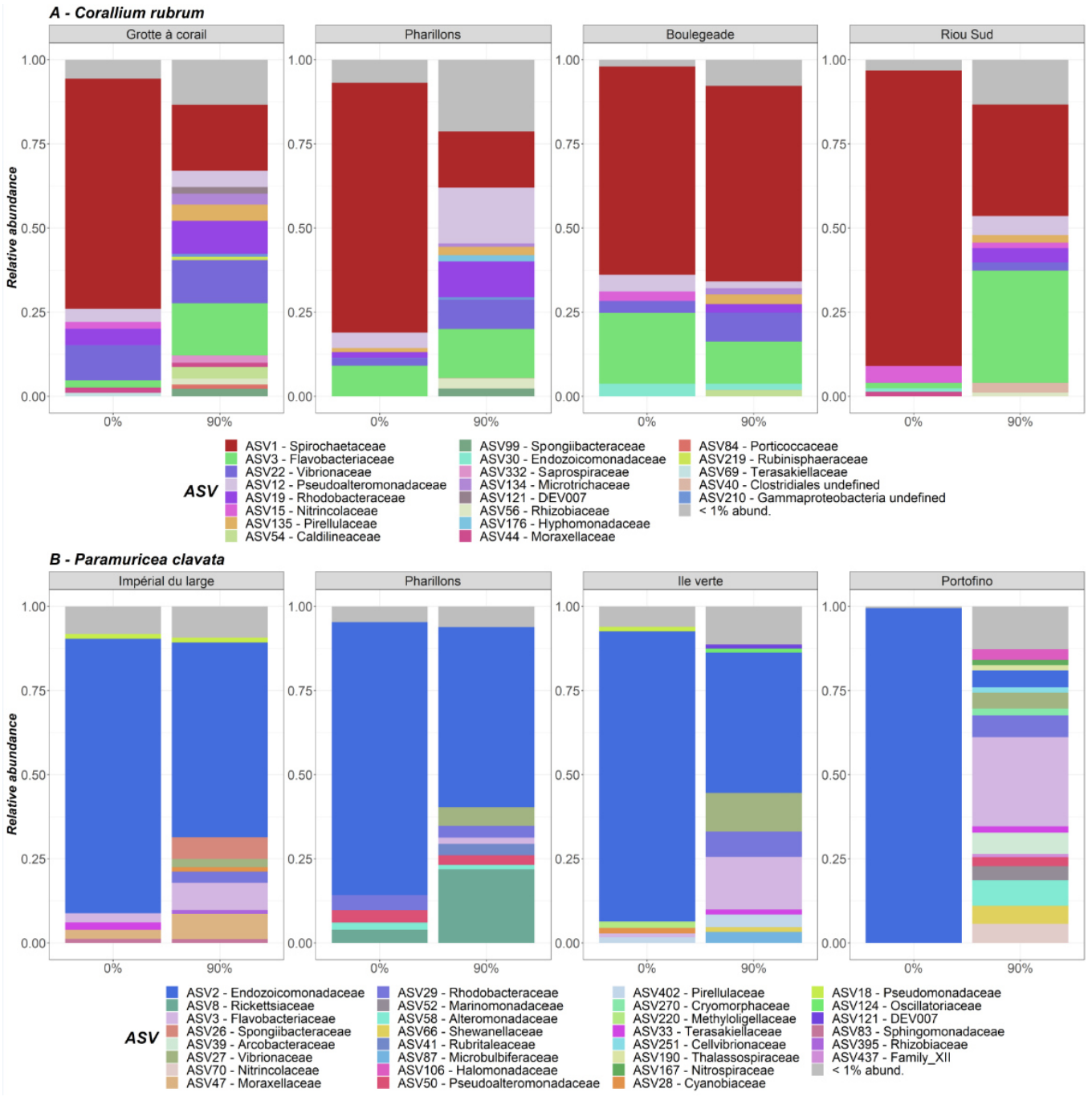

Figure 5: Relative abundance of the ASVs associated with *C. rubrum* (A) and *P. clavata* (B) depending on the collection site and the percentage of tissue loss (0% and 90%).

Differential abundance analyses based on compositional data

Overall, the bacterial communities associated with the colonies with 0% tissue loss were dominated by ASV1- *Spirochaetaceae* (72%), ASV5- *Spirochaetaceae* (11%) and ASV7- *Flavobacteriaceae* (6.1%) in *C. rubrum*, and by three *Endozoicomonadaceae*, ASV2, ASV6 and ASV4 (78%, 9% and 4% on average, respectively) in *P. clavata* (Fig. 5 and S4). For *C. rubrum*, no site-specific differences were observed in the structure of the bacterial communities associated with 0% tissue loss colonies (post-hoc tests $0.18 < p < 0.62$; Fig. 5A, S3, S4 and Table S8). In *P. clavata*, the structure of the bacterial communities associated with 0% tissue loss colonies collected in *Portofino* and *Ile verte* were significantly different from the other sites (post-hoc tests $0.02 < p < 0.03$, Figure 5B, S3, S4 and Table S8).

For both species, overall, the structure of the bacterial communities significantly differed between the two health (tissue loss) conditions ($F = 3.2$; d.f. = 1; $p = 1 \times 10^{-4}$ and $F = 1.5$; d.f. = 1; $p = 0.002$ for *C. rubrum* and *P. clavata*, respectively) (Fig. 5 and Table S8). Additionally, the bacterial communities associated with *C. rubrum* colonies showing 90% tissue loss displayed distinct structural patterns between all sites (post-hoc tests $0.02 < p < 0.05$; Table S8), except between *Pharillons* and *Boulegeade* (post-hoc test $p = 0.11$; Table S8). Considering all sites together, 53 ASVs were differentially abundant, with 41 ASVs less abundant and 12 ASVs more abundant in the 90% tissue loss condition compared to the 0% tissue loss condition (Fig. 6). Among the dominant ASVs that significantly decreased, the ASV1- *Spirochaetaceae* and ASV5- *Spirochaetaceae* decreased by two to three times in the colonies with 90% tissue loss (ASV1: average relative abundance of 60% and 25% in the 0% and 90% tissue loss condition, respectively, and ASV5: average relative abundance of 10% and 3% in the 0% and 90% tissue loss condition, respectively; Fig. 5 and 6A). The ASVs whose abundance increased in the samples with 90% tissue loss were composed of 42% of *Rhodobacteraceae*, including ASV29 and ASV57 which were 39 times more abundant on average (average relative abundance of 0.015% and 0.36% in colonies with 0% and 90% tissue loss, respectively; Fig. 5 and 6A). When the differential analysis is conducted by site, *Grotte à corail* and *Pharillons* showed a larger number of differentially abundant ASVs between tissue loss conditions (390 and 140 ASVs, respectively) compared to *Riou Sud* and *Boulegeade* (41

and 12 ASVs, respectively; Fig. 6B). Moreover, around 15% of the differentially abundant ASVs in *Grotte à corail* and *Pharillons* belonged to the *Rhodobacteraceae* family, while this percentage dropped to 0.09% in *Riou Sud* and 0% in *Boulegeade*.

In *P. clavata*, differential abundance analyses identified 14 ASVs, including 7 *Endozoicomonadaceae*, that were significantly less abundant in the 90% tissue loss condition compared to the 0% tissue loss condition (Fig.7 and Table S9) The first two differentially abundant ASVs, ASV2- *Endozoicomonadaceae* and ASV6- *Endozoicomonadaceae*, both decreased by two times (ASV2: average relative abundance of 62% and 29% in colonies with 0% and 90% tissue loss, respectively; ASV6: average relative abundance of 7% and 3% in colonies with 0% and 90% of tissue loss, respectively; Fig. 5, 7 and Table S9). Only ASV55-*Rhodobacteraceae* was found to be 44 times more abundant in *P. clavata* colonies with 90% of tissue loss compared to the colonies with 0% tissue loss (Fig. 7 and Table S9). Differential abundance analyses were not done per site due to the insufficient number of samples in certain sites and conditions (≤ four samples).

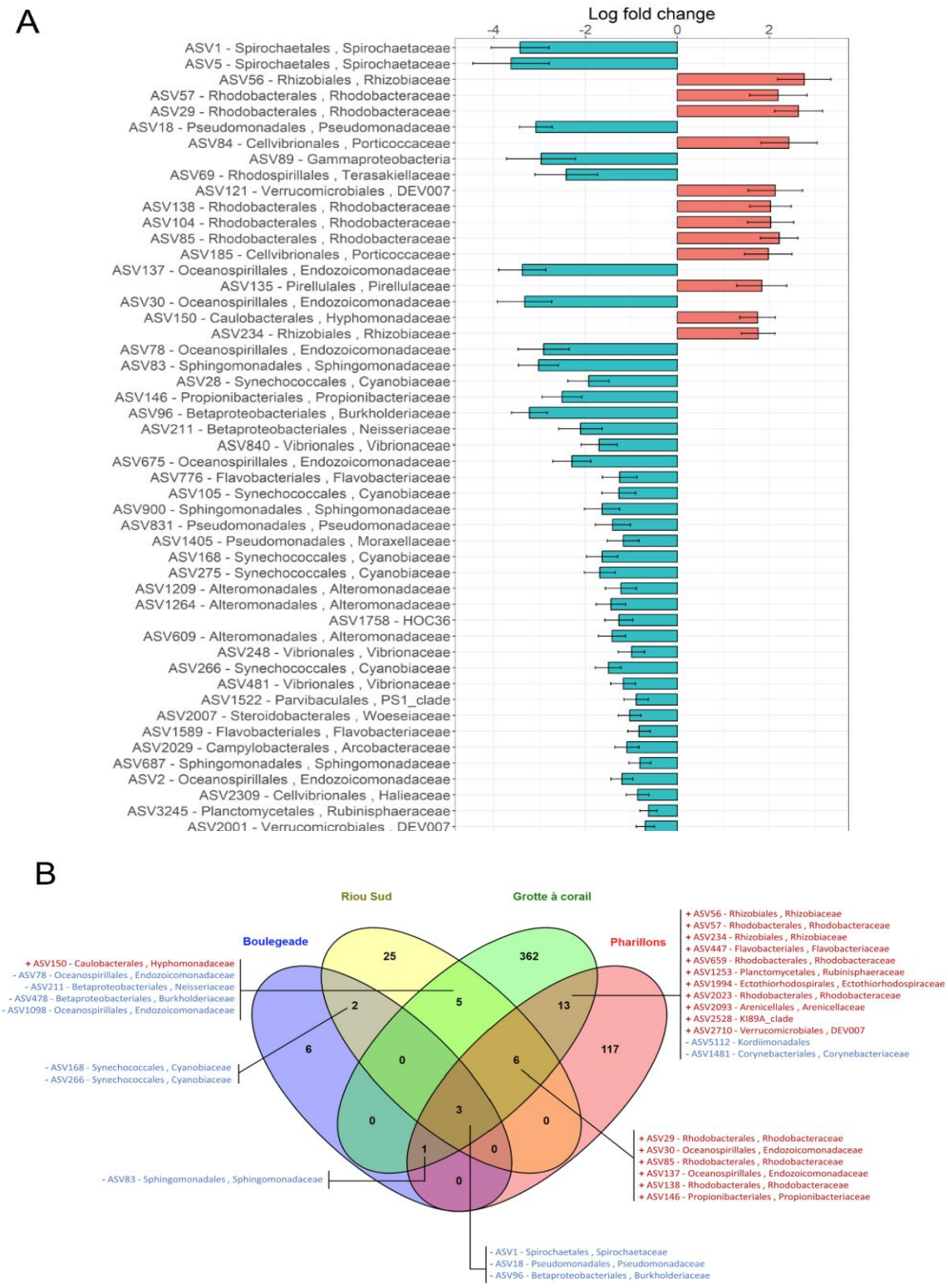

Figure 6: Bacterial ASVs differentially abundant between *C. rubrum* colonies with 0% and 90% tissue loss. (**A**) Difference in relative abundance calculated as log fold change (natural log) in the 90% tissue loss condition compared to the 0% tissue loss condition, all sites combined. (**B**) Venn diagram of the bacterial ASVs differentially abundant between tissue loss percentages and common between sites ('+' in red and '-' in blue indicating a significant increase or decrease of the ASV in the 90% tissue loss condition, respectively).

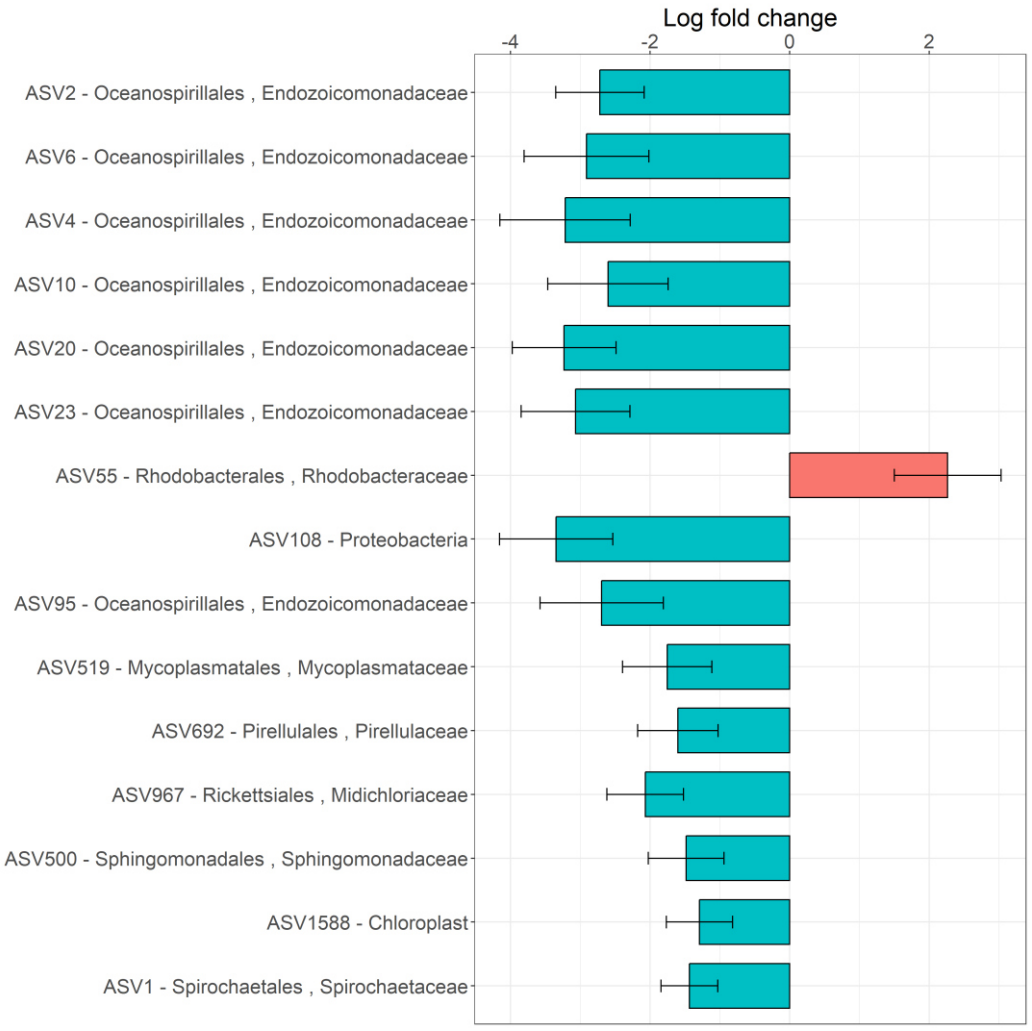

Figure 7: Bacterial ASVs differentially abundant in colonies of *P. clavata* with 0% and 90% tissue loss, all sites combined. The difference in relative abundance is calculated as log fold change (natural log) in the 90% compared to 0% tissue loss condition.

Comparative absolute quantification of specific bacterial taxa based on qPCR analyses

For *C. rubrum*, the total concentration of bacteria per host cell significantly increased in the colonies with 90% tissue loss compared to the colonies showing no tissue loss in *Grotte à corail* ($p = 0.003$; 4 times higher on average in the 90% tissue loss condition) and *Pharillons* ($p = 0.005$; 70 times higher on average in 90% tissue loss condition) (Fig. 8 and Table S13). For *P. clavata*, the total bacterial concentration only increased in the 90% tissue loss colonies collected in *Ile Verte* ($p = 0.005$; 2.8 times higher on average in the 90% tissue loss condition; Fig. 8 and Table S13).

For both octocoral species, the concentration of *Vibrio* per host cell was higher in colonies showing 90% tissue loss compared to colonies with 0% tissue loss in all sites (p values < 0.05; Fig. 8 and Table S13), increasing up to 313 times (*Riou Sud*) and 3126 times (*Portofino*) in *C. rubrum* and *P. clavata*, respectively, in the 90% tissue loss condition.

The concentration of *Spirochaetaceae* per host cell was higher in colonies with 90% tissue loss compared to the colonies with no tissue loss in *C. rubrum* at the sites *Grotte à corail* (p = 0.003; 2.7 times higher on average in the 90% tissue loss condition) and *Pharillons* (p = 0.005; 2 times higher on average in the 90% tissue loss condition) (Fig. 8 and Table S13).

Only in colonies of *P. clavata* from *Portofino*, the concentration of *Endozoicomonas* per host cell was lower in colonies with 90% tissue loss compared to the colonies with no tissue loss (p = 0.01; 14.3 times lower on average in the 90% tissue loss condition) (Fig. 8 and Table S13).

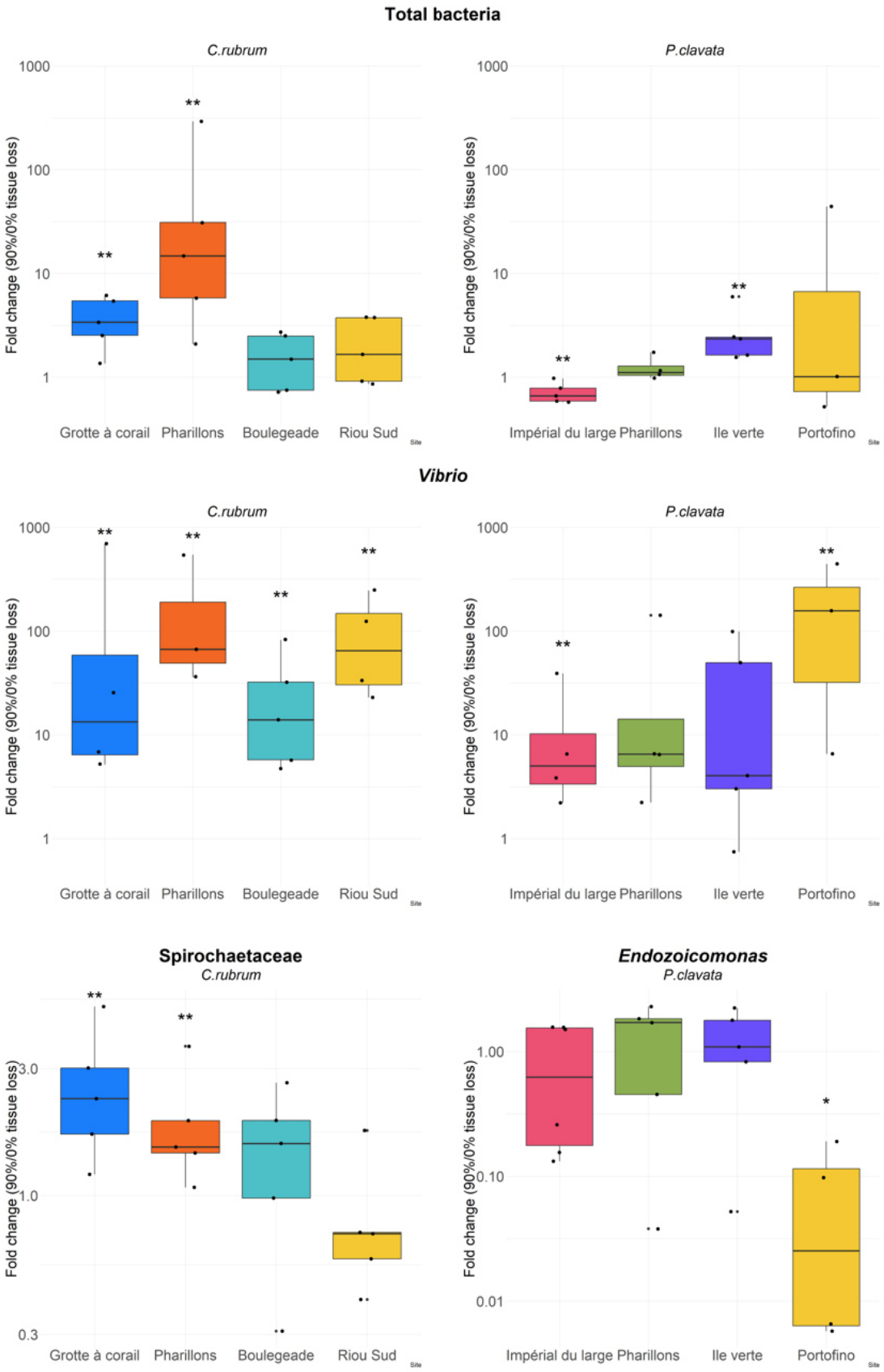

Figure 8: Relative expression ratio (fold change) between the 90% and 0% tissue loss conditions of the different targeted genes. Concentration per host cell of the total bacteria (A), *Vibrio* bacteria (B), *Spirochaetaceae* (C) and *Endozoicomonas* bacteria (D) per site. Graphs are presented in logarithmic scale. Statistical significance levels of differences between octocorals experiencing tissue loss or not are indicated by stars (* for $p < 0.05$ and ** for $p < 0.01$).

Discussion

The aim of this study was to get a clearer picture of the impact of MHWs on MAFs, particularly on the intricate relationship between the tissue loss of Mediterranean octocorals and the observed changes in their associated bacterial microbiome. Therefore, we investigated changes in the microbiota of octocorals following record-breaking MHWs that hit the Western Mediterranean Sea in summer 2022 (Juza et al. 2022; Quade 2022; Grenier et al. 2023), affecting up to 80% of the colonies of the red coral *C. rubrum* and 100% of the colonies of the gorgonian *P. clavata* depending on the site. In this study, we collected samples of *C. rubrum* and *P. clavata* with either 0% or 90% tissue loss at different sites. Using taxon-specific qPCR analyses, we demonstrated that the absolute abundance of the dominant symbionts (*Spirochaetacae* and *Endozoicomonas* in *C. rubrum* and *P. clavata*, respectively) did not change with thermal stress, suggesting that colony tissue loss was not associated with a diminution of their abundance in the microbiome. However, the relative abundance of these symbionts decreased in corals with 90% tissue loss due to a significant increase in the total abundance of other bacteria, including putative pathogens such as *Vibrio* and *Rhodobacterales*. Taken together, our study suggests that octocoral tissue loss during MHWs is due to the combination of heat stress and overgrowth of putative pathogenic bacteria. Finally, we found a site- and species-specific response of the octocoral microbiome to heat stress. While *C. rubrum* was more affected at the shallowest (and warmest) depths, the greatest changes in the microbiome of *P. clavata* were not related to temperature alone. These findings contribute to our understanding of the intricate relationships between host organisms, their microbiota and environmental stressors, and provide valuable insights into the impact of MHWs on MAFs in the Mediterranean Sea.

The 2022 Mediterranean heatwaves: the worst ever recorded

An analysis of seawater temperature records in *Riou Sud* (Marseille) at 15 and 30 m depths shows that the summer of 2022 was the warmest in the last 20 years. While temperatures above 24°C had never been measured at 30 m depth before 2022 and only on a maximum of four days per year at 15 m depth (in 2009 and 2012), the year 2022 showed three and ten days with temperatures above 24°C at 30 and 15 m depth,

respectively, indicating that the water column warmed for the first time on record down to 30 m depth in Marseille. Laboratory experiments have identified a temperature of 23-24°C as a thermal threshold for many Mediterranean octocoral species, above which tissue loss and mortality have been observed (Previati et al. 2010; Haguenauer et al. 2013; Tignat-Perrier et al. 2022; 2023; Torrents et al. 2008; Cau et al. 2018). Thus, after several months (from May to September 2022) of exposure to MHWs, many octocoral colonies showed impaired health and tissue loss throughout the Northwestern Mediterranean Sea (Grenier et al. 2023; Estaque et al. 2023). A significantly higher percentage of affected colonies of octocorals has been observed at shallower depths than at greater depths in the Calanques National Park (Marseille) (Estaque et al. 2023), suggesting that octocoral tissue loss is closely related to the duration and magnitude of thermal stress as observed in tropical corals (Leggat et al. 2022; Evensen et al. 2023; Aichelman et al. 2021). However, visual observation of the tissue showed that not all colonies were in the same state of health, as some showed 90% tissue loss or were dead, while other colonies showed 0% tissue loss. Within a population, this could be due to small-scale differences in water flow and 'perceived' temperature (Brown et al. 2023), food availability (Ezzat et al. 2019) or host genotype (Palacio-Castro et al. 2022; Kavousi et al. 2020). To explore whether changes in the bacterial microbiome could explain the observed tissue loss in Mediterranean octocorals, we examined bacterial abundance variations in colonies with 0% and 90% tissue loss. Even if the observed microbiome changes could be either responses to environmental shifts or the tissue loss itself, or potentially drivers of the tissue loss, the results suggest that the microbiome may influence host resilience or recovery, ultimately contributing to an explanation for the observed tissue loss in Mediterranean octocorals.

Colony tissue loss is not associated with a decrease in the abundance of the main bacterial symbionts

The bacterial microbiome of colonies with 0% tissue loss showed a high relative abundance of the main symbionts, comparable to non-stressed or healthy colonies, which are dominated by *Endozoicomonas* in *P. clavata* (van de Water et al. 2017; La Rivière et al. 2015; Ransome et al. 2014) and *Spirochaetaceae* in *C. rubrum* (van de Water et al. 2016; 2018), regardless of depth, season, or geographic location. The absence of tissue loss or significant changes in the microbiota suggests that these colonies were

potentially healthy at the time of sampling, even if they should have suffered from heat stress, as thermal anomalies were recorded to depth of 30 m. It would have been interesting to tag these colonies and revisit them after the MHWs to assess their overall well-being. If they continued to show no tissue loss later in the season, these colonies may represent heat stress resistant genotypes that warrant in-depth characterization.

In octocoral colonies with 90% tissue loss, we observed a significant decrease in the relative abundance of the main symbionts compared to those with 0% tissue loss (47% and 38% decrease for *C. rubrum* and *P. clavata*, respectively). This is in agreement with previous observations of a decrease in the relative abundance of the dominant bacteria in the microbiome of heat-stressed corals (Tignat-Perrier et al. 2022; Voolstra et al. 2021; Woo 2021; Palacio-Castro et al. 2022). However, this pattern is not always associated with tissue loss, as evidenced in recent studies of Tignat-Perrier et al. (2022; 2023) and Corinaldesi et al. (2022) on Mediterranean octocorals. This inconsistency is maybe due to the fact that the relative quantification of the symbionts does not accurately reflect actual changes occurring within the microbiota (Damhorst et al. 2021; Galazzo et al. 2020), and the quantification of the absolute abundance of symbionts is necessary to understand microbial dynamics.

A limited number of studies have investigated the response of coral symbionts by absolute quantification of microbiota members, primarily due to the challenge of designing taxa-specific primers caused by the lack of knowledge regarding the genomes of most symbionts (Shiu et al. 2020; Pogoreutz et al. 2022). In this study, the use of primers specific to the *16S rRNA* gene of *Spirochaetaceae* and *Endozoicomonas* revealed that colonies with 90% tissue loss did not exhibit a significant decrease in the abundance of their dominant symbionts. Instead, our study provides compelling evidence that the decline in the relative abundance of the dominant symbionts within colonies of *C. rubrum* and *P. clavata* experiencing tissue loss is, in most cases, due to the proliferation of opportunistic bacteria (saprophytic or commensal) on the octocoral tissue (Fig. 9). This pattern is largely observed in colonies sampled in Marseille. However, *P. clavata* colonies collected in *Portofino* actually showed a decrease in the absolute abundance in *Endozoicomonas* as well as the most significant changes in bacterial community composition, despite being at the deepest and coldest collection site. This suggests that

P. clavata populations from *Portofino* might be more susceptible to heat stress, or that other factors could have altered their microbiota. For example, *Vibrio* bacteria, which has been monitored by qPCR, increased 120 times more in *P. clavata* colonies collected in *Portofino* in comparison to the ones sampled in Marseille, suggesting that the overgrowth of opportunistic bacteria could have been more important in the *Portofino* population. *P. clavata* has been identified as particularly sensible to stress-related diseases, which may explain this overgrowth of opportunistic bacteria, and the higher impact of the MHWs (Tignat-Perrier et al. 2022; Previati et al. 2010; Bally et al. 2007) on this coral species. Additionally, the Portofino Marine Protected Area is known to be exposed to various anthropogenic stressors, including water contamination and organic matter enrichment (Di Carro et al. 2018; Misic et al. 2011; Paliaga et al. 2020), which could have represented additional stressors for *P. clavata* colonies during MHWs. In Marseille, none of the octocoral colonies showed a decrease in the absolute abundance of the dominant symbionts after the 2022 MHWs. Changes observed in the microbiome were directly related to the thermal stress intensity. Indeed, the colonies of *C. rubrum* which displayed the most substantial changes in the composition of the bacterial communities between colonies with 0% and 90% tissue loss as well as the highest alpha diversity in both 0% and 90% tissue loss conditions, were sampled in the shallowest sampling sites (*Grotte à corail*-15 m depth and *Pharillons*-23 m depth), which were also the warmest.

The lack of substantial decrease in the absolute abundance of the dominant symbionts (*Spirochaetaceae* in *C. rubrum* and *Endozoicomonas* in *P. clavata*) in the Marseille populations suggests that there is a promising potential for these octocorals to restore their microbiota to a 'healthy' state after the MHWs, if their functions remain unaffected. This recovery process may occur rapidly in colonies with 0% tissue loss, or within the remaining tissue in colonies with 90% tissue loss. Future studies should consider the recovery of microbiota after MHWs to identify potential reversals, in microbiome community composition but also in their functions. Functional profiling of the microbiome (e.g., metagenomic and metatranscriptomic analyses) would allow to document changes in gene presence or expression and identify actively participating members of the microbiome.

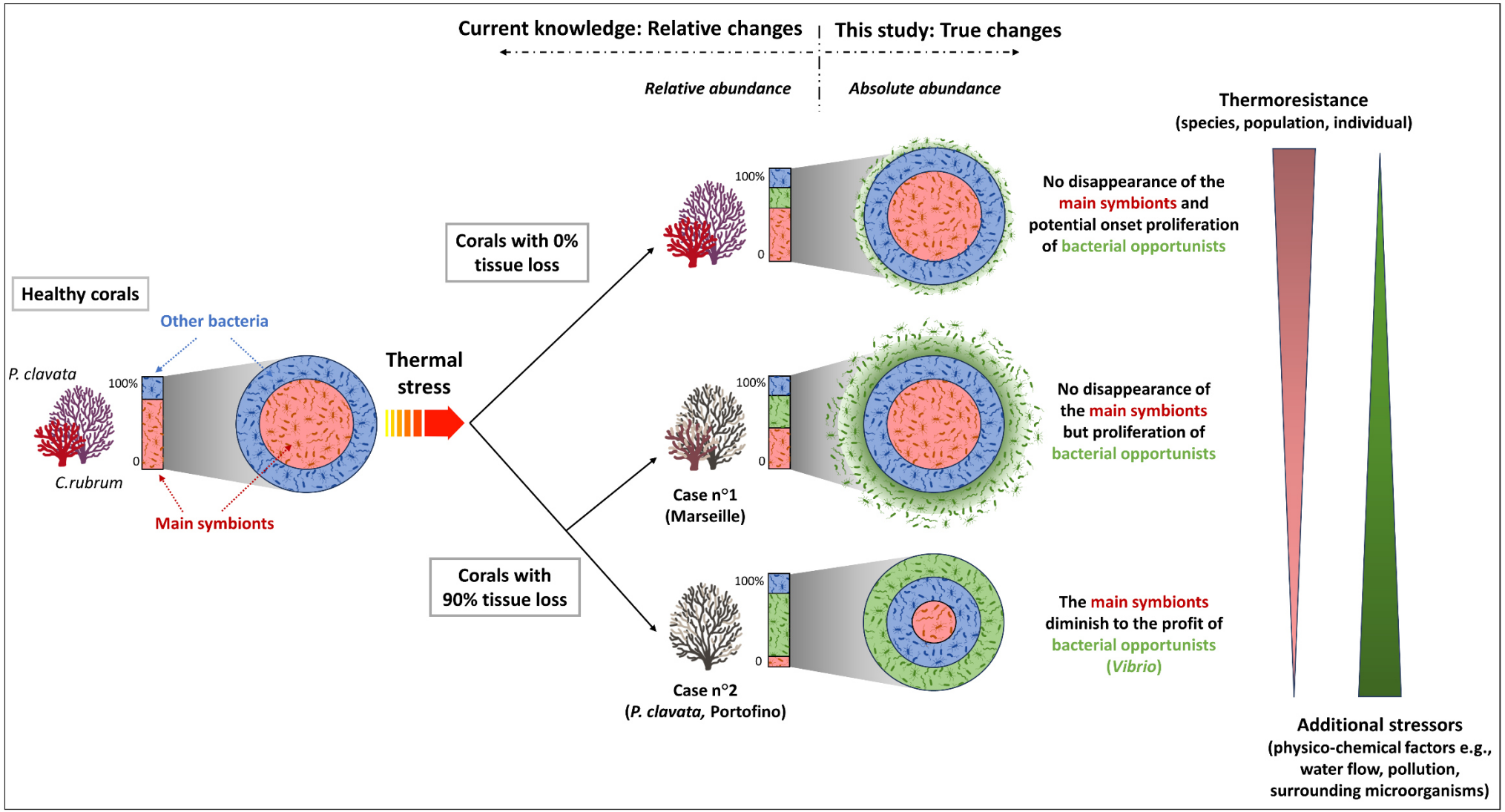

Figure 9: Differential responses of the octocoral microbiota to the marine heatwaves of 2022. By providing complimentary qPCR-based data to amplicon sequencing information, our study brings valuable insight on the microbiota changes occurring in two octocoral species experiencing the marine heatwaves of 2022. Biological and environmental factors were also identified as putative drivers of the differential responses

Octocoral tissue loss is associated with a relative increase in *Rhodobacterales* and site-specific bacterial opportunists

In colonies with 90% tissue loss, we observed a significant increase in bacterial diversity, which is likely attributed to the proliferation of opportunistic bacteria. The shift towards a more diverse bacterial community is a commonly observed phenomenon in heat-stressed organisms (De Castro-Fernández et al. 2023; Rubio-Portillo et al. 2021; Strano et al. 2023; Tignat-Perrier et al. 2022; 2023), including octocorals and may be a consequence of the temperature-induced changes in the bacterial growth dynamics and/or the octocoral loss of control over the microbiota (Jessen et al. 2013; Rubio-Portillo et al.2021; McDevitt-Irwin et al. 2017). Among the opportunistic bacteria, *Vibrio sp.* have been shown to frequently increase in the microbiota of heat-stressed corals (Tout et al. 2015; Tignat-Perrier et al. 2022; Martin et al. 2002). Although the sequencing results did not reveal an increase in the relative abundance of *Vibrio sp.* in octocorals with 90% of tissue loss, we observed a significant increase in the qPCR based-absolute abundance of these bacteria (464 and 487 times increase on average in *C. rubrum* and *P. clavata*, respectively), regardless of the sampling site. The impact of the proliferation of *Vibrio sp.* on coral stress tolerance and mortality however remains largely unknown, but some *Vibrio sp*. have been shown to be pathogenic for corals (Sun et al. 2023; Martin et al. 2002). Additionally, we observed a higher relative abundance of *Rhodobacterales* in the microbiome of *P. clavata* and *C. rubrum* colonies with 90% of tissue loss in the Calanques National Park (Marseille). *Rhodobacterales* have a widespread distribution in various oceanic regions and are particularly prevalent as primary surface colonizers in temperate coastal waters (Dang et al. 2008). They exhibit a capacity to thrive and multiply during phytoplankton blooms that often occur during heatwaves, as they can use newly generated organic matter by attaching themselves to marine particles (Buchan et al. 2014). Furthermore, *Rhodobacterales* have been implicated in coral diseases, including tissue loss diseases that affect stony corals (Rosales et al. 2023; 2020; Clark et al. 2021; Gajigan et al. 2017). Hence, the potential relative increase of these bacteria, if confirmed to correspond to an actual increase in absolute abundance, could potentially contribute to the observed tissue loss in our colonies. However, further research is necessary to confirm this hypothesis.

Bacteria that proliferated within the microbiome of colonies exhibiting 90% tissue loss were site-dependent, suggesting that both the surrounding physicochemical conditions and the seawater microorganisms may play a role in the observed bacterial changes. It also suggests that coral tissue loss is not associated to specific pathogens. The variation in seawater bacterial communities and the prevalence of specific bacteria in the vicinity of the colonies might have influenced the diversity of opportunistic bacteria that thrived within the stressed octocoral microbiota. Indeed, no *Rhodobacterales* were observed in *Portofino* samples, although *P. clavata* colonies lost their tissue to the same extent as those sampled in Marseille. In particular, the microbiota of the *Portofino* gorgonians showing tissue loss was characterized by a large increase in the relative abundance of *Alteromonadales* and *Flavobacteriales*, a group of species associated with tissue loss in tropical corals (McDevitt-Irwin et al. 2017; Meyer et al. 2019; Rosales et al. 2023).

Conclusion

Our study sheds light on the complex dynamics of the coral's microbiota in response to the 2022 MHWs, which severely affected Mediterranean octocorals down to 30 m depth. The results highlight the importance of considering both relative and absolute quantification methods when assessing the effects of thermal stress on the coral microbiome. Based on the measurements of the absolute abundance of the total bacteria and specific taxa, we showed that the abundance of the main symbionts was not affected in most colonies showing 90% tissue loss, and we suggest that octocoral tissue loss was probably the consequence of both heat stress and the proliferation of putative pathogens. Still, further studies should investigate the functional changes in the microbiota using a combination of metatranscriptomics and metagenomics, as heat stress might alter the microbiota's functions, for example by down-regulating genes related to metabolic functions that normally benefit the host and the holobiont. The loss of the main symbiont *Endozoicomonas* in *P. clavata* population in *Portofino,* while exposed to smaller thermal anomalies, suggests that additional factors (surrounding physico-chemical factors, seawater microorganisms, host genotypes) than heat stress might have contributed to

the observation of more drastic changes in the microbiota. Considering the above suggestions, future studies are urgently needed to elucidate the underlying processes that confer higher thermotolerance to some individuals and populations as the frequency and intensity of MHWs are expected to increase (Smale et al. 2019), threatening the survival of MAFs in shallow and mesophotic habitats.

Chapter 5

Response of the eurakyome of *Corallium rubrum* to the 2022 marine heatwaves



Chapter 5: Response of the eurakyome of *Corallium rubrum* to the 2022 marine heatwaves

I. Overview of the chapter

As described in the previous chapter, global warming is exacerbating marine heatwaves (MHWs), particularly in the Mediterranean Sea, leading to more frequent and severe temperature extremes that affect octocoral populations. There is growing evidence that the health of Mediterranean corals during thermal stress is linked to their bacterial microbiome (Vezzulli et al. 2010a; Corinaldesi et al. 2022; Tignat-Perrier et al. 2022; 2023). However, other microbial partners, such as the microeukaryotes, remain poorly characterized, and their role in coral responses to thermal stress is largely unknown (del Campo et al. 2020; Bonacolta et al. 2023). To date, only one study has investigated the eukaryome of a Mediterranean octocoral, the gorgonian *P. clavata* (Bonacolta et al. 2024). This emphasizes the need for further research to determine how microeukaryotes contribute to coral holobiont health and response to stress.

This chapter investigate the impact of the 2022 MHWs on the microeukaryotic communities of *C. rubrum*. Using *18S rRNA* gene-based metabarcoding, with the primer pairs described in chapter 2 that specifically exclude coral sequences, this study explores how thermal stress alters the richness and composition of the red coral eukaryome. The study is based on *in-situ* sampling of *C. rubrum* colonies in the Mediterranean, conducted during the 2022 MHWs (see in chapter 4) and during the winter of 2023 for the control colonies. Three sampling groups were considered: (1) colonies affected by the MHWs at shallow depths (16-28 m), which experienced severe thermal stress (16-23 days with temperatures exceeding 23 °C) and included both healthy and tissue-loss colonies; (2) colonies from deeper waters (35-37 m), which were less impacted (5-12 days with temperatures above 23 °C) but also displayed both healthy and tissue-loss phenotypes; and (3) control colonies collected in winter 2023 from depths greater than 30 m, which have not been exposed to thermal stress.

While the species richness between the control and the heat-stressed corals was not different, there were considerable differences in the eukaryome composition between the two groups. In particular, Dino-Group I dinoflagellates and Licnophoridae ciliates showed lower abundances under stress, possibly due to their thermosensitivity (Martinez 1980; Karajan et al. 2019). Depth-dependent responses revealed further complexity in the dynamics of the eukaryome. In deep-water corals, exposed to less intense MHW effects, the eukaryome shifted towards an increased presence of Warnowiaceae and Corallicolidae. In contrast, the shallow corals, which were more exposed to thermal stress, exhibited an increased abundance of Ephelotidae and Exobasidiomycetes. These observations highlight the sensitivity of the eukaryome to temperature.

Tissue loss in corals was, however, associated to a significant increase in eukaryotic diversity and beta-dispersion, suggesting a transition toward a more opportunistic microbial community. Key microeukaryotic groups associated with tissue loss included Labyrinthulomycetes and Phaeophyceae. Labyrinthulomycetes are recognized as opportunistic pathogens that can exploit bacterial blooms, potentially exacerbating coral mortality (Raghukumar and Damare 2011; Burge et al. 2012). Phaeophyceae, a brown macroalgae, can promote harmful bacterial growth in bleached tropical corals and are epibionts in necrotic tissue of *Paramuricea clavata* (Chimienti et al. 2021).

The findings of this study show the sensitivity of the eukaryome of *C. rubrum* to MHW-induced heat stress. Furthermore, this chapter highlights the importance of integrating eukaryome data into coral health monitoring for the development of adaptive management strategies in the face of climate change.

II. Publication

Unraveling the Impact of Marine Heatwaves on the Eukaryome of the Emblematic Mediterranean Red Coral *Corallium rubrum*

ISME Communications | January 2025

DOI: https://doi.org/10.1093/ismeco/ycaf035

Camille Prioux[1,2,3], Christine Ferrier-Pagès[3], Javier del Campo[4,5], Laure Guillou[6], Tristan Estaque[7], Denis Allemand[3] and Romie Tignat-Perrier[2,3]

[1]Sorbonne Université, Collège Doctoral, Paris, France

[2]Unité de Recherche sur la Biologie des Coraux Précieux CSM - CHANEL, Centre Scientifique de Monaco, 8 Quai Antoine 1er, MC 98000, Monaco, Principality of Monaco

[3]Centre Scientifique de Monaco, 8 Quai Antoine 1er, MC 98000, Principality of Monaco

[4]Department of Marine Biology and Ecology, Rosenstiel School of Marine, Atmospheric and Earth Science, University of Miami, Miami, Florida, USA

[5]Biodiversitat, Institut de Biologia Evolutiva (CSIC-Universitat Pompeu Fabra), Barcelona, Catalonia, Spain

[6]Sorbonne Université, CNRS, UMR7144 Adaptation et Diversité en Milieu Marin, Ecology of Marine Plankton (ECOMAP), Station Biologique de Roscoff SBR, Roscoff, France.

[7]Septentrion Environnement, Campus Nature Provence, 89 Traverse Parangon, 13008, Marseille, France

Abstract

Global warming is intensifying heatwaves worldwide, resulting in more frequent and severe temperature extremes. This study investigates the impact of the unprecedented 2022 Mediterranean heatwaves on the coral eukaryome, which received

limited attention despite its known importance in the functioning of the coral holobiont. Fifty-six colonies of the Mediterranean emblematic red coral *Corallium rubrum* were collected at different sites, depths and health states. Microeukaryotic communities were analyzed using a *18S rRNA* gene metabarcoding approach, with primers designed to reduce amplification of red coral *18S rRNA* gene sequences while remaining universal for amplifying microeukaryotes. Our results showed that the red coral eukaryome was dominated by Dino-Group I, Licnophoridae and Labyrinthulomycetes in the control sites unimpacted by marine heatwaves. In heat-affected colonies, the composition of the coral eukaryome changed, with an increase in the relative abundances of Ephelotidae, Exobasidiomycetes, Corallicolidae, Labyrinthulomycetes and/or the epibionts Phaeophyceae depending on the intensity of heat stress experienced by the colonies. It was therefore possible to relate the colony's health status to changes in the eukaryome. Finally, we illustrated putative interactions (competition, predator-prey and parasitism relations) that may occur within the *C. rubrum*'s eukaryome and that might explain the compositional changes observed in the microeukaryotic communities under heat stress. Our findings enhance our comprehension of the ecological implications of heatwaves on marine ecosystems.

Introduction

Unicellular microeukaryotes, which include phototrophs, decomposers, predators, and symbionts, are fundamental components of marine and terrestrial ecosystems. As microeukaryotes have varied functional roles, they contribute to the length and connectivity of food webs across trophic levels (Singer et al. 2021; Bachy et al. 2022; del Campo et al. 2020; Bonacolta et al. 2023; Amundsen et al. 2009). In marine environments, ciliates regulate bacterial communities (Mandal 2024), fungi degrade organic matter (Masigol et al. 2019; Tant et al. 2015), and diatoms and dinoflagellates play a central role in the global carbon cycle (Falkowski et al. 1998; Mitra et al. 2014). Microeukaryotes are also a key component of the microbiome in animals, including corals. Together with the host organism and other microbial communities, they form a holobiont which functions as an integrated unit (Ainsworth et al. 2017). In corals, the

microeukaryotic community, or eukaryome, likely plays important roles in processes such as nutrient cycling and immune responses (Ainsworth et al. 2017). However, despite its potential significance, the coral eukaryome remains poorly understood, highlighting the need for more research (Bonacolta et al. 2023).

Symbiotic dinoflagellates from the Symbiodiniaceae family are the most well-studied microeukaryotic partners of corals, providing their host with photosynthates and meeting the majority of its energy requirements (Muscatine et al. 1981; Tremblay et al. 2012). Many other microeukaryotes are associated with corals, although our understanding of these associations is limited. Marine alveolates related to Syndiniales dinoflagellates, particularly the Dino-Group I subgroup, have been shown to dominate the eukaryome of the tropical coral *Pocillopora damicornis* (Clerissi et al. 2018) and the thermally resistant colonies of the Mediterranean octocoral *Paramuricea clavata* (Bonacolta et al. 2024). In *P. damicornis*, their presence in healthy, unstressed colonies suggests a commensal relationship with the coral host. Furthermore, their abundance in *P. clavata* colonies described as thermally resistant raises questions about their potential role in coral heat resistance. Another group of microeukaryotes which are frequently found in corals are the apicomplexan corallicolids. These alveolates are associated with 70% of the coral genera studied with a relative abundance sometimes as high as that of the Symbiodiniaceae (Bonacolta et al. 2023; Kwong et al. 2021; 2019). Despite their heterotrophic behavior and role as human pathogens, such as in the malaria disease, corallicolids appear to be commensals in corals, as they are widely distributed and present in healthy individuals (Bonacolta et al. 2024; Kwong et al. 2019). While pioneering studies have begun to unravel the diversity of coral-associated microeukaryotes, further research is necessary to understand their role in the coral holobiont.

Mediterranean octocorals are good models for studying host-microbiome relationships because they tend to have strong and stable associations with their microorganisms (van de Water, Voolstra, et al. 2018a). Previous studies have shown that bacteria from the Oceanospirillales family (*i.e.*, *Endozoicomonas*) or from the Spirochaetaceae family constitute more than 50% of the bacterial community in gorgonians (Bayer et al. 2013a; van de Water et al. 2017; 2018) and in the precious red coral *Corallium rubrum* (van de Water et al. 2017; 2016), respectively. The coral

microbiome remains highly stable through time and space, except during thermal stress when the coral health is impaired (Corinaldesi et al. 2022; Vezzulli et al. 2010a; Prioux et al. 2023; Tignat-Perrier et al. 2022; 2023; Estaque et al. 2024). Research has therefore linked the health of the Mediterranean corals to the decline in the main bacterial symbionts and the presence of pathogenic or opportunistic bacteria (Vezzulli et al. 2010a; Prioux et al. 2023; Tignat-Perrier et al. 2022; 2023; Estaque et al. 2024). However, only one study was conducted on the octocoral eukaryome (Bonacolta et al. 2024). This experimental study investigated the eukaryome of the Mediterranean gorgonian *P. clavata* prior to heat stress exposure, and subsequently recorded coral mortality rate. It was found that thermally resistant gorgonians had an eukaryome enriched with Dino-Group I Clade 1, while thermally susceptible gorgonians had an eukaryome enriched with apicomplexan corallicolids. This suggests that certain microeukaryotes, such as Dino-Group I, may contribute to holobiont fitness. However, as the study did not analyze the microeukaryotic communities during or after the heat stress event, it does not allow an understanding of the heat-induced changes occurring in the coral eukaryome.

In light of the pioneering findings by Bonacolta et al. (2024), and given the increasing die-off of corals in the Mediterranean Sea due to ocean warming (Cerrano et al. 2000; Estaque et al. 2023; Garrabou et al. 2009a), it is crucial to further investigate changes in the microeukaryotic communities associated with corals under experimental heat stress and natural marine heatwave events. Coral populations are facing repeated mass mortality events (Cerrano et al. 2000; Estaque et al. 2023; Garrabou et al. 2009a), caused by the increasing frequency, duration and intensity of marine heatwaves (MHWs) due to climate change (Darmaraki 2019; Darmaraki et al. 2019; Omneya et al. 2021; Juza et al. 2022). In 2022, the north-western Mediterranean Sea experienced three to seven MHWs between May and September, leading to local sea surface temperature anomalies of up to 4.3°C above the summer average and exceeding the previous maximum of +2–3°C recorded during the 2003 MHWs (Guinaldo et al. 2023; Quade 2022; T-MEDNet 2023). The harmful impacts of the MHWs have been mostly felt above 30 m depth, where the Mediterranean seawater temperatures exceeded 23°C-24°C and affected coral health (Tignat-Perrier et al. 2023). In contrast, coral populations living below 30 m depth

remained relatively unaffected by MHWs as the temperature did not exceed 23°C (T-MEDNet 2023).

To better understand the impact of heat stress on the coral eukaryome, we studied the changes occurring in the microeukaryotic communities associated with the Mediterranean red coral *Corallium rubrum* (Linnaeus, 1758), during the 2022 MHWs. Together with other octocoral species, *C. rubrum* is one of the ecosystem engineer species of the Mediterranean marine animal forests, which provide complex habitats for numerous organisms and therefore contribute significantly to biodiversity (Ponti et al. 2019; Rossi et al. 2017c; Paoli et al. 2017). We collected *C. rubrum* samples at different locations from colonies affected by the MHWs of the summer 2022 (16-28 m depth) and from mesophotic colonies deep enough to escape MHWs (35-37 m depth). We also collected control colonies in winter 2023. Using a *18S rRNA* gene metabarcoding approach with specific primers which excluded the red coral *18S rRNA* sequences, we aimed to gain a comprehensive overview of the eukaryome of *C. rubrum* and assess the impact of thermal stress disturbances on the associated microeukaryotic communities.

Material and Methods

Study areas, sample collection and biological material

Sampling was conducted at the end of the summers of 2022 (September-November) and 2023 (November), after severe marine heatwave events (MHWs) at three locations in the NW Mediterranean Sea, within the photic (from 16 m to 28 m depth) and mesophotic zone (from 35 to 37 m depth; Figure 1). Corals of different health conditions were collected depending on the site (as detailed below). Hourly seawater temperature measurements in these locations were extracted from the T-MEDNet database (www.t-mednet.org) and from Somlit (www.somlit.fr), covering the entire depth range (Figure 2). During the summer, seawater temperatures above 30 m depth frequently exceeded 23°C-24°C, which are known to be detrimental to the health of *C. rubrum* (Figure 2; Tignat-Perrier et al. 2023). In contrast, temperatures below 30 m depth remained below 23°C. Thus, mesophotic sites below 30 m depth were designated as control sites, while sites

above 30 m depth were considered as MHW-impacted sites. Red coral colonies collected from the latter sites were considered as heat-stressed colonies.

Heat-stressed samples of *C. rubrum* were collected in MHW-impacted sites (<30 m) in September 2022 in the Calanques National Park (Marseille, France) and in October 2022 in the *Portofino* Marine Protected Area (Italy), with the consent of the respective park authorities (Figure 1). In Marseille, 48 individual samples of *C. rubrum* (3 cm long), showing different health status (0% or 90% tissue loss), were collected at four sampling sites: *Grotte à corail* (16 m depth), *Pharillons* (23 m depth), *Boulegeade* (25 m depth), and *Riou Sud* (28 m depth), according to the protocol described in Prioux et al. (2023). At these sites, temperatures reached 23°C during 23 days at 15 m depth and 5 days at 30 m depth (*Riou Sud*, Calanques National Park, Marseille, France; Figure 2).

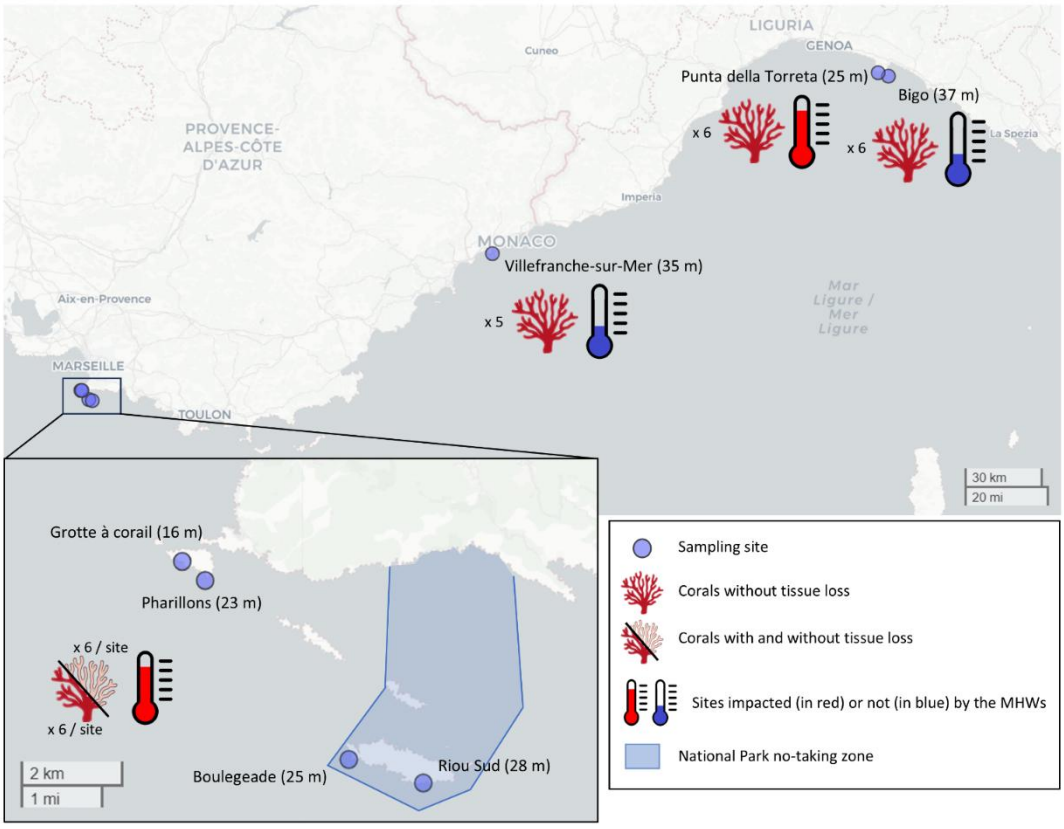

Figure 1: Locations of the different sampling sites. Colony health condition (with or without tissue loss) and intensity of the MHWs are indicated for each site.

In Portofino, at the MHW-impacted site *Punta della Torreta* (25 m), 6 samples of 3 cm in length from different colonies were collected, which showed no tissue loss. At this

location and depth, corals experienced 12 days with temperatures exceeding 23°C (Marine Protected Area, Portofino, Italy; Figure 2). Additionally, six replicates of 1 L seawater were collected and filtered through 0.2 µm Whatman Nuclepore Track-Etched filters (Sigma-Aldrich), with the retentate stored in RNAlater at 4°C.

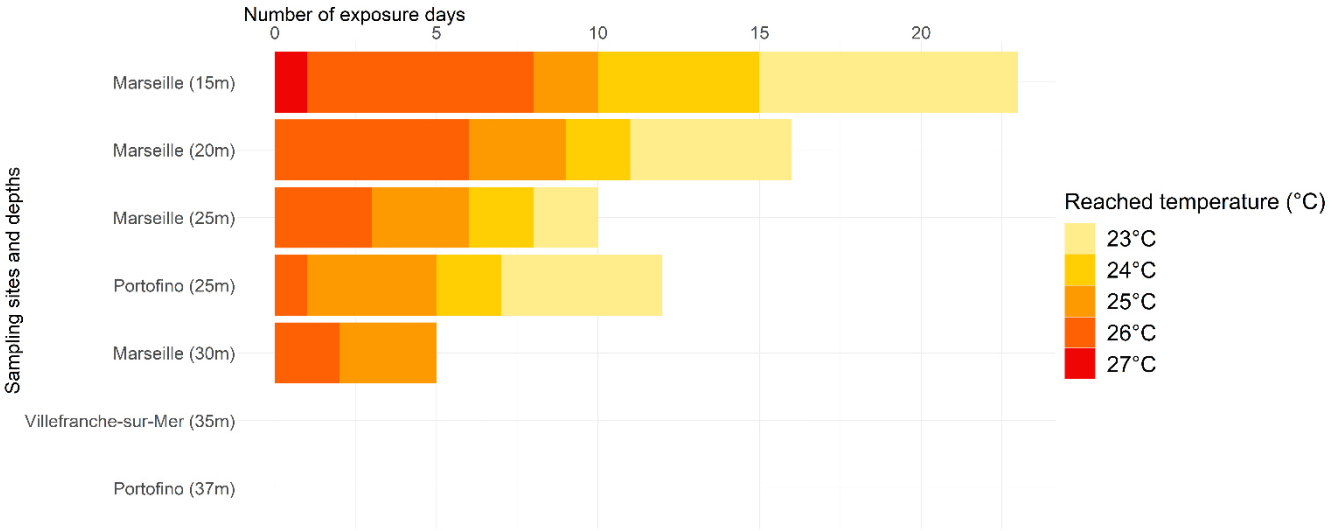

Figure 2: Number of days for which temperatures reached 23°C in the different sampling sites and depths, in 2022 (Marseille, Portofino) or 2023 (Villefranche-sur-Mer). Values of seawater temperature were extracted from the T-MEDNet database (www.t-mednet.org) at Riou Sud (Calanques National Park, France, 2022) and Portofino (MPA, Italy, 2022) and from Somlit (www.somlit.fr) at Villefranche-sur-Mer (Point B, France, 2022 and 2023).

Two sets of control samples of *C. rubrum* were collected in the mesophotic zone (>30 m; control sites or sites unaffected by MHWs) in the *Portofino* Marine Protected Area (MPA, Italy) in October 2022 (concurrently with the samples collected at <30 m depth) and in *Villefranche-sur-Mer* (France) in November 2023 (Figure 1). In *Portofino*, 6 samples of 3 cm in length from different colonies with no signs of tissue loss were collected at the site *Bigo* (37 m), where temperatures remained below 23°C in 2022 (MPA, *Portofino*, Italy; Figure 2). Six replicates of 1 L seawater were also collected and filtered through 0.2 µm Whatman Nuclepore Track-Etched filters (Sigma-Aldrich), with the retentate stored in RNAlater at 4°C. In *Villefranche-sur-Mer,* 5 samples of 3 cm in length, with no signs of tissue loss, were collected at a depth of 35 m, where temperatures remained below 23°C in both 2022 and 2023 (Point B, *Villefranche-sur-Mer*, France; Figure 2). All coral samples were immediately placed in separate Ziploc® plastic bags containing natural seawater after collection. Onboard, the samples were transferred to Eppendorf tubes, flash-frozen

in liquid nitrogen (~ 190°C, ©CX100 Worthington Industries) and then stored at – 80°C in the lab until further processing.

DNA extraction

Genetic material was extracted from approximately 1.5 cm of tissue using the DNeasy PowerBiofilm kit (QIAGEN, Hilden, Germany) with some adjustments. During cell lysis, 2 µL of proteinase K (600 U/ml) was added to each sample, followed by an incubation period of 2 hours at 60°C. Subsequently, bead beating was performed for 2 min using the CryoMill (Retch, Germany) set at a frequency of 30 Hz at room temperature. DNA concentration was determined using a Qubit fluorometer, and the extracted DNA was stored at -20°C.

MiSeq amplicon sequencing of the *18S rRNA* gene

Design of primers targeting the eukaryotic V4 region and minimizing host signal

Previous studies on the coral microbiome (Clerissi et al. 2018; Bonacolta et al. 2024; del Campo et al. 2019) have shown that the different universal *18S rRNA* gene primer pairs amplify the coral host sequences over the microeukaryotic sequences which are in fewer numbers. We tested the universal *18S rRNA* gene primers TAReuk454FWD1 (5'-CCAGCASCYGCGGTAATTCC-3') and TAReukREV3 (5'-ACTTTCGTTCTTGATYRA-3'), which target the V4 region (Stoeck et al. 2010), and mainly obtained reads corresponding to the red coral sequences (99,96% of reads were coral-derived; Supp. File 2 Table S1 and Figure S2).

To overcome this bias, we used customized primers derived from the UNonMet-PCR primers targeting the V4 region of the *18S rRNA* gene, initially described in Bower et al. (2004) and further validated for Illumina amplicon sequencing by del Campo et al. (2019). Originally, the UNonMet-PCR primers were designed to reduce the signal from metazoan hosts while amplifying that of microeukaryotes. Because these primers did not successfully reduce the signal from *C. rubrum* (Supp. File 2 Table S1), new primers, named 18S-NonMet_Cr-F (5'-AAGTCTGGTGCCAGCASCC-3') and 18S-NonMet_Cr-R (5'-TTTAAGTTTCAGCCTTGCGAT-3'). The NonMet_Cr-F primer was modified from the UNonMet-PCR forward primer, while the 18S-NonMet_Cr-R primer was fully designed. We

used a manually curated database containing 544 *18S rRNA* gene sequences from a diverse array of eukaryotes, including *C. rubrum* and microeukaryotic lineages previously detected in coral microbiota and available from the nr (non-redundant) nucleotide database of NCBI. Each nucleotide in the designed primers was carefully screened to ensure maximum dissimilarity to *C. rubrum* sequences within the V4 region while simultaneously maintaining universality to target microeukaryote sequences, particularly paying attention to lineages yet described as being part of coral microbiome in previous literature. The alignment of the primers on the database is available as Supp. file 1.

In-silico PCRs were done against the sequences from the PR2 microeukaryotic database (https://app.pr2-primers.org/pr2-primers/; v. 2.0.0) using the newly designed primers 18S-NonMet_Cr to test their universality in targeting the different microeukaryotic taxonomic groups. A sequence was considered amplified by the primers set if each primer had ≤ two mismatches with the sequence, and the percentage of sequences amplified for each microeukaryotic taxonomic group was calculated. As a comparison, the same analysis was done using the universal primers TAReuk454FWD1 and TAReukREV3 known to amplify the *18S rRNA* gene V4 region of both microeukaryotes and eukaryotes (Stoeck et al. 2010).

Library preparation and sequencing

PCR reactions were performed on coral and seawater samples along with three negative controls. They were done in a total volume of 25 µL. The reaction mixture comprised 5 µL of the 5X Q5® reaction buffer, 0.5 µL dNTPs, 1.25 µL of each of the forward and reverse primers with Illumina adaptors (10 µM), 0.25 µL of the Q5® High-Fidelity DNA Polymerase, and 2 µL of genomic DNA (or DNA-free water for negative control). Cycle parameters involved an initial denaturation at 98°C for 30 s, followed by 35 cycles of denaturation at 98°C for 10 s, annealing at 63°C for 30 s, and extension at 72°C for 30 s, with a final elongation step at 72°C for 2 min. For comparison purpose, PCRs using the universal *18S rRNA* primers (Stoeck et al. 2010) with Illumina adaptors were also done on the DNA of four coral samples from the dataset. An agarose gel electrophoresis was performed on the PCR products to confirm successful amplification (Figure S1). DNA fragments with the expected size (~500-730 bp) were excised from the gel and purified using the GFX™ PCR DNA and Gel Band Purification kit (Illustra™). DNA concentration was

determined using a Qubit fluorometer and amplicons were sent to STAB-VIDA (Portugal) for a paired-end sequencing (2 × 300 bp, 600 cycles) with the V3 chemistry on an Illumina MiSeq platform. All further steps of the amplicon library preparation were conducted using Illumina's standard "16S Metagenomic Sequencing Library Preparation" protocol (Illumina 2013). The fastq files containing the raw sequencing data have been deposited in the NCBI's Short Read Archive (SRA) under the BioProject accession number PRJNA1147612.

Bioinformatics data processing

The *18S rRNA* gene amplicon data were processed using the DADA2 pipeline (version 1.16; https://benjjneb.github.io/dada2/index.html; Callahan et al. 2016). Sequencing resulted in 7,899,126 reads ranging from 51,974 to 153,314 reads per sample (Supp. File 2, Table S2). Negative controls contained from 1,104 to 123,664 reads per sample. Primer sequences were trimmed at the 5'-end of each read using Cutadapt v3.1 (Martin 2011).

Read quality profiles were inspected, and reads were filtered and trimmed with the following settings: maxN=0, rm.phix=TRUE, maxEE=c(2,2), truncLen=c(298,240). As the size of most of the amplicons exceeded 600 bp (Supp. Figure S4), only 10% of reads successfully merged on average, with 35% of the samples having a merging ratio below 5% (Supp. File 2 Table S3). Following this observation, it was decided neither to merge nor to use R1 reads only but concatenate R1 and R2 reads using mergePairs(justConcatenate=TRUE) as it could offer a slight improvement in taxonomic resolution (Dacey and Chain 2021). Error rates were computed and used for sequence inference. An amplicon sequence variant (ASV) table was constructed based on concatenated and de-noised reads. Chimeras were detected and removed from the table using the removeBimeraDenovo() function. The number of reads and sequences per sample passing through the different steps of the pipeline is presented in Supp. File 2 Table S3.

Taxonomy was assigned to the 14,495 ASVs using the assignTaxonomy() function and the PR2 reference database v4.13.0 (Guillou et al. 2012). The ratio between the number of sequences assigned to microeukaryotic ASVs (*i.e.*, removing sequences

corresponding to Metazoa ASVs) and all sequences was calculated for both primer sets (*i.e.*, the newly designed 18S-NonMet_Cr primer set and the universal *18S rRNA* gene primer set TAReuk454FWD1 and TAReukREV3).

ASVs corresponding to Metazoa and Embryophyceae were then removed from the dataset, resulting in 8188 ASVs across eighty samples (Supp. File 2 Table S4). The ASV table and metadata are available in Supp. File 2 as Tables S5 and S6, respectively, and the sequences of the ASVs are available as Supp. File 3. Highly abundant ASVs from coral samples (ASV4, ASV5, ASV13, ASV18, ASV20, ASV21, ASV40, ASV41, ASV49 and ASV71) underwent BLAST analysis to assess their similarity to previously documented sequences deposited in the nr nucleotide database of NCBI. Detailed results from these analyses can be found in Supplementary File 4.

All statistical analyses were conducted in the R environment (version 4.2.1) using the R-package *phyloseq* (McMurdie and Holmes 2013). The R-package *decontam* (Davis et al. 2018) was used to identify contaminant ASVs in the samples based on the negative control samples (isContaminant function), however, no ASVs were identified as contaminants. Observed species richness and evenness (Shannon index) were calculated using the R-package *vegan* (Oksanen et al. 2022).

Alpha diversity analyses were conducted on the unrarefied ASV count table, given that rarefaction curves mostly reached the plateau (Figure S2) and the current debate concerning the applicability of unrarefied versus rarefied data (McMurdie and Holmes 2014; Willis 2019). Differences in observed richness and Shannon index were explored by fitting a generalized linear model (GLM) using a negative binomial distribution and a normal distribution, respectively. Two models were considered: one including the sampling site as a fixed factor on samples without tissue loss, and another including both sampling sites and tissue loss condition as fixed factors for samples collected in Marseille. The interaction term was excluded from consideration due to its lack of significance (Supp. File 2 Table S7). Post-hoc tests were performed to identify potential pairwise differences (R-package *emmeans*, Lenth 2023).

To examine potential changes in the composition of the microeukaryotic communities of *C. rubrum* across sampling sites and tissue loss conditions,

compositional data based analyses (CoDA; Gloor et al. 2017; Quinn et al. 2018) were used. The raw ASV abundances underwent a center log-ratios (clr) transformation using the R-package *compositions* (van den Boogaart and Tolosana-Delgado 2008a). Zero counts were imputed via Bayesian multiplicative replacement (Bayes-LaPlace BM method) using the cmultRepl() function in the R-package *zCompositions* (Palarea-Albaladejo and Martín-Fernández 2015). An Aitchison distance matrix was constructed by computing the Euclidean distance between samples using the clr-transformed data table. Principal component analyses (PCA) and permutational multivariate analysis of variance (performed with the adonis() function from the R-package *vegan*) were carried out to assess variations in the microeukaryotes community structure between groups of sites, *i.e.* control versus MHW-impacted sites and between deep (≥25 m depth) versus shallow (<25 m depth) MHW-impacted sites, and between colonies without and with 90% tissue loss (Supp. File 2 Table S8). Subsequently, potential pairwise differences were examined using the permanova_pairwise() function from the R-package *ecole* (Smith 2021), with p-values adjusted for false discovery rate (Supp. File 2 Table S8).

All graphs for alpha and beta diversity were done using R-package *ggplot2* (Wickham 2016). For the representations of the composition of the communities (*i.e.*, barplot and bubble plot), replicates of each Condition-Site couple were merged by averaging the counts of each ASV or family across all samples using the merge_samples() function from the R-package *phyloseq* (McMurdie and Holmes 2013). Following this, the transform_sample_counts() function was applied to normalize the data, converting raw counts into relative abundances.

Differential abundance analyses were performed to identify ASVs that were differentially abundant between sampling sites and tissue loss conditions using the R-package *ANCOM-BC* ((Lin and Peddada 2020; version 02–2023; ancombc2() function using prv_cut = 0.1 and alpha = 0.05; pairwise = TRUE for sampling sites; Supp. File 2 Table S9 and S10). The core eukaryome of the red coral colonies showing no tissue loss was identified using the core_members() function at the ASV level (arguments: detection = 0.01, prevalence = 98/100, include.lowest = FALSE) from the R-package *microbiome* (Lahti et al. 2017) and a custom made function with the R-package *dplyr* (Wickham and Francois 2015) for other taxonomic levels (Supp. File 2 Table S11).

To provide a phylogenetic context for the eight most prevalent taxonomic families (*i.e.*, Dino-Group I Clade 1, Licnophoridae, Warnowiaceae, Corallicolidae, Exobasidiomycetes, Ephelotidae, Labyrinthulaceae and Philasterida), we did a multiple sequence alignment (MSA) using the Super5 algorithm in Muscle5 (Edgar 2022) for each family (Supp. File 2 Table S12). The MSAs included the most abundant ASVs of each family (those representing >50% of the total microeukaryotic community in at least one coral sample), public ASV sequences obtained from a BLAST analysis (98% similarity threshold) of the representative ASV sequence of each family (*i.e.*, the most abundant ASV for each family) on the nr nucleotide database of NCBI, and, when available, ASV sequences documented in other coral studies and annotated as belonging to the same microeukaryotic families (Bonacolta et al. 2023; Clerissi et al. 2018). All trees were rooted with an ASV sequence (or a sequence from NCBI when it was not available) of an outgroup selected as belonging to the same taxonomic order but from a different family (Supp. File 2 Table S12). PhyML (Guindon et al. 2010) was used to calculate the phylogenetic distances between the ASV sequences and construct rooted trees based on the maximum-likelihood principle. Different substitution models were selected (Supp. File 2 Table S12) according to the microeukaryotic family using the Smart Model Selection (SMS) software implemented in the PhyML environment (Lefort et al. 2017) with the Akaike's Information Criteria (AIC). To ensure statistical consistency, the non-parametric variant of approximate likelihood-ratio test (SH-aLRT; Guindon et al. 2010) was applied to the datasets. The resulting trees were modified for publication using ggtree (Yu et al. 2017). In addition, the percentage of similarity between the representative ASVs from each family and the ASV sequences documented in the other coral studies and belonging to the same microeukaryotic families (Bonacolta et al., 2024, Clerissi et al., 2019; Siboni et al. 2010) were calculated using NCBI blastn suite-2sequences website.

Results

Specificity and universality tests on the newly designed primers

The non-metazoan primers designed specifically for *C. rubrum* notably reduced the coral host signal compared to the universal eukaryotic *18S rRNA* gene primers (Stoeck et al. 2010; Figure S2). Indeed, they yielded an average ratio of 22% microeukaryotic sequences per sample, markedly higher than the 0.04% ratio obtained with universal primers (Supp. File 2 Table S1; Figure S2). Rarefaction curves indicated that these primers were efficient in characterizing the microeukaryotic communities associated with *C. rubrum*, as most curves reached the plateau (Figure S3). Results of the *in-silico* PCRs on the PR2 database of microeukaryotes indicated that the 18S-NonMet_Cr primers successfully amplified more than 84% of the sequences of most microeukaryotic groups when setting the maximum number of mismatchs per primer to two (>60% of sequences amplified for all taxonomic groups; Figure S4). However, our primers only amplified 40%, 45% and 60% of the sequences corresponding to the microeukaryotic species from the Obazoa and Excavata supergroups, as well as from the Eukaryota_X group (*i.e.*, unclassified microeukaryotes), respectively. Therefore, our primers might be less universal for these groups than the universal *18S rRNA* gene primers (V4 region; Figure S4). After sequencing, using the 18S-NonMet_Cr primers, we captured a wide range of microeukaryotic groups, resulting in 8187 different ASVs spanning across 4 domains, 30 divisions, 131 classes, 261 orders, and 479 families of microeukaryotes (Supp. File 2 Table S4). It included groups which have already been found associated with other coral species, such as members of the Alveolata division, including dinoflagellates, ciliates and apicomplexans.

Overview of the eukaryome of *C. rubrum*

Microeukaryotic communities were structurally different between the coral and seawater samples, although both communities were predominantly dominated by the Alveolata division ($F = 2.7$; d.f. = 1; $p = 0.016$; Figure S5 and Supp. File 2 Table S4, S5 and S6). The microeukaryotic communities associated with corals contained on average 10

times less ASVs than seawater (94 ASVs and 1157 ASVs per sample on average in the coral and seawater samples, respectively; Supp. File 2 Table S7).

The eukaryome of *C. rubrum* was not significantly different between the control sites (*Bigo* and *Villefranche-sur-Mer*, pairwise analysis; F = 0.4; p = 0.8; Supp. File 2 Table S11) and was composed of microeukaryotes from the Dino-Group I and Licnophoridae which collectively formed ~45.5% of the total community. Overall, colonies without tissue loss were also dominated by the Dino-Group I, but also Gymnodiniales and Labyrinthulomycetes (Stramenopiles division), which collectively formed ~34% of the total community. In colonies exhibiting tissue loss, the relative abundance of Labyrinthulomycetes increased significantly, reaching up to 12% in some sites (Figures 6 and 8). Additionally, there was an emergence of Phaeophyceae, averaging 5% in these colonies (Figures 6 and 8).

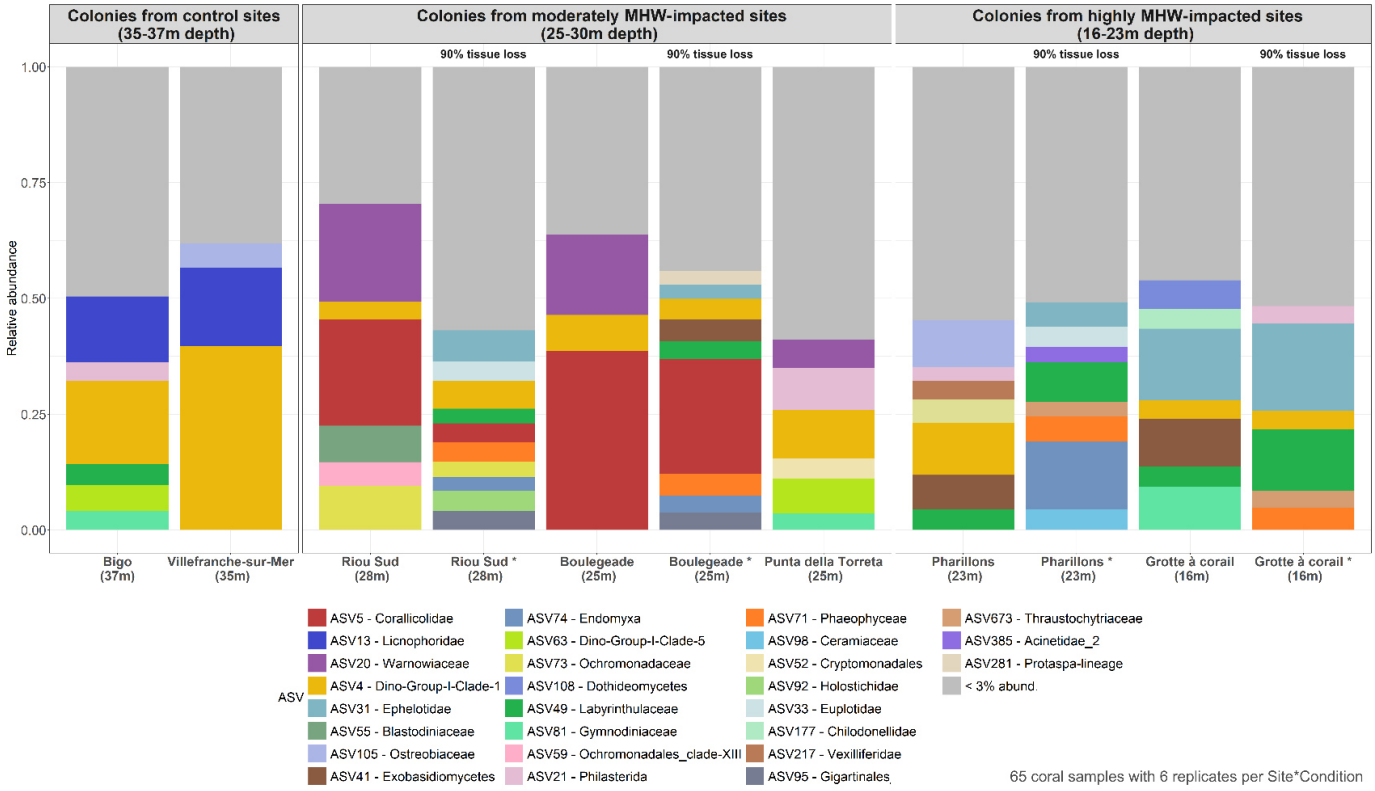

Figure 4: Composition of the microeukaryote communities associated with *C. rubrum* colonies (ASV level). Relative abundance and taxonomy of the most abundant microeukaryote ASVs associated with *C. rubrum* colonies of different health conditions and collected at different sites. Microeukaryotic taxa with an average relative abundance below 3% are aggregated.

Changes in the microeukaryotic communities associated with heat-stressed colonies without tissue loss

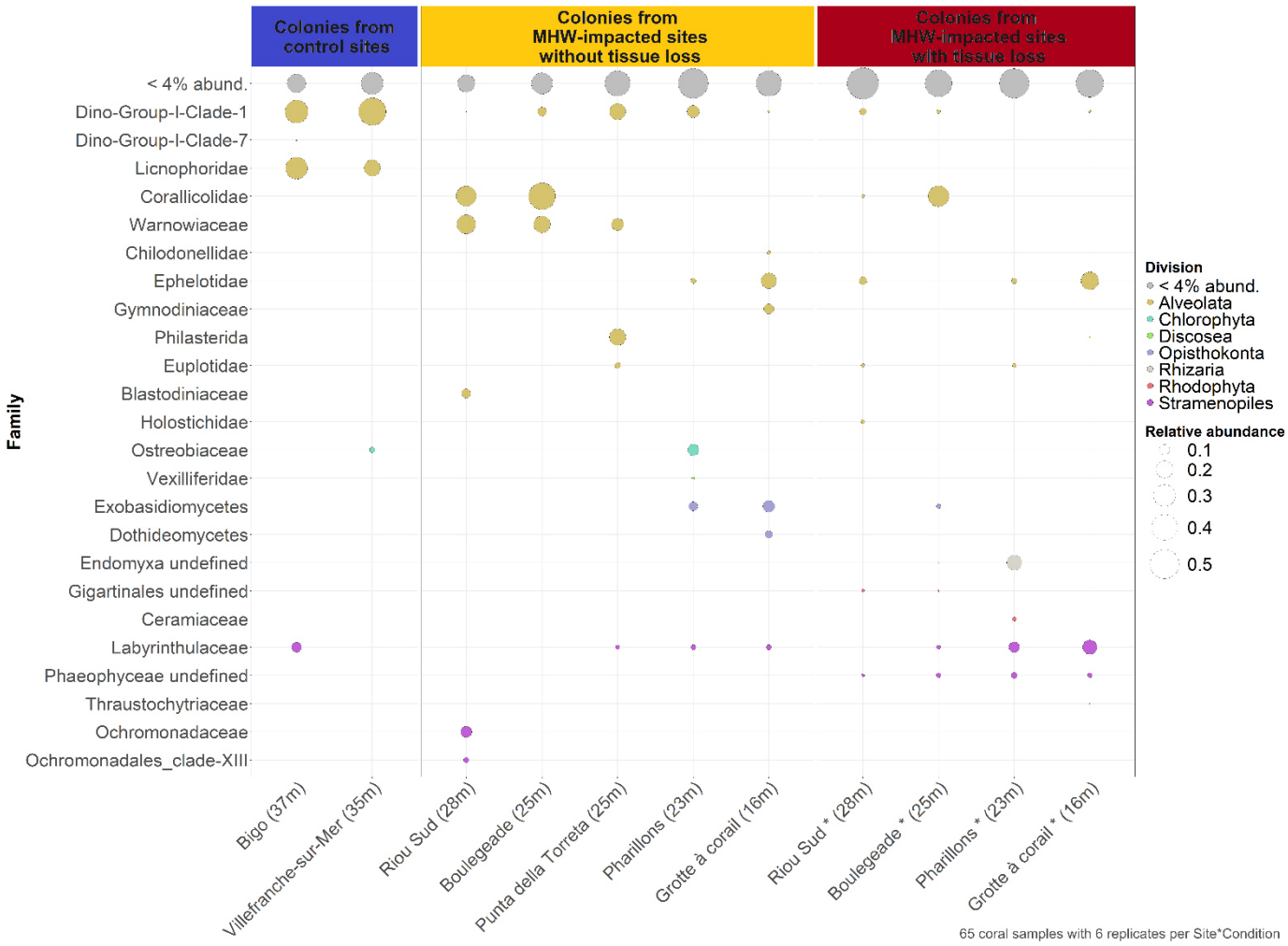

Figure 3: Relative abundance of the microeukaryotic families associated with *C. rubrum* colonies depending on the colony health condition (0% or 90% tissue loss) and collection site. Microeukaryotic taxa are ordered by taxonomic division for those with an average relative abundance above 1%.

While the observed species richness and Shannon index were not significantly different between colonies collected at the control and MHW-impacted sites, the structure of the microeukaryotic communities differed ($F = 3.8$; d.f. = 1; $p = 0.001$; Figure 8, Supp. File 2 Table S7 and S8). Differential abundance analyses identified 39 ASVs whose relative abundance was different between the colonies collected in the control and MHW-impacted sites (Figure 7). ASV4 and ASV517-Dino-Group I Clade 1, as well as ASV13-Licnophoridae exhibited significantly lower relative abundances in colonies

sampled in MHW-impacted sites compared to the colonies at control sites. ASV4 and ASV517-Dino-Group I Clade 1 relative abundances collectively decreased from 35% to 3%, and the ASV13 relative abundance decreased from 22% to 1% on average from control to heat-stressed colonies (Figure S9, Supp. File 2 Table S5 and S9). On the contrary, other ASVs were significantly more abundant in colonies collected in the MHW-impacted sites, such as ASV41-Exobasidiomycetes and ASV86-Peronosporomycetes whose relative abundances increased from 0.006% and 0.02% on average in the control colonies to 3% and 0.9% on average in the heat-stressed colonies, respectively (Figure S9 and Supp. File 2 Table S5 and S9).

Different microeukaryotes dominated the communities depending on the location and depth. Colonies from the deepest sites (≥25 m; *Riou Sud*, *Boulegeade* and *Punta della Torreta*) were characterized by a higher proportion of Warnowiaceae and especially ASV18 and ASV20 (18% on average in the deep MHW-impacted sites versus and 2% in control sites*;* Figure 4, 6 and Figure S9). Furthermore, ASV21-Philasterida was in a higher proportion in colonies from *Punta della Torreta* (20% on average), while ASV5-Corallicolidae was relatively abundant in colonies collected in *Riou Sud* (20% on average) and *Boulegeade* (60% on average; Figure 4). In the shallowest sites (<25 m; *Pharillons* and *Grotte à corail*), the microeukaryotic communities showed a higher relative abundance of ASV41-Exobasidiomycete (*Malassezia* genus) and ASV36-Ephelotidae (Figure 6, S9).

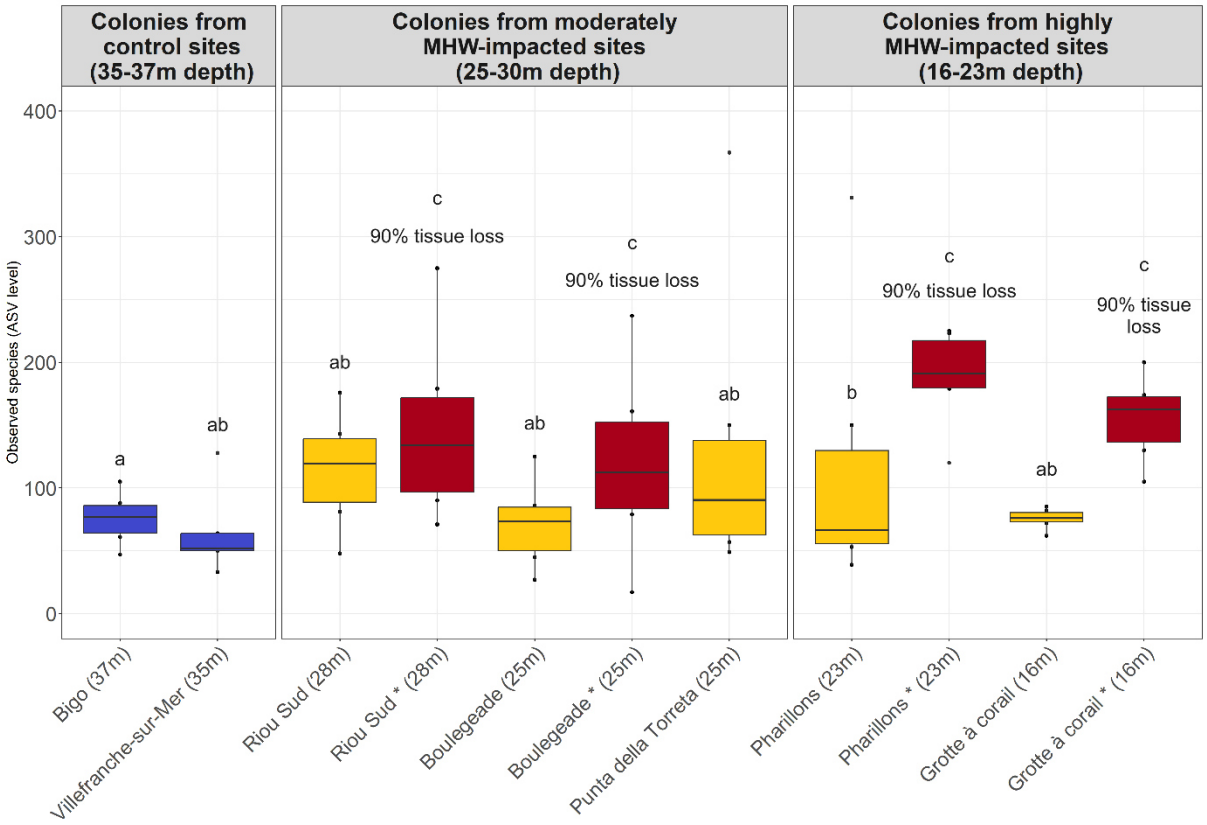

Figure 5: Microeukaryote species richness associated with *C. rubrum* colonies depending on the collection site and the colony health condition. Colonies collected at the control sites are represented in blue. Heat-stressed colonies without tissue loss but collected in MHWs-impacted sites are represented in yellow, while those with tissue loss are represented in red. Significant statistical differences (p-value < 0.05) between groups are indicated by letters.

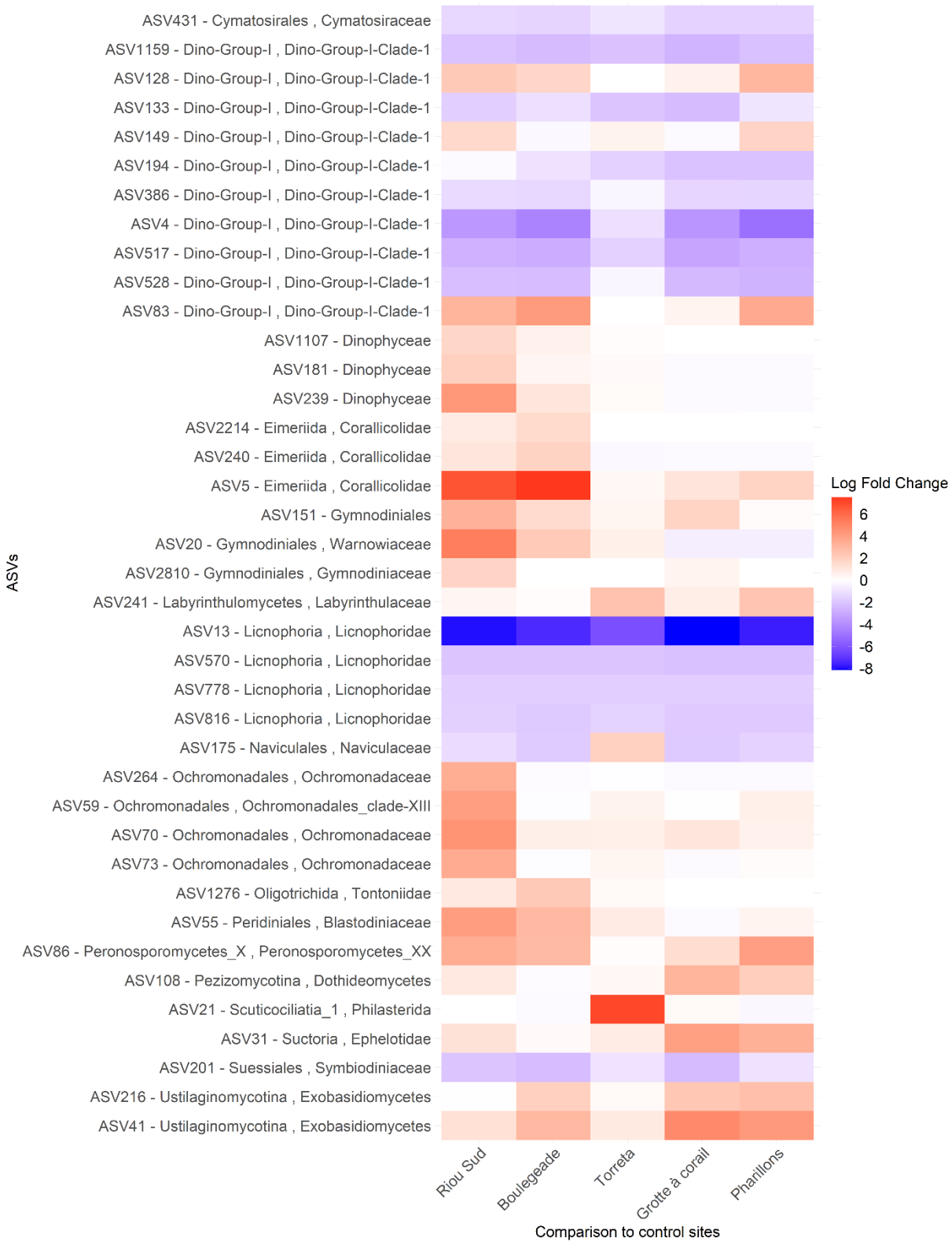

Figure 6: Microeukaryote ASVs differentially abundant (ANCOM-BC results) between the *C. rubrum* colonies collected at the control sites (*Villefranche-sur-Mer* and *Bigo*) and the *C. rubrum* colonies collected at the other sampling sites. Differences in relative abundance calculated as log fold change (natural log).

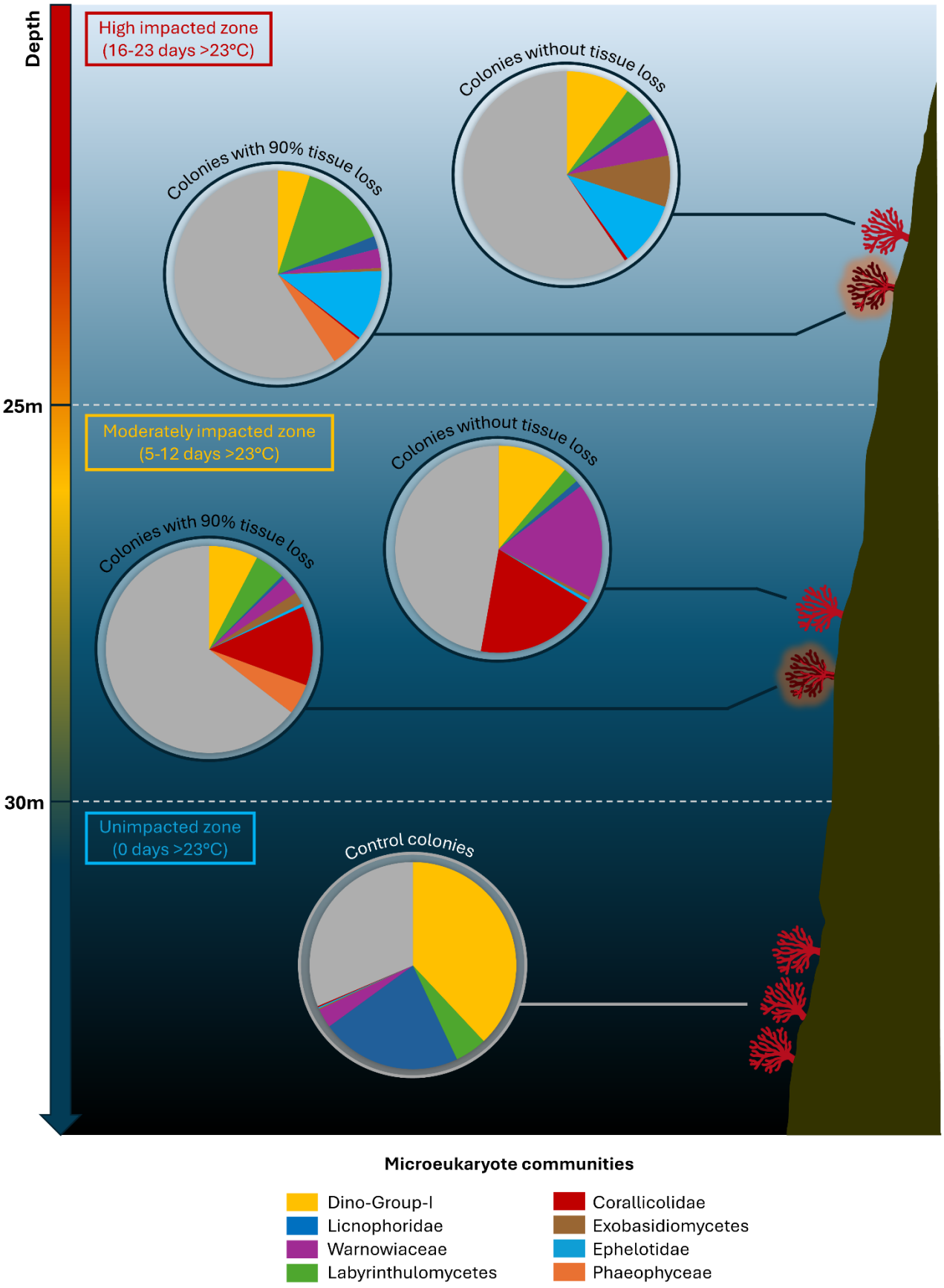

Figure 7: Schematic representation of the composition of the microeukaryote communities associated with *C. rubrum* colonies according to the sampling site and coral health condition. Only the most prevalent microeukaryote groups are represented.

Changes in the microeukaryotic communities associated with colonies showing tissue loss

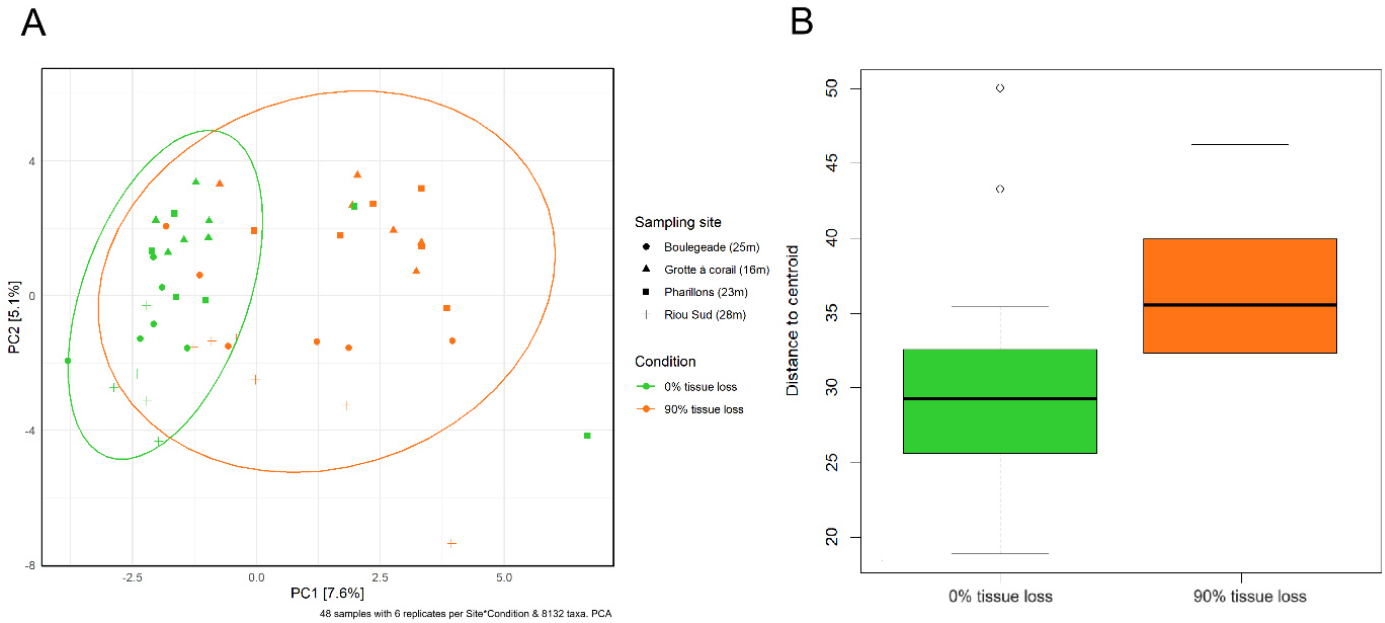

Figure 8: **Structure of the microeukaryote communities associated with *C. rubrum* colonies with 0% and 90% tissue loss in the Calanques National Park (Marseille). (A)** Principal component analysis of the Aitchison distance matrix based on the composition of the microeukaryote communities (ASV level), showing the distribution and dispersion of the *C. rubrum* samples collected at the different sites. **(B)** Beta-dispersion assessment using the distance to centroids of samples with and without tissue loss.

At the MHW-impacted sites of the Calanques National Park in Marseille, where most colonies with 90% tissue loss were collected, a higher species richness in microeukaryotes was observed in the colonies with tissue loss compared to the ones without tissue loss (1.6 times more on average; estimate std. = 0.49; error = 0.13; z-value = 3.6; p = 0.0003; Figure 3 and Supp. File 2 Table S7). Furthermore, the composition of the communities between the colonies with and without tissue loss differed (F = 1.75; d.f. = 1; p = 0.001; Figure 4, 5, and Supp. File 2 Table S8), with a higher beta-dispersion of the samples corresponding to the colonies with tissue loss (F = 12.2; d.f. = 1; p = 0.001; Figure 5 and Supp. File 2 Table S8). The differential analysis identified eight differentially abundant ASVs in the colonies with tissue loss, including three Phaeophyceae ASVs (ASV71, ASV184 and ASV394) and three Labyrinthulaceae ASVs (ASV252, ASV389, ASV691) whose relative abundance increased (Figure 4, 6, Supp. File 2 Table S10).

Analyses on each site showed that a difference in composition between colonies with and without tissue loss was observed in *Riou Sud* and *Boulegeade*, but not in *Pharillons* and *Grotte à corail* (Supp. File 2 Table S8 and S10).

Phylogenetic analyses of *C. rubrum* associated microeukaryotes

Phylogenetic analyses were done on the ASVs belonging to microeukaryotic taxa found in high relative abundances in control colonies (*i.e.*, Dino-Group I Clade I and Licnophoridae), as well as in heat-stressed colonies (*i.e.,* Warnowiaceae, Corallicolidae, *Malassezia*, Ephelotidae and Labyrinthulaceae).

Dino-Group I Clade 1 ASVs (ASV4, ASV133 and ASV143) clustered together and with Dino-Group I sequences recovered from the Mediterranean gorgonian *P. clavata* (98.42% sequence similarity) and the tropical scleractinian coral *Pocillopora damicornis* (100% sequence similarity; Figure S6 and Supp. File 4 Table S12). ASV13-Licnophoridae clustered with the other ASVs assigned as Licnophoridae and was 96% similar with *Ciliophora* spp. sequences recovered from diseased sea urchins (*Diadema antillarum*; Figure S7 and Supp. File 4 Table S12). ASVs assigned to the Warnowiaceae family (ASV18 and ASV20) clustered with dinoflagellate sequences and especially to sequences of seawater *Warnowia* spp. (99-100% sequence similarity; Figure S9 and Supp. File 4 Table S12). ASV5-Corallicolidae sequence was 100% similar to an unclassified microeukaryotic sequence recovered from the tropical coral *Porites astreoides* and 99.21% similar to the sequence of a Corallicolidae ASV found in association with the Mediterranean gorgonian *P. clavata* (Bonacolta et al. 2024; Figure S10 and Supp. File 4 Table S12). ASV41-*Malassezia* sequence showed 100% similarity to *Malassezia* spp. sequences described as pathogen of the skin of humans and terrestrial animals (NCBI nr nucleotide database, Cabañes 2014). Exobasidiomycetes (*Malassezia* genus) and Ephelotidae ASVs respectively clustered with sequences of *Malassezia* spp. (98% sequence similarity) and *Ephelota* spp. (95% sequence similarity), both associated with the Mediterranean gorgonian *P. clavata* (Figure S11 and S12; Supp. File 4 Table S12). ASV49-Labyrinthulaceae sequence was 98% similar to a *Labyrinthula* spp. sequence recovered from seagrass lesioned tissue (Supp. File 4 Table S12; Wahid et al. 2007). The closest public sequences

to the other Labyrinthulaceae ASVs were Stramenopiles sequences recovered from *Favia* spp. tropical corals (95% sequence similarity; Figure S13 and Supp. File 4 Table S12).

Discussion

Using a *18S rRNA* gene metabarcoding approach, we observed that the microeukaryotic community associated with the octocoral *C. rubrum* was composed of dinoflagellates Dino-Group I and Warnowiaceae, Stramenopiles belonging to Labyrinthulomycetes and ciliates Licnophoridae. These microeukaryotic groups were already found in other coral species. The eukaryome of *C. rubrum* was highly responsive to thermal stress and some microeukatyotes might be bioindicators of coral stress. Our work demonstrates the importance of modifying the initial *18S rRNA*-based UnNonMet primer set designed to study the biodiversity of microeukaryotes associated with metazoan hosts, to adapt them to the studied coral species and efficiently reduce the host's signal. Here, the primers designed for *C. rubrum* significantly reduced host signal while amplifying most microeukaryotic sequences. Overall, these findings underscore the importance of monitoring microeukaryotic communities to understand coral responses to environmental stress and highlight the technical need for species-specific primer optimization.

The eukaryome of *C. rubrum* colonies showing no tissue loss

The microeukaryotic community associated with *C. rubrum* had a lower richness and different composition than seawater, suggesting that only certain microeukaryotes associate with *C. rubrum*. Microeukaryotes found in all colonies without tissue loss were composed of dinoflagellates Dino-Group I and Warnowiaceae, ciliates Licnophoridae, and Stramenopiles belonging to Labyrinthulomycetes. These dominant groups may be essential for the functioning of *C. rubrum*, and more generally for coral holobionts. Microeukaryotes from the Dinoflagellata and Ciliophora subdivisions for example have been observed in association with other coral species from both temperate and tropical environment (Bonacolta et al. 2024; Clerissi et al. 2018; del Campo et al. 2020; Ainsworth et al. 2017). Specifically, several Dino-Group I ASVs observed in the red coral eukaryome were closely related to Dino-Group I ASVs found in the temperate octocoral *Paramuricea*

clavata (Bonacolta et al. 2024) and the tropical coral *Pocillopora damicornis* (Clerissi et al. 2018). Even if the role of Dino-Group I within the coral holobiont is still unclear, the Syndiniales class, to which these dinoflagellates belong, is exclusively found in marine environments and has been described as potentially parasitic due to its broad distribution across ocean food webs (Guillou et al. 2008). Warnowiaceae, other dinoflagellates from the Gymnodiniales order found in the red coral eukaryome, have been observed on sick tropical corals, and were suspected to be responsible, with bacterial infection, to the black band disease in producing paralytic shellfish toxins (Hold et al. 2001b; Green et al. 2004; Sala et al. 2005). Labyrinthulomycetes, a group of ubiquitous and diverse unicellular Stramenopiles, were also observed in the tissue of tropical corals, but also other marine organisms such as clams, nudibranchs and seagrasses (Raghukumar and Raghukumar 1991; Ben-Dov et al. 2009; Siboni et al. 2010; Kramarsky-Winter et al. 2006; Pan et al. 2017; McLean and Porter 1982; Ragone Calvo et al. 1998; Ragan et al. 2000; Muehlstein et al. 1991). They are known to be involved in saprotrophic nutrient uptake (Raghukumar and Damare 2011; Damare and Raghukumar 2010; Bongiorni et al. 2005; Taoka et al. 2009; Nagano et al. 2011). Their osmotrophic (uptake of dissolved organic matter) and phagotrophic (feeding on algae, bacteria, and small organic matter) abilities make them ecologically important in nutrient cycling by contributing to various decomposition processes in marine ecosystems (Raghukumar and Damare 2011; Damare and Raghukumar 2010; Bongiorni et al. 2005; Taoka et al. 2009; Nagano et al. 2011). Some species in this family are also known to produce high levels of omega-3 polyunsaturated fatty acids which has made Labyrinthulomycetes commercially valuable (Carmona et al. 2003; Lee Chang et al. 2012). Further studies are needed to determine whether the Labyrinthulomycetes species that form the eukaryome of *C. rubrum* may be a nutritional symbiont which transfer lipids to the coral host. Finally, Licnophoridae ciliates have been previously observed associated with the Mediterranean gorgonian *P. clavata* (Bonacolta et al. 2024) as well as the tropical coral *P. damicornis* (Clerissi et al. 2018). Some Licnophoridae have been described as predators of other ciliates (Sweet and Séré 2016). This relationship with other ciliates might explain their variability in relative abundance in our samples depending on the site (Clerissi et al. 2018).

Thus, some microeukaryotes (*i.e.*, Dino-Group I, Warnowiaceae and Labyrinthulomycetes) might be universal and found in association with many coral species, like the bacteria *Endozoicomonas* in the coral bacterial microbiome (Pogoreutz et al. 2022; McCauley et al. 2023; van de Water, Allemand, et al. 2018). These microeukaryotes might be relevant for the functioning of the coral holobiont and for understanding coral's response to environmental change. Further studies investigating the eukaryome of other coral species (including temperate, tropical, scleractinian but also octocoral species) are needed to identify universal and potentially relevant microeukaryotes in order to gain a deeper understanding of the coral holobiont.

Microeukaryotic indicators of heat stress conditions

While species richness did not differ between the control and heat-stressed colonies, the composition of the eukaryome did (Figure 8). Specifically, the relative abundance of Dino-Group I dinoflagellates and Licnophoridae ciliates was lower in colonies collected in the MHW-impacted sites. Dinoflagellates are sensitive to temperature fluctuations, and in scleractinian corals for example, the decrease in the abundance of Symbiodiniaceae dinoflagellates often marks the beginning of a deterioration in coral health (Douglas 2003; Jiang et al. 2021). A decline in Symbiodiniaceae abundance (commonly referred to as "coral bleaching") is indeed systematically observed during heat stress, and corals may die if bleaching persists for a prolonged period (Douglas 2003; Jiang et al. 2021). The decrease in the relative abundance of the Licnophoridae ciliates in the heat-stressed corals could also be due to temperature fluctuations, as marine ciliates are generally heat sensitive as well (Martinez 1980; Karajan et al. 2019). Temperature increase can indirectly affect their food sources, such as bacteria and other protists, or directly affect their metabolic rate, reproduction and survival (Martinez 1980; Karajan et al. 2019).

In the MHW-impacted sites, the composition of the eukaryome was different depending on the sampling depth, probably because colonies were differentially heat-affected. Warnowiaceae and Corallicolidae became dominant groups in the moderately (deep) MHW-impacted sites, while Ephelotidae and the fungi Exobasidiomycetes became dominant in the highly (shallow) MHW-impacted sites (Figure 8). While the latter,

especially *Malassezia*, are known as pathogens of the skin of humans and terrestrial animals (Cabañes 2014), it is unlikely that this change in microeukaryotic community composition is related to human proximity, and potential trophic drivers behind this change are currently unknown as for the other microeukaryotes. To identify their roles and therefore the consequences of their increase under heat stress in the holobiont functioning, these microeukaryotes need to be better characterized through other techniques such as metagenomics and cultures.

These specific microeukaryotes whose relative abundance increased in the heat-stressed colonies might be markers of the stress level that the holobiont is experiencing. They might serve as valuable bioindicators of coral health, such as certain associated bacteria (Pootakham et al. 2019a; Montaño-Salazar et al. 2023a; Glasl et al. 2019), although the latter have been shown to be more reliable proxies of host health than microeukaryotes in other marine holobionts (Wegner et al. 2025).

Increased microeukaryotic diversity and epibiont proliferation in colonies with tissue loss

Colonies with tissue loss showed greater richness and beta-dispersion, alongside marked differences in the eukaryome composition, compared to colonies without tissue loss. This suggests that numerous opportunistic microeukaryotes might have taken advantage of the high level of stress of their host to settle in and potentially jeopardize coral health. This is consistent with findings on the bacterial communities of heat-stressed corals, in which opportunistic bacteria, whether saprophytic or commensal, proliferate, increasing the observed richness (Jessen et al. 2013; Rubio-Portillo et al. 2021a; McDevitt-Irwin et al. 2017). The transition to a more diverse bacterial community is a well-documented phenomenon in heat-stressed organisms, including octocorals (De Castro-Fernández et al. 2023; Rubio-Portillo et al. 2021a; Strano et al. 2023; Tignat-Perrier et al. 2022) and specifically *C. rubrum* (Prioux et al. 2023; Tignat-Perrier et al. 2023). A similar trend can be observed in the associated microeukaryotic communities under heat stress, presumably due to changes in microeukaryotic population dynamics and/or reduced control of the coral host over its microbiota. The analysis on each site showed that the compositional difference between colonies with and without tissue loss

was significant in *Riou Sud* (28 m) and *Boulegeade* (25 m), but not in *Pharillons* (23 m) and *Grotte à corail* (16 m). In these shallow colonies, which do not show tissue loss yet but still highly suffered from heat, might have an eukaryome composition starting to look like the one associated with colonies with tissue loss. Monitoring these colonies after the MHWs would have helped to determine whether these healthy-looking colonies (*i.e.*, without tissue loss) collected in the shallowest sites of *Pharillons* and *Grotte à corail* had subsequently suffered tissue loss.

Within the colonies that exhibited tissue loss, we observed the presence of microeukaryotes previously associated with diseased organisms. Labyrinthulomycetes, which are found more abundant in the colonies with tissue loss, represent an ubiquitous and diverse group of unicellular Stramenopiles, known for their parasitic tendencies in various marine organisms (Pan et al. 2017; Raghukumar and Damare 2011; Damare and Raghukumar 2010). They were discovered for their possible role in multifocal purple spot disease which affects Caribbean Sea fans, although they have been found in both healthy and diseased tissues (Burge et al. 2012; Dennis et al. 2020). They probably act as opportunistic pathogens (Burge et al. 2012), engaging in "left-over scavenging" behavior following bacterial growth (Raghukumar and Damare 2011). The sequence of the Labyrinthulomycetes ASV49 was similar to sequences of Labyrinthulomycetes found at the interface of seagrass lesioned tissue, where they grow on dead bacterial cells (Wahid et al. 2007). This behavior could be the reason for their relatively high abundance in colonies with tissue loss, where they may take advantage of the heat-induced proliferation of opportunistic bacteria (Prioux et al. 2023). Colonies with tissue loss were also associated with a higher relative abundance of Phaeophyceae macroalgae, which have been described to harbor and promote the growth of pathogenic bacteria in bleached tropical corals (Vieira, Thomas, et al. 2016; Vieira, Engelen, et al. 2016). Species of Phaeophyceae were also found as epibionts covering the necrotic branches of MHW-affected *P. clavata* colonies (Chimienti et al. 2021). Considering that *P. clavata* and *C. rubrum* inhabit similar environments, it is not surprising that *C. rubrum* colonies suffering from MHWs experience the same algal proliferation.

Summary of putative interactions occurring within the eukaryome of *C. rubrum*

Microorganisms associated with *C. rubrum* are likely closely interacting through competition and predator-prey relationships. Based on the relative abundance of the dominant microeukaryotes in association with the red coral, and their trophic mode inferred from their taxonomy, Figure 9 illustrates three types (competition, predator-prey and parasitism relations) of putative interactions that may occur between them. Licnophoridae are dominant microeukaryotes under control conditions. When the temperature increases, as these microeukaryotes are likely thermosensitive (see discussion above; Martinez 1980; Karajan et al. 2019), their abundance would decrease, giving way to the proliferation of other microeukaryotes which compete for the same resources (mainly bacteria) and niche such as Ephelotidae (Mandal 2024), Labyrinthulomycetes (Raghukumar and Raghukumar 1991) and the mixotrophic Warnowiaceae (Mitra et al. 2014); Figure 9). In the same way, the decrease of the abundance of the thermosensitive Dino-Group I Clade I under hot temperatures might promote the proliferation of Corallicolidae in the heat-stressed colonies. This predation relationship has already been suggested within the holobiont of the Mediterranean octocoral *P. clavata* (Bonacolta et al. 2024). Finally, the fungi Exobasidiomycetes and macroalgae Phaeophyceae could take advantage of the compromised coral health in colonies with tissue loss to proliferate (Cabañes 2014; Chimienti et al. 2021); Figure 9). The assumptions above need to be validated by further studies and may be used as new research paths in our understanding of the interactions occurring between the microorganisms of the coral holobiont.

Conclusion

The study is the first assessing the composition of the eukaryome of the Mediterranean emblematic coral species *C. rubrum*. Using a *18S rRNA* gene metabarcoding approach and newly designed primers to reduce host signal, we investigated the microeukaryotic communities associated with red coral colonies collected in unimpacted (control) and MHW-impacted sites. The eukaryome of the

colonies collected in the control sites was dominated by Dino-Group I, Licnophoridae and Labyrinthulomycetes, suggesting a physiological importance of these microeukaryotic taxa in the coral holobiont. We showed that the eukaryome composition was different between the unimpacted and MHW-impacted sites, but also between the MHW-impacted sites depending on the depth. We thus identified putative bioindicators of the heat stress level experienced by *C. rubrum* colonies during the MHW episodes. These findings enhance our understanding of the response of *C. rubrum* to the Mediterranean MHWs and the role of the microbiome in the health status of corals.

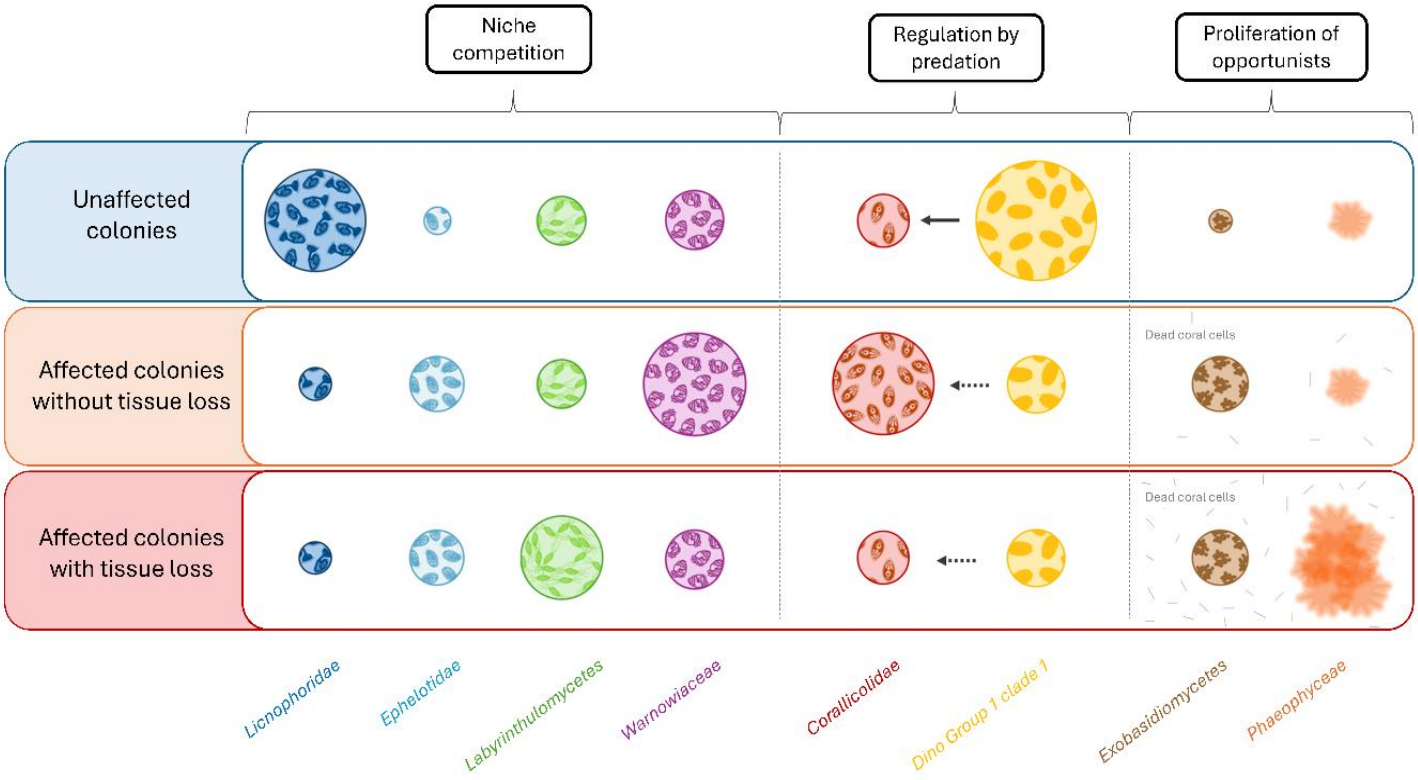

Figure 9: Conceptual diagram illustrating potential interrelationships and feeding dynamics among the most prevalent microeukaryote groups associated with *C. rubrum* colonies.

Chapter 6

Assessing the short-term resilience of *Corallium rubrum* holobiont to thermal stress



Chapter 6: Assessing the short-term resilience of *Corallium rubrum* holobiont to thermal stress

I. Overview of the chapter

In recent decades, the increasing frequency and severity of marine heatwaves (MHWs) have led to growing concern about the long-term viability of octocoral species. The microbiome, which is essential to coral functioning, likely plays a critical role in how corals cope with and recover from thermal stress (Voolstra et al. 2024c). However, our understanding of microbiome resilience, the ability of microbial communities to recover from disturbances, is still at an early stage. While numerous studies have demonstrated that thermal stress can significantly impact the composition of the coral microbiome, relatively few have examined the capacity of the microbiome to return to its original state (Epstein et al. 2019; Maher et al. 2020; Chapron et al. 2021; Dunphy et al. 2021; Girija et al. 2024; Vompe et al. 2024). However, a more comprehensive understanding of the recovery dynamics of the microbiome is essential for accurately predicting the survival and adaptability of coral species in the context of ongoing climate change.

This study investigates the structural dynamics of the red coral microbiome under two heat stress scenarios (from 15°C to 19°C and 23°C). The microbiome (bacteria and microeukaryotes) was analyzed using metabarcoding and qPCR, and co-occurrence analyses were conducted to identify potential interactions among microbial taxa. The expression levels of key stress marker genes in the host, heat shock protein 70 (HSP70) and tumor necrosis factor-related apoptosis-inducing ligand receptor 1 (TNFR1), were also monitored.

The coral host showed increased expression levels of HSP70 and TNFR1 genes at both 19°C and 23°C, with higher levels at 23°C. Although the applied stress was of short duration (8 days), the overexpression of these stress markers indicated that the host was physiologically challenged. However, after a week recovery at 15°C, gene expression levels returned to baseline, indicating that the host was able to recover quickly. The eukaryotic component of the microbiome showed a clear response to temperature.

Labyrinthulomycetes, Ostreobiaceae, and Philasterida were the dominant microeukaryotes under control conditions. During thermal stress, changes in community composition were observed, with the Labyrinthulomycetes community undergoing reorganization. Different phylotypes dominated during the stress phase compared to those present in the control and recovery phases. Furthermore, Ostreobiaceae phylotypes disappeared entirely during the stress and did not recover during the recovery phase. The absence of these dominant taxa may affect the functional dynamics of the holobiont. Interestingly, certain microeukaryotes such as Holostichidae ciliates and Endomyxa protozoa emerged under stress and persisted after recovery. These taxa could be opportunistic or stress-adapted species that could either enhance or impair the coral resilience, depending on their role within the holobiont. The ecological significance of these changes remains to be elucidated.

The bacterial microbiome exhibited a more gradual response to thermal stress. While the 23°C treatment triggered immediate compositional shifts, the 19°C treatment induced delayed changes, occurring after 8 days. The relative and absolute abundance of the dominant symbionts Spirochaetaceae remained stable under both temperature treatments. However, the abundance of putative opportunists, such as Vibrionaceae and Rhodobacteraceae, increased under thermal stress. Vibrionaceae, a family with known pathogenic potential (Martin et al. 2002; Vezzulli et al. 2010a; Vidal-Dupiol et al. 2011; Gibbin et al. 2018; Sun et al. 2023), proliferated significantly at both 19°C and 23°C and persisted even after the recovery phase. This persistence raises concerns regarding their potential role in reducing coral resilience, especially under repeated heat stress events typical of MHWs. Some members of the Rhodobacteraceae family can have a protective role in mitigating pathogenic *Vibrio* infections (Rosado et al. 2019; Kitamura et al. 2021; Xu et al. 2024), but their impact in the red coral remains to be investigated.

While the red coral microbiome demonstrated some plasticity and ability to recover under short-term thermal stress, persistent changes in community composition, particularly the proliferation of opportunistic and potentially pathogenic taxa (Vibrionaceae, Endomyxa and Holostichidae), might pose a threat to the long-term resilience of the red coral. These results suggest that the functional role of these opportunistic taxa and their possible impact on coral health need to be further

investigated. Moreover, the different responses observed between the eukaryotic and bacterial components of the microbiome highlight the complexity of the holobiont and the importance of integrating multi-kingdom analyses in future studies.

II. Publication

Heatwave-driven persistent microbes threaten the resilience of Mediterranean coral holobionts

Environmental Microbiome | August 2025

DOI: https://doi.org/10.1186/s40793-025-00765-8

Camille Prioux[1,2,3], Christine Ferrier-Pagès[3], Thibaut Lamarca[2,3], Denis Allemand[3], Romie Tignat-Perrier[2,3]

[1]Sorbonne Université, Collège Doctoral, Paris, France

[2]Unité de Recherche sur la Biologie des Coraux Précieux CSM - CHANEL, Centre Scientifique de Monaco, 8 Quai Antoine 1er, MC 98000, Monaco, Principality of Monaco

[3]Centre Scientifique de Monaco, 8 Quai Antoine 1er, MC 98000, Principality of Monaco

Abstract

Background: The climate crisis poses a serious threat to octocorals in the Mediterranean Sea as marine heatwaves (MHWs) not only impair coral metabolism but also disrupt the complex symbiosis between the coral host and its microbiome. Since octocorals are the foundation species of the Mediterranean animal forests, understanding their resilience, i.e. ability to recover and survive to MHWs, is crucial to predict their viability under future climatic conditions. Using amplification of *16S* and *18S rRNA* genes for metabarcoding and *qPCR* analyses to follow the changes in bacterial microbiome and eukaryome as well as host response under stress and recovery conditions, this study provides the first comprehensive assessment of the resilience of an iconic Mediterranean octocoral (the red coral *Corallium rubrum*) to a mild (19°C) and more severe (23°C) heat stress.

Results: The results of this work indicate a stress response of the host to elevated temperatures, even under mild temperature. The eukaryome was highly sensitive to heat stress and underwent rapid structural changes among the dominant microeukaryotes. In contrast, the relative and absolute abundance of the major bacterial symbionts remained stable throughout the stress. However, heat stress led to a significant increase in the abundance of some taxa such as Vibrionaceae that persisted after a week of recovery.
Conclusions: While the host recovered from the stress, and the microbiome largely returned to its original composition during recovery, the results highlight the persistent presence of some taxa that might compromise the short-term resilience of octocoral holobionts. This study provides new information on how octocoral holobionts respond to MHWs in the Mediterranean Sea. This knowledge is crucial for the development of effective, science-based strategies for coral protection and restauration.

Introduction

Corals are foundational species that build complex three-dimensional habitats supporting rich marine biodiversity. In tropical regions, scleractinian corals form the basis of coral reefs (Wilkinson 2008), while in temperate waters, gorgonian octocorals such as *Paramuricea clavata* and *Corallium rubrum* shape coralligenous assemblages, key components of Marine Animal Forests (MAFs; Rossi et al. 2017). These benthic systems, composed of large sessile invertebrates, provide structural complexity and support essential ecological processes (Paoli et al. 2017; Orejas et al. 2022). However, they are increasingly threatened by climate-driven stressors, with seawater warming and marine heatwaves posing major risks for coral health and biodiversity (Cerrano et al. 2000; Huete-Stauffer et al. 2011; Luigi Piazzi et al. 2021c; Verdura et al. 2019b; Garrabou et al. 2009a; 2022, 202). Corals are complex functional units known as holobionts, which consist of the animal host and its microbiome (*i.e.*, bacteria, archaea, viruses, protists and fungi). The microbial partners provide a wide range of benefits to the host, but the specific functions that drive these benefits are still largely unexplored (Lema et al. 2012; Matthews et al. 2020; Peixoto et al. 2017; Kvennefors et al. 2012; Nissimov et al. 2009; Ritchie 2006). Some bacteria, for example, can support coral resistance to environmental stressors by producing antioxidants, osmolytes or antimicrobial compounds (Kvennefors et al. 2012;

Nissimov et al. 2009; Shnit-Orland et al. 2012; Raina et al. 2016; Ushijima et al. 2023; Voolstra et al. 2024c). However, temperature stress may disrupt microbial community structure, leading to a loss of symbiotic partners and the proliferation of opportunistic microbes, including potentially pathogenic species such as those of the genus *Vibrio* (Voolstra et al. 2024c; van Oppen and Blackall 2019; Voolstra et al. 2021; Pootakham et al. 2019a; Tignat-Perrier et al. 2022; 2023; Prioux et al. 2023; Vezzulli et al. 2010a). These shifts, known as dysbiosis, can lead to temperature-dependent diseases and may precede tissue loss and coral mortality (Vezzulli et al. 2010a; Pootakham et al. 2019b; Rosales et al. 2020; Tignat-Perrier et al. 2023; 2022; Prioux et al. 2023; Voolstra et al. 2024c). Although microbiome shifts in various coral species during heat stress have been well characterized (Voolstra et al. 2024c; van Oppen and Blackall 2019; Voolstra et al. 2021; Tignat-Perrier et al. 2022; 2023; Prioux et al. 2023; Prioux, Ferrier-Pagès, Del Campo, et al. 2025; Pootakham et al. 2019b; Ahmed et al. 2019; Chapron et al. 2021), several knowledge gaps persist to fully understand the response of the coral holobiont to heat stress. For example, our understanding of microbiome resilience, the ability to withstand and recover from stress, remains limited. While many studies have shown that the composition of coral microbiomes changes significantly under thermal stress, fewer investigated the ability to recover their original state (Chapron et al. 2021; Maher et al. 2020; Girija et al. 2024; Dunphy et al. 2021; Epstein et al. 2019; Vompe et al. 2024). Since the microbiome may play a key role in the overall health and resistance of the host, its recovery capacity is a critical factor in coral health under heat stress. Therefore, the ability of the microbiome to restore homeostasis after disturbance may be central to predicting coral survival in the face of climate-driven stressors. A second major knowledge gap lies in the fact that most research has focused on the dynamics and recovery of bacterial communities, while the response to heat stress of other microbes, such as microeukaryotes, remains poorly understood. Most studies focused on the photosynthetic dinoflagellates from the family Symbiodiniaceae but the coral eukaryome contains other microeukaryotic members that have been poorly investigated despite their likely relevance for the coral holobiont (Maire et al. 2022; Ainsworth et al. 2017; Bonacolta et al. 2023). Some of these microeukaryotes such as the dinoflagellates Dino Group I Clade I have been linked to thermally tolerant corals, suggesting they may play a role in host's stress response (Bonacolta et al. 2024). However, excluding the ones on

Symbiodiniaceae, fewer than ten studies have investigated changes in coral-associated microeukaryotic communities under thermal stress (Bonacolta et al. 2024; Prioux, Ferrier-Pagès, Del Campo, et al. 2025; Martin-Cuadrado et al. 2024). Without a clearer picture of how these communities respond, our understanding of how coral holobionts will face rising temperatures remains incomplete. Finally, attention has been focused mainly on tropical corals, while the microbiome of other important coral species, such as temperate octocorals forming the Mediterranean MAFs, is largely unexplored.

The potential of Mediterranean octocorals to recover from temperature stress is a key topic as the Mediterranean Sea is warming 20% faster than the global average, with frequent and intense marine heatwaves (MHWs; MedECC 2020; Juza et al. 2022; T-MEDNet 2023). Recurrent MHWs induce disease outbreaks and mass mortality of octocoral species, such as *Paramuricea* spp., *Eunicella* spp. and *Corallium rubrum*, even in marine protected areas (Grenier et al. 2023; Gómez-Gras et al. 2021; Capdevila et al. 2023; 2024). These Mediterranean octocorals are good models to investigate dysbiosis and resilience to thermal stress, because they harbor a highly specific bacterial microbiome, that is normally stable across seasons, geographic locations and depths, and dominated by bacteria from the Endozoicomonadaceae or Spirochaetaceae family (van de Water et al. 2016a; van de Water, Voolstra, et al. 2018a). Recent studies have begun to investigate the changes in bacterial communities of these coral species during heat stress events (Tignat-Perrier et al. 2022; Corinaldesi et al. 2022; Rubio-Portillo et al. 2021a; Prioux et al. 2023). However, several important questions remain unanswered, including the potential recovery of bacterial communities after the stress event, and the response of other holobiont-associated microbial members, such as microeukaryotes. Addressing these gaps is crucial for a better understanding of the resistance and resilience of octocorals to heat stress.

In this study, we used the emblematic red coral *Corallium rubrum* as an octocoral model, due to its ecological and structural importance in Mediterranean marine ecosystems (Casas-Güell et al. 2015). As a long-lived, habitat-forming octocoral, *C. rubrum* contributes significantly to local biodiversity by providing complex three-dimensional structures that provide refuge and substrate for approximately 10% of marine Mediterranean species (Boudouresque 2004). Its population is already on the

verge of collapse as overfishing by the jewelry industry (Montero-Serra et al. 2015) and environmental stressors, such as ocean acidification and global warming, reduce the density and biomass of *C. rubrum* populations (Bramanti et al. 2013; Gómez-Gras et al. 2021; Garrabou et al. 2001; Garrabou and Harmelin 2002; Garrabou et al. 2022). Due to late sexual maturity, slow growth rates, and low recruitment rates, the ability of *C. rubrum* to recover from mortality events is low (Garrabou and Harmelin 2002; Ledoux et al. 2010). However, the decline of *C. rubrum* and other habitat-forming species rapidly disrupts community structure and poses a significant threat to the ecological functioning of Mediterranean animal forests (MAFs) and the organisms that depend on them (Garrabou et al. 2021; Gómez-Gras et al. 2019; 2021). To test the effect of thermal stress on *C. rubrum* holobiont, colonies were exposed to two short-term temperature increases (*i.e.*, 8 days at 19 °C or 23 °C instead of the control temperature of 15°C) simulating thermal anomalies experienced by Mediterranean octocorals during MHWs down to 40 m depth. To assess the impact of these treatments, we analyzed changes in the composition of the associated bacterial and microeukaryotic communities using amplicon sequencing of *16S* and *18S rRNA* genes and taxon-specific qPCR analyses. The concomitant coral host response was also assessed by measuring expression levels of two stress-response genes: *TNFR1*, involved in the regulation of the apoptosis cascade, and *HSP70*, a stress-response gene associated with cellular repair processes. Our findings provide insights into the short-term recovery capacity of octocoral holobionts after thermal anomalies and highlight how MHWs may contribute to disease outbreaks and mass mortality of octocoral populations in the Mediterranean Sea.

Material and Methods

Biological material and experimental design

Nine distinct multi-branched colonies of *Corallium rubrum* (7-8 cm long) were collected at 40 m depth in Villefranche-sur-Mer (France), with the permission of the Direction Inter-Régionale de la Mer Méditerranée (France). The seawater temperature near the colonies at the time of collection in June was 15°C (divers' computers and SOMLIT; www.somlit.fr). After collection, the colonies were transported to the aquarium

facility of the Centre Scientifique de Monaco. Each colony was divided into 9 nubbins (3 cm long) which were tagged according to their original colony. The 81 nubbins were suspended on fishing lines and maintained in open-flow aquaria at 15°C in darkness for 2 weeks to acclimate before being distributed over the experimental aquaria.

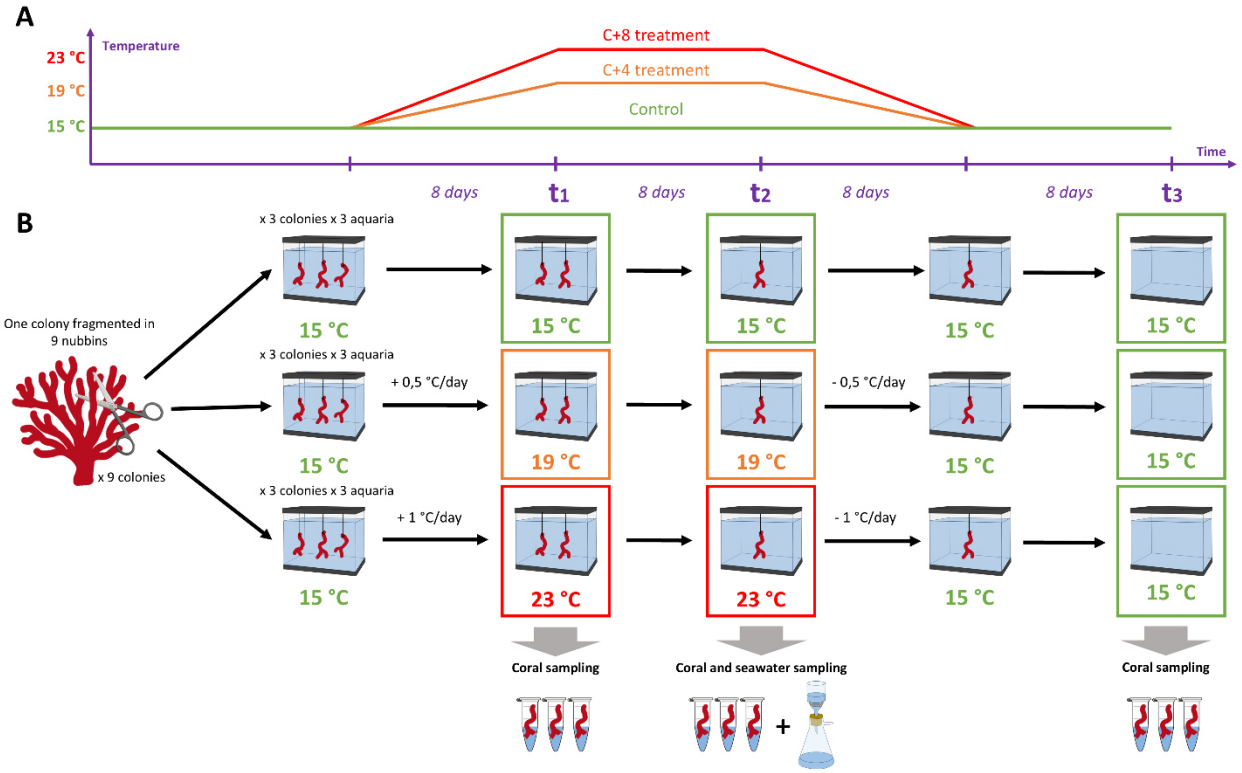

Figure 1: Schematic representation of the experimental design. (**A)** Experimental temperature regimes applied to the corals, with the three sample collection time points. **(B)** Nine colonies were cut in nine nubbins randomly allocated into groups of three in the aquaria. One nubbin per colony and thermal treatment was removed at each sampling time point.

The experimental setup consisted of nine 25 L aquaria, which were kept in the dark throughout the experiment to reflect their natural habitat conditions (Ballesteros 2006). Each aquarium received a continuous flow of seawater (15 L/h) pumped from a depth of 50 m and filtered through a 5 µm pore size filter, to prevent large particles or algae from entering the tanks. Nevertheless, it was possible to maintain the natural bacteria and microeukaryotes as under *in situ* conditions. Inside each aquarium, a pump ensured continuous mixing of the seawater, while a heater, regulated by a temperature controller, maintained a constant temperature. Nubbins were fed with fresh *Artemia salina* nauplii twice a week. Three aquaria were assigned for each of the three thermal regimes as detailed below. Each aquarium contained 9 nubbins, *i.e.* 3 nubbins originating from 3

distinct colonies, ensuring that the 9 colonies were represented in each of the thermal regime, allowing statistical correction for colony.

Nubbins were exposed to 3 thermal regimes: a control condition (15°C; Supplementary Figure S1), a moderate increase (+4°C, reaching 19°C), which corresponds to an automnal temperature at 40 m depth in Villefranche-sur-Mer, and a high increase (+8°C, reaching 23°C), simulating maximum temperatures reached during and after summer heatwave episodes (Supplementary Figure S1). In contrast to surface waters, the warmest temperatures at this depth occur in the fall following the seasonal mixed layer depth deepening (Supplementary Figure S1;Darmaraki 2019; Bahamon et al. 2020). In this experiment, colonies, acclimatized at 15°C, were exposed to 23°C for 8 days only. This limited exposure period was chosen to avoid tissue loss and mortality while eliciting a response from the host and its microbiome. As expected, colonies showed no sign of tissue loss or mortality in either thermal treatment, in agreement with previous studies indicating that the red coral shows partial mortality after 3 weeks at 23°C (Tignat-Perrier et al. 2023).

For simplicity, the different treatments are referred to as Control, C+4 treatment, and C+8 treatment, respectively, throughout the study. Except for the control aquaria, temperature was gradually heated to 19°C or 23°C in 8 days (+0.5°C or +1°C per day, respectively), maintained during the subsequent 8 days, followed by a gradual temperature decrease (-0.5°C or -1°C per day, respectively) in order to reach the control temperature condition of 15°C after 8 days (Figure 1). The rate of temperature increase differed between the two thermal treatments (0.5°C/day and 1°C/day) to ensure that corals across both conditions reached their respective target temperatures simultaneously. This design allowed all samples to be exposed to thermal stress over the same time frame and under the same water supply. Three nubbins per aquarium (originating from different colonies), were sampled at 3 time points during the experiment (Figure 1): just after the peak temperature was reached (*t1*), 8 days after the peak temperature was reached (*t2*) and finally 8 days after the temperature returned to normal (*i.e.*, 15°C; *t3*). None of the nubbins presented signs of tissue necrosis or polyp retraction. At each sampling point, nubbins were immediately rinsed with 0.22 µm filtered seawater to avoid introducing transient microorganisms from the surrounding water into the DNA

extraction and placed in separate Ziploc® plastic bags and flash-frozen in liquid nitrogen (~ 190°C, ©CX100 Worthington Industries). Two seawater samples were collected for each thermal treatment at *t2* by filtering 2 L of seawater per sample through a 0.2 µm Nuclepore Track-Etch Membrane filter (Whatman, diameter of 47 mm). Both coral and seawater samples were then stored at − 80°C until further processing.

DNA and RNA extraction

Total RNA and DNA were extracted from approximately 1 cm of tissue or 1 seawater filter using the AllPrep® DNA/ RNA Micro kit (Qiagen) with the following modifications: samples were transferred in pre-filled bead tubes (Qiagen) containing 346.5 µL of Buffer RLT Plus and 3.5 µL of beta-mercaptoethanol, followed by 2 times 2 min of bead beating using the CryoMill (Retch, Germany) at a frequency of 30 Hz. Two negative extraction control samples (*i.e.*, extraction without sample material) were processed at the same time as the rest of the samples to account for contaminants. DNA and RNA concentrations were measured using a Qubit fluorometer, DNA samples were stored at − 20°C and RNA samples at -80°C.

DNA-based MiSeq amplicon sequencing of the *16S* and *18S rRNA* gene

Library preparation and sequencing

The V3-V4 region of the *16S rRNA* gene was amplified to assess the composition of the bacterial communities using the forward primer 341F (5'-CCTACGGGNGGCWGCAG-3') and the reverse primer 785R (5'-GACTACHVGGGTATCTAATCC-3'), as described by Klindworth et al. (2013). To assess the composition of the microeukaryotic communities, customized primers 18S-NonMet_Cr-F (5'-AAGTCTGGTGCCAGCASCC-3') and 18S-NonMet_Cr-R (5'-TTTAAGTTTCAGCCTTGCGAT-3') were used, targeting the V4 region of the *18S rRNA* gene. These primers were derived from the UNonMet-PCR primers designed to minimize signals from metazoan hosts, as initially described by Bower et al. (2004). Their efficacy for Illumina amplicon sequencing was further validated by del Campo et al. (2019) and Prioux et al.(2025).

PCR amplifications were conducted on both coral and seawater samples, along with the two negative controls, in a total reaction volume of 25 µL. Each reaction

contained 5 µL of 5X Q5® reaction buffer, 0.5 µL of dNTPs, 1.25 µL of each forward and reverse primers (10 µM) with Illumina adapters, 0.25 µL of Q5® High-Fidelity DNA Polymerase, and 2 µL of template genomic DNA (or DNA-free water for the controls). The thermocycling program included an initial denaturation at 98°C for 30 s, followed by 35 cycles comprising denaturation at 98°C for 10 s, primer annealing at either 55°C (for *16S rRNA* gene primers) or 63°C (for *18S rRNA* gene primers) for 30 s, and extension at 72°C for 30 s, with a final extension at 72°C for 2 min. The success of amplification was verified by running the PCR products on an agarose gel. Bands corresponding to the target sizes were cut from the gel and purified using the GFX™ PCR DNA and Gel Band Purification Kit (Illustra™). DNA concentration was measured with a Qubit fluorometer, and amplicons were sent to STAB-VIDA (Portugal) for paired-end sequencing (2 × 300 bp, 600 cycles) on an Illumina MiSeq platform. All subsequent library preparation steps followed Illumina's "16S Metagenomic Sequencing Library Preparation" protocol (Illumina 2013). The raw sequencing data (fastq files) have been submitted to the NCBI Short Read Archive (SRA) under the BioProject accession number PRJNA1211024.

Bioinformatics data processing

The amplicon data were processed using the DADA2 pipeline (version 1.16; https://benjjneb.github.io/dada2/index.html; Callahan et al. 2016). Samples with less than 15, 000 reads were removed from the dataset, resulting in 74 and 71 samples for the bacterial and microeukaryotic communities, respectively. Sequencing of the *16S rRNA* gene amplicons resulted in 3,142,312 reads ranging from 21,901 to 109,992 reads per sample (Supp. File 1, Table S1). Sequencing of the *18S rRNA* gene amplicons resulted in 2,401,825 reads ranging from 15,955 to 109,874 reads per sample (Supp. File 1, Table S1). From both sequencing, negative controls contained from 12,337 to 92,207 reads per sample. Primer sequences were trimmed at the 5'-end of each read using Cutadapt v3.1 (Martin 2011).

Read quality profiles were inspected, and reads were filtered and trimmed with the following settings: maxN=0, rm.phix=TRUE, maxEE=c(2, 2), truncLen=c(295, 230) for the *16S rRNA* reads and truncLen=c(298, 200) for the *18S rRNA* reads. For both datasets, error rates were computed and used for sequence inference. For the *16S rRNA* gene sequencing, sequences were merged, and those smaller than 390 bp and longer than 450

bp were removed. For the *18S rRNA* gene sequencing, as the expected size of some amplicons exceeded 600 bp, R1 and R2 sequences were not merged but concatenated using mergePairs(justConcatenate=TRUE) following procedure choices from Prioux et al. (2025). Amplicon sequence variant (ASV) tables were created. Chimeras were detected and removed from the table using the removeBimeraDenovo() function. The number of reads and sequences per sample passing through the different steps of the pipeline for both datasets is presented in Supp. File 1, Table S1.

Taxonomy was assigned to the 5,034 ASVs (*16S rRNA* gene) and 8,617 ASVs (*18S rRNA* gene) using the assignTaxonomy() function and the SILVA SSU reference database (version 138.1) or the PR2 reference database v4.13.0 (Guillou et al. 2012) for the *16S* and *18S rRNA* gene sequencing, respectively. For the *16S rRNA* gene sequencing, ASVs corresponding to Archaea were removed, resulting in 4,991 ASVs. For the *18S rRNA* gene sequencing, ASVs corresponding to Metazoa and Embryophyceae were removed, resulting in 1,556 ASVs (Supp. File 1, Table S1). The ratio between the number of sequences assigned to microeukaryotic ASVs (*i.e.*, removing sequences corresponding to Metazoa ASVs) and the total of sequences was calculated. The ASV tables, the taxonomic annotation and metadata tables are available in Supp. File 1 as Tables S2, S3, S4, S5 and S6 respectively, and the sequences of the ASVs are available as Supp. File 2 and 3.

Analysis of the bacterial 16S rRNA gene and microeukaryotic 18S rRNA gene sequencing data

All statistical analyses were conducted in the R environment (version 4.2.1) using the R-package *phyloseq* (McMurdie and Holmes 2013). The R-package *decontam* (Davis et al. 2018) was used to identify contaminant ASVs in the samples based on the negative control samples (isContaminant function), however, no ASV was identified as contaminant. Observed species richness and evenness (Shannon index) were calculated using the R-package *vegan* (Oksanen et al. 2022). Alpha diversity analyses were performed on the unrarefied ASV count table, according to the ongoing debate about the use of unrarefied versus rarefied data (McMurdie and Holmes 2014; Willis 2019). To examine differences in observed richness and evenness, generalized linear mixed effects models were fitted including thermal treatment and sampling time as fixed factors and colony as random factor to assess whether an effect of colony existed. As no significant

random effect was observed, alpha diversity data were analyzed using generalized linear models (GLM) with thermal treatment and sampling time as fixed factors (observed richness ~ sampling time * thermal treatment; Supp. File 1 Table S7). Post-hoc tests were conducted to identify potential pairwise differences using a corrected α for multiple hypothesis testing of < 0.05 (Supp. File 1 Table S7; R-package *emmeans*; Lenth 2023).

The composition of the bacterial and microeukaryotic communities associated with *C. rubrum* exposed to the thermal treatments C+4 (increase to 19°C) and C+8 (increase to 23°C) was compared to the 15°C control condition at the three sampling times: *t1* or when the temperature of 19°C and 23°C was reached; *t2* or after 8 days of thermal exposure; and *t3* or after 8 days of recovery time (*i.e.*, temperatures back to 15°C). As no differences in community composition were detected in the 15°C control condition over time (*i.e.*, *t1* to *t3*), control samples of the three sampling times were pooled and used for statistical analyses. Differences in microbial community composition were also tested between the two thermal treatments C+4 and C+8. To examine compositional changes, compositional data based analyses (CoDA; Gloor et al. 2017; Quinn et al. 2018) were used, following the same data manipulation as in Prioux et al. (2023; 2025) exploiting the R-packages *compositions* and *zCompositions* (van den Boogaart and Tolosana-Delgado 2008a; Palarea-Albaladejo and Martín-Fernández 2015). After these procedures, an Aitchison distance matrix was generated by calculating the Euclidean distance between samples from a clr-transformed data table. To evaluate differences in the microbial community structure across sampling times and thermal treatments, principal component analysis (PCA) and permutational multivariate analysis of variance (using the adonis() function from the R-package vegan) were done (Supp. File 1 Table S8). Following this, potential pairwise differences were analyzed using the permanova_pairwise() function from the R-package *ecole* (Smith 2021), with p-values adjusted for false discovery rate (Supp. File 1 Table S8). Differential abundance analyses were conducted to detect differentially abundant ASVs between sampling times within each thermal treatments, using the R-package *ANCOM-BC* (ancombc2() function, using prv_cut = 0.1 and alpha = 0.01; pairwise = TRUE for sampling sites; version 02–2023; Supp. File 1 Table S9 and S10; Lin and Peddada 2020). The core microbiome of the bacterial and microeukaryotic communities in the control samples was identified at the ASV level using

the core_members() function (arguments: detection = 0.0001, prevalence = 0.99, include.lowest = FALSE) of the R-package *microbiome* (Supp. File 1 Table S9 and S11; Lahti et al. 2017).

Co-occurrence patterns between microorganisms (*i.e.*, between bacteria, between microeukaryotes and between bacteria and microeukaryotes) were analyzed across all samples, regardless of temperature treatment, to identify general patterns of co-presence or exclusion among taxa, reflecting potential ecological interactions rather than direct responses to thermal stress. It was performed using the R-package *SpiecEasi* (Sparse Inverse Covariance Estimation for Ecological Association Inference; Kurtz et al. 2015). Spiec-Easi is a statistical method developed specifically for compositional data. Network inference is done under the assumption of sparsity, using sparse neighborhood and inverse covariance selection algorithms (Kurtz et al. 2015). Non-normalized count ASV tables from both datasets were first filtered to remove low-abundant ASVs (*i.e.*, < 0.3 %). A multi-sample sparse inverse covariance estimation was done using the multi.spiec.easi() function of the R-package *SpiecEasi*. The method used for this analysis was 'mb' (Meinshausen-Bühlmann), which infers sparse graphical models by solving neighborhood selection problems. The parameters included sel.criterion = "stars" to use the StARS (Stability Approach to Regularization Selection) model selection criterion and pulsar.select = TRUE to enable automatic model selection using the Pulsar framework. The regularization path was determined with a minimum lambda ratio (lambda.min.ratio) of 1e-2 and nlambda set to 10. The adjacency matrix of the network was obtained using the "symBeta" function, and an undirected graph was created with the R-package *igraph* (Csárdi and Nepusz 2006). Edge weights, representing the strength and type of associations between ASVs, are available in Supp. File 1 Table S12. The network was then visualized in a circular layout to display relationships.

Quantitative PCR (qPCR)

Gene expression of heat stress protein 70 (HSP70) and tumor necrosis factor receptor 1 (TNFR1)

The host response to thermal stress was assessed following the gene expressions of *HSP70* and *TNFR1* using the primers designed in Haguenauer et al. (2013) and Tignat-

Perrier et al. (2023), respectively (details on primer pairs including primer efficiencies provided in Supp. File 1 Table S13). Additionally, a pair of primers targeting the *beta-actin* gene of *C. rubrum* (Prioux et al. 2023) was used to serve as internal control (Supp. File 1 Table S13). The efficiency of the different primer pairs was verified using a tenfold dilution series of a combined DNA sample mix. The amplification results were plotted as Ct vs. log10[DNA] and amplification efficiency was calculated using the formula $E=10^{(-1/slope)}$ (Supp. File 1 Table S13; (Pfaffl 2001).

For the reverse transcription qPCR analyses, cDNA was synthesized from 500 ng of total RNA in a final reaction volume of 20 µL using the SuperScript IV Reverse Transcriptase (ThermoFisher). Quantitative PCR reactions were performed in duplicate in a total volume of 10 µL with 1:10 dilution of cDNA template aliquots and 1 µM of primers using SYBR-green-based detection (SensiFAST™ SYBR ® No-ROX kit, ThermoFisher) on a QuantStudio3 qPCR machine (Applied Biosystems). Cycle parameters were 95°C 5 min then 40 cycles 95°C 10 s/60°C 30 s. Following amplification, the specificity of the product was assessed from a melting curve program.

Expression of specific bacterial gene markers

Comparative qPCR was used to follow the changes in the abundance of total bacteria, the abundance of bacteria belonging to the *Spirochaetaceae* family and the *Vibrio* genus in the red coral cells. The three primer pairs including the universal *16S rRNA* gene primers (total bacteria; (Fierer et al. 2005), primers specific to the *Spirochaetaceae* group (Husmann et al. 2010) and the *Vibrio* genus (Thompson et al. 2004) had their specificity and efficiency for *C. rubrum* tested in Prioux et al. (2023; details on primer pairs including primer efficiencies provided in Supp. File 1 Table S13; (Prioux et al. 2023).

qPCR assays were conducted in duplicate using a QuantStudio3 qPCR machine (Applied Biosystems). Each reaction consisted of 0.4 µL of each primer (4 µM), 10 µL of SensiFAST SYBR master mix (ThermoFisher), and 2 µL of DNA (10 ng/µL), in a total volume of 20 µL. The thermal cycling protocol included an initial denaturation at 95°C for 10 min, followed by 40 cycles 95°C 15 s/60°C 1 min.

qPCR data analysis

Relative gene expression was calculated using the Pfaffl method (Pfaffl 2001), normalized to the *beta-actin* reference gene. Fold changes in gene expression under the thermal treatments were calculated relative to the control conditions. Statistical differences in total bacterial abundances as well as of *Spirochaetaceae* and *Vibrio*, as well as in *HSP70* and *TNFR1* gene expression across sampling times and thermal treatments were evaluated using two-way non-parametric Kruskal-Wallis tests (Supp. File 1 Table S14).

Results

Alpha diversity in bacterial and microeukaryotic communities

A higher richness was observed in the seawater microbial communities (on average 671 bacterial ASVs and 117 microeukaryote ASVs) compared to the coral communities, (on average 241 bacterial ASVs and 51 microeukaryote ASVs; Supp. File 1 Table S7; $p= 2.1 \times 10^{-8}$ and estimate $p = 3 \times 10^{-3}$ for the bacterial and microeukaryotic communities, respectively; Supp. File 1 Table S7). There was no significant differences in alpha diversity of the bacterial and microeukaryotic communities in the coral samples between sampling times or thermal conditions (observed richness and Shannon index; p values > 0.05; Supp. File 1 Table S7). Although the limited number of samples did not allow statistical testing, the observed richness of microeukaryotic ASVs in seawater increased by 4 times with temperature (31, 60 and 260 ASVs on average at 15°C, 19°C and 23°C, respectively; Supp. File 1 Table S7).

Composition of the microbiome in the control colonies

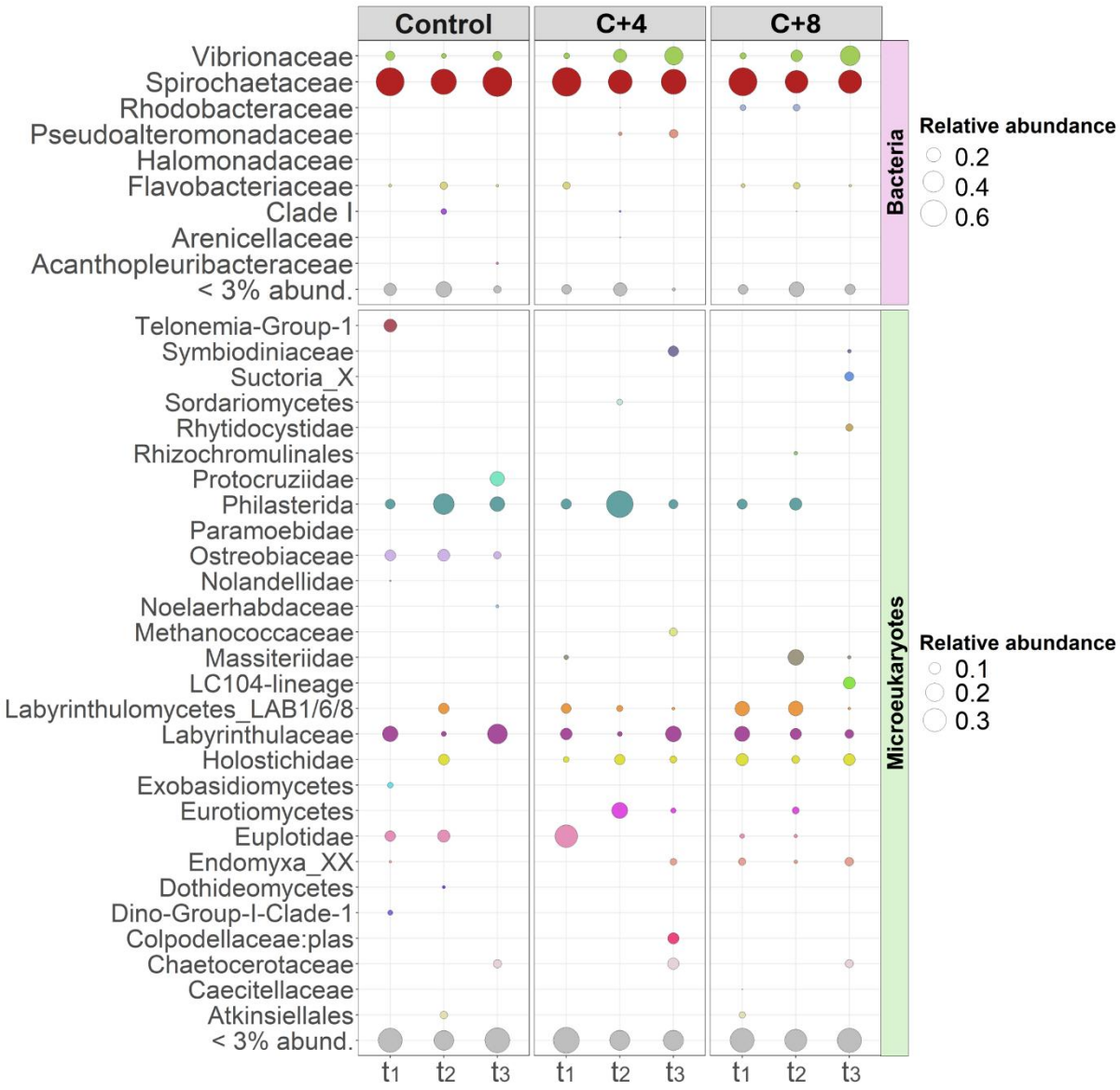

Figure 2: Relative abundance of the bacterial and microeukaryotic families associated with *C. rubrum* colonies depending on the sampling time and thermal treatment. Taxa with an average relative abundance below 3% are grouped.

No significant difference in community composition was found between the different sampling points in the control condition. The bacterial communities were therefore dominated by the Spirochaetaceae (representing on average 70% of the total community) and the Vibrionaceae family (10%), while the microeukaryotic communities were dominated by the Labyrinthulomycetes order (Labyrinthulaceae and LAB1/6/8 families; 25%), the Philasterida (15%) and the Ostreobiaceae family (10%; Figure 2). At

the ASV level, the core microbiome was composed of three bacterial ASVs (ASV1 and ASV2 from the Spirochaetaceae family and ASV3 from the Vibrionaceae family; Supp. File 1 Table S11) and 145 microeukaryotic ASVs (comprising 30 ASVs from the Labyrinthulomycetes order, 13 ASVs from the Philasterida family and two ASVs from the Ostreobiaceae family; Supp. File 1 Table S11). The composition of the bacterial and microeukaryotic communities was different between the negative control, seawater and coral samples (Supp. File 1 Table S8). Although present at low abundances, dominant coral-associated taxa such as Spirochaetaceae, Vibrionaceae, Labyrinthulomycetes, and Philasterida were detected in the seawater samples (Figure S2 and S3).

Differences in the composition of the microbial communities between temperature treatments and sampling times

The composition of the bacterial and microeukaryotic communities significantly changed between temperature treatments and sampling times.

Bacterial communities

There was no difference in betadispersion between temperature treatments ($p = 0.2$; Supp. File 1 Table S8) and sampling times ($p = 0.3$; Supp. File 1 Table S8). However, the composition of the bacterial communities was different between temperature treatments ($p = 1 \times 10^{-3}$; Supp. File 1 Table S8) and sampling times ($p = 1 \times 10^{-3}$; Supp. File 1 Table S8), and an interaction between temperature and time was detected ($p = 0.058$; Supp. File 1 Table S8). Compared to the control condition, the bacterial community composition changed after 8 days at 19°C (C+4 treatment at *t2*) and immediately at 23°C (C+8 treatment at *t1*; $p = 0.04$ for both; Supp. File 1 Table S8). In addition, at 23°C, the composition changed over time (C+8 treatment at *t1* versus *t2*; $p = 0.006$; Supp. File 1 Table S8). After 8 days of recovery (*i.e.*, temperatures back to 15°C; *t3*), the bacterial community composition in both temperature treatments was no longer different compared to the control condition (post-hoc tests p values > 0.05; Supp. File 1 Table S8).

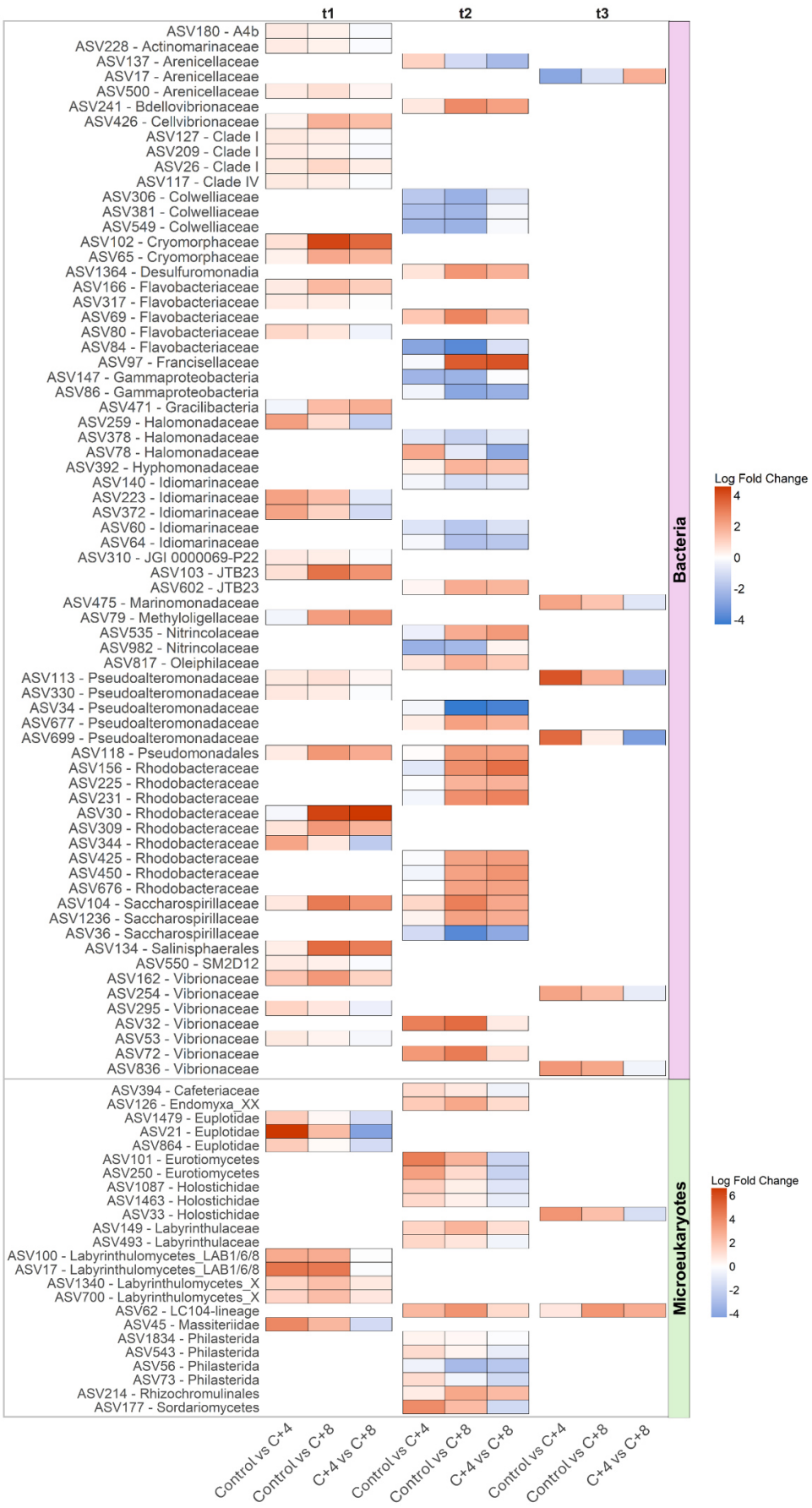

Figure 3: Bacteria and microeukaryote ASVs differentially abundant (ANCOM-BC results) between the sampling times and thermal treatments. Differences in relative abundance are calculated as log fold change (natural log).

At the family level, and compared to the control condition, we observed an increase in Vibrionaceae at 19°C and 23°C, as well as in Pseudoalteromonadaceae at 19°C and Rhodobacteraceae at 23°C (Figure 2). At the ASV level, several ASVs were differentially abundant between the control condition and the C+4 treatment (Figure 3 and Supp. File 1 Table S9). In particular, 22 ASVs (including Vibrionaceae and Rhodobacteraceae ASVs) increased at *t1* and 6 ASVs (including Vibrionaceae and Pseudoalteromonadaceae ASVs) increased at t3. In contrast, 5 ASVs (including Colwelliaceae, Flavobacteraceae, and Nitrincolaceae ASVs) decreased at *t2* and ASV17 (Arenicellaceae) decreased at *t3*. Several ASVs were also differentially abundant between the control condition and the C+8 treatment (Figure 3 and Supp. File 1 Table S9). In particular, 10 ASVs (including Vibrionaceae and Cellvibrionaceae) increased at *t1* and 13 ASVs (including Vibrionaceae) at *t2* while ASV30 (Rhodobacteraceae,) decreased at *t1* and 14 ASVs (including Rhodobacteraceae and Colwelliaceae) decreased at *t2*.

Microeukaryotic communities

There was no significant difference in the betadispersion between temperature treatments ($p = 0.3$; Supp. File 1 Table S8) or sampling times ($p = 0.6$; Supp. File 1 Table S8). However, the composition of the microeukaryotic communities showed significant changes across temperature treatments ($p = 5 \times 10^{-3}$; Supp. File 1 Table S8) and sampling times ($p = 1 \times 10^{-3}$; Supp. File 1 Table S8), with an interaction between these two factors ($p = 0.002$; Supp. File 1 Table S8). The composition of the microeukaryotic communities changed as soon as the temperature reached 19°C (C+4 treatment at *t1*) and 23°C (C+8 treatment at *t1*) in comparison to the control condition (p-values < 0.05; Supp. File 1 Table S8), and changed over time (*t1* versus *t2*; $p = 0.003$ and $p = 0.002$, respectively). After 8 days of recovery (C+4 and C+8 treatments at *t3*), the composition of the microeukaryotic communities was no longer different compared to the control condition (post-hoc tests p-values > 0.05; Supp. File 1 Table S8).

At the family level, both C+4 and C+8 treatments induced a relative decrease of Ostreobiaceae (*t1*, *t2*, *t3*) and Labyrinthulaceae (*t1* and *t2*), compared to the control condition (Figure 2). On the contrary, there was a relative increase in Holostichidae (*t1*, *t2*, *t3*) and in a specific Labyrinthulomycetes group (LAB1/6/8; *t1* and *t2*). Additionally, in the C+8 treatment, the relative abundance of the Philasterida family decreased over time

while the relative abundance of the Endomyxa family increased and members of the Massiteriidae family appeared briefly at *t2* before decreasing at *t3* (Figure 2). At the ASV level, several ASVs were differentially abundant between the control condition and the C+4 treatment (Figure 3 and Supp. File 1 Table S10). 6 ASVs (including Labyrinthulomycetes LAB1/6/8 and Euplotidae ASVs) increased at *t1*, 10 ASVs (including Labyrinthulaceae, Holostichidae, and Philasterida ASVs) increased at *t2* and one ASV (ASV33-Holostichidae) increased at *t3*. Several ASVs were also differentially abundant between the control condition and the C+8 treatment (Figure 3 and Supp. File 1 Table S10. Three ASVs (including Labyrinthulomycetes ASVs) increased at *t1*, 4 ASVs (including one Endomyxa and one Eurotiomycetes ASVs) increased at *t2* and ASV62 (LC104-lineage) increased at *t3*. Only ASV56 (Philasterida) decreased at *t2*.

Co-occurrence patterns between microorganisms

Co-occurrence analysis of the 60 and 56 most abundant bacterial and microeukaryotic ASVs, respectively, revealed 33 negative correlations (weights ranging from -0.0004 to -0.1; Supp. File 1 Table S12) and 134 positive correlations between taxa (weights ranging from 0.0002 to 0.05; Supp. File 1 Table S12). Correlations were more prevalent among bacterial taxa than among microeukaryote taxa (91 and 49 correlations for bacterial and microeukaryotic ASVs, respectively; Figure 4 and Supp. File 1 Table S12). In addition, 27 interactions were found between bacterial and microeukaryotic ASVs (Figure 4 and Supp. File 1 Table S12).

Positive co-occurrences among bacteria

The two strongest positive correlations were between ASV40 and ASV10 (Pseudoalteromonadaceae; weight = 0.57; Supp. File 1 Table S12), and between ASV73 and ASV59 (Vibrionaceae; weight=0.56; Supp. File 1 Table S12). ASVs from the Vibrionaceae family were present in several positive and strong co-occurrence correlations (27% of the correlations with 46% of the weights higher than 0.1; Figure 4 and Supp. File 1 Table S12). Furthermore, members of the Vibrionaceae family frequently co-occurred with each other (84% of the co-occurrences including the Vibrionaceae family were between two Vibrionaceae ASVs), as for the Rhodobacteraceae family (30% of the

co-occurrences including the Rhodobacteraceae family were between two Rhodobacteraceae ASVs; Figure 4 and Supp. File 1 Table S12).

Positive co-occurrences among microeukaryotes

The two strongest positive correlations were between ASV283 and ASV657 (Ostreobiaceae), and between ASV250-Eurotiomycetes and ASV177-Sordariomycetes (weight = 0.49 and 0.47, respectively; Supp. File 1 Table S12). Labyrinthulomycetes (including Labyrinthulaceae and Labyrinthulomycetes LAB1/6/8) represented 15% of the positive co-occurrence relations. Furthermore, 28% of the co-occurrences which included the Labyrinthulomycetes class were between two Labyrinthulomycetes ASVs (Figure 4 and Supp. File 1 Table S12). The Philasterida family represented 9% of the positive co-occurrence relations, and Philasterida ASVs mostly co-occurred with each other (56% of the co-occurrences including the Philasterida family were between two Philasterida ASVs; Figure 4 and Supp. File 1 Table S12).

Inter-kingdom co-occurrences

Among the 27 cross-domain interactions between bacteria and microeukaryotes, we observed 25 positive co-occurrences, with the four strongest associations between ASV47-Acanthopleuribacteraceae and ASV266-Protocruziidae, ASV53-Vibrionaceae and ASV191-Chaetocerotaceae, ASV60-Idiomarinaceae and ASV113-Dothideomycetes, and ASV30-Rhodobacteraceae and ASV394-Cafeteriaceae (weights ranging from 0.080 to 0.34; Supp. File 1 Table S12).

Negative co-occurrences

While negative correlations were not dominant, both intra- and inter-kingdom interactions were still observed. For example, a negative correlation was identified between the abundant ASV2-Spirochaetaceae and the microalgae Chlorarachniophyceae LC104 lineage (ASV62; weight = -0.07; Supp. File 1 Table S12). However, the overall strength of these negative interactions was low, with weights ranging from -0.0004 to -0.1 (Figure 4 and Supp. File 1 Table S12).

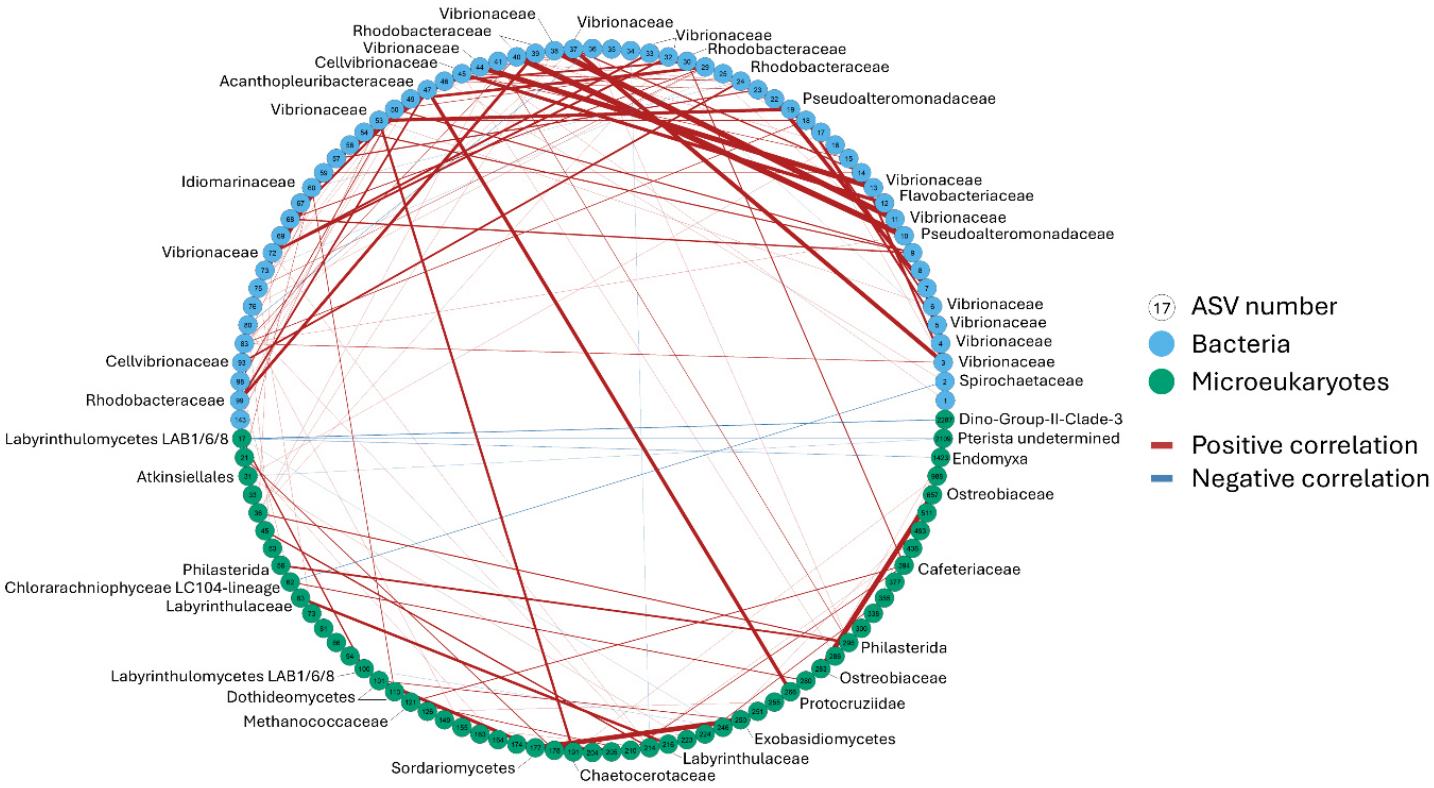

Figure 4: Network representation of significant microbial associations inferred from *16S* (prokaryotic) and *18S* (microeukaryotic) *rRNA* genes metabarcoding datasets. Nodes represent ASVs, with colors distinguishing bacterial (blue) and microeukaryotic (green) taxa. Edges indicate associations: red edges denote positive correlations, and blue edges denote negative correlations. Edge thickness corresponds to the strength of the association. Families of the ASVs of the 6 higher positive correlations for each group (intra-kingdom and inter-kingdom) as well as the first 3 higher negative correlations are labeled next to the nodes.

Quantitative PCR (qPCR)

Host response to temperature

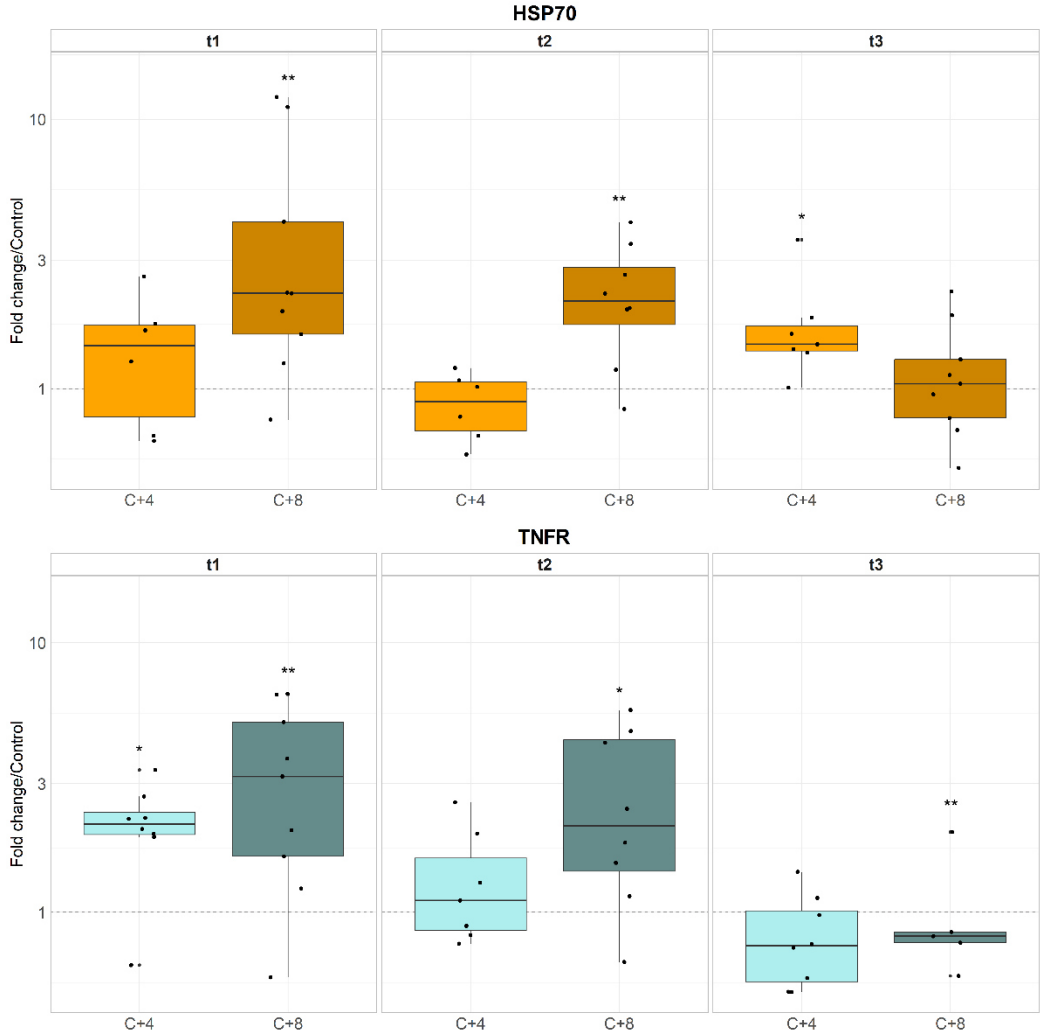

Figure 5: Relative expression ratio of stress response genes in fold change (TNFR1 and HSP70) between control and thermally treated colonies (C+4 and C+8) at the different sampling times. Graphs are presented in logarithmic scale. Statistical significance levels of differences compared to the controls are indicated by stars (* for $p < 0.05$ and ** for $p < 0.01$).

The gene expression of *HSP70* did not change at *t1* and *t2* in the C+4 treatment, compared to the control condition ($p = 0.7$ and $p = 0.3$, respectively; Figure 5 and Supp. File 1 Table S14), but significantly increased at *t3*, during the recovery ($p = 0.01$; Figure 5 and Supp. File 1 Table S14). In the C+8 treatment, mRNA levels of *HSP70* increased with a mean log fold change of 4 at *t1* ($p = 0.01$) and 2.3 at *t2* ($p = 0.009$; Figure 5 and Supp. File 1 Table S14). No significant difference with the control condition was observed at *t3* (recovery; $p = 0.7$, respectively; Figure 5 and Supp. File 1 Table S14). The gene expression

of *TNFR1* increased at *t1* in both the C+4 and C+8 treatments, with mean log fold changes of 1.9 (p = 0.05) and 3.4 (p = 0.01), respectively (Figure 5 and Supp. File 1 Table S14). At *t2* and *t3*, mRNA levels of *TNFR1* did not change in the C+4 treatment (p = 1 and p = 0.1, respectively; Figure 5 and Supp. File 1 Table S14), while they first increased (*t2*) then decreased in the C+8 treatment compared to the control condition (mean log fold change of 2.8, p = 0.02 at t2; mean log fold change of 0.7, p = 0.01 at *t3*; Figure 5 and Supp. File 1 Table S14).

Quantification of specific bacterial taxa

At *t1*, the total concentration of bacteria per host cell was not different between the control condition and the temperature treatments (p > 0.05; Figure 6 and Supp. File 1 Table S14). At *t2*, the concentration significantly increased in the C+8 treatment compared to the control condition (p = 0.02; 3.2 times higher on average; Figure 6 and Supp. File 1 Table S14). At *t3* (recovery), the total concentration of bacteria was higher only in the C+4 treatment (p = 0.01; 2 times higher on average; Figure 6 and Supp. File 1 Table S14).

Under both temperature treatments, the concentration of *Vibrio* per host cell was not different compared to the control condition at *t1* (p > 0.05; Figure 6 and Supp. File 1 Table S14). However, at *t2* and *t3*, *Vibrio* concentrations were higher under both temperature treatments compared to the control condition (p-values between 0.006 and 0.05; Supp. File 1 Table S14). In the C+4 treatment, concentrations were 9 times higher at *t2* and 6 times higher at *t3*, while under the C+8 treatment, concentrations were 17.5 times higher at *t2* and 6 times higher at *t3* (Figure 6 and Supp. File 1 Table S14). The concentration of Spirochaetaceae per host cell did not differ compared to the control condition at *t1*, *t2* and *t3* for both temperature treatments (p > 0.05; Figure 6 and Supp. File 1 Table S14).

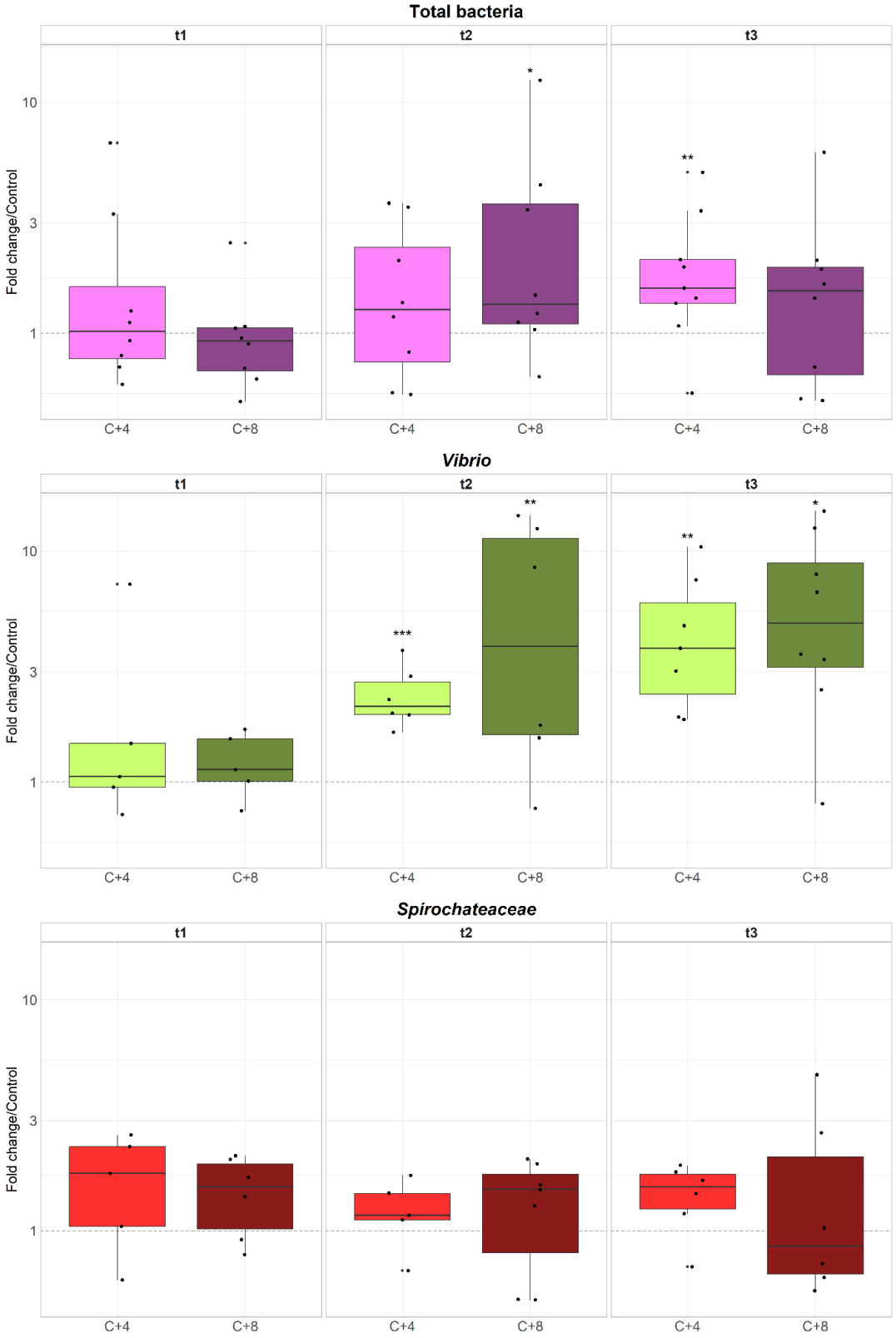

Figure 6: Relative expression ratio (fold change) between control and thermally treated colonies (C+4 and C+8) at the different sampling times of the different targeted genes. Concentration per host cell of the total bacteria, *Vibrio* and Spirochaetaceae bacteria. Graphs are presented in logarithmic scale. Statistical significance levels of differences compared to the controls are indicated by stars (* for $p < 0.05$, ** for $p < 0.01$ and *** for $p < 0.001$).

Discussion

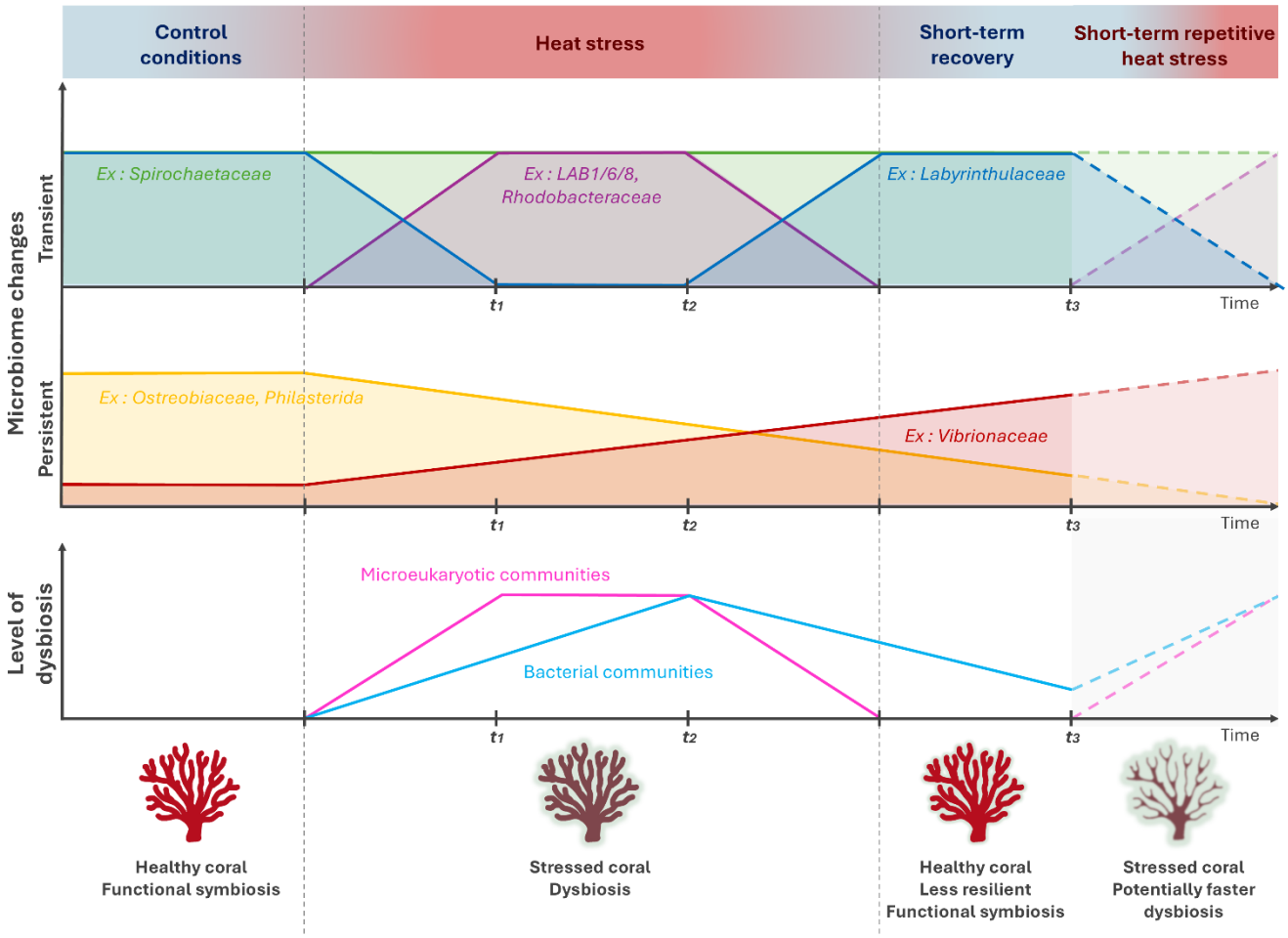

Figure 7: Microbiome dynamics of the red coral observed in this study during and after the heat stress. Under control conditions, the coral microbiome remained stable and was primarily composed of Spirochaetaceae bacteria and Labyrinthulaceae microeukaryotes. Exposure to elevated temperatures induced compositional changes in the microbiome: first in the eukaryome then in the bacterial communities. We observed an increase in opportunistic taxa and a decline in the relative abundance of microbial taxa consistently associated with healthy corals. As conditions normalize post-stress (2-weeks recovery period), the abundance of most original community members returned to baseline levels while the relative abundance of most opportunistic taxa declined. However, the coral microbiome did not fully recovered as some heat stress-associated microorganisms persisted at elevated relative abundances.

In this study, we investigated the resilience of the Mediterranean octocoral *Corallium rubrum* exposed to moderate (15°C to 19°C) and severe (15°C to 23°C) heat stress. The results of this work indicate that both the coral host and its associated

eukaryome responded rapidly to a temperature increase, while the bacterial microbiome showed a delayed response to the moderate heat stress. The magnitude of the responses was stress-dependent, with larger changes observed in the microbiome at 23°C compared to 19°C. qPCR analyses also showed that the concentration of opportunistic or potentially pathogenic bacteria, such as *Vibrio*, increased significantly during heat stress. Although the overall eukaryome and bacterial microbiome returned to their original composition after a week of recovery at control temperature, some stress-emergent microbes, Holostichidae ciliates, Endomyxa protozoa and Vibrionaceae bacteria, remained present at the same relative abundance. Future studies should therefore investigate the duration required for complete microbiome recovery, the impact of repeated heat stress on the resilience of the microbiome of *C. rubrum*, and whether the persistence of stress-associated microbial taxa influences the coral's resistance to successive heat stress as observed during MHWs.

Rapid eukaryome response to early signs of host stress

Both the eukaryome and the animal host responded promptly to temperature fluctuations. At 19°C, host gene expression of *TNFR1*, involved in the regulation of the apoptosis cascade, increased twofold. At 23°C, the expression of *TNFR1* but also *HSP70*, a stress-response gene associated with cellular repair processes, increased 4-fold and 3.4-fold, respectively. The rapid upregulation of these stress-induced genes is consistent with previous studies on heat-stressed colonies of *C. rubrum* (Tignat-Perrier et al. 2023) and tropical corals (Barshis et al. 2013). The *TNFR1* signaling pathway likely plays a critical role in regulating immune and stress responses in corals by leading to caspase activation and apoptosis (Barshis et al. 2013; Chuang and Mitarai 2020; Quistad et al. 2014; Waters et al. 2013; Van De Water et al. 2018). Concomitantly, the upregulation of *HSP70* might help colonies maintain protein structure and function under thermal stress. Heat shock proteins are commonly overexpressed in stressed corals, providing resistance to bleaching or serving as a protective mechanism during infection and disease progression (Barshis et al. 2013; Franzellitti et al. 2018; Brown et al. 2013). In particular, expression of *HSP70* increased significantly in corals exposed to pathogens such as *Vibrio coralliilyticus* and *Alteromonas* species (Brown et al. 2013).

Structural changes occurred in the microeukaryotic community immediately after the increase in temperature from 15°C to 19°C and 23°C. This contrasts with the response of the bacterial microbiome, which only showed compositional changes at 23°C or after 8 days of incubation at 19°C (see below). These results suggest that the coral eukaryome might be an early responder to environmental change, likely affecting the overall functional dynamics of the holobiont (Maire et al. 2022). Still, the changes in the coral eukaryome under environmental stress, whether beneficial or detrimental, remain poorly understood as only a few studies investigated this part of the coral microbiome (Ainsworth et al. 2017; Martin-Cuadrado et al. 2024; Wang et al. 2018; Bonacolta et al. 2024; 2023; Prioux, Ferrier-Pagès, Del Campo, et al. 2025). Concerning *C. rubrum*, the eukaryome appears to be closely linked to the physico-chemical environment in which the colonies live. In particular, differences in community composition were observed between corals maintained in the laboratory and those *in situ*. In colonies cultured in laboratory (this study), members of Philasterida and Ostreobiaceae dominated the eukaryome, whereas members of Dino-Group-I and Licnophoridae were the dominant microeukaryotes associated with colonies living in a natural environment (Prioux, Ferrier-Pagès, Del Campo, et al. 2025). Some microeukaryotic orders, such as the Labyrinthulomycetes, were found in both conditions, but showed differences in relative abundances and were represented by different ASVs (Prioux, Ferrier-Pagès, Del Campo, et al. 2025). Overall, these observations emphasize the need for broader geographical and temporal studies to assess the dynamic of the coral eukaryome across seasons and at different sites in the Mediterranean Sea.

Dysbiosis states are shaped by the intensity of heat stress

The response of the holobiont was stress and time dependent, although some major changes were common across heat treatments. In the microeukaryotic community, a shift within the dominant order of Labyrinthulomycetes from the Labyrinthulaceae to the LAB1/6/8 group was observed in both thermal treatments. This shift could indicate that the less abundant members of the community proliferate, while other members lose their competitive advantage. Interestingly, both Labyrinthulomycetes orders were detected in the seawater microbial community (Figure S3). This suggests a potential exchange between the coral microeukaryotic community

and the surrounding seawater, involving either the release or integration of certain symbionts in the eukaryome based on environmental conditions. Further investigation is needed to explore this phenomenon. While Labyrinthulomycetes are often found in dense communities in the mucus of some coral species (Siboni et al. 2010; Harel et al. 2008; Kramarsky-Winter et al. 2006), their precise role within coral holobionts is still unknown and requires further study. It has been shown that free-living marine members of Labyrinthulomycetes produce polyunsaturated fatty acids (Lee Chang et al. 2012) and carotenoids (Carmona et al. 2003; Lee Chang et al. 2012), and can have a bacteriolytic activity on dead bacterial cells (Wahid et al. 2007). These predatory protists have been shown to develop opportunistically on diseased *C. rubrum* colonies and sea fans (Burge et al. 2012; Prioux, Ferrier-Pagès, Del Campo, et al. 2025), where they might grow on bacterial invaders. Compared to the mild stress of 19°C, additional changes were observed in the dominant microeukaryotes at 23°C, with a significant decrease in the relative abundance of members of the Philasterida family. A study on free-living Philasterida species showed that these ciliates were more abundant in deep (below 200 m) than in surface waters, suggesting that they might be thermosensitive and more adapted to living at low temperatures and stable environments (Wan et al. 2024).

In the bacterial microbiome, compositional changes were detected immediately upon reaching 23 °C, whereas at 19 °C, changes only appeared after 8 days. This could either be due to the temperature stress or to the fact that the temperature rose much faster at 23°C than at 19°C, triggering a faster reaction of the bacterial microbiome. Although the specific changes in the bacterial community differed depending on the heat treatment, common changes occurred, characterized by the increase in the relative and absolute (qPCR-based) abundance of Vibrionaceae ASVs, as frequently observed in heat-stressed corals (Martin et al. 2002; Tignat-Perrier et al. 2023; Tout et al. 2015; Prioux et al. 2023). Although several *Vibrio* species, such as *V. coralliilyticus*, are known coral pathogens capable of inducing tissue necrosis (Martin et al. 2002; Sun et al. 2023; Gibbin et al. 2018; Vezzulli et al. 2010a; Vidal-Dupiol et al. 2011), we cannot confirm that the ASVs detected here correspond to pathogenic strains. Nonetheless, their proliferation in heat-stressed corals is potentially concerning and warrants further investigation to assess possible impacts on coral health. Furthermore, it is worth noting that quantifying

bacterial abundance using qPCR with universal *16S rRNA* gene primers can be affected by variation in rRNA operon copy numbers across the different bacteria. In addition to the apparent increase in Vibrionaceae, Rhodobacteraceae tended to proliferate at 23°C. While members of the Rhodobacteraceae family are not exclusively associated with stress or disease and can be part of the microbiome of healthy corals (Delgadillo-Ordoñez et al. 2022), an increase of their relative abundance has frequently been reported in corals experiencing thermal stress (Pootakham et al. 2019a; Tignat-Perrier et al. 2023; Prioux et al. 2023; Rosales et al. 2020; Clark et al. 2021; Rosales et al. 2023). Recent work suggest that some Rhodobacteraceae may play a protective role under stress, for example by mitigating *Vibrio coralliilyticus* infections (Rosado et al. 2019; Kitamura et al. 2021; Xu et al. 2024). Here again, the impact of their proliferation in heat-stressed red corals remains to be investigated. In contrast to the changes observed in the abundance of several bacterial symbionts, the Spirochaetaceae, which are the dominant symbionts of the red coral (constituting up to 70% of the bacterial community), appeared to be highly thermoresistant, as neither their relative abundance nor their qPCR-based absolute abundance were affected by heat stress, as previously observed (Tignat-Perrier et al. 2023; Prioux et al. 2023).

Some changes observed in the eukaryome and bacterial microbiome co-occurred, suggesting that members of the coral microbiome may have specific relationships. Close and interactive relationships, including predation, niche competition or mutualistic and symbiotic relationships, are expected between microbes from different kingdoms like bacteria and microeukaryotes. The strongest co-occurrences were observed within bacteria. Vibrionaceae ASVs as well as Rhodobacteraceae ASVs co-occurred positively with each other. This might be because both are more heat-tolerant than other microbes in the community. The proliferation of one species can drive the growth of other species from the same taxonomic group, potentially mediated by quorum sensing as already observed in *Vibrio* bacteria (Sun et al. 2023). Prioux et al. (2025; (Prioux, Ferrier-Pagès, Del Campo, et al. 2025) proposed putative relationships and nutritional dynamics between the major microeukaryotic taxa associated with *C. rubrum*. However, our co-occurrence analyses did not reveal these relationships, as the dominant microeukaryotic

symbionts identified in our study differed from those reported by Prioux et al. (Prioux, Ferrier-Pagès, Del Campo, et al. 2025).

The persistence of temperature-induced proliferations after thermal stress might threaten coral resilience

In contrast to the 19°C treatment, the stress marker genes remained overexpressed in the colonies throughout the 23°C treatment. Although colonies showed no visible signs of disease or tissue loss, due to the short-term stress (*i.e.*, 8 days) applied in this experiment, these results suggest that the coral holobiont was under stress at this temperature and if the stress persisted, health problems and tissue loss could have occurred, as it has been observed with long-term heat stress (≥ 2 weeks) in the laboratory (Tignat-Perrier et al. 2023). However, after one week of recovery time at the initial temperature of 15°C, both *HSP70* and *TNFR1* gene expression levels returned to baseline. These results highlight the sensitivity of *C. rubrum* to temperature fluctuations, whereby even short-term exposure to suboptimal temperatures (23°C) can induce stress. Still, as signs of coral stress disappeared after a week of recovery time, it suggests a rapid resilience capacity of the red coral to short-term thermal anomalies.

While mechanisms controlling coral resilience are still misunderstood, microbiome resilience after thermal stress likely plays a role in coral recovery. The composition of the coral microbiome in the recovery phase was not significantly different from that of the control samples, suggesting that the overall structure of the microbiome recovered after the dysbiosis observed at 19°C and 23°C (Figure 7). For example, the changes observed in the Labyrinthulomycetes microeukaryotes and in the Rhodobacteraceae bacteria under thermal stress were transient and reverted during the recovery phase. These findings highlight the inherent plasticity and overall capacity of the red coral microbiome to recover from short-term heat stress. However, while the microbiome globally returned to its original structure after stress, some notable changes persisted after one week of recovery time (Figure 7). Some dominant microeukaryotes under control conditions disappeared under thermal stress but no longer occurred after recovery, such as the endolithic boring algae of the genus Ostreobiaceae. While their role in the coral holobiont remains debated (*i.e.*, either mutualistic or parasitic;(Fine et al.

2006; Fine and Loya 2002; Verbruggen and Tribollet 2011), their absence from the recovered eukaryome may affect the holobiont functioning. In contrast, some microbes which emerged during thermal stress remained present and persisted in the same relative abundance after recovery, such as Holostichidae ciliates, Endomyxa protozoans and Vibrionaceae bacteria. This persistence of stress-emergent microbes could be detrimental to corals facing multiple heat stresses, such as the successive heatwaves observed in some areas in the Mediterranean Sea (Figure S1; (Grenier et al. 2023; Estaque et al. 2023). The relative abundance of some Vibrionaceae ASVs (e.g., ASV254 and ASV836) showed significant increase only during the recovery phase (Figure 3), suggesting that different members of this family may exhibit distinct thermal preferences or ecological strategies, as observed in free-living marine *Vibrios* (Takemura et al. 2014; Materna et al. 2012; Sampaio et al. 2022). To understand the long-term health of *C. rubrum*, future studies need to investigate the effects of recurrent heat stress on the resilience of its microbiome and the persistence of stress-emergent microbes.

Conclusion

Within the coral holobiont, the eukaryome showed a rapid responsiveness to thermal fluctuations. It was highly sensitive to both moderate (19°C) and high (23°C) temperature increase, with notable shifts in community structure. These included changes in the dominant microeukaryotes from the Labyrinthulomycetes, Ostreobiaceae and Philasterida taxa. In contrast, the bacterial microbiome showed a more graduated response. While an acute thermal stress at 23°C induced immediate changes, the response to the milder stress at 19°C was delayed. Interestingly, the abundance of dominant bacterial symbionts, such as Spirochaetaceae, remained stable under these conditions. After the end of the thermal stress, both the eukaryome and the bacterial microbiome partially returned to their initial compositions, though certain temperature-induced changes persisted. In the eukaryome, Ostreobiaceae, a group of boring endolithic algae which dominated under control conditions, completely disappeared, even after a week of recovery following the stress. In the bacterial microbiome, opportunistic taxa such as Vibrionaceae, a family with known pathogenic potential, proliferated and persisted, raising concern about their role in enhancing coral vulnerability to heat stress. The persistent changes in the coral microbiome could

undermine coral resilience, especially during repeated heat stress events such as occurring during MHW events in the Mediterranean Sea.

General discussion



Discussion

I. General discussion

The main goal of this work was to deepen our understanding of the response of Mediterranean octocoral holobionts to global warming. Investigations on the symbiosis between temperate octocorals and their microbiome remain limited, both under non-stressful and stressful environmental conditions, leaving significant knowledge gaps on our understanding of the holobiont functioning. In the first axis (**Axis I**), we focused our investigations on the diversity of the microbial communities associated with multiple octocoral species under non stressful conditions, and identified their naturally associated symbionts. We assessed whether some bacterial symbionts share a common evolutionary history with their host. For the Mediterranean red coral *Corallium rubrum*, we also investigated the diversity of the associated microeukaryotes, which represent an essential yet largely overlooked component of the microbiome.

In the Mediterranean Sea, rising global temperatures are leading to increasingly frequent and intense marine heatwaves, posing a serious threat to octocoral populations. In this context of accelerating climate change, a better understanding of the holobiont functioning is crucial to better assess, predict, and possibly mitigate the impact of global warming on these key Mediterranean organisms. The second axis of the thesis focused on the microbiome of two octocoral species, the gorgonian *Paramuricea clavata* and the emblematic red coral *Corallium rubrum*, and its response to warming (**Axis II**). For this purpose, we used both *in situ* measurements and controlled laboratory experiments to investigate the resistance and recovery capacity of the microbiome to thermal stress.

The two axes mainly answered the following questions (further details can be found in the Introduction - Aims of the thesis section):

I. Diversity of the microbiome of temperate octocorals

a. Do the bacterial symbionts of *C. rubrum* and other octocorals, that have already been characterized, share a common evolutionary history with their hosts?

b. What is the composition of the eukaryome of *C. rubrum* and does it remain stable across temporaaly and spatially distinct environments?

II. Response of the microbiome of *C. rubrum* and *P. clavata* to thermal stress

a. How octocoral holobionts respond to marine heatwaves and is dysbiosis linked to tissue loss?

b. Can the host and its microbiome recover after thermal stress?

To achieve these objectives, different methods were used, combining culture-based techniques, high-throughput amplicon sequencing, and taxon-specific quantitative PCR (qPCR). This integrative strategy allowed us to obtain a comprehensive view of the microbial communities associated with these corals and to identify potential microbial indicators of stress.

The key results of this thesis were presented at the beginning of each chapter and are also summarized below (as well as in Figure 1), in order to answer the main research questions. We then present an integrative approach of the results before addressing the limitations of the current work. We finally suggest future research directions to continue our efforts on the study of octocoral holobionts.

A. Summary of the key results

Axis I: Diversity of the microbiome of Mediterranean octocorals

In **Chapter 1**, we showed that mesophotic octocoral species harbor rich and distinct bacterial communities. Phylosymbiotic patterns were observed in the temperate Mediterranean octocoral species, but not in the tropical Red Sea species. Within the Mediterranean species, cophylogenetic associations between corals and specific bacterial taxa, mainly *Endozoicomonas* and Spirochaetaceae which are the main symbionts of *P. clavata* and *C. rubrum*, respectively - were also found, suggesting that

these octocorals might have long-term evolutionary relationships with some bacterial symbionts.

In **Chapter 2**, microeukaryotic (non-metazoan) primers targeting the *18S rRNA* gene were designed and used to analyze the diversity of the eukaryome of *C. rubrum* using amplicon sequencing. These primers significantly reduced the host signal compared to the *18S rRNA* based universal primers. They were then used to study the stability of the associated microeukaryotes at different times (year, season) and locations. They revealed a small group of consistently detected families, including *Licnophoridae* ciliates and *Dino-Group I Clade 1* dinoflagellates, which were present at all locations. This suggests that these taxa may play important functional roles in the coral holobiont. However, despite this common microbial core, the overall composition of the eukaryome showed considerable variation between sites and sampling years, in contrast to the more stable and homogeneous bacterial microbiome. This spatial and temporal variability indicates that the red coral eukaryome is strongly influenced by local environmental conditions and emphasizes the need for further research into the functional roles of the coral eukaryome and its potential importance in conservation and management strategies.

In **Chapter 3**, we explored the fungal diversity associated with *C. rubrum* , within the tissue and the skeleton, using preferentially culture-based methods. Indeed, as fungal diversity remains underrepresented in the metabarcoding data, we used a culture-based approach which proved to be effective in identifying a rich and previously underexplored mycobiome. The most abundant isolates belonged to the phylum Ascomycota, particularly the genera *Penicillium*, *Cladosporium*, and *Aspergillus*. Notably, 61% of the isolated species (24 species) were newly reported in association with corals, highlighting the extent of unexplored fungal diversity in marine ecosystems. In contrast, some isolates, such as *Aspergillus sydowii*, might be of concern due to their potential pathogenic behavior under elevated temperatures such as during the episodes of marine heatwaves in the Mediterranean Sea. The study showed distinct fungi inhabiting the tissue and skeleton. Overall, we suggested that the structure of the fungal community associated with *C. rubrum* is likely shaped by abiotic factors like temperature, energy resources and host-specific selection pressures.

Axis II: Response of the microbiome of *C. rubrum* and *P. clavata* to thermal stress

In **Chapter 4**, we examined the effects of the unprecedented Mediterranean heatwaves of 2022 on the bacterial microbiome of corals by comparing the microbiome of corals that had lost 90% of their tissue with that of corals that were visibly unaffected. We found a decrease in the relative abundance of the main bacterial symbionts (Spirochaetaceae in *C. rubrum* and *Endozoicomonas* in *P. clavata*). However, their absolute abundance (based on qPCR analyses) remained largely unchanged, even in colonies with 90% tissue loss. This suggests that tissue degradation was not due to the loss of the main symbionts. It may, however, result from alterations in the metabolic functions of these key symbionts, but Gervais et al. (unpublished data) suggested that only limited functional changes in Spirochaetaceae bacteria were detected in response to thermal stress in *C. rubrum*. It remains to be investigated for *Endozoicomonas*. Tissue loss could also be driven by the overgrowth of opportunistic bacteria, including putative pathogens such as *Vibrio*. These microbial changes (or absence of change for the main symbionts) could only be detectable by qPCR analyses, emphasizing the need for both relative and absolute approaches when assessing changes in microbial abundances. Our results suggest that the proliferation of microbes on the holobiont might be a key factor in the decline of octocorals during marine heatwaves.

In **Chapter 5,** the impact of the Mediterranean marine heatwaves of 2022 on the eukaryotic microbiome of *C. rubrum* was studied. Key microeukaryotes such as Licnophoridae ciliates, Warnowiaceae and Dino-Group I dinoflagellates and Labyrinthulomycetes stramenopiles were consistently present in all colonies regardless of their health state or habitat. Colonies with tissue loss showed a higher species diversity and an altered eukaryome composition. Specific taxa, such as Corallicolidae, Ephelotidae, Labyrinthulomycetes and Exobasidiomycetes increased with the intensity of heat stress, suggesting that these microeukaryotes may serve as bioindicators of thermal stress and coral health.

Finally, **Chapter 6** presented the first comprehensive assessment of the resilience of the microbiome of a Mediterranean octocoral (*C.rubrum*) to both mild (19 °C) and severe (23 °C) heat stress. The study showed that the eukaryome responded faster to an increase in temperature than the bacterial microbiome. Both the eukaryome and the

bacterial microbiome changed at 19°C and 23°C, particularly due to an increase in opportunistic and potentially pathogenic bacteria such as Vibrionaceae. While the holobiont partially recovered post-stress, the persistence of these putative pathogens might alter coral resistance to successive heatwaves. These results emphasize the role of marine heatwaves in promoting dysbiosis and highlight the vulnerability of Mediterranean octocorals under future climate scenarios. This chapter also identified positive co-occurrence patterns within bacterial taxa, especially among Vibrionaceae and Rhodobacteraceae, suggesting synergistic interactions under heat stress. In contrast, almost no significant interactions were found between bacterial and microeukaryotic symbionts.

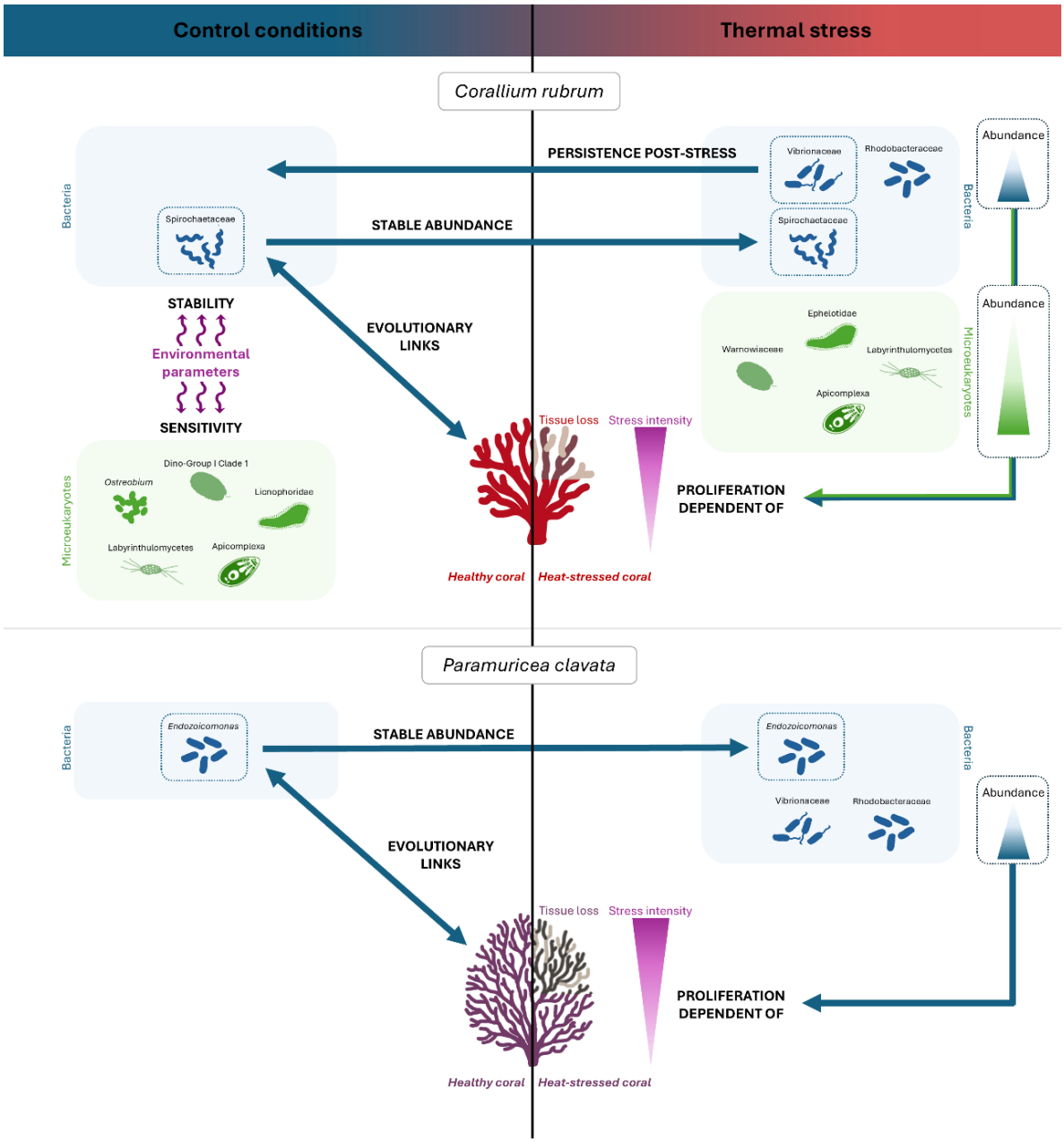

Figure 1: Schematic overview of the key results presented in this thesis

B. Integrative approach of experimental results

Axis I: Diversity of the microbiome of temperate octocorals

Prior to this work, the bacterial microbiome of Mediterranean octocorals had already been characterized, with members of the genus *Endozoicomonas* identified as the predominant symbionts in numerous species (van de Water et al. 2016; 2017; 2018; Bayer et al. 2013; La Rivière et al. 2015; Ransome et al. 2014). Such dominance is confirmed across the different studies presented in this thesis. This genus has been observed not only in a variety of host species but also along different environmental gradients, including both shallow and mesophotic reef zones, emphasizing its ecological versatility and potential importance for host physiology. There are a number of suggestions for the functions of these bacteria, including contributions to host fitness through nutrient supply, vitamin synthesis, chitin degradation and participation in sulfur metabolism (Tandon et al. 2022; Alex and Antunes 2019; Speck and Donachie 2012; Bourne et al. 2016; Morrow et al. 2012; Da Silva et al. 2023). However, the exact nature of the interaction between *Endozoicomonas* and its host remains controversial, with recent studies questioning the assumption of a purely mutualistic relationship (Pogoreutz and Ziegler 2024). In contrast to the *Endozoicomonas*-dominated microbiomes of most Mediterranean octocorals, the red coral *C. rubrum*, which is also the only one to secrete a hard calcitic skeleton, exhibits a distinct microbial composition characterized by a marked and consistent dominance of Spirochaetales, which can constitute up to 70% of the bacterial community (van de Water et al. 2016a). The geographical consistency of this association across *C. rubrum* populations suggests a long-standing, possibly co-evolved relationship (van de Water et al. 2016a). Although the precise role of Spirochaetales is not yet fully understood, it has been suggested that they may contribute to host metabolism through functions such as nitrogen fixation (Lilburn et al. 2001) and carbon cycling (Leadbetter et al. 1999).

The systematic presence and consistent dominance of *Endozoicomonas* and Spirochaetaceae in the microbiome of Mediterranean octocoral species, especially *P. clavata* and *C. rubrum*, suggests that these taxa are central components of the octocoral holobiont, and that there is an evolutionary relationship between the hosts and their

symbionts. Nevertheless, the evolutionary origins and mechanisms underlying coral-microbe symbioses remain poorly understood. While evidence of evolutionary associations between hosts and microbial partners is emerging in scleractinian corals, as evidenced by processes such as vertical transmission and co-diversification (Pollock et al. 2018; O'Brien et al. 2020), such relationships have barely been explored in octocorals and only in tropical species (O'Brien et al. 2020; 2021). This is an important area of research, particularly given the ecological and evolutionary significance of these symbiotic interactions. The study presented in **Chapter 1** aimed to examine the structure of the microbial communities associated with multiple Mediterranean and tropical octocoral species sampled at mesophotic depths, and to explore potential patterns of shared evolutionary history between the coral hosts and their associated microbiome. The bacterial community composition was species-specific and remained stable across different depths and locations within the same species, suggesting that host phylogeny or specific functional traits may be more influential than abiotic environmental factors in shaping microbial community structure. The detection of cophylogenetic signals between selected bacterial lineages and their respective octocoral hosts (such as between *C. rubrum* and Spirochaetaceae and between *P. clavata*, *Eunicella* spp. and *Endozoicomonas*) further supports the hypothesis of long-term evolutionary interactions. These signals are indicative of processes such as co-speciation, vertical transmission of microbial symbionts, or host-specific selection pressures. For *C. rubrum*, however, Tignat-Perrier et al. (2025) did not observe a vertical transmission of Spirochaetaceae between the mother colonies and the offsprings, suggesting an environmental acquisition of these symbionts. Collectively, these results contribute to a growing understanding of the associations between microbes and octocorals. This chapter thus provides a foundational framework for future research into the evolutionary and ecological dimensions of symbiotic relationships within octocoral holobionts, offering insights into the potential drivers of microbial community organization and host specificity.

While bacterial partners of corals are increasingly well characterized, the other members of the microbiome such as microeukaryotes, comprising protists and fungi, remains largely unexplored, partly due to technical challenges in metabarcoding approaches. The dominance of host sequences in *18S rRNA* gene-based sequencing

obscures microeukaryotic signals, and comprehensive studies using this method are still limited, especially in coral ecosystems (Clerissi et al. 2018; Bonacolta et al. 2023; Del Campo et al. 2019). Overcoming these biases is essential to better understand the diversity, functions, and dynamics of microeukaryotic communities within coral holobionts. To address the challenge of host DNA contamination in 18S rDNA metabarcoding, customized *18S rRNA* gene primers specific for *C.rubrum* were designed based on the UNonMet-PCR primers, to effectively reduce host amplification while preserving a broad taxonomic coverage of the microeukaryotic diversity (Bower et al. 2004; Del Campo et al. 2019). These primers were subsequently applied in several studies described in this thesis to investigate the diversity of the microeukaryotic communities associated with *C. rubrum*. This approach allowed us to uncover several microeukaryotic lineages, including Dino Group I, Warnowiaceae, Licnophoridae, Corallicolidae and Labyrinthulomycetes, which repeatedly appeared in the eukaryome of the red coral *C. rubrum*. Their consistent detection across three independent studies, in different environments, and under varying host conditions (**Chapters 2, 5, and 6**) suggests that these taxa are not transient members but potentially stable, functionally important symbionts. While research on coral microbiomes has traditionally focused on bacterial partners, these findings expand the scope of holobiont studies to include understudied eukaryotic symbionts, offering new perspectives on the complexity of coral-associated microbial communities (Bonacolta et al. 2023; del Campo et al. 2020; Ainsworth et al. 2017).

In natural and healthy colonies of *C. rubrum*, Dino Group I and Licnophoridae together made up almost half of the microeukaryotic community (**Chapter 2 and 5**). These taxa, together with Warnowiaceae and Labyrinthulomycetes, were also abundant in colonies that had suffered from heat stress but that showed no tissue loss (**Chapter 5**). The repeated occurrence of these microeukaryotes in healthy coral tissue suggests a potential ecological importance of these symbionts. Dino Group I, for instance, belongs to the Syndiniales, a group that is widespread in marine environments and often characterized as parasitic (Guillou et al. 2008). Some members have also been linked to coral disease and toxin production (Hold et al. 2001b; Green et al. 2004; Sala et al. 2005), raising important questions about their functional roles and context-dependent

interactions within the holobiont. As Dino Group I, Licnophoridae ciliates have been detected in both temperate and tropical coral species (Bonacolta et al. 2024; Clerissi et al. 2018). They may influence the microbiome composition through their predation activity on other protists (Sweet and Séré 2016), which could explain their differential abundance depending on the environmental conditions. Labyrinthulomycetes, another dominant group observed in natural colonies of *C. rubrum*, are saprotrophic stramenopiles known to contribute to nutrient cycling via osmotrophy and phagotrophy (Raghukumar and Damare 2011; Bongiorni et al. 2005). Their ubiquity in various marine hosts, from corals to seagrasses and mollusks, suggests broad ecological adaptability (C. Raghukumar and Raghukumar 1991; Siboni et al. 2010; Pan et al. 2017). Some species also synthesize high levels of omega-3 polyunsaturated fatty acids, making them potential nutritional symbionts (Carmona et al. 2003; Chang et al. 2012). However, their increased abundance in colonies with tissue loss questions their role within the red coral holobiont, as some species are known for their parasitic tendencies in various marine organisms (Pan et al. 2017; S. Raghukumar and Damare 2011; Damare and Raghukumar 2010).

The similarities between the core eukaryome of *C. rubrum* and that of other coral species (e.g., Dino Group I, Licnophoridae and Labyrinthulomycetes), including the tropical hexacoral *Pocillopora damicornis* and the temperate octocoral *Paramuricea clavata*, suggest that these microeukaryotes may play a fundamental role in phylogenetically and geographically distant coral taxa (Bonacolta et al. 2024; Clerissi et al. 2018). In this sense, they could represent eukaryotic analogues of bacterial symbionts such as *Endozoicomonas* or Spirochaetaceae, which have a cophylogenetic relationship with their hosts. However, despite the presence of these core taxa, the composition of the eukaryome in *C. rubrum* appears to be highly responsive depending on the environmental conditions. Differences in the dominant eukaryotic taxa were observed not only between sampling sites (**Chapter 2**) but also between corals collected *in-situ* (**Chapters 2 and 5**) and those maintained under laboratory conditions for several weeks (**Chapter 6**). For instance, *in-situ* samples were typically dominated by either Dino Group I, Licnophoridae or Corallicolidae while laboratory-maintained corals showed a prevalence of Philasterida and Ostreobiaceae. While some taxa such as

Labyrinthulomycetes were present in both conditions, they varied in relative abundance, and they were represented under different ASVs. These shifts emphasize the plasticity of the eukaryome and suggest that it may be more responsive to physico-chemical changes than the bacterial microbiome. This raises questions about the mechanisms of symbiont acquisition, whether through horizontal transmission or environmental acquisition, and their ability to help coral holobionts to cope with different environmental conditions. Although these site-specific dominant microeukaryotes may not be essential for core coral functioning, they may confer local ecological advantages, such as resource assimilation or stress resistance.

Although the metabarcoding-based approach has proven effective for exploring the microeukaryotic communities, it also revealed limitations for fungal detection in *C. rubrum*, as the fungal fraction was consistently underrepresented. This under-coverage is likely due to several factors, including low fungal biomass and limited reference database coverage. We then chose to use culture-based methods which proved to be effective in detecting a diverse fungal community, including fungal taxa with putative ecological and biotechnological interest. **Chapter 3** of this thesis aimed to study the cultivable mycobiome associated with *C. rubrum*. The red coral mycobiome turned out to be a rich fungal community dominated by Ascomycota, particularly *Penicillium*, *Cladosporium*, and *Aspergillus*, with many isolates known to produce bioactive secondary metabolites in other organisms (see **Chapter 3**). Notably, 61% of the isolated species were detected for the first time in association with corals, revealing a considerable reservoir of previously undescribed fungal diversity in coral ecosystems. Moreover, distinct fungi inhabiting were observed in the tissue and skeleton of the red coral. These observations suggest that the associated fungal community might be shaped by the host microenvironment (Roik et al. 2022; Amend et al. 2012).

Importantly, the study presented in **Chapter 3** also revealed fungal taxa with potential pathogenic traits, such as *Aspergillus sydowii*, a species known to cause disease in tropical corals under thermal stress (e.g., 25 °C; Roik et al. 2022). As marine heatwaves in the Mediterranean Sea become more frequent and severe, such opportunistic fungi may pose an increasing threat to red coral populations.

Understanding whether these taxa exist as latent pathogens, mutualists, or commensals is interesting for predicting holobiont responses to climate change and for developing mitigation strategies. Overall, the discovery of both generalist fungi, which may occur across multiple coral species or habitats, and specialist taxa specifically associated with *C. rubrum*, suggests an ecologically structured and evolutionarily relevant mycobiome. These findings call for a renewed effort to investigate the coral mycobiome using integrated methodological approaches and to explore the potential roles of fungi in coral health, nutrient dynamics, and resistance to environmental stressors.

In conclusion, this work emphasizes the importance of considering the entire community of microbial partners to understand coral physiology. It also emphasizes the value of integrating different approaches to uncover the true diversity of coral-associated microbes.

Axis II: Response of the microbiome of *C. rubrum* and *P. clavata* to thermal stress

Marine heatwaves (MHWs), prolonged periods of elevated sea surface temperatures (SST), have become more frequent and intense over the last decades (Darmaraki et al. 2019; Oliver et al. 2018). This phenomenon's intensification has been attributed to the accelerating pace of global climate change. As outlined in the introduction, the Mediterranean Sea has proven to be one of the fastest-warming Seas on Earth. Studies showed that SST in the Mediterranean is rising about 20% faster than the global average, and the region has also seen a marked increase in the frequency of MHW events over the last two decades (MedECC 2020; Cos et al. 2022b; Pastor et al. 2020; Darmaraki 2019; Juza et al. 2022; Omneya et al. 2021). This trend has caused alarm among marine biologists as MHWs are associated with mass mortality events in marine populations.

It is therefore crucial to understand how Mediterranean octocorals respond to such extreme thermal conditions. Octocorals, including the species *E. cavolini*, *E. singularis*, *P. clavata*, and *C. rubrum*, are key components of marine animal forests (MAFs), which are among the most ecologically rich habitats in the Mediterranean region (Paoli et al. 2017; Orejas et al. 2022; Rossi et al. 2017c). However, these organisms are

also particularly vulnerable to environmental disturbances. MHWs have already been associated with large-scale mortality events, with reports of microbial disease outbreaks and colony losses reaching up to 90% in some shallow water populations (Cerrano et al. 2000; Huete-Stauffer et al. 2011; Luigi Piazzi et al. 2021a; Verdura et al. 2019a; Garrabou et al. 2009b; 2022). These events are likely the result of a complex interplay between host physiological stress due to elevated temperatures, and microbial dysbiosis (Bourne et al. 2016; Mouchka et al. 2010; Vezzulli et al. 2010).

In our studies, we analyzed octocoral samples collected during the unprecedented 2022 MHW episodes in the Mediterranean, which was made possible by the organization Septentrion Environment (**Chapters 4 and 5**). In 2022, between May and September, the Mediterranean experienced between three and seven record-breaking MHW episodes, with temperature anomalies reaching up to +4.3°C in some areas, far exceeding the previously recorded highs of +2-3°C during the 2003 MHWs (T-MEDNet 2023; Quade 2022; Guinaldo et al. 2023). In the Northwestern Mediterranean, for instance, MHWs were characterized by either short bursts of extreme heat, peaking at 27°C in shallow waters, or by prolonged periods of stable and high temperatures around 23-24°C (Crisci et al. 2011; Estaque et al. 2023). At one of the sampling sites, *Riou Sud* (Marseille), temperatures at 15 m and 30 m depths reached 27°C and 26°C respectively during the summer. Prior to 2022, temperatures above 24°C at 30 m depth had never been recorded, and at 15 m depth, such occurrences were limited to no more than four days per year (in 2009 and 2012). However, in *Riou Sud*, in 2022, the number of days with temperatures above 24°C reached ten days at 15 m depth and three days at 30 m, indicating a warming of the water column that extended deeper than previously observed. Laboratory studies suggested that 23-24°C is a critical thermal threshold for many Mediterranean octocoral species. Above this threshold, tissue loss and coral mortality are commonly observed (Previati et al. 2010; Haguenauer et al. 2013; Tignat-Perrier et al. 2022; 2023; Torrents et al. 2008; Cau et al. 2018). During the 2022 MHW event, Septentrion Environment conducted a survey in the Calanques National Park to assess colony mortality of *C. rubrum* and *P. clavata* across different sites. The methodology used was based on a well-established approach involving the quantification of affected colonies and the percentage of tissue loss (Garrabou et al. 2009b; 2022), as detailed in

Estaque et al. (2023). The results revealed different mortality rates depending on the species and the site. Overall, *C. rubrum* populations were less impacted than *P. clavata* populations, with 45% and 81% of colonies affected, respectively. Moreover, they observed different levels of damage depending on the individual, with some colonies showing 0% tissue loss while others were nearly fully degraded (90% of tissue loss) within populations.

Several factors were suggested to influence coral response to abnormally high temperatures, such as water flow and temperature perception (Brown et al. 2023), food availability (Ezzat et al. 2019), genotype (Palacio-Castro et al. 2022; Kavousi et al. 2020), and the microbiome. Previous studies on Mediterranean octocorals have demonstrated that MHWs can trigger microbial dysbiosis. Microbial dysbiosis is typically marked by a reduction in the relative abundance of the main symbionts, such as *Endozoicomonas* and Spirochaetaceae, alongside an increase in the relative abundance of opportunistic taxa (Tignat-Perrier et al. 2022; 2023; Rubio-Portillo et al. 2021b; Corinaldesi et al. 2022; Vezzulli et al. 2010b; Bally and Garrabou 2007b). Overall, several knowledge gaps remain and considerably limit our understanding of the response of the coral holobiont to thermal stress. For example, the cause-and-effect relationship between the microbiome response (dysbiosis) and the coral response (such as tissue loss) to MHWs has not been clearly established. Moreover, the microeukaryotic communities associated with corals have been largely unexplored, both in terms of diversity and responsiveness to change, which makes it difficult to gain a full picture of what is happening inside the coral holobiont during thermal stress. Finally, we have no idea about the recovery capacity of the coral microbiome following stress events. And above all that, our knowledge on the response of the bacterial communities mainly rely on metabarcoding techniques and relative proportions, which have notable biases as shifts in relative abundances may not correspond to changes in raw abundances. As a result, some ecological dynamics may be misinterpreted, and the functional complexity of the microbiome may be underestimated. In this thesis work, we used different techniques to get relative and raw abundances of microbial taxa, a combination of *in-situ* observations (**Chapters 4 and 5**) with controlled laboratory experiments (**Chapter 6**) to investigate as effectively as

possible the response of the holobiont (host, bacteria and microeukaryotes) of *C. rubrum* and *P. clavata* to thermal stress.

The study on the impact of the 2022 MHWs on the bacterial communities of *C. rubrum* and *P. clavata* (**Chapter 4**) using taxon-specific qPCR analyses, revealed that the absolute abundance of their dominant bacterial symbionts (Spirochaetaceae in *C. rubrum* and *Endozoicomonas* in *P. clavata*) did not change significantly under thermal stress, even in colonies that had lost their tissue. This finding suggests that, contrary to previous assumptions, thermal stress and the subsequent tissue loss were not associated with a reduction in these key symbionts (Tignat-Perrier et al. 2022; Voolstra et al. 2021; Woo 2021; Palacio-Castro et al. 2022). Spirochaetaceae and *Endozoicomonas* appear to be highly thermotolerant (the latter with some exceptions, as a slight decrease in absolute abundance was observed in certain *P. clavata* colonies from Portofino (Italy) likely due to a combination of stressors; see **Chapter 4** for details). This thermotolerance, especially for the Spirochaetaceae in *C. rubrum* was further confirmed in a laboratory-based thermal stress study (**Chapter 5**), where both their relative and absolute abundance remained stable under stress.

The observed decrease in the relative abundance of the main symbionts is probably the consequence of a significant increase in the total abundance of other bacterial taxa, including putative pathogens such as *Vibrio*, as observed in our studies (**Chapters 4 and 6**). An increase in Vibrionaceae ASVs is a well-documented response in heat-stressed corals (Martin et al. 2002; Tignat-Perrier et al. 2023; Tout et al. 2015), and several *Vibrio* species are recognized coral pathogens such as the Mediterranean *Vibrio coralliilyticus* (Martin et al. 2002; Sun et al. 2023; Gibbin et al. 2018; Vezzulli et al. 2010; Vidal-Dupiol et al. 2011). **Chapter 6**, which also examined the recovery of *C. rubrum* and its microbiome after a heatwave, revealed that opportunistic pathogens persisted within the holobiont after thermal stress. Notably, some bacterial taxa, particularly Vibrionaceae species, were still present in high relative abundance after recovery, even when colonies showed no tissue loss. This persistent presence of potential pathogens may undermine coral resilience, especially in the face of the increasingly frequent MHWs in the Mediterranean (see Introduction Part III). In certain marine *Vibrio* species,

pathogenic virulence is triggered when seawater temperatures exceed 23°C (Billaud et al. 2022; Kimes et al. 2012) and/or when quorum sensing thresholds are reached (Sun et al. 2023). These conditions are commonly met during MHWs and may partly explain coral mortality after such events. Although virulence factors may become inactive once temperatures return to normal, they can be rapidly reactivated during subsequent heatwaves, potentially accelerating microbial dysbiosis and increasing the risk of coral mortality. The persistence of such opportunistic bacteria may accelerate microbial shifts during repeated heat stress, and promote tissue loss, necrosis, and eventually, colony death. This mechanism could explain why some colonies can withstand thermal stress longer than others: their resilience could be influenced by the extent of dysbiosis and the abundance of these "ready-to-respond" pathogens in their microbiome.

In addition to Vibrionaceae, Rhodobacteraceae also proliferated in colonies with tissue loss, as observed in **Chapters 4 and 6**. This pattern has already been observed in tropical corals and red corals exposed to heat stress (Pootakham et al. 2019a; Tignat-Perrier et al. 2023; Rosales et al. 2020; 2023; Clark et al. 2021). Rhodobacteraceae are known to proliferate during heat stress and disease outbreaks, which can undermine coral health (Ziegler et al. 2019; Pootakham et al. 2019a; Tignat-Perrier et al. 2023; Rosales et al. 2020; 2023; Clark et al. 2021). However, recent works challenge this view, and suggest that some Rhodobacteraceae may play a protective role under stress, for example by mitigating *Vibrio coralliilyticus* infections (Rosado et al. 2019; Kitamura et al. 2021; Xu et al. 2024). Their role in heat-stressed red corals has yet to be clarified. Overall, these results indicate that tissue loss in octocorals during MHWs is not due to the loss of dominant, beneficial symbionts such as Spirochaetaceae or *Endozoicomonas*. It could otherwise be due to the overgrowth of opportunistic or pathogenic bacteria.

Regarding the microeukaryotic component of the coral holobiont, very little was known about the associated microeukaryotic communities in Mediterranean octocorals prior to the research presented in this thesis. While the work described in **Chapters 2 and 3** shed light on the richness and composition of these microeukaryotic communities, **Chapters 5 and 6** contributed to a more comprehensive understanding of the holobiont response to thermal stress by incorporating these previously underexplored microbial

partners. Depth-related differences in the microeukaryotic composition were observed (**Chapter 5**): moderately stressed (deeper) colonies were dominated by Warnowiaceae and Corallicolidae, while more severely stressed (shallower) colonies hosted greater abundances of Ephelotidae and fungi like Exobasidiomycetes. These differences between depths might be due to differences in heat stress intensity or trophic factors as suggested by Maire et al. (2022). As demonstrated in **Chapter 2**, the eukaryome of *C. rubrum* seems strongly influenced by the physico-chemical environment, and more significantly than the bacterial microbiome.

Our thermal stress experiment where the response of the host, the bacterial and the microeukaryotic communities was assessed (**Chapter 6**) showed that microeukaryotes responded to thermal stress more rapidly than their bacterial counterparts. While shifts in the composition of the bacterial microbiome were only observed at 23°C or after prolonged exposure (8 days) to 19°C, structural changes in the eukaryome occurred immediately after the temperature increased from 15°C to 19°C or 23°C. This rapid response suggests that microeukaryotes may serve as early warning indicators of environmental disturbances. In **Chapter 5**, the composition of the eukaryome differed significantly between control and heat-stressed colonies. Specifically, a decrease in the relative abundance of Dino-Group I dinoflagellates and Licnophoridae ciliates was observed in colonies collected in MHW-impacted sites. Dinoflagellates, known to be highly sensitive to temperature fluctuations, might play a crucial role in coral health. Indeed, in scleractinian corals, the loss of Symbiodiniaceae dinoflagellates often marks the onset of bleaching and subsequent mortality (Douglas 2003; Jiang et al. 2021). Licnophoridae ciliates, also sensitive to thermal changes, may decline due to heat-driven metabolic impacts, or indirect effects such as changes in prey availability (Martinez 1980; Karajan et al. 2019). However, it remains important to determine whether these relative decreases reflect a true loss of symbionts, or if it is an artifact caused by the relative increase of other microeukaryotes. While bacteria remain reliable indicators of coral health condition in various marine holobionts (Wegner et al. 2025; Pootakham et al. 2019; Montaño-Salazar et al. 2023; Glasl et al. 2019), we show here that microeukaryotes could just as well serve as early-warning indicators of coral disturbances. To elucidate their

biomarker relevance and their overall functional roles, further investigations across Mediterranean coral populations are greatly needed.

Overall, these studies underscore the critical importance of investigating all parts of the microbiome to understand the response of Mediterranean octocorals to stress and assess their resilience to climate change. This thesis work underscores the necessity for continued research into the symbiosis between octocorals and their microbiome, and its implication for coral ecosystem health.

C. Limitations of this PhD

1. *In-situ* experiments/sampling: Limited consideration of environmental parameters beyond temperature

This thesis primarily focused on the impact of abnormally high temperatures, as observed during marine heatwaves (MHWs), on the composition and dynamics of coral-associated microbial communities. However, as observed in other coral species, the structure of the microbial communities is influenced by a variety of environmental factors such as nutrient levels, pH, salinity, hydrodynamics, and organic matter input (Zaneveld et al. 2016; Wang et al. 2018; Gissi et al. 2019; Morrow et al. 2015; Caughman et al. 2021; Lan et al. 2025; Nelson et al. 2023; Röthig et al. 2016; van Oppen and Blackall 2019). These factors were not systematically measured in our *in-situ* studies/sampling, potentially overlooking some drivers of microbiome variability. Future studies would benefit from a more holistic environmental monitoring approach to better disentangle the relative contribution of temperature versus other environmental stressors.

2. *In-situ* experiments/sampling: Inability to sample colonies before MHWs

A major challenge in studying natural MHWs is their unpredictability in both timing and intensity. As a result, it was not possible to conduct pre-stress baseline sampling of the same coral colonies that were later impacted. This limited our ability to track microbiome changes over time within individual holobionts, which would have strengthened our conclusions about cause-effect relationships. A more robust approach would involve tagging individual colonies *in-situ* and implementing a long-term monitoring strategy, allowing for repeated, temporally resolved sampling. This would also

make it possible to identify colony-specific microbiome features (e.g., particular taxa or community structures) that may predispose corals to thermo-sensitivity or resilience.

3. Laboratory experiments: Technical limitations

To compensate for the limitations of field sampling, a controlled laboratory experiment was conducted (Chapter 5). However, its relatively short duration limited the ability to assess long-term microbiome dynamics under sustained thermal stress. Extending the experimental period and including a wider range of temperatures, especially those mimicking more extreme or prolonged MHW scenarios, would allow for a more nuanced understanding of coral stress responses. For instance, such a design could help refine the relationship between temperature thresholds and the timing of physiological decline, such as tissue loss, as started in a laboratory experiment by Tignat-Perrier et al. (2022). Furthermore, it would allow testing of the hypothesis proposed in Chapter 5: that a reservoir of potentially pathogenic bacteria may remain in the coral microbiome even after thermal stress and may rapidly expand during subsequent MHWs. This persistent pathogenic reservoir could weaken microbiome resilience over time and increase coral vulnerability. Nonetheless, conducting such extended and complex experiments poses logistical challenges, requiring large numbers of aquaria and multiple fragments from genetically identical colonies.

4. Differences between laboratory and natural microeukaryotic communities

While laboratory conditions were successful in maintaining bacterial communities similar to those observed in natural environments, this was not the case for microeukaryotes. As mentioned in the previous paragraphs, the composition of the eukaryome in laboratory-maintained colonies diverged substantially from that observed *in-situ* (Chapter 4). This discrepancy suggests that microeukaryotic communities are more sensitive to artificial environmental conditions and may not be accurately represented under laboratory constraints. Consequently, conclusions drawn about their response to thermal stress must be interpreted with caution, and future research should aim to understand the differences between laboratory observations and field data.

5. Limited use of taxon-specific qPCR for tracking key microbes

Although quantitative PCR (qPCR) was used to monitor the absolute abundance of some important symbionts such as Spirochaetaceae, *Endozoicomonas* and Vibrionaceae, the approach was applied to only a small number of bacterial taxa. Yet, the results presented in chapter 4 clearly demonstrate the value of combining qPCR with metabarcoding to validate and quantify key microbial shifts. Expanding qPCR assays to include opportunistic or pathogenic bacterial groups like Rhodobacteraceae, as well as ecologically relevant microeukaryotes (e.g., Dino Group I, Licnophoridae, Labyrinthulomycetes), would provide more robust insights into microbial responses to heat stress.

However, despite remaining a valuable tool for gaining insights into microbial dynamics within the host, it is also essential to consider that quantifying bacterial abundance using qPCR targeting the *16S rRNA* gene can be influenced by differences in the number of rRNA operon copies among bacterial species within the same group (e.g., *Spirochaetaceae*, *Endozoicomonas*, or *Vibrionaceae* in our case). The rRNA operon (comprising the *5S*, *16S*, and *23S rRNA* genes) can vary in copy number from 1 to 15, depending on the bacterial genome (Klappenbach 2001; Acinas et al. 2004; Stoddard et al. 2015). For example, within the *Vibrio* genus, *V. parahaemolyticus* contains 11 rrn copies with identical *16S rRNA* genes (Gonzalez-Escalona et al. 2005), whereas *V. cholerae* has only 9 copies of *16S rRNA* genes (Ki 2009). As a result, in our studies, an observed increase in the abundance of a bacterial group like *Vibrionaceae* may not necessarily indicate a true increase in cell numbers, but rather a shift in species composition, such as the emergence of a species with a higher rRNA operon copy number compared to the control. To overcome this limitation, more specific qPCR assays targeting individual species, such as *V. corallilyticus*, could be a solution.

II. Future directions in microbial ecology research on octocorals

1. Investigating all microbial compartments

While this thesis focused primarily on the associated bacteria and microeukaryotes, other microbial groups such as viruses and archaea may also play a crucial role in coral health and stress response (Thompson et al. 2015; Voolstra et al. 2024; van de Water et al. 2018). These communities are still poorly understood in octocorals but could potentially explain some of the heterogeneity observed in coral mortality and resilience under thermal stress. Future studies should incorporate these microbes to provide a more holistic view of the holobiont. The fungi within the coral holobiont remain also a relatively unexplored group. Future research should aim to investigate their ecological roles more deeply, including potential symbiotic, pathogenic, or opportunistic interactions. This could include investigating traits with biotechnological potential (e.g., secondary metabolite production), pathogenicity profiling, and conducting targeted heat-stress experiments to assess their stability under changing conditions. As the present thesis suggests, certain fungal taxa such as *Malassezia* (Cabañes 2014) occur in stressed corals or at least have a preference for elevated temperatures such as *Aspergillus sydowii* (Roik et al. 2022), but their specific role remains unclear. An ecological approach, that builds on the stress experiments already developed, could help determine whether fungal communities are mere indicators of dysbiosis or active contributors to coral decline.

2. Elucidating the role of *Vibrio* spp. (and other microbes) in coral mortality

An important direction for future research is the experimental investigation of the role of *Vibrio* species as primary pathogens contributing to the mortality of *C. rubrum* under thermal stress. While observational data and sequencing analyses suggest a strong association between the increased abundance of *Vibrionaceae* and impacted coral colonies, causality has yet to be clearly established. This could be achieved through controlled infection experiments, in which *Vibrio* strains isolated from thermally stressed corals are reintroduced into healthy colonies under laboratory conditions. Such studies should monitor host response and tissue integrity over time to assess pathogenicity. In parallel, further investigation of the regulatory mechanisms of *Vibrio* virulence is

warranted, particularly those related to thermal activation (e.g., above 23°C; (Billaud et al. 2022; Kimes et al. 2012; Martin et al. 2002) and quorum sensing thresholds (Sun et al. 2023). Understanding how environmental conditions modulate the expression of virulence genes could clarify why certain *Vibrio* populations remain quiescent post-stress yet rapidly reactivate during subsequent thermal anomalies. However, focusing exclusively on *Vibrio* may introduce a taxonomic bias, given its well-established reputation as a coral pathogen. It remains possible that other, less-characterized bacterial taxa (such as Alteromonadaceae and Pseudoalteromonadaceae) also contribute to host decline under thermal stress. Broader pathogen screening efforts are therefore necessary to determine whether *Vibrio* is indeed the primary causative agent or part of a more complex pathogenic consortium. Moreover, this line of research could be extended to explore microbiome-mediated mitigation strategies. For instance, the potential antagonistic role of *Rhodobacteraceae* in suppressing *Vibrio* virulence, as documented in other coral systems (Rosado et al. 2019; Kitamura et al. 2021; Xu et al. 2024), could offer new insights into microbiome-based resilience mechanisms. Such work would not only test a key ecological hypothesis but also contribute to applied strategies aimed at enhancing coral resistance to climate-induced stressors.

3. Expanding and optimizing qPCR assays for broader microbial coverage

As demonstrated in this thesis, qPCR is a powerful complement to metabarcoding and enables a more precise quantification of specific microbial taxa. To improve the resolution of community dynamics observed in this thesis, future studies should develop qPCR assays targeting other key bacterial families such as Rhodobacteraceae, and major microeukaryotic groups that respond to stress, such as Dino Group I, Licnophoridae, and Labyrinthulomycetes. This would allow for more accurate tracking of microbial responses during thermal events and strengthen the interpretation of functional shifts in the microbiome.

4. Shifting toward functional and multi-omics approaches

As emphasized in a recent coral microbiome review (Voolstra et al. 2024c), the field must now move beyond compositional studies and develop functional approaches. This includes metagenomics, metatranscriptomics, and metabolomics, which can reveal the

metabolic potential and activity of the microbiome and its interaction with the host. Applying these techniques before, during (with multiple time points), and after thermal stress events would provide a more comprehensive picture of microbial dynamics and help identify the molecular mechanisms underlying coral responses to stress.

5. **In an ideal scenario: implement long-term holistic monitoring programs**

In an ideal scenario, where resources, time, and infrastructure are not limited, a comprehensive, geographical monitoring program would significantly contribute to advancing our understanding of octocoral-microbiome dynamics. Such a program would integrate:

- **Comprehensive environmental data**, including temperature, salinity, pH, turbidity, nutrient load, and pollution levels.
- **Expand microbial community profiling** to encompass multiple taxonomic kingdoms, including for example viruses and archaea in addition to bacteria and microeukaryotes**.**
- **A large scale geographical and depth sampling,** encompassing many octocoral species (not only *C. rubrum* and *P. clavata*) from both shallow and mesophotic reefs across the Mediterranean, to ensure the dataset represents the full diversity of environmental contexts in which these octocorals species occur and compare their response. **This is particularly relevant for microbes other than bacteria, such as microeukaryotes, which have been much less studied.** For example, a large-scale geographic survey of microeukaryotic communities associated with octocorals across the Mediterranean would provide valuable insights into the spatial variability of these communities and help identify ecological patterns. Such studies should be combined with extensive environmental metadata to decipher the environmental drivers shaping microeukaryotic diversity and distribution. Understanding these patterns would help distinguish between naturally occurring biogeographic variability and stress-induced shifts in the microbiome.
- **Time-series sampling** before, during, and after environmental disturbances (e.g., marine heatwaves), combined with **detailed coral physiological assessments**,

such as measurements of respiration, calcification, and oxidative stress responses. Additionally, **tagging individual colonies** and revisiting them over time would allow to track within-host microbial trajectories and assess whether specific microbiome configurations predispose corals to thermal sensitivity or resilience such as the work initiated in Bonacolta et al. (2024) for the microeukaryotes community associated with *P. clavata* .

- **Multi-omics approaches**, including metabarcoding, metagenomics, metatranscriptomics and metabolomics, to resolve functional changes.

While such program would be logistically and financially demanding, requiring substantial infrastructure (e.g., sampling vessels, molecular laboratories, advanced sequencing facilities), it represents the type of integrative, large-scale effort needed to generate predictive models of coral holobiont responses under climate change. These efforts would align with calls in the literature for more mechanistic and systems-level investigations into host-microbiome-environment interactions (Voolstra et al. 2019).

III. Conclusion: insights into understanding the role of the microbiome in the health and resilience of Mediterranean octocorals in a changing world

In an era characterized by rapid environmental change and an increase in the frequency and intensity of extreme events such as marine heatwaves (MHWs), understanding the resilience of foundational species of the marine animal forests (MAFs) has become essential. These ecosystems harbor a rich diversity of species that contribute significantly to regional biodiversity and provide important ecosystem services to human societies (Bianchi et al. 2000; Ballesteros 2006; Tonin 2018; Buonocore et al. 2020). This is particularly evident in the Mediterranean Sea, a recognized biodiversity hotspot that is also experiencing some of the most pronounced effects of global climate change (MedECC 2020; Pastor et al. 2020; Cos et al. 2022; Tuel et al. 2020). Consequently, it is essential to preserve the structure and functionality of these ecosystems as much as possible to maintain the vital services they provide to marine life and human societies.

It is increasingly recognized that the health and resilience of these marine organisms is closely linked to the microbiome (Bourne et al. 2009; Apprill 2017; Thompson et al. 2015). The concept that a host and its microbial community form a cohesive unit, referred to as a holobiont, has gained considerable momentum in recent years (Simon et al. 2019b; Dittami et al. 2021). In this framework, the physiological performance and overall health of the host are determined not only by its own genetic and cellular processes, but also by the composition and functions of its symbiotic microbial partners. This new perspective represents a paradigm shift and emphasizes the need for holistic strategies for the conservation and management of marine ecosystems, strategies that protect both the host species and the integrity of their microbiome.

This thesis contributes to the evolving scientific discourse on host-microbiome interactions by examining the complex relationships between Mediterranean octocorals and their associated microbial communities. As foundational species of the MAFs, octocorals such as *Paramuricea clavata* and *Corallium rubrum* play a crucial ecological

role. A detailed understanding of their microbiome is essential to develop and refine ecosystem management strategies, especially in view of the increasing impacts of climate change. By characterizing the basic composition of healthy microbial communities associated with these species, this research provides a basis for detecting microbiome changes that may indicate environmental stress or disease.

In the future, by comparing microbial communities under healthy and stress conditions, it will be possible to identify microbial species which can serve as early indicators of stress, and which can be used as tools for monitoring ecosystem health. Although beyond the immediate scope of this thesis, such findings hold promise for advancing microbiome-based conservation strategies. This could include the prediction of host thermal sensitivity based on microbiome profiles, and the development of microbial-based interventions such as probiotics, an area of growing interest in coral research (Peixoto et al. 2021; 2022; Rosado et al. 2019; Doering et al. 2023).

Résumé en français

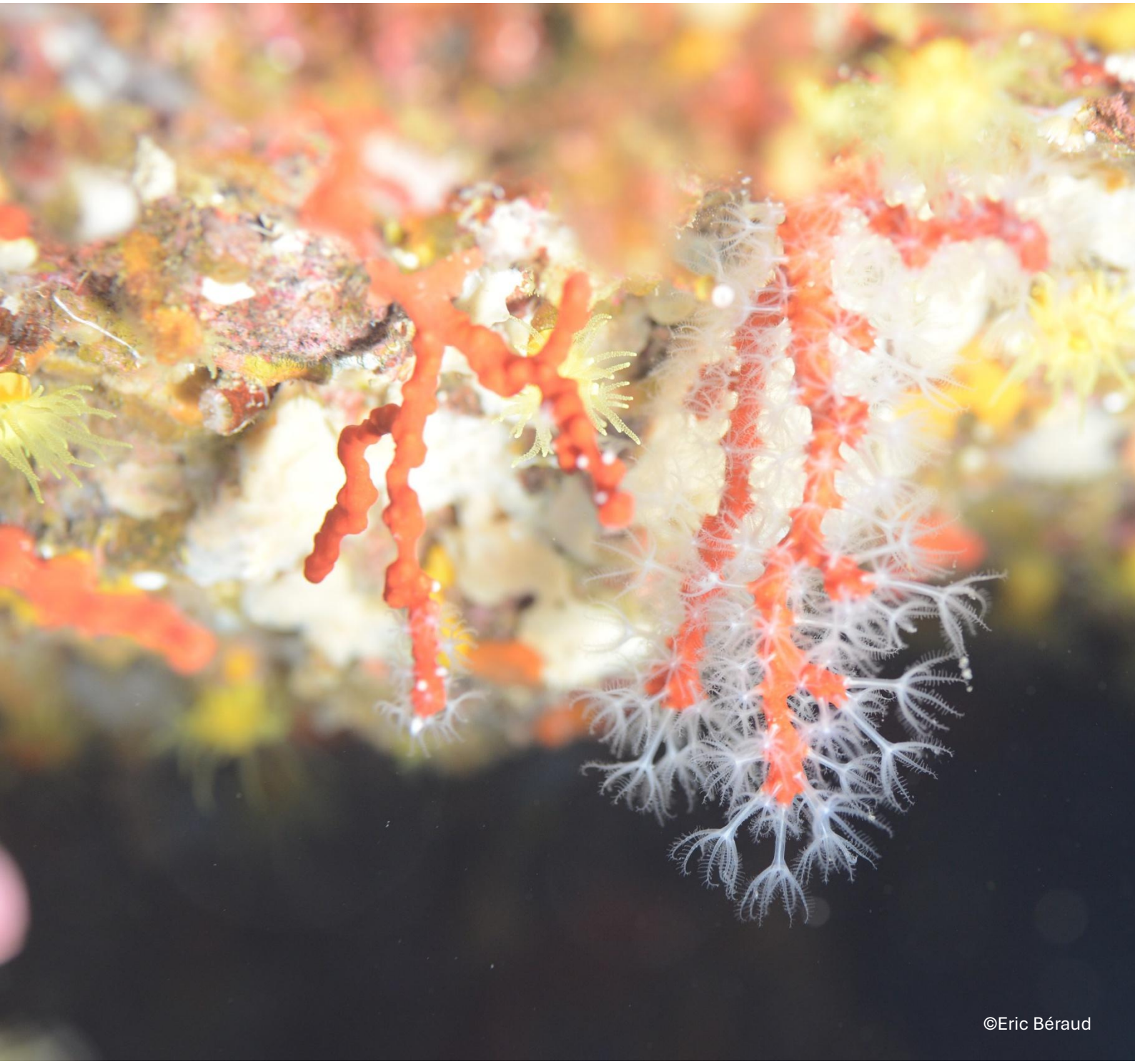

©Eric Béraud

Résumé général de la thèse en français

Introduction

IV. Rôle écologique et économique des forêts animales marines méditerranéennes

Les forêts animales marines (MAFs, pour Marine Animal Forests), un concept introduit par Alfred Wallace en 1869 et développé par Rossi et al. (2017), désignent des écosystèmes benthiques dominés par des invertébrés sessiles, tels que coraux, gorgones et éponges. Ces espèces forment des structures tridimensionnelles rappelant des canopées d'arbres, fournissant refuge à de multiples organismes marins (L. Piazzi et al. 2021) et favorisant la biodiversité (Paoli et al. 2017). Ces écosystèmes sont parmi les plus diversifiés et productifs au monde (Bianchi and Morri 2000; Ballesteros 2006; Wilkinson 2008; Gori et al. 2011), apportant des bénéfices sociaux et économiques majeurs (Bianchi and Morri 2000; Ballesteros 2006; Tonin 2018; Buonocore et al. 2020), contribuant localement à la pêche commerciale, au tourisme et à la protection des côtes contre l'érosion (Ferrario et al. 2014; Randone et al. 2017; Spalding et al. 2017).

Contrairement aux récifs coralliens tropicaux, qui sont construits par des coraux durs, formant des structures calcaires (Allemand et al. 2004), les forêts animales méditerranéennes (ou coralligène) sont formées par des octocoralliaires comme les gorgones du genre *Eunicella*, *Paramuricea* et *Callogorgia* ainsi que par le corail rouge *Corallium rubrum* (Gibson et al. 2006). Ces écosystèmes vivent à différentes profondeurs, de 40 à 200 mètres, et se développent aussi bien sur des pentes côtières, que sur le plateau continental ou les monts sous-marins (Gori et al. 2017). Ils servent d'habitats pour de nombreuses espèces de poissons, crustacés et mollusques (Santín et al. 2021; Cartes et al. 2022) et constituent des sites de ponte et de refuge pour les juvéniles (Bo et al. 2015). Cette thèse s'est particulièrement intéressée au corail rouge, *Corallium rubrum*, ainsi qu'à sa capacité à résister aux stress anthropiques.

Corallium rubrum (Linnaeus, 1758) est en effet une espèce emblématique, connue pour son squelette rouge vif, bien que l'origine de sa pigmentation reste inconnue. Il est principalement présent dans la Méditerranée occidentale (Cattaneo-Vietti et al.

2016). C'est une espèce sciaphile, observée aux abords de grottes, surplombs et crevasses (Ballesteros 2006) à des profondeurs allant de de 10 à 1 000 m (Costantini et al. 2010; Knittweis et al. 2016; Pratlong et al. 2021). Cette espèce est caractérisée par une croissance lente, un renouvellement des populations faible et une forte mortalité post-larvaire, ce qui augmente sa vulnérabilité aux pressions naturelles et anthropiques (Gallmetzer et al. 2010). Utilisé depuis l'Antiquité, le corail rouge est présent dans des objets décoratifs, spirituels et des bijoux (Cattaneo-Vietti et al. 2016; Tsounis et al. 2006; 2010; 2013). En raison de sa grande valeur commerciale, *C. rubrum* a été largement exploité, devenant l'une des ressources marines les plus importantes sur le plan économique en Méditerranée (Santangelo and Abbiati 2001b; Tsounis et al. 2010).

II. Les coraux sont des holobiontes

Le concept d'holobionte a profondément transformé notre compréhension des systèmes biologiques en considérant l'hôte et son microbiome comme une unité fonctionnelle unique (Margulis et Fester 1991 ; Baedke et al. 2020 ; Simon et al. 2019). Les coraux forment des associations symbiotiques complexes avec des microorganismes variés tels que les bactéries, archées, champignons, virus et microeucaryotes (van de Water et al. 2018 ; Stévenne et al. 2021 ; Voolstra et al. 2024). Le microbiome contribue à des processus clés comme le recyclage des nutriments, la dégradation de la matière organique, la production de composés antimicrobiens et l'augmentation de la résistance au stress (Voolstra et al. 2024a). Bien que les communautés bactériennes commencent à être bien étudiées, la diversité et le rôle des autres microorganismes restent largement inexplorés.

A. Communautés procaryotes associées aux holobiontes coralliens

La diversité taxonomique des bactéries associées aux coraux est importante, avec au moins 39 phyla (Huggett et al. 2019) et des dizaines à des milliers de taxons identifiés au niveau de l'espèce (Hernandez-Agreda et al. 2017). Les partenaires bactériens les plus connus des coraux appartiennent à la famille des Endozoicomonadaceae, notamment le genre *Endozoicomonas* (Neave et al. 2016). Chez les gorgones méditerranéennes (genres *Paramuricea*, *Leptogorgia*, *Eunicella*), *Endozoicomonas* représente plus de 96 % de la communauté bactérienne (van de Water et al. 2018 ; Ransome et al. 2014). Ces bactéries

participent notamment à la synthèse d'acides aminés, au métabolisme des composés soufrés, à la production de vitamine B (Tandon et al. 2022), ainsi qu'à la dégradation de molécules complexes comme le DMSP (Raina et al. 2009 ; 2010) et la chitine (Da Silva et al. 2023). Toutefois, leur fonction exacte dans le métabolisme des coraux reste débattue, notamment en raison de preuves émergentes de leur potentiel pathogène et de l'insuffisance de données fonctionnelles (Ziegler et al. 2019 ; Pogoreutz et Ziegler 2024). Contrairement aux autres octocoralliaires méditerranéens, le microbiome du corail rouge *Corallium rubrum* est dominé par les Spirochaetaceae, pouvant représenter jusqu'à 70 % de la communauté bactérienne, (van de Water et al. 2016). Présents également chez des invertébrés comme les arthropodes et les vers, les Spirochaetaceae interviennent parfois dans la dégradation du bois et la fixation de l'azote (Brune 2014 ; Lilburn et al. 2001), mais leur rôle exact chez les coraux reste inconnu. Leur association stable avec *Corallium rubrum* suggère qu'ils pourraient contribuer au métabolisme de l'holobionte ainsi formé, et donc à la santé du corail.

Les microbiotes des coraux comprennent d'autres familles bactériennes importantes, notamment les Vibrionaceae, les Rhodobacteraceae et l'ordre des Alteromonadales (Hernandez-Agreda et al., 2017 ; van Oppen et al., 2019 ; Bourne et al., 2016). Les Vibrionaceae, particulièrement les *Vibrio* spp., sont ubiquistes dans les environnements marins et souvent associées aux coraux (Rubio-Portillo et al., 2018 ; Sharon et al., 2010). Leur prolifération est fortement dépendante de la température, avec une augmentation en été et sous l'effet du changement climatique, en particulier en Méditerranée (Vezzulli et al., 2010, 2012, 2013). Souvent liées à des maladies coralliennes (Munn, 2015), certaines espèces, comme *Vibrio coralliilyticus*, peuvent induire des nécroses sous stress thermique, particulièrement chez les gorgones méditerranéennes (Tout et al., 2015 ; Tignat-Perrier et al., 2023). Néanmoins, des souches de *Vibrio* isolées de coraux sains démontrent des interactions mutualistes, telles que la fixation d'azote (Chimetto et al., 2008) ou la défense contre les pathogènes (Ritchie, 2006). Les Rhodobacteraceae, quant à elles, augmentent en abondance sous stress environnemental mais pourraient interagir positivement avec les symbiotes coralliens, renforçant ainsi la résilience (Pootakham et al., 2019 ; Rosales et al., 2020) ; (Xu et al., 2024). Enfin, les Alteromonadales, fréquemment observées dans le mucus des coraux

tropicaux, présentent des propriétés antibactériennes, antioxydantes et participent à la régulation osmotique (Ng et al., 2015 ; Raina et al., 2009a). Leur présence pourrait également être corrélée avec une résistance accrue à l'infection (Wright et al., 2017), bien que leur rôle reste parfois ambigu (Gignoux-Wolfsohn et al., 2017 ; Ziegler et al., 2019).

Ces associations stables entre coraux et bactéries suggèrent une évolution parallèle entre ces organismes, voire une coévolution marquée par des changements réciproques entre les espèces en interaction. Ainsi, la phylosymbiose décrit une communauté microbienne reflétant la phylogénie de l'hôte (Lim et Bordenstein, 2020), déjà observée chez les coraux tropicaux (Pollock et al., 2018). La cophylogénie identifie des symbiotes partageant une histoire évolutive avec les coraux (Blasco-Costa et al., 2021), notamment *Endozoicomonas* (O'Brien et al., 2023). La caractérisation de ces interactions est une étape clé pour comprendre l'adaptation des coraux.

B. Communautés microeucaryotes associées aux coraux

D'autres microorganismes, appelés microeucaryotes, comme des microalgues, des protistes et des champignons, font partie du microbiome des coraux, mais restent mal connus (Bonacolta et al., 2023 ; Ainsworth et al., 2017 ; Keeling et al., 2017), à part l'association mutualiste entre les coraux et des protistes dinoflagellés de la famille Symbiodiniaceae. Ces derniers, du fait de leur activité photosynthétique, fournissent jusqu'à 95 % des besoins énergétiques de l'animal hôte (Muscatine et al., 1981 ; Treignier et al., 2008). Ils sont présents chez seulement 38 % des octocoralliaires (Schubert et al., 2016), et seulement chez *Eunicella singularis* en Méditerranée. D'autres dinoflagellés peuvent être associés aux coraux comme l'ordre des Syndiniales, par exemple (Clerissi et al. 2018 ; Qiu et al. 2021). Beaucoup de ces espèces sont parasitaires, capables de tuer leurs hôtes en libérant des dinospores infectieuses (Guillou et al. 2008). Certains dinoflagellés peuvent également offrir des avantages protecteurs tels que la résistance aux UV grâce à la production d'acides aminés de type mycosporine (Klisch et al. 2001).

Au-delà des dinoflagellés, les coraux sont associés à d'autres microeucaryotes, notamment des protistes, comme les ciliés, souvent observés dans les coraux tropicaux malades (Sweet et al., 2016 ; Ravindran et al., 2022), les Apicomplexa qui apparaissent en abondance chez certains octocoralliaires (Vohsen et al., 2020 ; Bonacolta et al., 2023),

ou les Labyrinthulomycetes, des stramenopiles qui peuvent jouer un rôle défensif ou opportuniste (Burge et al., 2012). Certaines microalgues ont également été observées dans les coraux comme *Ostreobium*. Elles contribueraient aux cycles biogéochimiques et à la récupération post-blanchissement (Massé et al., 2018 ; Galindo-Martínez et al., 2022). Les champignons (mycobiome) comprennent à la fois des symbiotes et des pathogènes, comme *Aspergillus sydowii*, responsable d'une maladie appelée aspergillose qui décime les coraux tropicaux (Nagelkerken et al., 1997 ; Smith et al., 1996). Certains champignons participent au recyclage des nutriments (Kohlmeyer, 1969 ; Wegley et al., 2007) ou inhibent des bactéries pathogènes (Xu et al., 2018). Néanmoins, pour la plupart, leur rôle exact, mutualiste ou pathogène, reste à clarifier (Roik et al., 2022).

En résumé, le rôle des microeucaryotes dans le corail est divers et important, mais reste largement sous-étudié par rapport aux bactéries.

C. Autres communautés microbiennes associées aux coraux

Au-delà des bactéries et des microeucaryotes, l'holobionte corallien abrite d'autres micro-organismes, notamment des archées et des virus, dont les rôles dans la santé et le fonctionnement des coraux sont probablement cruciaux. Toutefois, nos connaissances sur ces partenaires microscopiques, en particulier chez les octocoralliaires, restent préliminaires, soulignant des lacunes majeures à explorer. Les archées, notamment les phyla Thermoproteota et Euryarchaeota, peuvent représenter jusqu'à la moitié de la communauté procaryote dans le mucus de certains coraux, où elles interviennent dans le cycle de l'azote (Siboni et al. 2008 ; 2012). Des études métagénomiques révèlent des génomes d'archées avec des voies métaboliques potentiellement bénéfiques à l'hôte, comme la fixation du carbone et la biosynthèse de vitamines (Robbins et al. 2019). Chez les octocoralliaires, les archées sont moins nombreuses et leur rôle reste largement inconnu (Keller-Costa et al. non publié). Les communautés virales associées aux coraux, bien que peu étudiées, incluent plus de 60 familles virales, notamment des phages bactériens qui régulent les communautés bactériennes (Correa et al. 2016 ; Cárdenas et al. 2020). Les Phycodnaviridae par exemple, sont présents lors des événements de blanchissement et pourraient affecter

les Symbiodiniaceae (Correa et al. 2013 ; 2016). Chez les octocoralliaires, les viromes restent peu caractérisés, mais des virus comme les Totiviridae pourraient impacter la virulence des champignons pathogènes (Gudenkauf et Hewson 2016). Malgré ces découvertes, les rôles fonctionnels des archées et des virus dans les octocoralliaires restent largement spéculatifs. Les défis techniques, comme la faible concentration virale dans les échantillons, compliquent leur étude (Weynberg et al. 2014 ; van de Water, Allemand, et al. 2018).

D. Méthodes d'étude des communautés microbiennes

Le gène *16S ARNr* est couramment utilisé pour analyser les communautés bactériennes, tandis que les gènes *ITS2* ou *18S ARNr* sont employés pour les Symbiodiniaceae, les algues ou les champignons. Toutefois, l'étude des microeucaryotes associés aux coraux rencontre un défi majeur : la contamination par l'ADN de l'hôte. Les amorces universelles pour le *18S ARNr* favorisent l'amplification de l'ADN du corail. Des solutions comme les amorces ciblées (*UNonMet-PCR*) ou les amorces bloquantes ont été proposées (Del Campo et al. 2019). La PCR imbriquée (nested PCR) améliore la résolution, mais peut introduire des biais.

Le métabarcoding indique uniquement la proportion de chaque espèce au sein d'une communauté (abondance relative), ce qui rend difficile la détermination du nombre absolu de taxons différents. Par conséquent, les changements dans l'abondance d'une espèce peuvent donner l'impression que d'autres espèces ont changé, même si la taille réelle de leur population reste inchangée. Par exemple, si une espèce microbienne particulière augmente considérablement, l'abondance relative d'autres espèces peut diminuer même si leur nombre absolu reste le même (Damhorst et al. 2021 ; Galazzo et al. 2020). La PCR quantitative (qPCR) permet de quantifier l'abondance absolue des micro-organismes, utile pour valider les résultats du métabarcoding. Seules quelques études, comme celles de Shiu et al. (2020) et Pogoreutz et al. (2022), ont combiné des approches relatives et absolues. Pour une compréhension fonctionnelle, la métagénomique, la méta-transcriptomique et la méta-protéomique sont utiles. Ces méthodes, bien qu'efficaces, sont coûteuses et peu utilisées en raison des exigences en expertise.

III. Pressions anthropiques en mer Méditerranée et leurs conséquences sur les espèces d'octocoralliaires

A. Perturbations anthropiques

Les activités anthropiques, notamment l'utilisation de combustibles fossiles et la déforestation, augmentent le réchauffement global par l'émission massive de gaz à effet de serre (Wigley et al. 1981 ; Houghton et al. 1990 ; Hawkins et al. 2012). Le bassin méditerranéen, classé comme une zone sensible au changement climatique, se réchauffe deux fois plus vite que la moyenne mondiale (MedECC 2020; Pastor et al. 2020; Cos et al. 2022), avec une hausse annuelle de 0,041°C à la surface des eaux (Pastor et al. 2020 ; Pisano et al. 2020). En conséquence, le nombre d'événements de vagues de chaleur marines (MHWs, pour Marine Heatwaves), définis comme des périodes prolongées de températures anormalement élevées, a fortement augmenté en Méditerranée, avec une moyenne de 1,3 événements supplémentaires par décennie (Hamdeno et al. 2023). En 2022, 3 à 7 MHWs ont été enregistrées, avec des anomalies locales atteignant +4,6°C, bien au-delà des +2 à +3°C observés en 2003 (T-MEDNet 2023; Quade 2022; Guinaldo et al. 2023). Ces événements extrêmes menacent la biodiversité marine, la résilience des écosystèmes et les pêcheries, soulignant l'urgence des stratégies d'atténuation et d'action.

En plus du réchauffement global, les organismes benthiques subissent d'autres menaces anthropiques, notamment l'acidification des océans, liée à l'augmentation du CO_2 atmosphérique, qui diminue la calcification et la croissance des coraux, les rendant plus vulnérables (Bramanti et al. 2013; Cerrano et al. 2013). Les polluants chimiques, tels que les métaux lourds, les pesticides et les microplastiques, affectent aussi la santé et la reproduction des espèces (Corinaldesi et al. 2021; Bavestrello et al. 2014; Ricolleau et al. 2019). Enfin, les filets perdus, appelés filets fantômes, endommagent les colonies coralliennes, augmentant leur mortalité (Canessa et al. 2024; Consoli et al. 2019). Ainsi, *Corallium rubrum*, classé comme « en danger » par l'UICN, reste menacé malgré les mesures de conservation (FAO-General Fisheries Commission for the Mediterranean; Cannas et al. 2019). Une action concertée et immédiate est indispensable pour préserver la biodiversité et la résilience des écosystèmes méditerranéens (Cannas et al. 2019).

B. Les conséquences du réchauffement de l'eau de mer sur les populations d'octocoralliaires

La mer Méditerranée, riche en biodiversité et abritant 7 à 10 % des espèces marines connues, notamment des espèces endémiques (Coll et al. 2010 ; Bianchi et al. 2000), sert de modèle privilégié pour étudier les impacts du changement climatique sur les écosystèmes marins. Les octocoralliaires, notamment les gorgones, sont particulièrement vulnérables aux vagues de chaleur marines (MHWs), qui provoquent des épisodes de mortalités massives, touchant jusqu'à 90 % des colonies dans certaines populations (Cerrano et al. 2000 ; Garrabou et al. 2009 ; 2022 ; Piazzi et al. 2021b ; 2019). Même si les écosystèmes profonds (50–200 m) offrent un certain refuge contre le stress thermique, des effets délétères y ont été récemment observés, comme des pertes tissulaires chez des gorgones profondes, soulignant leur vulnérabilité grandissante (Cerrano et al. 2019 ; Corinaldesi et al. 2022). De plus, des espèces jugées résistantes, comme *Eunicella singularis*, montrent désormais des signes de déclin, en particulier en reproduction et survie (Ramirez-Calero et al. 2024 ; Sarda et al. 2024). Les études suggèrent que les octocoralliaires de surface sont mieux adaptés au stress thermique que leurs homologues profondes, notamment chez *Corallium rubrum* (Pratlong et al. 2021 ; Cau et al. 2018) et *Paramuricea clavata* (Pivotto et al. 2015 ; Ramirez-Calero et al. 2025). La dégradation des assemblages dominés par les octocoralliaires menace non seulement la biodiversité, mais aussi des fonctions écologiques essentielles. Face à l'augmentation des MHWs, des actions urgentes et des recherches approfondies sont indispensables pour atténuer ces effets et comprendre les mécanismes liés à la mortalité (Garrabou et al. 2021).

Le stress thermique chez les coraux provoque des réponses métaboliques variées, comme l'accumulation de lipides et de glucides et la surexpression des gènes d'HSP (Heat stress proteins), tout en impliquant des mécanismes oxydatifs (Pupier et al. 2024 ; Barshis et al. 2013 ; Montalbetti et al. 2023). Cependant, au-delà de l'hôte, la réponse des coraux doit être analysée au niveau de l'holobionte, en intégrant les interactions avec le microbiote. Cette approche intégrée permet de mieux saisir les mécanismes

d'adaptation, de résistance ou de vulnérabilité face aux changements environnementaux.

Les réponses des microbiomes des octocoralliaires méditerranéens au stress thermique montrent des tendances communes. Chez *Paramuricea clavata* (Bally & Garrabou, 2007 ; Vezzulli et al., 2010), *Eunicella cavolini* (Bally & Garrabou, 2007 ; Vezzulli et al., 2010 ; Bonacolta et al., 2024), et *Corallium rubrum* (Wessels et al., 2017 ; Keller-Costa et al., 2021), le stress thermique entraîne une diminution relative des principaux symbiotes (*Endozoicomonas* et Spirochaetaceae), et une augmentation des bactéries opportunistes, notamment des Rhodobacteraceae, Alteromonadaceae et Vibrionaceae. Ces dernières peuvent sécréter des enzymes extracellulaires (protéinase, gélatinase, DNase) qui participent à la nécrose tissulaire (Billaud et al., 2022 ; Kimes et al., 2012 ; Ushijima et al., 2023). Cependant, les études basées sur le metabarcoding présentent des biais en ne mesurant que les abondances relatives et non l'abondance absolue (Dunphy et al., 2021) ne permettant pas de distinguer si la dégradation de la santé des coraux est due à la perte de symbiotes clés ou à la prolifération de pathogènes. De plus, chez certains coraux tropicaux, les changements microbiens associés au stress thermique peuvent persister longtemps après l'événement, modifiant durablement la composition bactérienne (Tracy et al., 2015 ; Girija et al., 2024) mais aucune étude n'existe sur les octocoralliaires méditerranéens. Les microeucaryotes, bien moins étudiés, jouent probablement un rôle important dans la réponse au stress thermique (Amend et al., 2012 ; Thurber et al., 2009 ; Bonacolta et al., 2024). Chez *P. clavata*, une association entre l'abondance de Dino-Group I et de Corallicolidae et la résistance au stress thermique a été suggérée (Bonacolta et al., 2024). Néanmoins, les mécanismes sous-jacents restent à élucider. En conclusion, si des schémas généraux émergent, la réponse du microbiome des octocoralliaires au stress thermique est fortement spécifique à l'espèce et nécessite une approche cas par cas pour une compréhension complète de leurs dynamiques et de leurs implications pour la survie des coraux.

Conclusion

Les canicules marines répétées provoquent des mortalités massives, notamment dans la mer Méditerranée, avec des pertes importantes chez plusieurs octocoralliaires.

Le stress thermique modifie la physiologie et la composition du microbiome, entraînant une dysbiose caractérisée par la perte de symbiotes clés et la prolifération de bactéries opportunistes, liée à une augmentation de la mortalité. Cependant, le lien causal entre ces changements microbiens et la perte de tissus reste partiellement inconnu, en raison de limitations des données de metabarcoding. De plus, des lacunes persistent notamment sur le rôle d'autres micro-organismes tels que les microeucaryotes ainsi que la récupération à long terme.

Objectifs de la thèse

La compréhension des interactions entre les coraux et leur microbiote associé est centrale en écologie marine, les symbiotes microbiens jouant un rôle clé dans la santé, la résilience et l'adaptation des coraux aux stress environnementaux. Alors que les microbiomes des coraux constructeurs de récifs tropicaux sont bien étudiés, ceux des octocoralliaires méditerranéens restent largement inexplorés, notamment en termes de diversité de réponse au changement climatique, et cela malgré le déclin majeur des octocoralliaires. Ce manque de données sur leur microbiome limite notre capacité à évaluer leur potentiel d'adaptation et à prédire leur résilience. Une étude approfondie de ces communautés microbiennes est donc indispensable pour mieux comprendre les interactions hôte-microbe dans les écosystèmes coralliens tempérés et orienter des stratégies de conservation.

L'objectif général de cette thèse est de caractériser le microbiome (bactéries et microeucaryotes) des octocoralliaires méditerranéens et d'évaluer leur réponse au réchauffement climatique, en mettant particulièrement l'accent sur le microbiome du corail rouge *Corallium rubrum*.

Nous avons donc étudié la composition des communautés bactériennes et microeucaryotes associées à certains octocoralliaires emblématiques de la Méditerranée, tels que la gorgone *Paramuricea clavata* et le corail rouge *Corallium rubrum*, et nous avons cherché à comprendre comment les vagues de chaleur marines (MHWs) affectent cette composition. L'objectif était d'explorer les interactions hôte-microbe et le rôle des symbiotes microbiens dans la santé et la résilience des octocoralliaires. Pour ce faire, nous avons utilisé la culture, le séquençage d'amplicons et la PCR quantitative (qPCR). L'impact des MHWs a été évalué à la fois par des observations *in-situ* et des expériences contrôlées en laboratoire.

Cette recherche s'est articulée autour de deux objectifs clés décrits ci-dessous.

I. Diversité du microbiome des octocoralliaires méditerranéens

Deux sous-objectifs principaux ont été poursuivis :

a. **Les symbiotes bactériens de *C. rubrum* et d'autres octocoralliaires, qui ont déjà été caractérisés, partagent-ils une histoire évolutive commune avec leurs hôtes ?**
b. **Quelle est la composition de l'eucaryome de *C. rubrum* et reste-t-elle constante dans des environnements temporellement et spatialement distincts ?**

a. Les symbiotes bactériens de *C. rubrum* et d'autres octocoralliaires, qui ont déjà été caractérisés, partagent-ils une histoire évolutive commune avec leurs hôtes ?

Les communautés bactériennes des octocoralliaires méditerranéens sous conditions stables sont bien connues, leur grande stabilité suggérant une conservation possible des associations microbiennes au sein de ces espèces, probablement liée à une histoire évolutive partagée (Lim et al. 2020 ; Page 2003 ; Balbuena et al. 2013). L'analyse de phylosymbiose et de cophylogénie peut mettre en évidence des interactions symbiotiques essentielles pour la résilience, le cycle des nutriments et la défense immunitaire des hôtes (O'Brien et al. 2020 ; 2021 ; Pollock et al. 2018). Les communautés procaryotes d'octocoralliaires des zones mésophotiques (60-150 m) de la Méditerranée et de la mer Rouge ont donc été étudiées, permettant d'explorer ces liens évolutifs avec 14 espèces d'octocoralliaires collectées lors des campagnes Gombessa V, VI et ENCOR.

b. Quelle est la composition de l'eukaryome de *C. rubrum* et reste-t-elle constante dans des environnements temporellement et spatialement distincts ?

En plus des communautés bactériennes, les microeucaryotes, tels que les champignons et les protistes, jouent un rôle-clé dans le fonctionnement des hôtes coralliens, mais restent peu étudiés, notamment chez les octocoralliaires méditerranéens (Bonacolta et al. 2023 ; Ainsworth et al. 2017). Une grande partie de cette thèse a donc porté sur la caractérisation des microeucaryotes associés à *C. rubrum*. Une méthode ciblant une région spécifique du gène *18S ARNr* a été développée pour minimiser l'interférence avec l'hôte et améliorer la précision de l'identification (Góes-

Neto et al. 2020 ; Marcelino et al. 2016). Cette méthodologie a ensuite été appliquée pour étudier la diversité et la composition des communautés microeucaryotes associées à *C. rubrum* dans des conditions naturelles, tout en évaluant la stabilité de ces associations dans le temps et l'espace.

Les difficultés rencontrées à récupérer des séquences fongiques ont souligné l'intérêt d'approches complémentaires, telles que les méthodes de culture. De plus, les communautés fongiques coralliennes sont souvent analysées sans distinction des compartiments (tissu, mucus, squelette), alors que des différences fonctionnelles existent entre ces micro-habitats (Bonthond et al. 2018 ; Rabbani et al. 2021). Une partie de ce travail a donc porté sur une telle analyse.

II. Réponse du microbiome de *C. rubrum* et *P. clavata* au stress thermique

Le second objectif était d'étudier la réponse du microbiome de *C. rubrum* (et *P. clavata*) au stress thermique et ses conséquences sur l'hôte. Les vagues de chaleur marines, liées au changement climatique, ont déjà provoqué des mortalités massives chez les octocoralliaires méditerranéens, mais le rôle du microbiome reste mal connu (Bonacolta et al. 2023). En analysant les modifications des communautés bactériennes et microeucaryotes sous des températures élevées, il est possible d'évaluer si le stress thermique entraîne une dysbiose microbienne et si cela contribue à la mortalité corallienne. La résilience du microbiome de *C. rubrum* après le stress thermique a également été examinée pour déterminer si les communautés microbiennes se rétablissent ou restent altérées, ce qui pourrait affaiblir la capacité du corail à résister à de futures perturbations.

Deux sous-objectifs principaux ont été poursuivis :

a. **Comment les holobiontes octocoralliaires réagissent-ils aux vagues de chaleur marines et la perte de tissus est-elle liée à la dysbiose ?**
b. **L'hôte et son microbiome peuvent-ils se rétablir après un stress thermique ?**

a. Comment les holobiontes octocoralliaires réagissent-ils aux vagues de chaleur marines et la perte de tissus est-elle liée à la dysbiose ?

Les vagues de chaleur marines perturbent la symbiose entre les octocoralliaires méditerranéens et leurs microbes, essentielle à la tolérance au stress et à la défense contre les pathogènes. Bien que des études aient observé une diminution relative de symbiotes majoritaires (comme Spirochaetaceae) en laboratoire et *in-situ*, aucune corrélation claire avec la perte de tissus n'a été trouvée (Tignat-Perrier et al. 2022 ; 2023 ; Corinaldesi et al. 2022). Pour approfondir ces liens, les changements subis par le microbiome de *C. rubrum* et *P. clavata*, avec ou sans nécrose tissulaire, ont été analysées après la vague de chaleur de 2022, via le séquençage d'amplicons (*16S ARNr*) et la qPCR. En parallèle, les dynamiques des microeucaryotes ont été étudiées, puisque leur rôle dans la résistance thermique des coraux reste mal connu (Bonacolta et al. 2024). Cette thèse apporte les premières données précises sur les changements de l'« eucaryome » corallien induits par la chaleur, établissant un lien entre ces modifications et la santé de l'holobionte.

b. L'hôte et son microbiome peuvent-ils se rétablir après un stress thermique ?

La résilience du microbiome, c'est-à-dire sa capacité à se rétablir après un stress thermique, est essentielle à la santé des coraux face au réchauffement climatique. Dans le contexte des vagues de chaleur marines de plus en plus fréquentes, cette thèse a évalué pour la première fois la résilience d'un octocoralliaire méditerranéen (*C. rubrum*) en analysant sa réponse physiologique et microbiologique à un stress thermique modéré (19°C) et plus intense (23°C). Les résultats, obtenus par séquençage des gènes *16S* et *18S ARNr* ainsi que par qPCR ciblée, fournissent des éléments révélateurs sur la capacité de rétablissement de l'holobionte après des épisodes de vagues de chaleur.

Conclusion

En poursuivant ces objectifs, cette recherche comble des lacunes essentielles sur le microbiome des octocoralliaires méditerranéens et leur réponse au changement climatique. Elle apporte des éléments de réponse essentiels pour expliquer la mortalité de *C. rubrum* (et *P. clavata*) après les vagues de chaleur et prédire leur résilience dans un

environnement en transformation rapide. Ces résultats contribuent aux efforts de conservation marine et ouvrent des perspectives pour des stratégies de conservation, notamment basées sur le microbiome, visant à renforcer la résilience corallienne au réchauffement climatique.

Résumé du chapitre 1 : Relations évolutives entre les octocoralliaires et leurs microbiomes bactériens

Les études sur les octocoralliaires méditerranéens ont révélé un microbiote hautement stable à l'échelle temporelle et géographique, ainsi que sur une large gamme de températures (Tignat-Perrier et al., 2022, 2023 ; van de Water et al., 2016, 2017, 2018). Cette remarquable stabilité suggère qu'il pourrait y avoir une histoire évolutive commune entre différentes espèces d'octocoralliaires méditerranéens et leur microbiote. L'exploration d'une telle perspective pourrait davantage souligner l'importance des relations corail-bactéries.

Pour étudier les liens évolutifs entre les coraux et leur microbiote, l'analyse de motifs tels que la phylosymbiose et la cophylogénie est une approche pertinente. La phylosymbiose désigne la concordance entre la structure des communautés microbiennes et la phylogénie de l'hôte (Lim et al., 2020). Observée chez les plantes, les mammifères, les insectes, les éponges et les coraux scléractiniaires (Van Bel et al., 2021 ; Bornbusch et al., 2023 ; Li et al., 2022 ; O'Brien et al., 2020 ; Pollock et al., 2018), la phylosymbiose peut être le signe d'associations hôte-microbes profondément ancrées. L'analyse de cophylogénie, par comparaison des phylogénies hôtes et de certains clades bactériens, associe leur congruence à une histoire évolutive partagée, bien que les mécanismes sous-jacents puissent inclure à la fois la coévolution et la biogéographie (Page, 2003 ; Balbuena et al., 2013 ; Hafner et al., 1988 ; Godsoe et al., 2009 ; Smith et al., 2008 ; Weckstein, 2004). Notamment, la cophylogénie a été documentée chez les coraux scléractiniaires, particulièrement en ce qui concerne *Endozoicomonas* (O'Brien et al., 2021 ; Pollock et al., 2018).

Ce chapitre explore ces motifs à travers l'analyse des communautés procaryotes des octocoralliaires des zones mésophotiques (60-150 m de profondeur) de la mer

Méditerranée et de la mer Rouge. Les écosystèmes mésophotiques sont idéaux pour étudier les liens évolutifs entre les coraux et leur microbiote, en raison d'une faible exposition aux facteurs physiques et anthropiques. Les données ont été collectées lors des campagnes Gombessa V et VI (2019, 2021) et ENCOR (2019), incluant 14 espèces d'octocoralliaires issues de 10 genres et 9 familles, incluant le corail rouge *Corallium rubrum*.

Les communautés bactériennes associées aux octocoralliaires mésophotiques ont été analysées par le séquençage d'amplicons du gène *16S ARNr*. La composition du microbiote diffère nettement entre les deux mers, probablement en raison d'un long isolement géographique et de conditions environnementales contrastées (Steininger et al., 1984 ; Manasrah et al., 2019 ; Tanhua et al., 2013). Les octocoralliaires méditerranéens présentent des microbiotes spécifiques, dont les compositions se regroupent principalement selon qu'ils sont dominés par *Endozoicomonas* ou Spirochaetaceae, comme l'ont montré des études précédentes (van de Water et al., 2016, 2017, 2018 ; Bayer et al., 2013). Des chevauchements, tels que des OTUs communs entre *P. clavata* et les *Eunicella* spp., pourraient refléter une convergence évolutive ou des schémas déterminés par des stratégies de vie (McFadden, 1999 ; Groot et al., 1982 ; Quintanilla et al., 2013). Les octocoralliaires de la mer Rouge présentent eux aussi couramment *Endozoicomonas* et Spirochaetaceae, mais les regroupements sont plutôt influencés par la présence de taxa tels que les Mollicutes et les Rhodobacteraceae (Haydon et al., 2022 ; O'Brien et al., 2020 ; Alsharif et al., 2023). Ces associations confirment celles observées dans d'autres études sur les octocoralliaires tropicaux et indo-pacifiques (Wessels et al., 2017 ; Morrow et al., 2012).

La phylosymbiose a été identifiée uniquement chez les octocoralliaires méditerranéens (Lim et al., 2020 ; Pollock et al., 2018 ; O'Brien et al., 2020). Le mucus, très présent dans les espèces de mer Rouge, abrite des communautés bactériennes instables qui pourraient masquer ces motifs évolutifs (Pollock et al., 2018 ; van de Water et al., 2018). Au-delà de la phylosymbiose, des signaux de cophylogénie ont été détectés chez 13 des 14 espèces d'octocoralliaires étudiés. Les analyses ont montré que seules certaines bactéries, principalement *Endozoicomonas* et Spirochaetaceae, présentent des histoires évolutives congruentes avec leurs hôtes (O'Brien et al., 2021 ; Pollock et al.,

2018). Le genre *Endozoicomonas* affiche une cophylogénie significative avec les octocoralliaires des deux mers, ce qui souligne un possible rôle important pour les coraux (Speck et al., 2012 ; Neave et al., 2017 ; Maire et al., 2023), bien que la nature précise de ces relations nécessite encore des clarifications (Pogoreutz et al., 2024). Certains taxa moins dominants, notamment les Mollicutes et les Spongiibacteraceae, montrent également des signes de cophylogénie (Keller-Costa et al., 2022 ; Rasmussen et al., 2023 ; Quintanilla et al., 2022). Cependant, tous les microbiotes abondants ne présentent pas de lien évolutif avec leurs hôtes coralliens, contestant ainsi l'hypothèse selon laquelle l'abondance équivaut à une association de longue durée.

Dans l'ensemble, les résultats de ce chapitre soulignent l'importance des *Endozoicomonas* et des Spirochaetaceae dans la symbiose chez les octocoralliaires, ainsi que l'intérêt d'explorer l'histoire évolutive entre les coraux et leur microbiome pour une compréhension approfondie de leurs interactions.

Résumé du chapitre 2 : Composition et stabilité spatiotemporelle de l'eucaryome de *C. rubrum*

Alors que les communautés bactériennes ont été largement étudiées pour leurs rôles dans le cycle des nutriments, la résistance au stress et la protection contre les pathogènes, les communautés de microeucaryotes (eucaryome), comprenant les protistes, les microalgues et les champignons, demeure peu caractérisée, à part l'association avec les dinoflagellés photosynthétiques (Symbiodiniaceae) qui contribuent largement à la nutrition des coraux. Comprendre la diversité, la stabilité et les rôles fonctionnels de ces communautés microeucaryotes, est essentiel pour élucider le fonctionnement de l'holobionte corallien et sa résistance face aux stress environnementaux tels que les vagues de chaleur marine et la dégradation des habitats. Cette thèse s'est donc attachée à caractériser l'eucaryome de *Corallium rubrum*, qui n'a jamais été étudié.

Un défi technique majeur dans l'étude des microeucaryotes associés aux coraux réside dans la présence dominante de l'ADN de l'hôte dans les données de métabarcoding du gène *18S ARNr*, ce qui masque la détection des microeucaryotes

associés (del Campo et al. 2019 ; Parfrey et al. 2014). Pour pallier ce problème, des amorces spécifiques ciblant une région du gène *18S ARNr* ont été développées afin de minimiser l'amplification des séquences de l'hôte *C. rubrum* tout en capturant une large diversité de microeucaryotes. Cette approche a été appliquée à 46 colonies de *C. rubrum* collectées sur cinq sites géographiquement distincts en Méditerranée nord-occidentale (*Porticcio*, *Cap de Creus*, *Cassis*, *Villefranche-sur-Mer* et *Portofino*), couvrant environ 44 670 km^2, afin d'évaluer la diversité microeucaryote et la stabilité spatiale.

Le métabarcoding a révélé une communauté microeucaryote diverse dont certaines familles ont été détectées de manière constante sur tous les sites, notamment les ciliés Licnophoridae et les dinoflagellés du groupe Dino-Group I Clade 1. Cette association constante suggère que ces taxons, déjà observés chez d'autres espèces coralliennes telles que l'hexacoralliaire tropical *Pocillopora damicornis* et la gorgone tempérée *Paramuricea clavata* (Clerissi et al. 2018 ; Bonacolta et al. 2024), jouent probablement un rôle écologique important au sein de l'holobionte du corail rouge. Les espèces de Licnophoridae sont connues comme des prédateurs d'autres ciliés (Sweet et Séré 2016), un trait qui pourrait contribuer à leur rôle fonctionnel dans le maintien de l'équilibre des communautés microbiennes au sein du corail. Par ailleurs, les colonies de *P. clavata* résistantes à la chaleur hébergeaient des eucaryomes enrichis en membres de la famille des Dino-Group I Clade 1, suggérant un rôle potentiel dans la tolérance au stress corallien, bien que cela nécessite des investigations complémentaires.

Cependant, la composition globale de l'eucaryome a montré une variabilité spatiale et temporelle significative entre les sites, contrastant avec le microbiome bactérien plus stable documenté chez *C. rubrum* (van de Water et al. 2016 ; 2017). Certains microeucaryotes, tels que les apicomplexes *Corallicolidae*, sont par exemple prévalents uniquement sur certains sites d'échantillonnage, ce qui suggère que les conditions environnementales locales influencent fortement la structure des communautés microeucaryotes.

Dans l'ensemble, ce chapitre démontre que l'eucaryome de *C. rubrum* est défini par un noyau stable de taxons microeucaryotes clés, principalement les ciliés Licnophoridae et les dinoflagellés Dino-Group I Clade 1, constamment associés au corail, accompagné d'une fraction variable fortement modulée par les facteurs

environnementaux locaux. Les taxons stables dans l'eucaryome fournissent probablement un soutien fonctionnel essentiel, tel que la nutrition ou la résistance au stress, tandis que les microeucaryotes spécifiques à certains sites peuvent conférer des bénéfices contextuels, comme une protection contre des stress locaux. La variabilité et la sensibilité de l'eucaryome aux conditions environnementales soulignent la nécessité de recherches approfondies pour élucider les rôles écologiques de ces microeucaryotes et leur contribution à la santé et à la résilience des coraux. La compréhension de ces dynamiques est cruciale pour prédire les réponses des coraux au changement climatique et pour développer des stratégies de conservation efficaces pour les populations vulnérables d'octocoralliaires en Méditerranée.

Résumé du chapitre 3 : Caractérisation de la communauté fongique cultivable de *C. rubrum*

Les champignons constituent une composante souvent négligée mais potentiellement importante de l'holobionte corallien, contribuant au cycle des nutriments, à la défense contre les pathogènes et à la santé globale du corail (Burgaud et al. 2022; Gladfelter et al. 2019; Golubic et al. 2005; Masigol et al. 2019; Raghukumar 2017b). Malgré leur importance, les communautés fongiques associées aux coraux, en particulier aux octocoralliaires méditerranéens tels que *C. rubrum*, restent peu caractérisées (Bonthond et al. 2018 ; Rabbani et al. 2021). Ce chapitre vise à explorer la diversité fongique associée à *C. rubrum* en utilisant des méthodes d'isolement et de culture, avec un focus sur les communautés spécifiques aux compartiments des tissus mous et du squelette.

En raison des limites des marqueurs génétiques couramment utilisés (gènes *18S ADNr* et régions *ITS*) pour récupérer les séquences fongiques chez les coraux (Góes-Neto et al. 2020 ; Marcelino et al. 2016), des méthodes de culture ont été employées dans ce chapitre et comparées aux approches de métabarcoding afin d'obtenir une vision plus complète de la communauté fongique. Les échantillons de tissus mous et de squelette de *C. rubrum* ont été analysés séparément pour évaluer les assemblages fongiques spécifiques à chaque compartiment, comblant ainsi une lacune dans la compréhension

de la structuration spatiale des champignons associés aux coraux (Bonthond et al. 2018 ; Rabbani et al. 2021).

Les données de métabarcoding ont largement sous-estimé la diversité fongique par rapport aux résultats issus des cultures, soulignant la nécessité d'améliorer les protocoles moléculaires, notamment la conception des amorces et le traitement des bases de données de référence, afin de mieux capturer le « mycobiome » corallien (Bonacolta et al. 2023). Les analyses basées sur la culture ont révélé une communauté fongique riche, dominée par des Ascomycètes tels que *Penicillium*, *Cladosporium* et *Aspergillus*, avec 61 % des espèces isolées observées pour la première fois en association avec des coraux. La communauté fongique présente une compartimentation marquée, avec des assemblages distincts dans les tissus mous et le squelette, probablement façonnés par des pressions de sélection dérivées de l'hôte ainsi que par des facteurs locaux tels que la disponibilité en nutriments. Notamment, certains champignons isolés, comme *Aspergillus sydowii*, sont reconnus comme des pathogènes potentiels, en particulier à des températures élevées (> 25 °C), conditions pouvant survenir lors des vagues de chaleur marine en Méditerranée, ce qui soulève des questions quant à leur impact sur la santé corallienne (Bonthond et al. 2018 ; Rabbani et al. 2021).

Les résultats démontrent que *C. rubrum* héberge une communauté fongique diverse et structurée, avec des assemblages spécifiques à chaque compartiment qui pourraient contribuer à la santé et à l'adaptation du corail. La présence de champignons potentiellement pathogènes souligne l'importance de surveiller la dynamique fongique, notamment face aux stress induits par le climat tels que les vagues de chaleur marine. L'utilisation en parallèle de méthodes basées sur la culture et des approches moléculaires est essentielle pour une compréhension exhaustive des champignons associés aux coraux. Par ailleurs, la découverte d'espèces fongiques connues pour produire des composés bioactifs ouvre des perspectives pour des applications biotechnologiques et des études écologiques. Dans l'ensemble, cette recherche met en lumière la diversité largement inexplorée des champignons associés aux coraux et l'importance écologique du mycobiome dans les holobiontes coralliens. Les études futures devraient se concentrer sur l'amélioration des méthodes moléculaires de détection et l'investigation des rôles fonctionnels des taxons fongiques afin de mieux

comprendre leurs contributions à la résilience corallienne et d'éclairer les efforts de conservation dans un contexte de changement climatiques.

Résumé du chapitre 4 : Réponses du microbiome bactérien de *Corallium rubrum* et *Paramuricea clavata* aux vagues de chaleur marines de 2022

Les vagues de chaleur marines (MHW) émergent comme l'une des menaces les plus importantes pour la biodiversité, notamment dans la mer Méditerranée, où le changement climatique a accéléré leur fréquence et leur intensité (Smale et al. 2019 ; Juza et al. 2022 ; Quade 2022 ; Grenier et al. 2023). Les octocoralliaires, tels que le corail rouge *Corallium rubrum* et la gorgone *Paramuricea clavata*, constituent le socle des forêts animales marines (MAFs) et sont particulièrement vulnérables à ces événements climatiques extrêmes. Ces octocoralliaires étant fortement dépendants de relations symbiotiques avec des communautés microbiennes, les MHW peuvent perturber cet équilibre délicat, entraînant une dégradation des tissus et une mortalité accrue (Voolstra et al. 2024).

Des études antérieures ont exploré l'impact du stress thermique sur le microbiome des octocoralliaires, mais les résultats ne permettent pas de mettre en évidence une corrélation entre les changements microbiens et la perte de tissus de l'animal (Corinaldesi et al. 2022 ; Tignat-Perrier et al. 2022, 2023). Cette lacune est due au fait que le métabarcoding ne quantifie que l'abondance relative des symbiotes, et non l'abondance absolue, et n'apporte donc pas d'information quantitative sur la dynamique complète des changements des communautés microbiennes. Cette étude comble cette lacune en combinant le séquençage d'amplicons et la qPCR spécifique sur certains taxons bactériens pour évaluer à la fois les abondances relative et absolue des communautés bactériennes dans des colonies de *C. rubrum* et *P. clavata* présentant ou non une nécrose tissulaire à la suite des épisodes de MHW de 2022 en Méditerranée occidentale. L'objectif étant de préciser le rôle de la dysbiose, notamment la prolifération de pathogènes potentiels tels que *Vibrio*, dans la dégradation de la santé des octocoralliaires.

Les données de ce chapitre reposent sur des échantillons collectés dans deux aires marines protégées (AMP), le Parc national des Calanques (France) et la réserve marine de Portofino (Italie). Un total de quatre-vingt-seize colonies d'octocoralliaires (*C. rubrum* et *P. clavata*) a été échantillonné à des profondeurs comprises entre 15 et 35 mètres, leur état de santé étant visuellement catégorisé en fonction d'une perte de tissus de 0 % ou de 90 %. Les MHWs de 2022 ont entraîné des anomalies thermiques allant jusqu'à +4,3 °C dans ces zones, avec des températures maximales de 27 °C et 26 °C respectivement à 15 m de profondeur dans les Calanques et Portofino (Crisci et al. 2011 ; Juza et al. 2022 ; Grenier et al. 2023). La composition bactérienne des coraux a été analysée par séquençage des amplicons du gène *16S ARNr* afin de caractériser la structure des communautés, et par qPCR spécifique pour évaluer l'abondance absolue des symbiotes majoritaires tels que Spirochaetaceae, *Endozoicomonas* et Vibrionaceae.

Les résultats révèlent une diminution significative de l'abondance relative des symbiotes dominants dans les colonies ayant subi une perte de tissus de 90 %, avec une réduction de 47 % et 38 % respectivement pour *C. rubrum* et *P. clavata*. Cependant, cette baisse ne traduit pas toujours une diminution de l'abondance absolue. En effet, la plupart des colonies ayant subi une perte de tissus importante n'ont pas montré de réduction significative de l'abondance absolue de leurs principaux symbiotes. Au contraire, la baisse de l'abondance relative a été attribuée à une prolifération de bactéries opportunistes, notamment *Vibrio*, dont l'abondance a augmenté jusqu'à 120 fois dans certaines colonies de *P. clavata* à Portofino. Le stress thermique s'est avéré être un facteur de dysbiose principal à Marseille, où les changements les plus marqués dans la composition des communautés microbiennes ont été observés dans les sites peu profonds et chauds. Au contraire, la population de Portofino a montré des modifications plus radicales malgré un environnement plus froid et profond. Cela suggère que des facteurs supplémentaires, tels que la pollution anthropique et l'enrichissement en matières organiques (Di Carro et al. 2018 ; Misic et al. 2011), ont pu contribuer au déséquilibre microbiologique dans cette région.

Ces résultats soulignent l'importance d'une approche basée sur l'abondance absolue pour comprendre les dynamiques microbiennes sous des contraintes environnementales. L'abondance relative seule peut être trompeuse, car elle n'inclut pas

l'émergence de taxa opportunistes (Shiu et al. 2020 ; Pogoreutz et al. 2022). En combinant les deux méthodes, cette étude fournit des preuves convaincantes sur le fait que la prolifération microbienne, notamment *Vibrio*, plutôt que la perte des symbiotes majoritaires, est un facteur probable de la dégradation des tissus chez les octocoralliaires soumis à des vagues de chaleur. Ce chapitre met en évidence le rôle critique de la dysbiose dans le déclin des octocoralliaires méditerranéens lors des MHWs. Cependant, la variabilité observée entre les AMPs souligne l'influence de facteurs environnementaux et anthropiques locaux, suggérant que l'impact des MHWs n'est pas uniforme entre les populations. Alors que la fréquence et l'intensité de ces événements continuent d'augmenter, la prise en compte de potentielles interactions entre ces événements est essentielle pour élaborer des stratégies de conservation ciblées destinées à protéger les habitats marins vulnérables.

Résumé du chapitre 5: Réponse de l'eucaryome de *Corallium rubrum* aux vagues de chaleur marines de 2022

Comme souligné dans le chapitre précédent, le réchauffement climatique accroît l'intensité et la fréquence des vagues de chaleur marines (MHWs), particulièrement dans la mer Méditerranée, affectant les populations d'octocoralliaires. La littérature scientifique met en évidence un lien entre la santé des coraux méditerranéens soumis à un stress thermique et leur microbiome bactérien (Vezzulli et al., 2010 ; Tignat-Perrier et al., 2022 ; 2023 ; Estaque et al., 2024). Cependant, d'autres partenaires microbiens, tels que le microbiome eucaryote, restent mal caractérisés et leurs rôles dans les réponses des coraux au stress thermique sont largement inconnus (Del campo et al. 2019 ; Bonacolta et al. 2023). A ce jour, une seule étude a examiné l'eucaryome d'un octocoralliaire méditerranéen, la gorgone *Paramuricea clavata* (Bonacolta et al., 2024), soulignant le besoin d'une recherche accrue sur la manière dont les microeucaryotes contribuent à la dynamique de l'holobionte corallien dans un contexte de stress thermique.

Ce chapitre avait pour objectif d'étudier l'impact des épisodes de MHWs de 2022 sur les communautés microeucaryotes associées à *Corallium rubrum*. L'analyse a été menée en utilisant le séquençage d'amplicons du gène *18S ARNr*, avec la paire d'amorces décrites au chapitre 2, spécifiquement conçues pour exclure les séquences du corail. Cela a permis d'explorer la manière dont le stress thermique modifie la composition et la diversité de l'eucaryome associé au corail rouge. L'étude s'appuie sur des prélèvements *in-situ* de colonies de *C. rubrum* dans la Méditerranée, effectués lors des épisodes de MHWs de 2022 ainsi qu'en hiver (Novembre 2023) pour les colonies témoins. Trois groupes d'échantillonnage ont été pris en compte : 1) les colonies touchées par les MHW à faible profondeur (16-28 m), qui ont subi un stress thermique sévère (16-23 jours avec des températures supérieures à 23 °C) et qui comprenaient à la fois des colonies saines et des colonies présentant une perte de tissus ; (ii) les colonies provenant d'eaux plus profondes (35-37 m), qui ont été moins touchées (5-12 jours avec des températures supérieures à 23 °C) mais qui présentaient également des phénotypes sains et des phénotypes présentant une perte de tissus ; et (iii) les colonies témoins prélevées au cours de l'hiver 2023 à des profondeurs supérieures à 30 m, qui n'ont pas été exposées à un stress thermique.

La richesse spécifique entre les colonies témoins et les colonies ayant subi un stress thermique, mais n'ayant pas perdu de tissu, reste globalement similaire mais la composition de l'eucaryome s'est significativement réorganisée. Plus précisément, les Dino-Group I et les Licnophoridae présentent des abondances réduites sous stress, qui pourraient être dues à leur sensibilité aux variations de température (Martinez, 1980 ; Karajan et al., 2019). Au-delà de ces changements globaux, des différences selon la profondeur des colonies ont été observées, révélant une complexité accrue dans la dynamique de l'eucaryome. Chez les coraux profonds, qui subissent des effets de MHWs plus modérés, l'eucaryome se caractérise par une plus grande présence de Warnowiaceae et de Corallicolidae. En revanche, les coraux peu profonds, plus exposés au stress thermique, montrent une augmentation notable de l'abondance d'Ephelotidae et d'Exobasidiomycetes. Ces observations illustrent la sensibilité de l'eucaryome au stress environnemental et soulignent l'influence d'autres paramètres que la température sur la composition de l'eucaryome de *C. rubrum*. Dans les colonies ayant perdu leur

tissu, une augmentation significative de la diversité et de la bêta-dispersion ont été observées, suggérant la prolifération de taxa opportunistes. Parmi les groupes microeucaryotes associés à cette perte de tissu, figurent les Labyrinthulomycetes. Ceux-ci sont reconnus comme des pathogènes opportunistes capables d'exploiter la prolifération bactérienne (Burge et al., 2012 ; Raghukumar et Damare, 2011). Ils pourraient donc profiter de cette dynamique microbienne dans les coraux ayant subi une perte de tissus, comme mis en évidence au chapitre précédent.

Les résultats de cette étude montrent la sensibilité de l'eucaryome de *C. rubrum* au stress thermique induit par les vagues de chaleur marines. De plus, ce chapitre souligne l'importance de l'intégration des données sur l'eucaryome dans les programmes de surveillance de la santé des coraux, afin de concevoir des stratégies d'adaptation et de gestion face aux changements climatiques (Browne et al., 2022 ; Bianchi et al., 2019).

Résumé du chapitre 6 : Évaluation de la résilience à court terme de l'holobionte *Corallium rubrum* au stress thermique

Au cours des dernières décennies, l'augmentation de la fréquence et de l'intensité des vagues de chaleur marines (MHWs) a suscité une inquiétude croissante concernant la viabilité à long terme des espèces d'octocoralliaires. Le microbiome, qui est essentiel au maintien de la santé globale et de la résilience de l'hôte, semble jouer un rôle crucial dans la capacité des coraux à faire face et à se remettre du stress thermique (Voolstra et al. 2024). Toutefois, notre compréhension de la résilience du microbiome, c'est-à-dire la capacité des communautés microbiennes à résister aux perturbations et à retrouver un équilibre fonctionnel et compositionnel après le stress, reste encore très partielle. Bien que de plus en plus d'études démontrent que le stress thermique entraîne des modifications marquées de la composition des microbiomes associés aux coraux, peu se sont concentrées sur la capacité de ces communautés à retrouver leur structure initiale après le stress (Chapron et al. 2021 ; Maher et al. 2020 ; Girija et al. 2024 ; Dunphy et al. 2021 ; Epstein et al. 2019 ; Vompe et al. 2024). Par conséquent, une compréhension

plus approfondie des dynamiques de récupération du microbiome est essentielle pour prédire avec précision la survie et l'adaptabilité des coraux dans le contexte des changements climatiques en cours.

Ce chapitre se concentre sur la dynamique structurelle du microbiome de *C. rubrum* soumis à des scénarios contrôlés de stress thermique. Deux traitements thermiques (19 °C et 23 °C) ont été appliqués à des colonies maintenues à leur température de base de 15 °C. Le microbiome (bactéries et microeucaryotes) a été analysé par métabarcoding et qPCR, et des analyses de co-occurrence ont été réalisées afin d'identifier les interactions potentielles entre les taxa microbiens. Les niveaux d'expression génique de marqueurs clés du stress, notamment la protéine de choc thermique 70 (HSP70) et le récepteur du ligand d'induction de l'apoptose lié au facteur de nécrose tumorale (TNFR1), ont également été suivis pour évaluer les réponses physiologiques de l'hôte.

Le corail a montré une sensibilité aux deux traitements thermiques, avec une surexpression notable des gènes HSP70 et TNFR1, particulièrement marquée sous le traitement à 23 °C. Bien que le stress ait été de courte durée (8 jours), cette surexpression met en évidence une perturbation physiologique de l'hôte, suggérant une réponse au stress. Après une semaine de récupération à 15 °C, les niveaux d'expression des gènes sont revenus à la normale, suggérant une capacité rapide de résilience de l'hôte. La composante eucaryote du microbiome a également réagi de manière marquante au stress thermique. Les Labyrinthulomycetes, les Ostreobiaceae et les Philasterida constituaient les microeucaryotes dominants dans les conditions contrôlées. À la suite du stress thermique, des changements structuraux ont été observés : des changements transitoires de taxa principaux au sein des Labyrinthulomycetes ont été observés, tandis que les Ostreobiaceae ont disparu complètement après le traitement et ne se sont pas rétablis au cours de la période de récupération. L'absence de ces taxa majoritaires pourrait avoir un impact sur la dynamique fonctionnelle de l'holobionte. D'autres microeucaryotes ont émergé lors du stress thermique, tels que les Holostichidae et les Endomyxa, et ont persisté après la récupération. Ces taxa pourraient représenter des organismes opportunistes ou bien adaptés à l'environnement stressant, capables de faciliter, ou inversement d'entraver, la résilience du corail en fonction de leur rôle précis

au sein de l'holobionte. L'importance écologique de ces modifications reste cependant à clarifier.

Le microbiome bactérien a montré une réponse plus progressive au stress thermique. Bien que le traitement à 23 °C ait induit des modifications immédiates de la composition de la communauté, le traitement à 19 °C a entraîné des changements plus tardifs, après 8 jours de stress. Les symbiotes bactériens dominants, notamment les Spirochaetaceae (jusqu'à 70 % de la communauté bactérienne sous conditions contrôlées), ont maintenu une abondance relativement stable sous les deux traitements thermiques, suggérant une haute tolérance à la chaleur. Cependant, l'abondance de certains taxa, notamment les Vibrionaceae et les Rhodobacteraceae, a augmenté en réponse au stress thermique. Certains membres de la famille des Rhodobacteraceae peuvent jouer un rôle protecteur dans les infections pathogènes causées par des *Vibrio* (Rosado et al. 2019 ; Kitamura et al. 2021 ; Xu et al. 2024), bien que leur rôle exact dans le corail rouge reste à déterminer. Les Vibrionaceae, famille bien connue pour son potentiel pathogène (Martin et al. 2002 ; Sun et al. 2023 ; Gibbin et al. 2018 ; Vezzulli et al. 2010 ; Vidal-Dupiol et al. 2011), se sont fortement multipliés sous les deux traitements thermiques et ont persisté même après la phase de récupération. Cette persistance soulève des préoccupations quant à leur rôle possible dans la réduction de la résilience corallienne, particulièrement dans le contexte des événements répétés de stress thermique associés aux MHWs.

Bien que le microbiome du corail rouge ait démontré une certaine plasticité et capacité de récupération face au stress thermique à court terme, des modifications persistantes dans la composition des communautés constituent une menace pour sa résilience à long terme. La persistance d'espèces microbiennes émergentes sous stress, telles que les Vibrionaceae et les Holostichidae, souligne la nécessité d'approfondir la connaissance de leurs rôles fonctionnels et de leur impact potentiel sur la santé du corail. De plus, les différences dans les réponses entre les composantes eucaryotes et bactériennes du microbiome mettent en évidence la complexité de l'holobionte et l'importance d'adopter une approche intégrative, couvrant plusieurs règnes microbiens, dans les recherches futures.

Discussion

I. Discussion générale

A. Axe I : Diversité du microbiome des octocoralliaires méditerranéens

Avant ces travaux, le microbiome bactérien des octocoralliaires méditerranéens avait déjà été caractérisé, les membres du genre *Endozoicomonas* ayant été identifiés comme les symbiotes prédominants chez de nombreuses espèces (van de Water et al. 2016 ; 2017 ; 2018 ; Bayer et al. 2013 ; La Rivière et al. 2015 ; Ransome et al. 2014). Cette dominance est confirmée par les différentes études présentées dans cette thèse. Ce genre a été observé non seulement chez diverses espèces hôtes, mais aussi le long de différents gradients environnementaux, y compris dans les zones de surface et mésophotiques, ce qui souligne sa polyvalence écologique et son importance potentielle pour la physiologie de l'hôte corallien. Plusieurs hypothèses ont été avancées quant aux fonctions de ces bactéries, notamment leur contribution à la santé de l'hôte par l'apport de nutriments, la synthèse de vitamines, ou la dégradation de la chitine et leur participation au métabolisme du soufre (Tandon et al. 2022 ; Alex et Antunes 2019 ; Speck et Donachie 2012 ; Bourne et al. 2016 ; Morrow et al. 2012 ; Da Silva et al. 2023). Cependant, la nature exacte de l'interaction entre *Endozoicomonas* et son hôte reste controversée, des études récentes remettant en question l'hypothèse d'une relation purement mutualiste (Pogoreutz et Ziegler 2024). Contrairement aux microbiomes dominés par *Endozoicomonas* de la plupart des octocoralliaires méditerranéens, le corail rouge *Corallium rubrum*, qui est également le seul à sécréter un squelette dur, présente une composition microbienne distincte caractérisée par une dominance marquée et constante des Spirochaetaceae, qui peuvent constituer jusqu'à 70 % de la communauté bactérienne (van de Water et al. 2016b). Bien que le rôle précis des Spirochaetaceae ne soit pas encore entièrement compris, il a été suggéré qu'ils pourraient contribuer au métabolisme de l'hôte par des fonctions telles que la fixation de l'azote (Lilburn et al. 2001) et le cycle du carbone (Leadbetter et al. 1999).

La présence systématique et la dominance constante d'*Endozoicomonas* et de Spirochaetaceae dans le microbiome des octocoralliaires méditerranéens suggère que

ces taxons sont des composants essentiels de l'holobionte et qu'il existe une relation évolutive entre les hôtes et leurs symbiotes. Néanmoins, les origines évolutives et les mécanismes sous-jacents aux symbioses corail-microbe restent mal compris. Si des preuves d'associations évolutives entre les hôtes et leurs partenaires microbiens apparaissent chez les coraux scléractiniaires, comme en témoignent des processus tels que la transmission verticale et la co-diversification (Pollock et al. 2018 ; O'Brien et al. 2021), ces relations ont à peine été explorées chez les octocoralliaires. L'étude présentée au **chapitre 1** visait à examiner la structure des communautés microbiennes associées à plusieurs espèces d'octocoralliaires méditerranéens et tropicaux échantillonnés à des profondeurs mésophotiques, et à explorer ces modèles potentiels d'histoire évolutive commune entre les coraux hôtes et leur microbiome associé. Cette étude a montré que la composition de la communauté bactérienne est spécifique à chaque espèce et reste stable à différentes profondeurs et à différents endroits au sein d'une même espèce, ce qui suggère que la phylogénie de l'hôte, ou des traits fonctionnels spécifiques, pourraient exercer une influence plus importante que les facteurs environnementaux dans la structure de la communauté microbienne. La détection de motifs de phylosymbiose et de signaux co-phylogénétiques entre certaines lignées bactériennes et leurs hôtes octocoralliaires respectifs (par exemple entre *C. rubrum* et Spirochaetaceae et entre *P. clavata*, *Eunicella* spp. et *Endozoicomonas*) renforce encore l'hypothèse d'interactions évolutives à long terme. Ces signaux sont révélateurs de processus tels que la co-spéciation, la transmission verticale de symbiotes microbiens ou les pressions de sélection spécifiques à l'hôte. Pour *C. rubrum*, cependant, Tignat-Perrier et al. (2025) n'ont pas observé de transmission verticale de Spirochaetaceae entre les colonies mères et les descendants, ce qui suggère une acquisition environnementale de ces symbiotes. Collectivement, ces résultats contribuent à une meilleure compréhension des associations entre les microbes et les octocoralliaires. Ce chapitre fournit ainsi un cadre fondamental pour les recherches futures sur les dimensions évolutives et écologiques des relations symbiotiques au sein des holobiontes octocoralliaires, offrant un aperçu des facteurs potentiels de l'organisation des communautés microbiennes et de la spécificité de l'hôte.

Alors que les partenaires bactériens des coraux sont de mieux en mieux caractérisés, les autres membres du microbiome, tels que les microeucaryotes, comprenant les microalgues, les protistes et les champignons, restent largement inexplorés, en partie en raison des défis techniques que posent les approches de métabarcoding. La prédominance des séquences hôtes dans le séquençage basé sur le gène *18S ARNr* masque la plupart des signaux microeucaryotes, et les études approfondies utilisant cette méthode sont encore limitées, en particulier dans les écosystèmes coralliens (Clerissi et al. 2018 ; Bonacolta et al. 2023 ; Del Campo et al. 2019). Dans le cadre de cette thèse, des amorces ciblant le gène de l'ARNr 18S spécifiques à *C. rubrum* ont été conçues sur la base des amorces UNonMet-PCR (Bower et al. 2004 ; Del Campo et al. 2019), afin de réduire efficacement l'amplification de l'hôte tout en préservant une large couverture taxonomique de la diversité microeucaryote. Ces amorces ont ensuite été utilisées dans plusieurs chapitres de cette thèse afin d'étudier la diversité des communautés microeucaryotes associées à *C. rubrum* (**chapitres 2, 5 et 6**). Cette approche nous a permis de découvrir plusieurs groupes de microeucaryotes, notamment Dino Group I, Warnowiaceae, Licnophoridae, Corallicolidae et Labyrinthulomycetes, qui apparaissaient de manière répétée dans l'eucaryome du corail rouge. Leur détection constante dans trois études indépendantes, dans des environnements différents et dans des conditions physiologiques de l'hôte variables (**chapitres 2, 5 et 6**) suggère que ces taxons ne sont pas des membres transitoires, mais des symbiotes potentiellement stables et fonctionnellement importants. Alors que la recherche sur les microbiomes coralliens s'est traditionnellement concentrée sur les partenaires bactériens, ces résultats élargissent le champ des études sur les holobiontes pour inclure les symbiotes eucaryotes peu étudiés, offrant ainsi de nouvelles perspectives sur la complexité des communautés microbiennes associées aux coraux (Bonacolta et al. 2023 ; del Campo et al. 2020 ; Ainsworth et al. 2017).

Dans les colonies naturelles et saines de *C. rubrum*, les Dino Group I et les Licnophoridae représentaient ensemble près de la moitié de la communauté microeucaryote (**chapitres 2 et 5**). Ces taxons, ainsi que les Warnowiaceae et les Labyrinthulomycetes, étaient également abondants dans les colonies qui avaient subi un stress thermique mais qui ne présentaient aucune perte de tissu (**chapitre 5**). La

présence répétée de ces microeucaryotes dans les tissus coralliens sains suggère une importance écologique potentielle de ces symbiotes. Les Dino Group I, par exemple, appartiennent aux Syndiniales, un groupe très répandu dans les environnements marins et souvent caractérisé comme parasite (Guillou et al. 2008). Certains membres ont également été associés à des maladies coralliennes et à la production de toxines (Hold et al. 2001 ; Green et al. 2004 ; Sala et al. 2005), soulevant d'importantes questions sur leurs rôles fonctionnels et leurs interactions dépendantes du contexte au sein de l'holobionte. Comme les Dino Group I, les ciliés Licnophoridae ont été détectés dans des espèces de coraux tempérés et tropicaux (Bonacolta et al. 2024 ; Clerissi et al. 2018). Ils peuvent influencer la composition du microbiome par leur activité prédatrice sur d'autres protistes (Sweet et Séré 2016), ce qui pourrait expliquer leur abondance différente en fonction des conditions environnementales. Les Labyrinthulomycetes, un autre groupe dominant observé dans les colonies naturelles de *C. rubrum*, sont des straménopiles saprotrophes connus pour contribuer au cycle des nutriments par osmose et phagocytose (Raghukumar et Damare 2011 ; Bongiorni et al. 2005). Leur omniprésence dans divers hôtes marins, des coraux aux herbiers en passant par les mollusques, suggère une grande adaptabilité écologique (C. Raghukumar et Raghukumar 1991 ; Siboni et al. 2010 ; Pan et al. 2017). Certaines espèces synthétisent également des niveaux élevés d'acides gras polyinsaturés oméga-3, ce qui en fait des symbiotes nutritionnels potentiels (Carmona et al. 2003 ; Chang et al. 2012). Cependant, leur abondance accrue dans les colonies présentant une perte de tissu remet en question leur rôle au sein de l'holobionte du corail rouge, car certaines espèces sont connues pour leurs tendances parasitaires chez divers organismes marins (Pan et al. 2017 ; S. Raghukumar et Damare 2011 ; Damare et Raghukumar 2010).

Les similitudes entre l'eucaryome de *C. rubrum* et celui d'autres espèces de coraux (par exemple, les Dino Group I, les Licnophoridae et les Labyrinthulomycetes), plus ou moins éloignés géographiquement et phylogénétiquement, notamment l'hexacoralliaire tropical *Pocillopora damicornis* et l'octocoralliaire tempéré *P. clavata*, suggèrent que ces microeucaryotes pourraient jouer un rôle fondamental dans l'holobionte corallien (Bonacolta et al. 2024 ; Clerissi et al. 2018). En ce sens, ils pourraient représenter des analogues eucaryotes de symbiotes bactériens tels que

Endozoicomonas ou Spirochaetaceae, qui ont une relation co-phylogénétique avec leurs hôtes. Cependant, malgré la présence de ces taxons principaux, la composition de l'eucaryome chez *C. rubrum* semble être très sensible aux conditions environnementales. Des différences dans les taxons eucaryotes dominants ont été observées non seulement entre les sites d'échantillonnage (**chapitre 2**), mais aussi entre les coraux collectés *in-situ* (**chapitres 2 et 5**) et ceux maintenus en laboratoire (**chapitre 6**). Par exemple, les échantillons prélevés *in-situ* étaient généralement dominés soit par les Dino Group I, soit par les Licnophoridae ou les Corallicolidae, tandis que les coraux conservés en laboratoire présentaient une prévalence de Philasterida et d'Ostreobiaceae. Si certains taxons tels que les Labyrinthulomycetes sont présents dans les deux conditions, leur abondance relative peut varier et ils sont représentés par différents ASV. Ces changements soulignent la plasticité de l'eucaryome et suggèrent qu'il pourrait être plus sensible aux changements physico-chimiques que le microbiome bactérien. Cela soulève des questions sur les mécanismes d'acquisition des symbiotes, que ce soit par transmission horizontale ou par acquisition environnementale, et sur leur capacité à aider les holobiontes coralliens à faire face à différentes conditions environnementales. Bien que ces microeucaryotes dominants spécifiques à certains sites ne soient pas indispensables au fonctionnement fondamental des coraux, ils peuvent conférer des avantages écologiques locaux, tels que l'assimilation des ressources ou la résistance au stress.

Bien que l'approche basée sur le métabarcoding se soit révélée efficace pour explorer les communautés microeucaryotes, elle a également révélé ses limites pour la détection des champignons dans *C. rubrum*, car la fraction fongique était systématiquement sous-représentée. Cette sous-représentation est probablement due à plusieurs facteurs, notamment la faible biomasse fongique et la couverture limitée de la base de données de référence. Nous avons alors choisi d'utiliser des méthodes de culture, qui se sont avérées efficaces pour détecter une communauté fongique diversifiée, y compris des taxons fongiques présentant un intérêt écologique et biotechnologique présumé. **Le chapitre 3** de cette thèse visait donc à étudier le mycobiome cultivable associé à *C. rubrum*. Le mycobiome du corail rouge s'est avéré être une communauté fongique riche dominée par les Ascomycota, en particulier les genres

Penicillium, *Cladosporium* et *Aspergillus*, avec de nombreux isolats connus pour produire des métabolites secondaires bioactifs dans d'autres organismes (voir chapitre 3). Il est à noter que 61 % des espèces isolées ont été détectées pour la première fois en association avec des coraux, révélant un réservoir considérable de diversité fongique jusqu'alors non décrite dans les écosystèmes coralliens. De plus, des champignons distincts ont été observés dans les tissus et le squelette du corail rouge. Ces observations suggèrent que la communauté fongique associée pourrait être façonnée par le microenvironnement de l'hôte (Roik et al. 2022 ; Amend et al. 2012).

Il est important de noter que l'étude présentée au chapitre 3 a également révélé l'existence de taxons fongiques présentant des caractéristiques pathogènes potentielles, tels que *Aspergillus sydowii*, une espèce connue pour provoquer des maladies chez les coraux tropicaux soumis à un stress thermique (par exemple, 25 °C ; Roik et al. 2022). À mesure que les vagues de chaleur marines dans la mer Méditerranée deviennent plus fréquentes et plus sévères, ces champignons opportunistes peuvent constituer une menace croissante pour les populations de coraux rouges. Il est intéressant de comprendre si ces taxons existent en tant que pathogènes latents, mutualistes ou commensaux afin de prédire les réponses des holobiontes au changement climatique et d'élaborer des stratégies d'atténuation. Dans l'ensemble, la découverte de champignons généralistes, qui peuvent être présents dans plusieurs espèces ou habitats de coraux, et de taxons spécialisés spécifiquement associés à *C. rubrum*, suggère un mycobiome structuré sur le plan écologique et pertinent sur le plan évolutif. Ces résultats appellent à un effort renouvelé pour étudier le mycobiome des coraux à l'aide d'approches méthodologiques intégrées et pour explorer les rôles potentiels des champignons dans la santé des coraux, la dynamique des nutriments et la résistance aux facteurs de stress environnementaux.

En conclusion, ces travaux soulignent l'importance de prendre en compte l'ensemble de la communauté des partenaires microbiens pour comprendre la physiologie des coraux. Ils soulignent également l'intérêt d'intégrer différentes approches pour explorer la diversité des microbes associés aux coraux.

B. Axe II : Réponse du microbiome de *C. rubrum* (et *P. clavata*) au stress thermique

Les MHWs sont devenues plus fréquentes et plus intenses au cours des dernières décennies (Darmaraki et al. 2019 ; Oliver et al. 2018). L'intensification de ce phénomène a été attribuée à l'accélération du changement climatique mondial. Comme indiqué dans l'introduction, la mer Méditerranée, en particulier, s'est avérée être l'une des régions de la Terre qui se réchauffe le plus rapidement. Des études ont montré que la température de surface en Méditerranée augmente environ 20 % plus vite que la moyenne mondiale, et la région a également connu une augmentation marquée de la fréquence des événements de MHW au cours des deux dernières décennies (MedECC 2020 ; Cos et al. 2022a ; Pastor et al. 2020 ; Darmaraki 2019 ; Juza et al. 2022 ; Omneya et al. 2021). Cette tendance a alarmé les biologistes marins, car les MHWs sont associés à des événements de mortalité massive dans les écosystèmes benthiques.

Il est donc essentiel de comprendre comment les octocoralliaires méditerranéens réagissent à ces conditions thermiques extrêmes. Les octocoralliaires, notamment les espèces *E. cavolini*, *E. singularis*, *P. clavata* et *C. rubrum*, sont des éléments-clés des forêts animales marines (MAFs), qui comptent parmi les habitats les plus riches sur le plan écologique en mer Méditerranée (Paoli et al. 2017 ; Orejas et al. 2022 ; Rossi et al. 2017). Cependant, ces organismes sont également particulièrement vulnérables aux perturbations environnementales. Les MHWs ont déjà été associées à des événements de mortalité à grande échelle, avec des rapports faisant état d'épidémies microbiennes et de pertes de colonies atteignant jusqu'à 90 % dans certaines populations (Cerrano et al. 2000 ; Huete-Stauffer et al. 2011 ; Piazzi et al. 2021 ; Verdura et al. 2019 ; Garrabou et al. 2009 ; 2022). Ces événements sont probablement le résultat d'une interaction complexe entre le stress physiologique de l'hôte dû à des températures élevées et la dysbiose microbienne (Bourne et al. 2016 ; Mouchka et al. 2010 ; Vezzulli et al. 2010).

Dans le cadre de cette thèse, nous avons analysé des échantillons d'octocoralliaires prélevés lors des épisodes sans précédent de MHWs en Méditerranée en 2022, ce qui a été rendu possible grâce à l'organisation *Septentrion Environnement* (**chapitres 4 et 5**). En 2022, entre mai et septembre, la Méditerranée a connu entre trois

et sept épisodes de MHWs record, avec des anomalies de température atteignant jusqu'à +4,3 °C dans certaines zones, dépassant de loin les records précédents de +2 à +3 °C enregistrés lors des MHWs de 2003 (T-MEDNet 2023 ; Quade 2022 ; Guinaldo et al. 2023). Dans le nord-ouest de la Méditerranée, par exemple, les MHWs se sont caractérisés soit par de courtes périodes de chaleur extrême, avec des pics à 27 °C dans les eaux peu profondes, soit par des périodes prolongées de températures stables et élevées autour de 23-24 °C (Crisci et al. 2011 ; Estaque et al. 2023). Sur l'un des sites d'échantillonnage, *Riou Sud* (Marseille), les températures à 15 m et 30 m de profondeur ont atteint respectivement 27 °C et 26 °C pendant l'été. Avant 2022, des températures supérieures à 24 °C à 30 m de profondeur n'avaient jamais été enregistrées, et à 15 m de profondeur, ces phénomènes étaient limités à quatre jours par an au maximum (en 2009 et 2012). Cependant, en 2022, à *Riou Sud*, le nombre de jours avec des températures supérieures à 24 °C a atteint dix jours à 15 m de profondeur et trois jours à 30 m, indiquant un réchauffement de la colonne d'eau qui s'est étendu plus profondément que ce qui avait été observé précédemment. Des études en laboratoire ont suggéré que 23-24 °C est un seuil thermique critique pour de nombreuses espèces d'octocoralliaires méditerranéens. Au-delà de ce seuil, on observe couramment une perte de tissus et une mortalité (Previati et al. 2010 ; Haguenauer et al. 2013 ; Tignat-Perrier et al. 2022 ; 2023 ; Torrents et al. 2008 ; Cau et al. 2018). Lors des événements de MHWs de 2022, *Septentrion Environnement* a mené une étude dans le parc national des Calanques afin d'évaluer la mortalité des colonies de *C. rubrum* et *P. clavata* sur différents sites. Dans l'ensemble, les populations de *C. rubrum* ont été moins touchées que celles de *P. clavata*, avec respectivement 45 % et 81 % de colonies affectées. Le niveau de mortalité des colonies variait d'un site à l'autre, ce qui suggère le rôle des conditions environnementales locales dans la réponse au stress. De plus, ils ont observé différents niveaux de dommages selon les individus, certaines colonies présentant une perte de tissu de 0 % tandis que d'autres étaient presque entièrement dégradées (90 % de perte de tissu) au sein des populations.

Plusieurs facteurs ont été suggérés comme influençant la réponse des coraux à des températures anormalement élevées, tels que les courants et la perception de la température de l'eau (Brown et al. 2023), la disponibilité en nutriments (Ezzat et al. 2019), le génotype (Palacio-Castro et al. 2022 ; Kavousi et al. 2020) et le microbiome. En effet,

des études antérieures sur les octocoralliaires méditerranéens ont démontré que les MHWs peuvent déclencher une dysbiose microbienne. La dysbiose microbienne se caractérise généralement par une réduction de l'abondance relative des principaux symbiotes, tels que les *Endozoicomonas* et les Spirochaetaceae, parallèlement à une augmentation de l'abondance relative des taxons opportunistes (Tignat-Perrier et al. 2022 ; 2023 ; Rubio-Portillo et al. 2021 ; Corinaldesi et al. 2022 ; Vezzulli et al. 2010a ; Bally et Garrabou 2007). Dans l'ensemble, plusieurs lacunes subsistent et limitent considérablement notre compréhension de la réponse de l'holobionte corallien au stress thermique. Par exemple, la relation de cause à effet entre la réponse du microbiome (dysbiose) et la réponse du corail (telle que la perte de tissu) aux MHWs n'a pas été clairement établie. De plus, les communautés microeucaryotes associées aux coraux ont été largement inexplorées, tant en termes de diversité que de réactivité au changement, ce qui rend difficile d'avoir une vue d'ensemble de ce qui se passe au sein de l'holobionte corallien pendant le stress thermique. Enfin, nous n'avions aucune idée de la capacité de récupération du microbiome corallien après des événements stressants. Et surtout, nos connaissances sur la réponse des communautés bactériennes reposent principalement sur des techniques de métabarcoding et d'abondances relatives, qui présentent des biais notables, car les variations d'abondance relative peuvent ne pas correspondre aux changements d'abondance absolue. En conséquence, certaines dynamiques écologiques peuvent être mal interprétées et la complexité fonctionnelle du microbiome peut être sous-estimée. Dans le cadre de cette thèse, nous avons utilisé différentes techniques pour obtenir les abondances relatives et absolues des taxons microbiens, en combinant des observations *in-situ* (**chapitres 4 et 5**) et des expériences contrôlées en laboratoire (**chapitre 6**) afin d'étudier aussi efficacement que possible la réponse de l'holobionte (hôte, bactéries et microeucaryotes) de *C. rubrum* et *P. clavata* au stress thermique.

L'étude sur l'impact des MHWs de 2022 sur les communautés bactériennes de *C. rubrum* et *P. clavata* (**chapitre 4**), à l'aide d'analyses qPCR spécifiques à chaque taxon, a révélé que l'abondance absolue de leurs symbiotes bactériens dominants (Spirochaetaceae chez *C. rubrum* et *Endozoicomonas* chez *P. clavata*) n'avait pas changé de manière significative sous l'effet du stress thermique, même dans les colonies qui

avaient perdu leurs tissus. Cette découverte suggère que, contrairement aux hypothèses précédentes, le stress thermique et la perte de tissu qui en a résulté n'étaient pas associés à une réduction de ces symbiotes majoritaires (Tignat-Perrier et al. 2022 ; Voolstra et al. 2021 ; Woo 2021 ; Palacio-Castro et al. 2022). Les Spirochaetaceae et les *Endozoicomonas* semblent être très thermotolérants (ces dernières avec quelques exceptions, car une légère diminution de l'abondance absolue a été observée dans certaines colonies de *P. clavata* de Portofino, en Italie, probablement due à une combinaison de facteurs de stress ; voir le chapitre 4 pour plus de détails). Cette thermotolérance, en particulier pour les Spirochaetaceae dans *C. rubrum*, a été confirmée par une étude de stress thermique en laboratoire (chapitre 5), où leur abondance relative et absolue est restée stable sous stress.

La diminution observée de l'abondance relative des principaux symbiotes est la conséquence d'une augmentation significative de l'abondance totale d'autres taxons bactériens, y compris des pathogènes putatifs tels que *Vibrio*, comme l'ont montré nos études (**chapitres 4 et 6**). Une augmentation des ASV Vibrionaceae est une réponse bien documentée chez les coraux soumis à un stress thermique (Martin et al. 2002 ; Tignat-Perrier et al. 2023 ; Tout et al. 2015), et plusieurs espèces de *Vibrio* sont reconnues comme des pathogènes des coraux, telle que l'espèce méditerranéenne *Vibrio coralliilyticus* (Martin et al. 2002 ; Sun et al. 2023 ; Gibbin et al. 2018 ; Vezzulli et al. 2010 ; Vidal-Dupiol et al. 2011). Le chapitre 6, qui a également examiné la récupération de *C. rubrum* et de son microbiome après une vague de chaleur, a révélé que des pathogènes opportunistes persistaient dans l'holobionte après un stress thermique. Il est à noter que certains taxons bactériens, en particulier les espèces Vibrionaceae, étaient encore présents après la récupération, même lorsque les colonies ne présentaient aucune perte de tissu. Cette présence persistante de micro-organismes pathogènes potentiels peut nuire à la résilience des coraux, en particulier face à la fréquence croissante des MHWs en Méditerranée (voir Introduction, partie III). Chez certaines espèces marines de *Vibrio*, la virulence pathogène est déclenchée lorsque la température de l'eau de mer dépasse 23 °C (Billaud et al. 2022 ; Kimes et al. 2012) et/ou lorsque les seuils de *quorum sensing* sont atteints (Sun et al. 2023). Ces conditions sont couramment réunies pendant les MHWs et peuvent expliquer en partie la mortalité des coraux après de tels événements.

Bien que les facteurs de virulence puissent devenir inactifs une fois que les températures reviennent à la normale, ils peuvent être rapidement réactivés lors de vagues de chaleur ultérieures, ce qui peut accélérer la dysbiose microbienne et augmenter le risque de mortalité des coraux. La persistance de ces bactéries opportunistes peut accélérer les changements microbiens lors de stress thermiques répétés et favoriser la perte de tissus, la nécrose et, finalement, la mort de la colonie. Ce mécanisme pourrait expliquer pourquoi certaines colonies peuvent résister plus longtemps que d'autres au stress thermique : leur résilience pourrait être influencée par l'ampleur de la dysbiose et l'abondance de ces pathogènes « prêts à réagir » dans leur microbiome.

Outre les Vibrionaceae, les Rhodobacteraceae se sont également multipliées dans les colonies présentant une perte de tissu, comme observé dans les **chapitres 4 et 6**. Ce phénomène a déjà été observé chez les coraux tropicaux et les coraux rouges exposés à un stress thermique (Pootakham et al. 2019 ; Tignat-Perrier et al. 2023 ; Rosales et al. 2020 ; 2023 ; Clark et al. 2021). Les Rhodobacteraceae sont connus pour proliférer lors de stress thermiques et d'épidémies (Clark et al. 2021 ; Rosales et al. 2020 ; 2023). Des travaux récents suggèrent que certaines Rhodobacteraceae pourraient jouer un rôle protecteur en cas de stress, par exemple en atténuant les infections à *Vibrio coralliilyticus* (Rosado et al. 2019 ; Kitamura et al. 2021 ; Xu et al. 2024). Leur rôle dans les coraux rouges soumis à un stress thermique reste à clarifier. Dans l'ensemble, ces résultats indiquent que la perte de tissus chez les octocoralliaires pendant les MHWs n'est pas due à la perte de symbiotes dominants et bénéfiques tels que les Spirochaetaceae ou les *Endozoicomonas*. Elle pourrait plutôt être due à la prolifération de bactéries opportunistes ou pathogènes.

En ce qui concerne la composante microeucaryote de l'holobionte corallien, peu de choses étaient connues avant les recherches présentées dans cette thèse. Alors que les travaux décrits dans les **chapitres 2 et 3** ont mis en lumière la richesse et la composition de ces communautés microeucaryotes, **les chapitres 5 et 6** ont contribué à une compréhension plus complète de la réponse de l'holobionte au stress thermique en intégrant ces partenaires microbiens jusqu'alors peu étudiés. Des différences liées à la profondeur ont été observées dans la composition microeucaryote (**chapitre 5**) : les colonies modérément stressées (plus profondes) étaient dominées par les

Warnowiaceae et les Corallicolidae, tandis que les colonies plus sévèrement stressées (moins profondes) abritaient une plus grande abondance d'Ephelotidae et de champignons tels que les Exobasidiomycetes. Ces différences entre les profondeurs pourraient être dues à des différences d'intensité du stress thermique ou à des facteurs trophiques, comme le suggèrent Maire et al. (2022). Comme démontré au **chapitre 2**, l'eucaryome de *C. rubrum* semble fortement influencé par l'environnement physico-chimique, et ce de manière plus significative que le microbiome bactérien.

L'expérience en laboratoire sur le stress thermique, dans laquelle nous avons évalué la réponse de l'hôte, des communautés bactériennes et microeucaryotes (**chapitre 6**), a montré que les microeucaryotes réagissaient plus rapidement au stress thermique que leurs homologues bactériens. Alors que les changements dans la composition du microbiome bactérien n'ont été observés qu'à 23 °C ou après une exposition prolongée (8 jours) à 19 °C, les changements structurels dans l'eucaryome se sont produits immédiatement après l'augmentation de la température de 15 °C à 19 °C ou 23 °C. Cette réponse rapide suggère que les microeucaryotes pourraient servir d'indicateurs précoces des perturbations environnementales. Dans le **chapitre 5**, la composition de l'eucaryome différait considérablement entre les colonies témoins et celles soumises à un stress thermique. Plus précisément, une diminution de l'abondance relative des dinoflagellés Dino Group I et des ciliés Licnophoridae a été observée dans les colonies prélevées sur les sites touchés par les MHWs. Les dinoflagellés, connus pour être très sensibles aux fluctuations de température, pourraient jouer un rôle crucial dans la santé des coraux. En effet, chez les coraux scléractiniaires, la perte des dinoflagellés Symbiodiniaceae marque souvent le début du blanchissement et la mortalité qui s'ensuit (Douglas 2003 ; Jiang et al. 2021). Les ciliés Licnophoridae, également sensibles aux changements thermiques, peuvent décliner en raison des impacts métaboliques liés à la chaleur ou d'effets indirects tels que les changements dans la disponibilité des proies (Martinez 1980 ; Karajan et al. 2019). Cependant, il reste important de déterminer si ces diminutions relatives reflètent une véritable perte de symbiotes ou s'il s'agit d'un artefact causé par l'augmentation relative d'autres microeucaryotes. Si les bactéries restent des indicateurs fiables de l'état de santé des coraux dans divers holobiontes marins (Wegner et al. 2025 ; Pootakham et al. 2019 ; Montaño-Salazar et al. 2023 ; Glasl et al. 2019), nous

montrons ici que les microeucaryotes pourraient tout aussi bien servir d'indicateurs précoces des perturbations coralliennes. Afin d'élucider leur pertinence en tant que biomarqueurs et leurs rôles fonctionnels globaux, des recherches supplémentaires sur les populations de coraux méditerranéens sont indispensables.

Dans l'ensemble, ces études soulignent l'importance cruciale d'étudier tous les composants du microbiome afin de comprendre la réponse des octocoralliaires méditerranéens au stress et d'évaluer leur résilience au changement climatique. Ce travail de thèse souligne la nécessité de poursuivre les recherches sur la symbiose entre les octocoralliaires et leur microbiome, ainsi que ses implications pour la santé de l'écosystème corallien.

II. Perspectives de recherche en écologie microbienne des octocoralliaires

Bien que cette thèse ait porté principalement sur les bactéries et microeucaryotes associés, d'autres groupes tels que les virus et les archées pourraient également jouer un rôle crucial dans la santé et la réponse au stress des coraux. Ces communautés restent mal comprises, mais pourraient expliquer certaines hétérogénéités dans la mortalité et la résilience des coraux face au stress thermique. Les études futures devraient les intégrer pour proposer une vue plus complète de l'holobionte. Les champignons constituent également un groupe encore peu étudié, surtout en termes de rôle écologique. Il est essentiel de mieux comprendre leurs interactions potentiellement symbiotiques, pathogènes ou opportunistes. Cela pourrait inclure l'analyse de caractéristiques biotechnologiques (comme la production de métabolites secondaires), les profils pathogéniques, et des expériences ciblées sous stress thermique.

Un autre sujet déterminant est l'investigation expérimentale du rôle de *Vibrio* spp. comme pathogènes dans la mortalité de *C. rubrum* sous stress thermique. Bien que des données observationnelles et des analyses de séquençage indiquent un lien fort entre l'abondance des Vibrionaceae et les colonies impactées, la causalité reste à établir. Cela pourrait être réalisé par des expériences de contamination contrôlées. Par ailleurs, une analyse des mécanismes régulant la virulence de *Vibrio*, notamment en lien avec les

températures élevées (> 23°C), pourrait aider à comprendre ses dynamiques. Il est également possible que d'autres bactéries, moins connues, contribuent à la dégradation de l'holobionte. Des recherches plus larges sont nécessaires pour évaluer si *Vibrio* est le principal agent pathogène ou s'inscrit dans un consortium complexe. De plus, des approches microbiome-dépendantes, comme l'action antagoniste des Rhodobacteraceae, pourraient offrir des pistes pour renforcer la résilience des coraux.

En termes de méthodologie, la qPCR s'est révélée un outil puissant pour quantifier certains taxa. Les études futures devraient développer des tests ciblant d'autres familles bactériennes et microeucaryotes, tels que les Rhodobacteraceae, Dino Group I, Licnophoridae, et Labyrinthulomycetes. Cela améliorera la compréhension des dynamiques microbiennes pendant les événements thermiques. De plus, le domaine doit progresser au-delà des études de composition vers des approches fonctionnelles, comme la métagénomique, la métatranscriptomique et la métabolomique. Ces méthodes pourraient révéler le potentiel métabolique du microbiome et son interaction avec l'hôte. Leur application avant, pendant et après les événements de stress thermique fournirait une image plus complète des dynamiques microbiennes et des mécanismes moléculaires associés aux réponses des coraux.

III. Conclusion : rôle du microbiome dans la résilience des octocoralliaires méditerranéens dans un contexte de changements environnementaux

À une époque caractérisée par des changements environnementaux rapides et une augmentation de la fréquence et de l'intensité des phénomènes extrêmes tels que les vagues de chaleur marines, il est devenu essentiel de comprendre la résistance et la résilience des espèces fondatrices des forêts animales marines (MAFs). Ces écosystèmes abritent une riche diversité d'espèces qui contribuent de manière significative à la biodiversité régionale et fournissent des services écosystémiques

importants aux sociétés humaines (Bianchi et al. 2000 ; Ballesteros 2006 ; Tonin 2018 ; Buonocore et al. 2020). Cela est particulièrement évident en mer Méditerranée, un haut lieu reconnu de la biodiversité qui subit également les effets les plus prononcés du changement climatique mondial (MedECC 2020 ; Pastor et al. 2020 ; Cos et al. 2022 ; Tuel et al. 2020). Il est donc essentiel de préserver autant que possible la structure et la fonctionnalité de ces écosystèmes afin de maintenir les services vitaux qu'ils fournissent à la vie marine et aux sociétés humaines.

Il est de plus en plus reconnu que la santé et la résilience de ces organismes marins sont étroitement liées au microbiome (Bourne et al. 2009 ; Apprill 2017 ; Thompson et al. 2015). Le concept selon lequel un hôte et sa communauté microbienne forment une unité cohésive, appelée holobionte, a pris un essor considérable ces dernières années (Simon et al. 2019 ; Dittami et al. 2021). Dans ce cadre, les performances physiologiques et la santé globale de l'hôte sont déterminées non seulement par ses propres processus génétiques et cellulaires, mais aussi par la composition et les fonctions de ses partenaires microbiens symbiotiques. Cette nouvelle perspective représente un changement de paradigme et souligne la nécessité de stratégies holistiques pour la conservation et la gestion des écosystèmes marins, des stratégies qui protègent à la fois les espèces hôtes et l'intégrité de leur microbiome.

Cette thèse contribue au débat scientifique en constante évolution sur les interactions entre l'hôte et le microbiome en examinant les relations complexes entre les octocoralliaires méditerranéens et leurs communautés microbiennes associées. En tant qu'espèces fondamentales des MAFs, les octocoralliaires tels que *P. clavata* et *C. rubrum* jouent un rôle écologique crucial. Une compréhension détaillée de leur microbiome est essentielle pour développer et affiner les stratégies de gestion des écosystèmes, en particulier compte tenu des impacts croissants du changement climatique. En caractérisant la composition des communautés microbiennes associées à ces espèces, en conditions saines et lors de stress thermique, cette recherche fournit une base de compréhension du rôle du microbiome dans la survie et la résilience des octocoralliaires. Il est ainsi possible d'identifier les espèces microbiennes qui peuvent servir d'indicateurs précoces du stress et qui peuvent être utilisées comme outils de surveillance de la santé des écosystèmes. Bien que cela dépasse le cadre immédiat de cette thèse, ces résultats

sont prometteurs pour faire progresser les stratégies de conservation basées sur le microbiome. Cela pourrait inclure la prédiction de la sensibilité thermique de l'hôte sur la base des profils microbiologiques et le développement d'interventions microbiennes telles que les probiotiques, un domaine qui suscite un intérêt croissant dans la recherche sur les coraux (Peixoto et al. 2021 ; 2022 ; Rosado et al. 2019 ; Doering et al. 2023).

Appendices



Appendix 1 – Introduction

Table S1 : Litterature review on coral's microbiome that include Spirochaetaceae

Study	Species	Class of coral	Origin	% (mean if several)	min %	max %	Details	16S primers	Sequencing technology
van de Water 2016	Corallium rubrum	Octocoral	Mediterranean		50	72		V1-V2	MiSeq
Lawler 2016	Anthothela grandiflora	Octocoral	USA		10	70		V4-V5	MiSeq
Lawler 2016	Alcyonium grandiflorum	Hexacoral	USA	1				V4-V5	MiSeq
Wessels 2017, Whalen et al. 2023	Lobophytum pauciflorum	Octocoral	Australia	43				V3-V4	MiSeq
Kellogg 2009	Lophelia pertusa	Hexacoral	Mexico	one clone				8F/1492R	DGGE
Ng 2015	Platygyra carnosus	Hexacoral	Hong Kong	2				V3-V5	454
Sekar 2008	Siderasrea siderea	Hexacoral	Caribbean	3 (diseased)				27F/1492R	cloning
Ainsworth 2015	Acropora granulosa	Hexacoral	Australia		17	80		27F/519R	454
Closek 2014	Orbicella faveolata	Hexacoral	Mexico		20	32	healthy/diseased	27F/1492R	Transcriptomics, philochips
Closek 2014	Plumarella superba	Octocoral	Alaska		3	7		Eco8F/1492R	cloning
Porporato 2013	Pennatula phosphorea	Octocoral	Mediterranean	3				8F/907R	ARISA
Porporato 2013	Pteroeides spinosum	Octocoral	Mediterranean	10				8F/907R	ARISA
Cleary 2019	Cladiella species	Octocoral			25	50		V3-V4	MiSeq

Chapron 2020	Lophelia pertusa	Hexacoral	Mediterranean		0	80		V1-V3	TruSeq
Chapron 2020	Madrepora oculata	Hexacoral	Mediterranean		25	75		V1-V3	TruSeq
O'Brien et al. 2021	Echinopora mammiformis	Hexacoral	Great Barrier Reef	10				V4	MiSeq
O'Brien et al. 2021	Pachyseris speciosa	Hexacoral	Great Barrier Reef	20				V4	MiSeq
O'Brien et al. 2021	Porites cylindrica	Hexacoral	Great Barrier Reef	5				V4	MiSeq
O'Brien et al. 2021	Sarcophyton sp.	Octocoral	Great Barrier Reef		45	55		V4	MiSeq
O'Brien et al. 2021	Sinularia sp.	Octocoral	Great Barrier Reef		20	55		V4	MiSeq
O'Brien et al. 2021	Cladellia sp.	Octocoral	Great Barrier Reef	20				V4	MiSeq
O'Brien et al. 2021	Pinnigorgia sp.	Octocoral	Great Barrier Reef	5				V4	MiSeq
O'Brien et al. 2021	Isis hippuris	Octocoral	Great Barrier Reef	5				V4	MiSeq
Williams et al. 2022	Acropora cervicornis	Hexacoral	Florida's Coral Reef		5	80		V4	MiSeq
Cleary et al. 2021	Melithaea maldivensis	Octocoral	Maldivian waters	8				V3-V4	MiSeq
Cleary et al. 2021	Paraminabea sp.	Octocoral	Maldivian waters	20				V3-V4	MiSeq
Heitzman et al. 2023	Porites heronensis	Hexacoral	Shidagaura, Shimoda, Japan	5			Coral with White Mat Syndrome (WMS)	V3-V4	MiSeq
Krishnaswamy et al. 2023	Porites lutea	Hexacoral	Indian Ocean	1,6				V3-V4	MiSeq
Montaño-Salazar et al. 2023	Pacifigorgia cairnsi	Octocoral	Tropical Eastern Pacific		18	48		V4	MiSeq

Dubé et al. 2021	Millepora platyphylla	Hydrozoa	Moorea Island, French Polynesia	10				V5-V6	HiSeq 2500
Boote 2021	Heliofungia actiniformis	Hexacoral		90					MiSeq
Jahajeeah et al. 2023	Sinularia polydactya	Octocoral	Mauritian Soft Corals	45				V3-V4	MiSeq
Greenwood 2020	Dipsastraea pallida	Hexacoral		47				V3-V4	MiSeq
Palacio-Castro et al. 2022	Acropora cervicornis	Hexacoral	Caribbean	1			Present in heat-resistant corals	V4	MiSeq
Haydon et al. 2021	Sarcophyton sp.	Octocoral	Great Barrier Reef	30				V1–V3	MiSeq
Steinum et al. 2024	Alcyonium acaule	Octocoral	Sea of Marmara	20					MiSeq
Steinum et al. 2024	Savalia savaglia	Octocoral	Sea of Marmara	40					MiSeq
Park et al. 2022	Litophyton sp.	Octocoral	Micronesia	20				V1–V3	MiSeq
Park et al. 2022	Sinularia sp.	Octocoral	Micronesia	64				V1–V3	MiSeq
Holm et al. 2016	Muricea californica	Octocoral	Pacific and western Atlantic oceans		6	64		V4–V6	MiSeq
Holm et al. 2016	Savalia lucifica	Hexacoral	Pacific and western Atlantic oceans		21	84		V4–V6	MiSeq
Gray et al. 2011	Plumarella superba	Octocoral	Aleutian islands		3	7			Culture

Frias-Lopez et al. 2002	Montastrea cavernosa	Hexacoral	Caribbean			0.01			MiSeq
Weiler et al. 2018	Paragorgia arborea	Octocoral	Cold-water gulf of Maine		7	36		V6-V8	MiSeq

Appendix 2 – Chapter 1

Tables S2, S3, S7 and S9 are not available due to the large size of the tables as well as supplementary figures (too large for the document) but all supplementary information of this chapter can be found on the web version of the paper following this link : https://animalmicrobiome.biomedcentral.com/articles/10.1186/s42523-024-00351-2#Sec21

Table S1: Summary table of the sites and sample collections for each expedition

Expedition	Sampling site	Collected samples	Number of samples
Gombessa V (July 2019)	- Le massif du Raventurier (-70 m) *43°33'13.6"N 7°08'54.0"E*	- *Corallium rubrum* - *Eunicella cavolini* - *Eunicella verrucosa* - *Paramuricea clavata*	6 5 6 12
	- St Martin (-77 m) *43°44'15.1"N 7°28'17.2"E*	- *Corallium rubrum* - *Eunicella cavolini* - *Eunicella verrucosa* - *Paramuricea clavata*	5 4 4 6
	- Tombant des Américains (-103 m) *43°41'04.5"N 7°18'18.7"E*	- *Eunicella cavolini* - *Eunicella verrucosa* - *Paramuricea. clavata*	5 4 5
Gombessa VI (July 2021)	- Capense (70 m) *43°57'30.5856”N 9°18'57.5928”E*	- *Eunicella cavolini* - *Paramuricea clavata* - Seawater	3 4 4
	- Scalo (-62 m) *43°55'20.1504”N 9°19'57.8712”E*	- *Corallium rubrum* - *Eunicella cavolini* - Seawater	4 5 4
	- Palagaccio (-88 m) *43°43'45.3828”N 9°29'4.362”E*	- *Callogorgia verticillata* - Seawater	1 1

	- Cap Corse 8A (-81 m) *43°7'50.9592”N 9°31'14.952”E*	- *Alcyonium coralloides* - *Corallium rubrum* - *Eunicella cavolini* - *Paramuricea clavata* - Seawater	5 6 3 5 6
	- Nord 1 site 1 (-95 m) *43°17'10.8888”N 9°26'0.3228”E*	- *Eunicella cavolini* - *Paramuricea clavata* - Seawater	5 5 6
	- Anneaux site A (-116 m) *43° 10' 59.4588”N 9° 30' 50.1588”E*	- *Callogorgia verticillata*	6
	- Anneaux DC (-105 m) *43° 14' 43.3788”N 9° 29' 56.1588”E*	- *Callogorgia verticillata* - Seawater	6 3
ENCOR (October 2019)	Eilat (-65 to -120 m) *29°30'03.1"N 34°55'20.4"E*	- *Klyxum utinomii* - *Ovabunda* spp. - *Paralemnalia thyrsoides* - *Sarcophyton glaucum* - *Sclerophytum eilatense* - *Sclerophytum loyai* - *Sclerophytum polydactylum* - *Sclerophytum vrijmoethi* - Seawater	4 15 10 11 8 3 2 11 6

Table S4 : Bacterial diversity data (Chao1 estimated richness) for each species and statistical tests.

Species	variable	n	mean	sd
Sclerophytum_loyai	S.chao1	3	95,786	16,769
Paralemnalia_thyrsoides	S.chao1	9	155,86	60,503
Eunicella_verrucosa	S.chao1	14	157,976	61,089
Sclerophytum_eilatense	S.chao1	7	169,048	64,599
Corallium_rubrum	S.chao1	20	162,292	118,693
Sarcophyton_glaucum	S.chao1	11	148,277	152,694
Alcyonium_coralloides	S.chao1	4	416,025	175,112
Eunicella_cavolini	S.chao1	30	190,257	220,389
Paramuricea_clavata	S.chao1	37	262,183	227,127
Klyxum_utinomii	S.chao1	4	298,25	291,049
Sclerophytum_vrijmoethi	S.chao1	11	223,318	352,096
Callogorgia_verticillata	S.chao1	12	667,58	413,127
Sclerophytum_polydactylum	S.chao1	2	1145,996	428,469
Ovabunda	S.chao1	15	355,427	444,587

Analysis of Variance Table (differences between species)

Response: log(S.chao1)

	Df	Sum Sq	Mean Sq	F value	Pr(>F)
Species	13	35.355	2.71958	5.3145	6.29e-08
Residuals	165	84.436	0.51173		

Tukey's Honestly Significant Difference (HSD) test for from the ANOVA comparison between species

names	Species.diff	Species.lwr	Species.upr	Species.p.adj
Eunicella_cavolini-Callogorgia_verticillata	-1,436724803	-2,263074168	-0,610375439	2,0394E-06
Corallium_rubrum-Callogorgia_verticillata	-1,444560267	-2,327964897	-0,561155637	1,09868E-05
Sarcophyton_glaucum-Callogorgia_verticillata	-1,551362042	-2,561236191	-0,541487893	5,14912E-05
Sclerophytum_vrijmoethi-Callogorgia_verticillata	-1,484180162	-2,494054311	-0,474306013	0,000139587
Eunicella_verrucosa-Callogorgia_verticillata	-1,337524288	-2,289273083	-0,385775492	0,00035419
Paramuricea_clavata-Callogorgia_verticillata	-1,060719345	-1,864424692	-0,257013998	0,001156827
Paralemnalia_thyrsoides-Callogorgia_verticillata	-1,334962433	-2,401774876	-0,26814999	0,002840728
Sclerophytum_polydactylum-Sarcophyton_glaucum	2,234782754	0,375049578	4,09451593	0,005298045
Sclerophytum_polydactylum-Eunicella_cavolini	2,120145515	0,353336255	3,886954775	0,005408659
Sclerophytum_polydactylum-Corallium_rubrum	2,127980979	0,333777694	3,922184264	0,006412008
Sclerophytum_vrijmoethi-Sclerophytum_polydactylum	-2,167600874	-4,02733405	-0,307867698	0,008200612
Sclerophytum_polydactylum-Eunicella_verrucosa	2,020945	0,192123669	3,84976633	0,016498058
Sclerophytum_eilatense-Callogorgia_verticillata	-1,246653958	-2,397262146	-0,09604577	0,020952895
Sclerophytum_polydactylum-Paralemnalia_thyrsoides	2,018383145	0,127126823	3,909639467	0,024993142
Ovabunda-Callogorgia_verticillata	-0,956717282	-1,893709388	-0,019725175	0,040496059
Sclerophytum_polydactylum-Sclerophytum_eilatense	1,93007467	-0,009683276	3,869832616	0,052517068
Sclerophytum_polydactylum-Paramuricea_clavata	1,744140057	-0,012192478	3,500472591	0,053529431
Sclerophytum_polydactylum-Ovabunda	1,640137994	-0,181047306	3,461323293	0,12438653
Sarcophyton_glaucum-Alcyonium_coralloides	-1,198731209	-2,611299958	0,213837541	0,188712174
Eunicella_cavolini-Alcyonium_coralloides	-1,08409397	-2,371866445	0,203678505	0,198618746
Corallium_rubrum-Alcyonium_coralloides	-1,091929434	-2,417036378	0,233177511	0,226347176
Sclerophytum_vrijmoethi-Alcyonium_coralloides	-1,131549329	-2,544118078	0,281019421	0,265792804
Sclerophytum_polydactylum-Klyxum_utinomii	1,63939495	-0,455783095	3,734572994	0,300679446
Eunicella_verrucosa-Alcyonium_coralloides	-0,984893454	-2,356509452	0,386722543	0,439275166
Klyxum_utinomii-Callogorgia_verticillata	-0,955974238	-2,352759601	0,440811125	0,519373355
Paralemnalia_thyrsoides-Alcyonium_coralloides	-0,9823316	-2,436151899	0,4714887	0,540535687
Paramuricea_clavata-Eunicella_cavolini	0,376005459	-0,218377316	0,970388233	0,64472723
Ovabunda-Eunicella_cavolini	0,480007522	-0,28504333	1,245058373	0,656984561
Sarcophyton_glaucum-Ovabunda	-0,59464476	-1,555006843	0,365717322	0,676249698
Sarcophyton_glaucum-Paramuricea_clavata	-0,490642697	-1,321475657	0,340190262	0,740561497
Ovabunda-Corallium_rubrum	0,487842985	-0,33850638	1,31419235	0,740957784
Sclerophytum_eilatense-Alcyonium_coralloides	-0,894023125	-2,410401665	0,622355416	0,742639157
Paramuricea_clavata-Corallium_rubrum	0,383840922	-0,287606283	1,055288128	0,779923985
Paramuricea_clavata-Alcyonium_coralloides	-0,708088511	-1,98144901	0,565271988	0,810180085
Sclerophytum_vrijmoethi-Ovabunda	-0,52746288	-1,487824963	0,432899202	0,822767711
Sclerophytum_vrijmoethi-Paramuricea_clavata	-0,423460817	-1,254293777	0,407372142	0,886291284
Sclerophytum_polydactylum-Alcyonium_coralloides	1,036051545	-1,059126499	3,13122959	0,906318862
Ovabunda-Alcyonium_coralloides	-0,604086448	-1,965504416	0,757331519	0,956010453
Ovabunda-Eunicella_verrucosa	0,380807006	-0,518234318	1,27984833	0,969064253
Sarcophyton_glaucum-Klyxum_utinomii	-0,595387804	-2,007956554	0,817180945	0,970222351
Sclerophytum_vrijmoethi-Klyxum_utinomii	-0,528205924	-1,940774674	0,884362825	0,988817543
Klyxum_utinomii-Eunicella_cavolini	0,480750565	-0,80702191	1,768523041	0,988973694
Paralemnalia_thyrsoides-Ovabunda	-0,378245151	-1,398312953	0,641822651	0,989595872
Sclerophytum_polydactylum-Callogorgia_verticillata	0,683420712	-1,164352641	2,531194065	0,989821503
Klyxum_utinomii-Corallium_rubrum	0,488586029	-0,836520916	1,813692974	0,990090936
Paramuricea_clavata-Eunicella_verrucosa	0,276804943	-0,482315192	1,035925078	0,991001834
Klyxum_utinomii-Alcyonium_coralloides	-0,603343405	-2,314049114	1,107362305	0,993289812
Paramuricea_clavata-Paralemnalia_thyrsoides	0,274243088	-0,624937871	1,173424048	0,998254337
Klyxum_utinomii-Eunicella_verrucosa	0,38155005	-0,990065948	1,753166047	0,999291762
Sclerophytum_eilatense-Ovabunda	-0,289936676	-1,397342986	0,817469633	0,999615851
Paralemnalia_thyrsoides-Klyxum_utinomii	-0,378988195	-1,832808494	1,074832104	0,999632464
Sclerophytum_eilatense-Sarcophyton_glaucum	0,304708084	-0,865009969	1,474426137	0,999635153
Callogorgia_verticillata-Alcyonium_coralloides	0,352630833	-1,04415453	1,749416196	0,999735547
Sarcophyton_glaucum-Eunicella_verrucosa	-0,213837754	-1,188602799	0,76092729	0,99993969
Sclerophytum_vrijmoethi-Sclerophytum_eilatense	-0,237526204	-1,407244257	0,932191849	0,999973822
Sarcophyton_glaucum-Paralemnalia_thyrsoides	-0,216399609	-1,30379554	0,870996321	0,999978994
Sclerophytum_eilatense-Klyxum_utinomii	-0,29067972	-1,80705826	1,22569882	0,999986069
Sclerophytum_eilatense-Eunicella_cavolini	0,190070845	-0,825432872	1,205574562	0,999989295
Sclerophytum_eilatense-Paramuricea_clavata	-0,185934613	-1,183098999	0,811229772	0,999989733
Sclerophytum_eilatense-Corallium_rubrum	0,197906309	-0,864542874	1,260355492	0,999989848
Sclerophytum_vrijmoethi-Eunicella_verrucosa	-0,146655874	-1,121420919	0,82810917	0,999999078
Paramuricea_clavata-Ovabunda	-0,104002063	-0,844536881	0,636532756	0,99999958
Sclerophytum_vrijmoethi-Paralemnalia_thyrsoides	-0,149217729	-1,236613659	0,938178201	0,999999678
Sarcophyton_glaucum-Eunicella_cavolini	-0,114637239	-0,967394176	0,738119699	0,999999746
Eunicella_verrucosa-Corallium_rubrum	0,107035979	-0,736008999	0,950080957	0,999999868
Eunicella_verrucosa-Eunicella_cavolini	0,099200516	-0,683853995	0,882255027	0,999999872
Sarcophyton_glaucum-Corallium_rubrum	-0,106801775	-1,014956422	0,801352871	0,999999946
Paralemnalia_thyrsoides-Corallium_rubrum	0,109597834	-0,861477783	1,08067345	0,999999966
Paralemnalia_thyrsoides-Eunicella_cavolini	0,10176237	-0,817714321	1,021239061	0,999999973
Paramuricea_clavata-Klyxum_utinomii	-0,104745107	-1,378105606	1,168615392	0,999999999
Sclerophytum_eilatense-Eunicella_verrucosa	0,09087033	-1,029049443	1,210790102	0,999999999
Sclerophytum_eilatense-Paralemnalia_thyrsoides	0,088308475	-1,130905745	1,307522695	1
Sclerophytum_vrijmoethi-Sarcophyton_glaucum	0,06718188	-0,964412477	1,098776238	1
Sclerophytum_vrijmoethi-Eunicella_cavolini	-0,047455359	-0,900212296	0,805301579	1
Eunicella_cavolini-Corallium_rubrum	0,007835463	-0,690557218	0,706228145	1
Sclerophytum_vrijmoethi-Corallium_rubrum	-0,039619895	-0,947774542	0,868534751	1
Paralemnalia_thyrsoides-Eunicella_verrucosa	0,002561855	-1,03107729	1,036201	1
Ovabunda-Klyxum_utinomii	-0,000743044	-1,362161012	1,360674924	1

Table S5 : Output of the PERMANOVA statistical tests.

Permutation test for adonis under reduced model
Terms added sequentially (first to last)
Permutation: free
Number of permutations: 9999

Test	Details	Df	SumOfSqs	R2	F	Pr(>F)
formula = otu_table_Dist ~ Type of sample (Seawater or coral)	Type	1	9.648	0.10391	24.004	0.001
	Residual	207	83.201	0.89609	NA	NA
	Total	208	92.849	1.00000	NA	NA
formula = otu_table_Dist ~ Sea + Species + Sea Species*	Sea	1	6,946	0,09637	42,955	1,00E-04
	Species	12	40,393	0,5604	20,817	1,00E-04
	Residual	153	24,741	0,34324	NA	NA
	Total	166	72,08	1	NA	NA

Pairwise PERMANOVA comparisons between mediteranean coral species

Comparison	R2	F	df	p	p.adj
Alcyonium_coralloides.Corallium_rubrum	0,189244	5 135 184	1;22	0,0001	0,000214
Alcyonium_coralloides.Eunicella_cavolini	0,148223	5 394 503	1;31	0,0001	0,000214
Alcyonium_coralloides.Paramuricea_clavata	0,209544	1 033 863	1;39	0,0001	0,000214
Callogorgia_verticillata.Eunicella_cavolini	0,210192	1 037 907	1;39	0,0001	0,000214
Callogorgia_verticillata.Eunicella_verrucosa	0,308456	9 812 886	1;22	0,0001	0,000214
Callogorgia_verticillata.Paramuricea_clavata	0,310155	2 113 126	1;47	0,0001	0,000214
Corallium_rubrum.Paramuricea_clavata	0,133229	8 453 908	1;55	0,0001	0,000214
Corallium_rubrum.Eunicella_cavolini	0,089831	4 638 746	1;47	0,0005	0,000938
Alcyonium_coralloides.Eunicella_verrucosa	0,293174	5 806 856	1;14	0,0006	0,001
Alcyonium_coralloides.Callogorgia_verticillata	0,37998	8 579 914	1;14	0,0008	0,0012
Eunicella_cavolini.Paramuricea_clavata	0,054028	3 655 275	1;64	0,0059	0,008045
Corallium_rubrum.Eunicella_verrucosa	0,090877	2 998 828	1;30	0,0155	0,019375
Callogorgia_verticillata.Corallium_rubrum	0,085289	2 797 248	1;30	0,0227	0,026192
Eunicella_cavolini.Eunicella_verrucosa	0,041523	1 689 565	1;39	0,1214	0,1289
Eunicella_verrucosa.Paramuricea_clavata	0,036063	1 758 395	1;47	0,1289	0,1289

Pairwise PERMANOVA comparisons between Red sea coral species

Comparison	R2	F	df	p	p.adj
Ovabunda.Paralemnalia_thyrsoides	0,106531	2 623 136	1;22	0,0011	0,0308
Paralemnalia_thyrsoides.Sarcophyton_glaucum	0,131632	2 728 534	1;18	0,004	0,056
Klyxum_utinomii.Paralemnalia_thyrsoides	0,14742	1 729 103	1;10	0,1442	0,637778
Ovabunda.Sclerophytum_eilatense	0,060902	1 232 189	1;19	0,1906	0,637778
Ovabunda.Sclerophytum_loyai	0,074367	1 205 126	1;15	0,1186	0,637778
Paralemnalia_thyrsoides.Sclerophytum_eilatense	0,100399	1 450 858	1;13	0,1284	0,637778
Paralemnalia_thyrsoides.Sclerophytum_polydactylum	0,141137	1 478 966	1;9	0,1663	0,637778
Sarcophyton_glaucum.Sclerophytum_eilatense	0,075228	1 220 214	1;15	0,195	0,637778
Sarcophyton_glaucum.Sclerophytum_loyai	0,106528	1 311 519	1;11	0,205	0,637778
Klyxum_utinomii.Sarcophyton_glaucum	0,084898	1 113 288	1;12	0,3601	0,7202
Klyxum_utinomii.Sclerophytum_loyai	0,274415	1 134 597	1;3	0,3	0,7202
Ovabunda.Sarcophyton_glaucum	0,044311	1 112 784	1;24	0,2896	0,7202
Ovabunda.Sclerophytum_vrijmoethi	0,047903	1 056 572	1;21	0,358	0,7202
Sarcophyton_glaucum.Sclerophytum_vrijmoethi	0,058917	10 643	1;17	0,3377	0,7202
Klyxum_utinomii.Sclerophytum_eilatense	0,119326	0,948457	1;7	0,512	0,751983
Klyxum_utinomii.Sclerophytum_vrijmoethi	0,088596	0,874879	1;9	0,6089	0,751983
Paralemnalia_thyrsoides.Sclerophytum_loyai	0,087976	0,868161	1;9	0,4469	0,751983
Paralemnalia_thyrsoides.Sclerophytum_vrijmoethi	0,054093	0,857797	1;15	0,5665	0,751983
Sarcophyton_glaucum.Sclerophytum_polydactylum	0,077307	0,921622	1;11	0,5618	0,751983
Sclerophytum_eilatense.Sclerophytum_loyai	0,140582	0,98147	1;6	0,5416	0,751983
Sclerophytum_eilatense.Sclerophytum_polydactylum	0,141614	0,989865	1;6	0,46	0,751983
Sclerophytum_loyai.Sclerophytum_vrijmoethi	0,092919	0,819502	1;8	0,6177	0,751983
Sclerophytum_polydactylum.Sclerophytum_vrijmoethi	0,104351	0,932071	1;8	0,5578	0,751983
Klyxum_utinomii.Sclerophytum_polydactylum	0,233218	0,912456	1;3	0,7	0,79184
Sclerophytum_eilatense.Sclerophytum_vrijmoethi	0,060777	0,776515	1;12	0,707	0,79184
Klyxum_utinomii.Ovabunda	0,047544	0,798683	1;16	0,7449	0,8022
Ovabunda.Sclerophytum_polydactylum	0,047103	0,741468	1;15	0,8985	0,931778
Sclerophytum_loyai.Sclerophytum_polydactylum	0,330132	0,985664	1;2	1	1

Table S6 : Outputs of the dispersion analyses

Output of the betadisper function between Mediteranean and Red Sea samples

Homogeneity of multivariate dispersions
Call: betadisper(d = otu_table_Dist, group = Sea)
No. of Positive Eigenvalues: 123
No. of Negative Eigenvalues: 43

Average distance to median:

MED	RED
0,5909	1

Eigenvalues for PCoA axes:
(Showing 8 of 166 eigenvalues)

PCoA1	PCoA2	PCoA3	PCoA4	PCoA5	PCoA6	PCoA7	PCoA8
13,594	9,88	6,707	3,942	3,673	3,436	2,424	2,305

Analysis of Variance of the betadispersion between Mediteranean and Red Sea samples

	Df	Sum Sq	Mean Sq	F value	Pr(>F)
Groups	1	0,1968	0,196799	13,55	0,000314
Residuals	165	2,3965	0,014524	NA	NA

Pairwise comparisons of betadispersion between mediteranean coral species

Comparison	F	df	p	p.adj
Alcyonium_coralloides.Eunicella_cavolini	90 585	1;31	0,0008	0,012
Eunicella_cavolini.Paramuricea_clavata	9 730 543	1;64	0,0034	0,0255
Alcyonium_coralloides.Corallium_rubrum	7 135 977	1;22	0,0134	0,05025
Corallium_rubrum.Paramuricea_clavata	730 201	1;55	0,0104	0,05025
Callogorgia_verticillata.Eunicella_cavolini	6 115 093	1;39	0,0186	0,0558
Alcyonium_coralloides.Eunicella_verrucosa	4 681 017	1;14	0,0456	0,097714
Callogorgia_verticillata.Corallium_rubrum	4 613 109	1;30	0,0402	0,097714
Alcyonium_coralloides.Paramuricea_clavata	2 563 272	1;39	0,1157	0,216938
Eunicella_verrucosa.Paramuricea_clavata	213 792	1;47	0,1496	0,249333
Callogorgia_verticillata.Eunicella_verrucosa	1 789 971	1;22	0,1966	0,2949
Callogorgia_verticillata.Paramuricea_clavata	0,659574	1;47	0,4141	0,513
Corallium_rubrum.Eunicella_verrucosa	0,577173	1;30	0,4446	0,513
Eunicella_cavolini.Eunicella_verrucosa	0,700271	1;39	0,4055	0,513
Alcyonium_coralloides.Callogorgia_verticillata	0,260849	1;14	0,6121	0,655821
Corallium_rubrum.Eunicella_cavolini	0,001269	1;47	0,97	0,97

Pairwise comparisons of betadispersion between Red sea coral species

Comparison	F	df	p	p.adj
Ovabunda.Sclerophytum_loyai	9 785 895	1;15	0,0078	0,1092
Ovabunda.Sclerophytum_polydactylum	9 419 735	1;15	0,0068	0,1092
Klyxum_utinomii.Ovabunda	5 100 215	1;16	0,0403	0,1547
Sclerophytum_eilatense.Sclerophytum_loyai	109 009	1;6	0,0371	0,1547
Sclerophytum_eilatense.Sclerophytum_polydactylum	1 041 272	1;6	0,0349	0,1547
Sclerophytum_loyai.Sclerophytum_polydactylum	1,49E+27	1;2	0,041667	0,1547
Sclerophytum_loyai.Sclerophytum_vrijmoethi	3 896 351	1;8	0,043	0,1547
Sclerophytum_polydactylum.Sclerophytum_vrijmoeth	3 728 899	1;8	0,0442	0,1547
Klyxum_utinomii.Sclerophytum_eilatense	2 502 474	1;7	0,1155	0,359333
Ovabunda.Paralemnalia_thyrsoides	2 028 981	1;22	0,1697	0,47516
Klyxum_utinomii.Sclerophytum_vrijmoethi	1 743 715	1;9	0,21	0,534545
Klyxum_utinomii.Sarcophyton_glaucum	0,464802	1;12	0,507	0,747158
Ovabunda.Sarcophyton_glaucum	0,57826	1;24	0,453	0,747158
Ovabunda.Sclerophytum_eilatense	0,626324	1;19	0,4348	0,747158
Paralemnalia_thyrsoides.Sarcophyton_glaucum	0,462985	1;18	0,499	0,747158
Paralemnalia_thyrsoides.Sclerophytum_eilatense	0,479544	1;13	0,482	0,747158
Paralemnalia_thyrsoides.Sclerophytum_vrijmoethi	0,685942	1;15	0,4221	0,747158
Sarcophyton_glaucum.Sclerophytum_loyai	0,961508	1;11	0,443	0,747158
Sarcophyton_glaucum.Sclerophytum_polydactylum	0,914534	1;11	0,4342	0,747158
Ovabunda.Sclerophytum_vrijmoethi	0,358668	1;21	0,5558	0,77812
Paralemnalia_thyrsoides.Sclerophytum_loyai	0,071111	1;9	0,693	0,882
Paralemnalia_thyrsoides.Sclerophytum_polydactylum	0,063274	1;9	0,6898	0,882
Klyxum_utinomii.Sclerophytum_loyai	0,381517	1;3	0,908333	0,950444
Klyxum_utinomii.Sclerophytum_polydactylum	0,337187	1;3	0,908333	0,950444
Sarcophyton_glaucum.Sclerophytum_eilatense	0,025552	1;15	0,8732	0,950444
Sarcophyton_glaucum.Sclerophytum_vrijmoethi	0,058133	1;17	0,7994	0,950444
Sclerophytum_eilatense.Sclerophytum_vrijmoethi	0,011087	1;12	0,9165	0,950444
Klyxum_utinomii.Paralemnalia_thyrsoides	0,000464	1;10	0,9709	0,9709

Table S8 : Tests of phylosymbiosis

Outputs from the TreeCmp pipeline						
	All species (Mediterranean and Red Seas)					
	Matching cluster test			Robinson-Foulds test		
	MatchingCluster	MatchingCluster_toYuleAvg	P-value	R-F	R-F_toYuleAvg	P-value
	44	0,8501	0,04585	8	0,6828	0,00033
	Mediterranean Sea species					
	Matching cluster test			Robinson-Foulds test		
	MatchingCluster	MatchingCluster_toYuleAvg	P-value	R-F	R-F_toYuleAvg	P-value
	4	0,3170	0,001	1	0,2773	0,01121
	Red Sea species					
	Matching cluster test			Robinson-Foulds test		
	MatchingCluster	MatchingCluster_toYuleAvg	P-value	R-F	R-F_toYuleAvg	P-value
	14	0,8546	0,1131	5	1,0808	0,9900

Mantel tests outputs				
All species (Mediterranean and Red Seas)				
Observation	Std.Obs	Expectation	Variance	Simulated p-value
0,1437472	1,153499755	-0,000447331	0,015626534	0,1029
Mediterranean Sea species				
Observation	Std.Obs	Expectation	Variance	Simulated p-value
0,5980036	2,488570692	-0,001599556	0,05805342	0,0027
Red Sea species				
Observation	Std.Obs	Expectation	Variance	Simulated p-value
0,5244712	1,576746821	0,002413739	0,109625788	0,1359

Appendix 3 – Chapter 2

Table S1: Number of reads and sequences throughout the DADA2 pipeline for each sample.

Sample	**input**	**filtered**	**denoisedF**	**denoisedR**	**merged**	**nonchim**	**After filtering**
C1_Cap de Creus	94691	76098	75715	75806	75445	65140	11 samples
C2_Cap de Creus	90532	69079	68647	68753	68352	54673	
C5_Cap de Creus	74280	60038	59683	59823	59492	48490	
C6_Cap de Creus	77802	61903	61689	61753	61562	56409	
C7_Cap de Creus	78142	61603	61199	61321	60939	49079	
C9_Cap de Creus	56899	43628	43130	43267	42806	24532	
C11_Cap de Creus	82007	64176	63846	63955	63649	47879	
C12_Cap de Creus	67533	52443	51340	51868	50834	36968	
C13_Cap de Creus	77655	62371	62139	62269	62055	46164	
C14_Cap de Creus	99946	78702	78287	78596	78192	56115	
C15_Cap de Creus	89359	71524	71022	71217	70737	50286	
C1_Cassis	63947	49890	49650	49740	49514	35248	15 samples
C2_Cassis	60597	46259	45873	46091	45735	27998	
C3_Cassis	66865	53152	52575	52894	52329	30200	
C4_Cassis	64912	50391	50174	50273	50073	36112	
C5_Cassis	69062	54340	53921	54088	53693	40361	
C6_Cassis	81555	63678	63064	63241	62657	39739	
C7_Cassis	78501	60695	60004	60284	59625	44420	
C8_Cassis	183202	136548	135296	135782	134569	61224	
C9_Cassis	56517	43422	43288	43341	43215	27632	
C10_Cassis	77041	62241	62032	62141	61944	41865	
C11_Cassis	80847	64827	64571	64605	64367	40512	
C12_Cassis	69434	55708	55414	55519	55242	34979	

C13_Cassis	72723	57721	57303	57565	57166	36899	
C14_Cassis	111226	86475	85786	86125	85488	66494	
C15_Cassis	93395	75343	75059	75219	74945	50584	
C2_Porticcio	89925	71567	71307	71401	71162	49140	12 samples
C3_Porticcio	56149	45344	45147	45255	45075	31329	
C4_Porticcio	53764	41798	41645	41727	41580	29420	
C5_Porticcio	68483	54574	54336	54383	54159	36002	
C6_Porticcio	73957	56349	56063	56202	55947	42719	
C7_Porticcio	84755	67312	66819	67047	66567	48456	
C8_Porticcio	73030	57797	57553	57585	57354	40927	
C10_Porticcio	78609	63221	62900	63057	62761	41778	
C11_Porticcio	65324	52427	52083	52234	51903	37988	
C12_Porticcio	51196	37163	36847	37036	36737	24196	
C13_Porticcio	56978	45758	45319	45609	45192	28107	
C15_Porticcio	71596	56716	56402	56542	56251	42248	
C1_Villefranche	62287	39283	39261	39240	39228	37506	4 samples
C2_Villefranche	59147	36691	36501	36533	36368	31018	
C3_Villefranche	64206	42579	42437	42539	42415	35653	
C4_Villefranche	62510	33330	33278	33283	33240	30015	
C2_Portofino	57617	39188	39119	39136	39078	34607	4 samples
C3_Portofino	46868	31320	31214	31231	31143	26289	
C5_Portofino	55398	35257	35157	35234	35146	29992	
C6_Portofino	67288	44995	44899	44944	44864	40059	
Sum	3417757						
Maximum	183202						
Minimum	46868						

Table S2 and S3 are not available due to the large size of the tables (ASV table of the microeukaryotic communities and Taxonomic annotation of microeukaryotic ASVs)

Table S4: Metadata

Sample	Site	Colonie	DNA concentration after extraction (ng/µL)
C1_Cap de Creus	Cap de Creus	C1	40,2
C2_Cap de Creus	Cap de Creus	C2	34,7
C5_Cap de Creus	Cap de Creus	C5	43,9
C6_Cap de Creus	Cap de Creus	C6	14,8
C7_Cap de Creus	Cap de Creus	C7	48,5
C9_Cap de Creus	Cap de Creus	C9	42,9
C11_Cap de Creus	Cap de Creus	C11	30,9
C12_Cap de Creus	Cap de Creus	C12	55,9
C13_Cap de Creus	Cap de Creus	C13	39
C14_Cap de Creus	Cap de Creus	C14	43,3
C15_Cap de Creus	Cap de Creus	C15	43,8
C1_Cassis	Cassis	C1	103
C2_Cassis	Cassis	C2	30,7
C3_Cassis	Cassis	C3	22,9
C4_Cassis	Cassis	C4	31,1
C5_Cassis	Cassis	C5	28,8
C6_Cassis	Cassis	C6	23,6
C7_Cassis	Cassis	C7	44,2
C8_Cassis	Cassis	C8	29,1
C9_Cassis	Cassis	C9	22,3
C10_Cassis	Cassis	C10	61,2
C11_Cassis	Cassis	C11	40,9
C12_Cassis	Cassis	C12	47,4
C13_Cassis	Cassis	C13	45
C14_Cassis	Cassis	C14	37,3
C15_Cassis	Cassis	C15	48,3

C2_Porticcio	Porticcio	C2	64,1
C3_Porticcio	Porticcio	C3	61,8
C4_Porticcio	Porticcio	C4	51,9
C5_Porticcio	Porticcio	C5	61,6
C6_Porticcio	Porticcio	C6	43,2
C7_Porticcio	Porticcio	C7	31,5
C8_Porticcio	Porticcio	C8	80
C10_Porticcio	Porticcio	C10	37
C11_Porticcio	Porticcio	C11	39,5
C12_Porticcio	Porticcio	C12	68
C13_Porticcio	Porticcio	C13	96
C15_Porticcio	Porticcio	C15	30,1
C1_Villefranche	Villefranche	C1	35,9
C2_Villefranche	Villefranche	C2	131
C3_Villefranche	Villefranche	C3	94,7
C4_Villefranche	Villefranche	C4	78
C2_Portofino	Portofino	C2	7,13
C3_Portofino	Portofino	C3	6,41
C5_Portofino	Portofino	C5	9,07
C6_Portofino	Portofino	C6	13

Table S5: Microeukaryotic diversity data (observed richness, Shannon, Simpson, InvSimpson) and statistical tests.

Alpha Diversity Statistic per Site (Raw Dataset vs Rarefied Dataset)							
Site	**Metric**	**Median (Raw Dataset)**	**Median (Rarefied Dataset)**	**Mean (Raw Dataset)**	**Mean (Rarefied Dataset)**	**Variance (Raw Dataset)**	**Variance (Rarefied Dataset)**
Cap de Creus	Observed	130	117	127	109.272727272727	1948	1004.0181818181818
Cassis	Observed	188	159	183.666666666667	155.133333333333	1133.2380952381	783.980952380952
Porticcio	Observed	141	134	161.333333333333	139.75	2488.9696969697	1817.29545454545
Portofino	Observed	102	96.5	98.75	93.5	118.916666666667	61.6666666666667
Villefranche	Observed	80.5	74.5	95.25	88	2238.25	1624.66666666667
Cap de Creus	Shannon	2.25069146197639	2.23996921659957	2.04296526409615	2.03257180875721	0.64912732864725	0.659249692669709
Cassis	Shannon	2.12301991469245	2.12352707401364	2.01927856030863	2.01073229658313	0.39915948030103	0.395336680188944
Porticcio	Shannon	1.64360476090402	1.65008019354377	1.75515378826509	1.75299681642642	0.450201089092882	0.440692801638148
Portofino	Shannon	2.10597047461184	2.09352945096736	2.04722876363616	2.04222672910586	0.122534123052694	0.125622109577061
Villefranche	Shannon	1.85793997803055	1.86148002778612	1.99643182544972	1.99021844237944	0.231636554444639	0.219190240654047
Cap de Creus	Simpson	0.777728883870215	0.778975595088210	0.642104855780789	0.640537821834160	0.069585075809381	0.070298566948642
Cassis	Simpson	0.706746662975779	0.703208073063093	0.624775138640284	0.625351814598864	0.038921165447473 2	0.038589263958178 6
Porticcio	Simpson	0.580372356021418	0.575120521100496	0.558822651057438	0.559336959192260	0.047406196251207 5	0.046776887254485 6

Portofino	Simpson	0.770479474378109	0.769892790542598	0.738570724841 1	0.737367931101497	0.008502161208388891	0.008769665858325 1
Villefranche	Simpson	0.676503927146005	0.674631463125462	0.705264722680711	0.704215899028249	0.006200130980226 11	0.006072587191066676
Cap de Creus	InvSimpson	4.49901011616865	4.52438725216384	4.4344559783537	4.40924025809092	7.5436709656464 5	7.3945842803304
Cassis	InvSimpson	3.4100208718764	3.36936388506478	3.32861054001999	3.32585114352373	2.0096399089520 6	1.9785647618520 6
Porticcio	InvSimpson	2.38321319861777	2.35516737470422	2.9850272784182	2.98458164212525	3.0399702318154 1	3.0205959390018 1
Portofino	InvSimpson	4.43272666172172	4.42570922356086	4.1403624447476 5	4.12859027861055	1.4641052468760 2	1.4861681462105 9
Villefranche	InvSimpson	3.09754812367275	3.08212022991573	3.6493421510346 4	3.6271964223461 2	1.6552107907589 6	1.5702428226552
Alpha Diversity Metrics per Sample (Raw Dataset)							
Sample	**Observed**	**Shannon**	**Simpson**	**InvSimpson**			
C1_Cap de Creus	125	2,84562136	0.835014017736 26	6.0611209890634 2			
C1_Cassis	107	1,18738153	0.383494408926826	1.6220453058004 9			
C1_Villefranche	56	2,015547356	0.691116790854746	3.2374696014303 1			
C10_Cassis	185	1,380279976	0.433173801332802	1.7642092097213 2			
C10_Porticcio	130	1,389619859	0.416710543567221	1.7144146683461 4			
C11_Cap de Creus	136	1,965977283	0.597094600788712	2.4819721998205			
C11_Cassis	188	2,123019915	0.643093757431629	2.8018562880934 6			

C11_Porticcio	182	1,972923188	0.577064588753484	2.364427223184 52			
C12_Cap de Creus	64	1,247813264	0.407692584337054	1.688312476859 23			
C12_Cassis	213	2,513936956	0.766675350045799	4.285873782286 99			
C12_Porticcio	227	2,762094984	0.820408992522717	5.568207529135 29			
C13_Cap de Creus	130	0,658118309	0.174654237421791	1.211613417479 98			
C13_Cassis	220	2,432554569	0.767541546577022	4.301843986634 53			
C13_Porticcio	251	2,525321794	0.786101989873197	4.675125305780 93			
C14_Cap de Creus	196	0,863351039	0.221634765947739	1.284743917445 9			
C14_Cassis	181	2,645170403	0.757517541689186	4.124009658126 28			
C15_Cap de Creus	178	1,896229726	0.621210931465 23	2.639991707966 11			
C15_Cassis	210	2,01791777	0.706746662975779	3.410020871876 4			
C15_Porticcio	141	1,394693807	0.388671569145738	1.635781929203 94			
C2_Cap de Creus	138	2,836736143	0.861876473374 74	7.239896232255 06			
C2_Cassis	169	1,326592767	0.358038850415512	1.557726664062 54			
C2_Porticcio	110	0,880882044	0.257279085483482	1.346400754920 12			
C2_Portofino	103	2,38547422	0.800496785952152	5.012450575157 97			

C2_Villefranche	164	2,66807915	0.820236271401958	5.562857467403 97			
C3_Cassis	135	0,812688775	0.219501941760883	1.281233168287 57			
C3_Porticcio	98	1,410299016	0.472016517890457	1.893998645572 26			
C3_Portofino	108	1,591499885	0.607586921812 21	2.548335046879 98			
C3_Villefranche	83	1,7003326	0.647814765028877	2.839414889389 09			
C4_Cassis	194	1,522182095	0.461089553380472	1.855595871768 29			
C4_Porticcio	133	1,489010451	0.583680123289352	2.401999174051 03			
C4_Villefranche	78	1,601768196	0.661891063437263	2.957626645915 19			
C5_Cap de Creus	103	2,717441185	0.859302731901069	7.107458542100 83			
C5_Cassis	150	2,327859697	0.796830649651496	4.922002252232 75			
C5_Porticcio	141	1,79819907	0.620642460351685	2.636035653666 07			
C5_Portofino	101	1,967041729	0.740462162804066	3.853002748285 46			
C6_Cap de Creus	45	2,250691462	0.816733369885 55	5.456530735439 93			
C6_Cassis	236	2,685267503	0.781877485443863	4.584579460010 93			
C6_Porticcio	119	0,689067824	0.194246414814166	1.241074217211 66			
C6_Portofino	83	2,24489922	0.805737028795972	5.147661408667 19			

C7_Cap de Creus	130	2,859583046	0.890210816860319	9.108365427291108			
C7_Cassis	199	2,639332532	0.798031033113858	4.951255707333715			
C7_Porticcio	213	2,669454662	0.844397720671 1	6.426641076936 16			
C8_Cassis	196	2,762548912	0.809912174657171	5.260726183786 2			
C8_Porticcio	191	2,080278759	0.744651806326655	3.916221163010 28			
C9_Cap de Creus	152	2,331055088	0.777728883870215	4.499010116168 65			
C9_Cassis	172	1,912445003	0.688102322201959	3.206179690274 95			

Table S6: Outputs of the PERMANOVA statistical tests.

Differences in microeukaryotes composition between sites					
PERMANOVA with 999 permutations					
adonis2(formula = Aitchison distance matrix ~ Site, data = ASV table)					
	Df	SumOfSqs	R2	F	Pr(>F)
Site	4	14109	0.14362	1.7189	0.001
Residual	41	84131	0.85638	.	.
Total	45	98240	1.00000	.	.
Pairwise permanova					
pairs	**SumOfSqs**	**F.Model**	**R2**	**pval**	**p.adj**
Cap de Creus vs Cassis	5471,881315	2,4271329	0,09184246	0,001	0,00333333
Cap de Creus vs Porticcio	3432,834224	1,75628474	0,07717801	0,001	0,00333333
Cap de Creus vs Portofino	2473,377707	1,32812134	0,09269333	0,013	0,01444444
Cap de Creus vs Villefranche	2664,382807	1,4353215	0,09943121	0,007	0,01
Cassis vs Porticcio	3015,404441	1,35640132	0,05146383	0,013	0,01444444
Cassis vs Portofino	3920,822552	1,72051305	0,09190523	0,002	0,00333333
Cassis vs Villefranche	3988,142317	1,75359411	0,0935071	0,002	0,00333333
Porticcio vs Portofino	3147,942	1,71615112	0,10919665	0,001	0,00333333
Villefranche vs Porticcio	3285,813429	1,79678615	0,11374378	0,002	0,00333333
Villefranche vs Portofino	2011,841907	1,37710812	0,18667316	0,027	0,027
ANOVA on the betadispersion values (distance to centroid) between sites					
anova(betadisper(Aitchison distance matrix, group= Site))					
	Df	Sum Sq	Mean Sq	F value	Pr(>F)

Groups	4	1185.6	296.410	4.2753	0.005539
Residuals	41	2842.6	69.331	.	.
Tukey multiple comparisons of means with 95% family-wise confidence level					
	diff	lwr	upr	p adj	
Villefranche-Cassis	-15.3860759	-28.753422	-2.018730	0.0169664	
Portofino-Cassis	-14.4207722	-27.788118	-1.053426	0.0288473	
Porticcio-Cassis	-6.9190811	-16.119120	2.280957	0.2210211	
Villefranche-Cap de Creus	-9.9833713	-23.852951	3.886209	0.2597149	
Portofino-Cap de Creus	-9.0180676	-22.887647	4.851512	0.3573065	
Villefranche-Porticcio	-8.4669948	-22.181602	5.247613	0.4094024	
Cassis-Cap de Creus	5.4027046	-4.026796	14.832206	0.4846618	
Portofino-Porticcio	-7.5016911	-21.216299	6.212916	0.5304587	
Porticcio-Cap de Creus	-1.5163765	-11.432021	8.399268	0.9921832	
Villefranche-Portofino	-0.9653037	-17.762199	15.831592	0.9998307	
BETADISPERSION :Average distance to centroid					
Cap de Creus	Cassis	Porticcio	Villefranche	Portofino	
42.11	47.51	40.60	32.13	33.09	
Sample	Distance to centroid				
C1_Cap de Creus	43,31591907				
C1_Cassis	34,82949594				
C1_Villefranche	28,68394011				

C10_Cassis	45,00476356				
C10_Porticcio	33,36199576				
C11_Cap de Creus	42,59197036				
C11_Cassis	46,75598266				
C11_Porticcio	47,15242903				
C12_Cap de Creus	36,27901211				
C12_Cassis	47,39006136				
C12_Porticcio	54,72349491				
C13_Cap de Creus	39,44249505				
C13_Cassis	58,44795725				
C13_Porticcio	63,29161055				
C14_Cap de Creus	50,85630073				
C14_Cassis	48,24806988				
C15_Cap de Creus	48,11096852				
C15_Cassis	44,32735175				
C15_Porticcio	37,77055278				
C2_Cap de Creus	44,8389687				
C2_Cassis	46,99380537				
C2_Porticcio	27,77782645				
C2_Portofino	39,45481953				
C2_Villefranche	47,44139872				
C3_Cassis	47,31778572				
C3_Porticcio	25,82765911				
C3_Portofino	32,5009096				
C3_Villefranche	27,39618012				
C4_Cassis	47,00267634				
C4_Porticcio	34,50291237				
C4_Villefranche	24,9936458				
C5_Cap de Creus	37,52312869				

C5_Cassis	42,63029673				
C5_Porticcio	32,36760582				
C5_Portofino	28,58683344				
C6_Cap de Creus	32,08383141				
C6_Cassis	56,26937				
C6_Porticcio	29,17131482				
C6_Portofino	31,83381705				
C7_Cap de Creus	40,69223286				
C7_Cassis	51,52543738				
C7_Porticcio	53,9236771				
C8_Cassis	53,95396604				
C8_Porticcio	47,2783537				
C9_Cap de Creus	47,49895997				
C9_Cassis	42,0259869				
Differences in microeukaryotes composition between sampling years					
PERMANOVA with 999 permutations					
adonis2(formula = Aitchison distance matrix ~ Year, data = ASV table)					
	Df	SumOfSqs	R2	F	Pr(>F)
Year	1	4133	0.04207	1.9323	0.001
Residual	44	94107	0.95793		
Total	45	98240	1.00000		

ANOVA on the betadispersion values (distance to centroid) between sites					
anova(betadisper(Aitchison distance matrix, group= Site))					
	Df	Sum Sq	Mean Sq	F value	Pr(>F)
Groups	1	656.0	656.02	8.8038	0.004846
Residuals	44	3278.7	74.52		
BETADISPERSION :Average distance to centroid					
2013	2023				
46.05	36.09				

Table S8: Core microbiome

#core microbiome at the ASV level	
core_microbiome <- core_members(ps, detection = 0.001, prevalence = 99/100, include.lowest = TRUE)	
ASV1 - Licnophoridae	
#core microbiome at the family level	
ps_fam <- tax_glom(ps, taxrank = "Family")	
fam_freq <- psmelt(ps_fam) %>%	
group_by(Sample, Family) %>%	
summarize(abundance = sum(Abundance))	
core_threshold <- 0,90	
core_microbiome <- fam_freq %>%	
group_by(Family) %>%	
summarize(presence = mean(abundance > 0)) %>%	
filter(presence >= core_threshold)	
Family	**Presence in samples**
Dino-Group-I-Clade-1	100%
Licnophoridae	100%

Table S7 and S8 are not available due to the large size of the tables (Outputs of the ANCOM-BC test comparing the sampling sites and Outputs of the ANCOM-BC test comparing the sampling years)

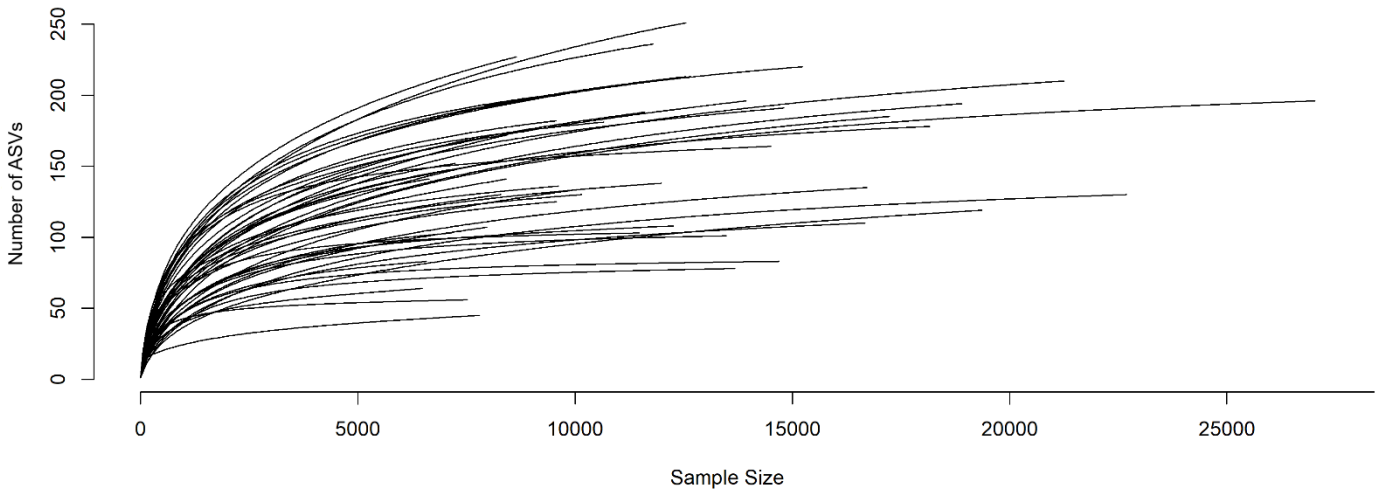

Figure S1: Rarefaction curves for each sample.

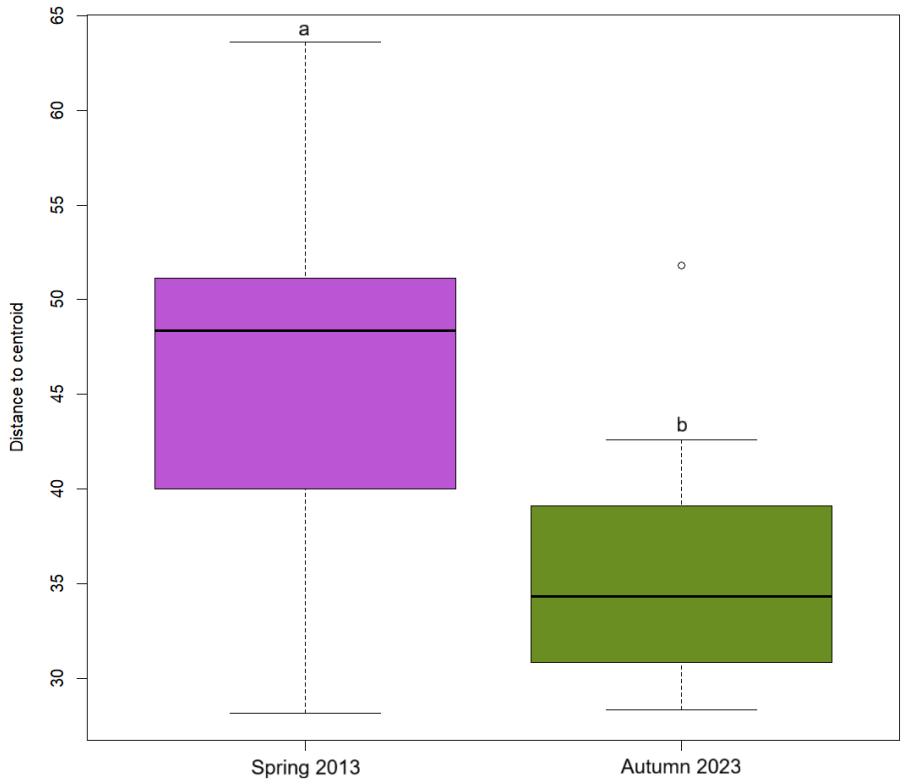

Figure S2: Beta dispersion (within-site variability) of the samples based on the community composition at the ASV level. Boxplots display value medians and interquartile ranges for each sampling year.

Appendix 4 – Chapter 3

Supplementary file 1 : Fungi identification

Primers sets

Internal Transcribed Spacer		**Tm**	**Amplicon expected size**
ITS1	TCCGTAGGTGAACCTGCGG	58°C	600 bp
ITS4	TCCTCCGCTTATTGATATGC		
Beta tubulin		**Tm**	**Amplicon expected size**
Bt2B	ACCCTCAGTGTAGTGACCCTTGGC	55°C	450 bp
Bt2A	GGTAACCAAATCGGTGCTGCTTTC		
D1/D2 region (26S rRNA)		**Tm**	**Amplicon expected size**
NL1	GCATATCAATAAGCGGAGGAAAAG	55°C	680 bp
NL4	GGTCCGTGTTTCAAGACGG		
Actin		**Tm**	**Amplicon expected size**
ACT-512F	ATGTGCAAGGCCGGTTTCGC	58°C	233-235 bp
ACT-783R	TACGAGTCCTTCTGGCCCAT		
Rpb2		**Tm**	**Amplicon expected size**
RPB2-5F	GAYGAYMGWGATCAYTTYGG	58°C	1000 bp
RPB2-7CR	CCCATRGCTTGYTTRCCCAT		
LSU		**Tm**	**Amplicon expected size**
LR7	TACTACCACCAAGATCT	60°C	bp
LR0R	ACCCGCTGAACTTAAGC		
SSU		**Tm**	**Amplicon expected size**
NS1	GTAGTCATATGCTTGTCTC	59°C	1000 bp
NS4	CTTCCGTCAATTCCTTTAAG		

Molecular and morphological identification

Fungal species	Molecular markers used
Acremonium implicatum	RPB2-5F/RPB2-7CR
Alternaria alternata	ITS1/IST4
Aspergillus fumigatus	Bt2B/Bt2A
Aspergillus sydowii	Bt2B/Bt2A
Aspergillus tubingensis	Bt2B/Bt2A
Aspergillus unguis	Bt2B/Bt2A
	ITS1/IST4
Aspergillus versicolor	Bt2B/Bt2A
Beauveria bassiana	ITS1/IST4
Bullera alba	NL1/NL4
Chrysosporium lobatum	ITS1/IST4
Cladosporium asperulatum	ACT-512F/ACT-783R
Cladosporium cladosporioides	ACT-512F/ACT-783R
Cladosporium halotolerans	ACT-512F/ACT-783R
Cladosporium perangustum	ACT-512F/ACT-783R
Cladosporium psychrotolerans	ACT-512F/ACT-783R
Cladosporium ramotenellum	ACT-512F/ACT-783R
Cladosporium sphaerospermum	ACT-512F/ACT-783R
Exophiala xenobiotica	ITS1/IST4
Flammulina velutipes	ITS1/IST4
Hortaea werneckii	ITS1/IST4
Penicillium biforme	Bt2B/Bt2A + morphological study

Penicillium brevicompactum	Bt2B/Bt2A
Penicillium charlesii	Bt2B/Bt2A
Penicillium chrysogenum	Bt2B/Bt2A
Penicillium commune	Bt2B/Bt2A
Penicillium fundyense	Bt2B/Bt2A + morphological study
Penicillium novae-zeelandiae	Bt2B/Bt2A
Penicillium rubens	Bt2B/Bt2A + morphological study
Penicillium sanguifluum	Bt2B/Bt2A
Penicillium terrigenum	Bt2B/Bt2A
Periconia cookei	ITS1/IST4
	RPB2-5F/RPB2-7CR
Pleosporales sp.	ITS1/IST4
Pseudogymnoascus pannorum	LR7/LR0R
	NS1/NS4
	RPB2-5F/RPB2-7CR
Sarocladium strictum	LR7/LR0R
	NS1/NS4
Simplicillium sympodiophorum	ITS1/IST4
Sporobolomyces roseus	NL1/NL4
	LR7/LR0R
Symmetrospora coprosmae	NL1/NL4
	LR7/LR0R
Tilachlidium brachiatum	ITS1/IST4
Tilletiopsis washingtonensis	NL1/NL4

Results of the isolation

Fungal species	Isolation temperature	Tissue	Media
Acremonium implicatum	15°c and 25°C	Soft tissue and skeleton	CMA-SW, GA-SW, P-CMA-SW and CA-SW
Alternaria alternata	15°C	Skeleton	CMA-SW and GA-SW
Aspergillus fumigatus	25°C	Soft tissue and skeleton	CMA-SW, GA-SW and P-CMA-SW
Aspergillus sydowii	25°C	Skeleton	CA-SW
Aspergillus tubingensis	15°c and 25°C	Soft tissue	GA-SW and P-CMA-SW
Aspergillus unguis	25°C	Soft tissue and skeleton	CMA-SW, GA-SW and CA-SW
Aspergillus versicolor	15°c and 25°C	Soft tissue and skeleton	CMA-SW, GA-SW, P-CMA-SW and CA-SW
Beauveria bassiana	25°C	Soft tissue	CMA-SW and CA-SW
Bullera alba	15°C	Skeleton	CMA-SW
Chrysosporium lobatum	25°C	Soft tissue	CMA-SW
Cladosporium asperulatum	25°C	Soft tissue	P-CMA-SW
Cladosporium cladosporioides	15°c and 25°C	Soft tissue and skeleton	CMA-SW, GA-SW, P-CMA-SW and CA-SW
Cladosporium halotolerans	15°c and 25°C	Soft tissue and skeleton	CMA-SW, GA-SW, P-CMA-SW and CA-SW
Cladosporium perangustum	25°C	Soft tissue	CMA-SW
Cladosporium psychrotolerans	25°C	Skeleton	CMA-SW
Cladosporium ramotenellum	25°C	Soft tissue and skeleton	CMA-SW, GA-SW, P-CMA-SW and CA-SW
Cladosporium sphaerospermum	15°c and 25°C	Soft tissue and skeleton	CMA-SW, GA-SW, P-CMA-SW and CA-SW
Exophiala xenobiotica	15°C	Soft tissue	CA-SW
Flammulina velutipes	15°c and 25°C	Soft tissue and skeleton	CMA-SW, GA-SW, P-CMA-SW and CA-SW
Hortaea werneckii	15°C	Soft tissue and skeleton	GA-SW and CA-SW
Penicillium biforme	25°C	Soft tissue	GA-SW
Penicillium brevicompactum	25°C	Soft tissue	CMA-SW
Penicillium charlesii	25°C	Skeleton	CMA-SW
Penicillium chrysogenum	25°C	Soft tissue	CMA-SW
Penicillium commune	15°c and 25°C	Soft tissue and skeleton	CMA-SW, GA-SW, P-CMA-SW and CA-SW

Penicillium fundyense	15°c and 25°C	Skeleton	CMA-SW and CA-SW
Penicillium novae-zeelandiae	15°c and 25°C	Soft tissue and skeleton	CMA-SW, GA-SW, P-CMA-SW and CA-SW
Penicillium rubens	25°C	Soft tissue and skeleton	CMA-SW, GA-SW, P-CMA-SW
Penicillium sanguifluum	15°c and 25°C	Soft tissue and skeleton	CMA-SW, GA-SW, P-CMA-SW and CA-SW
Penicillium terrigenum	25°C	Soft tissue and skeleton	CMA-SW and P-CMA-SW
Periconia cookei	15°c and 25°C	Skeleton	CMA-SW
Pleosporales sp.	15°C	Skeleton	CA-SW
Pseudogymnoascus pannorum	15°c and 25°C	Soft tissue and skeleton	CMA-SW and GA-SW
Sarocladium strictum	15°C	Soft tissue	P-CMA-SW
Simplicillium sympodiophorum	25°C	Soft tissue	GA-SW
Sporobolomyces roseus	15°C	Soft tissue	P-CMA-SW
Symmetrospora coprosmae	15°C	Skeleton	CMA-SW
Tilachlidium brachiatum	15°c and 25°C	Skeleton	CA-SW
Tilletiopsis washingtonensis	15°C	Soft tissue	CMA-SW

CFU per conditions

Sample	Coral	Media	Isolation_temperature	Tissue	CFU/g_dry_weight
C1_15C_S_CMA-SW	C1	CMA-SW	15C	S	0
C2_15C_S_CMA-SW	C2	CMA-SW	15C	S	1,54292415
C3_15C_S_CMA-SW	C3	CMA-SW	15C	S	0
C4_15C_S_CMA-SW	C4	CMA-SW	15C	S	6,839225589
C5_15C_S_CMA-SW	C5	CMA-SW	15C	S	1,465330285
C6_15C_S_CMA-SW	C6	CMA-SW	15C	S	5,643022403
C1_15C_T_CMA-SW	C1	CMA-SW	15C	T	18,82484436
C2_15C_T_CMA-SW	C2	CMA-SW	15C	T	4,584632312
C3_15C_T_CMA-SW	C3	CMA-SW	15C	T	0
C4_15C_T_CMA-SW	C4	CMA-SW	15C	T	0
C5_15C_T_CMA-SW	C5	CMA-SW	15C	T	0
C6_15C_T_CMA-SW	C6	CMA-SW	15C	T	0
C1_15C_S_CA-SW	C1	CA-SW	15C	S	0,704569512
C2_15C_S_CA-SW	C2	CA-SW	15C	S	7,714620749
C3_15C_S_CA-SW	C3	CA-SW	15C	S	0
C4_15C_S_CA-SW	C4	CA-SW	15C	S	0
C5_15C_S_CA-SW	C5	CA-SW	15C	S	0

C6_15C_S_CA-SW	C6	CA-SW	15C	S	2,351259334
C1_15C_T_CA-SW	C1	CA-SW	15C	T	37,64968873
C2_15C_T_CA-SW	C2	CA-SW	15C	T	0
C3_15C_T_CA-SW	C3	CA-SW	15C	T	0
C4_15C_T_CA-SW	C4	CA-SW	15C	T	0
C5_15C_T_CA-SW	C5	CA-SW	15C	T	6,091617934
C6_15C_T_CA-SW	C6	CA-SW	15C	T	0
C1_15C_S_GA-SW	C1	GA-SW	15C	S	0
C2_15C_S_GA-SW	C2	GA-SW	15C	S	0
C3_15C_S_GA-SW	C3	GA-SW	15C	S	0
C4_15C_S_GA-SW	C4	GA-SW	15C	S	0
C5_15C_S_GA-SW	C5	GA-SW	15C	S	2,442217142
C6_15C_S_GA-SW	C6	GA-SW	15C	S	0
C1_15C_T_GA-SW	C1	GA-SW	15C	T	6,274948121
C2_15C_T_GA-SW	C2	GA-SW	15C	T	0
C3_15C_T_GA-SW	C3	GA-SW	15C	T	21,22241087
C4_15C_T_GA-SW	C4	GA-SW	15C	T	12,01634223
C5_15C_T_GA-SW	C5	GA-SW	15C	T	6,091617934
C6_15C_T_GA-SW	C6	GA-SW	15C	T	6,23596907
C1_15C_S_P-CMA-SW	C1	P-CMA-SW	15C	S	0
C2_15C_S_P-CMA-SW	C2	P-CMA-SW	15C	S	0
C3_15C_S_P-CMA-SW	C3	P-CMA-SW	15C	S	0
C4_15C_S_P-CMA-SW	C4	P-CMA-SW	15C	S	0
C5_15C_S_P-CMA-SW	C5	P-CMA-SW	15C	S	0

C6_15C_S_P-CMA-SW	C6	P-CMA-SW	15C	S	0
C1_15C_T_P-CMA-SW	C1	P-CMA-SW	15C	T	6,274948121
C2_15C_T_P-CMA-SW	C2	P-CMA-SW	15C	T	0
C3_15C_T_P-CMA-SW	C3	P-CMA-SW	15C	T	0
C4_15C_T_P-CMA-SW	C4	P-CMA-SW	15C	T	9,012256669
C5_15C_T_P-CMA-SW	C5	P-CMA-SW	15C	T	0
C6_15C_T_P-CMA-SW	C6	P-CMA-SW	15C	T	0
C1_25C_S_CMA-SW	C1	CMA-SW	25C	S	3,522847559
C2_25C_S_CMA-SW	C2	CMA-SW	25C	S	1,54292415
C3_25C_S_CMA-SW	C3	CMA-SW	25C	S	8,355614973
C4_25C_S_CMA-SW	C4	CMA-SW	25C	S	24,2003367
C5_25C_S_CMA-SW	C5	CMA-SW	25C	S	4,395990856
C6_25C_S_CMA-SW	C6	CMA-SW	25C	S	0,470251867
C1_25C_T_CMA-SW	C1	CMA-SW	25C	T	37,64968873
C2_25C_T_CMA-SW	C2	CMA-SW	25C	T	9,169264625
C3_25C_T_CMA-SW	C3	CMA-SW	25C	T	159,1680815

C4_25C_T_CMA-SW	C4	CMA-SW	25C	T	27,03677001
C5_25C_T_CMA-SW	C5	CMA-SW	25C	T	51,77875244
C6_25C_T_CMA-SW	C6	CMA-SW	25C	T	28,06186081
C1_25C_S_CA-SW	C1	CA-SW	25C	S	0
C2_25C_S_CA-SW	C2	CA-SW	25C	S	3,0858483
C3_25C_S_CA-SW	C3	CA-SW	25C	S	0
C4_25C_S_CA-SW	C4	CA-SW	25C	S	4,734848485
C5_25C_S_CA-SW	C5	CA-SW	25C	S	17,09552
C6_25C_S_CA-SW	C6	CA-SW	25C	S	15,51831161
C1_25C_T_CA-SW	C1	CA-SW	25C	T	18,82484436
C2_25C_T_CA-SW	C2	CA-SW	25C	T	18,33852925
C3_25C_T_CA-SW	C3	CA-SW	25C	T	445,6706282
C4_25C_T_CA-SW	C4	CA-SW	25C	T	6,008171113
C5_25C_T_CA-SW	C5	CA-SW	25C	T	6,091617934
C6_25C_T_CA-SW	C6	CA-SW	25C	T	137,1913195
C1_25C_S_GA-SW	C1	GA-SW	25C	S	9,159403653
C2_25C_S_GA-SW	C2	GA-SW	25C	S	1,54292415
C3_25C_S_GA-SW	C3	GA-SW	25C	S	3,713606655
C4_25C_S_GA-SW	C4	GA-SW	25C	S	4,208754209
C5_25C_S_GA-SW	C5	GA-SW	25C	S	23,933728
C6_25C_S_GA-SW	C6	GA-SW	25C	S	2,821511201
C1_25C_T_GA-SW	C1	GA-SW	25C	T	37,64968873
C2_25C_T_GA-SW	C2	GA-SW	25C	T	36,6770585
C3_25C_T_GA-SW	C3	GA-SW	25C	T	233,4465195
C4_25C_T_GA-SW	C4	GA-SW	25C	T	21,02859889
C5_25C_T_GA-SW	C5	GA-SW	25C	T	54,8245614
C6_25C_T_GA-SW	C6	GA-SW	25C	T	34,29782988

C1_25C_S_P-CMA-SW	C1	P-CMA-SW	25C	S	1,409139024
C2_25C_S_P-CMA-SW	C2	P-CMA-SW	25C	S	11,3147771
C3_25C_S_P-CMA-SW	C3	P-CMA-SW	25C	S	25,06684492
C4_25C_S_P-CMA-SW	C4	P-CMA-SW	25C	S	1,578282828
C5_25C_S_P-CMA-SW	C5	P-CMA-SW	25C	S	1,465330285
C6_25C_S_P-CMA-SW	C6	P-CMA-SW	25C	S	0,470251867
C1_25C_T_P-CMA-SW	C1	P-CMA-SW	25C	T	6,274948121
C2_25C_T_P-CMA-SW	C2	P-CMA-SW	25C	T	9,169264625
C3_25C_T_P-CMA-SW	C3	P-CMA-SW	25C	T	201,6129032
C4_25C_T_P-CMA-SW	C4	P-CMA-SW	25C	T	18,02451334
C5_25C_T_P-CMA-SW	C5	P-CMA-SW	25C	T	57,87037037
C6_25C_T_P-CMA-SW	C6	P-CMA-SW	25C	T	18,70790721

Supplementary table 2 – The metabarcoding approaches

Primer sets

Primer pair	Forward primer	Reverse primer	Hibridization temperature	References
UnNonMet_18S_Cr	AAGTCTGGTGCCAGCASCC	TTTAAGTTTCAGCCTTGCGAT	63°C	Prioux et al. 2025
Universal_18S	CCAGCASCYGCGGTAATTCC	ACTTTCGTTCTTGATYRA	49°C	Stoeck et al. 2010
Fungi_18S	CGATAACGAACGAGACCT	ANCCATTCAATCGGTANT	48°C	Banos et al. 2018
ITS2	AACTTTYRRCAAYGGATCWCT	AGCCTCCGCTTATTGATATGCTTAART	58°C	Taylor et al. 2016

Blocking primers	Sequence (add 3' spacer)
BP_1	GTCGCTCCTACCGATTGA
BP_2	TTAACGAACGAGACCTCGA
BP_3	TCGCACCTACCGATTGAA
BP_4	GACCTTAACCTACTAAATAGTTA

Pipeline track

ITS2									Total reads	Reads fungi
sample.names	input	filtered	denoisedF	denoisedR	merged	nonchim	NonMet	Fungi		
C1-Ske	97790	14544	14501	14522	11133	10264				
C1-Tiss	71526	6885	6874	6875	5411	5406			37504	0
C2-Ske	90024	17101	17073	17070	13382	12414				
C2-Tiss	69678	12072	12062	12062	9426	9420				

Universal_18S									*In silico* PCR against PR2 database	
sample.names	input	filtered	denoisedF	denoisedR	concatenated	nonchim	NonMet	Fungi		
C1-Ske	71066	4717	4603	4466	4452	3411	147	0		
C1-Tiss	53577	20679	20374	20141	19952	15615	580	0		
C2-Ske	46577	15888	15340	14978	14901	11833	125	0		
C2-Tiss	54956	26694	26021	25987	25570	21212	367	0		
C3-Ske	70346	1058	907	866	858	729	27	0		
C3-Tiss	51955	21470	20750	20628	20200	16654	321	0	164547	41
C4-Ske	44339	21963	21702	21511	21383	18025	711	41		
C4-Tiss	31144	20786	20234	20097	19889	16238	573	0		
C5-Ske	55120	6745	6501	6453	6335	5481	136	0		
C5-Tiss	52103	33228	32734	32556	32277	24885	594	0		
C6-Ske	31250	15679	14936	14766	14438	11531	255	0		
C6-Tiss	36845	24406	23766	23756	23387	18933	719	0		
SW	27604	20088	19484	18561	18102	15089	11963	18		

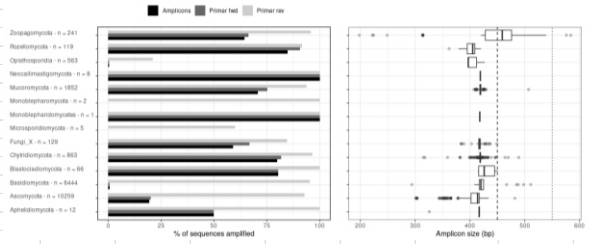

Fungi_18S									*In silico* PCR against PR2 database	
sample.names	input	filtered	denoisedF	denoisedR	merged	nonchim	NonMet	Fungi		
C1-Ske	95070	74994	74891	74844	71908	52174	0	0		
C1-Tiss	85830	68696	68640	68662	67205	58842	0	0		
C2-Ske	105194	68925	68866	68908	67323	61665	0	0		
C2-Tiss	92401	77716	77651	77572	75758	68453	0	0		
C3-Ske	84956	63402	63370	63362	61721	51266	0	0		
C3-Tiss	94427	75776	75682	75718	73382	53151	0	0	624764	0
C4-Ske	93138	70433	70370	70406	67903	57867	0	0		
C4-Tiss	65494	53291	53265	53226	52112	48035	2	0		
C5-Ske	90156	70111	70009	70086	65916	44612	0	0		
C5-Tiss	59152	48681	48652	48650	46682	39196	0	0		
C6-Ske	101677	81974	81870	81941	78672	55403	13	0		
C6-Tiss	79309	63535	63423	63475	59285	34100	0	0		
SW	86961	62916	61523	62409	59160	44358	15216	835		

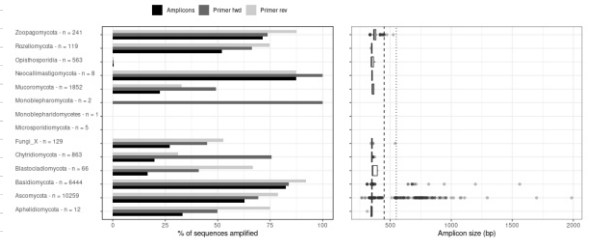

UnNonMet_18S_Cr									*In silico* PCR against PR2 database	
Sample	input	filtered	denoisedF	denoisedR	concatenated	nonchim	NonMet	Fungi		
C1-Ske	32475	22516	20585	19703	18229	13997	937	4		
C1-Tiss	23711	14414	14263	14147	14038	11324	394	3		
C2-Ske	30559	22132	21934	21857	21720	19799	61	35		
C2-Tiss	24841	17101	16357	15919	15314	12187	720	8		
C3-Ske	26804	19646	19435	19321	19166	17342	601	38		
C3-Tiss	25029	13474	13260	13147	13004	9821	945	2		
C4-Ske	22860	16110	15902	15773	15615	13881	1153	88	174416	240
C4-Tiss	31093	19424	19093	18887	18650	15812	427	47		
C5-Ske	17474	8278	7902	7884	7659	6115	5629	0		
C5-Tiss	21659	15903	15688	15580	15416	13413	848	15		
C6-Ske	24821	17716	17055	17005	16499	14079	1296	0		
C6-Tiss	24579	17551	17199	16989	16722	14112	1224	0		
SW	20937	15076	14573	14451	14064	12534	4332	29		

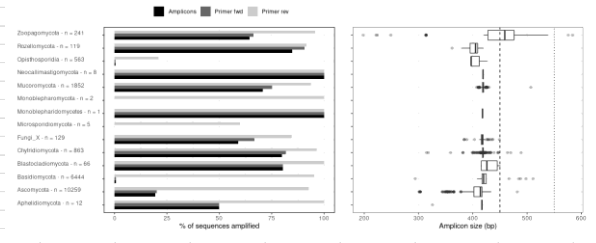

The taxonomic annotations are not available due to the large size of the tables.

Supplementary file 3 - Review on fungi species retrieved from other coral species

Octocorals	Hexacorals	References	Potential interest for corals hosts	Pathogenicity	Biotechnological application		
Cladiella krempfi, Sarcophyton tortuosum	*Favia gravida, Alythoa caribaeorum, Palythoa variabilis, Zoanthus sociatus, Porites lutea, Favites sp., Acropora sp., Galaxea fascicularis, Favia sp.*	Paulino et al. 2019, Zhang et al. 2019, Xu et al. 2018	Antifouling activity (Zhang et al. 2019)	Human (Kaur et al. 2023; Sandoval-Denis et al. 2015), plants (Pouralibaba et al. 2021)	Cytotoxicity (Wang et al. 2021), Biodegradation of polyester polyurethane (Zhang et al. 2022), antibacterial and cytotoxic activity (Sandrawati et al. 2020)		**Color code**
Cladiella krempfi and Sarcophyton tortuosum, Echinogorgia rebekka, Dichotella gemmacea, Gorgonia ventalina, Lepidisis	*Favia gravida, Alythoa caribaeorum, Palythoa variabilis, Zoanthus sociatus, Palythoa caribaeorum, Porites lutea*	Paulino et al. 2020, Zhang et al. 2019, Da Silva et al. 2008, Wang et al. 2011, Zhang et al. 2012, Toledo-Hernández et al. 2008, Marchese et al. 2021, Liu et al. 2021	Antioxidant capacity (Couttolenc et al. 2022), Antiangiogenic, wound healing and antioxidant activity (Hulikere et al. 2016), antimicrobial activity (Zhang et al. 2019, Zhang et al. 2021)	Pandas (Ma et al. 2013), humans (Sellart-Altisent et al. 2007; Gugnani et al. 2000)	Antiproliferative activity against cancer cell lines (Espinoza et al. 2021), Polyurethane degradation (Álvarez-Barragán et al. 2016)		In corals
Cladiella krempfi, Sarcophyton tortuosum, Echinogorgia rebekka, Muricella flexuosa, Gorgonia ventalina, Paralemnalia thyrsoides, Leptogorgia sp., Leptogorgia obscura	*Montastrea annularis, Porites spp.*	Zhang et al. 2019, Wang et al. 2011, Zhang et al. 2012, Toledo-Hernández et al. 2008, , Kendrick et al. 1982, Taher Mohie El-Dien et al. 2023, Liu et al. 2021, Soler-Hurtado et al. (2016)	Antimicrobial activity (Zhang et al. 2021)				In other marine organisms
				Mangroves (Liu et al. 2015)	Production of azaphilones (Fan et al. 2016), Synthesis of silver nanoparticles and their antioxidant, anticancer and nano-toxicological applications (Govindappa et al. 2020)		In a terrestrial organism
				Humans (Sandoval-Denis et al. 2015), Plants (Temperini et al. 2017; Chen et al. 2024)	Polyurethane degradation (Álvarez-Barragán et al. 2016)		Free-living (terrestrial or marine)
			Enhancement of plant biomass and antifungal activity against pathogens (González-Pérez et al. 2024)				
	Parantipathes sp., Bathypathes sp.	Marchese et al. 2021		Plants (Temperini et al. 2017; Hu 2023; Jang et al. 2013)			
Dichotella gemmacea, Echinogorgia aurantiaca, Subergorgia suberosa, Leptogorgia sp., Leptogorgia obscura	*Acropora cervicornis, Acropora humilis, Stylophora pistillata, Pavona clavus, Porites astreoides, Favites spp., Montipora spp., Stylophora pistillata, Acropora tenius*	Abd El-Rahman et al. 2020, Zhang et al. 2012, Wegley et al. 2007,Soler-Hurtado et al. (2016)	Antimicrobial activity (Abd El-Rahman et al. 2020)	Humans (Latgé et al. 1999, 2019)	Polyurethane degradation (Álvarez-Barragán et al. 2016)		
Cladiella krempfi, Sarcophyton tortuosum, Dichotella gemmacea ,Echinogorgia rebekka, Melitodes squamata, Subergorgia suberosa, Verrucella umbraculum, Gorgonia ventalina, Hemicorallium imperiale, Carijoa sp.	*Favia gravida, Alythoa caribaeorum, Palythoa variabilis, Zoanthus sociatus, Porites lutea, Favites sp., Acropora sp., Galaxea fascicularis, Favia sp., Favia speciosa, Porites pukoensis, Montastraea annularis, Sidrastrea siderea, Stephanocoenia intersepta, Acropora spp., Acropora hyacinthus, Goniastrea retiformis, Porites autralensis*	Paulino et al. 2019, Zhang et al. 2019, Dong et al. 2024, Li et al. 2014, Wang et al. 2011, Zhang et al. 2012, Rongen et al. 2018, Toledo-Hernández et al. 2008, El-Morsy et al. 2017, Dong et al. 2023, Kendrick et al. 1982, Hou et al. 2017	Cytotoxicity, radical-scavenging activity and antimicrobial activity (Zhuang et al. 2011; 2011; Zhang et al. 2019), Antifouling activity (Zhang et al. 2019), antioxidant activity (Chen et al. 2012), antibacterial activity and inhibitory effects against Vibrio harveyi and V. parahaemolyticus (Dong et al; 2023; Setyati et al. 2023)		Bioremoval of reactive dye and heavy metals (Taştan et al. 2010; Das et al. 2007; Bairagi et al. 2011), bioactive metabolites with cancer cell inhibitory activity (He et al. 2024), production of polyketides (Putri et al. 2015)		
Sinularia spp., Gorgonia ventalina		EL-Shahid et al. 2021, Putri et al. 2015, Toledo-Hernández et al. 2008	Antibacterial activity and inhibitory effects against Vibrio harveyi and V. parahaemolyticus (Setyati et al. 2023)		Anti-Osteoclastogenic and Antibacterial of produced polyketides (Zhang et al. 2022)		
Echinogorgia aurantiaca, Subergorgia suberosa	*Favia gravida, Alythoa caribaeorum, Palythoa variabilis, Zoanthus sociatus, Agaricia agaricites, Madracis mirabilis, Montastraea annularis, Montastraea cavernosa, Sidrastrea siderea, Stephanocoenia intersepta*	Paulino et al. 2019, Rongen et al. 2018					
Dichotella gemmacea, Echinogorgia aurantiaca, Melitodes squamata, Muricella flexuosa, Subergorgia suberosa, Verrucella umbraculum, Gorgonia ventalina, Leptogorgia sp., Leptogorgia obscura	*Favia gravida, Alythoa caribaeorum, Palythoa variabilis, Zoanthus sociatus, Oculina arbuscula, Montastraea annularis, Sidrastrea siderea, Stephanocoenia intersepta, Porites lutea, Favites sp., Acropora sp., Galaxea fascicularis, Favia sp., Porites porites, Acropora palmata*	Paulino et al. 2019, Abd El-Rahman et al. 2020, Zhang et al. 2012, Rongen et al. 2018, Toledo-Hernández et al. 2008, Kendrick et al. 1982, Xu et al. 2018, Soler-Hurtado et al. (2016)		Leptogorgia sp. and Leptogorgia obscura (Soler-Hurtado et al. 2016), Gorgonia spp. (Alker et al. 2001; Kim et al. 2015)	Antibacterial and cytotoxic activity (Sandrawati et al. 2020)		
Gorgonia ventalina, Muricella abnormalis		Toledo-Hernández et al. 2008, Chen et al. 2013	Production of polysaccharides (Chen et al. 2013), production of antimicrobial aromatic polyketides (Wang et al. 2012)				
	Favia gravida, Alythoa caribaeorum, Palythoa variabilis, Zoanthus sociatus	Paulino et al. 2019			Inhibition of the proliferation of cancer cells (Wu et al. 2024)		
Unknown coral	*Unknown coral*	Ying et al. 2023;2023	Antibacterial counpounds (Ying et al. 2023;2023) including rubensteroid exhibiting strong antibacterial activity against E. coli and Vibrio parahaemolyticus				

Supplementary file 4 – Statistical tests

Kruskal-Wallis statistical tests

> kruskal.test(Number of isolates ~ Isolation_temperature)
Kruskal-Wallis chi-squared = 2.693, df = 1, p-value = 0.1008

> kruskal.test(Number of isolates ~ Media)
Kruskal-Wallis chi-squared = 4.8417, df = 3, p-value = 0.1838

> kruskal.test(Number of isolates ~ Tissue)
Kruskal-Wallis chi-squared = 0.58382, df = 1, p-value = 0.4448

Differences in fungal community

PERMANOVA with 999 permutations

adonis2(formula = distance matrix (Bray-Curtis)~ Isolation temperature + Tissue + Media)

	Df	SumOfSqs	R2	F	Pr(>F)
Isolation temperature	1	0.6432	0.02209	1.4562	0.052
Tissue	1	1.2808	0.04399	2.8998	0.001
Media	3	1.1307	0.03884	0.8533	0.818
Residual	59	26.0599	0.89508		
Total	64	29.1146	1.00000		

Appendix 5 – Chapter 4

Tables S4, S10 and S11 are not available due to the large size of the tables but all supplementary information of this chapter can be found on the web version of the paper following this link :

https://microbiomejournal.biomedcentral.com/articles/10.1186/s40168-023-01711-x#citeas

Table S1: Percentage of colonies affected by the marine heatwaves of 2022 at the different sites. A colony was considered as affected when tissue loss represented at least 10% of the colony surface area.

Location (depth)	Mean (%)	Standard error	Number of surveys	Species
Boulegeade (25 m)	33,27642	7,108195543	2	*C.rubrum*
Grotte à corail (16 m)	83,19328	NA	1	*C.rubrum*
Pharillons (23 m)	50,54945	6,593406593	2	*C.rubrum*
Riou Sud (28 m)	13,46154	NA	1	*C.rubrum*
Impérial du large (15m)	68,51948	12,84428887	5	*P.clavata*
Ile verte (30 m)	75,2	16,49969697	5	*P.clavata*
Pharillons (23 m)	100	0	3	*P.clavata*
Average % P.clavata - all sites	81,23983			
Average % C.rubrum - all sites	45,12017			

Table S2: DNA concentration of the samples and sequencing libraries, read number and length obtained from each library

Sample	Sample Concentration [ng/uL]	Library Concentration [ng/uL]	Sequencing	Number of Sequencing Reads	Read Length [bp]
50_Pc_Iv	57,4 ng/uL	0 ng/uL	-	-	-
51_Pc_Iv	19 ng/uL	0 ng/uL	-	-	-
52_Pc_Iv	17,5 ng/uL	0,64 ng/uL	ok	104456	300
53_Pc_Iv	20,6 ng/uL	1,36 ng/uL	ok	178142	300
54_Pc_Iv	57,4 ng/uL	1,32 ng/uL	ok	123310	300
55_Pc_Iv	24,4 ng/uL	1,29 ng/uL	ok	159426	300
56_Pc_Iv	28 ng/uL	2,22 ng/uL	ok	184138	300
57_Pc_Iv	23,2 ng/uL	1,76 ng/uL	ok	123546	300
58_Pc_Iv	69,8 ng/uL	4,56 ng/uL	ok	199036	300
59_Pc_Iv	36,7 ng/uL	2,38 ng/uL	ok	172564	300
60_Pc_Iv	43,7 ng/uL	0,568 ng/uL	ok	89796	300
61_Pc_Iv	19,7 ng/uL	7,96 ng/uL	ok	226402	300
74_Pc_Pha	21,6 ng/uL	0,54 ng/uL	ok	42720	300
75_Pc_Pha	23,4 ng/uL	0,732 ng/uL	ok	156024	300
76_Pc_Pha	23,1 ng/uL	2,39 ng/uL	ok	183162	300
77_Pc_Pha	14,8 ng/uL	0 ng/uL	-	-	-
78_Pc_Pha	21,3 ng/uL	0 ng/uL	-	-	-
79_Pc_Pha	24,4 ng/uL	0 ng/uL	-	-	-
80_Pc_Pha	36,2 ng/uL	1,47 ng/uL	ok	193190	300
81_Pc_Pha	38,8 ng/uL	0,74 ng/uL	ok	140670	300
82_Pc_Pha	25,7 ng/uL	2,16 ng/uL	ok	141578	300
83_Pc_Pha	8,38 ng/uL	0,584 ng/uL	ok	107434	300
84_Pc_Pha	47,2 ng/uL	1,94 ng/uL	ok	194146	300
85_Pc_Pha	32 ng/uL	0,796 ng/uL	ok	116918	300
113_Pc_Idl	44,1 ng/uL	1,35 ng/uL	ok	188060	300
114_Pc_Idl	66,3 ng/uL	1,29 ng/uL	ok	163100	300
115_Pc_Idl	84,7 ng/uL	3,42 ng/uL	ok	175048	300

116_Pc_Idl	98,5 ng/uL	2,4 ng/uL	ok	139368	300
117_Pc_Idl	55,3 ng/uL	1,71 ng/uL	ok	104994	300
118_Pc_Idl	111 ng/uL	0,764 ng/uL	ok	130500	300
101_Pc_Idl	56,7 ng/uL	1,53 ng/uL	ok	148540	300
102_Pc_Idl	34 ng/uL	1,71 ng/uL	ok	128718	300
103_Pc_Idl	15,5 ng/uL	1,67 ng/uL	ok	175300	300
104_Pc_Idl	28,8 ng/uL	0,86 ng/uL	ok	145568	300
105_Pc_Idl	42,4 ng/uL	1,07 ng/uL	ok	157506	300
106_Pc_Idl	42,1 ng/uL	0 ng/uL	-	-	-
1_Cr_GaC	28,1 ng/uL	2,4 ng/uL	ok	114820	300
2_Cr_GaC	42,8 ng/uL	3,34 ng/uL	ok	168874	300
3_Cr_GaC	28,6 ng/uL	2,61 ng/uL	ok	178918	300
4_Cr_GaC	63 ng/uL	4,36 ng/uL	ok	130074	300
5_Cr_GaC	61,5 ng/uL	3,85 ng/uL	ok	163034	300
6_Cr_GaC	59,2 ng/uL	5,48 ng/uL	ok	205632	300
7_Cr_GaC	13,8 ng/uL	7,68 ng/uL	ok	216260	300
8_Cr_GaC	0 ng/uL	30,2 ng/uL	ok	212304	300
9_Cr_GaC	1,38 ng/uL	17,4 ng/uL	ok	177118	300
10_Cr_GaC	29,1 ng/uL	24,5 ng/uL	ok	206640	300
11_Cr_GaC	11,2 ng/uL	21 ng/uL	ok	191160	300
12_Cr_GaC	43,3 ng/uL	7,6 ng/uL	ok	182162	300
13_Cr_Pha	3,66 ng/uL	7,64 ng/uL	ok	219894	300
14_Cr_Pha	34,1 ng/uL	9,16 ng/uL	ok	193612	300
15_Cr_Pha	33,7 ng/uL	8,6 ng/uL	ok	198588	300
16_Cr_Pha	32,5 ng/uL	13,2 ng/uL	ok	258862	300
17_Cr_Pha	29,7 ng/uL	14,9 ng/uL	ok	119112	300
18_Cr_Pha	0 ng/uL	13,4 ng/uL	ok	208220	300
19_Cr_Pha	40,8 ng/uL	6,68 ng/uL	ok	171214	300
20_Cr_Pha	22,6 ng/uL	8,52 ng/uL	ok	160494	300

21_Cr_Pha	55,8 ng/uL	3,22 ng/uL	ok	171632	300
22_Cr_Pha	65,4 ng/uL	2,82 ng/uL	ok	176444	300
23_Cr_Pha	30 ng/uL	10,7 ng/uL	ok	210406	300
24_Cr_Pha	27,1 ng/uL	2,02 ng/uL	ok	198884	300
25_Cr_Riou	125 ng/uL	2,53 ng/uL	ok	104792	300
26_Cr_Riou	133 ng/uL	2,37 ng/uL	ok	195444	300
27_Cr_Riou	121 ng/uL	2,08 ng/uL	ok	178626	300
28_Cr_Riou	145 ng/uL	2,68 ng/uL	ok	153616	300
29_Cr_Riou	106 ng/uL	1,72 ng/uL	ok	181900	300
30_Cr_Riou	97,4 ng/uL	1,31 ng/uL	ok	178016	300
31_Cr_Riou	133 ng/uL	2,55 ng/uL	ok	194938	300
32_Cr_Riou	70 ng/uL	6,56 ng/uL	ok	264000	300
33_Cr_Riou	88,8 ng/uL	1,55 ng/uL	ok	45418	300
34_Cr_Riou	112 ng/uL	2,78 ng/uL	ok	170718	300
35_Cr_Riou	89,7 ng/uL	18,4 ng/uL	ok	260514	300
36_Cr_Riou	106 ng/uL	15,2 ng/uL	ok	159834	300
37_Cr_Blg	135 ng/uL	11 ng/uL	ok	239392	300
38_Cr_Blg	177 ng/uL	3,37 ng/uL	ok	174698	300
39_Cr_Blg	79,7 ng/uL	5,6 ng/uL	ok	201262	300
40_Cr_Blg	108 ng/uL	2,99 ng/uL	ok	168822	300
41_Cr_Blg	117 ng/uL	1,38 ng/uL	ok	103586	300
42_Cr_Blg	83,9 ng/uL	10 ng/uL	ok	158792	300
43_Cr_Blg	71,9 ng/uL	8,32 ng/uL	ok	216358	300
44_Cr_Blg	47,4 ng/uL	2,19 ng/uL	ok	137666	300
45_Cr_Blg	22,4 ng/uL	0 ng/uL	-	-	-
46_Cr_Blg	44 ng/uL	7,4 ng/uL	ok	231946	300
47_Cr_Blg	79,6 ng/uL	5,44 ng/uL	ok	180910	300
48_Cr_Blg	58,3 ng/uL	2,94 ng/uL	ok	168180	300
P1Para7_O	2,43 ng/uL	0 ng/uL	-	-	-

P1Para8_O	9,06 ng/uL	22,4 ng/uL	ok	172220	300
P1Para9_O	36,2 ng/uL	15,2 ng/uL	ok	198854	300
P1Para10_O	2,15 ng/uL	0 ng/uL	-	-	-
P1Para11_O	5,14 ng/uL	1,25 ng/uL	ok	136816	300
P1Para12_O	6,83 ng/uL	14,3 ng/uL	ok	124714	300
P3Para13	18,2 ng/uL	6,2 ng/uL	ok	176960	300
P3Para14	4,62 ng/uL	0 ng/uL	-	-	-
P3Para15	7,69 ng/uL	0 ng/uL	-	-	-
P3Para16	3,48 ng/uL	39 ng/uL	ok	197382	300
P3Para17	7,55 ng/uL	2,88 ng/uL	ok	141742	300
P3Para18	28 ng/uL	15,2 ng/uL	ok	217874	300
			Sum	14363708	
			Max	264000	
			Min	42720	

Table S3: Number of reads and sequences throughout the DADA2 pipeline for each sample.

Sample	Paired input reads	Paired filtered reads	Denoised forward reads	Denoised reverse reads	Merged sequences	Non-chimeric sequences
1-Cr-GaC	57410	32975	32263	32535	31465	30991
10-Cr-GaC	103320	60894	59288	59901	56794	54478
101-Pc-Idl	74270	45544	45277	45251	44757	43329
102-Pc-Idl	64359	31005	30878	30875	30222	29853
103-Pc-Idl	87650	50661	50508	50531	49748	48887
104-Pc-Idl	72784	40787	40689	40687	40075	38541
105-Pc-Idl	78753	47436	47320	47303	46000	45459
11-Cr-GaC	95580	54185	50993	52792	47124	46029
113-Pc-Idl	94030	51586	51091	51110	49337	48311
114-Pc-Idl	81550	48442	48355	48350	47140	46123
115-Pc-Idl	87524	56550	56478	56468	54955	54465
116-Pc-Idl	69684	44082	43980	44018	42758	42360
117-Pc-Idl	52497	28470	28420	28453	28185	28073
118-Pc-Idl	65250	38220	38073	38078	37463	35648
12-Cr-GaC	91081	40498	39189	39505	36817	36593
13-Cr-Pha	109947	57745	54373	55722	49828	48706
14-Cr-Pha	96806	56574	56043	56174	54864	47457
15-Cr-Pha	99294	59292	58031	58447	55930	55540
16-Cr-Pha	129431	78269	76984	77492	75011	74245
17-Cr-Pha	59556	31487	30341	31013	28809	27961
18-Cr-Pha	104110	54890	51064	53223	46478	45958
19-Cr-Pha	85607	50407	49543	49698	47982	47239
2-Cr-GaC	84437	53986	53798	53797	53436	52110
20-Cr-Pha	80247	43285	43129	43036	42867	42588
21-Cr-Pha	85816	50784	50656	50609	50390	49041
22-Cr-Pha	88222	52375	52263	52282	52042	50392

23-Cr-Pha	105203	64225	62698	63087	60146	59490
24-Cr-Pha	99442	64324	64196	64198	63832	63309
25-Cr-Riou	52396	29414	29297	29335	29084	28930
26-Cr-Riou	97722	61221	60940	61051	60633	59682
27-Cr-Riou	89313	52068	51934	51941	51633	50647
28-Cr-Riou	76808	41592	41508	41520	41113	40593
29-Cr-Riou	90950	52173	52008	52010	51817	50619
3-Cr-GaC	89459	56434	56049	56083	55411	54153
30-Cr-Riou	89008	54805	54703	54705	54484	53061
31-Cr-Riou	97469	56091	55596	55584	54180	53449
32-Cr-Riou	132000	75830	75439	75585	74947	74511
33-Cr-Riou	22709	9327	9165	9264	9014	9002
34-Cr-Riou	85359	54981	54740	54810	54459	53512
35-Cr-Riou	130257	80292	79093	79523	77493	75638
36-Cr-Riou	79917	41605	41186	41307	40645	40169
37-Cr-Blg	119696	76033	75941	75943	75771	75302
38-Cr-Blg	87349	54256	54150	54167	53288	52764
39-Cr-Blg	100631	62461	62375	62393	62159	61330
4-Cr-GaC	65037	30062	29931	29946	29829	29406
40-Cr-Blg	84411	52437	52302	52354	52104	51318
41-Cr-Blg	51793	28386	28277	28303	28136	27748
42-Cr-Blg	79396	50174	49955	49996	49625	48822
43-Cr-Blg	108179	69898	69622	69663	69078	67791
44-Cr-Blg	68833	21673	21399	21421	21256	20695
46-Cr-Blg	115973	71990	71740	71743	71052	70195
47-Cr-Blg	90455	51246	50636	50738	49705	48812
48-Cr-Blg	84090	47611	46758	46870	45077	43494
5-Cr-GaC	81517	52865	52682	52711	52321	51357
52-Pc-Iv	52228	31777	31726	31743	31428	30709

53-Pc-Iv	89071	54629	54445	54514	53279	52862
54-Pc-Iv	61655	33445	33308	33308	32941	32388
55-Pc-Iv	79713	47040	46960	46989	45902	44510
56-Pc-Iv	92069	55571	55353	55362	53641	52653
57-Pc-Iv	61773	27377	27105	27039	25914	25449
58-Pc-Iv	99518	57026	56030	56132	53947	52961
59-Pc-Iv	86282	47574	47406	47408	46880	41001
6-Cr-GaC	102816	61747	61462	61487	60757	59863
60-Pc-Iv	44898	26464	26366	26348	26086	25478
61-Pc-Iv	113201	57830	55691	56056	50537	50069
7-Cr-GaC	108130	62660	61559	61883	59464	58845
74-Pc-Pha	21360	10509	10434	10472	10261	10227
75-Pc-Pha	78012	47615	47575	47551	46596	45730
76-Pc-Pha	91581	58901	58829	58836	57082	56259
8-Cr-GaC	106152	61529	59041	59936	55458	54938
80-Pc-Pha	96595	61434	61338	61323	59307	59087
81-Pc-Pha	70335	43484	43349	43343	42117	41634
82-Pc-Pha	70789	39674	39019	39173	37506	37289
83-Pc-Pha	53717	32625	32558	32558	32419	31422
84-Pc-Pha	97073	60035	59864	59892	59056	58297
85-Pc-Pha	58459	30779	30668	30643	29701	29444
9-Cr-GaC	88559	42048	37627	39948	32681	32383
P1Para11-O	68408	42001	41958	41972	40924	40375
P1Para12-O	62357	34136	34071	34062	33131	32324
P1Para8-O	86110	52130	52050	52069	50724	48063
P1Para9-O	99427	57945	57858	57859	56321	55378
P3Para13	88480	47512	46209	46516	44376	43964
P3Para16	98691	58777	57624	58241	53479	47574
P3Para17	70871	35674	35374	35489	35002	34759

P3Para18	108937	58387	55932	56815	51434	47570

Table S5: Metadata

Sample	Coral_species	Site	Condition (% of tissue loss)	Type	Mission
1-Cr-GaC-S-N0348-16SV3V4	C.rubrum	Grotte_a_corail	0%	Coral	Septentrion
2-Cr-GaC-S-N0349-16SV3V4	C.rubrum	Grotte_a_corail	0%	Coral	Septentrion
3-Cr-GaC-S-N0350-16SV3V4	C.rubrum	Grotte_a_corail	0%	Coral	Septentrion
4-Cr-GaC-S-N0351-16SV3V4	C.rubrum	Grotte_a_corail	0%	Coral	Septentrion
5-Cr-GaC-S-N0352-16SV3V4	C.rubrum	Grotte_a_corail	0%	Coral	Septentrion
6-Cr-GaC-S-N0353-16SV3V4	C.rubrum	Grotte_a_corail	0%	Coral	Septentrion
7-Cr-GaC-N-N0354-16SV3V4	C.rubrum	Grotte_a_corail	90%	Coral	Septentrion
8-Cr-GaC-N-N0355-16SV3V4	C.rubrum	Grotte_a_corail	90%	Coral	Septentrion
9-Cr-GaC-N-N0356-16SV3V4	C.rubrum	Grotte_a_corail	90%	Coral	Septentrion
10-Cr-GaC-N-N0357-16SV3V4	C.rubrum	Grotte_a_corail	90%	Coral	Septentrion
11-Cr-GaC-N-N0358-16SV3V4	C.rubrum	Grotte_a_corail	90%	Coral	Septentrion
12-Cr-GaC-N-N0359-16SV3V4	C.rubrum	Grotte_a_corail	90%	Coral	Septentrion
13-Cr-Pha-S-N0360-16SV3V4	C.rubrum	Pharillons	90%	Coral	Septentrion
14-Cr-Pha-S-N0361-16SV3V4	C.rubrum	Pharillons	90%	Coral	Septentrion
15-Cr-Pha-S-N0362-16SV3V4	C.rubrum	Pharillons	90%	Coral	Septentrion
16-Cr-Pha-S-N0363-16SV3V4	C.rubrum	Pharillons	90%	Coral	Septentrion
17-Cr-Pha-S-N0364-16SV3V4	C.rubrum	Pharillons	90%	Coral	Septentrion
18-Cr-Pha-S-N0365-16SV3V4	C.rubrum	Pharillons	90%	Coral	Septentrion
19-Cr-Pha-N-N0366-16SV3V4	C.rubrum	Pharillons	0%	Coral	Septentrion
20-Cr-Pha-N-N0367-16SV3V4	C.rubrum	Pharillons	0%	Coral	Septentrion
21-Cr-Pha-N-N0368-16SV3V4	C.rubrum	Pharillons	0%	Coral	Septentrion
22-Cr-Pha-N-N0369-16SV3V4	C.rubrum	Pharillons	0%	Coral	Septentrion
23-Cr-Pha-N-N0370-16SV3V4	C.rubrum	Pharillons	0%	Coral	Septentrion
24-Cr-Pha-N-N0371-16SV3V4	C.rubrum	Pharillons	0%	Coral	Septentrion
25-Cr-Riou-S-N0372-16SV3V4	C.rubrum	Riou_Sud	0%	Coral	Septentrion
26-Cr-Riou-S-N0373-16SV3V4	C.rubrum	Riou_Sud	0%	Coral	Septentrion
27-Cr-Riou-S-N0374-16SV3V4	C.rubrum	Riou_Sud	0%	Coral	Septentrion

28-Cr-Riou-S-N0375-16SV3V4	C.rubrum	Riou_Sud	0%	Coral	Septentrion
29-Cr-Riou-S-N0376-16SV3V4	C.rubrum	Riou_Sud	0%	Coral	Septentrion
30-Cr-Riou-S-N0377-16SV3V4	C.rubrum	Riou_Sud	0%	Coral	Septentrion
31-Cr-Riou-N-N0378-16SV3V4	C.rubrum	Riou_Sud	90%	Coral	Septentrion
32-Cr-Riou-N-N0379-16SV3V4	C.rubrum	Riou_Sud	90%	Coral	Septentrion
33-Cr-Riou-N-N0380-16SV3V4	C.rubrum	Riou_Sud	90%	Coral	Septentrion
34-Cr-Riou-N-N0381-16SV3V4	C.rubrum	Riou_Sud	90%	Coral	Septentrion
35-Cr-Riou-N-N0382-16SV3V4	C.rubrum	Riou_Sud	90%	Coral	Septentrion
36-Cr-Riou-N-N0383-16SV3V4	C.rubrum	Riou_Sud	90%	Coral	Septentrion
37-Cr-Blg-S-N0384-16SV3V4	C.rubrum	Boulegeade	0%	Coral	Septentrion
38-Cr-Blg-S-N0385-16SV3V4	C.rubrum	Boulegeade	0%	Coral	Septentrion
39-Cr-Blg-S-N0386-16SV3V4	C.rubrum	Boulegeade	0%	Coral	Septentrion
40-Cr-Blg-S-N0387-16SV3V4	C.rubrum	Boulegeade	0%	Coral	Septentrion
41-Cr-Blg-S-N0388-16SV3V4	C.rubrum	Boulegeade	0%	Coral	Septentrion
42-Cr-Blg-S-N0389-16SV3V4	C.rubrum	Boulegeade	0%	Coral	Septentrion
43-Cr-Blg-N-N0390-16SV3V4	C.rubrum	Boulegeade	90%	Coral	Septentrion
44-Cr-Blg-N-N0391-16SV3V4	C.rubrum	Boulegeade	90%	Coral	Septentrion
46-Cr-Blg-N-N0393-16SV3V4	C.rubrum	Boulegeade	90%	Coral	Septentrion
47-Cr-Blg-N-N0394-16SV3V4	C.rubrum	Boulegeade	90%	Coral	Septentrion
48-Cr-Blg-N-N0395-16SV3V4	C.rubrum	Boulegeade	90%	Coral	Septentrion
52-Pc-Iv-S-N0314-16SV3V4	P.clavata	Ile_verte	0%	Coral	Septentrion
53-Pc-Iv-S-N0315-16SV3V4	P.clavata	Ile_verte	0%	Coral	Septentrion
54-Pc-Iv-S-N0316-16SV3V4	P.clavata	Ile_verte	0%	Coral	Septentrion
55-Pc-Iv-S-N0317-16SV3V4	P.clavata	Ile_verte	0%	Coral	Septentrion
56-Pc-Iv-N-N0318-16SV3V4	P.clavata	Ile_verte	90%	Coral	Septentrion
57-Pc-Iv-N-N0319-16SV3V4	P.clavata	Ile_verte	90%	Coral	Septentrion
58-Pc-Iv-N-N0320-16SV3V4	P.clavata	Ile_verte	90%	Coral	Septentrion
59-Pc-Iv-N-N0321-16SV3V4	P.clavata	Ile_verte	90%	Coral	Septentrion
60-Pc-Iv-N-N0322-16SV3V4	P.clavata	Ile_verte	90%	Coral	Septentrion

61-Pc-Iv-N-N0323-16SV3V4	P.clavata	Ile_verte	90%	Coral	Septentrion
74-Pc-Pha-S-N0324-16SV3V4	P.clavata	Pharillons	0%	Coral	Septentrion
75-Pc-Pha-S-N0325-16SV3V4	P.clavata	Pharillons	0%	Coral	Septentrion
76-Pc-Pha-S-N0326-16SV3V4	P.clavata	Pharillons	0%	Coral	Septentrion
80-Pc-Pha-N-N0330-16SV3V4	P.clavata	Pharillons	90%	Coral	Septentrion
81-Pc-Pha-N-N0331-16SV3V4	P.clavata	Pharillons	90%	Coral	Septentrion
82-Pc-Pha-N-N0332-16SV3V4	P.clavata	Pharillons	90%	Coral	Septentrion
83-Pc-Pha-N-N0333-16SV3V4	P.clavata	Pharillons	90%	Coral	Septentrion
84-Pc-Pha-N-N0334-16SV3V4	P.clavata	Pharillons	90%	Coral	Septentrion
85-Pc-Pha-N-N0335-16SV3V4	P.clavata	Pharillons	90%	Coral	Septentrion
101-Pc-Idl-N-N0342-16SV3V4	P.clavata	Imperial_du_Large	90%	Coral	Septentrion
102-Pc-Idl-N-N0343-16SV3V4	P.clavata	Imperial_du_Large	90%	Coral	Septentrion
103-Pc-Idl-N-N0344-16SV3V4	P.clavata	Imperial_du_Large	90%	Coral	Septentrion
104-Pc-Idl-N-N0345-16SV3V4	P.clavata	Imperial_du_Large	90%	Coral	Septentrion
105-Pc-Idl-N-N0346-16SV3V4	P.clavata	Imperial_du_Large	90%	Coral	Septentrion
113-Pc-Idl-S-N0336-16SV3V4	P.clavata	Imperial_du_Large	0%	Coral	Septentrion
114-Pc-Idl-S-N0337-16SV3V4	P.clavata	Imperial_du_Large	0%	Coral	Septentrion
115-Pc-Idl-S-N0338-16SV3V4	P.clavata	Imperial_du_Large	0%	Coral	Septentrion
116-Pc-Idl-S-N0339-16SV3V4	P.clavata	Imperial_du_Large	0%	Coral	Septentrion
117-Pc-Idl-S-N0340-16SV3V4	P.clavata	Imperial_du_Large	0%	Coral	Septentrion
118-Pc-Idl-S-N0341-16SV3V4	P.clavata	Imperial_du_Large	0%	Coral	Septentrion
P1Para8-O-N0408-16SV3V4	P.clavata	Portofino	0%	Coral	Portofino
P1Para9-O-N0409-16SV3V4	P.clavata	Portofino	0%	Coral	Portofino
P1Para11-O-N0411-16SV3V4	P.clavata	Portofino	0%	Coral	Portofino
P1Para12-O-N0412-16SV3V4	P.clavata	Portofino	0%	Coral	Portofino
P3Para13-N-N0419-16SV3V4	P.clavata	Portofino	90%	Coral	Portofino
P3Para16-N-N0422-16SV3V4	P.clavata	Portofino	90%	Coral	Portofino
P3Para17-N-N0423-16SV3V4	P.clavata	Portofino	90%	Coral	Portofino
P3Para18-N-N0424-16SV3V4	P.clavata	Portofino	90%	Coral	Portofino

Table S6: Bacterial diversity data (observed richness, Shannon diversity) for each sample of C. rubrum and statistical tests

Table S7: Bacterial diversity data (observed richness, Shannon diversity) for each sample of P. clavata and statistical tests.

Coral_sample	Coral_species	Site	Condition	Mission	Observed	Shannon
101-Pc-Idl	P.clavata	Impérial du large	90%	Septentrion	540	3,09769731
102-Pc-Idl	P.clavata	Impérial du large	90%	Septentrion	237	2,83526014
103-Pc-Idl	P.clavata	Impérial du large	90%	Septentrion	518	3,75237232
104-Pc-Idl	P.clavata	Impérial du large	90%	Septentrion	370	3,09487485
105-Pc-Idl	P.clavata	Impérial du large	90%	Septentrion	288	1,5811763
113-Pc-Idl	P.clavata	Impérial du large	0%	Septentrion	968	4,09046981
114-Pc-Idl	P.clavata	Impérial du large	0%	Septentrion	167	1,49220923
115-Pc-Idl	P.clavata	Impérial du large	0%	Septentrion	111	0,54388448
116-Pc-Idl	P.clavata	Impérial du large	0%	Septentrion	126	1,0063955
117-Pc-Idl	P.clavata	Impérial du large	0%	Septentrion	105	1,01986099
118-Pc-Idl	P.clavata	Impérial du large	0%	Septentrion	141	2,40082597
52-Pc-Iv	P.clavata	Ile verte	0%	Septentrion	103	2,16694776
53-Pc-Iv	P.clavata	Ile verte	0%	Septentrion	199	1,80087923
54-Pc-Iv	P.clavata	Ile verte	0%	Septentrion	218	2,99983366
55-Pc-Iv	P.clavata	Ile verte	0%	Septentrion	105	1,79465493
56-Pc-Iv	P.clavata	Ile verte	90%	Septentrion	445	1,67968371
57-Pc-Iv	P.clavata	Ile verte	90%	Septentrion	484	2,66636196
58-Pc-Iv	P.clavata	Ile verte	90%	Septentrion	1240	3,24512505
59-Pc-Iv	P.clavata	Ile verte	90%	Septentrion	274	2,68890694
60-Pc-Iv	P.clavata	Ile verte	90%	Septentrion	280	2,74076477
61-Pc-Iv	P.clavata	Ile verte	90%	Septentrion	2045	6,07959198
74-Pc-Pha	P.clavata	Pharillons	0%	Septentrion	87	1,20049219
75-Pc-Pha	P.clavata	Pharillons	0%	Septentrion	149	2,17888028
76-Pc-Pha	P.clavata	Pharillons	0%	Septentrion	101	1,15808574
80-Pc-Pha	P.clavata	Pharillons	90%	Septentrion	179	1,07294114
81-Pc-Pha	P.clavata	Pharillons	90%	Septentrion	397	2,51698851
82-Pc-Pha	P.clavata	Pharillons	90%	Septentrion	958	3,80465633
83-Pc-Pha	P.clavata	Pharillons	90%	Septentrion	163	1,59884627
84-Pc-Pha	P.clavata	Pharillons	90%	Septentrion	218	1,44722769
85-Pc-Pha	P.clavata	Pharillons	90%	Septentrion	201	1,75043819
P1Para11-O	P.clavata	Portofino	0%	Portofino	39	0,93524185
P1Para12-O	P.clavata	Portofino	0%	Portofino	53	0,79877643
P1Para8-O	P.clavata	Portofino	0%	Portofino	54	0,88363899
P1Para9-O	P.clavata	Portofino	0%	Portofino	42	0,62853092
P3Para13	P.clavata	Portofino	90%	Portofino	1099	5,02574071
P3Para16	P.clavata	Portofino	90%	Portofino	326	3,9474249
P3Para17	P.clavata	Portofino	90%	Portofino	293	3,05862456
P3Para18	P.clavata	Portofino	90%	Portofino	684	4,19639388

GLM model with negative binomial distribution

glm.nb(formula = Observed ~ Condition + Site, data = RichnessPc, init.theta = 2.154093587, link = log)

Deviance Residuals:

Min	1Q	Median	3Q	Max
-1.4037	-0.8522	-0.5606	0.0614	3.2053

Coefficients:

	Estimate	Std. Error	z value	Pr(>|z|)
(Intercept)	5.23042	0.25564	20.460	< 2e-16
Condition90%	1.34466	0.22672	5.931	3.01e-09
SiteImperial_du_Large	0.03239	0.30054	0.108	0.9142
SitePharillons	-0.63885	0.31482	-2.029	0.0424
SitePortofino	-0.60373	0.32560	-1.854	0.0637

(Dispersion parameter for Negative Binomial(2.1541) family taken to be 1)

Null deviance: 74.057 on 37 degrees of freedom

Residual deviance: 40.708 on 33 degrees of freedom

AIC: 511.29

Number of Fisher Scoring iterations: 1

Theta: 2.154

Std. Err.: 0.465

Tukey test : Differences 0%/90% tissue loss between sites (only for the relevant comparisons)

contrast	estimate	SE	df	z.ratio	p.value
0% Ile_verte - 90% Ile_verte	-1,3446616	0,226721	Inf	-5,9308979	8,4133E-08
0% Imperial_du_Large - 90% Imperial_du_Large	-1,3446616	0,226721	Inf	-5,9308979	8,4133E-08
0% Pharillons - 90% Pharillons	-1,3446616	0,226721	Inf	-5,9308979	8,4133E-08
0% Portofino - 90% Portofino	-1,3446616	0,226721	Inf	-5,9308979	8,4133E-08
90% Imperial_du_Large - 90% Pharillons	0,6712428	0,311465	Inf	2,15511788	0,37938209
0% Ile_verte - 0% Pharillons	0,6388493	0,314815	Inf	2,0292836	0,46185176
90% Ile_verte - 90% Pharillons	0,6388493	0,314815	Inf	2,0292836	0,46185176
0% Imperial_du_Large - 0% Portofino	0,636126	0,318475	Inf	1,99741131	0,48353623
90% Imperial_du_Large - 90% Portofino	0,636126	0,318475	Inf	1,99741131	0,48353623
0% Ile_verte - 0% Portofino	0,6037325	0,325595	Inf	1,85424143	0,58264811
90% Ile_verte - 90% Portofino	0,6037325	0,325595	Inf	1,85424143	0,58264811
0% Ile_verte - 0% Imperial_du_Large	-0,0323935	0,300537	Inf	-0,1077853	0,99999999
90% Ile_verte - 90% Imperial_du_Large	-0,0323935	0,300537	Inf	-0,1077853	0,99999999
0% Pharillons - 0% Portofino	-0,0351168	0,335214	Inf	-0,1047592	0,99999999
90% Pharillons - 90% Portofino	-0,0351168	0,335214	Inf	-0,1047592	0,99999999

Table S8: Output of the PERMANOVA statistical tests.

C.rubrum

PERMANOVA on *C.rubrum* samples

vegan::adonis2(formula = aitchison_dists_Cr ~ Condition + Site, data = metadata, permutations = 9999)

Number of permutations: 9999

	Df	SumOfSqs	R2	F	Pr(>F)
Condition	1	24711	0.06356	3.2412	1,00E-04
Site	3	43354	0.11151	1.8955	1,00E-04
Residual	42	320205	0.82358		
Total	46	388799	1.00000		

Pairwise permanova for differences 0%/90% tissue loss between sites (only for the relevant comparisons)

pairs	SumOfSqs	F.Model	R2	pval	p.adj
Grotte_a_corail_0% vs Grotte_a_corail_90%	0,64769825	2,036106818	0,16916656	0,003	0,024
Grotte_a_corail_90% vs Riou_Sud_90%	0,71125678	2,592471821	0,20587474	0,003	0,024
Pharillons_90% vs Riou_Sud_90%	0,66463805	2,113744242	0,1744914	0,005	0,02666667
Riou_Sud_90% vs Boulegeade_90%	0,51312982	1,706636717	0,15939989	0,01	0,04
Grotte_a_corail_90% vs Pharillons_90%	0,50643803	1,517746808	0,13177463	0,016	0,048
Grotte_a_corail_90% vs Boulegeade_90%	0,47497996	1,474880642	0,14080167	0,018	0,048
Pharillons_90% vs Pharillons_0%	0,49202217	1,383155567	0,12150898	0,046	0,092
Boulegeade_0% vs Boulegeade_90%	0,47635556	1,526314659	0,14499991	0,043	0,092
Pharillons_90% vs Boulegeade_90%	0,45944787	1,25333051	0,12223643	0,066	0,11733333
Grotte_a_corail_0% vs Pharillons_0%	0,4216461	1,239577532	0,11028684	0,137	0,18215385
Grotte_a_corail_0% vs Boulegeade_0%	0,41812456	1,352496439	0,11913648	0,138	0,18215385
Pharillons_0% vs Boulegeade_0%	0,40714762	1,327568551	0,11719802	0,144	0,18215385
Riou_Sud_0% vs Riou_Sud_90%	0,41099697	1,26389825	0,11220789	0,148	0,18215385
Riou_Sud_0% vs Boulegeade_0%	0,34569776	1,030496496	0,09342249	0,425	0,48571429
Pharillons_0% vs Riou_Sud_0%	0,36543623	0,997179023	0,09067589	0,467	0,49813333
Grotte_a_corail_0% vs Riou_Sud_0%	0,35087641	0,951055846	0,08684604	0,624	0,624

P.clavata

PERMANOVA on *P.clavata* samples

vegan::adonis2(formula = aitchison_dists_Pc ~ Condition + Site, data = metadata, permutations = 9999)

Number of permutations: 9999

	Df	SumOfSqs	R2	F	Pr(>F)
Condition	1	8713	0.03816	1.5107	0.0024
Site	3	29093	0.12742	1.6815	0.0001
Residual	33	190323	0.83355		
Total	37	228327	1.00000		

Pairwise permanova for differences 0%/90% tissue loss between sites (only for the relevant comparisons)

pairs	SumOfSqs	F.Model	R2	pval	p.adj
Imperial_du_Large_90% vs Portofino_90%	0,09310786	9,321837932	0,57112673	0,0022	0,02112
Ile_verte_0% vs Portofino_0%	0,04771409	12,57341469	0,67695762	0,0062	0,02112
Pharillons_0% vs Portofino_0%	0,00690482	4,0551017	0,44782509	0,0036	0,02112
Pharillons_90% vs Portofino_90%	0,10456296	6,801524799	0,45951514	0,0066	0,02112
Portofino_0% vs Portofino_90%	0,25738288	207,417478	0,97188609	0,0058	0,02112
Imperial_du_Large_90% vs Imperial_du_Large_0%	0,05070389	4,41489188	0,3291038	0,0108	0,02468571
Ile_verte_90% vs Portofino_90%	0,08369136	4,771639924	0,37361216	0,0102	0,02468571
Imperial_du_Large_0% vs Ile_verte_0%	0,02618718	3,360155252	0,29578427	0,0146	0,02844444
Ile_verte_0% vs Pharillons_0%	0,02869667	4,787522543	0,48914549	0,016	0,02844444
Imperial_du_Large_0% vs Portofino_0%	0,00830252	1,624321342	0,16877256	0,0384	0,06144
Pharillons_0% vs Pharillons_90%	0,03209408	1,810943984	0,20553348	0,0498	0,07243636
Ile_verte_0% vs Ile_verte_90%	0,02165392	1,113037849	0,12213686	0,059	0,07866667
Imperial_du_Large_0% vs Pharillons_0%	0,00445453	0,64837347	0,08477273	0,1026	0,12627692
Imperial_du_Large_90% vs Pharillons_90%	0,00983042	0,493366986	0,05196965	0,1164	0,13302857
Ile_verte_90% vs Pharillons_90%	0,00887664	0,355457728	0,03432564	0,1274	0,13589333
Imperial_du_Large_90% vs Ile_verte_90%	0,00490599	0,224526436	0,02434016	0,1588	0,1588

Table S9: Output of the Beta-dispersion tests.

Dataset	Test Dispersion	Details	Df	SumOfSqs	Mean Sq	F value	Pr(>F)
C.rubrum	0%/90%	Groups	1	0.00595	0.0059525	0.2544	0.6164
		Residuals	45	1.05272	0.0233938		
P.clavata	0%/90%	Groups	1	0.18258	0.182579	9.2621	0.004352
		Residuals	36	0.70965	0.019713		

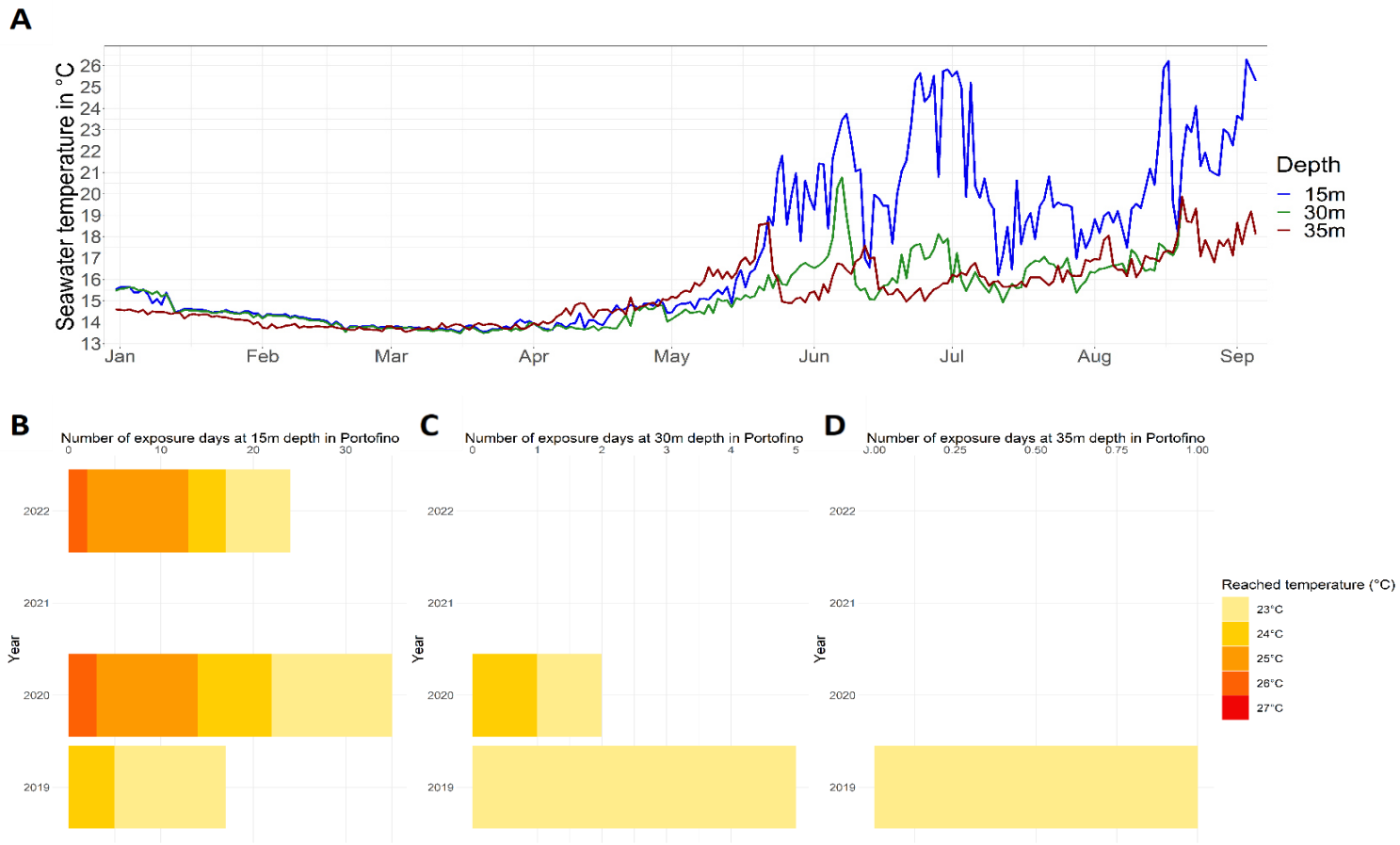

Figure S1: Temperature regime in 2022 and in the past twenty years in Portofino. Seawater temperature at 15 m, 30 m, and 35 m depth during the 2022 heatwaves (A), and number of exposure days at temperatures between 23°C and 27°C at 15 m (B), 30 m (C) and 35 m depth (D) over the past three years

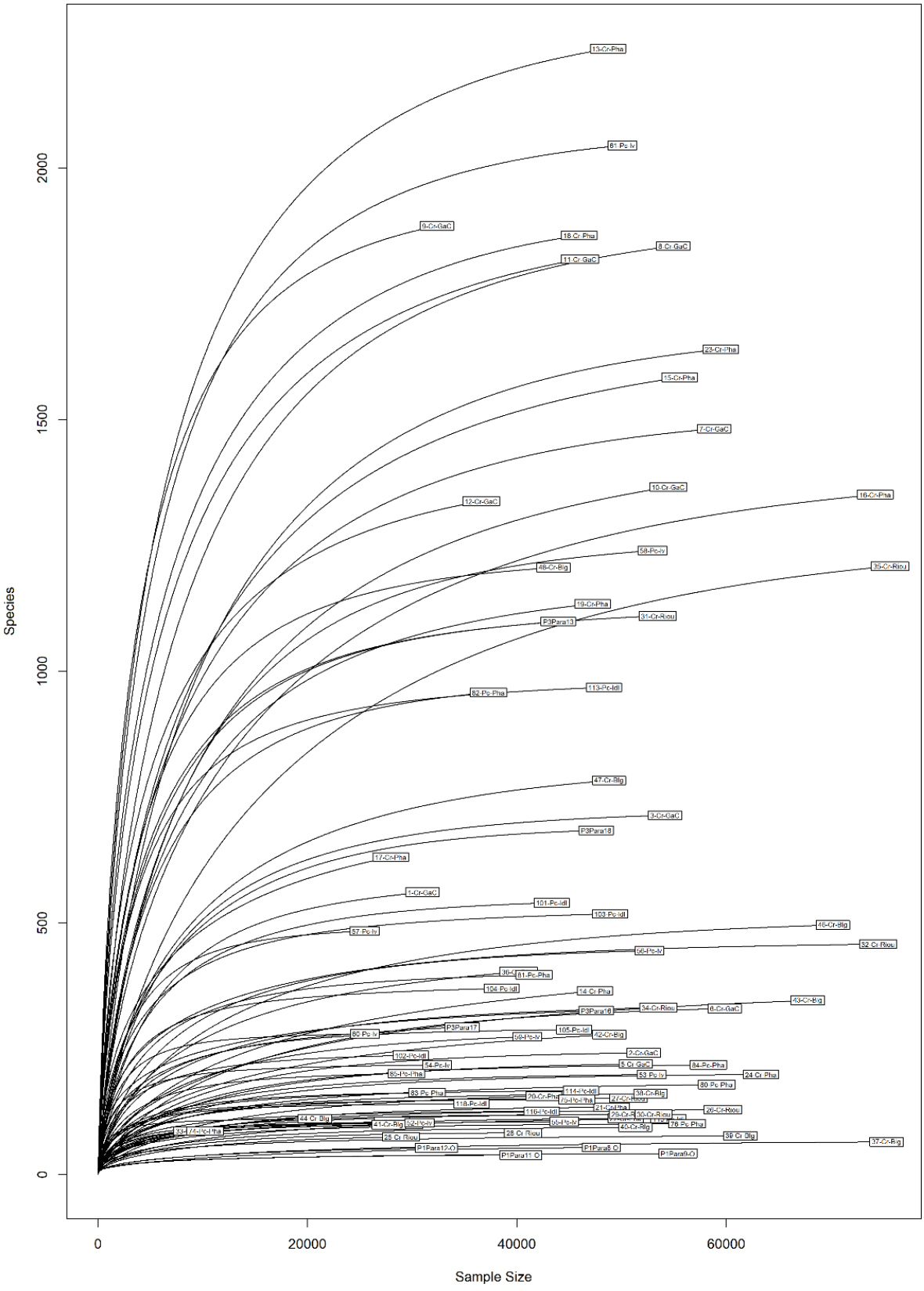

Figure S2: Rarefaction curves for all the samples of the two coral species.

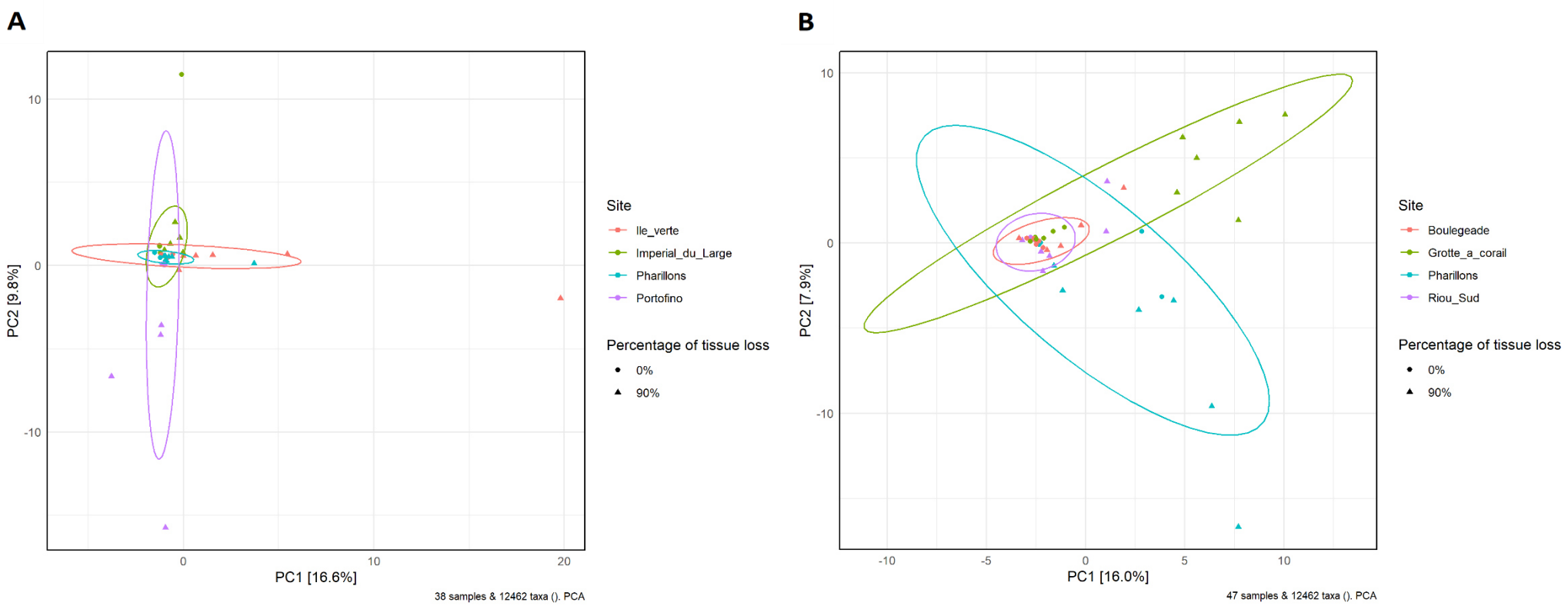

Figure S3: Principal component analysis of the Aitchison distance matrix based on the composition of the bacterial community (ASV level) associated with *P.clavata* (A) and *C. rubrum* (B) grouped according to the site and health state of the corals.

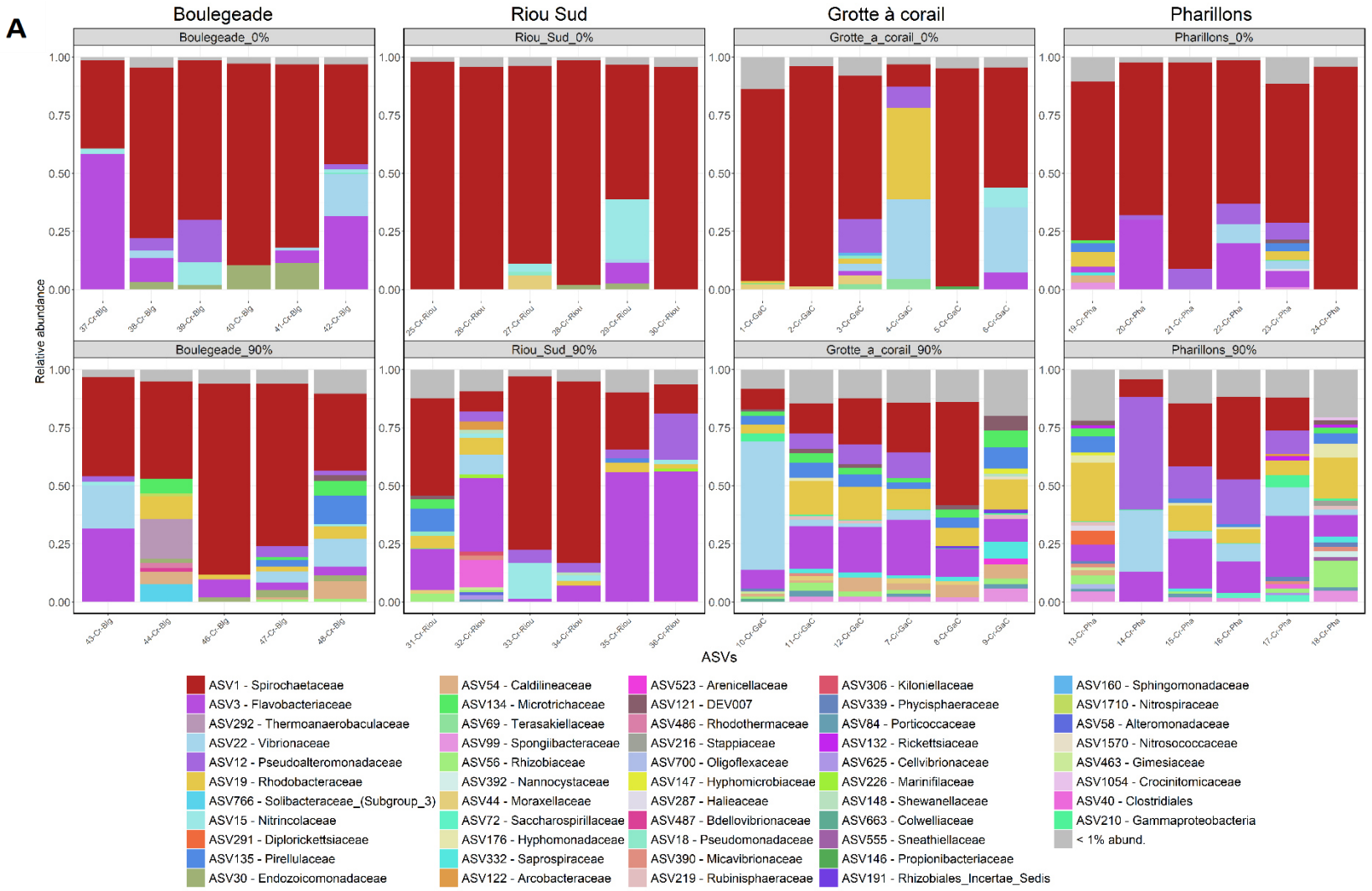
A
Boulegeade
Riou Sud
Grotte à corail
Pharillons
Boulegeade_0%
Riou_Sud_0%
Grotte_a_corail_0%
Pharillons_0%
Boulegeade_90%
Riou_Sud_90%
Grotte_a_corail_90%
Pharillons_90%
Relative abundance
1.00
0.75
0.50
0.25
0.00
37-Cr-Blg
38-Cr-Blg
39-Cr-Blg
40-Cr-Blg
41-Cr-Blg
42-Cr-Blg
25-Cr-Riou
26-Cr-Riou
27-Cr-Riou
28-Cr-Riou
29-Cr-Riou
30-Cr-Riou
1-Cr-GaC
2-Cr-GaC
3-Cr-GaC
4-Cr-GaC
5-Cr-GaC
6-Cr-GaC
19-Cr-Pha
20-Cr-Pha
21-Cr-Pha
22-Cr-Pha
23-Cr-Pha
24-Cr-Pha
43-Cr-Blg
44-Cr-Blg
46-Cr-Blg
47-Cr-Blg
48-Cr-Blg
31-Cr-Riou
32-Cr-Riou
33-Cr-Riou
34-Cr-Riou
35-Cr-Riou
36-Cr-Riou
10-Cr-GaC
11-Cr-GaC
12-Cr-GaC
7-Cr-GaC
8-Cr-GaC
9-Cr-GaC
13-Cr-Pha
14-Cr-Pha
15-Cr-Pha
16-Cr-Pha
17-Cr-Pha
18-Cr-Pha
ASVs
ASV1 - Spirochaetaceae
ASV3 - Flavobacteriaceae
ASV292 - Thermoanaerobaculaceae
ASV22 - Vibrionaceae
ASV12 - Pseudoalteromonadaceae
ASV19 - Rhodobacteraceae
ASV766 - Solibacteraceae_(Subgroup_3)
ASV15 - Nitrincolaceae
ASV291 - Diplorickettsiaceae
ASV135 - Pirellulaceae
ASV30 - Endozoicomonadaceae
ASV54 - Caldilineaceae
ASV134 - Microtrichaceae
ASV69 - Terasakiellaceae
ASV99 - Spongiibacteraceae
ASV56 - Rhizobiaceae
ASV392 - Nannocystaceae
ASV44 - Moraxellaceae
ASV72 - Saccharospirillaceae
ASV176 - Hyphomonadaceae
ASV332 - Saprospiraceae
ASV122 - Arcobacteraceae
ASV523 - Arenicellaceae
ASV121 - DEV007
ASV486 - Rhodothermaceae
ASV216 - Stappiaceae
ASV700 - Oligoflexaceae
ASV147 - Hyphomicrobiaceae
ASV287 - Halieaceae
ASV487 - Bdellovibrionaceae
ASV18 - Pseudomonadaceae
ASV390 - Micavibrionaceae
ASV219 - Rubinisphaeraceae
ASV306 - Kiloniellaceae
ASV339 - Phycisphaeraceae
ASV84 - Porticoccaceae
ASV132 - Rickettsiaceae
ASV625 - Cellvibrionaceae
ASV226 - Marinifilaceae
ASV148 - Shewanellaceae
ASV663 - Colwelliaceae
ASV555 - Sneathiellaceae
ASV146 - Propionibacteriaceae
ASV191 - Rhizobiales_Incertae_Sedis
ASV160 - Sphingomonadaceae
ASV1710 - Nitrospiraceae
ASV58 - Alteromonadaceae
ASV1570 - Nitrosococcaceae
ASV463 - Gimesiaceae
ASV1054 - Crocinitomicaceae
ASV40 - Clostridiales
ASV210 - Gammaproteobacteria
< 1% abund.

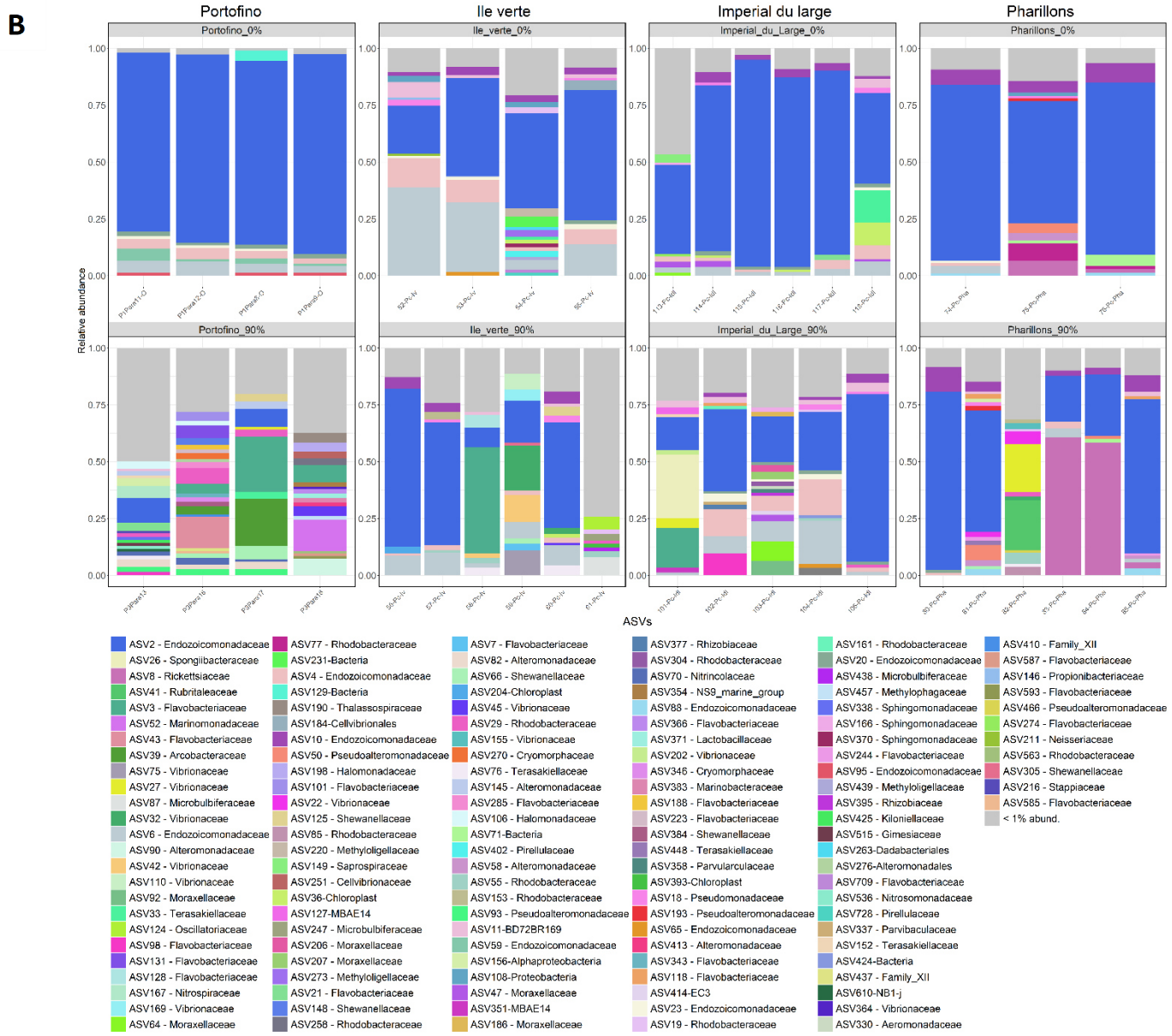

Figure S4: Relative abundance of all ASVs associated with *C. rubrum* (A) and *P. clavata* (B) depending on the samples, collection site and the colony health status based on the tissue loss percentage (0% and 90%).

Appendix 6 – Chapter 5

Supplementary file 1, 2 and 4 as well as tables S4, S5, S9 and S10 from supplementary file 3 are not available due to the large size of the tables but all supplementary information of this chapter can be found on the web version of the paper following this link :

https://academic.oup.com/ismecommun/article/5/1/ycaf035/8029725#supplementary-data

Table S1: Results of amplicons sequencing tests with universal primers of the 18S rRNA gene

Sequencing test	Samples	Total reads	Sequences Non-Met	Ratio Non-Met/Total reads
Universal 18S rRNA gene primers TAReuk454FWD1 (5'-CCAGCASCYGCGGTAATTCC-3') and TAReukREV3 (5'-ACTTTCGTTCTTGATYRA-3')	Cr1	70639	15	0,0002
	Cr2	65262	41	0,0006
	Cr3	74492	45	0,0006
	Cr4	71478	16	0,0002
UnNonMet universal primers from del Campo et al. 2019 : 616*F_MiSeq (5'-TTAAARVGYTCGTAGTYG-3') and UNonMet_DB_R (5'-CTTTAARTTTCASYCTTGCG-3')	Cr1	67607	267	0,0039
	Cr2	33514	389	0,0116
	Cr3	51530	4205	0,0816

Table S2: DNA concentration of the samples and sequencing libraries, read number and length obtained from each library

Sample	Sample Concentration [ng/uL]	Library Concentration [ng/uL]	Sequencing	Number of Sequencing Reads	Read Length [bp]
1_Cr_GaC	6	32,3 ng/uL	ok	64174	300
2_Cr_GaC	4,54	31,1 ng/uL	ok	135644	300
3_Cr_GaC	6,73	18,1 ng/uL	ok	114564	300
4_Cr_GaC	7,8	31,8 ng/uL	ok	66928	300
5_Cr_GaC	6,73	42 ng/uL	ok	98260	300
6_Cr_GaC	7,07	36,2 ng/uL	ok	97088	300
7_Cr_GaC	7,27	38,2 ng/uL	ok	108222	300
8_Cr_GaC	9,33	32,8 ng/uL	ok	153314	300
9_Cr_GaC	11,3	48,4 ng/uL	ok	57896	300
10_Cr_GaC	12,2	39 ng/uL	ok	122202	300
11_Cr_GaC	14,5	40,4 ng/uL	ok	114186	300
12_Cr_GaC	10,3	16,1 ng/uL	ok	93684	300
13_Cr_Pha	3,7	23,4 ng/uL	ok	82068	300
14_Cr_Pha	16	29,5 ng/uL	ok	85460	300
15_Cr_Pha	16,7	39,1 ng/uL	ok	94204	300
16_Cr_Pha	14,7	35,6 ng/uL	ok	93002	300
17_Cr_Pha	18,3	48,4 ng/uL	ok	62852	300
18_Cr_Pha	9,4	42 ng/uL	ok	97832	300
19_Cr_Pha	6,8	42 ng/uL	ok	91728	300
20_Cr_Pha	1,92	18,5 ng/uL	ok	70838	300
21_Cr_Pha	4,67	22,6 ng/uL	ok	75506	300
22_Cr_Pha	5,71	28,5 ng/uL	ok	82998	300
23_Cr_Pha	4,81	46 ng/uL	ok	122072	300
24_Cr_Pha	3,52	21,4 ng/uL	ok	105516	300
25_Cr_Riou	11,2	50,4 ng/uL	ok	99742	300
26_Cr_Riou	10,4	46 ng/uL	ok	98660	300

27_Cr_Riou	9,27	18,4 ng/uL	ok	86732	300
28_Cr_Riou	11,3	39,7 ng/uL	ok	79836	300
29_Cr_Riou	9	45,2 ng/uL	ok	75112	300
30_Cr_Riou	11,7	17,6 ng/uL	ok	126700	300
31_Cr_Riou	3,66	17 ng/uL	ok	118418	300
32_Cr_Riou	10	34,6 ng/uL	ok	93628	300
33_Cr_Riou	1,19	8,08 ng/uL	ok	54880	300
34_Cr_Riou	5,76	15,4 ng/uL	ok	95648	300
35_Cr_Riou	8,87	36,8 ng/uL	ok	104258	300
36_Cr_Riou	4,06	46,8 ng/uL	ok	82958	300
37_Cr_Blg	9,27	57,6 ng/uL	ok	149282	300
38_Cr_Blg	9,27	23,9 ng/uL	ok	90230	300
39_Cr_Blg	11,6	21,8 ng/uL	ok	88938	300
40_Cr_Blg	9,33	23,2 ng/uL	ok	101842	300
41_Cr_Blg	10,9	23,5 ng/uL	ok	61758	300
42_Cr_Blg	11,8	34,6 ng/uL	ok	103626	300
43_Cr_Blg	8	23,5 ng/uL	ok	94084	300
44_Cr_Blg	1,85	33,9 ng/uL	ok	109132	300
45_Cr_Blg	10,7	37,5 ng/uL	ok	94512	300
46_Cr_Blg	11,5	17,2 ng/uL	ok	88538	300
47_Cr_Blg	4,37	21,2 ng/uL	ok	103520	300
48_Cr_Blg	12,6	28,7 ng/uL	ok	132424	300
1_Cr_Bigo	7,13	41,6 ng/uL	ok	54508	300
2_Cr_Bigo	6,41	28,3 ng/uL	ok	115894	300
3_Cr_Bigo	9,07	42 ng/uL	ok	94224	300
4_Cr_Bigo	13	33,8 ng/uL	ok	98980	300
5_Cr_Bigo	8,33	36,6 ng/uL	ok	120720	300
6_Cr_Bigo	6,26	20,9 ng/uL	ok	138326	300
7_Cr_Torreta	4,19	14,1 ng/uL	ok	139196	300

8_Cr_Torreta	9,6	36 ng/uL	ok	140526	300
9_Cr_Torreta	6,13	28,4 ng/uL	ok	51974	300
10_Cr_Torreta	7,6	41,6 ng/uL	ok	77166	300
11_Cr_Torreta	0,103	0,972 ng/uL	ok	52406	300
12_Cr_Torreta	15,1	76 ng/uL	ok	74228	300
1_SW_Bigo	10,3	52,8 ng/uL	ok	125610	300
2_SW_Bigo	10,7	51,6 ng/uL	ok	123226	300
3_SW_Bigo	4,28	24,7 ng/uL	ok	114156	300
4_SW_Bigo	6,1	20,5 ng/uL	ok	110060	300
5_SW_Bigo	11,3	25,3 ng/uL	ok	66260	300
6_SW_Bigo	10,3	43,2 ng/uL	ok	135582	300
1_SW_Torreta	4,21	35,2 ng/uL	ok	143860	300
2_SW_Torreta	3,8	20 ng/uL	ok	94054	300
3_SW_Torreta	6,07	17,7 ng/uL	ok	116232	300
4_SW_Torreta	2,78	9,84 ng/uL	ok	124138	300
5_SW_Torreta	1,75	5,72 ng/uL	ok	137304	300
6_SW_Torreta	2,1	13,2 ng/uL	ok	116502	300
Neg_Septentrion	0	0,936 ng/uL	ok	1104	300
Neg_Portofino	0	4,6 ng/uL	ok	123664	300
1_Cr_Vlfc	1,13	13,1 ng/uL	ok	126094	300
2_Cr_Vlfc	18,3	53,6 ng/uL	ok	119142	300
3_Cr_Vlfc	17,6	48 ng/uL	ok	129206	300
4_Cr_Vlfc	3,61	24,7 ng/uL	ok	126936	300
5_Cr_Vlfc	8	5 ng/uL	ok	77086	300
Neg_Villefranche	0,001	Out of range	ok	6066	300
			Max sample	153314	
			Min samples	51974	
			Max negative	123664	

			Min negative	1104	
			Sum	7899126	

Table S3: Number of reads and sequences throughout the DADA2 pipeline for each sample.

					Concatenation				Merging			Only R1
Sample	**Paired input reads**	**Paired filtered reads**	**Denoised forward reads**	**Denoised reverse reads**	**Concatenated sequences**	**Non-chimeric sequences**	**Sequences Non-Met**	**Ratio Non-Met/Total reads**	**merged**	**nonchim**	**merge_ratio**	**nonchim**
1_Cr_GaC	31149	17860	17779	17796	17733	16627	2592	0,155891021	2324	2294	7	17416
10_Cr_GaC	57778	33409	33065	33040	32739	30432	4595	0,150992376	6081,9	5904,6	10	32776
11_Cr_GaC	52873	29857	29445	29453	29102	26429	3184	0,120473722	6192	6002,1	11	29145
12_Cr_GaC	45937	21248	20922	20986	20717	18433	1197	0,064937883	4144,5	4049,4	9	20366
13_Cr_Pha	31589	16542	16232	16316	16070	15414	4393	0,285000649	3089,7	3033,3	10	16118
14_Cr_Pha	33915	19095	18917	18963	18812	17802	4341	0,243849006	2503,8	2486,1	7	18597
15_Cr_Pha	37803	21972	21584	21616	21296	19492	5932	0,304329982	3288	3218,1	9	21261
16_Cr_Pha	38383	21648	21284	21345	21049	19192	4657	0,242653189	3130,5	3051,9	8	20791
17_Cr_Pha	12414	5717	5452	5552	5348	4998	1382	0,276510604	903,6	896,7	7	5402
18_Cr_Pha	41201	23096	22489	22642	22129	20019	4088	0,204206004	4748,1	4599	11	22277
19_Cr_Pha	44815	27294	27050	27157	26942	25186	3104	0,123243072	3131,1	3068,1	7	26540
2_Cr_GaC	66812	43760	43614	43613	43486	38224	3691	0,096562369	1404	1395	2	41915
20_Cr_Pha	34410	17489	17443	17430	17400	16438	4724	0,287382893	2065	2052	6	17113
21_Cr_Pha	36867	21909	21838	21858	21802	20234	1086	0,053672037	2087	2004	5	21345
22_Cr_Pha	40958	26056	26018	26026	26000	24251	1391	0,057358459	1311	1305	3	25398
23_Cr_Pha	58126	35009	34458	34560	34141	31562	5940	0,188201001	16311	15929	27	33830
24_Cr_Pha	50868	31450	31391	31416	31365	29408	3610	0,122755713	5394	5364	11	30733
25_Cr_Riou	49548	14871	14360	14390	14122	11596	3737	0,322266299	1037	921	2	13463
26_Cr_Riou	47870	21801	21069	20997	20685	17643	5409	0,306580514	2596	2346	5	19864
27_Cr_Riou	42082	28280	28216	28230	28180	24972	5676	0,22729457	2227	2224	5	26686
28_Cr_Riou	39326	22034	21991	22001	21974	19358	2229	0,115146193	1361	1352	3	20679
29_Cr_Riou	37311	24402	24304	24340	24253	20516	5953	0,290163775	1096	1086	3	22660
3_Cr_GaC	55905	37064	36970	36998	36927	34316	6533	0,190377666	4917	4899	9	35873
30_Cr_Riou	62539	40089	39791	39784	39503	34040	9831	0,288807286	2853	2825	5	37714
31_Cr_Riou	58294	36570	36455	36458	36364	35187	4456	0,126637679	16875	16668	29	36067
32_Cr_Riou	36984	21987	21732	21891	21656	20230	8003	0,395600593	5754	5742	16	21306
33_Cr_Riou	25850	14855	14719	14781	14682	13984	3113	0,222611556	1052	1036	4	14454
34_Cr_Riou	45490	29845	29742	29805	29714	26848	2768	0,103098927	5529	5486	12	28396
35_Cr_Riou	49819	29656	29171	29327	28907	25567	5551	0,217115813	13682	13253	27	28362
36_Cr_Riou	39522	19021	18812	18849	18678	17085	4589	0,268598186	7520	7396	19	18355
37_Cr_Blg	74360	12683	11804	11592	11269	8664	3243	0,374307479	1998	1635	2	10670
38_Cr_Blg	43022	27308	27247	27263	27215	23449	3061	0,130538616	2126	2122	5	25452
39_Cr_Blg	43094	29842	29783	29813	29763	26643	443	0,016627257	3406	3277	8	28199
4_Cr_GaC	32875	18425	18365	18378	18341	15448	783	0,050686173	1144	1138	3	17305
40_Cr_Blg	49651	33550	33493	33517	33469	30132	2662	0,088344617	2514	2510	5	32164
41_Cr_Blg	30529	16933	16732	16730	16636	13479	5551	0,411825803	688	675	2	15273
42_Cr_Blg	51222	33381	33319	33344	33288	30608	11074	0,361800836	1243	1241	2	32219
43_Cr_Blg	45983	29219	29099	29151	29046	27391	6685	0,244058267	4452	4433	10	28524

44_Cr_Blg	54074	20544	20320	20409	20202	17516	4204	0,240009135		13967	12582	23	18535
45_Cr_Blg	37564	20890	20576	20694	20428	18638	6290	0,337482563		7580	7427	20	20091
46_Cr_Blg	42241	24438	24260	24303	24145	21509	2062	0,095866846		4906	4775	11	23159
47_Cr_Blg	49334	30842	30697	30735	30621	27577	6270	0,227363383		7938	7855	16	29570
48_Cr_Blg	64257	37710	37507	37538	37348	34169	3589	0,105036729		18474	18029	28	36604
5_Cr_GaC	46969	29205	29148	29156	29108	26543	5451	0,20536488		3712	3681	8	28191
6_Cr_GaC	47769	30134	29887	30064	29831	25170	1501	0,059634485		2520	2510	5	28215
7_Cr_GaC	46089	28929	28807	28729	28632	26637	2498	0,09377933		12814	12622	27	28151
8_Cr_GaC	74276	44430	44144	44118	43866	41466	7514	0,181208701		25629	25155	34	43689
9_Cr_GaC	28489	13026	12477	12602	12173	10561	1841	0,174320614		6802	6483	23	12389
Neg_Portofino	59820	34476	34273	34307	34182	32855				4781	4749	8	33917
Neg_Septentrion	527	85	64	71	60	54				26	26	5	64
1_Cr_Bigo	27127	15399	15344	15372	15322	12883	1923	0,149266475		888	882	3	14028
10_Cr_Torreta	37117	22673	22619	22644	22596	20545	3310	0,161109759		1059	1054	3	21802
11_Cr_Torreta	24260	14309	13904	14131	13800	12656	1676	0,132427307		4077	3991	16	13617
12_Cr_Torreta	30762	12949	12564	12630	12307	10792	3572	0,330985915		4935	4790	16	12214
2_Cr_Bigo	57617	35524	35468	35429	35387	31506	10148	0,322097378		2124	2116	4	33779
3_Cr_Bigo	46868	27369	27292	27292	27230	23091	10400	0,450391928		775	774	2	25137
4_Cr_Bigo	49104	23803	23755	23734	23697	19640	757	0,038543788		921	921	2	21564
5_Cr_Bigo	55398	28876	28835	28816	28780	24651	10141	0,411382905		1270	1266	2	26580
6_Cr_Bigo	67288	39057	38479	38986	38422	34046	5427	0,159401986		914	912	1	36488
7_Cr_Torreta	68577	43474	42974	43440	42957	40249	3429	0,085194663		1607	1603	2	41664
8_Cr_Torreta	68763	43803	43659	43715	43582	38482	16474	0,428096253		1701	1700	2	40979
9_Cr_Torreta	25595	13729	13680	13695	13657	11978	4036	0,336951077		466	463	2	12850
1_SW_Bigo	61823	34214	32396	33420	31815	20483	8828	0,430991554		13316	11013	18	30674
2_SW_Bigo	60126	31933	30314	31309	29855	19879	9189	0,462246592		11884	10187	17	29088
3_SW_Bigo	54299	30053	28435	29365	27921	18129	10504	0,579403166		8166	7241	13	27704
4_SW_Bigo	54365	29967	28389	29283	27898	17994	8155	0,453206624		10934	9394	17	27245
5_SW_Bigo	32631	15391	14356	14994	14096	9390	4083	0,434824281		5863	4987	15	13742
6_SW_Bigo	66915	37302	35398	36560	34885	22688	10264	0,452397743		13783	11824	18	34050
1_SW_Torreta	70928	40002	38518	39366	38084	29777	12748	0,42811566		6356	6170	9	37717
2_SW_Torreta	46471	20846	19759	20362	19446	14325	9739	0,679860384		4077	4000	9	19620
3_SW_Torreta	57515	31992	30558	31368	30108	22037	14845	0,673639788		6885	6703	12	30278
4_SW_Torreta	61528	32280	30835	31574	30329	20675	14416	0,697267231		6212	5872	10	30334
5_SW_Torreta	68029	37814	36164	36986	35569	23859	14247	0,597133157		9657	9113	13	35522
6_SW_Torreta	57778	31270	29845	30589	29334	19934	12844	0,644326277		7238	6808	12	29345
1_Cr_Vlfc	62287	25111	25059	25048	25007	23800	4217	0,177184874		3841	3823	6	24790
2_Cr_Vlfc	59147	25393	25221	25184	25035	21357	9474	0,443601629		945	941	2	23608
3_Cr_Vlfc	64206	29895	29755	29749	29621	25158	10341	0,411042213		1078	1034	2	27836
4_Cr_Vlfc	62510	15614	15581	15503	15479	13790	5834	0,423060189		3618	3375	6	14679
5_Cr_Vlfc	38097	15387	15253	15208	15091	9807	1853	0,188946671		2169	2053	6	13150
Neg_Villefranche	2980	361	222	190	164	163				131	124	4	222

Table S6: Metadata

Samples	Sample_type	Origin	Sampling_site	Condition	Impact
1_Cr_GaC	Coral	Septentrion	Grotte à corail	0% tissue loss	Impacted
2_Cr_GaC	Coral	Septentrion	Grotte à corail	0% tissue loss	Impacted
3_Cr_GaC	Coral	Septentrion	Grotte à corail	0% tissue loss	Impacted
4_Cr_GaC	Coral	Septentrion	Grotte à corail	0% tissue loss	Impacted
5_Cr_GaC	Coral	Septentrion	Grotte à corail	0% tissue loss	Impacted
6_Cr_GaC	Coral	Septentrion	Grotte à corail	0% tissue loss	Impacted
7_Cr_GaC	Coral	Septentrion	Grotte à corail	90% tissue loss	Impacted
8_Cr_GaC	Coral	Septentrion	Grotte à corail	90% tissue loss	Impacted
9_Cr_GaC	Coral	Septentrion	Grotte à corail	90% tissue loss	Impacted
10_Cr_GaC	Coral	Septentrion	Grotte à corail	90% tissue loss	Impacted
11_Cr_GaC	Coral	Septentrion	Grotte à corail	90% tissue loss	Impacted
12_Cr_GaC	Coral	Septentrion	Grotte à corail	90% tissue loss	Impacted
13_Cr_Pha	Coral	Septentrion	Pharillons	90% tissue loss	Impacted
14_Cr_Pha	Coral	Septentrion	Pharillons	90% tissue loss	Impacted
15_Cr_Pha	Coral	Septentrion	Pharillons	90% tissue loss	Impacted
16_Cr_Pha	Coral	Septentrion	Pharillons	90% tissue loss	Impacted
17_Cr_Pha	Coral	Septentrion	Pharillons	90% tissue loss	Impacted
18_Cr_Pha	Coral	Septentrion	Pharillons	90% tissue loss	Impacted
19_Cr_Pha	Coral	Septentrion	Pharillons	0% tissue loss	Impacted
20_Cr_Pha	Coral	Septentrion	Pharillons	0% tissue loss	Impacted
21_Cr_Pha	Coral	Septentrion	Pharillons	0% tissue loss	Impacted
22_Cr_Pha	Coral	Septentrion	Pharillons	0% tissue loss	Impacted
23_Cr_Pha	Coral	Septentrion	Pharillons	0% tissue loss	Impacted
24_Cr_Pha	Coral	Septentrion	Pharillons	0% tissue loss	Impacted
25_Cr_Riou	Coral	Septentrion	Riou Sud	0% tissue loss	Impacted
26_Cr_Riou	Coral	Septentrion	Riou Sud	0% tissue loss	Impacted
27_Cr_Riou	Coral	Septentrion	Riou Sud	0% tissue loss	Impacted
28_Cr_Riou	Coral	Septentrion	Riou Sud	0% tissue loss	Impacted
29_Cr_Riou	Coral	Septentrion	Riou Sud	0% tissue loss	Impacted
30_Cr_Riou	Coral	Septentrion	Riou Sud	0% tissue loss	Impacted
31_Cr_Riou	Coral	Septentrion	Riou Sud	90% tissue loss	Impacted
32_Cr_Riou	Coral	Septentrion	Riou Sud	90% tissue loss	Impacted
33_Cr_Riou	Coral	Septentrion	Riou Sud	90% tissue loss	Impacted
34_Cr_Riou	Coral	Septentrion	Riou Sud	90% tissue loss	Impacted
35_Cr_Riou	Coral	Septentrion	Riou Sud	90% tissue loss	Impacted
36_Cr_Riou	Coral	Septentrion	Riou Sud	90% tissue loss	Impacted
37_Cr_Blg	Coral	Septentrion	Boulegeade	0% tissue loss	Impacted
38_Cr_Blg	Coral	Septentrion	Boulegeade	0% tissue loss	Impacted
39_Cr_Blg	Coral	Septentrion	Boulegeade	0% tissue loss	Impacted
40_Cr_Blg	Coral	Septentrion	Boulegeade	0% tissue loss	Impacted

41_Cr_Blg	Coral	Septentrion	Boulegeade	0% tissue loss	Impacted
42_Cr_Blg	Coral	Septentrion	Boulegeade	0% tissue loss	Impacted
43_Cr_Blg	Coral	Septentrion	Boulegeade	90% tissue loss	Impacted
44_Cr_Blg	Coral	Septentrion	Boulegeade	90% tissue loss	Impacted
45_Cr_Blg	Coral	Septentrion	Boulegeade	90% tissue loss	Impacted
46_Cr_Blg	Coral	Septentrion	Boulegeade	90% tissue loss	Impacted
47_Cr_Blg	Coral	Septentrion	Boulegeade	90% tissue loss	Impacted
48_Cr_Blg	Coral	Septentrion	Boulegeade	90% tissue loss	Impacted
1_Cr_Bigo	Coral	Portofino	Bigo	0% tissue loss	Control site
2_Cr_Bigo	Coral	Portofino	Bigo	0% tissue loss	Control site
3_Cr_Bigo	Coral	Portofino	Bigo	0% tissue loss	Control site
4_Cr_Bigo	Coral	Portofino	Bigo	0% tissue loss	Control site
5_Cr_Bigo	Coral	Portofino	Bigo	0% tissue loss	Control site
6_Cr_Bigo	Coral	Portofino	Bigo	0% tissue loss	Control site
7_Cr_Torreta	Coral	Portofino	Punta della Torreta	0% tissue loss	Impacted
8_Cr_Torreta	Coral	Portofino	Punta della Torreta	0% tissue loss	Impacted
9_Cr_Torreta	Coral	Portofino	Punta della Torreta	0% tissue loss	Impacted
10_Cr_Torreta	Coral	Portofino	Punta della Torreta	0% tissue loss	Impacted
11_Cr_Torreta	Coral	Portofino	Punta della Torreta	0% tissue loss	Impacted
12_Cr_Torreta	Coral	Portofino	Punta della Torreta	0% tissue loss	Impacted
1_SW_Bigo	SW	Portofino	Bigo	0% tissue loss	Control site
2_SW_Bigo	SW	Portofino	Bigo	0% tissue loss	Control site
3_SW_Bigo	SW	Portofino	Bigo	0% tissue loss	Control site
4_SW_Bigo	SW	Portofino	Bigo	0% tissue loss	Control site
5_SW_Bigo	SW	Portofino	Bigo	0% tissue loss	Control site
6_SW_Bigo	SW	Portofino	Bigo	0% tissue loss	Control site
1_SW_Torreta	SW	Portofino	Punta della Torreta	0% tissue loss	Impacted
2_SW_Torreta	SW	Portofino	Punta della Torreta	0% tissue loss	Impacted
3_SW_Torreta	SW	Portofino	Punta della Torreta	0% tissue loss	Impacted
4_SW_Torreta	SW	Portofino	Punta della Torreta	0% tissue loss	Impacted
5_SW_Torreta	SW	Portofino	Punta della Torreta	0% tissue loss	Impacted
6_SW_Torreta	SW	Portofino	Punta della Torreta	0% tissue loss	Impacted
Neg_Septentrion	Negative	Septentrion	Negative	Negative	Negative
Neg_Portofino	Negative	Portofino	Negative	Negative	Negative
1_Cr_Vlfc	Coral	Villefranche-sur-Mer	Villefranche-sur-Mer	0% tissue loss	Control site
2_Cr_Vlfc	Coral	Villefranche-sur-Mer	Villefranche-sur-Mer	0% tissue loss	Control site
3_Cr_Vlfc	Coral	Villefranche-sur-Mer	Villefranche-sur-Mer	0% tissue loss	Control site
4_Cr_Vlfc	Coral	Villefranche-sur-Mer	Villefranche-sur-Mer	0% tissue loss	Control site
5_Cr_Vlfc	Coral	Villefranche-sur-Mer	Villefranche-sur-Mer	0% tissue loss	Control site
Neg_Villefranche	Negative	Villefranche	Negative	Negative	Negative

Table S7: Microeukaryote diversity data (observed richness, Shannon diversity) for each sample of C. rubrum and statistical tests.

Differences in observed richness between coral samples from Portofino and seawater samples

GLM model with negative binomial distribution

glm.nb(formula = Observed ~ Sample_type, data = Richness, init.theta = 3.730140657, link = log)

Coefficients:	Estimate	Std. Error	z value	Pr(>|z|)
(Intercept)	4.6532	0.1227	37.92	<2e-16
Sample_type	2.4000	0.1714	14.00	<2e-16

(Dispersion parameter for Negative Binomial(5.8441) family taken to be 1)

Null deviance: 188.654 on 23 degrees of freedom

Residual deviance: 25.009 on 22 degrees of freedom

AIC: 310.81

Number of Fisher Scoring iterations: 1

Theta: 5.84

Std. Err.: 1.72

2 x log-likelihood: -304.81

Differences in observed richness between coral samples and seawater samples

GLM model with negative binomial distribution

glm.nb(formula = Observed ~ Sample_type, data = Richness, init.theta = 3.730140657, link = log)

Coefficients:	Estimate	Std. Error	z value	Pr(>|z|)
(Intercept)	4.75213	0.06525	72.83	<2e-16
Sample_type	2.30102	0.16331	14.09	<2e-16

(Dispersion parameter for Negative Binomial(3.7301) family taken to be 1)

Null deviance: 373.538 on 76 degrees of freedom

Residual deviance: 80.621 on 75 degrees of freedom

AIC: 897.73

Number of Fisher Scoring iterations: 1

Theta: 3.730

Std. Err.: 0.598

2 x log-likelihood: -891.730

Differences in observed richness between samples without tissue loss from the different sampling sites

GLM model with negative binomial distribution

glm.nb(formula = Observed_richness ~ Sampling_site, data =Richness, init.theta = 3.837888888, link = log)

Coefficients:	Estimate	Std. Error	z value	Pr(>|z|)
(Intercept)	4.1836	0.2349	17.813	< 2e-16
Sampling_siteBigo	0.1450	0.3175	0.457	0.64794
Sampling_siteBoulegeade	0.3782	0.2788	1.356	0.17501
Sampling_siteGrotte à corail	0.5664	0.2786	2.033	0.04201
Sampling_sitePharillons	0.8463	0.2782	3.042	0.00235
Sampling_siteRiou Sud	0.6910	0.2784	2.482	0.01307
Sampling_sitePunta della Torreta	0.7143	0.3160	2.261	0.02378

(Dispersion parameter for Negative Binomial(3.8379) family taken to be 1)

Null deviance: 82.565 on 64 degrees of freedom

Residual deviance: 67.618 on 58 degrees of freedom

AIC: 716.85

Number of Fisher Scoring iterations: 1

Theta: 3.838

Std. Err.: 0.672

2 x log-likelihood: -700.846

Tukey test : pairwise differences between sampling sites

contrast	estimate	SE	df	z.ratio	p.value
Villefranche-sur-Mer - Pharillons	-0,8463174	0,27824279	Inf	-3,0416509	0,03800483
Bigo - Pharillons	-0,7013552	0,26054316	Inf	-2,6918962	0,10021264
Villefranche-sur-Mer - Riou Sud	-0,6909853	0,2784073	Inf	-2,4819223	0,16575551
Villefranche-sur-Mer - Punta della Torreta	-0,7142641	0,31596075	Inf	-2,2606102	0,26339195
Boulegeade - Pharillons	-0,4681525	0,21175914	Inf	-2,2107782	0,28949537
Bigo - Riou Sud	-0,546023	0,26071885	Inf	-2,0942983	0,35592778
Villefranche-sur-Mer - Grotte à corail	-0,5664161	0,27855892	Inf	-2,0333798	0,39336275
Bigo - Punta della Torreta	-0,5693019	0,30049108	Inf	-1,8945716	0,48386479
Bigo - Grotte à corail	-0,4214538	0,26088074	Inf	-1,6155038	0,67230178
Boulegeade - Riou Sud	-0,3128204	0,21197526	Inf	-1,4757399	0,75943635
Villefranche-sur-Mer - Boulegeade	-0,3781649	0,27882685	Inf	-1,3562716	0,8249633
Grotte à corail - Pharillons	-0,2799013	0,21140623	Inf	-1,3239976	0,84091066
Boulegeade - Punta della Torreta	-0,3360992	0,25933392	Inf	-1,2960093	0,85408382
Bigo - Boulegeade	-0,2332027	0,26116681	Inf	-0,8929262	0,97373744
Boulegeade - Grotte à corail	-0,1882511	0,21217435	Inf	-0,8872474	0,97456774
Pharillons - Riou Sud	0,15533212	0,21120641	Inf	0,73545173	0,99040261
Grotte à corail - Riou Sud	-0,1245692	0,21162271	Inf	-0,5886382	0,99715175
Grotte à corail - Punta della Torreta	-0,147848	0,25904583	Inf	-0,5707408	0,99760237
Pharillons - Punta della Torreta	0,13205331	0,25870585	Inf	0,51043805	0,99872164
Villefranche-sur-Mer - Bigo	-0,1449623	0,31746688	Inf	-0,4566217	0,99932293
Riou Sud - Punta della Torreta	-0,0232788	0,25888279	Inf	-0,0899203	0,99999996

Differences in observed richness between samples with 0% and 90% tissue loss

GLM model with negative binomial distribution

glm.nb(formula = Observed ~ Condition + Sampling_site, data = Richness, init.theta = 4.782107885, link = log)

Coefficients:	**Estimate**	**Std. Error**	**z value**	**Pr(>|z|)**
(Intercept)	4.2847	0.1517	28.252	< 2e-16
Condition	0.4892	0.1348	3.630	0.000284
Sampling_siteGrotte à corail	0.1647	0.1912	0.861	0.389050
Sampling_sitePharillons	0.4733	0.1907	2.482	0.013054
Sampling_siteRiou Sud	0.3433	0.1909	1.799	0.072061

(Dispersion parameter for Negative Binomial(4.7821) family taken to be 1)

Null deviance: 69.226 on 47 degrees of freedom

Residual deviance: 49.817 on 43 degrees of freedom

AIC: 526.5

Number of Fisher Scoring iterations: 1

Theta: 4.782

Std. Err.: 0.994

Tukey test : pairwise differences between sampling sites

contrast	**estimate**	**SE**	**df**	**z.ratio**	**p.value**
Boulegeade 0% - Pharillons 90%	-0,9624388	0,23365158	Inf	-4,1191197	0,00099229
Boulegeade 0% - Boulegeade 90%	-0,4891662	0,13476437	Inf	-3,6297886	0,0068827
Grotte à corail 0% - Grotte à corail 90%	-0,4891662	0,13476437	Inf	-3,6297886	0,0068827
Pharillons 0% - Pharillons 90%	-0,4891662	0,13476437	Inf	-3,6297886	0,0068827
Riou 0%ud 0% - Riou 0%ud 90%	-0,4891662	0,13476437	Inf	-3,6297886	0,0068827
Boulegeade 0% - Riou 0%ud 90%	-0,8324893	0,23378218	Inf	-3,5609612	0,00884
Grotte à corail 0% - Pharillons 90%	-0,7977467	0,2332835	Inf	-3,4196448	0,01451782
Grotte à corail 0% - Riou 0%ud 90%	-0,6677972	0,23341434	Inf	-2,8609946	0,08068621
Boulegeade 0% - Grotte à corail 90%	-0,6538583	0,23399223	Inf	-2,7943588	0,09630696
Riou 0%ud 0% - Pharillons 90%	-0,6191157	0,23294558	Inf	-2,6577698	0,13575877
Boulegeade 0% - Pharillons 0%	-0,4732727	0,19066047	Inf	-2,4822799	0,20288711
Boulegeade 90% - Pharillons 90%	-0,4732727	0,19066047	Inf	-2,4822799	0,20288711
Boulegeade 0% - Riou 0%ud 0%	-0,3433231	0,19086939	Inf	-1,7987331	0,62096467
Boulegeade 90% - Riou 0%ud 90%	-0,3433231	0,19086939	Inf	-1,7987331	0,62096467
Grotte à corail 0% - Pharillons 0%	-0,3085806	0,19029315	Inf	-1,6216063	0,73734423
Grotte à corail 90% - Pharillons 90%	-0,3085806	0,19029315	Inf	-1,6216063	0,73734423
Pharillons 0% - Riou 0%ud 90%	-0,3592166	0,23286544	Inf	-1,542593	0,78425197
Grotte à corail 0% - Boulegeade 90%	-0,3244741	0,23385572	Inf	-1,3874968	0,86331475
Riou 0%ud 0% - Grotte à corail 90%	-0,3105352	0,23328744	Inf	-1,3311268	0,88718886
Grotte à corail 0% - Riou 0%ud 0%	-0,178631	0,19050252	Inf	-0,9376831	0,98240051
Grotte à corail 90% - Riou 0%ud 90%	-0,178631	0,19050252	Inf	-0,9376831	0,98240051
Boulegeade 0% - Grotte à corail 0%	-0,1646921	0,19120407	Inf	-0,861342	0,9893212
Boulegeade 90% - Grotte à corail 90%	-0,1646921	0,19120407	Inf	-0,861342	0,9893212
Pharillons 0% - Grotte à corail 90%	-0,1805856	0,23307647	Inf	-0,7747912	0,99438359
Pharillons 0% - Riou 0%ud 0%	0,12994956	0,18995669	Inf	0,68410101	0,99742108
Pharillons 90% - Riou 0%ud 90%	0,12994956	0,18995669	Inf	0,68410101	0,99742108
Riou 0%ud 0% - Boulegeade 90%	-0,1458431	0,23351877	Inf	-0,6245454	0,99855944
Pharillons 0% - Boulegeade 90%	-0,0158935	0,23330804	Inf	-0,0681224	1

Differences in Shannon indexes between samples without tissue loss from the different sampling sites

GLM model with negative binomial distribution

glm.nb(formula = Observed_richness ~ Sampling_site, data =Richness, init.theta = 3.837888888, link = log)

Coefficients:	Estimate	Std. Error	z value	Pr(>|z|)
(Intercept)	2.2634	0.3118	7.259	2.1e-08
Sampling_siteBigo	-0.1228	0.4222	-0.291	0.773
Sampling_siteBoulegeade	-0.3004	0.4222	-0.712	0.482
Sampling_siteGrotte à corail	0.6331	0.4222	1.500	0.143
Sampling_sitePharillons	1.1896	0.4222	2.818	0.008
Sampling_sitePunta della Torreta	0.2374	0.4222	0.562	0.578
Sampling_siteRiou Sud	0.5271	0.4222	1.248	0.220

(Dispersion parameter for gaussian family taken to be 0.4860914)
Null deviance: 25.948 on 40 degrees of freedom
Residual deviance: 16.527 on 34 degrees of freedom
AIC: 95.102
Number of Fisher Scoring iterations: 2

Tukey test : pairwise differences between sampling sites

contrast	estimate	SE	df	z.ratio	p.value
Boulegeade (25m) - Pharillons (23m)	-1,4899974	0,40253006	34	-3,7015804	0,01208354
Bigo (37m) - Pharillons (23m)	-1,3124356	0,40253006	34	-3,2604659	0,03677574
(Villefranche-sur-Mer (35m)) - Pharillons (23m)	-1,1896178	0,42217709	34	-2,8178172	0,10095758
Pharillons (23m) - Riou Sud (28m)	0,95221628	0,40253006	34	2,36557805	0,24409738
Boulegeade (25m) - Grotte à corail (16m)	-0,9334819	0,40253006	34	-2,3190364	0,2645822
Boulegeade (25m) - Punta della Torreta (25m)	-0,8274414	0,40253006	34	-2,0556016	0,4006137
Bigo (37m) - Grotte à corail (16m)	-0,75592	0,40253006	34	-1,8779219	0,50786289
Pharillons (23m) - Punta della Torreta (25m)	0,66255597	0,40253006	34	1,64597886	0,65467147
Bigo (37m) - Punta della Torreta (25m)	-0,6498796	0,40253006	34	-1,6144871	0,67424197
(Villefranche-sur-Mer (35m)) - Grotte à corail (16m)	-0,6331023	0,42217709	34	-1,4996132	0,74305564
Grotte à corail (16m) - Pharillons (23m)	-0,5565155	0,40253006	34	-1,382544	0,8070432
Boulegeade (25m) - Riou Sud (28m)	-0,5377811	0,40253006	34	-1,3360024	0,83023409
(Villefranche-sur-Mer (35m)) - Punta della Torreta (25m)	-0,5270619	0,42217709	34	-1,2484379	0,86982617
Grotte à corail (16m) - Riou Sud (28m)	0,39570076	0,40253006	34	0,98303405	0,95432033
Bigo (37m) - Riou Sud (28m)	-0,3602193	0,40253006	34	-0,8948879	0,97089758
Punta della Torreta (25m) - Riou Sud (28m)	0,2896603	0,40253006	34	0,71959919	0,99040945
(Villefranche-sur-Mer (35m)) - Boulegeade (25m)	0,30037955	0,42217709	34	0,71150131	0,99096484
(Villefranche-sur-Mer (35m)) - Riou Sud (28m)	-0,2374016	0,42217709	34	-0,562327	0,9974751
Bigo (37m) - Boulegeade (25m)	0,17756185	0,40253006	34	0,44111451	0,99935677
(Villefranche-sur-Mer (35m)) - Bigo (37m)	0,1228177	0,42217709	34	0,29091513	0,99994257
Grotte à corail (16m) - Punta della Torreta (25m)	0,10604045	0,40253006	34	0,26343486	0,99996797

Differences in observed richness between samples with 0% and 90% tissue loss

GLM model with negative binomial distribution

glm.nb(formula = Observed ~ Condition + Sampling_site, data = Richness, init.theta = 4.782107885, link = log)

Coefficients:	Estimate	Std. Error	z value	Pr(>|z|)
(Intercept)	2.0480	0.2077	9.859	1.32e-12
Condition	0.8233	0.1858	4.431	6.36e-05
Sampling_siteGrotte à corail	0.9139	0.2628	3.478	0.001168
Sampling_sitePharillons	1.1067	0.2628	4.212	0.000127
Sampling_siteRiou Sud	0.6005	0.2628	2.285	0.027291

(Dispersion parameter for gaussian family taken to be 0.4142432)
Null deviance: 34.383 on 47 degrees of freedom
Residual deviance: 17.812 on 43 degrees of freedom
AIC: 100.64
Number of Fisher Scoring iterations: 2

Tukey test : pairwise differences between sampling sites

contrast	estimate	SE	df	z.ratio	p.value
Boulegeade (25m) S - Pharillons (23m) N	-1,9300141	0,32180864	43	-5,9973967	9,718E-06
Boulegeade (25m) S - Grotte à corail (16m) N	-1,7371869	0,32180864	43	-5,3981984	6,9954E-05
Boulegeade (25m) S - Boulegeade (25m) N	-0,8232653	0,1857963	43	-4,4310099	0,00151587
Grotte à corail (16m) S - Grotte à corail (16m) N	-0,8232653	0,1857963	43	-4,4310099	0,00151587
Pharillons (23m) S - Pharillons (23m) N	-0,8232653	0,1857963	43	-4,4310099	0,00151587
Riou Sud (28m) S - Riou Sud (28m) N	-0,8232653	0,1857963	43	-4,4310099	0,00151587
Boulegeade (25m) S - Riou Sud (28m) N	-1,4237256	0,32180864	43	-4,4241373	0,00154813
Boulegeade (25m) S - Pharillons (23m) S	-1,1067488	0,26275565	43	-4,2120837	0,0029432
Boulegeade (25m) N - Pharillons (23m) N	-1,1067488	0,26275565	43	-4,2120837	0,0029432
Riou Sud (28m) S - Pharillons (23m) N	-1,3295537	0,32180864	43	-4,1315041	0,00374167
Riou Sud (28m) S - Grotte à corail (16m) N	-1,1367265	0,32180864	43	-3,5323059	0,02042381
Boulegeade (25m) S - Grotte à corail (16m) S	-0,9139216	0,26275565	43	-3,4782187	0,02359236
Boulegeade (25m) N - Grotte à corail (16m) N	-0,9139216	0,26275565	43	-3,4782187	0,02359236
Grotte à corail (16m) S - Pharillons (23m) N	-1,0160924	0,32180864	43	-3,157443	0,05344925
Boulegeade (25m) S - Riou Sud (28m) S	-0,6004603	0,26275565	43	-2,2852423	0,32489923
Boulegeade (25m) N - Riou Sud (28m) N	-0,6004603	0,26275565	43	-2,2852423	0,32489923
Pharillons (23m) S - Grotte à corail (16m) N	-0,6304381	0,32180864	43	-1,9590465	0,52005318
Pharillons (23m) S - Riou Sud (28m) S	0,50628846	0,26275565	43	1,92684135	0,54091667
Pharillons (23m) N - Riou Sud (28m) N	0,50628846	0,26275565	43	1,92684135	0,54091667
Grotte à corail (16m) S - Riou Sud (28m) N	-0,509804	0,32180864	43	-1,5841836	0,75680598
Grotte à corail (16m) S - Riou Sud (28m) S	0,31346129	0,26275565	43	1,19297638	0,92960148
Grotte à corail (16m) N - Riou Sud (28m) N	0,31346129	0,26275565	43	1,19297638	0,92960148
Pharillons (23m) S - Riou Sud (28m) N	-0,3169768	0,32180864	43	-0,9849854	0,97421103
Pharillons (23m) S - Boulegeade (25m) N	0,28348354	0,32180864	43	0,88090718	0,98629566
Grotte à corail (16m) S - Pharillons (23m) S	-0,1928272	0,26275565	43	-0,733865	0,99539824
Grotte à corail (16m) N - Pharillons (23m) N	-0,1928272	0,26275565	43	-0,733865	0,99539824
Riou Sud (28m) S - Boulegeade (25m) N	-0,2228049	0,32180864	43	-0,6923522	0,99679007
Grotte à corail (16m) S - Boulegeade (25m) N	0,09065637	0,32180864	43	0,28170894	0,99999177

Table S8: Outputs of the PERMANOVA statistical tests.

Differences in microeukaryotes composition between samples without tissue loss accross the different sampling sites

PERMANOVA on the different sampling sites

adonis2(formula = Aitchison_distance_matrix ~ Sampling_site, data = ASV_table)

Number of permutations: 999

	Df	SumOfSqs	R2	F	Pr(>F)
as.factor(ASV_table$Sampling_site)	6	8967	0.23635	1.7538	0.001
Residual	34	28974	0.76365		
Total	40	37941	1.00000		

ANOVA on the betadispersion values (distance to centroid) between sampling sites

anova(betadisper(Aitchison_distance_matrix, group=ASV_table$Sampling_site))

	Df	Sum Sq	Mean Sq	F value	Pr(>F)
Groups	6	497.93	82.988	2.9551	0.01977
Residuals	34	954.83	28.083		

Pairwise permanova for differences between sites

pairs	SumOfSqs	F.Model	R2	pval	p.adj
Grotte à corail vs Punta della Torreta	17632307,2	2,08668165	0,172643056	0,002	0,0126
Grotte à corail vs Villefranche	12909584,4	8,38172293	0,482214736	0,003	0,0126
Pharillons vs Villefranche	14789699,1	6,5103628	0,41974278	0,002	0,0126
Riou Sud vs Villefranche	18310932	4,02127097	0,308823231	0,003	0,0126
Boulegeade vs Punta della Torreta	31011096,5	2,02145853	0,168154182	0,002	0,0126
Pharillons vs Punta della Torreta	18150095,3	1,99270155	0,166159521	0,006	0,018
Riou Sud vs Punta della Torreta	21695590,8	1,94371711	0,162739715	0,006	0,018
Pharillons vs Bigo	13058945	2,59971268	0,206331108	0,008	0,021
Riou Sud vs Bigo	16739543,8	2,36539539	0,191291529	0,009	0,021
Boulegeade vs Villefranche	25049736,1	2,7237151	0,232325255	0,012	0,0252
Boulegeade vs Bigo	24270763,8	2,15627199	0,17737938	0,019	0,036272727
Grotte à corail vs Bigo	11275333,4	2,58320193	0,205289714	0,021	0,03675
Grotte à corail vs Riou Sud	6176244,17	1,65559407	0,142042873	0,032	0,051692308
Grotte à corail vs Pharillons	2595322,25	1,54768249	0,134025376	0,056	0,084
Grotte à corail vs Boulegeade	13516968,5	1,7089376	0,145951551	0,164	0,2296
Bigo vs Punta della Torreta	10248683,9	0,86880906	0,079935994	0,491	0,606529412
Punta della Torreta vs Villefranche	9102439,54	0,92907707	0,093571343	0,482	0,606529412
Pharillons vs Boulegeade	7939103,58	0,92660663	0,084802781	0,527	0,614833333
Pharillons vs Riou Sud	2740133,58	0,62433414	0,058764543	0,746	0,79
Riou Sud vs Boulegeade	6960028,5	0,65527398	0,061497619	0,79	0,79
Bigo vs Villefranche	2121125,4	0,4033833	0,042897677	0,788	0,79

Differences in microeukaryotes composition between samples impacted or not by the MHWs

PERMANOVA on the differences between control sites and sites impacted by the MHWs

adonis2(formula = Aitchison_distance_matrix ~ Impact, data =ASV_table)

Number of permutations: 999

	Df	SumOfSqs	R2	F	Pr(>F)
as.factor(ASV_table$Impact)	1	0.3952	0.08932	3.8251	0.001
Residual	39	4.0290	0.91068		
Total	40	4.4242	1.00000		

ANOVA on the betadispersion values (distance to centroid) between control and impacted sites

anova(betadisper(Aitchison_distance_matrix, group=ASV_table$Impact))

	Df	Sum Sq	Mean Sq	F value	Pr(>F)
Groups	1	0.02601	0.026013	2.1894	0.147
Residuals	39	0.46337	0.011881		

Differences in microeukaryotes composition between coral from Portofino and seawater samples

PERMANOVA on the differences between coral from Portofino and seawater samples

adonis2(formula = Aitchison_distance_matrix ~ Sample_type, data =ASV_table)

Number of permutations: 999

	Df	SumOfSqs	R2	F	Pr(>F)
as.factor(ASV_table$Sample_type)	1	12076	0.27775	8.4602	0.001
Residual	22	31404	0.72225		
Total	23	43480	1.00000		

ANOVA on the betadispersion values (distance to centroid) coral from Portofino and seawater samples

anova(betadisper(Aitchison_distance_matrix, group=ASV_table$Sample_type))

	Df	Sum Sq	Mean Sq	F value	Pr(>F)
Groups	1	1614.87	1614.87	61.525	8.177e-08
Residuals	22	577.44	26.25		

Differences in microeukaryotes composition between coral and seawater samples

PERMANOVA on the differences between coral and seawater samples

adonis2(formula = Aitchison_distance_matrix ~ Sample_type, data =ASV_table)

Number of permutations: 999

	Df	SumOfSqs	R2	F	Pr(>F)
as.factor(ASV_table$Sample_type)	1	0.2095	0.03524	2.7392	0.016
Residual	75	5.7354	0.96476		
Total	76	5.9449	1.00000		

ANOVA on the betadispersion values (distance to centroid) coral and seawater samples

anova(betadisper(Aitchison_distance_matrix, group=ASV_table$Sample_type))

	Df	Sum Sq	Mean Sq	F value	Pr(>F)
Groups	1	0.09297	0.092971	5.8391	0.01811
Residuals	75	1.19417	0.015922		

Differences in microeukaryotes composition between samples with 0% and 90% tissue loss accross the different sampling sites

PERMANOVA on the differences between samples with 0% and 90% tissue loss

adonis2(formula = Aitchison_distance_matrix ~ Sampling_site*Condition, data = ASV_table)

Number of permutations: 999

	Df	SumOfSqs	R2	F	Pr(>F)
as.factor(ASV_table$Sampling_site)	3	5738	0.10417	1.7516	0.001
as.factor(ASV_table$Condition)	1	2730	0.04957	2.5003	0.001
as.factor(ASV_table$Sampling_site):as.factor(ASV_table$Condition)	3	4026	0.07309	1.2290	0.009
Residual	39	42590	0.77316		
Total	46	55085	1.00000		

ANOVA on the betadispersion values (distance to centroid) between samples with 0% and 90% tissue loss

anova(betadisper(Aitchison_distance_matrix, group=ASV_table$Condition))

	Df	Sum Sq	Mean Sq	F value	Pr(>F)
Groups	1	453.07	453.07	12.186	0.00109
Residuals	45	1673.06	37.18		

Pairwise permanova for differences between sites

pairs	SumOfSqs	F.Model	R2	pval	p.adj
0%_Grotte à corail vs 0%_Pharillons	2200,43751	1,97404656	0,164860438	0,001	0,009333333
0%_Grotte à corail vs 0%_Riou Sud	1962,45265	1,4594483	0,12735764	0,003	0,009333333
90%_Grotte à corail vs 90%_Riou Sud	1896,73272	1,92754669	0,161604623	0,002	0,009333333
0%_Pharillons vs 0%_Riou Sud	1481,35416	1,42314681	0,12458448	0,003	0,009333333
0%_Riou Sud vs 90%_Riou Sud	1612,13846	1,63541707	0,140555088	0,001	0,009333333
0%_Pharillons vs 0%_Boulegeade	1460,32289	1,56359871	0,13521731	0,008	0,020363636
90%_Riou Sud vs 90%_Boulegeade	1537,33732	1,50822138	0,143527751	0,01	0,023333333
0%_Boulegeade vs 90%_Boulegeade	1581,72282	1,29941913	0,126164312	0,019	0,035466667
90%_Grotte à corail vs 90%_Boulegeade	1718,16419	1,28784307	0,125181057	0,023	0,04025
0%_Grotte à corail vs 0%_Boulegeade	1566,97194	1,26603204	0,112376038	0,028	0,046117647
90%_Grotte à corail vs 90%_Pharillons	1624,00952	1,34491848	0,118548096	0,034	0,052888889
90%_Pharillons vs 0%_Pharillons	1214,31136	1,23998248	0,110318898	0,051	0,073333333
90%_Pharillons vs 90%_Boulegeade	1505,48489	1,18762846	0,116575556	0,054	0,073333333
0%_Grotte à corail vs 90%_Grotte à corail	1483,88584	1,1049847	0,099503487	0,118	0,13216
0%_Riou Sud vs 0%_Boulegeade	1237,97363	1,06362434	0,096137062	0,221	0,238
90%_Pharillons vs 90%_Riou Sud	956,384364	1,03486581	0,093781458	0,324	0,324

Table S11: Core microbiome of different groups of C. rubrum samples.

All samples			All 0% samples			Control sites			Impacted sites	
Order	**presence**		**Order**	**presence**		**Order**	**presence**		Order	presence
Dino-Group-I	1		Dino-Group-I	0,984615385		Dino-Group-I	1		NA	NA
Labyrinthulomycetes	0,87804878		Labyrinthulomycetes	0,923076923		Licnophoria	1			
			Gymnodiniales	0,876923077		Isochrysidales	0,909090909			
						Suessiales	0,909090909			

Table S12 : Selected sequences for each most prevalent taxonomic families

Corallicolidae		
Sequence	Source	Other information
ASV5	Corallium rubrum	
KF579894.1	Porites astreoides	Blast of ASV5
KF579893.1	Porites astreoides	Blast of ASV5
KF579892.1	Porites astreoides	Blast of ASV5
MN022453.1	Callogorgia delta	Blast of ASV5
MN022434.1	Muricea pendula	Blast of ASV5
ASV240	Corallium rubrum	
ASV2214	Corallium rubrum	
ASV2403	Corallium rubrum	
ASV2436	Corallium rubrum	
Cluster21	Pocillopora damicornis	Cluster21 from Clerissi et al. 2018
JX943876.1	Montastraea faveolata	Blast of Cluster21 from Clerissi et al. 2018
Cluster76	Pocillopora damicornis	Cluster76 from Clerissi et al. 2018
MH304760.1	NA	Corallicola aquarius, Blast of Cluster76 from Clerissi et al. 2018
Cluster77	Pocillopora damicornis	Cluster77 from Clerissi et al. 2018
JX943880.1	Pocillopora damicornis	Blast of Cluster77 from Clerissi et al. 2018
ASV6-Bonacolta	Paramuricea clavata	ASV6 from Bonacolta et al. 2024
MN022452.1	Callogorgia delta	Blast of ASV6 from Bonacolta et al. 2024
ASV16-Bonacolta	Paramuricea clavata	ASV6 from Bonacolta et al. 2024
ASV19-Bonacolta	Paramuricea clavata	ASV6 from Bonacolta et al. 2024
ASV22-Bonacolta	Paramuricea clavata	ASV6 from Bonacolta et al. 2024
MN022429.1	Leiopathes glaberrima	Blast of ASV16, ASV19, ASV22 from Bonacolta et al. 2024
ASV105-Bonacolta	Paramuricea clavata	ASV6 from Bonacolta et al. 2024
JX943883.1	Porites astreoides	Blast of ASV105 from Bonacolta et al. 2024
EF023195.1	Outgroup	Eimeriidae

Dino-Group-I-Clade 1		
Sequence	Source	Other information
ASV4	Corallium rubrum	
ASV83	Corallium rubrum	
ASV128	Corallium rubrum	
ASV133	Corallium rubrum	
ASV136	Corallium rubrum	
ASV143	Corallium rubrum	
ASV149	Corallium rubrum	
ASV170	Corallium rubrum	
KF129971.1	Seawater	Dinoflagellata Blast of ASV4
KF129765.1	Seawater	Dinoflagellata Blast of ASV5
KF031941.1	Seawater	Dinoflagellata Blast of ASV6
KF031929.1	Seawater	Dinoflagellata Blast of ASV7
Cluster15	Pocillopora damicornis	Cluster15 from Clerissi et al. 2018
KF129971.1	Seawater	Blast of Cluster15 from Clerissi et al. 2018
ASV12-Bonacolta	Paramuricea clavata	ASV12 from Bonacolta et al. 2024
KP187805.1	Seawater	Blast of ASV12 from Bonacolta et al. 2024
ASV13-Bonacolta	Paramuricea clavata	ASV12 from Bonacolta et al. 2024
ASV256	Outgroup	Dino-Group-III

Ephelotidae		
Sequence	Source	Other information
ASV31	Corallium rubrum	
ASV40	Corallium rubrum	
HQ696558.1	Contaminated seawate	Ciliate Blast of ASV40
MZ687485.1	Seawater	Ciliate Blast of ASV40
MZ663406.1	Seawater	Ciliate Blast of ASV40
DQ115965.1	Contaminated seawate	Ciliate Blast of ASV40
KM486062.1	Crustacean	Suctoria Blast of ASV40
ASV91	Corallium rubrum	
ASV251	Corallium rubrum	
ASV261	Corallium rubrum	
ASV333	Corallium rubrum	
ASV7-Bonacolta	Paramuricea clavata	ASV7 from Bonacolta et al. 2024
ASV46-Bonacolta	Paramuricea clavata	ASV46 from Bonacolta et al. 2024
ASV65-Bonacolta	Paramuricea clavata	ASV65 from Bonacolta et al. 2024
ASV233-Out	Outgroup	Endogenida

Exobasidiomycetes		
Sequence	Source	Other information
ASV41	Corallium rubrum	
ASV216	Corallium rubrum	
ASV283	Corallium rubrum	
ASV14611-Bonacolta	Paramuricea clavata	Malassezia globosa from Bonacolta et al. 2024
ASV3263-Bonacolta	Paramuricea clavata	Malassezia restricta from Bonacolta et al. 2024
ASV3805-Bonacolta	Paramuricea clavata	Malassezia restricta from Bonacolta et al. 2024
KP173676.1	Copepod	Blast of ASV41
OM190398.1	Human skin	Malassezia restricta Blast of ASV41
KC666033.1	Rhizosphere	Glomus Blast of ASV41
KC487833.1	Hypersaline lake	Malassezia Blast of ASV41
KC675175.1	Human skin	Malassezia Blast of ASV41
OQ128060.1	Other coral	Microstromataceae from Papan et al. 2023
MT535806.1	Sediments	Exobasidiomycetes from Marchese et al. 2021
AY743636.1	Sponge	Malassezia restricta from Gao et al. 2008
DQ900961.1	Sponge	Malassezia restricta from Gao et al. 2008
AM260792.1	Sponge	Malassezia restricta from Gao et al. 2008
AJ437695.1	Sponge	Malassezia restricta from Gao et al. 2008
AY387136.1	Sponge	Malassezia globosa from Gao et al. 2008
ASV3604	Outgroup	Ustilaginomycetes

Labyrinthulomycetes		
Sequence	Source	Other information
ASV49	Corallium rubrum	
KU559378.1	Seagrass	Labyrinthula Blast of ASV49
EF100254.1	Sediments	Blast of ASV49
EU431330.1-Labyrinth	Amoeba	Labyrinthula Blast of ASV49
PP496752.1-Labyrinth	Seagrass	Labyrinthula Blast of ASV49
ASV78	Corallium rubrum	
ASV85	Corallium rubrum	
ASV226	Corallium rubrum	
ASV241	Corallium rubrum	
ASV252	Corallium rubrum	
ASV289	Corallium rubrum	
ASV300	Corallium rubrum	
FJ389843.1-Stramenor	Favia spp.	Stramenopile from Siboni et al. 2010
FJ389842.1-Stramenor	Favia spp.	Stramenopile from Siboni et al. 2010
FJ389840.1-Stramenor	Favia spp.	Stramenopile from Siboni et al. 2010
FJ389861.1-Stramenor	Favia spp.	Stramenopile from Siboni et al. 2010
EF371005.1-Strameno	Fungiid coral	Stramenopile from Ben-Dov et al. 2009
EF371006.1-Strameno	Fungiid coral	Stramenopile from Ben-Dov et al. 2009
EF371010.1-Strameno	Fungiid coral	Stramenopile from Ben-Dov et al. 2009
DQ073058.1-Stramen	Fungia granulosa	Stramenopile from Kramarsky-Winter et al. 2006
DQ073059.1-Stramen	Fungia granulosa	Stramenopile from Kramarsky-Winter et al. 2006
DQ073060.1-Stramen	Fungia granulosa	Stramenopile from Kramarsky-Winter et al. 2006
JN675242.1-Thraustoc	Producing fatty acids	
JN675243.1-Thraustoc	Producing fatty acids	
JN675245.1-Thraustoc	Producing fatty acids	
JN675277.1-Thraustoc	Producing fatty acids	
ASV995	Outgroup	Oblongichytridiaceae

Licnophoridae		
Sequence	Source	Other information
ASV13	Corallium rubrum	
OR525732.1-Ciliophora	Urchin	Blast of ASV13
OR525728.1-Ciliophora	Urchin	Blast of ASV13
OR525730.1-Ciliophora	Urchin	Blast of ASV13
ASV193	Corallium rubrum	
ASV257	Corallium rubrum	
ASV544	Corallium rubrum	
ASV570	Corallium rubrum	
ASV588	Corallium rubrum	
ASV684	Corallium rubrum	
ASV732	Corallium rubrum	
ASV3-Bonacolta	Paramuricea clavata	from Bonacolta et al. 2024
AF527758.1	Sea cucumber	Blast of Cluster7 from Clerissi et al. 2018
Cluster7-Clerissi	Pocillopora damicornis	from Clerissi et al. 2018
Cluster56-Clerissi	Pocillopora damicornis	from Clerissi et al. 2018
ASV33	Outgroup	Euplotidae

Warnowiaceae		
Sequence	Source	Other information
ASV18	Corallium rubrum	
FJ914412.1	Seawater	Dinoflagellata Blast ASV18
FJ467492.1	Seawater	Warnowia Blast ASV18
AB827549.1	Seawater	Dinoflagellata Blast ASV18
EU500023.1	Seawater	Dinoflagellata Blast ASV18
ASV20	Corallium rubrum	
ASV28	Corallium rubrum	
ASV294	Corallium rubrum	
ASV612	Corallium rubrum	
ASV631	Corallium rubrum	
ASV675	Corallium rubrum	
ASV757	Corallium rubrum	
FM211468.1	Isolated toxic strain	Alexandrium catenella strain ACT1
FM211470.1	Isolated toxic strain	Alexandrium catenella strain ACTEM17
KJ781424.2	Isolated toxic strain	Alexandrium minutum
KJ781426.1	Isolated toxic strain	Alexandrium minutum
GU362426.1	Isolated toxic strain	Gymnodinium catenatum strain ZX9
JQ638928.1	Isolated toxic strain	Gymnodinium catenatum
JF906999.1	Isolated toxic strain	Alexandrium lusitanicum strain-AL-1
JF901327.1	Isolated toxic strain	Alexandrium tamarense
JX173250.1	Isolated toxic strain	Alexandrium tamarense strain ATDH56
ASV81	Outgroup	Gymnodiniaceae

Philasterida		
Sequence	Source	Other information
ASV21	Corallium rubrum	
ASV224	Corallium rubrum	
ASV416	Corallium rubrum	
ASV491	Corallium rubrum	
ASV644	Corallium rubrum	
MN189136.1	Herbivorous fish	
JF831359.1	Diseased corals	Tropical corals with signs of White and Brown Band diseases
KP792999.1	Echinopora lamellosa	
JN641995.1	Diseased corals	Tropical corals with signs of White and Brown Band diseases
JN641994.1	Diseased corals	Tropical corals with signs of White and Brown Band diseases
JN626268.1	Diseased corals	Tropical corals with signs of White and Brown Band diseases
ASV3003-Bonacolta	Paramuricea clavata	from Bonacolta et al. 2024
ASV1653-Bonacolta	Paramuricea clavata	from Bonacolta et al. 2025
ASV1014-Bonacolta	Paramuricea clavata	from Bonacolta et al. 2026
ASV180	Outgroup	Cohnilembidae

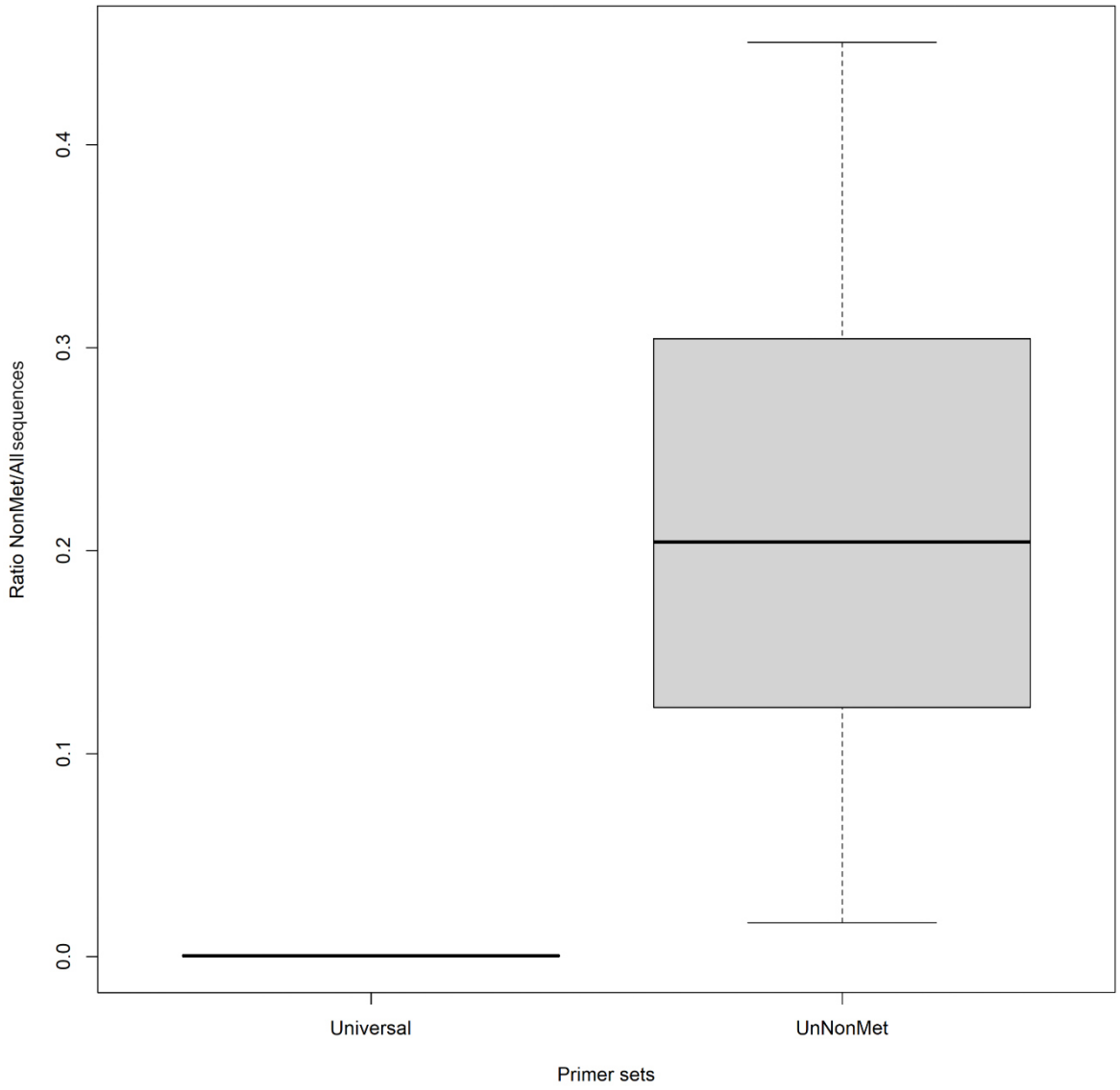

Figure S1: Ratios between the number of sequences assigned as non-metazoan and the total number of sequences (*i.e.*, non-metazoan and metazoan assigned sequences) obtained on the *C. rubrum* samples using the UnNonMet primers designed for this study and the universal *rRNA 18S* V4 primers TAReuk454FWD1 (5'-CCAGCASCYGCGGTAATTCC-3') and TAReukREV3 (5'-ACTTTCGTTCTTGATYRA-3'), respectively. Mean of 0.04% for the universal primers (4 samples) and 22% for the newly designed UnNonMet primers (65 samples).

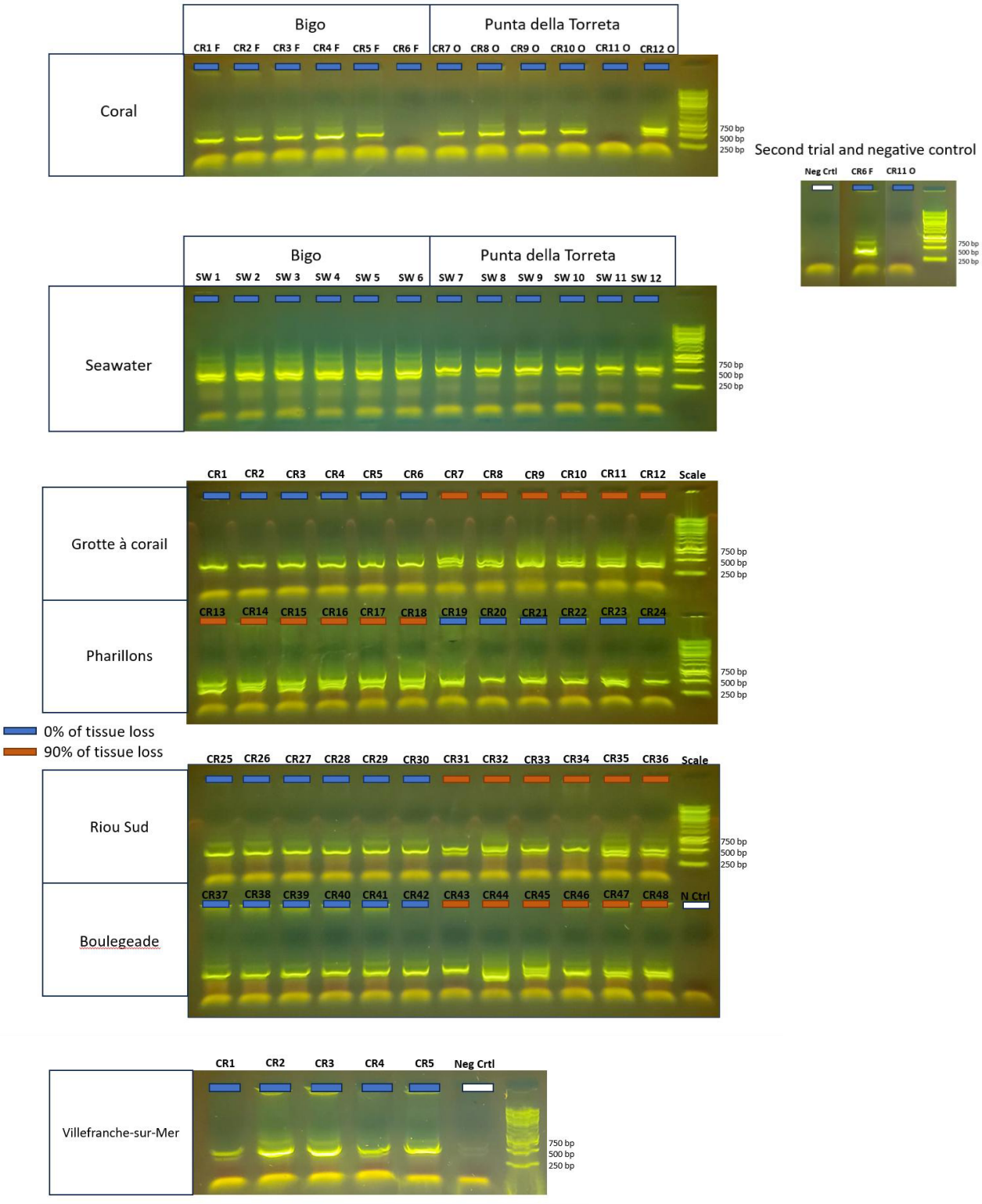

Figure S2: Images of the electrophoresis agarose gels showing the PCR products using the newly designed primers (product size between 500 and 730 bp), for each sample of the different sampling sites.

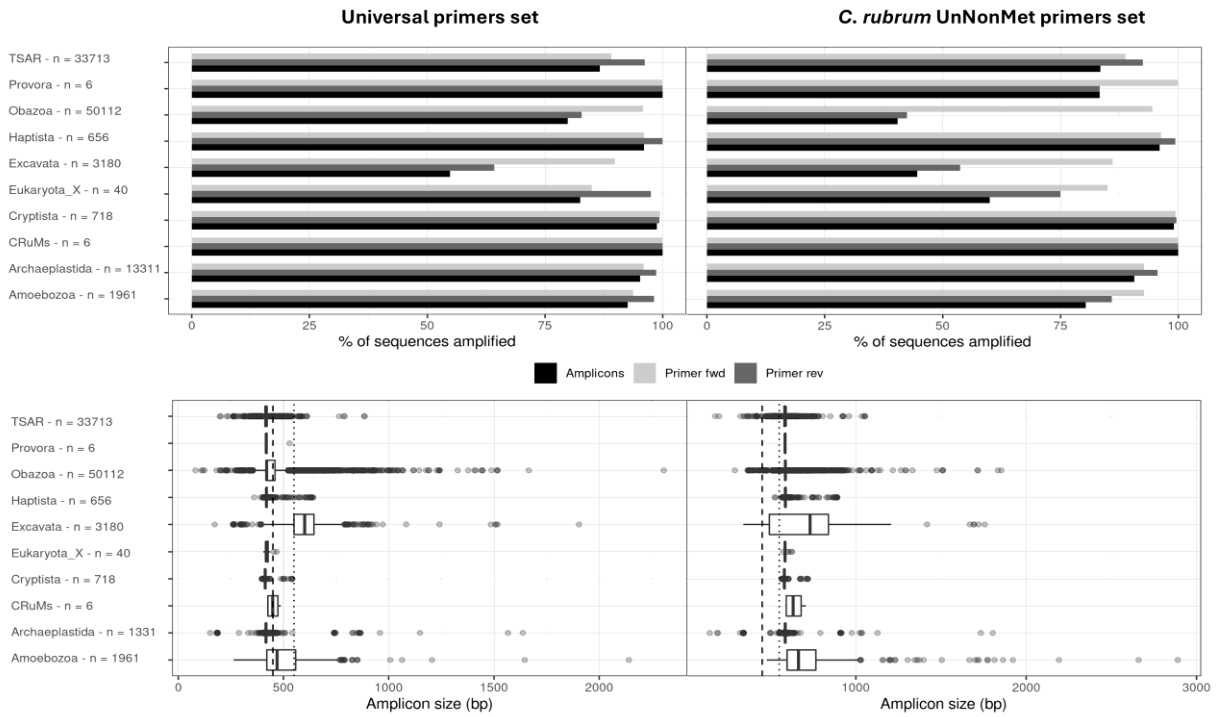

Figure S3: In-silico PCR searches. Percentage of sequences and amplicon expected size per phylum recovered from the PR2 primer database (https://app.pr2-primers.org/pr2-primers/; v. 2.0.0) using the universal *rRNA 18S* V4 primers TAReuk454FWD1 (5'-CCAGCASCYGCGGTAATTCC-3') and TAReukREV3 (5'-ACTTTCGTTCTTGATYRA-3') and the UnNonMet primers designed for this study. Primers were allowed a maximum of 2 mismatches.

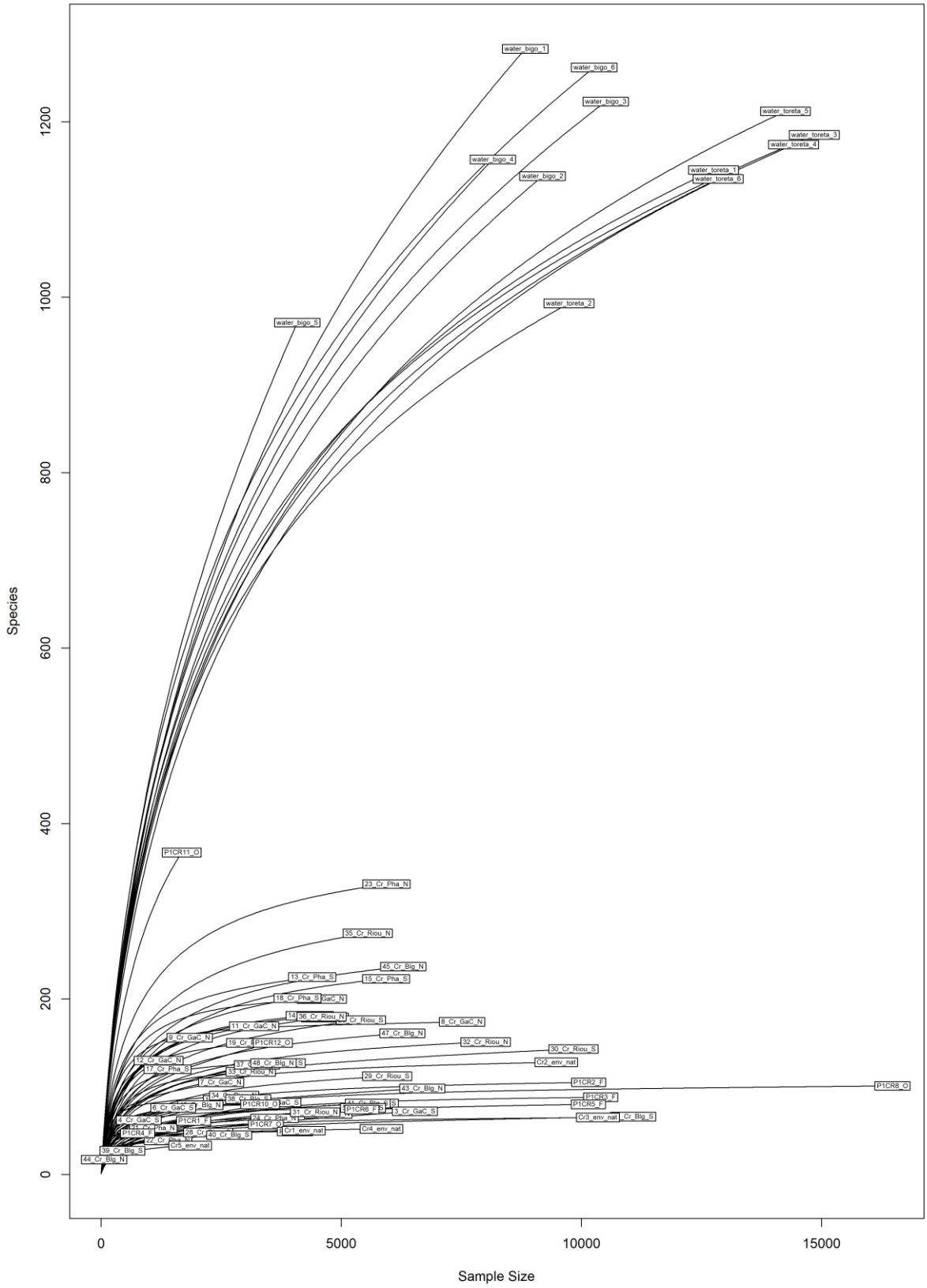

Figure S4: Rarefaction curves for all samples.

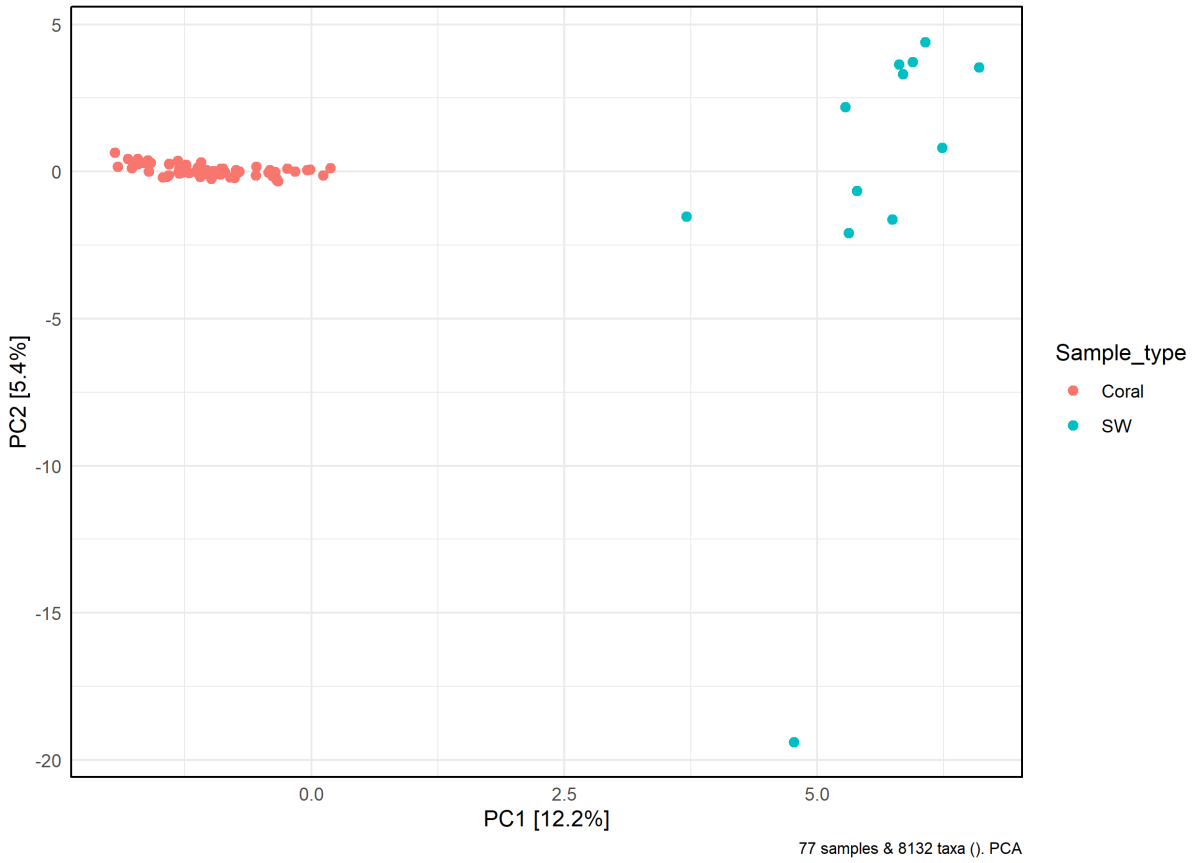

Figure S5: Beta diversity of the microeukaryote community of *C. rubrum* ("Coral", in red) and the seawater samples ("SW", in blue). Principal component analysis based on the Aitchison distance matrix showing the distribution and dispersion of the samples.

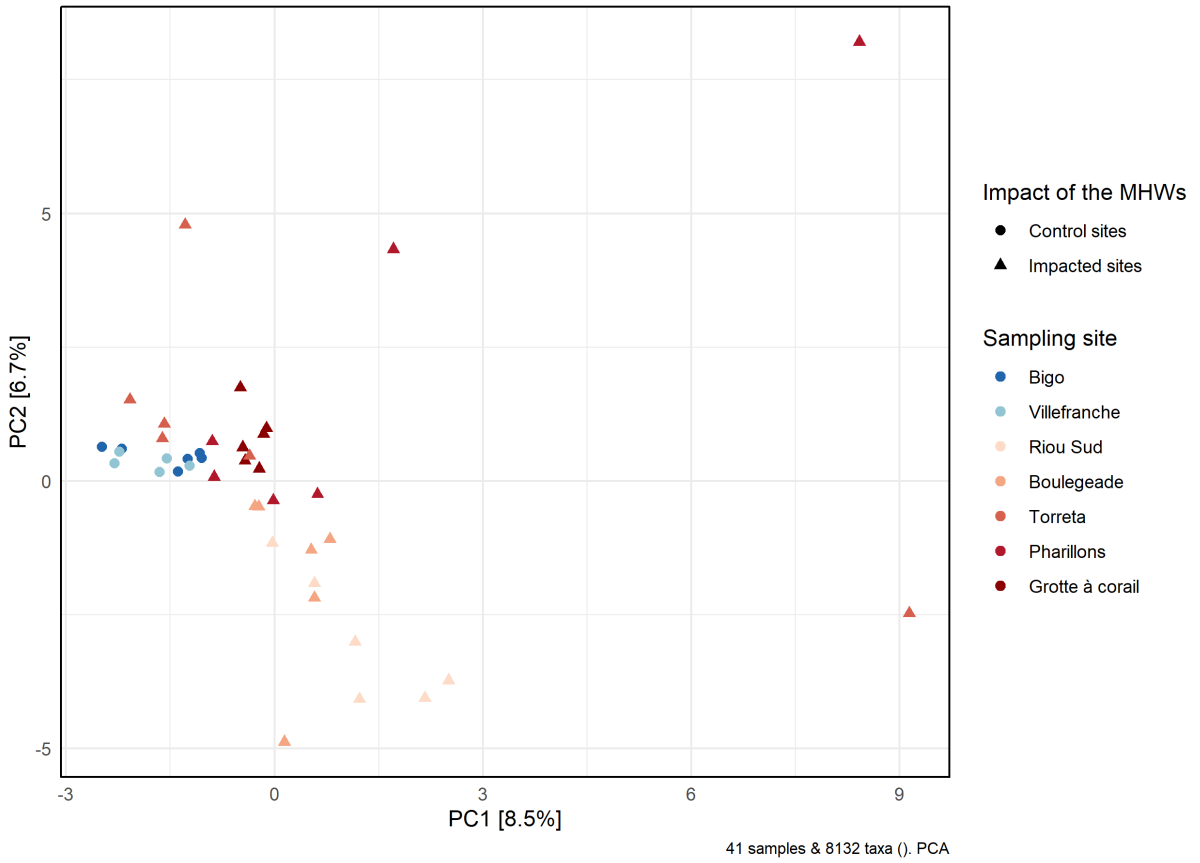

Figure S6: Principal component analysis of the Aitchison distance matrix based on the composition of the microeukaryote community (ASV level) associated with *C. rubrum* samples according to the sampling site and the impact of the MHWs.

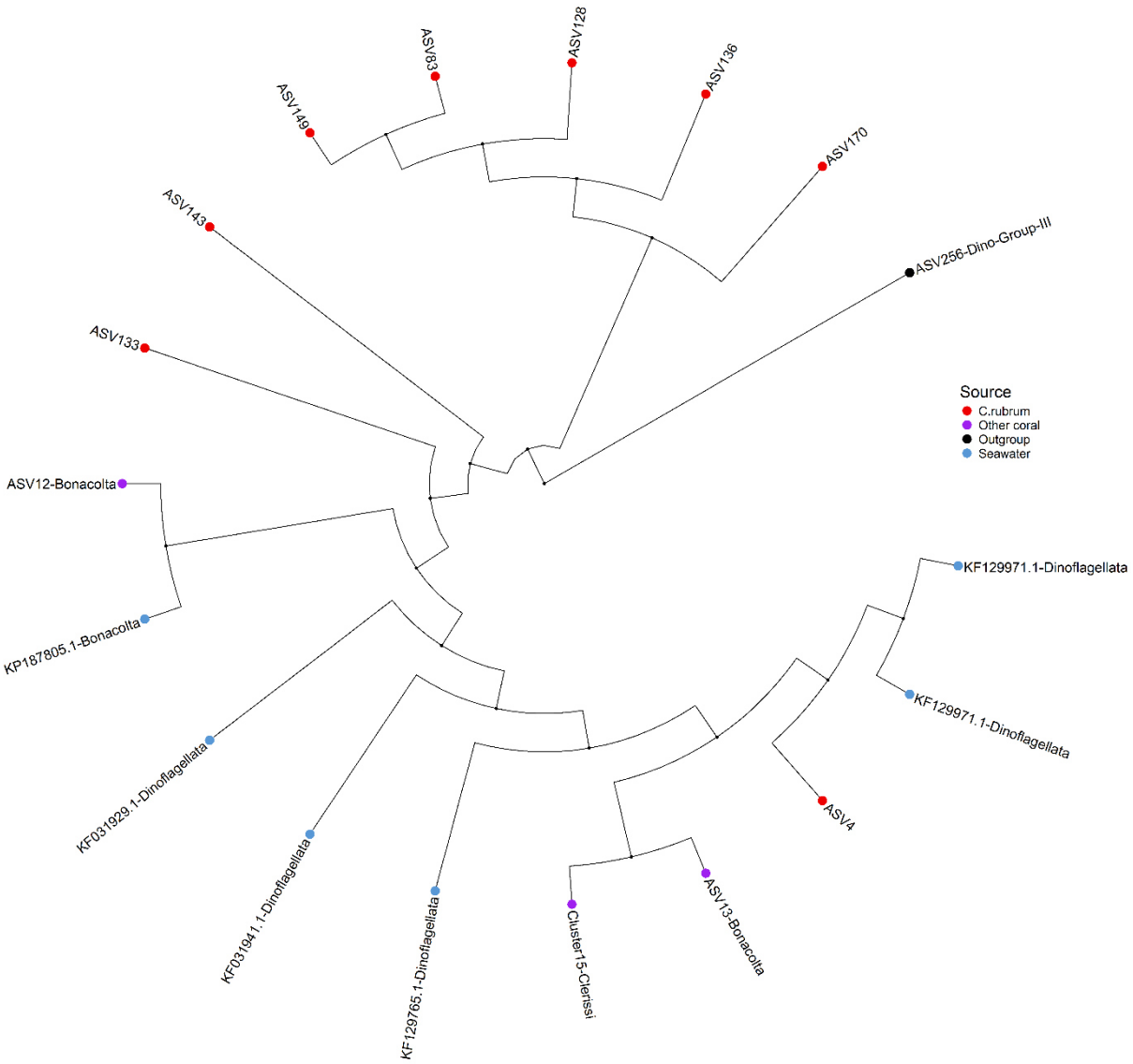

Figure S7: Dendrogram illustrating the phylogenetic relationships (PhyML, GTR model) between all the ASVs annotated as belonging to the Dino Group I Clade 1 family, public ASV sequences recovered after a BLASTn search on the NCBI nucleotide collection using the ASV4 (as the ASV4 is the most prevalent ASV annotated as belonging to the Dino Group I Clade 1 family) as well as ASV sequences recovered from two studies and annotated as belonging to the Dino Group I Clade 1 family (Sequences recovered from *Paramuricea clavata* in Bonacolta et al., 2024 and from *Pocillopora damicornis* in Clerissi et al., 2018).

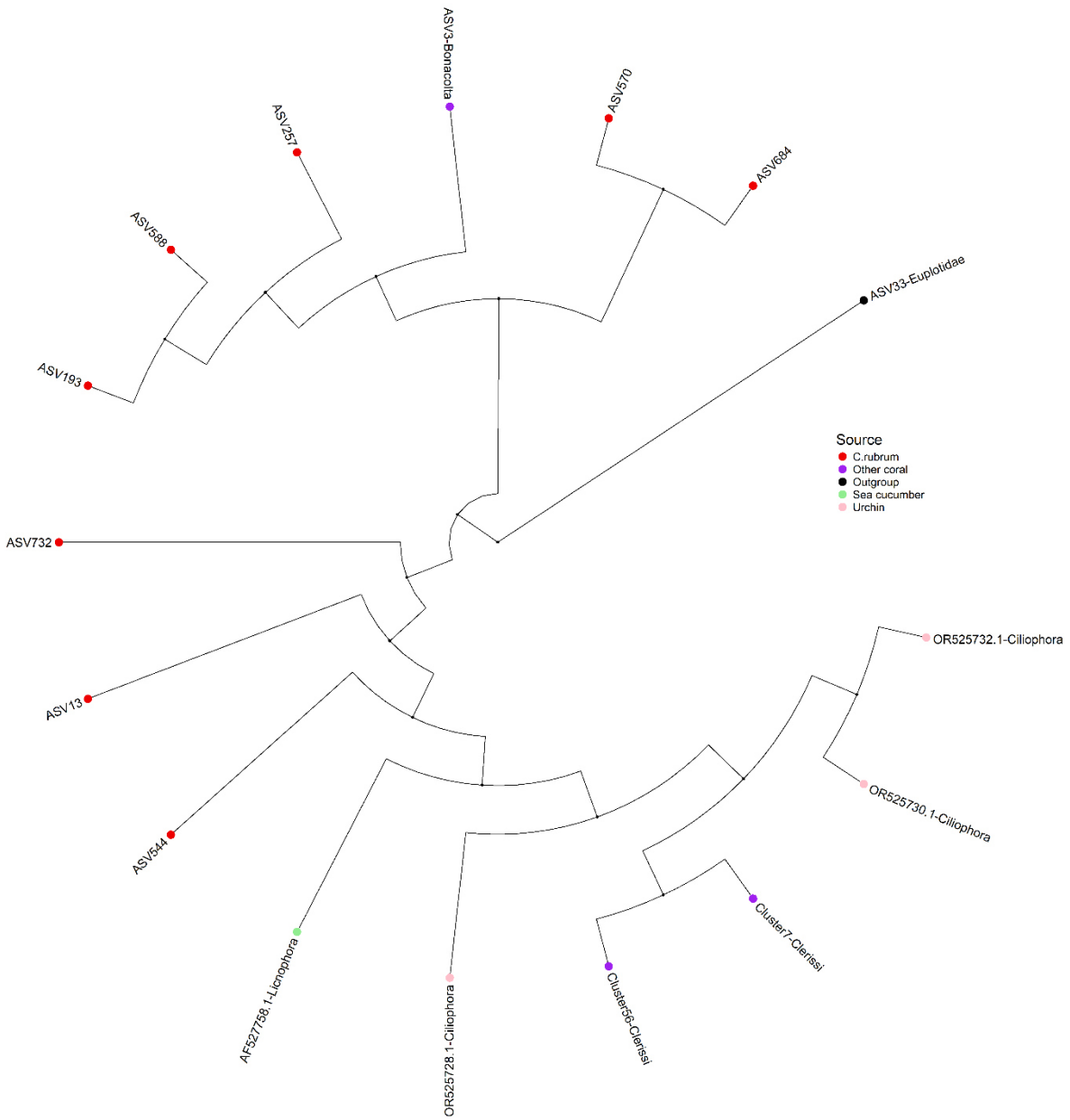

Figure S8: Dendrogram illustrating the phylogenetic relationships (PhyML, TN93 model) between all the ASVs annotated as belonging to the Licnophoridae family, public ASV sequences recovered after a BLASTn search on the NCBI nucleotide collection using the ASV13 (as the ASV13 is the most prevalent ASV annotated as belonging to the Licnophoridae family) as well as ASV sequences recovered from two studies and annotated as belonging to the Licnophoridae family (Sequences recovered from *Paramuricea clavata* in Bonacolta et al., 2024 and from *Pocillopora damicornis* in Clerissi et al., 2018).

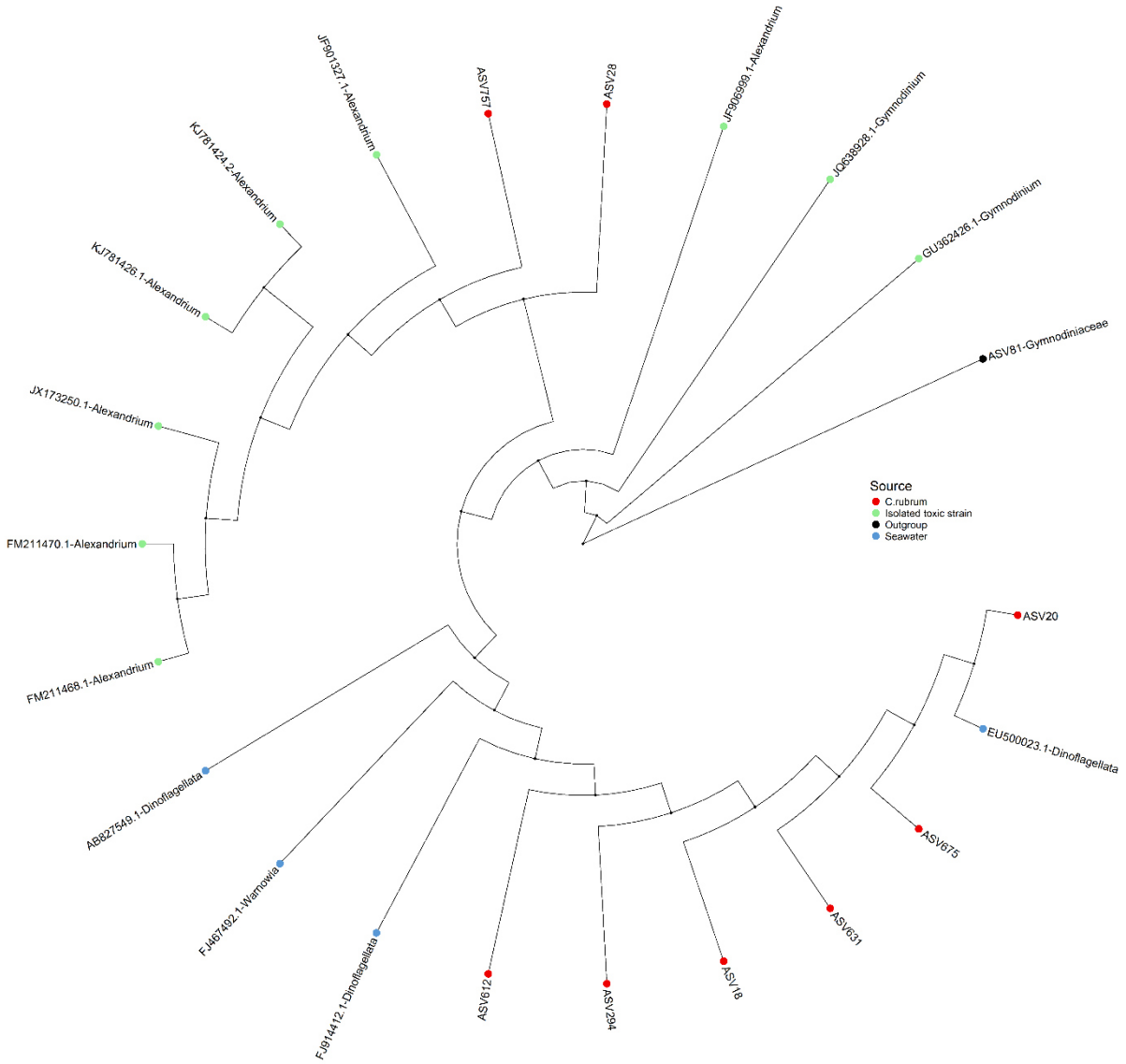

Figure S9: Dendrogram illustrating the phylogenetic relationships (PhyML, GTR model) between all the ASVs annotated as belonging to the Warnowiaceae family, public ASV sequences recovered after a BLASTn search on the NCBI nucleotide collection using the ASV4 (as the ASV4 is the most prevalent ASV annotated as belonging to the Warnowiaceae family).

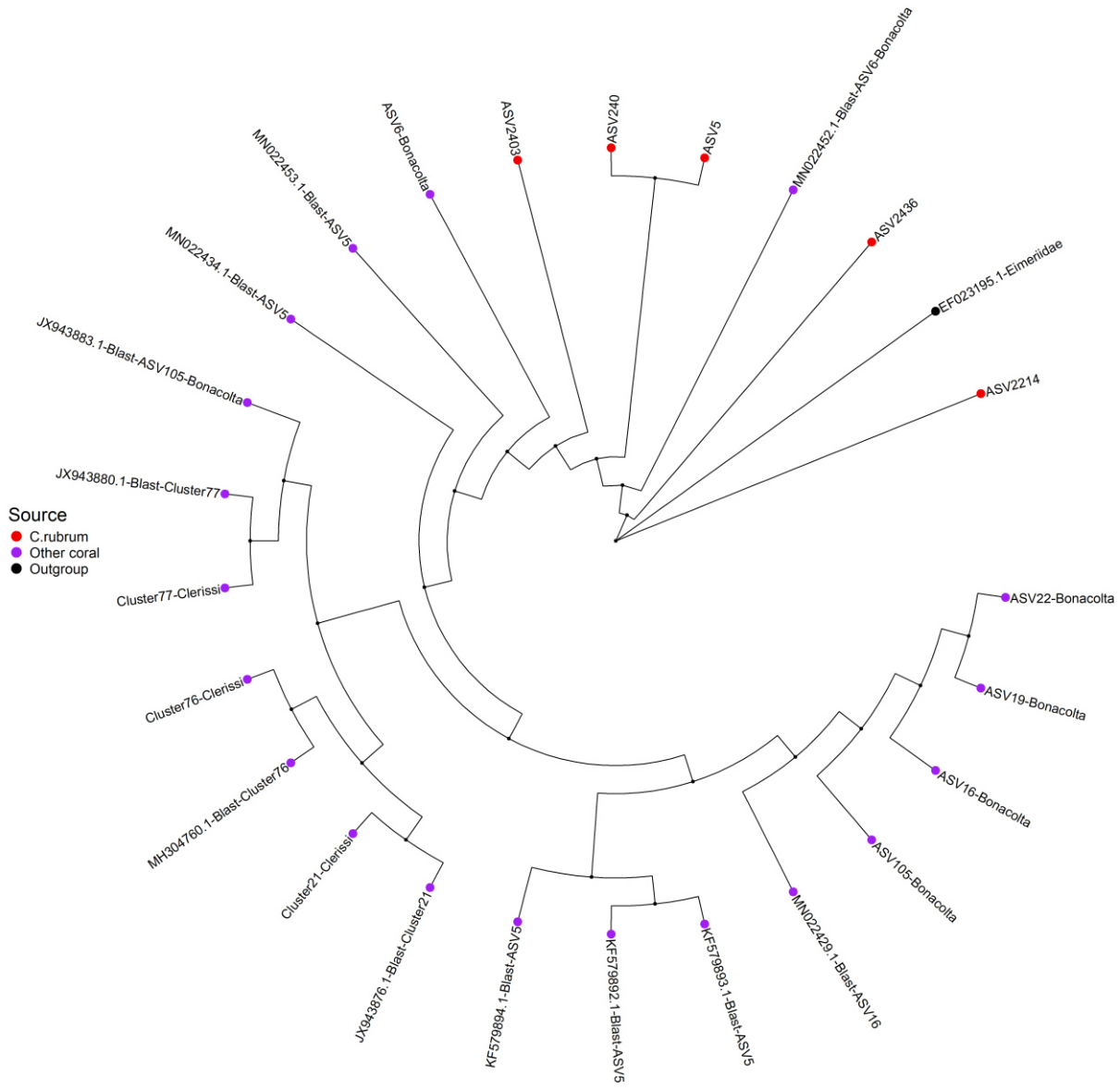

Figure S10: Dendrogram illustrating the phylogenetic relationships (PhyML, TN93 model) between all the ASVs annotated as belonging to the Corallicolidae family, public ASV sequences recovered after a BLASTn search on the NCBI nucleotide collection using the ASV5 (as the ASV5 is the most prevalent ASV annotated as belonging to the Corallicolidae family) as well as ASV sequences recovered from two studies and annotated as belonging to the Corallicolidae family (Sequences recovered from *Paramuricea clavata* in Bonacolta et al., 2024 and from *Pocillopora damicornis* in Clerissi et al., 2018).

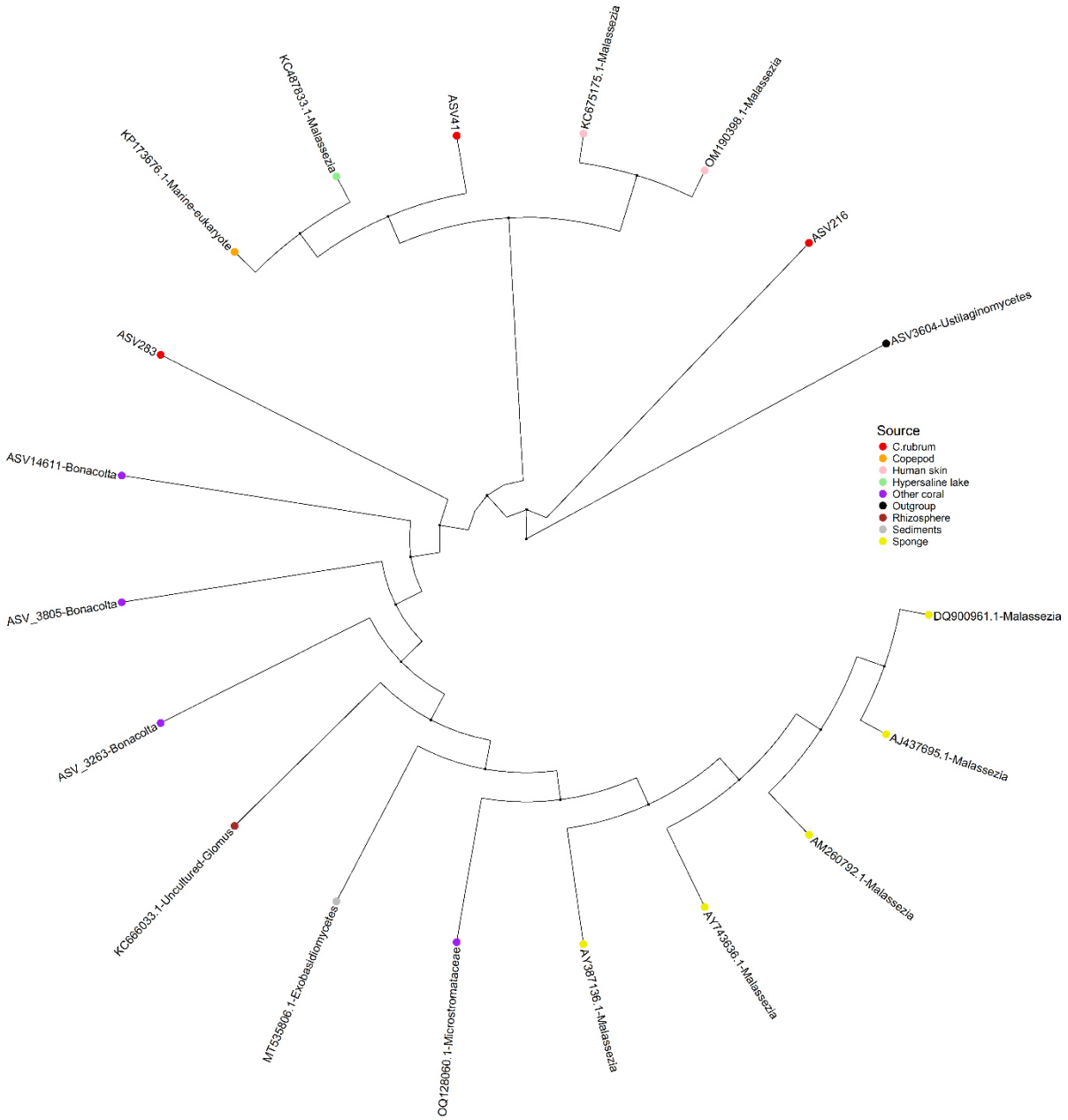

Figure S11: Dendrogram illustrating the phylogenetic relationships (PhyML, TN93 model) between all the ASVs annotated as belonging to the Exobasidiomycetes family, public ASV sequences recovered after a BLASTn search on the NCBI nucleotide collection using the ASV41 (as the ASV41 is the most prevalent ASV annotated as belonging to the Exobasidiomycetes family) as well as ASV sequences recovered from two studies and annotated as belonging to the Exobasidiomycetes family (Sequences recovered from *Paramuricea clavata* in Bonacolta et al., 2024 and from *Pocillopora damicornis, Pavona decussata* and *Porites lutea* in Papan et al., 2023).

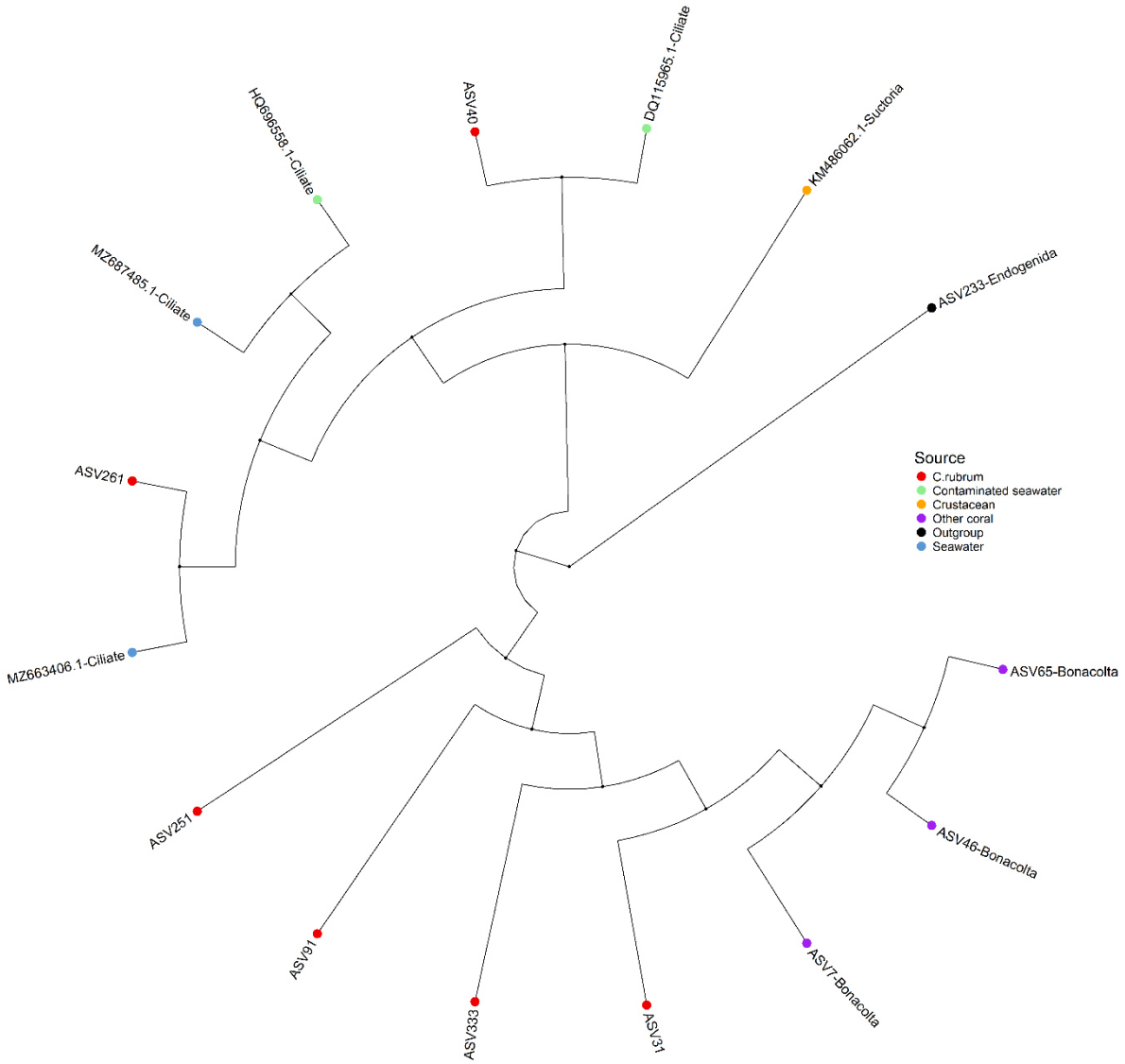

Figure S12: Dendrogram illustrating the phylogenetic relationships (PhyML, GTR model) between all the ASVs annotated as belonging to the Ephelotidae family, public ASV sequences recovered after a BLASTn search on the NCBI nucleotide collection using the ASV40 (as the ASV40 is the most prevalent ASV annotated as belonging to the Ephelotidae family) as well as ASV sequences recovered from one study and annotated as belonging to the Ephelotidae family (Sequences recovered from *Paramuricea clavata* in Bonacolta et al., 2024).

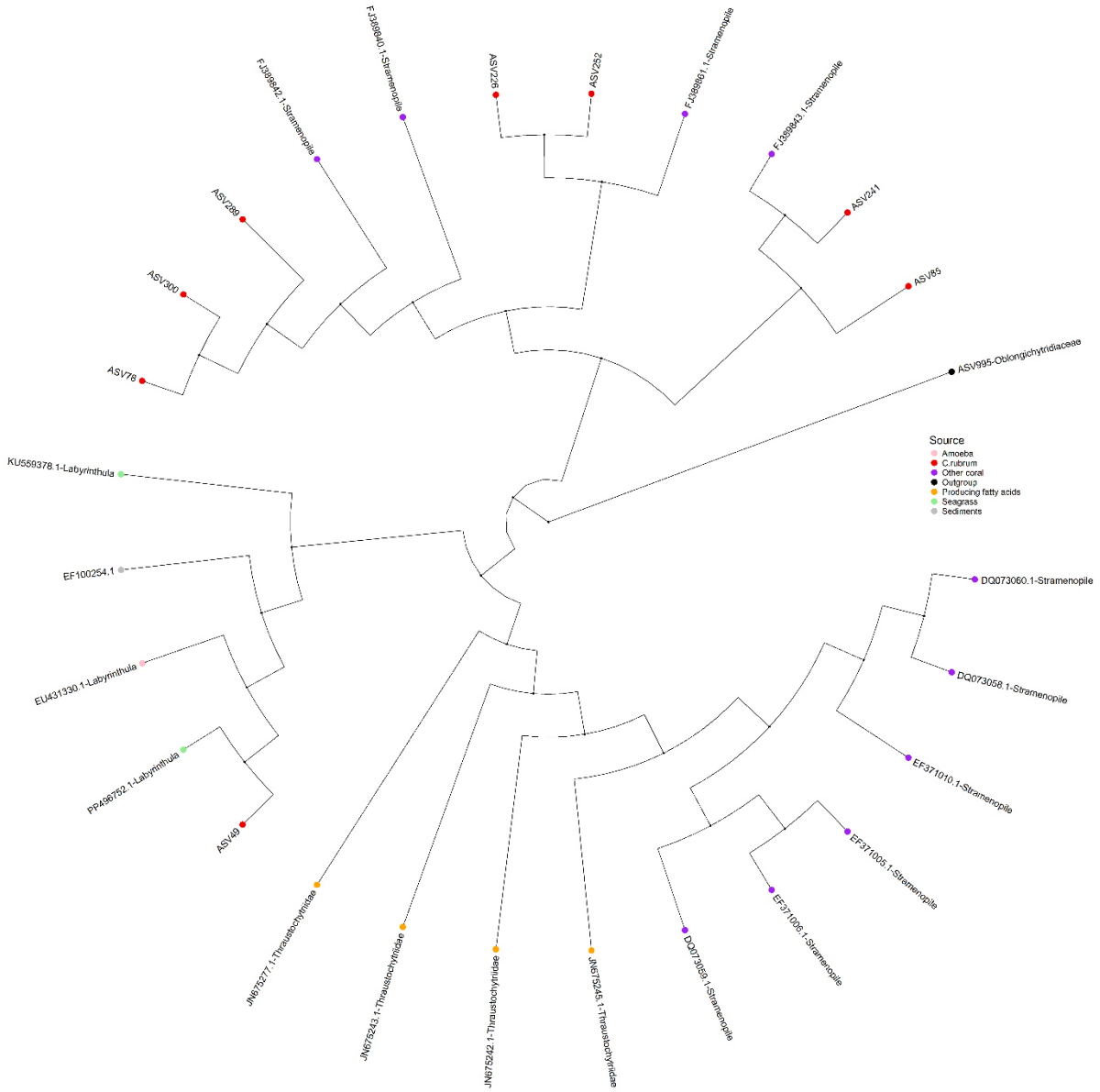

Figure S13: Dendrogram illustrating the phylogenetic relationships (PhyML, HKY85 model) between all the ASVs annotated as belonging to the Labyrinthulaceae family, public ASV sequences recovered after a BLASTn search on the NCBI nucleotide collection using the ASV49 (as the ASV49 is the most prevalent ASV annotated as belonging to the Labyrinthulaceae family) as well as ASV sequences recovered from three studies and annotated as belonging to the Labyrinthulaceae family (Sequences recovered from *Favia* spp. in Siboni et al. 2010, from fungiid corals in Ben-Dov et al. 2009 and from *Fungia granulosa* in Kramarsky-Winter et al. 2006).

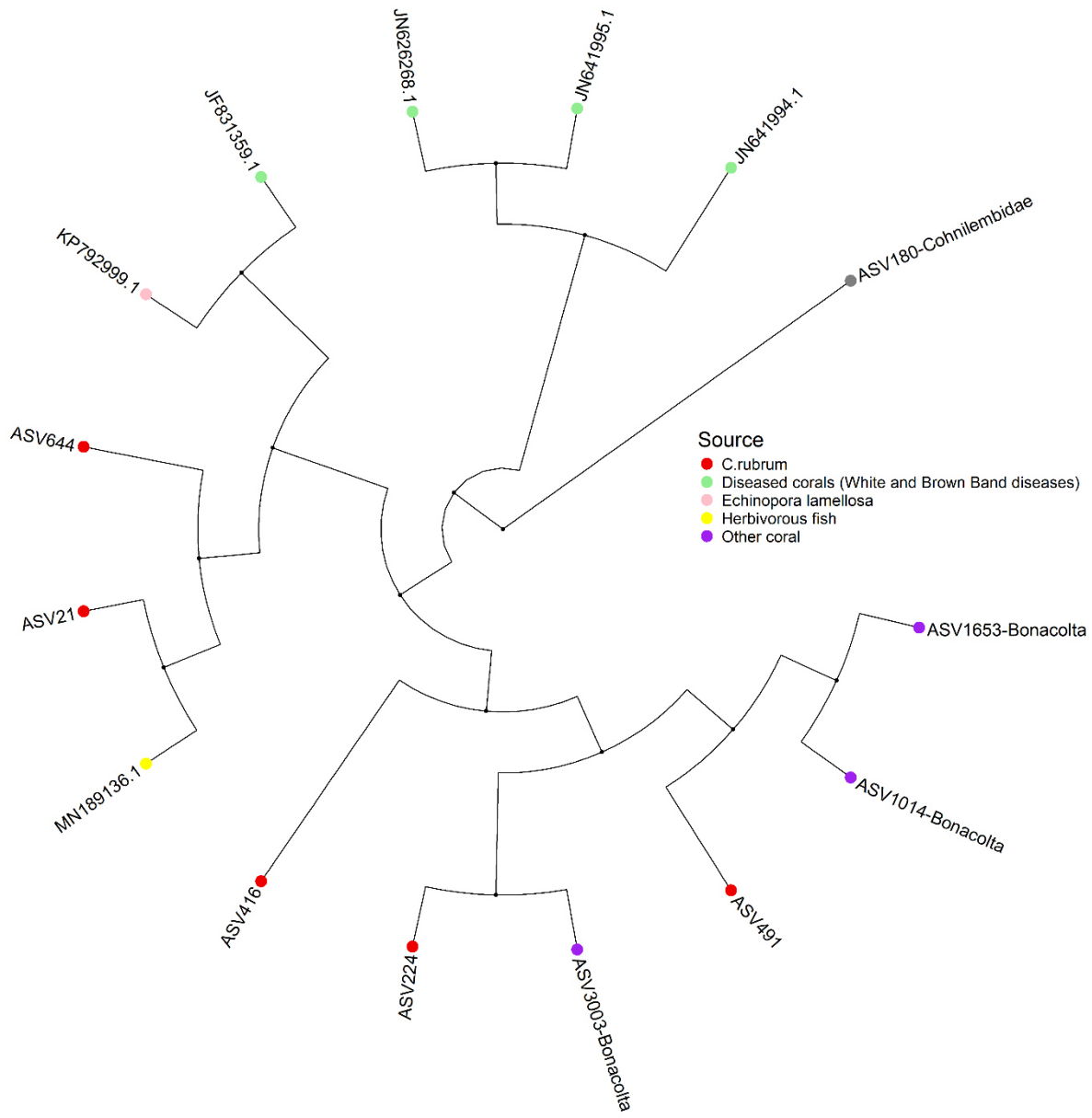

Figure S14: Dendrogram illustrating the phylogenetic relationships (PhyML, GTR model) between all the ASVs annotated as belonging to the Philasterida family, public ASV sequences recovered after a BLASTn search on the NCBI nucleotide collection using the ASV21 (as the ASV21 is the most prevalent ASV annotated as belonging to the Philasterida family) as well as ASV sequences recovered from one study and annotated as belonging to the Philasterida family (Sequences recovered from *Paramuricea clavata* in Bonacolta et al., 2024).

Appendix 7 – Chapter 6

Tables S2-S5, S9-S12 from supplementary file 1 as well as supplementary files 2 and 3 not available due to the large size of the tables but all supplementary information of this chapter can be found on the web version of the paper following this link:

https://environmentalmicrobiome.biomedcentral.com/articles/10.1186/s40793-025-00765-8

Table S1: Number of reads and sequences throughout the DADA2 pipeline for each sample.

	16S						18S						
Sample	input	filtered	denoisedF	denoisedR	merged	nonchim	input	filtered	denoisedF	nonchim	denoisedR	concatenated	NonMet
t1_Cr1_C	32156	20716	19527	20327	17948	10910	31345	17171	16991	17031	16917	13695	365
t1_Cr2_C							109874	71772	71457	71597	71335	62407	3650
t1_Cr3_C	42578	29379	28161	28870	25852	18279	35042	20842	20718	20775	20673	18260	129
t1_Cr4_C	34407	19396	18685	19106	17483	10478							
t1_Cr5_C	35734	25999	24743	25415	22384	15701	35084	22097	21906	22002	21827	18528	332
t1_Cr6_C	38049	27572	27152	27350	25517	19893	21663	14015	13926	13963	13898	10925	158
t1_Cr7_C	29402	23665	23521	23611	23305	18986							
t1_Cr8_C	38779	29032	27492	28373	24276	19016							
t1_Cr9_C	23969	18018	17832	17880	16960	13081							
t1_Cr1_C+4	43398	31897	31606	31743	30808	27615	25815	17579	17492	17514	17453	15330	415
t1_Cr2_C+4	41552	31195	30130	30737	26497	21815	29820	20449	20301	20364	20254	17849	3623
t1_Cr3_C+4	38828	26461	26282	26350	25733	22239	24809	14734	14584	14634	14521	12866	4447
t1_Cr4_C+4	28511	20030	19431	19714	17446	12730	38988	26251	26057	26176	26010	22050	4325
t1_Cr5_C+4	42683	30840	30557	30659	29622	26978	34832	22888	22766	22794	22706	19974	3765
t1_Cr6_C+4	40635	31569	31320	31442	30529	27751	42283	29465	29291	29364	29232	25691	1166
t1_Cr7_C+4	49887	36744	36425	36625	35603	28896	30809	19454	19328	19382	19278	17312	2394
t1_Cr8_C+4	33685	24804	24337	24583	23244	20665							
t1_Cr9_C+4	54326	33878	32988	33497	31331	24448	45739	30588	30413	30471	30326	27186	803
t1_Cr1_C+8	38288	26993	26757	26887	26463	25302	21948	14961	14806	14883	14745	12182	4764

t1_Cr2_C+8	50642	31958	28570	30603	22575	17506	28271	19057	18938	18990	18890	16450	1785
t1_Cr3_C+8	36632	15561	15001	15163	12836	8983	31552	20858	20661	20719	20546	17716	2186
t1_Cr4_C+8	39315	28426	27496	27987	25421	19854	25610	17110	17017	17048	16979	14143	141
t1_Cr5_C+8	38381	26116	24467	25252	19275	11917	35730	24387	24223	24311	24172	19825	2101
t1_Cr6_C+8	28015	21662	21191	21396	19578	17477	22415	12970	12824	12891	12760	10378	2315
t1_Cr7_C+8	43129	32226	31077	31673	27220	17883	33702	21563	21354	21453	21278	18606	769
t1_Cr8_C+8	34525	24748	23598	24139	19228	11831	30520	20709	20590	20614	20514	17993	1227
t1_Cr9_C+8	33674	22757	22091	22457	19855	15741	30795	21020	20937	20975	20907	18016	325
t2_Cr1_C	43670	32684	32188	32435	30461	25711	25044	15820	15680	15738	15641	15089	125
t2_Cr2_C													
t2_Cr3_C	36927	26792	26400	26584	24796	20086	46495	30149	29864	30000	29780	27976	166
t2_Cr4_C	56656	26001	25758	25888	25203	21791	26078	15209	15062	15091	14992	14225	146
t2_Cr5_C	44145	32444	31514	31888	28198	21338	39246	25239	24941	25113	24871	22601	50
t2_Cr6_C	109992	84749	82613	83817	78451	65544							
t2_Cr7_C	37988	28385	27861	28134	26866	23195							
t2_Cr8_C	35444	25382	23723	24650	20605	17036							
t2_Cr9_C	43021	31573	30495	31010	26777	19664	37320	23857	22352	23009	21645	15469	8094
t2_Cr1_C+4	44988	33929	32333	33105	28647	22809	23334	15288	15068	15101	14924	9710	3541
t2_Cr2_C+4	40714	26645	23353	25380	19725	17606	37529	24040	23144	23553	22714	17244	3010
t2_Cr3_C+4	43303	33187	32873	33051	31501	23355	40584	25379	25172	25246	25098	20764	3731
t2_Cr4_C+4	43212	33444	32944	33087	29263	19732	20210	13647	13515	13549	13468	11065	3770
t2_Cr5_C+4	77431	60387	59517	59897	52398	35494	31763	20520	20324	20401	20246	17373	5067
t2_Cr6_C+4	46388	36495	36076	36286	34675	28213	38894	22079	21853	21981	21792	20329	762
t2_Cr7_C+4	25132	18529	18134	18206	15861	11301	40350	24660	24346	24468	24279	23306	737
t2_Cr8_C+4	89436	63193	62474	62879	61318	54450	24835	15344	15166	15243	15112	14302	238
t2_Cr9_C+4	33238	25703	25193	25398	22924	17850	33787	22153	21930	22019	21844	21338	518
t2_Cr1_C+8							42776	24479	24125	24288	23970	21954	168
t2_Cr2_C+8	44716	29807	29260	29493	27571	22953	43153	25761	25580	25664	25512	23661	2379
t2_Cr3_C+8	39047	29360	27876	28707	24328	17687	24991	16200	16105	16135	16056	15688	101

t2_Cr4_C+8	47772	33698	33004	33326	31224	27620	36287	23634	23431	23505	23338	19585	361
t2_Cr5_C+8	40605	31539	30774	31121	28522	25537	30949	17408	17222	17294	17161	15207	214
t2_Cr6_C+8	48680	37880	37220	37513	35514	31969	26793	16986	16833	16865	16730	13528	3717
t2_Cr7_C+8	21901	15616	14963	15357	13840	11010	22997	15612	15561	15568	15533	12742	2009
t2_Cr8_C+8	38632	28983	28669	28821	27606	22730	21121	14256	14156	14183	14102	12131	2301
t2_Cr9_C+8	28839	21243	20924	21079	20266	16973	15955	9487	9319	9345	9208	7792	725
t3_Cr1_C													
t3_Cr2_C	59237	44880	44594	44765	43915	37115							
t3_Cr3_C	36580	26588	24921	25868	23402	17170	43022	29218	29003	29098	28931	25935	3177
t3_Cr4_C	45655	35452	35050	35252	33853	27743							
t3_Cr5_C							27935	18734	18586	18625	18504	15889	1933
t3_Cr6_C	38864	29677	29422	29498	28895	25378	25281	16489	16315	16387	16224	13084	542
t3_Cr7_C	40444	31265	30287	30901	28435	23538							
t3_Cr8_C							26605	17792	17631	17713	17585	14744	763
t3_Cr9_C							30410	20208	20027	20107	19952	17689	115
t3_Cr1_C+4							37234	25427	25238	25323	25174	21278	314
t3_Cr2_C+4	107706	50045	49800	49901	49175	42997	34777	23714	23565	23604	23491	20897	587
t3_Cr3_C+4	39182	29186	28986	29040	27962	19894	30107	16740	16611	16668	16575	14782	734
t3_Cr4_C+4	31549	24126	23966	23966	22615	14687	28758	16971	16796	16867	16717	14965	119
t3_Cr5_C+4													
t3_Cr6_C+4	37488	30671	30060	30287	27412	19303	34602	22999	22876	22889	22799	19526	1006
t3_Cr7_C+4													
t3_Cr8_C+4	26727	20750	20211	20508	18379	10231	37086	24643	24464	24551	24393	20778	866
t3_Cr9_C+4													
t3_Cr1_C+8							35947	23643	23362	23433	23176	19458	817
t3_Cr2_C+8	28388	22124	21997	22059	21580	15852	39146	25077	24948	24977	24870	21194	432
t3_Cr3_C+8	47918	36283	32563	34620	24549	16301	45688	28024	27388	27734	27132	21668	2242
t3_Cr4_C+8	52684	39310	39022	39201	38020	28201	31894	21219	20918	21064	20782	17527	5262
t3_Cr5_C+8	58601	46864	46221	46558	44616	31046	34407	20927	20804	20847	20742	17337	371

t3_Cr6_C+8	57509	43285	37615	40840	30957	18612	45219	27096	26834	26962	26713	22463	2589
t3_Cr7_C+8	29195	21657	21368	21547	20406	13538	41996	27906	27785	27838	27732	25409	474
t3_Cr8_C+8	50326	37937	34958	36817	29585	21086	43415	29942	29641	29754	29480	25497	7766
t3_Cr9_C+8	40046	31284	30825	31070	29382	20376	47153	30486	30299	30379	30217	26751	1226
t2_SW1_C	38789	26623	22905	25044	18385	14525	46209	30224	30103	30084	29997	26383	1176
t2_SW2_C	42366	32357	23500	28899	17234	13416	22705	14195	14004	14090	13926	12112	455
t2_SW1_C+4	47973	33879	29651	31949	22969	15071	28022	19294	19211	19217	19161	17280	381
t2_SW2_C+4	36310	27951	25531	26948	21754	18733	31004	18760	18558	18660	18487	17023	6804
t2_SW1_C+8	38860	28852	24831	27078	20872	17054	27675	15250	14378	14601	13906	12119	4825
t2_SW2_C+8							28391	18690	17830	18111	17351	13936	7234
Neg_1	58356	5523	5315	5422	5137	3992	12337	6554	6215	6325	6150	5651	
Neg_2	92207	5210	4717	4943	4109	3242	48706	32840	32711	32789	32683	31042	

Table S6: Metadata

Sample	Sample type	Colony number	Thermal treatment	Sampling time
t1_Cr1_C	Coral	1	Control	t1
t1_Cr2_C	Coral	2	Control	t1
t1_Cr3_C	Coral	3	Control	t1
t1_Cr4_C	Coral	4	Control	t1
t1_Cr5_C	Coral	5	Control	t1
t1_Cr6_C	Coral	6	Control	t1
t1_Cr7_C	Coral	7	Control	t1
t1_Cr8_C	Coral	8	Control	t1
t1_Cr9_C	Coral	9	Control	t1
t1_Cr1_C+4	Coral	1	C+4	t1
t1_Cr2_C+4	Coral	2	C+4	t1
t1_Cr3_C+4	Coral	3	C+4	t1
t1_Cr4_C+4	Coral	4	C+4	t1
t1_Cr5_C+4	Coral	5	C+4	t1
t1_Cr6_C+4	Coral	6	C+4	t1
t1_Cr7_C+4	Coral	7	C+4	t1
t1_Cr8_C+4	Coral	8	C+4	t1
t1_Cr9_C+4	Coral	9	C+4	t1
t1_Cr1_C+8	Coral	1	C+8	t1
t1_Cr2_C+8	Coral	2	C+8	t1
t1_Cr3_C+8	Coral	3	C+8	t1
t1_Cr4_C+8	Coral	4	C+8	t1
t1_Cr5_C+8	Coral	5	C+8	t1
t1_Cr6_C+8	Coral	6	C+8	t1
t1_Cr7_C+8	Coral	7	C+8	t1
t1_Cr8_C+8	Coral	8	C+8	t1

t1_Cr9_C+8	Coral	9	C+8	t1
t2_Cr1_C	Coral	1	Control	t2
t2_Cr3_C	Coral	3	Control	t2
t2_Cr4_C	Coral	4	Control	t2
t2_Cr5_C	Coral	5	Control	t2
t2_Cr6_C	Coral	6	Control	t2
t2_Cr7_C	Coral	7	Control	t2
t2_Cr8_C	Coral	8	Control	t2
t2_Cr9_C	Coral	9	Control	t2
t2_Cr1_C+4	Coral	1	C+4	t2
t2_Cr2_C+4	Coral	2	C+4	t2
t2_Cr3_C+4	Coral	3	C+4	t2
t2_Cr4_C+4	Coral	4	C+4	t2
t2_Cr5_C+4	Coral	5	C+4	t2
t2_Cr6_C+4	Coral	6	C+4	t2
t2_Cr7_C+4	Coral	7	C+4	t2
t2_Cr8_C+4	Coral	8	C+4	t2
t2_Cr9_C+4	Coral	9	C+4	t2
t2_Cr1_C+8	Coral	1	C+8	t2
t2_Cr2_C+8	Coral	2	C+8	t2
t2_Cr3_C+8	Coral	3	C+8	t2
t2_Cr4_C+8	Coral	4	C+8	t2
t2_Cr5_C+8	Coral	5	C+8	t2
t2_Cr6_C+8	Coral	6	C+8	t2
t2_Cr7_C+8	Coral	7	C+8	t2
t2_Cr8_C+8	Coral	8	C+8	t2
t2_Cr9_C+8	Coral	9	C+8	t2
t3_Cr2_C	Coral	2	Control	t3
t3_Cr3_C	Coral	3	Control	t3

t3_Cr4_C	Coral	4	Control	t3
t3_Cr5_C	Coral	5	Control	t3
t3_Cr6_C	Coral	6	Control	t3
t3_Cr7_C	Coral	7	Control	t3
t3_Cr8_C	Coral	8	Control	t3
t3_Cr9_C	Coral	9	Control	t3
t3_Cr1_C+4	Coral	1	C+4	t3
t3_Cr2_C+4	Coral	2	C+4	t3
t3_Cr3_C+4	Coral	3	C+4	t3
t3_Cr4_C+4	Coral	4	C+4	t3
t3_Cr6_C+4	Coral	6	C+4	t3
t3_Cr8_C+4	Coral	8	C+4	t3
t3_Cr1_C+8	Coral	1	C+8	t3
t3_Cr2_C+8	Coral	2	C+8	t3
t3_Cr3_C+8	Coral	3	C+8	t3
t3_Cr4_C+8	Coral	4	C+8	t3
t3_Cr5_C+8	Coral	5	C+8	t3
t3_Cr6_C+8	Coral	6	C+8	t3
t3_Cr7_C+8	Coral	7	C+8	t3
t3_Cr8_C+8	Coral	8	C+8	t3
t3_Cr9_C+8	Coral	9	C+8	t3
t2_SW1_C	Seawater	NA	Control	t2
t2_SW2_C	Seawater	NA	Control	t2
t2_SW1_C+4	Seawater	NA	C+4	t2
t2_SW2_C+4	Seawater	NA	C+4	t2
t2_SW1_C+8	Seawater	NA	C+8	t2
t2_SW2_C+8	Seawater	NA	C+8	t2
Neg_1	Negative control	NA	NA	NA

Neg_2	Negative control	NA	NA	NA

Table S7: Bacteria and microeukaryote diversity data (observed richness, Shannon diversity) for each sample and statistical tests.

Differences in observed richness between coral samples and seawater samples

Bacterial communities					Microeukaryotic communities				
GLM model on observed richness with negative binomial distribution									
glm.nb(formula = Observed ~ Sample type, data = Alpha, init.theta = 6.482308512, link = log)					glm.nb(formula = Observed ~ Sample type, data = Alpha, init.theta = 2.387198674, link = log)				
Coefficients:	**Estimate**	**Std. Error**	**z value**	**Pr(>|z|)**	**Coefficients:**	**Estimate**	**Std. Error**	**z value**	**Pr(>|z|)**
(Intercept)	5.48420	0.04792	114.455	<2,00E-16	(Intercept)	3.92287	0.08153	48.117	<2,00E-16
Sample type	1.02428	0.18289	5.601	2.14e-08	Sample type	0.84072	0.27908	3.012	0.00259
(Dispersion parameter for Negative Binomial(6.4823) family taken to be 1)					(Dispersion parameter for Negative Binomial(2.3872) family taken to be 1)				
Null deviance: 117.907 on 73 degrees of freedom					Null deviance: 90.733 on 71 degrees of freedom				
Residual deviance: 75.867 on 72 degrees of freedom					Residual deviance: 79.396 on 70 degrees of freedom				
AIC: 893.54					AIC: 704.17				
Number of Fisher Scoring iterations: 1					Number of Fisher Scoring iterations: 1				
Theta: 6.48					Theta: 2.387				
Std. Err.: 1.07					Std. Err.: 0.404				
2 x log-likelihood: -887.537					2 x log-likelihood: -698.168				

Differences in observed richness between sampling times and thermal treatments

Bacterial communities					Microeukaryotic communities				
GLM model on observed richness with negative binomial distribution									
glm.nb(formula = Observed ~ Sampling_time * Thermal_stress + Colony number, data = Alpha, init.theta = 7.382312797, link = log)					glm.nb(formula = Observed ~ Sampling_time * Thermal_stress + Colony number, data = Alpha, init.theta = 7.382312797, link = log)				
Coefficients:	**Estimate**	**Std. Error**	**z value**	**Pr(>|z|)**	**Coefficients:**	**Estimate**	**Std. Error**	**z value**	**Pr(>|z|)**
(Intercept)	5.378919	0.165853	32.432	<2e-16	(Intercept)	3.51303	0.27429	12.808	<2e-16
t1 vs t2	0.307526	0.186798	1.646	0.0997	t1 vs t2	0.12074	0.36436	0.331	0.7404
t1 vs t3	-0.051307	0.214333	-0.239	0.8108	t1 vs t3	0.51827	0.36926	1.404	0.1604
Control vs C+4	0.000949	0.182072	0.005	0.9958	Control vs C+4	0.55992	0.32189	1.739	0.0820
Control vs C+8	0.095592	0.181942	0.525	0.5993	Control vs C+8	0.59623	0.32177	1.853	0.0639
Colony number	-0.005137	0.018592	-0.276	0.7823	Colony number	-0.03163	0.02793	-1.132	0.2574
Control vs t2:C+4	-0.070357	0.256779	-0.274	0.7841	Control vs t2:C+4	0.28663	0.45022	0.637	0.5244
Control vs t3:C+4	-0.246671	0.299440	-0.824	0.4101	Control vs t3:C+4	-0.91830	0.48101	-1.909	0.0562
Control vs t2:C+8	-0.070501	0.260512	-0.271	0.7867	Control vs t2:C+8	0.06255	0.45048	0.139	0.8896
Control vs t3:C+8	0.166826	0.281609	0.592	0.5536	Control vs t3:C+8	-0.64957	0.45519	-1.427	0.1536
(Dispersion parameter for Negative Binomial(7.3823) family taken to be 1)					(Dispersion parameter for Negative Binomial(3.3542) family taken to be 1)				
Null deviance: 84.774 on 68 degrees of freedom					Null deviance: 90.172 on 65 degrees of freedom				
Residual deviance: 70.442 on 59 degrees of freedom					Residual deviance: 73.401 on 56 degrees of freedom				
AIC: 830.29					AIC: 634.13				
Number of Fisher Scoring iterations: 1					Number of Fisher Scoring iterations: 1				
Theta: 7.38					Theta: 3.354				
Std. Err.: 1.27					Std. Err.: 0.629				
2 x log-likelihood: -808.29					2 x log-likelihood: -612.130				
GLM model on Shannon index with Gamma distribution (log link)									
glm(formula = Shannon ~ Sampling_time * Thermal_stress + Colony_number, family = Gamma(link = "log"), data = Alpha)									
Coefficients:	**Estimate**	**Std. Error**	**z value**	**Pr(>|z|)**	**Coefficients:**	**Estimate**	**Std. Error**	**z value**	**Pr(>|z|)**
(Intercept)	0.773095	0.146116	5.291	1.87e-06	(Intercept)	0.956073	0.128949	7.414	7.9e-10
t1 vs t2	-0.076222	0.164817	-0.462	0.645	t1 vs t2	0.009393	0.170969	0.055	0.956
t1 vs t3	-0.167950	0.188599	-0.891	0.377	t1 vs t3	-0.043794	0.174571	-0.251	0.803
Control vs C+4	-0.126234	0.160291	-0.788	0.434	Control vs C+4	-0.043829	0.154515	-0.284	0.778
Control vs C+8	-0.032069	0.160291	-0.200	0.842	Control vs C+8	0.057190	0.151852	0.377	0.708
Colony number	-0.001308	0.016397	-0.080	0.937	Colony number	-0.012608	0.013490	-0.935	0.354
Control vs t2:C+4	0.238408	0.226519	1.052	0.297	Control vs t2:C+4	-0.021798	0.215096	-0.101	0.920
Control vs t3:C+4	0.184733	0.263074	0.702	0.485	Control vs t3:C+4	-0.028537	0.228833	-0.125	0.901
Control vs t2:C+8	0.381221	0.229972	1.658	0.103	Control vs t2:C+8	0.017428	0.212999	0.082	0.935
Control vs t3:C+8	0.380909	0.248102	1.535	0.130	Control vs t3:C+8	-0.136889	0.215901	-0.634	0.529
(Dispersion parameter for Gamma family taken to be 0.1086584)					(Dispersion parameter for Gamma family taken to be 0.07262119)				
Null deviance: 8.6586 on 68 degrees of freedom					Null deviance: 4.9899 on 64 degrees of freedom				
Residual deviance: 7.3554 on 59 degrees of freedom					Residual deviance: 4.6014 on 55 degrees of freedom				
AIC: 164.04					AIC: 143.82				
Number of Fisher Scoring iterations: 5					Number of Fisher Scoring iterations: 5				

Table S8: Outputs of the PERMANOVA statistical tests.

Differences in microbial composition between samples and negative control

PERMANOVA with 999 permutations

adonis2(formula = distance matrix ~ Sample type, data = ASV table)

Bacterial communities

	Df	SumOfSqs	R2	F	Pr(>F)
Sample type	2	625425856	0.08178	3.2508	0.042
Residual	73	7022320010	0.91822		
Total	75	7647745866	1.00000		

Microeukaryotic communities

	Df	SumOfSqs	R2	F	Pr(>F)
Sample type	1	10573070	0.09365	6.8195	0.033
Residual	66	102327812	0.90635		
Total	67	112900882	1.00000		

Differences in microbial composition between coral and seawater samples

PERMANOVA with 999 permutations

adonis2(formula = distance matrix ~ Sample type, data = ASV table)

Bacterial communities

	Df	SumOfSqs	R2	F	Pr(>F)
Sample type	1	0.9573	0.12342	10.137	0.001
Residual	72	6.7994	0.87658		
Total	73	7.7568	1.00000		

Microeukaryotic communities

	Df	SumOfSqs	R2	F	Pr(>F)
Sample type	1	1701	0.02885	2.0798	0.003
Residual	70	57240	0.97115		
Total	71	58940	1.00000		

Differences in microbial composition between sampling times for the control condition

PERMANOVA with 999 permutations

adonis2(formula = Aitchison distance matrix ~ Sampling time, data = ASV table Control)

Bacterial communities

	Df	SumOfSqs	R2	F	Pr(>F)
Sampling time	2	0.24967	0.10479	1.1705	0.295
Residual	20	2.13300	0.89521		
Total	22	2.38268	1.00000		

Microeukaryotic communities

	Df	SumOfSqs	R2	F	Pr(>F)
Sampling time	2	0.27585	0.12197	0.9724	0.493
Residual	14	1.98569	0.87803		
Total	16	2.26154	1.00000		

Differences in microeukaryotes composition between samples without tissue loss accross the different sampling sites

PERMANOVA with 999 permutations

adonis2(formula = Aitchison distance matrix ~ Thermal stress * Sampling time +Thermal stress:Colony number + Sampling time:Colony number, data = ASV table)

Bacterial communities

	Df	SumOfSqs	R2	F	Pr(>F)
Thermal stress	2	8882	0.05527	2.1499	0.001
Sampling time	2	14345	0.08927	3.4722	0.001
Thermal stress:Sampling time	2	5219	0.03248	1.2632	0.058
Thermalstress:Colony number	24	53106	0.33050	1.0712	0.156
Samplingtime:Colony number	15	31623	0.19680	1.0206	0.401
Residual	23	47510	0.29567		
Total	68	160685	1.00000		

Microeukaryotic communities

	Df	SumOfSqs	R2	F	Pr(>F)
Thermal stress	2	1872	0.03870	1.3154	0.005
Sampling time	2	2658	0.05495	1.8677	0.001
Thermal stress	2	1846	0.03817	1.2974	0.002
Thermal stress	23	16163	0.33419	0.9878	0.571
Sampling time:	16	11598	0.23980	1.0189	0.383
Residual	20	14229	0.29420		
Total	65	48366	1.00000		

Pairwise permanova for differences between sites

Bacterial communities

pairs	SumOfSqs	F.Model	R2	pval	p.adj
Control vs C+8_t2	7427,55789	2,07155063	0,06459153	0,001	0,002625
Control vs C+8_t3	6787,07879	1,88168653	0,06093212	0,001	0,002625
C+4_t1 vs C+8_t2	6680,99144	2,21077817	0,12139943	0,001	0,002625
C+4_t1 vs C+8_t3	6048,09538	1,99882335	0,11758598	0,001	0,002625
C+4_t2 vs C+8_t3	6385,43947	1,71775552	0,09177145	0,001	0,002625
C+8_t1 vs C+4_t3	5040,13218	2,10126478	0,1490125	0,001	0,002625
C+8_t1 vs C+8_t3	6025,57243	1,80440977	0,10737716	0,001	0,002625
C+8_t2 vs C+8_t3	6685,16962	1,63012223	0,09802226	0,001	0,002625
C+4_t1 vs C+4_t3	4843,141	2,41348039	0,16744605	0,002	0,0042
C+8_t2 vs C+4_t3	5914,9531	1,76528947	0,12824209	0,002	0,0042
C+4_t1 vs C+4_t2	4345,9891	1,56358176	0,07992308	0,003	0,00525
C+4_t1 vs C+8_t1	3391,50061	1,46948701	0,08411735	0,003	0,00525
C+8_t1 vs C+8_t2	5050,71307	1,52315966	0,08692266	0,004	0,00646154
C+4_t2 vs C+8_t1	4172,99035	1,3723399	0,07084017	0,02	0,028
C+4_t2 vs C+8_t2	5376,89175	1,46289874	0,07516346	0,02	0,028
Control vs C+4_t3	4971,24455	1,55177013	0,05632198	0,025	0,0328125
C+4_t2 vs C+4_t3	5079,64313	1,69776611	0,10815336	0,027	0,03335294
Control vs C+4_t2	4592,93332	1,34536993	0,04034653	0,035	0,04083333
Control vs C+8_t1	4200,04895	1,31060093	0,04185806	0,045	0,04973684
Control vs C+4_t1	3747,99712	1,22969476	0,03937582	0,107	0,11235
C+4_t3 vs C+8_t3	3027,22589	0,89409811	0,07517158	0,715	0,715

Microeukaryotic communities

pairs	SumOfSqs	F.Model	R2	pval	p.adj
Control vs C+4_	1444,66812	1,90052835	0,07337798	0,001	0,00233333
Control vs C+8_	1666,45835	2,20449902	0,08412674	0,001	0,00233333
C+4_t1 vs C+4_	1599,35998	2,28115372	0,11247653	0,001	0,00233333
C+4_t1 vs C+8_	1373,93683	1,97543194	0,09889308	0,001	0,00233333
C+4_t2 vs C+8_	1567,46462	1,91543927	0,09617861	0,001	0,00233333
C+4_t2 vs C+8_	1509,35237	2,03122194	0,11265027	0,001	0,00233333
C+8_t1 vs C+8_	1498,72496	1,84407417	0,0929282	0,001	0,00233333
C+8_t2 vs C+4_	1333,38808	1,86107604	0,12523158	0,001	0,00233333
C+8_t2 vs C+8_	1360,98209	1,84723188	0,10350243	0,001	0,00233333
C+4_t1 vs C+4_	1029,95951	1,57037618	0,0947701	0,002	0,0035
C+4_t1 vs C+8_	1141,87066	1,66935763	0,08487098	0,002	0,0035
C+4_t2 vs C+4_	1351,91729	1,86671132	0,12556316	0,002	0,0035
Control vs C+8_	1175,07134	1,47051446	0,05353065	0,003	0,00484615
Control vs C+4_	1159,77835	1,61542228	0,05849711	0,004	0,0056
C+4_t2 vs C+8_	1175,61939	1,55503787	0,08858072	0,004	0,0056
C+8_t1 vs C+8_	1091,73957	1,36257819	0,07037173	0,015	0,0196875
Control vs C+8_	970,975264	1,29928584	0,05135662	0,017	0,021
C+4_t1 vs C+8_	1019,86332	1,34608079	0,06305986	0,032	0,03733333
Control vs C+4_	926,341157	1,25818862	0,056527	0,037	0,04089474
C+8_t1 vs C+4_	1008,80573	1,26651119	0,07786004	0,072	0,0756
C+4_t3 vs C+8_	770,124024	1,09931985	0,07796971	0,189	0,189

ANOVA on the betadispersion values (distance to centroid) between sampling times

anova(betadisper(Aitchison distance matrix, group= Sampling time))

Bacterial communities

	Df	Sum Sq	Mean Sq	F value	Pr(>F)
Groups	3	1488.1	496.03	1.6707	0.1812
Residuals	70	20783.4	296.91		

Microeukaryotic communities

	Df	Sum Sq	Mean Sq	F value	Pr(>F)
Groups	3	28.58	9.5282	0.5915	0.6227
Residuals	68	1095.46	16.1097		

ANOVA on the betadispersion values (distance to centroid) between thermal treatments

anova(betadisper(Aitchison distance matrix, group= Thermal treatment))

Bacterial communities

	Df	Sum Sq	Mean Sq	F value	Pr(>F)
Groups	2	690.8	345.41	1.2099	0.3043
Residuals	71	20269.0	285.48		

Microeukaryotic communities

	Df	Sum Sq	Mean Sq	F value	Pr(>F)
Groups	2	39.91	19.954	1.3026	0.2784
Residuals	69	1057.02	15.319		

Table S12: Sequences and amplification efficiencies of the different qPCR primer pairs used for each targeted gene

Target	Gene	Sequences 5'- 3		Efficacies	Reference
Bacteria	*16s bacteria*	Forward	ACTCCTACGGGAGGCAGCAG	2,0178	Fierer et al. (2005)
		Reverse	ATTACCGCGGCTGCTGG		
	16s Spirocheataceae	Forward	YCCTGGGCTACACACGT	1,966	Husmann et al. (2010)
		Reverse	GTTACGACTTCACCCTCCT		
	16s vibrio	Forward	GGCGTAAAGCGCATGCAGGT	2,07	Thompson et al. (2004)
		Reverse	GAAATTCTACCCCCCTCTACAG		
Host	HSP70	Forward	TCGACCAAAGTTGAATCC	2,346	Haguenauer et al. (2013)
		Reverse	TGCATCTTTTGTCGCTTGAC		
	TNRF	Forward	GCGTTACTTCCTTGGCCTTT	2,1017	Tignat-Perrier et al. (2023)
		Reverse	AAGGAAGAGCTCTGCGGATC		
Reference	*Beta actin*	Forward	GCCAGCAGTTCAAGTTTGGA	2,009	Tignat-Perrier et al. (2023)
		Reverse	ACCAGCAGATTCCATTCCCA		
NB : The efficacy is calculated as 10^(-1/Slope value) for the Pfaffl method					

Table S13: Output of the statistical tests on the qPCR data

Host

	Kruskal-Wallis rank sum test for HSP70 by thermal treatment				Kruskal-Wallis rank sum test for TNRF by thermal treatment			
t1	**Test: HSP70 at t1 by Thermal treatment**				**Test: TNRF at t1 by Thermal treatment**			
	Kruskal-Wallis chi-squared = 9.2525, df = 2, p-value = 0.009791				Kruskal-Wallis chi-squared = 9.0658, df = 2, p-value = 0.01075			
	Pairwise comparisons using Wilcoxon rank sum test with continuity correction				**Pairwise comparisons using Wilcoxon rank sum test with continuity correction**			
		Control	C+4			Control	C+4	
	C+4	0.706	-	P value adjustment method: BH	C+4	0.054	-	P value adjustment method: BH
	C+8	0.010	0.028		C+8	0.010	0.297	
t2	**Test: HSP70 at t2 by Thermal treatment**				**Test: TNRF at t2 by Thermal treatment**			
	Kruskal-Wallis chi-squared = 11.327, df = 2, p-value = 0.00347				Kruskal-Wallis chi-squared = 6.9508, df = 2, p-value = 0.03095			
	Pairwise comparisons using Wilcoxon rank sum test with continuity correction				**Pairwise comparisons using Wilcoxon rank sum test with continuity correction**			
		Control	C+4			Control	C+4	
	C+4	0.3758	-	P value adjustment method: BH	C+4	1.000	-	P value adjustment method: BH
	C+8	0.0086	0.0056		C+8	0.017	0.124	
t3	**Test: HSP70 at t3 by Thermal treatment**				**Test: TNRF at t3 by Thermal treatment**			
	Kruskal-Wallis chi-squared = 5.4657, df = 2, p-value = 0.06503				Kruskal-Wallis chi-squared = 8.4066, df = 2, p-value = 0.01495			
	Pairwise comparisons using Wilcoxon rank sum test with continuity correction				**Pairwise comparisons using Wilcoxon rank sum test with continuity correction**			
		Control	C+4			Control	C+4	
	C+4	0.017	-	P value adjustment method: BH	C+4	0.10	-	P value adjustment method: BH
	C+8	0.706	0.415		C+8	0.01	0.37	

Bacteria

	Kruskal-Wallis rank sum test for total bacteria by thermal treatment				Kruskal-Wallis rank sum test for *Vibrio* by thermal treatment				Kruskal-Wallis rank sum test for Spirochaetaceae by thermal treatment			
t1	**Test: total bacteria at t1 by Thermal treatment**				**Test: *Vibrio* at t1 by Thermal treatment**				**Test: Spirochaetaceae at t1 by Thermal treatment**			
	Kruskal-Wallis chi-squared = 0.79818, df = 2, p-value = 0.6709				Kruskal-Wallis chi-squared = 0.064617, df = 2, p-value = 0.9682				Kruskal-Wallis chi-squared = 0.1327, df = 2, p-value = 0.9358			
	Pairwise comparisons using Wilcoxon rank sum test with continuity correction				**Pairwise comparisons using Wilcoxon rank sum test with continuity correction**				**Pairwise comparisons using Wilcoxon rank sum test with continuity correction**			
		Control	C+4			Control	C+4			Control	C+4	
	C+4	0.71	-	P value adjustment method: BH	C+4	1	-	P value adjustment method: BH	C+4	1	-	P value adjustment method: BH
	C+8	0.71	0.71		C+8	1	1		C+8	1	1	
t2	**Test: total bacteria at t2 by Thermal treatment**				**Test: *Vibrio* at t2 by Thermal treatment**				**Test: Spirochaetaceae at t2 by Thermal treatment**			
	Kruskal-Wallis chi-squared = 5.5935, df = 2, p-value = 0.06101				Kruskal-Wallis chi-squared = 13.396, df = 2, p-value = 0.001233				Kruskal-Wallis chi-squared = 1.5895, df = 2, p-value = 0.4517			
	Pairwise comparisons using Wilcoxon rank sum test with continuity correction				**Pairwise comparisons using Wilcoxon rank sum test with continuity correction**				**Pairwise comparisons using Wilcoxon rank sum test with continuity correction**			
		Control	C+4			Control	C+4			Control	C+4	
	C+4	0.505	-	P value adjustment method: BH	C+4	0.00065	-	P value adjustment method: BH	C+4	1.00	-	P value adjustment method: BH
	C+8	0.017	0.505		C+8	0.00864	0.95913		C+8	0.56	0.56	
t3	**Test: total bacteria at t3 by Thermal treatment**				**Test: *Vibrio* at t3 by Thermal treatment**				**Test: Spirochaetaceae at t3 by Thermal treatment**			
	Kruskal-Wallis chi-squared = 5.8473, df = 2, p-value = 0.05374				Kruskal-Wallis chi-squared = 8.0406, df = 2, p-value = 0.01795				Kruskal-Wallis chi-squared = 0.99225, df = 2, p-value = 0.6089			
	Pairwise comparisons using Wilcoxon rank sum test with continuity correction				**Pairwise comparisons using Wilcoxon rank sum test with continuity correction**				**Pairwise comparisons using Wilcoxon rank sum test with continuity correction**			
		Control	C+4			Control	C+4			Control	C+4	
	C+4	0.01	-	P value adjustment method: BH	C+4	0.010	-	P value adjustment method: BH	C+4	0.71	-	P value adjustment method: BH
	C+8	0.71	0.51		C+8	0.050	0.931		C+8	0.66	0.71	

References

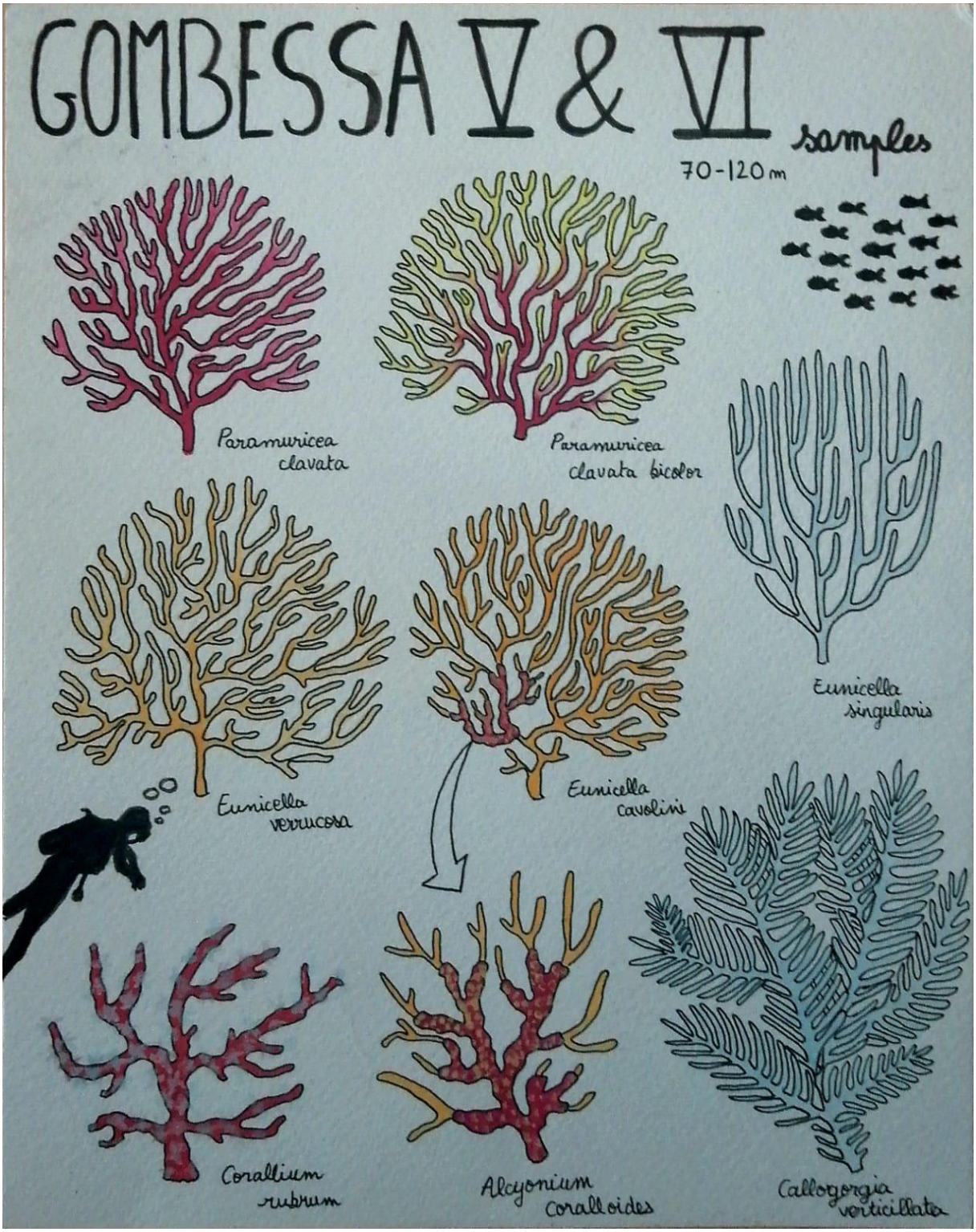

©Personal illustation

References

Abarenkov, Kessy, Allan Zirk, Timo Piirmann, et al. 2025. “UNITE General FASTA Release for Fungi.” UNITE Community, February 19. Application/gzip. https://doi.org/10.15156/BIO/3301229.

Abd El-Rahman, Tahany M.A., Nagwa A. Tharwat, Sayed M.S. Abo El-Souad, Ahmed A. El-Beih, and Ahmed I. El-Diwany. 2020. “Biological Activities and Variation of Symbiotic Fungi Isolated from Coral Reefs Collected from Red Sea in Egypt.” *Mycology* 11 (3): 243–55. https://doi.org/10.1080/21501203.2020.1741470.

Abrego, David, Karin E Ulstrup, Bette L Willis, and Madeleine J.H Van Oppen. 2008. “Species–Specific Interactions between Algal Endosymbionts and Coral Hosts Define Their Bleaching Response to Heat and Light Stress.” *Proceedings of the Royal Society B: Biological Sciences* 275 (1648): 2273–82. https://doi.org/10.1098/rspb.2008.0180.

Acinas, Silvia G., Luisa A. Marcelino, Vanja Klepac-Ceraj, and Martin F. Polz. 2004. “Divergence and Redundancy of 16S rRNA Sequences in Genomes with Multiple *Rrn* Operons.” *Journal of Bacteriology* 186 (9): 2629–35. https://doi.org/10.1128/JB.186.9.2629-2635.2004.

Ahmed, Hanin Ibrahim, Marcela Herrera, Yi Jin Liew, and Manuel Aranda. 2019. “Long-Term Temperature Stress in the Coral Model Aiptasia Supports the ‘Anna Karenina Principle’ for Bacterial Microbiomes.” *Frontiers in Microbiology* 10 (May): 975. https://doi.org/10.3389/fmicb.2019.00975.

Aichelman, Hannah E., Colleen B. Bove, Karl D. Castillo, et al. 2021. “Exposure Duration Modulates the Response of Caribbean Corals to Global Change Stressors.” *Limnology and Oceanography* 66 (8): 3100–3115. https://doi.org/10.1002/lno.11863.

Ainsworth, T.D., A.J. Fordyce, and E.F. Camp. 2017. “The Other Microeukaryotes of the Coral Reef Microbiome.” *Trends in Microbiology* 25 (12): 980–91. https://doi.org/10.1016/j.tim.2017.06.007.

Ainsworth, Tracy D, Lutz Krause, Thomas Bridge, et al. 2015. “The Coral Core Microbiome Identifies Rare Bacterial Taxa as Ubiquitous Endosymbionts.” *The ISME Journal* 9 (10): 10. https://doi.org/10.1038/ismej.2015.39.

Alex, Anoop, and Agostinho Antunes. 2019. “Comparative Genomics Reveals Metabolic Specificity of Endozoicomonas Isolated from a Marine Sponge and the Genomic Repertoire for Host-Bacteria Symbioses.” *Microorganisms* 7 (12): 635. https://doi.org/10.3390/microorganisms7120635.

Alker, Alisa P., Garriet W. Smith, and Kiho Kim. 2001. “Characterization of Aspergillus Sydowii (Thom et Church), a Fungal Pathogen of Caribbean Sea Fan Corals.” *Hydrobiologia* 460 (1/3): 105–11. https://doi.org/10.1023/A:1013145524136.

Allemand, Denis, Christine Ferrier-Pagès, Paola Furla, et al. 2004. “Biomineralisation in Reef-Building Corals: From Molecular Mechanisms to Environmental Control.” *Comptes Rendus Palevol* 3 (6–7): 453–67. https://doi.org/10.1016/j.crpv.2004.07.011.

Allers, Elke, Christina Niesner, Christian Wild, and Jakob Pernthaler. 2008. “Microbes Enriched in Seawater after Addition of Coral Mucus.” *Applied and Environmental Microbiology* 74 (10): 3274–78. https://doi.org/10.1128/AEM.01870-07.

Alsharif, Sultan M., Moayad S. Waznah, Mohamed Ismaeil, and Wael S. El-Sayed. 2023. “16S rDNA-Based Diversity Analysis of Bacterial Communities Associated with Soft Corals of the Red Sea, Al Rayyis, White Head, KSA.” *Journal of Taibah University for Science* 17 (1): 2156762. https://doi.org/10.1080/16583655.2022.2156762.

Amend, Anthony S, Daniel J Barshis, and Thomas A Oliver. 2012. “Coral-Associated Marine Fungi Form Novel Lineages and Heterogeneous Assemblages.” *The ISME Journal* 6 (7): 1291–301. https://doi.org/10.1038/ismej.2011.193.

Amundsen, Per-Arne, Kevin D. Lafferty, Rune Knudsen, Raul Primicerio, Anders Klemetsen, and Armand M. Kuris. 2009. “Food Web Topology and Parasites in the Pelagic Zone of a Subarctic Lake.” *Journal of Animal Ecology* 78 (3): 563–72. https://doi.org/10.1111/j.1365-2656.2008.01518.x.

Angiolillo, Michela, and Simonepietro Canese. 2018. “Deep Gorgonians and Corals of the Mediterranean Sea.” In *Corals in a Changing World*, edited by Carmenza Duque Beltran and Edisson Tello Camacho. InTech. https://doi.org/10.5772/intechopen.69686.

Anthony, Sl, Ca Page, Dg Bourne, and Bl Willis. 2008. “Newly Characterized Distinct Phases of the Coral Disease ‘Atramentous Necrosis’ on the Great Barrier Reef.” *Diseases of Aquatic Organisms* 81 (September): 255–59. https://doi.org/10.3354/dao01962.

Antonius, Arnfried. 1999. “Halofolliculina Corallasia, a New Coral-Killing Ciliate on Indo-Pacific Reefs.” *Coral Reefs* 18 (3): 300–300. https://doi.org/10.1007/s003380050199.

Antonius, Arnfried A., and Diana Lipscomb. 2000. “First Protozoan Coral-Killer Identified in the Indo-Pacific.” *Atoll Research Bulletin* 481. https://doi.org/10.5479/si.00775630.481.

Apprill, Amy. 2017. “Marine Animal Microbiomes: Toward Understanding Host–Microbiome Interactions in a Changing Ocean.” *Frontiers in Marine Science* 4 (July): 222. https://doi.org/10.3389/fmars.2017.00222.

Ashraf, Nizam, Abdulaziz Anas, Vrinda Sukumaran, Girish Gopinath, K.K. Idrees Babu, and P.K. Dinesh Kumar. 2023. “Recent Advancements in Coral Health, Microbiome Interactions and Climate Change.” *Science of The Total Environment* 878 (June): 163085. https://doi.org/10.1016/j.scitotenv.2023.163085.

Avalos, Javier, and M. Carmen Limón. 2015. “Biological Roles of Fungal Carotenoids.” *Current Genetics* 61 (3): 309–24. https://doi.org/10.1007/s00294-014-0454-x.

Bachy, Charles, Elisabeth Hehenberger, Yu-Chen Ling, et al. 2022. “Marine Protists: A Hitchhiker’s Guide to Their Role in the Marine Microbiome.” In *The Marine Microbiome*, edited by Lucas J. Stal and Mariana Silvia Cretoiu, vol. 3. The Microbiomes of Humans, Animals, Plants, and the Environment. Springer International Publishing. https://doi.org/10.1007/978-3-030-90383-1_4.

Baedke, Jan, Alejandro Fábregas-Tejeda, and Abigail Nieves Delgado. 2020. “The Holobiont Concept before Margulis.” *Journal of Experimental Zoology Part B: Molecular and Developmental Evolution* 334 (3): 149–55. https://doi.org/10.1002/jez.b.22931.

Bahamon, Nixon, Jacopo Aguzzi, Miguel Ángel Ahumada-Sempoal, et al. 2020. “Stepped Coastal Water Warming Revealed by Multiparametric Monitoring at NW Mediterranean Fixed Stations.” *Sensors* 20 (9): 2658. https://doi.org/10.3390/s20092658.

Baker, Andrew C. 2003. “Flexibility and Specificity in Coral-Algal Symbiosis: Diversity, Ecology, and Biogeography of *Symbiodinium*.” *Annual Review of Ecology, Evolution, and Systematics* 34 (1): 661–89. https://doi.org/10.1146/annurev.ecolsys.34.011802.132417.

Baker-Austin, Craig, Joaquin A. Trinanes, Nick G. H. Taylor, Rachel Hartnell, Anja Siitonen, and Jaime Martinez-Urtaza. 2013. “Emerging Vibrio Risk at High Latitudes in Response to Ocean Warming.” *Nature Climate Change* 3 (1): 73–77. https://doi.org/10.1038/nclimate1628.

Balabanova, Larissa, Lubov Slepchenko, Oksana Son, and Liudmila Tekutyeva. 2018. “Biotechnology Potential of Marine Fungi Degrading Plant and Algae Polymeric Substrates.” *Frontiers in Microbiology* 9 (July): 1527. https://doi.org/10.3389/fmicb.2018.01527.

Balbuena, Juan Antonio, Raúl Míguez-Lozano, and Isabel Blasco-Costa. 2013. “PACo: A Novel Procrustes Application to Cophylogenetic Analysis.” *PLoS ONE* 8 (4): e61048. https://doi.org/10.1371/journal.pone.0061048.

Balbuena, Juan Antonio, Óscar Alejandro Pérez-Escobar, Cristina Llopis-Belenguer, and Isabel Blasco-Costa. 2020. “Random Tanglegram Partitions (Random TaPas): An Alexandrian Approach to the Cophylogenetic Gordian Knot.” *Systematic Biology* 69 (6): 1212–30. https://doi.org/10.1093/sysbio/syaa033.

Ballesteros, Enric. 2006. “Mediterranean Coralligenous Assemblages : A Synthesis of Present Knowledge.” In *Oceanography and Marine Biology*, 0 ed. CRC Press. https://doi.org/10.1201/9781420006391-7.

Bally, Marc, and Joaquim Garrabou. 2007a. “Thermodependent Bacterial Pathogens and Mass Mortalities in Temperate Benthic Communities: A New Case of Emerging Disease Linked to Climate Change.” *Global Change Biology* 13 (10): 2078–88. https://doi.org/10.1111/j.1365-2486.2007.01423.x.

Bally, Marc, and Joaquim Garrabou. 2007b. “Thermodependent Bacterial Pathogens and Mass Mortalities in Temperate Benthic Communities: A New Case of Emerging Disease Linked to Climate Change.” *Global Change Biology* 13 (10): 2078–88. https://doi.org/10.1111/j.1365-2486.2007.01423.x.

Banos, Stefanos, Guillaume Lentendu, Anna Kopf, Tesfaye Wubet, Frank Oliver Glöckner, and Marlis Reich. 2018. “A Comprehensive Fungi-Specific 18S rRNA Gene Sequence Primer Toolkit Suited for Diverse Research Issues and Sequencing Platforms.” *BMC Microbiology* 18 (1): 190. https://doi.org/10.1186/s12866-018-1331-4.

Bärlocher, Felix, and Lynne Boddy. 2016. “Aquatic Fungal Ecology – How Does It Differ from Terrestrial?” *Fungal Ecology* 19 (February): 5–13. https://doi.org/10.1016/j.funeco.2015.09.001.

Barr, Jeremy J., Rita Auro, Mike Furlan, et al. 2013. “Bacteriophage Adhering to Mucus Provide a Non–Host-Derived Immunity.” *Proceedings of the National Academy of Sciences* 110 (26): 10771–76. https://doi.org/10.1073/pnas.1305923110.

Barshis, Daniel J., Jason T. Ladner, Thomas A. Oliver, François O. Seneca, Nikki Traylor-Knowles, and Stephen R. Palumbi. 2013. “Genomic Basis for Coral Resilience to Climate Change.” *Proceedings of the National Academy of Sciences* 110 (4): 1387–92. https://doi.org/10.1073/pnas.1210224110.

Bavestrello, G., M. Bo, S. Canese, R. Sandulli, and R. Cattaneo-Vietti. 2014. “The Red Coral Populations of the Gulfs of Naples and Salerno: Human Impact and Deep Mass Mortalities.” *Italian Journal of Zoology* 81 (4): 552–63. https://doi.org/10.1080/11250003.2014.950349.

Bayer, T, C Arif, C Ferrier-Pagès, D Zoccola, M Aranda, and Cr Voolstra. 2013a. “Bacteria of the Genus Endozoicomonas Dominate the Microbiome of the Mediterranean Gorgonian Coral Eunicella Cavolini.” *Marine Ecology Progress Series* 479 (April): 75–84. https://doi.org/10.3354/meps10197.

Bayer, T, C Arif, C Ferrier-Pagès, D Zoccola, M Aranda, and Cr Voolstra. 2013b. “Bacteria of the Genus Endozoicomonas Dominate the Microbiome of the Mediterranean Gorgonian Coral Eunicella Cavolini.” *Marine Ecology Progress Series* 479 (April): 75–84. https://doi.org/10.3354/meps10197.

Belivermiş, Murat, Önder Kılıç, H. Barış Özalp, et al. 2025. “Phenotypic Plasticity in Mediterranean Gorgonians Eunicella Singularis and Paramuricea Clavata at High Temperature and Low pH.” *Science of The Total Environment* 990 (August): 179845. https://doi.org/10.1016/j.scitotenv.2025.179845.

Ben-Dov, Eitan, Esti Kramarsky-Winter, and Ariel Kushmaro. 2009. “An in Situ Method for Cultivating Microorganisms Using a Double Encapsulation Technique: In Situ Method for Cultivating Microorganisms.” *FEMS Microbiology Ecology* 68 (3): 363–71. https://doi.org/10.1111/j.1574-6941.2009.00682.x.

Ben-Haim, Y., F. L. Thompson, C. C. Thompson, et al. 2003. “Vibrio Coralliilyticus Sp. Nov., a Temperature-Dependent Pathogen of the Coral Pocillopora Damicornis.” *International Journal of Systematic and Evolutionary Microbiology* 53 (1): 309–15. https://doi.org/10.1099/ijs.0.02402-0.

Ben-Haim, Yael, Maya Zicherman-Keren, and Eugene Rosenberg. 2003. “Temperature-Regulated Bleaching and Lysis of the Coral *Pocillopora Damicornis* by the Novel Pathogen *Vibrio Coralliilyticus*.” *Applied and Environmental Microbiology* 69 (7): 4236–42. https://doi.org/10.1128/AEM.69.7.4236-4242.2003.

Bennett, Reuel M., D. Honda, Gordon W. Beakes, and Marco Thines. 2017. “Labyrinthulomycota.” In *Handbook of the Protists*, edited by John M. Archibald, Alastair G.B. Simpson, and Claudio H. Slamovits. Springer International Publishing. https://doi.org/10.1007/978-3-319-28149-0_25.

Bentis, Cj, L Kaufman, and S Golubic. 2000. “Endolithic Fungi in Reef-Building Corals (Order : Scleractinia) Are Common, Cosmopolitan, and Potentially Pathogenic.” *The Biological Bulletin* 198 (2): 254–60. https://doi.org/10.2307/1542528.

Berzins, Ilze K., Roy P. E. Yanong, Elise E.B. LaDouceur, and Esther C. Peters. 2021. “Cnidaria.” In *Invertebrate Histology*, 1st ed., edited by Elise E.B. LaDouceur. Wiley. https://doi.org/10.1002/9781119507697.ch3.

Bianchi, C.Nike, and Carla Morri. 2000. “Marine Biodiversity of the Mediterranean Sea: Situation, Problems and Prospects for Future Research.” *Marine Pollution Bulletin* 40 (5): 367–76. https://doi.org/10.1016/S0025-326X(00)00027-8.

Bilewitch, Jaret P, and Sandie M Degnan. 2011. “A Unique Horizontal Gene Transfer Event Has Provided the Octocoral Mitochondrial Genome with an Active Mismatch Repair Gene That Has Potential for an Unusual Self-Contained Function.” *BMC Evolutionary Biology* 11 (1): 228. https://doi.org/10.1186/1471-2148-11-228.

Billaud, Mélanie, François Seneca, Eric Tambutté, and Dorota Czerucka. 2022. “An Increase of Seawater Temperature Upregulates the Expression of Vibrio Parahaemolyticus Virulence Factors Implicated in Adhesion and Biofilm Formation.” *Frontiers in Microbiology* 13 (March): 840628. https://doi.org/10.3389/fmicb.2022.840628.

Blasco-Costa, Isabel, Alexander Hayward, Robert Poulin, and Juan A. Balbuena. 2021. “Next-Generation Cophylogeny: Unravelling Eco-Evolutionary Processes.” *Trends in Ecology & Evolution* 36 (10): 907–18. https://doi.org/10.1016/j.tree.2021.06.006.

Bo, Marzia, Giorgio Bavestrello, Michela Angiolillo, et al. 2015. “Persistence of Pristine Deep-Sea Coral Gardens in the Mediterranean Sea (SW Sardinia).” *PLOS ONE* 10 (3): e0119393. https://doi.org/10.1371/journal.pone.0119393.

Bo, Marzia, Simonepietro Canese, Costanza Spaggiari, et al. 2012. “Deep Coral Oases in the South Tyrrhenian Sea.” *PLoS ONE* 7 (11): e49870. https://doi.org/10.1371/journal.pone.0049870.

Bo, Marzia, Carlo Cerrano, Simonepietro Canese, et al. 2014. “The Coral Assemblages of an Off-shore Deep M Editerranean Rocky Bank (NW S Icily, I Taly).” *Marine Ecology* 35 (3): 332–42. https://doi.org/10.1111/maec.12089.

Boavida, Joana, Jorge Assis, Inga Silva, and Ester A. Serrão. 2016. “Overlooked Habitat of a Vulnerable Gorgonian Revealed in the Mediterranean and Eastern Atlantic by Ecological Niche Modelling.” *Scientific Reports* 6 (1): 36460. https://doi.org/10.1038/srep36460.

Boessenkool, Sanne, Laura S. Epp, James Haile, et al. 2012. “Blocking Human Contaminant DNA during PCR Allows Amplification of Rare Mammal Species from Sedimentary Ancient DNA.” *Molecular Ecology* 21 (8): 1806–15. https://doi.org/10.1111/j.1365-294X.2011.05306.x.

Bogdanowicz, Damian, and Krzysztof Giaro. 2013. “On a Matching Distance between Rooted Phylogenetic Trees.” *International Journal of Applied Mathematics and Computer Science* 23 (3): 669–84. https://doi.org/10.2478/amcs-2013-0050.

Bogdanowicz, Damian, Krzysztof Giaro, and Borys Wróbel. 2012. “TreeCmp: Comparison of Trees in Polynomial Time.” *Evolutionary Bioinformatics* 8 (January): EBO.S9657. https://doi.org/10.4137/EBO.S9657.

Bonacolta, Anthony M., Jordi Miravall, Daniel Gómez-Gras, et al. 2024. “Differential Apicomplexan Presence Predicts Thermal Stress Mortality in the Mediterranean Coral

Paramuricea Clavata." *Environmental Microbiology*, 1462-2920.16548. https://doi.org/10.1111/1462-2920.16548.

Bonacolta, Anthony M., Bradley A. Weiler, Teresa Porta-Fitó, Michael Sweet, Patrick Keeling, and Javier Del Campo. 2023. "Beyond the Symbiodiniaceae: Diversity and Role of Microeukaryotic Coral Symbionts." *Coral Reefs* 42 (2): 567–77. https://doi.org/10.1007/s00338-023-02352-0.

Bongiorni, L, A Pusceddu, and R Danovaro. 2005. "Enzymatic Activities of Epiphytic and Benthic Thraustochytrids Involved in Organic Matter Degradation." *Aquatic Microbial Ecology* 41: 299–305. https://doi.org/10.3354/ame041299.

Bonifaz, A., H. Badali, G.S. De Hoog, et al. 2008. "Tinea Nigra by Hortaea Werneckii, a Report of 22 Cases from Mexico." *Studies in Mycology* 61: 77–82. https://doi.org/10.3114/sim.2008.61.07.

Bonthond, Guido, Daniel G. Merselis, Katherine E. Dougan, et al. 2018. "Inter-Domain Microbial Diversity within the Coral Holobiont *Siderastrea Siderea* from Two Depth Habitats." *PeerJ* 6 (February): e4323. https://doi.org/10.7717/peerj.4323.

Boogaart, K. Gerald van den, and R. Tolosana-Delgado. 2008a. "'Compositions': A Unified R Package to Analyze Compositional Data." *Computers & Geosciences* 34 (4): 4. https://doi.org/10.1016/j.cageo.2006.11.017.

Boogaart, K. Gerald van den, and R. Tolosana-Delgado. 2008b. "'Compositions': A Unified R Package to Analyze Compositional Data." *Computers & Geosciences* 34 (4): 320–38. https://doi.org/10.1016/j.cageo.2006.11.017.

Boote, Chloë Georgina. 2021. "Molecular Insights into a Novel Coral Model, Heliofungia Actiniformis." https://researchonline.jcu.edu.au/75791/1/JCU_75791_Boote_2021_thesis.pdf.

Bornbusch, Sally L, Carly R Muletz-Wolz, Ekaterina Lopez-Bondarchuk, Michael T Maslanka, and Erin L Kendrick. 2023. "Gut Microbiomes of Captive Primates Show Phylosymbiosis, Respond to Dietary Sugar Reduction, and Select for Host-Specific Dietary Microbes." *FEMS Microbiology Ecology* 99 (8): fiad069. https://doi.org/10.1093/femsec/fiad069.

Bornmann, Lutz, and Werner Marx. 2011. "The Anna Karenina Principle: A Concept for the Explanation of Success in Science." Version 2. Preprint, arXiv. https://doi.org/10.48550/ARXIV.1104.0807.

Borzykh, O. G., and L. V. Zvereva. 2015. "Mycobiota of the Bivalve Mollusk Anadara Broughtoni (Schrenck, 1867) from Various Parts of Peter the Great Bay, Sea of Japan." *Russian Journal of Marine Biology* 41 (4): 321–23. https://doi.org/10.1134/S1063074015040033.

Boudouresque, Charles F. 2004. "Marine Biodiversity in the Mediterranean: Status of Species, Populations and Communities." *Scientific Reports* 20 (January): 97–146.

Bourne, David G., Holly V. Boyett, Meegan E. Henderson, Andrew Muirhead, and Bette L. Willis. 2008. "Identification of a Ciliate (Oligohymenophorea: Scuticociliatia) Associated with Brown Band Disease on Corals of the Great Barrier Reef." *Applied and Environmental Microbiology* 74 (3): 883–88. https://doi.org/10.1128/AEM.01124-07.

Bourne, David G., Melissa Garren, Thierry M. Work, Eugene Rosenberg, Garriet W. Smith, and C. Drew Harvell. 2009. “Microbial Disease and the Coral Holobiont.” *Trends in Microbiology* 17 (12): 554–62. https://doi.org/10.1016/j.tim.2009.09.004.

Bourne, David G., Kathleen M. Morrow, and Nicole S. Webster. 2016. “Insights into the Coral Microbiome: Underpinning the Health and Resilience of Reef Ecosystems.” *Annual Review of Microbiology* 70 (1): 317–40. https://doi.org/10.1146/annurev-micro-102215-095440.

Bovio, Elena, Marilyne Fauchon, Yannick Toueix, Mohamed Mehiri, Giovanna Cristina Varese, and Claire Hellio. 2019. “The Sponge-Associated Fungus Eurotium Chevalieri MUT 2316 and Its Bioactive Molecules: Potential Applications in the Field of Antifouling.” *Marine Biotechnology* 21 (6): 743–52. https://doi.org/10.1007/s10126-019-09920-y.

Bovio, Elena, Giorgio Gnavi, Valeria Prigione, et al. 2017. “The Culturable Mycobiota of a Mediterranean Marine Site after an Oil Spill: Isolation, Identification and Potential Application in Bioremediation.” *Science of The Total Environment* 576 (January): 310–18. https://doi.org/10.1016/j.scitotenv.2016.10.064.

Bower, Susan M., Ryan B. Carnegie, Benjamin Goh, Simon R. M. Jones, Geoffrey J. Lowe, and Michelle W. S. Mak. 2004. “Preferential PCR Amplification of Parasitic Protistan Small Subunit rDNA from Metazoan Tissues.” *Journal of Eukaryotic Microbiology* 51 (3): 325–32. https://doi.org/10.1111/j.1550-7408.2004.tb00574.x.

Boyett, Holly V., David G. Bourne, and Bette L. Willis. 2007. “Elevated Temperature and Light Enhance Progression and Spread of Black Band Disease on Staghorn Corals of the Great Barrier Reef.” *Marine Biology* 151 (5): 1711–20. https://doi.org/10.1007/s00227-006-0603-y.

Bramanti, L., J. Movilla, M. Guron, et al. 2013. “Detrimental Effects of Ocean Acidification on the Economically Important Mediterranean Red Coral (*C Orallium Rubrum*).” *Global Change Biology* 19 (6): 1897–908. https://doi.org/10.1111/gcb.12171.

Brannock, Pamela M., Alice C. Ortmann, Anthony G. Moss, and Kenneth M. Halanych. 2016. “Metabarcoding Reveals Environmental Factors Influencing Spatio-temporal Variation in Pelagic Micro-eukaryotes.” *Molecular Ecology* 25 (15): 3593–604. https://doi.org/10.1111/mec.13709.

Bray, J. Roger, and J. T. Curtis. 1957. “An Ordination of the Upland Forest Communities of Southern Wisconsin.” *Ecological Monographs* 27 (4): 325–49. https://doi.org/10.2307/1942268.

Brooks, Andrew W., Kevin D. Kohl, Robert M. Brucker, Edward J. van Opstal, and Seth R. Bordenstein. 2016. “Phylosymbiosis: Relationships and Functional Effects of Microbial Communities across Host Evolutionary History.” *PLOS Biology* 14 (11): e2000225. https://doi.org/10.1371/journal.pbio.2000225.

Brown, B. E. 1997. “Coral Bleaching: Causes and Consequences.” *Coral Reefs* 16 (0): S129–38. https://doi.org/10.1007/s003380050249.

Brown, Kristen T., Gal Eyal, Sophie G. Dove, and Katie L. Barott. 2023. “Fine-Scale Heterogeneity Reveals Disproportionate Thermal Stress and Coral Mortality in Thermally Variable Reef

Habitats during a Marine Heatwave." *Coral Reefs* 42 (1): 131–42. https://doi.org/10.1007/s00338-022-02328-6.

Brown, Tanya, David Bourne, and Mauricio Rodriguez-Lanetty. 2013. "Transcriptional Activation of C3 and Hsp70 as Part of the Immune Response of Acropora Millepora to Bacterial Challenges." *PLoS ONE* 8 (7): e67246. https://doi.org/10.1371/journal.pone.0067246.

Bruckner, Andrew W. 2016. "Advances in Management of Precious Corals to Address Unsustainable and Destructive Harvest Techniques." In *The Cnidaria, Past, Present and Future*, edited by Stefano Goffredo and Zvy Dubinsky. Springer International Publishing. https://doi.org/10.1007/978-3-319-31305-4_46.

Brune, Andreas. 2014. "Symbiotic Digestion of Lignocellulose in Termite Guts." *Nature Reviews Microbiology* 12 (3): 168–80. https://doi.org/10.1038/nrmicro3182.

Buchan, Alison, Gary R. LeCleir, Christopher A. Gulvik, and José M. González. 2014. "Master Recyclers: Features and Functions of Bacteria Associated with Phytoplankton Blooms." *Nature Reviews Microbiology* 12 (10): 686–98. https://doi.org/10.1038/nrmicro3326.

Buonocore, Elvira, Luigia Donnarumma, Luca Appolloni, Antonino Miccio, Giovanni F. Russo, and Pier Paolo Franzese. 2020. "Marine Natural Capital and Ecosystem Services: An Environmental Accounting Model." *Ecological Modelling* 424 (May): 109029. https://doi.org/10.1016/j.ecolmodel.2020.109029.

Burgaud, Gaëtan, Virginia Edgcomb, Brandon T. Hassett, et al. 2022. "Marine Fungi." In *The Marine Microbiome*, edited by Lucas J. Stal and Mariana Silvia Cretoiu, vol. 3. The Microbiomes of Humans, Animals, Plants, and the Environment. Springer International Publishing. https://doi.org/10.1007/978-3-030-90383-1_5.

Burge, Ca, N Douglas, I Conti-Jerpe, et al. 2012. "Friend or Foe: The Association of Labyrinthulomycetes with the Caribbean Sea Fan Gorgonia Ventalina." *Diseases of Aquatic Organisms* 101 (1): 1–12. https://doi.org/10.3354/dao02487.

Burriesci, Matthew S., Theodore K. Raab, and John R. Pringle. 2012. "Evidence That Glucose Is the Major Transferred Metabolite in Dinoflagellate–Cnidarian Symbiosis." *Journal of Experimental Biology* 215 (19): 3467–77. https://doi.org/10.1242/jeb.070946.

Busing, Jordan D., Matthew Buendia, Yash Choksi, Girish Hiremath, and Suman R. Das. 2021. "Microbiome in Eosinophilic Esophagitis—Metagenomic, Metatranscriptomic, and Metabolomic Changes: A Systematic Review." *Frontiers in Physiology* 12 (September): 731034. https://doi.org/10.3389/fphys.2021.731034.

Cabañes, F. Javier. 2014. "Malassezia Yeasts: How Many Species Infect Humans and Animals?" *PLoS Pathogens* 10 (2): e1003892. https://doi.org/10.1371/journal.ppat.1003892.

Cabanillas-Bojórquez, Luis A., Octavio Valdez-Baro, Erick Paul Gutiérrez-Grijalva, and J. Basilio Heredia. 2023. "Microbial Production of Bioactive Compounds." In *Microbial Products for Future Industrialization*, edited by Angana Sarkar and Idris Adewale Ahmed. Interdisciplinary Biotechnological Advances. Springer Nature Singapore. https://doi.org/10.1007/978-981-99-1737-2_10.

Callahan, Benjamin J, Paul J McMurdie, Michael J Rosen, Andrew W Han, Amy Jo A Johnson, and Susan P Holmes. 2016. “DADA2: High-Resolution Sample Inference from Illumina Amplicon Data.” *Nature Methods* 13 (7): 581–83. https://doi.org/10.1038/nmeth.3869.

Campo, Javier del, David Bass, and Patrick J. Keeling. 2020. “The Eukaryome: Diversity and Role of Microeukaryotic Organisms Associated with Animal Hosts.” *Functional Ecology* 34 (10): 2045–54. https://doi.org/10.1111/1365-2435.13490.

Campo, Javier del, Maria J. Pons, Maria Herranz, et al. 2019. “Validation of a Universal Set of Primers to Study Animal-associated Microeukaryotic Communities.” *Environmental Microbiology* 21 (10): 3855–61. https://doi.org/10.1111/1462-2920.14733.

Canessa, Martina, Rosella Bertolotto, Federico Betti, et al. 2024. “Variation in the Health Status of the Mediterranean Gorgonian Forests: The Synergistic Effect of Marine Heat Waves and Fishing Activity.” *Biology* 13 (8): 642. https://doi.org/10.3390/biology13080642.

Cannas, Rita, Maria Cristina Follesa, Alessandro Cau, Angelo Cau, and Kim Friedman. 2019. *Global Report on the Biology, Fishery and Trade of Precious Corals*.

Capdevila, Pol, Yanis Zentner, Graciel·la Rovira, Joaquim Garrabou, Alba Medrano, and Cristina Linares. 2023. “Marine Heatwaves Favour Resistant Mediterranean Octocoral Populations at the Expense of Their Speed of Recovery.” Preprint, November 30. https://doi.org/10.1101/2023.11.29.569041.

Capdevila, Pol, Yanis Zentner, Graciel·la Rovira, Joaquim Garrabou, Alba Medrano, and Cristina Linares. 2024. “Mediterranean Octocoral Populations Exposed to Marine Heatwaves Are Less Resilient to Disturbances.” *Journal of Animal Ecology*, September 14, 1365-2656.14147. https://doi.org/10.1111/1365-2656.14147.

Carareto Alves, Lucia Maria, Jackson Antônio Marcondes De Souza, Alessandro De Mello Varani, and Eliana Gertrudes De Macedo Lemos. 2014. “The Family Rhizobiaceae.” In *The Prokaryotes*, edited by Eugene Rosenberg, Edward F. DeLong, Stephen Lory, Erko Stackebrandt, and Fabiano Thompson. Springer Berlin Heidelberg. https://doi.org/10.1007/978-3-642-30197-1_297.

Cardénas, Anny, and Christian R Voolstra. 2021. “Genomes and Full-Length 16S Reference Sequences for 27 Alpha- and Gamma-Proteobacterial Isolates from Red Sea Acropora Corals.” Version 1. Zenodo, February 1. https://doi.org/10.5281/ZENODO.4485821.

Cárdenas, Anny, Jin Ye, Maren Ziegler, et al. 2020. “Coral-Associated Viral Assemblages From the Central Red Sea Align With Host Species and Contribute to Holobiont Genetic Diversity.” *Frontiers in Microbiology* 11 (September): 572534. https://doi.org/10.3389/fmicb.2020.572534.

Carmona, Marvelisa L., Takeshi Naganuma, and Yukiho Yamaoka. 2003. “Identification by HPLC-MS of Carotenoids of the *Thraustochytrium* CHN-1 Strain Isolated from the Seto Inland Sea.” *Bioscience, Biotechnology, and Biochemistry* 67 (4): 884–88. https://doi.org/10.1271/bbb.67.884.

Caron, David A. 2005. “Marine Microbial Ecology in a Molecular World: What Does the Future Hold?” *Scientia Marina* 69 (S1): 97–110. https://doi.org/10.3989/scimar.2005.69s197.

Carpine, Christian, and Manfred Grasshoff. 1975. *Les Gorgonaires de la Méditerranée*. 140.

Cartes, J. E., D. Díaz-Viñolas, J. M. González-Irusta, A. Serrano, S. Mohamed, and A. Lombarte. 2022. “The Macrofauna Associated to the Bamboo Coral Isidella Elongata: To What Extent the Impact on Isideidae Affects Diversification of Deep-Sea Fauna.” *Coral Reefs* 41 (4): 1273–84. https://doi.org/10.1007/s00338-022-02243-w.

Carugati, Laura, Lorenzo Bramanti, Bruna Giordano, et al. 2021. “Colonization of Plastic Debris by the Long-Lived Precious Red Coral Corallium Rubrum: New Insights on the ‘Plastic Benefits’ Paradox.” *Marine Pollution Bulletin* 165 (April): 112104. https://doi.org/10.1016/j.marpolbul.2021.112104.

Casas-Güell, Edgar, Núria Teixidó, Joaquim Garrabou, and Emma Cebrian. 2015. “Structure and Biodiversity of Coralligenous Assemblages over Broad Spatial and Temporal Scales.” *Marine Biology* 162 (4): 4. https://doi.org/10.1007/s00227-015-2635-7.

Cattaneo-Vietti, R., M. Bo, R. Cannas, et al. 2016. “An Overexploited Italian Treasure: Past and Present Distribution and Exploitation of the Precious Red Coral *Corallium Rubrum* (L., 1758) (Cnidaria: Anthozoa).” *Italian Journal of Zoology* 83 (4): 443–55. https://doi.org/10.1080/11250003.2016.1255788.

Cau, Alessandro, Lorenzo Bramanti, Rita Cannas, et al. 2018. “Differential Response to Thermal Stress of Shallow and Deep Dwelling Colonies of Mediterranean Red Coral Corallium Rubrum (L., 1758).” *Advances in Oceanography and Limnology* 9 (1). https://doi.org/10.4081/aiol.2018.7275.

Cau, Alessandro, M. Cristina Follesa, Davide Moccia, et al. 2015. “Deepwater Corals Biodiversity along Roche Du Large Ecosystems with Different Habitat Complexity along the South Sardinia Continental Margin (CW Mediterranean Sea).” *Marine Biology* 162 (9): 1865–78. https://doi.org/10.1007/s00227-015-2718-5.

Caughman, Alicia M., Zoe A. Pratte, Nastassia V. Patin, and Frank J. Stewart. 2021. “Coral Microbiome Changes over the Day–Night Cycle.” *Coral Reefs* 40 (3): 921–35. https://doi.org/10.1007/s00338-021-02097-8.

Ceccarelli, Daniela, and Rita R. Colwell. 2014. “Vibrio Ecology, Pathogenesis, and Evolution.” *Frontiers in Microbiology* 5 (May). https://doi.org/10.3389/fmicb.2014.00256.

Ceh, Janja, Matt R. Kilburn, John B. Cliff, Jean-Baptiste Raina, Mike Van Keulen, and David G. Bourne. 2013. “Nutrient Cycling in Early Coral Life Stages: *Pocillopora Damicornis* Larvae Provide Their Algal Symbiont (*Symbiodinium*) with Nitrogen Acquired from Bacterial Associates.” *Ecology and Evolution* 3 (8): 2393–400. https://doi.org/10.1002/ece3.642.

Cerrano, C., A. Bastari, B. Calcinai, et al. 2019. “Temperate Mesophotic Ecosystems: Gaps and Perspectives of an Emerging Conservation Challenge for the Mediterranean Sea.” *The European Zoological Journal* 86 (1): 370–88. https://doi.org/10.1080/24750263.2019.1677790.

Cerrano, C., G. Bavestrello, C.N. Bianchi, et al. 2000. “A Catastrophic Mass-Mortality Episode of Gorgonians and Other Organisms in the Ligurian Sea (North-Western Mediterranean), Summer 1999.” *Ecology Letters* 3 (4): 284–93. https://doi.org/10.1046/j.1461-0248.2000.00152.x.

Cerrano, Carlo, Ulisse Cardini, Silvia Bianchelli, Cinzia Corinaldesi, Antonio Pusceddu, and Roberto Danovaro. 2013. “Red Coral Extinction Risk Enhanced by Ocean Acidification.” *Scientific Reports* 3 (1): 1457. https://doi.org/10.1038/srep01457.

Chapron, Leila, Pierre E. Galand, Audrey M. Pruski, et al. 2021. “Resilience of Cold-Water Coral Holobionts to Thermal Stress.” *Proceedings of the Royal Society B: Biological Sciences* 288 (1965): 20212117. https://doi.org/10.1098/rspb.2021.2117.

Chapron, Leila, Franck Lartaud, Nadine Le Bris, Erwan Peru, and Pierre E. Galand. 2020. “Local Variability in Microbiome Composition and Growth Suggests Habitat Preferences for Two Reef-Building Cold-Water Coral Species.” *Frontiers in Microbiology* 11 (February): 275. https://doi.org/10.3389/fmicb.2020.00275.

Chemel, Mathilde, Erwan Peru, Mohammad Binsarhan, Ramiro Logares, Franck Lartaud, and Pierre E. Galand. 2024. “Cold-Water Coral Mortality under Ocean Warming Is Associated with Pathogenic Bacteria.” *Environmental Microbiome* 19 (1): 76. https://doi.org/10.1186/s40793-024-00622-0.

Chen, Biao, Yuxin Wei, Kefu Yu, et al. 2024. “The Microbiome Dynamics and Interaction of Endosymbiotic Symbiodiniaceae and Fungi Are Associated with Thermal Bleaching Susceptibility of Coral Holobionts.” *Applied and Environmental Microbiology* 90 (4): e01939-23. https://doi.org/10.1128/aem.01939-23.

Chen, Yin, Wenjun Mao, Yupin Yang, et al. 2012. “Structure and Antioxidant Activity of an Extracellular Polysaccharide from Coral-Associated Fungus, *Aspergillus Versicolor* LCJ-5-4.” *Carbohydrate Polymers* 87 (1): 218–26. https://doi.org/10.1016/j.carbpol.2011.07.042.

Chen, Ying, Xiaoyan Pang, Yanchun He, et al. 2022a. “Secondary Metabolites from Coral-Associated Fungi: Source, Chemistry and Bioactivities.” *Journal of Fungi* 8 (10): 1043. https://doi.org/10.3390/jof8101043.

Chen, Ying, Xiaoyan Pang, Yanchun He, et al. 2022b. “Secondary Metabolites from Coral-Associated Fungi: Source, Chemistry and Bioactivities.” *Journal of Fungi* 8 (10): 1043. https://doi.org/10.3390/jof8101043.

Chen, Yu-Hsin, Jimmy Kuo, Ping-Jung Sung, et al. 2012. “Isolation of Marine Bacteria with Antimicrobial Activities from Cultured and Field-Collected Soft Corals.” *World Journal of Microbiology and Biotechnology* 28 (12): 3269–79. https://doi.org/10.1007/s11274-012-1138-7.

Chimetto, Luciane A., Marcelo Brocchi, Cristiane C. Thompson, Roberta C.R. Martins, Heloiza R. Ramos, and Fabiano L. Thompson. 2008. “Vibrios Dominate as Culturable Nitrogen-Fixing Bacteria of the Brazilian Coral Mussismilia Hispida.” *Systematic and Applied Microbiology* 31 (4): 312–19. https://doi.org/10.1016/j.syapm.2008.06.001.

Chimienti, Giovanni, Diana De Padova, Maria Adamo, et al. 2021. “Effects of Global Warming on Mediterranean Coral Forests.” *Scientific Reports* 11 (1): 20703. https://doi.org/10.1038/s41598-021-00162-4.

Chintiroglou, H., C. Dounas, and Ath. Koukouras. 1989. “The Presence of *Corallium Rubrum* (Linnaeus, 1758) in the Eastern Mediterranean Sea.” *Mitteilungen Aus Dem Museum Für*

Naturkunde in Berlin. Zoologisches Museum Und Institut Für Spezielle Zoologie (Berlin) 65 (1): 145–49. https://doi.org/10.1002/mmnz.19890650106.

Chuang, Po-Shun, and Satoshi Mitarai. 2020. "Signaling Pathways in the Coral Polyp Bail-out Response." *Coral Reefs* 39 (6): 1535–48. https://doi.org/10.1007/s00338-020-01983-x.

Clark, Abigail S., Sara D. Williams, Kerry Maxwell, et al. 2021. "Characterization of the Microbiome of Corals with Stony Coral Tissue Loss Disease along Florida's Coral Reef." *Microorganisms* 9 (11): 2181. https://doi.org/10.3390/microorganisms9112181.

Claverie, Jean-Michel, Renata Grzela, Audrey Lartigue, et al. 2009. "Mimivirus and Mimiviridae: Giant Viruses with an Increasing Number of Potential Hosts, Including Corals and Sponges." *Journal of Invertebrate Pathology* 101 (3): 172–80. https://doi.org/10.1016/j.jip.2009.03.011.

Clerissi, Camille, Sébastien Brunet, Jeremie Vidal-Dupiol, et al. 2018. "Protists Within Corals: The Hidden Diversity." *Frontiers in Microbiology* 9 (August): 2043. https://doi.org/10.3389/fmicb.2018.02043.

Coll, Marta, Chiara Piroddi, Jeroen Steenbeek, et al. 2010. "The Biodiversity of the Mediterranean Sea: Estimates, Patterns, and Threats." *PLoS ONE* 5 (8): 8. https://doi.org/10.1371/journal.pone.0011842.

Consoli, Pierpaolo, Teresa Romeo, Michela Angiolillo, et al. 2019. "Marine Litter from Fishery Activities in the Western Mediterranean Sea: The Impact of Entanglement on Marine Animal Forests." *Environmental Pollution* 249 (June): 472–81. https://doi.org/10.1016/j.envpol.2019.03.072.

"Copernicus Marine Service." 2023. https://marine.copernicus.eu/access-data.

Corinaldesi, Cinzia, Sara Canensi, Antonio Dell'Anno, et al. 2021. "Multiple Impacts of Microplastics Can Threaten Marine Habitat-Forming Species." *Communications Biology* 4 (1): 431. https://doi.org/10.1038/s42003-021-01961-1.

Corinaldesi, Cinzia, Stefano Varrella, Michael Tangherlini, et al. 2022. "Changes in Coral Forest Microbiomes Predict the Impact of Marine Heatwaves on Habitat-Forming Species down to Mesophotic Depths." *Science of The Total Environment* 823 (June): 153701. https://doi.org/10.1016/j.scitotenv.2022.153701.

Correa, Adrienne M. S., Tracy D. Ainsworth, Stephanie M. Rosales, Andrew R. Thurber, Christopher R. Butler, and Rebecca L. Vega Thurber. 2016. "Viral Outbreak in Corals Associated with an In Situ Bleaching Event: Atypical Herpes-Like Viruses and a New Megavirus Infecting Symbiodinium." *Frontiers in Microbiology* 7 (February). https://doi.org/10.3389/fmicb.2016.00127.

Correa, Hebelin, Brad Haltli, Carmenza Duque, and Russell Kerr. 2013. "Bacterial Communities of the Gorgonian Octocoral Pseudopterogorgia Elisabethae." *Microbial Ecology* 66 (4): 972–85. https://doi.org/10.1007/s00248-013-0267-3.

Cos, Josep, Francisco Doblas-Reyes, Martin Jury, Raül Marcos, Pierre-Antoine Bretonnière, and Margarida Samsó. 2022a. "The Mediterranean Climate Change Hotspot in the CMIP5 and CMIP6 Projections." *Earth System Dynamics* 13 (1): 321–40. https://doi.org/10.5194/esd-13-321-2022.

Cos, Josep, Francisco Doblas-Reyes, Martin Jury, Raül Marcos, Pierre-Antoine Bretonnière, and Margarida Samsó. 2022b. “The Mediterranean Climate Change Hotspot in the CMIP5 and CMIP6 Projections.” *Earth System Dynamics* 13 (1): 321–40. https://doi.org/10.5194/esd-13-321-2022.

Costantini, Federica, Marco Taviani, Alessandro Remia, Eleonora Pintus, Patrick J. Schembri, and Marco Abbiati. 2010. “Deep-water *Corallium Rubrum* (L., 1758) from the Mediterranean Sea: Preliminary Genetic Characterisation.” *Marine Ecology* 31 (2): 261–69. https://doi.org/10.1111/j.1439-0485.2009.00333.x.

Costanza, Robert, Rudolf De Groot, Paul Sutton, et al. 2014. “Changes in the Global Value of Ecosystem Services.” *Global Environmental Change* 26 (May): 152–58. https://doi.org/10.1016/j.gloenvcha.2014.04.002.

Couceiro, Joana Fernandes, Tina Keller-Costa, Matilde Marques, et al. 2021. “The Roseibium Album (Labrenzia Alba) Genome Possesses Multiple Symbiosis Factors Possibly Underpinning Host-Microbe Relationships in the Marine Benthos.” *Microbiology Resource Announcements* 10 (34): e00320-21. https://doi.org/10.1128/MRA.00320-21.

Creer, Simon, Kristy Deiner, Serita Frey, et al. 2016. “The Ecologist’s Field Guide to Sequence-based Identification of Biodiversity.” *Methods in Ecology and Evolution* 7 (9): 1008–18. https://doi.org/10.1111/2041-210X.12574.

Crisci, Carolina, Nathaniel Bensoussan, Jean-Claude Romano, and Joaquim Garrabou. 2011. “Temperature Anomalies and Mortality Events in Marine Communities: Insights on Factors behind Differential Mortality Impacts in the NW Mediterranean.” *PLoS ONE* 6 (9): e23814. https://doi.org/10.1371/journal.pone.0023814.

Csárdi, Gábor, and Tamás Nepusz. 2006. “The Igraph Software Package for Complex Network Research.” https://api.semanticscholar.org/CorpusID:16923281.

Cui, Lijia, Alison Morris, and Elodie Ghedin. 2013. “The Human Mycobiome in Health and Disease.” *Genome Medicine* 5 (7): 63. https://doi.org/10.1186/gm467.

Cziesielski, Maha J., Yi Jin Liew, Guoxin Cui, et al. 2018. “Multi-Omics Analysis of Thermal Stress Response in a Zooxanthellate Cnidarian Reveals the Importance of Associating with Thermotolerant Symbionts.” *Proceedings of the Royal Society B: Biological Sciences* 285 (1877): 20172654. https://doi.org/10.1098/rspb.2017.2654.

Cziesielski, Maha J., Sebastian Schmidt-Roach, and Manuel Aranda. 2019. “The Past, Present, and Future of Coral Heat Stress Studies.” *Ecology and Evolution* 9 (17): 10055–66. https://doi.org/10.1002/ece3.5576.

Da Silva, Daniela M G, Filipa R Pedrosa, M Ângela Taipa, Rodrigo Costa, and Tina Keller-Costa. 2023. “Widespread Occurrence of Chitinase-Encoding Genes Suggests the *Endozoicomonadaceae* Family as a Key Player in Chitin Processing in the Marine Benthos.” *ISME Communications* 3 (1): 109. https://doi.org/10.1038/s43705-023-00316-7.

Dacey, Daniel P., and Frédéric J. J. Chain. 2021. “Concatenation of Paired-End Reads Improves Taxonomic Classification of Amplicons for Profiling Microbial Communities.” *BMC Bioinformatics* 22 (1): 493. https://doi.org/10.1186/s12859-021-04410-2.

Daly, Marymegan, Mercer R. Brugler, Paulyn Cartwright, et al. 2007. “The Phylum Cnidaria: A Review of Phylogenetic Patterns and Diversity 300 Years after Linnaeus*.” *Zootaxa* 1668 (1). https://doi.org/10.11646/zootaxa.1668.1.11.

Damare, V, and S Raghukumar. 2010. “Association of the Stramenopilan Protists, the Aplanochytrids, with Zooplankton of the Equatorial Indian Ocean.” *Marine Ecology Progress Series* 399 (January): 53–68. https://doi.org/10.3354/meps08277.

Damhorst, Gregory L, Max W Adelman, Michael H Woodworth, and Colleen S Kraft. 2021. “Current Capabilities of Gut Microbiome–Based Diagnostics and the Promise of Clinical Application.” *The Journal of Infectious Diseases* 223 (Supplement_3): S270–75. https://doi.org/10.1093/infdis/jiaa689.

Dang, Hongyue, Tiegang Li, Mingna Chen, and Guiqiao Huang. 2008. “Cross-Ocean Distribution of *Rhodobacterales* Bacteria as Primary Surface Colonizers in Temperate Coastal Marine Waters.” *Applied and Environmental Microbiology* 74 (1): 52–60. https://doi.org/10.1128/AEM.01400-07.

Darmaraki, Sofia. 2019. “Past Variability of Mediterranean Sea Marine Heatwaves.” *Geophysical Research Letters* 46 (16): 9813–23. https://doi.org/10.1029/2019GL082933.

Darmaraki, Sofia, Samuel Somot, Florence Sevault, et al. 2019. “Future Evolution of Marine Heatwaves in the Mediterranean Sea.” *Climate Dynamics* 53 (3–4): 1371–92. https://doi.org/10.1007/s00382-019-04661-z.

Davis, Nicole M., Diana M. Proctor, Susan P. Holmes, David A. Relman, and Benjamin J. Callahan. 2018. “Simple Statistical Identification and Removal of Contaminant Sequences in Marker-Gene and Metagenomics Data.” *Microbiome* 6 (1): 1. https://doi.org/10.1186/s40168-018-0605-2.

Davy, Je, and Nl Patten. 2007. “Morphological Diversity of Virus-like Particles within the Surface Microlayer of Scleractinian Corals.” *Aquatic Microbial Ecology* 47 (April): 37–44. https://doi.org/10.3354/ame047037.

De Castro-Fernández, Paula, Elisenda Ballesté, Carlos Angulo-Preckler, Jason Biggs, Conxita Avila, and Cristina García-Aljaro. 2023. “How Does Heat Stress Affect Sponge Microbiomes? Structure and Resilience of Microbial Communities of Marine Sponges from Different Habitats.” *Frontiers in Marine Science* 9 (January): 1072696. https://doi.org/10.3389/fmars.2022.1072696.

De Leo, Filomena, Angelina Lo Giudice, Chiara Alaimo, et al. 2019. “Occurrence of the Black Yeast Hortaea Werneckii in the Mediterranean Sea.” *Extremophiles* 23 (1): 9–17. https://doi.org/10.1007/s00792-018-1056-1.

Deidun, A., F. Andaloro, G. Bavestrello, et al. 2014. “First Characterisation of a *Leiopathes Glaberrima* (Cnidaria: Anthozoa: Antipatharia) Forest in Maltese Exploited Fishing Grounds.” *Italian Journal of Zoology*, December 3, 1–10. https://doi.org/10.1080/11250003.2014.986544.

Del Campo, Javier, Maria J. Pons, Maria Herranz, et al. 2019. “Validation of a Universal Set of Primers to Study Animal-associated Microeukaryotic Communities.” *Environmental Microbiology* 21 (10): 3855–61. https://doi.org/10.1111/1462-2920.14733.

Delgadillo-Ordoñez, Nathalia, Inês Raimundo, Adam R. Barno, et al. 2022. “Red Sea Atlas of Coral-Associated Bacteria Highlights Common Microbiome Members and Their Distribution across Environmental Gradients—A Systematic Review.” *Microorganisms* 10 (12): 2340. https://doi.org/10.3390/microorganisms10122340.

Dennis, Mm, Aamj Becker, and Ma Freeman. 2020. “Pathology of Multifocal Purple Spots, a Nonspecific Lesion Morphology of Caribbean Sea Fans Gorgonia Spp.” *Diseases of Aquatic Organisms* 141 (September): 79–89. https://doi.org/10.3354/dao03523.

Desalvo, M. K., C. R. Voolstra, S. Sunagawa, et al. 2008. “Differential Gene Expression during Thermal Stress and Bleaching in the Caribbean Coral *Montastraea Faveolata*.” *Molecular Ecology* 17 (17): 3952–71. https://doi.org/10.1111/j.1365-294X.2008.03879.x.

DeSalvo, Mk, S Sunagawa, Cr Voolstra, and M Medina. 2010. “Transcriptomic Responses to Heat Stress and Bleaching in the Elkhorn Coral Acropora Palmata.” *Marine Ecology Progress Series* 402 (March): 97–113. https://doi.org/10.3354/meps08372.

Di Carro, Marina, Emanuele Magi, Francesco Massa, et al. 2018. “Untargeted Approach for the Evaluation of Anthropic Impact on the Sheltered Marine Area of Portofino (Italy).” *Marine Pollution Bulletin* 131 (June): 87–94. https://doi.org/10.1016/j.marpolbul.2018.03.059.

Dittami, Simon M., Enrique Arboleda, Jean-Christophe Auguet, et al. 2021. “A Community Perspective on the Concept of Marine Holobionts: Current Status, Challenges, and Future Directions.” *PeerJ* 9 (February): e10911. https://doi.org/10.7717/peerj.10911.

Dixon, Groves, Evelyn Abbott, and Mikhail Matz. 2020. “Meta-analysis of the Coral Environmental Stress Response: *Acropora* Corals Show Opposing Responses Depending on Stress Intensity.” *Molecular Ecology* 29 (15): 2855–70. https://doi.org/10.1111/mec.15535.

Dixon, Philip. 2003. “VEGAN, a Package of R Functions for Community Ecology.” *Journal of Vegetation Science* 14 (6): 927–30. https://doi.org/10.1111/j.1654-1103.2003.tb02228.x.

Doering, Talisa, Justin Maire, Madeleine J. H. Van Oppen, and Linda L. Blackall. 2023. “Advancing Coral Microbiome Manipulation to Build Long-Term Climate Resilience.” *Microbiology Australia* 44 (1): 36–40. https://doi.org/10.1071/MA23009.

Domart-Coulon, I. J., C. S. Sinclair, R. T. Hill, S. Tambutt, S. Puverel, and G. K. Ostrander. 2004. “A Basidiomycete Isolated from the Skeleton of Pocillopora Damicornis (Scleractinia) Selectively Stimulates Short-Term Survival of Coral Skeletogenic Cells.” *Marine Biology* 144 (3): 583–92. https://doi.org/10.1007/s00227-003-1227-0.

Dong, Yu-Liang, Xiao-Ming Li, Xiao-Shan Shi, Yi-Ran Wang, Bin-Gui Wang, and Ling-Hong Meng. 2023. “Diketopiperazine Alkaloids and Bisabolene Sesquiterpenoids from Aspergillus Versicolor AS-212, an Endozoic Fungus Associated with Deep-Sea Coral of Magellan Seamounts.” *Marine Drugs* 21 (5): 5. https://doi.org/10.3390/md21050293.

D’Onghia, Gianfranco, Porzia Maiorano, Roberto Carlucci, et al. 2012. “Comparing Deep-Sea Fish Fauna between Coral and Non-Coral ‘Megahabitats’ in the Santa Maria Di Leuca Cold-Water Coral Province (Mediterranean Sea).” *PLoS ONE* 7 (9): e44509. https://doi.org/10.1371/journal.pone.0044509.

Douglas, A.E. 2003. “Coral Bleaching—How and Why?” *Marine Pollution Bulletin* 46 (4): 385–92. https://doi.org/10.1016/S0025-326X(03)00037-7.

Dray, Stéphane, and Anne-Béatrice Dufour. 2007. “The Ade4 Package: Implementing the Duality Diagram for Ecologists.” *Journal of Statistical Software* 22 (4). https://doi.org/10.18637/jss.v022.i04.

Dungan, Ashley M., Dieter Bulach, Heyu Lin, Madeleine J. H. Van Oppen, and Linda L. Blackall. 2021. “Development of a Free Radical Scavenging Bacterial Consortium to Mitigate Oxidative Stress in Cnidarians.” *Microbial Biotechnology* 14 (5): 2025–40. https://doi.org/10.1111/1751-7915.13877.

Dunphy, Courtney M., Steven V. Vollmer, and Tarik C. Gouhier. 2021. “Host–Microbial Systems as Glass Cannons: Explaining Microbiome Stability in Corals Exposed to Extrinsic Perturbations.” *Journal of Animal Ecology* 90 (5): 1044–57. https://doi.org/10.1111/1365-2656.13466.

Easson, Cole G., Deborah J. Gochfeld, and Marc Slattery. 2024. “Microbiome Changes in Sinularia Spp. Soft Corals Relative to Health Status.” *Marine Biology* 171 (2): 53. https://doi.org/10.1007/s00227-023-04362-6.

Eckman, James E., David O. Duggins, and Amy T. Sewell. 1989. “Ecology of under Story Kelp Environments. I. Effects of Kelps on Flow and Particle Transport near the Bottom.” *Journal of Experimental Marine Biology and Ecology* 129 (2): 173–87. https://doi.org/10.1016/0022-0981(89)90055-5.

Edgar, Robert C. 2022. “Muscle5: High-Accuracy Alignment Ensembles Enable Unbiased Assessments of Sequence Homology and Phylogeny.” *Nature Communications* 13 (1): 6968. https://doi.org/10.1038/s41467-022-34630-w.

El-Gendy, Mervat Morsy Abbas Ahmed, Shaymaa M. M. Yahya, Ahmed R. Hamed, Maha M. Soltan, and Ahmed Mohamed Ahmed El-Bondkly. 2018. “Phylogenetic Analysis and Biological Evaluation of Marine Endophytic Fungi Derived from Red Sea Sponge Hyrtios Erectus.” *Applied Biochemistry and Biotechnology* 185 (3): 755–77. https://doi.org/10.1007/s12010-017-2679-x.

Elsawy, Mohammed B. D., and Abderrahim Lakhouit. 2020. “A Review on the Impact of Salinity on Foundation Soil of Coastal Infrastructures and Its Implications to North of Red Sea Coastal Constructions.” *Arabian Journal of Geosciences* 13 (13): 555. https://doi.org/10.1007/s12517-020-05601-6.

Epstein, Hannah E., Gergely Torda, and Madeleine J. H. Van Oppen. 2019. “Relative Stability of the Pocillopora Acuta Microbiome throughout a Thermal Stress Event.” *Coral Reefs* 38 (2): 373–86. https://doi.org/10.1007/s00338-019-01783-y.

Erlandson, Sonya, Xiaojing Wei, Jessica Savage, Jeannine Cavender-Bares, and Kabir Peay. 2018. “Soil Abiotic Variables Are More Important than Salicaceae Phylogeny or Habitat Specialization in Determining Soil Microbial Community Structure.” *Molecular Ecology* 27 (8): 2007–24. https://doi.org/10.1111/mec.14576.

Espinoza, César, Carlos D. Herrera-García, Victoria Espinosa-García, et al. 2021. “The Antiproliferative Potential of Fungi Associated with Coral and Algae Collected from a

Veracruz Reef System, Gulf of Mexico." *Latin American Journal of Aquatic Research* 49 (5): 843–49. https://doi.org/10.3856/vol49-issue5-fulltext-2704.

Estaque, Tristan, Solène Basthard-Bogain, Olivier Bianchimani, et al. 2024. "Investigating the Outcomes of a Threatened Gorgonian in Situ Transplantation: Survival and Microbiome Diversity in Paramuricea Clavata (Risso, 1827)." *Marine Environmental Research* 196 (April): 106384. https://doi.org/10.1016/j.marenvres.2024.106384.

Estaque, Tristan, Justine Richaume, Olivier Bianchimani, et al. 2023. "Marine Heatwaves on the Rise: One of the Strongest Ever Observed Mass Mortality Event in Temperate Gorgonians." *Global Change Biology*, September 8, gcb.16931. https://doi.org/10.1111/gcb.16931.

Evensen, Nicolas R., Timothy G. Bateman, Courtney N. Klepac, et al. 2023. "The Roles of Heating Rate, Intensity, and Duration on the Response of Corals and Their Endosymbiotic Algae to Thermal Stress." *Journal of Experimental Marine Biology and Ecology* 567 (October): 151930. https://doi.org/10.1016/j.jembe.2023.151930.

Ezzat, Leïla, Jean-François Maguer, Renaud Grover, Cécile Rottier, Pascale Tremblay, and Christine Ferrier-Pagès. 2019. "Nutrient Starvation Impairs the Trophic Plasticity of Reef-building Corals under Ocean Warming." *Functional Ecology* 33 (4): 643–53. https://doi.org/10.1111/1365-2435.13285.

Fabri, M-C., L. Pedel, L. Beuck, F. Galgani, D. Hebbeln, and A. Freiwald. 2014. "Megafauna of Vulnerable Marine Ecosystems in French Mediterranean Submarine Canyons: Spatial Distribution and Anthropogenic Impacts." *Deep Sea Research Part II: Topical Studies in Oceanography* 104 (June): 184–207. https://doi.org/10.1016/j.dsr2.2013.06.016.

Fabricius, Katharina, and Philip Alderslade. 2001. *Soft Corals and Sea Fans: A Comprehensive Guide to the Tropical Shallow Water Genera of the Central-West Pacific, the Indian Ocean and the Red Sea*. Australian Institute of Marine Science.

Falkowski, Paul G., Richard T. Barber, and Victor Smetacek. 1998. "Biogeochemical Controls and Feedbacks on Ocean Primary Production." *Science* 281 (5374): 200–206. https://doi.org/10.1126/science.281.5374.200.

Ferrario, Filippo, Michael W. Beck, Curt D. Storlazzi, Fiorenza Micheli, Christine C. Shepard, and Laura Airoldi. 2014. "The Effectiveness of Coral Reefs for Coastal Hazard Risk Reduction and Adaptation." *Nature Communications* 5 (1): 3794. https://doi.org/10.1038/ncomms4794.

Fierer, Noah, Jason A. Jackson, Rytas Vilgalys, and Robert B. Jackson. 2005. "Assessment of Soil Microbial Community Structure by Use of Taxon-Specific Quantitative PCR Assays." *Applied and Environmental Microbiology* 71 (7): 4117–20. https://doi.org/10.1128/AEM.71.7.4117-4120.2005.

Fine, M., G. Roff, T. D. Ainsworth, and O. Hoegh-Guldberg. 2006. "Phototrophic Microendoliths Bloom during Coral 'White Syndrome.'" *Coral Reefs* 25 (4): 577–81. https://doi.org/10.1007/s00338-006-0143-4.

Fine, Maoz, and Yossi Loya. 2002. "Endolithic Algae: An Alternative Source of Photoassimilates during Coral Bleaching." *Proceedings of the Royal Society of London. Series B: Biological Sciences* 269 (1497): 1205–10. https://doi.org/10.1098/rspb.2002.1983.

Forcioli, D, Pl Merle, C Caligara, et al. 2011. “Symbiont Diversity Is Not Involved in Depth Acclimation in the Mediterranean Sea Whip Eunicella Singularis.” *Marine Ecology Progress Series* 439 (October): 57–71. https://doi.org/10.3354/meps09314.

France, Scott C., and Loretta L. Hoover. 2002. “DNA Sequences of the Mitochondrial COI Gene Have Low Levels of Divergence among Deep-Sea Octocorals (Cnidaria: Anthozoa).” *Hydrobiologia* 471 (1/3): 149–55. https://doi.org/10.1023/A:1016517724749.

Franzellitti, Silvia, Valentina Airi, Diana Calbucci, et al. 2018. “Transcriptional Response of the Heat Shock Gene Hsp70 Aligns with Differences in Stress Susceptibility of Shallow-Water Corals from the Mediterranean Sea.” *Marine Environmental Research* 140 (September): 444–54. https://doi.org/10.1016/j.marenvres.2018.07.006.

Frias-Lopez, Jorge, Aubrey L. Zerkle, George T. Bonheyo, and Bruce W. Fouke. 2002. “Partitioning of Bacterial Communities between Seawater and Healthy, Black Band Diseased, and Dead Coral Surfaces.” *Applied and Environmental Microbiology* 68 (5): 2214–28. https://doi.org/10.1128/AEM.68.5.2214-2228.2002.

Frölicher, Thomas L., Erich M. Fischer, and Nicolas Gruber. 2018. “Marine Heatwaves under Global Warming.” *Nature* 560 (7718): 360–64. https://doi.org/10.1038/s41586-018-0383-9.

Fu, Jingyun, Ying Li, Lihong Zhao, Chunguang Wu, and Zengguo He. 2022. “Characterization and Genomic Analysis of a Bacteriophage with Potential in Lysing Vibrio Alginolyticus.” *Viruses* 15 (1): 135. https://doi.org/10.3390/v15010135.

Fukushima-Sakuno, Emi. 2020. “Bioactive Small Secondary Metabolites from the Mushrooms Lentinula Edodes and Flammulina Velutipes.” *The Journal of Antibiotics* 73 (10): 687–96. https://doi.org/10.1038/s41429-020-0354-x.

Gajigan, Andrian P., Leomir A. Diaz, and Cecilia Conaco. 2017. “Resilience of the Prokaryotic Microbial Community of *Acropora Digitifera* to Elevated Temperature.” *MicrobiologyOpen* 6 (4): e00478. https://doi.org/10.1002/mbo3.478.

Galazzo, Gianluca, Niels van Best, Birke J. Benedikter, et al. 2020. “How to Count Our Microbes? The Effect of Different Quantitative Microbiome Profiling Approaches.” *Frontiers in Cellular and Infection Microbiology* 10 (August): 403. https://doi.org/10.3389/fcimb.2020.00403.

Galindo-Martínez, Claudia Tatiana, Michele Weber, Viridiana Avila-Magaña, et al. 2022. “The Role of the Endolithic Alga Ostreobium Spp. during Coral Bleaching Recovery.” *Scientific Reports* 12 (1): 2977. https://doi.org/10.1038/s41598-022-07017-6.

Galkiewicz, Julia P., Sarah H. Stellick, Michael A. Gray, and Christina A. Kellogg. 2012. “Cultured Fungal Associates from the Deep-Sea Coral Lophelia Pertusa.” *Deep Sea Research Part I: Oceanographic Research Papers* 67 (September): 12–20. https://doi.org/10.1016/j.dsr.2012.05.001.

Gallmetzer, Ivo, Alexandra Haselmair, and Branko Velimirov. 2010. “Slow Growth and Early Sexual Maturity: Bane and Boon for the Red Coral Corallium Rubrum.” *Estuarine, Coastal and Shelf Science* 90 (1): 1–10. https://doi.org/10.1016/j.ecss.2010.04.018.

Gardner, Stephanie G., Daniel A. Nielsen, Olivier Laczka, et al. 2016. "Dimethylsulfoniopropionate, Superoxide Dismutase and Glutathione as Stress Response Indicators in Three Corals under Short-Term Hyposalinity Stress." *Proceedings of the Royal Society B: Biological Sciences* 283 (1824): 20152418. https://doi.org/10.1098/rspb.2015.2418.

Garrabou, J., R. Coma, N. Bensoussan, et al. 2009a. "Mass Mortality in Northwestern Mediterranean Rocky Benthic Communities: Effects of the 2003 Heat Wave." *Global Change Biology* 15 (5): 1090–103. https://doi.org/10.1111/j.1365-2486.2008.01823.x.

Garrabou, J., R. Coma, N. Bensoussan, et al. 2009b. "Mass Mortality in Northwestern Mediterranean Rocky Benthic Communities: Effects of the 2003 Heat Wave." *Global Change Biology* 15 (5): 1090–103. https://doi.org/10.1111/j.1365-2486.2008.01823.x.

Garrabou, J, Daniel Gómez-Gras, Alba Medrano, et al. 2022. "Marine Heatwaves Drive Recurrent Mass Mortalities in the Mediterranean Sea." *Global Change Biology* 28 (19): 5708–25. https://doi.org/10.1111/gcb.16301.

Garrabou, J., and J. G. Harmelin. 2002. "A 20-year Study on Life-history Traits of a Harvested Long-lived Temperate Coral in the NW Mediterranean: Insights into Conservation and Management Needs." *Journal of Animal Ecology* 71 (6): 966–78. https://doi.org/10.1046/j.1365-2656.2002.00661.x.

Garrabou, J, T Perez, S Sartoretto, and Jg Harmelin. 2001. "Mass Mortality Event in Red Coral Corallium Rubrum Populations in the Provence Region (France, NW Mediterranean)." *Marine Ecology Progress Series* 217: 263–72. https://doi.org/10.3354/meps217263.

Garrabou, Joaquim, Daniel Gómez-Gras, Jean-Baptiste Ledoux, et al. 2019. "Collaborative Database to Track Mass Mortality Events in the Mediterranean Sea." *Frontiers in Marine Science* 6 (November): 707. https://doi.org/10.3389/fmars.2019.00707.

Garrabou, Joaquim, Jean-Baptiste Ledoux, Nathaniel Bensoussan, Daniel Gómez-Gras, and Cristina Linares. 2021. "Sliding Toward the Collapse of Mediterranean Coastal Marine Rocky Ecosystems." In *Ecosystem Collapse and Climate Change*, edited by Josep G. Canadell and Robert B. Jackson, vol. 241. Ecological Studies. Springer International Publishing. https://doi.org/10.1007/978-3-030-71330-0_11.

Garzoli, Laura, Giorgio Gnavi, Giovanna C. Varese, and Anna M. Picco. 2015. "Mycobiota Associated with the Rhodophyte Alien Species *A Sparagopsis Taxiformis* (D Elile) T Revisan de S Aint- L Éon in the M Editerranean S Ea." *Marine Ecology* 36 (4): 959–68. https://doi.org/10.1111/maec.12189.

Gazulla, Carlota R., Paula López-Sendino, Agostinho Antunes, et al. 2021. "Demo-Genetic Approach for the Conservation and Restoration of a Habitat-Forming Octocoral: The Case of Red Coral, Corallium Rubrum, in the Réserve Naturelle de Scandola." *Frontiers in Marine Science* 8 (June): 633057. https://doi.org/10.3389/fmars.2021.633057.

Gegner, Hagen M., Nils Rädecker, Michael Ochsenkühn, et al. 2019. "High Levels of Floridoside at High Salinity Link Osmoadaptation with Bleaching Susceptibility in the Cnidarian-Algal Endosymbiosis." *Biology Open* 8 (12): bio045591. https://doi.org/10.1242/bio.045591.

Gegner, Hagen M., Maren Ziegler, Nils Rädecker, Carol Buitrago-López, Manuel Aranda, and Christian R. Voolstra. 2017. “High Salinity Conveys Thermotolerance in the Coral Model Aiptasia.” *Biology Open*, January 1, bio.028878. https://doi.org/10.1242/bio.028878.

Ghanem, Raouia, Jamila Ben Souissi, Jean-Baptiste Ledoux, Cristina Linares, and Joaquim Garrabou. 2021. “Population Structure and Conservation Status of the White Gorgonian Eunicella Singularis (Esper, 1791) in Tunisian Waters (Central Mediterranean).” *Mediterranean Marine Science*, ahead of print, March 8. https://doi.org/10.12681/mms.24984.

Gibbin, E., A. Gavish, I. Domart-Coulon, et al. 2018. “Using NanoSIMS Coupled with Microfluidics to Visualize the Early Stages of Coral Infection by Vibrio Coralliilyticus.” *BMC Microbiology* 18 (1): 39. https://doi.org/10.1186/s12866-018-1173-0.

Gibson, R. N., R. J. A. Atkinson, J. D. M. Gordon, and E Ballesteros, eds. 2006. “Mediterranean Coralligenous Assemblages: A Synthesis of Present Knowledge.” In *Oceanography and Marine Biology : An Annual Review*, 0 ed. CRC Press. https://doi.org/10.1201/9781420006391-7.

Gignoux-Wolfsohn, Sarah A., Felicia M. Aronson, and Steven V. Vollmer. 2017. “Complex Interactions between Potentially Pathogenic, Opportunistic, and Resident Bacteria Emerge during Infection on a Reef-Building Coral.” *FEMS Microbiology Ecology* 93 (7). https://doi.org/10.1093/femsec/fix080.

Gili, Josep-Maria, and Rafel Coma. 1998. “Benthic Suspension Feeders: Their Paramount Role in Littoral Marine Food Webs.” *Trends in Ecology & Evolution* 13 (8): 316–21. https://doi.org/10.1016/S0169-5347(98)01365-2.

Girija, Gowri Krishna, Li-Chun Tseng, Priyanka Muthu, Yu-Ling Chen, Ying-Ning Ho, and Jiang-Shiou Hwang. 2024. “Microbiome Flexibility Enhances the Resilience of the Potentially Invasive Coral Tubastraea Aurea to Abrupt Environmental Changes: Insights from a Shallow Water Hydrothermal Vent Transplantation Study.” *Science of The Total Environment* 954 (December): 176792. https://doi.org/10.1016/j.scitotenv.2024.176792.

Gissi, Francesca, Amanda J. Reichelt-Brushett, Anthony A. Chariton, et al. 2019. “The Effect of Dissolved Nickel and Copper on the Adult Coral Acropora Muricata and Its Microbiome.” *Environmental Pollution* 250 (July): 792–806. https://doi.org/10.1016/j.envpol.2019.04.030.

Gladfelter, Amy S., Timothy Y. James, and Anthony S. Amend. 2019. “Marine Fungi.” *Current Biology* 29 (6): R191–95. https://doi.org/10.1016/j.cub.2019.02.009.

Glasl, Bettina, David G. Bourne, Pedro R. Frade, Torsten Thomas, Britta Schaffelke, and Nicole S. Webster. 2019. “Microbial Indicators of Environmental Perturbations in Coral Reef Ecosystems.” *Microbiome* 7 (1): 94. https://doi.org/10.1186/s40168-019-0705-7.

Gleason, Frank H., Geoffrey M Gadd, John I Pitt, and Anthony W. D Larkum. 2017. “The Roles of Endolithic Fungi in Bioerosion and Disease in Marine Ecosystems. I. General Concepts.” *Mycology* 8 (3): 205–15. https://doi.org/10.1080/21501203.2017.1352049.

Gloor, Gregory B., Jean M. Macklaim, Vera Pawlowsky-Glahn, and Juan J. Egozcue. 2017. “Microbiome Datasets Are Compositional: And This Is Not Optional.” *Frontiers in Microbiology* 8 (November): 2224. https://doi.org/10.3389/fmicb.2017.02224.

Glynn, Peter W. 1983. “Extensive ‘Bleaching’ and Death of Reef Corals on the Pacific Coast of Panamá.” *Environmental Conservation* 10 (2): 149–54. https://doi.org/10.1017/S0376892900012248.

Glynn, Peter W. 1984. “Widespread Coral Mortality and the 1982–83 El Niño Warming Event.” *Environmental Conservation* 11 (2): 133–46. https://doi.org/10.1017/S0376892900013825.

Godinho, Valéria Martins, Maria Theresa Rafaela de Paula, Débora Amorim Saraiva Silva, et al. 2019. “Diversity and Distribution of Hidden Cultivable Fungi Associated with Marine Animals of Antarctica.” *Fungal Biology* 123 (7): 507–16. https://doi.org/10.1016/j.funbio.2019.05.001.

Godsoe, William, Eva Strand, Christopher Irwin Smith, Jeremy B. Yoder, Todd C. Esque, and Olle Pellmyr. 2009. “Divergence in an Obligate Mutualism Is Not Explained by Divergent Climatic Factors.” *New Phytologist* 183 (3): 589–99. https://doi.org/10.1111/j.1469-8137.2009.02942.x.

Góes-Neto, Aristóteles, Vanessa Rossetto Marcelino, Heroen Verbruggen, Felipe Ferreira Da Silva, and Fernanda Badotti. 2020. “Biodiversity of Endolithic Fungi in Coral Skeletons and Other Reef Substrates Revealed with 18S rDNA Metabarcoding.” *Coral Reefs* 39 (1): 229–38. https://doi.org/10.1007/s00338-019-01880-y.

Golubic, Stjepko, Gudrun Radtke, and Therese Le Campion-Alsumard. 2005. “Endolithic Fungi in Marine Ecosystems.” *Trends in Microbiology* 13 (5): 229–35. https://doi.org/10.1016/j.tim.2005.03.007.

Gómez-Gras, D., C. Linares, A. López-Sanz, et al. 2021. “Population Collapse of Habitat-Forming Species in the Mediterranean: A Long-Term Study of Gorgonian Populations Affected by Recurrent Marine Heatwaves.” *Proceedings of the Royal Society B: Biological Sciences* 288 (1965): 20212384. https://doi.org/10.1098/rspb.2021.2384.

Gómez-Gras, Daniel, Cristina Linares, Sonia De Caralt, et al. 2019. “Response Diversity in Mediterranean Coralligenous Assemblages Facing Climate Change: Insights from a Multispecific Thermotolerance Experiment.” *Ecology and Evolution* 9 (7): 4168–80. https://doi.org/10.1002/ece3.5045.

Gómez-Gras, Daniel, Cristina Linares, Maria Dornelas, et al. 2021. “Climate Change Transforms the Functional Identity of Mediterranean Coralligenous Assemblages.” *Ecology Letters* 24 (5): 1038–51. https://doi.org/10.1111/ele.13718.

Gonzalez-Escalona, Narjol, Jaime Romero, and Romilio T. Espejo. 2005. “Polymorphism and Gene Conversion of the 16S rRNA Genes in the Multiple rRNA Operons of *Vibrio Parahaemolyticus*.” *FEMS Microbiology Letters* 246 (2): 213–19. https://doi.org/10.1016/j.femsle.2005.04.009.

González-Pech, Raúl A., Vivian Y. Li, Vanessa Garcia, et al. 2024. “The Evolution, Assembly, and Dynamics of Marine Holobionts.” *Annual Review of Marine Science* 16 (1): 443–66. https://doi.org/10.1146/annurev-marine-022123-104345.

Goreau, Thomas F. 1964. “Mass Expulsion of Zooxanthellae from Jamaican Reef Communities after Hurricane Flora.” *Science* 145 (3630): 383–86. https://doi.org/10.1126/science.145.3630.383.

Gori, Andrea, Giorgio Bavestrello, Jordi Grinyó, Carlos Dominguez-Carrió, Stefano Ambroso, and Marzia Bo. 2017. “Animal Forests in Deep Coastal Bottoms and Continental Shelf of the Mediterranean Sea.” In *Marine Animal Forests*, edited by Sergio Rossi, Lorenzo Bramanti, Andrea Gori, and Covadonga Orejas. Springer International Publishing. https://doi.org/10.1007/978-3-319-17001-5_5-1.

Gori, Andrea, Lorenzo Bramanti, Pablo López-González, et al. 2012. “Characterization of the Zooxanthellate and Azooxanthellate Morphotypes of the Mediterranean Gorgonian Eunicella Singularis.” *Marine Biology* 159 (7): 1485–96. https://doi.org/10.1007/s00227-012-1928-3.

Gori, Andrea, Sergio Rossi, Elisa Berganzo, Joan Lluis Pretus, Mark R. T. Dale, and Josep-Maria Gili. 2011. “Spatial Distribution Patterns of the Gorgonians Eunicella Singularis, Paramuricea Clavata, and Leptogorgia Sarmentosa (Cape of Creus, Northwestern Mediterranean Sea).” *Marine Biology* 158 (1): 143–58. https://doi.org/10.1007/s00227-010-1548-8.

Granit, Lior, Rotem Levi, Nofar Lifshitz, et al. 2025. “Beneficial and Detrimental Fungi within the Culturable Mycobiome of the Red Sea Coral *Stylophora Pistilatta*.” *The ISME Journal* 19 (1). https://doi.org/10.1093/ismejo/wraf090.

Gray, Michael A., Robert P. Stone, Molly R. McLaughlin, and Christina A. Kellogg. 2011. “Microbial Consortia of Gorgonian Corals from the Aleutian Islands: Microbial Consortia of Aleutian Gorgonians.” *FEMS Microbiology Ecology* 76 (1): 109–20. https://doi.org/10.1111/j.1574-6941.2010.01033.x.

Green, David H, Lyndon E Llewellyn, Andrew P Negri, Susan I Blackburn, and Christopher J.S Bolch. 2004. “Phylogenetic and Functional Diversity of the Cultivable Bacterial Community Associated with the Paralytic Shellfish Poisoning Dinoflagellate Gymnodinium Catenatum.” *FEMS Microbiology Ecology* 47 (3): 345–57. https://doi.org/10.1016/S0168-6496(03)00298-8.

Grenier, Marie, Tal Idan, Pierre Chevaldonné, and Thierry Pérez. 2023. “Mediterranean Marine Keystone Species on the Brink of Extinction.” *Global Change Biology*, January 28, 16597. https://doi.org/10.1111/gcb.16597.

Grieneisen, Laura E., Marie J. E. Charpentier, Susan C. Alberts, et al. 2019. “Genes, Geology and Germs: Gut Microbiota across a Primate Hybrid Zone Are Explained by Site Soil Properties, Not Host Species.” *Proceedings of the Royal Society B: Biological Sciences* 286 (1901): 20190431. https://doi.org/10.1098/rspb.2019.0431.

Grigg, Richard W. 1984. “Resource Management of Precious Corals: A Review and Application to Shallow Water Reef Building Corals.” *Marine Ecology* 5 (1): 57–74. https://doi.org/10.1111/j.1439-0485.1984.tb00307.x.

Grigg, Richard W. 2002. “Precious Corals in Hawaii: Discovery of a New Bed and Revised Management Measures for Existing Beds.” *Marine Fisheries Review*.

Grinyó, Jordi, Andrea Gori, Stefano Ambroso, et al. 2016. “Diversity, Distribution and Population Size Structure of Deep Mediterranean Gorgonian Assemblages (Menorca Channel, Western Mediterranean Sea).” *Progress in Oceanography* 145 (June): 42–56. https://doi.org/10.1016/j.pocean.2016.05.001.

Grinyó, Jordi, Andrea Gori, Pablo J. López-González, Andreu Santín, Patricia Baena, and Josep-Maria Gili. 2018. “Morphological Features of the Gorgonian *Paramuricea Macrospina* on the Continental Shelf and Shelf Edge (Menorca Channel, Western Mediterranean Sea).” *Marine Biology Research* 14 (1): 30–40. https://doi.org/10.1080/17451000.2017.1375118.

Groot, Steven, and Steven Weinberg. 1982. “Biogeography, Taxonomical Status and Ecology of Alcyonium (Parerythropodium) Coralloides (PALLAS, 1766).” *Marine Ecology* 3 (4): 293–312. https://doi.org/10.1111/j.1439-0485.1982.tb00281.x.

Grover, Renaud, Jean-François Maguer, Stephanie Reynaud-Vaganay, and Christine Ferrier-Pagès. 2002. “Uptake of Ammonium by the Scleractinian Coral *Stylophora Pistillata* : Effect of Feeding, Light, and Ammonium Concentrations.” *Limnology and Oceanography* 47 (3): 782–90. https://doi.org/10.4319/lo.2002.47.3.0782.

Gudenkauf, Brent M., and Ian Hewson. 2016. “Comparative Metagenomics of Viral Assemblages Inhabiting Four Phyla of Marine Invertebrates.” *Frontiers in Marine Science* 3 (March). https://doi.org/10.3389/fmars.2016.00023.

Guillou, L., M. Viprey, A. Chambouvet, et al. 2008. “Widespread Occurrence and Genetic Diversity of Marine Parasitoids Belonging to *Syndiniales* (*Alveolata*).” *Environmental Microbiology* 10 (12): 3349–65. https://doi.org/10.1111/j.1462-2920.2008.01731.x.

Guillou, Laure, Dipankar Bachar, Stéphane Audic, et al. 2012. “The Protist Ribosomal Reference Database (PR2): A Catalog of Unicellular Eukaryote Small Sub-Unit rRNA Sequences with Curated Taxonomy.” *Nucleic Acids Research* 41 (D1): D597–604. https://doi.org/10.1093/nar/gks1160.

Guinaldo, Thibault, Aurore Voldoire, Robin Waldman, Stéphane Saux Picart, and Hervé Roquet. 2023. “Response of the Sea Surface Temperature to Heatwaves during the France 2022 Meteorological Summer.” *Ocean Science* 19 (3): 629–47. https://doi.org/10.5194/os-19-629-2023.

Guindon, Stéphane, Jean-François Dufayard, Vincent Lefort, Maria Anisimova, Wim Hordijk, and Olivier Gascuel. 2010. “New Algorithms and Methods to Estimate Maximum-Likelihood Phylogenies: Assessing the Performance of PhyML 3.0.” *Systematic Biology* 59 (3): 307–21. https://doi.org/10.1093/sysbio/syq010.

Häder, Donat-P. 2021. “Bioreactive Substances from Coral Reefs and Gorgonians.” In *Natural Bioactive Compounds*. Elsevier. https://doi.org/10.1016/B978-0-12-820655-3.00019-7.

Hafner, Mark S., and Steven A. Nadler. 1988. “Phylogenetic Trees Support the Coevolution of Parasites and Their Hosts.” *Nature* 332 (6161): 258–59. https://doi.org/10.1038/332258a0.

Haguenauer, A., F. Zuberer, J.-B. Ledoux, and D. Aurelle. 2013. “Adaptive Abilities of the Mediterranean Red Coral Corallium Rubrum in a Heterogeneous and Changing Environment: From Population to Functional Genetics.” *Journal of Experimental Marine Biology and Ecology* 449 (November): 349–57. https://doi.org/10.1016/j.jembe.2013.10.010.

Hamdeno, Manal, and Aida Alvera-Azcaráte. 2023. “Marine Heatwaves Characteristics in the Mediterranean Sea: Case Study the 2019 Heatwave Events.” *Frontiers in Marine Science* 10 (March): 1093760. https://doi.org/10.3389/fmars.2023.1093760.

Harada, Ai, Susumu Ohtsuka, and Takeo Horiguchi. 2007. “Species of the Parasitic Genus Duboscquella Are Members of the Enigmatic Marine Alveolate Group I.” *Protist* 158 (3): 337–47. https://doi.org/10.1016/j.protis.2007.03.005.

Harel, Moshe, Eitan Ben-Dov, Diana Rasoulouniriana, et al. 2008. “A New Thraustochytrid, Strain Fng1, Isolated from the Surface Mucus of the Hermatypic Coral Fungia Granulosa: New Coral Mucus-Associated Thraustochytrid.” *FEMS Microbiology Ecology* 64 (3): 378–87. https://doi.org/10.1111/j.1574-6941.2008.00464.x.

Harvell, Drew, Kiho Kim, Craig Quirolo, Julianna Weir, and Garriet Smith. 2001. “Coral Bleaching and Disease: Contributors to 1998 Mass Mortality in Briareum Asbestinum (Octocorallia, Gorgonacea).” *Hydrobiologia* 460 (1–3): 97–104. https://doi.org/10.1023/A:1013169331913.

Hawkins, E., and R. Sutton. 2012. “Time of Emergence of Climate Signals.” *Geophysical Research Letters* 39 (1): n/a-n/a. https://doi.org/10.1029/2011GL050087.

Haydon, Trent D., David J. Suggett, Nachshon Siboni, Tim Kahlke, Emma F. Camp, and Justin R. Seymour. 2022. “Temporal Variation in the Microbiome of Tropical and Temperate Octocorals.” *Microbial Ecology* 83 (4): 1073–87. https://doi.org/10.1007/s00248-021-01823-7.

Helgoe, Joshua, Simon K. Davy, Virginia M. Weis, and Mauricio Rodriguez-Lanetty. 2024. “Triggers, Cascades, and Endpoints: Connecting the Dots of Coral Bleaching Mechanisms.” *Biological Reviews* 99 (3): 715–52. https://doi.org/10.1111/brv.13042.

Henríquez, Marlene, Karen Vergara, Javiera Norambuena, et al. 2014. “Diversity of Cultivable Fungi Associated with Antarctic Marine Sponges and Screening for Their Antimicrobial, Antitumoral and Antioxidant Potential.” *World Journal of Microbiology and Biotechnology* 30 (1): 65–76. https://doi.org/10.1007/s11274-013-1418-x.

Hernandez-Agreda, Alejandra, Ruth D. Gates, and Tracy D. Ainsworth. 2017. “Defining the Core Microbiome in Corals’ Microbial Soup.” *Trends in Microbiology* 25 (2): 125–40. https://doi.org/10.1016/j.tim.2016.11.003.

Hernandez-Agreda, Alejandra, William Leggat, Pim Bongaerts, and Tracy D. Ainsworth. 2016. “The Microbial Signature Provides Insight into the Mechanistic Basis of Coral Success across Reef Habitats.” *mBio* 7 (4): 4. https://doi.org/10.1128/mBio.00560-16.

Hewson, I., J. M. Brown, C. A. Burge, et al. 2012. “Description of Viral Assemblages Associated with the Gorgonia Ventalina Holobiont.” *Coral Reefs* 31 (2): 487–91. https://doi.org/10.1007/s00338-011-0864-x.

Hino, Akina, Haruhiko Maruyama, and Taisei Kikuchi. 2016. “A Novel Method to Assess the Biodiversity of Parasites Using 18S rDNA Illumina Sequencing; Parasitome Analysis Method.” *Parasitology International* 65 (5): 572–75. https://doi.org/10.1016/j.parint.2016.01.009.

Hoegh-Guldberg, Ove. 1999. “Climate Change, Coral Bleaching and the Future of the World’s Coral Reefs.” *Marine and Freshwater Research*, ahead of print. https://doi.org/10.1071/MF99078.

Hold, Georgina L., Elizabeth A. Smith, T. Harry Birkbeck, and Susan Gallacher. 2001a. “Comparison of Paralytic Shellfish Toxin (PST) Production by the Dinoflagellates Alexandrium Lusitanicum NEPCC 253 and Alexandrium Tamarense NEPCC 407 in the Presence and Absence of Bacteria.” *FEMS Microbiology Ecology* 36 (2–3): 223–34. https://doi.org/10.1111/j.1574-6941.2001.tb00843.x.

Hold, Georgina L., Elizabeth A. Smith, T. Harry Birkbeck, and Susan Gallacher. 2001b. “Comparison of Paralytic Shellfish Toxin (PST) Production by the Dinoflagellates Alexandrium Lusitanicum NEPCC 253 and Alexandrium Tamarense NEPCC 407 in the Presence and Absence of Bacteria.” *FEMS Microbiology Ecology* 36 (2–3): 223–34. https://doi.org/10.1111/j.1574-6941.2001.tb00843.x.

Holm, Johanna B., and Karla B. Heidelberg. 2016. “Microbiomes of Muricea Californica and M. Fruticosa: Comparative Analyses of Two Co-Occurring Eastern Pacific Octocorals.” *Frontiers in Microbiology* 7 (June). https://doi.org/10.3389/fmicb.2016.00917.

Hopkins, Frances E., Thomas G. Bell, Mingxi Yang, David J. Suggett, and Michael Steinke. 2016. “Air Exposure of Coral Is a Significant Source of Dimethylsulfide (DMS) to the Atmosphere.” *Scientific Reports* 6 (1): 36031. https://doi.org/10.1038/srep36031.

Hou, Xue-Mei, Yang Hai, Yu-Cheng Gu, Chang-Yun Wang, and Chang-Lun Shao. 2019. “Chemical and Bioactive Marine Natural Products of Coral-Derived Microorganisms (2015-2017).” *Current Medicinal Chemistry* 26 (38): 6930–41. https://doi.org/10.2174/0929867326666190626153819.

Houghton, J.T., G. J. Jenkins, and J. J. Ephraums. 1990. *Climate Change 1990*. The IPCC Scientific Assessment No. 1. Intergovernmental Panel on Climate Change.

Howe-Kerr, Lauren I, Carsten G B Grupstra, Kristen M Rabbitt, et al. 2023. “Viruses of a Key Coral Symbiont Exhibit Temperature-Driven Productivity across a Reefscape.” *ISME Communications* 3 (1): 27. https://doi.org/10.1038/s43705-023-00227-7.

Hu, J. 2023. “First Report of *Cladosporium Ramotenellum* Causing Sooty Spot on Postharvest Clementines in the United States.” *Plant Disease* 107 (10): 3281. https://doi.org/10.1094/PDIS-02-23-0210-PDN.

Huete-Stauffer, Carla, Ilaria Vielmini, Marco Palma, et al. 2011. “Paramuricea Clavata (Anthozoa, Octocorallia) Loss in the Marine Protected Area of Tavolara (Sardinia, Italy) Due to a Mass Mortality Event: P. Clavata Loss in the MPA of Tavolara.” *Marine Ecology* 32 (April): 107–16. https://doi.org/10.1111/j.1439-0485.2011.00429.x.

Huggett, Megan J., and Amy Apprill. 2019. “Coral Microbiome Database: Integration of Sequences Reveals High Diversity and Relatedness of Coral-associated Microbes.” *Environmental Microbiology Reports* 11 (3): 372–85. https://doi.org/10.1111/1758-2229.12686.

Hughes, Terry P., James T. Kerry, Andrew H. Baird, et al. 2018. “Global Warming Transforms Coral Reef Assemblages.” *Nature* 556 (7702): 492–96. https://doi.org/10.1038/s41586-018-0041-2.

Husmann, Gunnar, Gunnar Gerdts, and Antje Wichels. 2010. “Spirochetes in Crystalline Styles of Marine Bivalves: Group-Specific PCR Detection and 16S rRNA Sequence Analysis.” *Journal of Shellfish Research* 29 (4): 1069–75. https://doi.org/10.2983/035.029.0409.

Iha, Cintia, Katherine E. Dougan, Javier A. Varela, et al. 2021. “Genomic Adaptations to an Endolithic Lifestyle in the Coral-Associated Alga Ostreobium.” *Current Biology* 31 (7): 1393-1402.e5. https://doi.org/10.1016/j.cub.2021.01.018.

Illumina. 2013. “16S Metagenomic Sequencing Library Preparation.”

Illumina I. 2013. “16S Metagenomic Sequencing Library Preparation.”

Jang, Yeongseon, Young Min Lee, Gyu-Hyeok Kim, and Jae-Jin Kim. 2013. “Two Species of *Cladosporium* Associated with Wood Discoloration in Korea.” *Mycotaxon* 124 (1): 21–29. https://doi.org/10.5248/124.21.

Jessen, Christian, Javier Felipe Villa Lizcano, Till Bayer, et al. 2013. “In-Situ Effects of Eutrophication and Overfishing on Physiology and Bacterial Diversity of the Red Sea Coral Acropora Hemprichii.” *PLoS ONE* 8 (4): e62091. https://doi.org/10.1371/journal.pone.0062091.

Jiang, Jiaoyun, Aoqi Wang, Xiangzi Deng, Wenxu Zhou, Qinhua Gan, and Yandu Lu. 2021. “How Symbiodiniaceae Meets the Challenges of Life during Coral Bleaching.” *Coral Reefs* 40 (4): 1339–53. https://doi.org/10.1007/s00338-021-02115-9.

Jones, E. B. Gareth, Satinee Suetrong, Jariya Sakayaroj, et al. 2015. “Classification of Marine Ascomycota, Basidiomycota, Blastocladiomycota and Chytridiomycota.” *Fungal Diversity* 73 (1): 1–72. https://doi.org/10.1007/s13225-015-0339-4.

Jovel, Juan, Aissata Nimaga, Tracy Jordan, et al. 2022. “Metagenomics Versus Metatranscriptomics of the Murine Gut Microbiome for Assessing Microbial Metabolism During Inflammation.” *Frontiers in Microbiology* 13 (February): 829378. https://doi.org/10.3389/fmicb.2022.829378.

Joye, Samantha B., Marshall W. Bowles, and Kai Ziervogel. 2022. “Marine Biogeochemical Cycles.” In *The Marine Microbiome*, edited by Lucas J. Stal and Mariana Silvia Cretoiu, vol. 3. The Microbiomes of Humans, Animals, Plants, and the Environment. Springer International Publishing. https://doi.org/10.1007/978-3-030-90383-1_15.

Juza, Mélanie, Àngels Fernández-Mora, and Joaquin Tintoré. 2022. “Sub-Regional Marine Heat Waves in the Mediterranean Sea From Observations: Long-Term Surface Changes, Sub-Surface and Coastal Responses.” *Frontiers in Marine Science* 9 (March): 785771. https://doi.org/10.3389/fmars.2022.785771.

Juza, Mélanie, and Joaquín Tintoré. 2021. “Multivariate Sub-Regional Ocean Indicators in the Mediterranean Sea: From Event Detection to Climate Change Estimations.” *Frontiers in Marine Science* 8. https://www.frontiersin.org/articles/10.3389/fmars.2021.610589.

Kahng, S. E., J. R. Garcia-Sais, H. L. Spalding, et al. 2010. “Community Ecology of Mesophotic Coral Reef Ecosystems.” *Coral Reefs* 29 (2): 2. https://doi.org/10.1007/s00338-010-0593-6.

Kamat, Siya, Madhuree Kumari, Sidhartha Taritla, and C. Jayabaskaran. 2020. “Endophytic Fungi of Marine Alga From Konkan Coast, India—A Rich Source of Bioactive Material.” *Frontiers in Marine Science* 7 (February): 31. https://doi.org/10.3389/fmars.2020.00031.

Karajan, Bella P., Olga G. Leonova, Nina N. Bobyleva, and Vladimir I. Popenko. 2019. “Effect of Heat Shock on the Cell Cycle Duration of Algae-Containing and Algae-Free Ciliates Climacostomum Virens.” *Protistology*, no. 4. https://doi.org/10.21685/1680-0826-2019-13-4-3.

Katz, Sefano M., F. Joseph Pollock, David G. Bourne, and Bette L. Willis. 2014. “Crown-of-Thorns Starfish Predation and Physical Injuries Promote Brown Band Disease on Corals.” *Coral Reefs* 33 (3): 705–16. https://doi.org/10.1007/s00338-014-1153-2.

Kavousi, Javid, Vianney Denis, Victoria Sharp, James Davis Reimer, Takashi Nakamura, and John Everett Parkinson. 2020. “Unique Combinations of Coral Host and Algal Symbiont Genotypes Reflect Intraspecific Variation in Heat Stress Responses among Colonies of the Reef-Building Coral, Montipora Digitata.” *Marine Biology* 167 (2): 23. https://doi.org/10.1007/s00227-019-3632-z.

Keeling, Patrick J., and Javier Del Campo. 2017. “Marine Protists Are Not Just Big Bacteria.” *Current Biology* 27 (11): R541–49. https://doi.org/10.1016/j.cub.2017.03.075.

Keller-Costa, T., A. Lago-Lestón, J. P. Saraiva, et al. 2021. “Metagenomic Insights into the Taxonomy, Function, and Dysbiosis of Prokaryotic Communities in Octocorals.” *Microbiome* 9 (1): 72. https://doi.org/10.1186/s40168-021-01031-y.

Keller-Costa, Tina, Dominic Eriksson, Jorge M. S. Gonçalves, Newton C.M. Gomes, Asunción Lago-Lestón, and Rodrigo Costa. 2017. “The Gorgonian Coral Eunicella Labiata Hosts a Distinct Prokaryotic Consortium Amenable to Cultivation.” *FEMS Microbiology Ecology* 93 (12). https://doi.org/10.1093/femsec/fix143.

Keller-Costa, Tina, Lydia Kozma, Sandra G. Silva, Rodolfo Toscan, Jorge Gonçalves, Asunción Lago-Lestón, Nikos C. Kyrpides, Ulisses Nunes Rocha, et al. 2022. *Evidence for Cross-Feeding, Metabolic Specialization, and Niche Partitioning in the Octocoral Holobiont*. Preprint. In Review. https://doi.org/10.21203/rs.3.rs-1630933/v1.

Keller-Costa, Tina, Lydia Kozma, Sandra G. Silva, Rodolfo Toscan, Jorge Gonçalves, Asunción Lago-Lestón, Nikos C. Kyrpides, Ulisses Nunes Da Rocha, et al. 2022. “Metagenomics-Resolved Genomics Provides Novel Insights into Chitin Turnover, Metabolic Specialization, and Niche Partitioning in the Octocoral Microbiome.” *Microbiome* 10 (1): 151. https://doi.org/10.1186/s40168-022-01343-7.

Keller-Costa, Tina, Rúben Silva, Asunción Lago-Lestón, and Rodrigo Costa. 2016. “Genomic Insights into *Aquimarina* Sp. Strain EL33, a Bacterial Symbiont of the Gorgonian Coral *Eunicella Labiata*.” *Genome Announcements* 4 (4): e00855-16. https://doi.org/10.1128/genomeA.00855-16.

Kellogg, Ca. 2004. “Tropical Archaea: Diversity Associated with the Surface Microlayer of Corals.” *Marine Ecology Progress Series* 273: 81–88. https://doi.org/10.3354/meps273081.

Kellogg, Christina A., John T. Lisle, and Julia P. Galkiewicz. 2009. “Culture-Independent Characterization of Bacterial Communities Associated with the Cold-Water Coral

Lophelia Pertusa in the Northeastern Gulf of Mexico." *Applied and Environmental Microbiology* 75 (8): 2294–303. https://doi.org/10.1128/AEM.02357-08.

Kendrick, B, M.J. Risk, J Michaelides, and K Bergman. 1982. "Amphibious Microborers: Bioeroding Isolated from Live Corals Fungi." *Mar. Sci. Bull.* 32: 862–67.

Kenkel, C. D., E. Meyer, and M. V. Matz. 2013. "Gene Expression under Chronic Heat Stress in Populations of the Mustard Hill Coral (*P Orites Astreoides*) from Different Thermal Environments." *Molecular Ecology* 22 (16): 4322–34. https://doi.org/10.1111/mec.12390.

Ki, Jang-Seu. 2009. "Heterogeneity Analysis of the 16S rRNA Gene Sequences of the Genus Vibrio." *The Korean Journal of Microbiology* 45 (January).

Kim, C. S. 1999. "Reactive Oxygen Species as Causative Agents in the Ichthyotoxicity of the Red Tide Dinoflagellate Cochlodinium Polykrikoides." *Journal of Plankton Research* 21 (11): 2105–15. https://doi.org/10.1093/plankt/21.11.2105.

Kim, Kiho, and Krystal Rypien. 2015. "Aspergillosis of Caribbean Sea Fan Corals, *Gorgonia* Spp." In *Diseases of Coral*, 1st ed., edited by Cheryl M. Woodley, Craig A. Downs, Andrew W. Bruckner, James W. Porter, and Sylvia B. Galloway. Wiley. https://doi.org/10.1002/9781118828502.ch16.

Kimes, Nikole E, Christopher J Grim, Wesley R Johnson, et al. 2012. "Temperature Regulation of Virulence Factors in the Pathogen *Vibrio Coralliilyticus*." *The ISME Journal* 6 (4): 835–46. https://doi.org/10.1038/ismej.2011.154.

Kitamura, Ruriko, Natsuko Miura, Michihiro Ito, et al. 2021. "Specific Detection of Coral-Associated Ruegeria, a Potential Probiotic Bacterium, in Corals and Subtropical Seawater." *Marine Biotechnology* 23 (4): 576–89. https://doi.org/10.1007/s10126-021-10047-2.

Klappenbach, J. A. 2001. "Rrndb: The Ribosomal RNA Operon Copy Number Database." *Nucleic Acids Research* 29 (1): 181–84. https://doi.org/10.1093/nar/29.1.181.

Klindworth, Anna, Elmar Pruesse, Timmy Schweer, et al. 2013. "Evaluation of General 16S Ribosomal RNA Gene PCR Primers for Classical and Next-Generation Sequencing-Based Diversity Studies." *Nucleic Acids Research* 41 (1): e1–e1. https://doi.org/10.1093/nar/gks808.

Klisch, Manfred, Rajeshwar P. Sinha, Peter R. Richter, and Donat-P. Häder. 2001. "Mycosporine-like Amino Acids (MAAs) Protect against UV-B-Induced Damage in Gyrodinium Dorsum Kofoid." *Journal of Plant Physiology* 158 (11): 1449–54. https://doi.org/10.1078/0176-1617-00552.

Knittweis, L, R Aguilar, H Alvarez, et al. 2016. *NEW DEPTH RECORD OF THE PRECIOUS RED CORAL CORALLIUM RUBRUM FOR THE MEDITERRANEAN*.

Knowlton, Nancy, and Forest Rohwer. 2003. "Multispecies Microbial Mutualisms on Coral Reefs: The Host as a Habitat." *The American Naturalist* 162 (S4): S4. https://doi.org/10.1086/378684.

Kogej, Tina, Cene Gostinčar, Marc Volkmann, Anna A. Gorbushina, and Nina Gunde-Cimerman. 2006. “Mycosporines in Extremophilic Fungi—Novel Complementary Osmolytes?” *Environmental Chemistry* 3 (2): 105. https://doi.org/10.1071/EN06012.

Kohlmeyer, Jan. 1969. “The Role of Marine Fungi in the Penetration of Calcareous Substances.” *American Zoologist* 9 (3): 741–46. https://doi.org/10.1093/icb/9.3.741.

Kramarsky-Winter, E, M Harel, N Siboni, et al. 2006. “Identification of a Protist-Coral Association and Its Possible Ecological Role.” *Marine Ecology Progress Series* 317 (July): 67–73. https://doi.org/10.3354/meps317067.

Kubin, Elisabeth, Milena Menna, Elena Mauri, Giulio Notarstefano, and Pierre-Marie Poulain. 2022. *Heat Content and Temperature Trends in the Mediterranean Sea as Derived by Argo Float Data (2005-2020)*. March 27. https://doi.org/10.5194/egusphere-egu22-4899.

Kurahashi, M., Y. Fukunaga, S. Harayama, and A. Yokota. 2008. “Sneathiella Glossodoripedis Sp. Nov., a Marine Alphaproteobacterium Isolated from the Nudibranch Glossodoris Cincta, and Proposal of Sneathiellales Ord. Nov. and Sneathiellaceae Fam. Nov.” *INTERNATIONAL JOURNAL OF SYSTEMATIC AND EVOLUTIONARY MICROBIOLOGY* 58 (3): 548–52. https://doi.org/10.1099/ijs.0.65328-0.

Kurtz, Zachary D., Christian L. Müller, Emily R. Miraldi, Dan R. Littman, Martin J. Blaser, and Richard A. Bonneau. 2015. “Sparse and Compositionally Robust Inference of Microbial Ecological Networks.” *PLOS Computational Biology* 11 (5): e1004226. https://doi.org/10.1371/journal.pcbi.1004226.

Kvennefors, E. Charlotte E., Eugenia Sampayo, Caroline Kerr, Genyess Vieira, George Roff, and Andrew C. Barnes. 2012. “Regulation of Bacterial Communities Through Antimicrobial Activity by the Coral Holobiont.” *Microbial Ecology* 63 (3): 3. https://doi.org/10.1007/s00248-011-9946-0.

Kwong, Waldan K., Javier del Campo, Varsha Mathur, Mark J. A. Vermeij, and Patrick J. Keeling. 2019. “A Widespread Coral-Infecting Apicomplexan with Chlorophyll Biosynthesis Genes.” *Nature* 568 (7750): 7750. https://doi.org/10.1038/s41586-019-1072-z.

Kwong, Waldan K., Nicholas A.T. Irwin, Varsha Mathur, et al. 2021. “Taxonomy of the Apicomplexan Symbionts of Coral, Including Corallicolida Ord. Nov., Reassignment of the Genus *Gemmocystis* , and Description of New Species *Corallicola Aquarius* Gen. Nov. Sp. Nov. and *Anthozoaphila Gnarlus* Gen. Nov. Sp. Nov.” *Journal of Eukaryotic Microbiology* 68 (4): e12852. https://doi.org/10.1111/jeu.12852.

La Rivière, Marie, Joaquim Garrabou, and Marc Bally. 2015. “Evidence for Host Specificity among Dominant Bacterial Symbionts in Temperate Gorgonian Corals.” *Coral Reefs* 34 (4): 1087–98. https://doi.org/10.1007/s00338-015-1334-7.

La Rivière, Marie, Marie Roumagnac, Joaquim Garrabou, and Marc Bally. 2013. “Transient Shifts in Bacterial Communities Associated with the Temperate Gorgonian Paramuricea Clavata in the Northwestern Mediterranean Sea.” *PLoS ONE* 8 (2): e57385. https://doi.org/10.1371/journal.pone.0057385.

Lahti, L, S Shetty, T Blake, and J Salojarvi. 2017. *Tools for Microbiome Analysis in R*. V. 1(5), 28. Released. https://github.com/microbiome/microbiome.

LaJeunesse, Todd C. 2001. “Investigating the Biodiversity, Ecology, and Phylogeny of Endosymbiotic Dinoflagellates in the Genus Symbiodinium Using the ITS Region: In Search of a ‘Species’ Level Marker.” *Journal of Phycology* 37 (5): 866–80. https://doi.org/10.1046/j.1529-8817.2001.01031.x.

LaJeunesse, Todd C., and Daniel J. Thornhill. 2011. “Improved Resolution of Reef-Coral Endosymbiont (Symbiodinium) Species Diversity, Ecology, and Evolution through psbA Non-Coding Region Genotyping.” *PLoS ONE* 6 (12): e29013. https://doi.org/10.1371/journal.pone.0029013.

Lan, Mengling, Kaixiang Gao, Zhenjun Qin, et al. 2025. “Coral Microbiome in Estuary Coral Community of Pearl River Estuary: Insights into Variation in Coral Holobiont Adaptability to Low-Salinity Conditions.” *BMC Microbiology* 25 (1): 278. https://doi.org/10.1186/s12866-025-04013-4.

Lasker, H. R. 2003. “Zooxanthella Densities within a Caribbean Octocoral during Bleaching and Non-Bleaching Years.” *Coral Reefs* 22 (1): 23–26. https://doi.org/10.1007/s00338-003-0276-7.

Le Campion-Alsumard, T, S Golubic, and K Priess. 1995. “Fungi in Corals: Symbiosis or Disease? Interaction between Polyps and Fungi Causes Pearl-like Skeleton Biomineralization.” *Marine Ecology Progress Series* 117: 137–47. https://doi.org/10.3354/meps117137.

Le Roux, Frédérique, and Melanie Blokesch. 2018. “Eco-Evolutionary Dynamics Linked to Horizontal Gene Transfer in Vibrios.” *Annual Review of Microbiology* 72 (1): 89–110. https://doi.org/10.1146/annurev-micro-090817-062148.

Leadbetter, J. R., T. M. Schmidt, J. R. Graber, and J. A. Breznak. 1999. “Acetogenesis from H_2 Plus CO_2 by Spirochetes from Termite Guts.” *Science* 283 (5402): 686–89. https://doi.org/10.1126/science.283.5402.686.

Ledoux, J.-B., J. Garrabou, O. Bianchimani, P. Drap, J.-P. Féral, and D. Aurelle. 2010. “Fine-Scale Genetic Structure and Inferences on Population Biology in the Threatened Mediterranean Red Coral, Corallium Rubrum: SPATIAL GENETIC STRUCTURE IN THE RED CORAL.” *Molecular Ecology* 19 (19): 4204–16. https://doi.org/10.1111/j.1365-294X.2010.04814.x.

Lee Chang, Kim Jye, Graeme A. Dunstan, Guy C. J. Abell, et al. 2012. “Biodiscovery of New Australian Thraustochytrids for Production of Biodiesel and Long-Chain Omega-3 Oils.” *Applied Microbiology and Biotechnology* 93 (5): 2215–31. https://doi.org/10.1007/s00253-011-3856-4.

Lefort, Vincent, Jean-Emmanuel Longueville, and Olivier Gascuel. 2017. “SMS: Smart Model Selection in PhyML.” *Molecular Biology and Evolution* 34 (9): 2422–24. https://doi.org/10.1093/molbev/msx149.

Leggat, William, Scott F. Heron, Alexander Fordyce, David J. Suggett, and Tracy D. Ainsworth. 2022. “Experiment Degree Heating Week (eDHW) as a Novel Metric to Reconcile and Validate Past and Future Global Coral Bleaching Studies.” *Journal of Environmental Management* 301 (January): 113919. https://doi.org/10.1016/j.jenvman.2021.113919.

Lejeusne, Christophe, Pierre Chevaldonné, Christine Pergent-Martini, Charles F. Boudouresque, and Thierry Pérez. 2010. “Climate Change Effects on a Miniature Ocean: The Highly Diverse, Highly Impacted Mediterranean Sea.” *Trends in Ecology & Evolution* 25 (4): 250–60. https://doi.org/10.1016/j.tree.2009.10.009.

Lema, Kimberley A., Bette L. Willis, and David G. Bourne. 2012. “Corals Form Characteristic Associations with Symbiotic Nitrogen-Fixing Bacteria.” *Applied and Environmental Microbiology* 78 (9): 9. https://doi.org/10.1128/AEM.07800-11.

Lenth, Russell V. 2023. *Emmeans: Estimated Marginal Means, Aka Least-Squares Means*. V. R package version 1.8.8. Released. https://CRAN.R-project.org/package=emmeans.

Levin, Rachel Ashley, Christian Robert Voolstra, Karen Dawn Weynberg, and Madeleine Josephine Henriette Van Oppen. 2017. “Evidence for a Role of Viruses in the Thermal Sensitivity of Coral Photosymbionts.” *The ISME Journal* 11 (3): 808–12. https://doi.org/10.1038/ismej.2016.154.

Ley, Ruth E., Micah Hamady, Catherine Lozupone, et al. 2008. “Evolution of Mammals and Their Gut Microbes.” *Science* 320 (5883): 1647–51. https://doi.org/10.1126/science.1155725.

Li, Jiaxing, Xianqin Wei, Dawei Huang, and Jinhua Xiao. 2022. “The Phylosymbiosis Pattern Between the Fig Wasps of the Same Genus and Their Associated Microbiota.” *Frontiers in Microbiology* 12 (February): 800190. https://doi.org/10.3389/fmicb.2021.800190.

Liang, Jiayuan, Kefu Yu, Yinghui Wang, et al. 2017. “Distinct Bacterial Communities Associated with Massive and Branching Scleractinian Corals and Potential Linkages to Coral Susceptibility to Thermal or Cold Stress.” *Frontiers in Microbiology* 8 (June): 979. https://doi.org/10.3389/fmicb.2017.00979.

Lilburn, T. G., K. S. Kim, N. E. Ostrom, K. R. Byzek, J. R. Leadbetter, and J. A. Breznak. 2001. “Nitrogen Fixation by Symbiotic and Free-Living Spirochetes.” *Science* 292 (5526): 2495–98. https://doi.org/10.1126/science.1060281.

Lim, Shen Jean, and Seth R. Bordenstein. 2020. “An Introduction to Phylosymbiosis.” *Proceedings of the Royal Society B: Biological Sciences* 287 (1922): 1922. https://doi.org/10.1098/rspb.2019.2900.

Lim, Shen Jean, Brenton G. Davis, Danielle E. Gill, et al. 2019. “Taxonomic and Functional Heterogeneity of the Gill Microbiome in a Symbiotic Coastal Mangrove Lucinid Species.” *The ISME Journal* 13 (4): 902–20. https://doi.org/10.1038/s41396-018-0318-3.

Lima, Laís F. O., Maya Weissman, Micheal Reed, et al. 2020. “Modeling of the Coral Microbiome: The Influence of Temperature and Microbial Network.” *mBio* 11 (2): e02691-19. https://doi.org/10.1128/mBio.02691-19.

Lin, Heyu, Min Yu, Xiaolei Wang, and Xiao-Hua Zhang. 2018. “Comparative Genomic Analysis Reveals the Evolution and Environmental Adaptation Strategies of Vibrios.” *BMC Genomics* 19 (1): 135. https://doi.org/10.1186/s12864-018-4531-2.

Lin, Huang, and Shyamal Das Peddada. 2020. “Analysis of Compositions of Microbiomes with Bias Correction.” *Nature Communications* 11 (1): 3514. https://doi.org/10.1038/s41467-020-17041-7.

Linares, Cristina, Rafel Coma, Joaquim Garrabou, David Díaz, and Mikel Zabala. 2008. “Size Distribution, Density and Disturbance in Two Mediterranean Gorgonians: *Paramuricea Clavata* and *Eunicella Singularis*.” *Journal of Applied Ecology* 45 (2): 688–99. https://doi.org/10.1111/j.1365-2664.2007.01419.x.

Linares, Cristina, Rafel Coma, Simone Mariani, David Díaz, Bernat Hereu, and Mikel Zabala. 2008. “Early Life History of the Mediterranean Gorgonian *Paramuricea Clavata:* Implications for Population Dynamics.” *Invertebrate Biology* 127 (1): 1–11. https://doi.org/10.1111/j.1744-7410.2007.00109.x.

Lionello, P., P. Malanotte-Rizzoli, R. Boscolo, et al. 2006. “The Mediterranean Climate: An Overview of the Main Characteristics and Issues.” In *Developments in Earth and Environmental Sciences*, vol. 4. Elsevier. https://doi.org/10.1016/S1571-9197(06)80003-0.

Lionello, Piero, and Luca Scarascia. 2018. “The Relation between Climate Change in the Mediterranean Region and Global Warming.” *Regional Environmental Change* 18 (5): 1481–93. https://doi.org/10.1007/s10113-018-1290-1.

Liu, Y., Y. Li, Q. Lin, and Y. Zhang. 2017. “Assessment of the Pathogenicity of Marine *Cladosporium* Spp. towards Mangroves.” *Forest Pathology* 47 (2): e12322. https://doi.org/10.1111/efp.12322.

Llaberia-Robledillo, Mar, J Ignacio Lucas-Lledó, Oscar A Pérez-Escobar, Boris R Krasnov, and Juan Antonio Balbuena. 2023. “Rtapas: An R Package to Assess Cophylogenetic Signal between Two Evolutionary Histories.” *Systematic Biology* 72 (4): 946–54. https://doi.org/10.1093/sysbio/syad016.

Lopes, Ana Rita, Filipa Faleiro, Inês C. Rosa, et al. 2018. “Physiological Resilience of a Temperate Soft Coral to Ocean Warming and Acidification.” *Cell Stress and Chaperones* 23 (5): 1093–100. https://doi.org/10.1007/s12192-018-0919-9.

López-Cortés, David J., Erick J. Núñez Vázquez, Juan J. Dorantes-Aranda, et al. 2019. “The State of Knowledge of Harmful Algal Blooms of Margalefidinium Polykrikoides (a.k.a. Cochlodinium Polykrikoides) in Latin America.” *Frontiers in Marine Science* 6 (August): 463. https://doi.org/10.3389/fmars.2019.00463.

Lu, Hao, Alireza Asem, Lu Wang, Weidong Li, and PeiZheng Wang. 2020. “Comparison of Symbiotic Bacterial Community of Soft Corals Sarcophyton and Sinularia of the Hainan Province, (South China Sea, China).” *Genetics of Aquatic Organisms* 5 (1): 19–28. https://doi.org/10.4194/2459-1831-v5_1_03.

Luan, Nguyen Trong, M. Azizur Rahman, Teruya Maki, Nozumu Iwasaki, and Hiroshi Hasegawa. 2013. “Growth Characteristics and Growth Rate Estimation of Japanese Precious Corals.” *Journal of Experimental Marine Biology and Ecology* 441 (March): 117–25. https://doi.org/10.1016/j.jembe.2013.01.012.

Luo, Danli, Xiaojun Wang, Xiaoyuan Feng, et al. 2021. “Population Differentiation of Rhodobacteraceae along with Coral Compartments.” *The ISME Journal* 15 (11): 3286–302. https://doi.org/10.1038/s41396-021-01009-6.

Liverino, Basilio. 1989. Red Coral: Jewel of the Sea. Edizioni Analisi.

Ma, Xuan, and Shu-Hua Qi. 2019. “Marine Natural Products from Marine Coral-Derived Microorganisms.” In *Symbiotic Microbiomes of Coral Reefs Sponges and Corals*, edited by Zhiyong Li. Springer Netherlands. https://doi.org/10.1007/978-94-024-1612-1_14.

Machida, Ryuji J., Matthew Kweskin, and Nancy Knowlton. 2012. “PCR Primers for Metazoan Mitochondrial 12S Ribosomal DNA Sequences.” *PLoS ONE* 7 (4): e35887. https://doi.org/10.1371/journal.pone.0035887.

Maher, Rebecca L., Emily R. Schmeltzer, Sonora Meiling, et al. 2020. “Coral Microbiomes Demonstrate Flexibility and Resilience Through a Reduction in Community Diversity Following a Thermal Stress Event.” *Frontiers in Ecology and Evolution* 8 (October): 555698. https://doi.org/10.3389/fevo.2020.555698.

Mai, Jeffrey C., and Annette W. Coleman. 1997. “The Internal Transcribed Spacer 2 Exhibits a Common Secondary Structure in Green Algae and Flowering Plants.” *Journal of Molecular Evolution* 44 (3): 258–71. https://doi.org/10.1007/PL00006143.

Maire, Justin, Patrick Buerger, Wing Yan Chan, et al. 2022. “Effects of Ocean Warming on the Underexplored Members of the Coral Microbiome.” *Integrative and Comparative Biology* 62 (6): 1700–1709. https://doi.org/10.1093/icb/icac005.

Maire, Justin, Kshitij Tandon, Astrid Collingro, et al. 2023. “Colocalization and Potential Interactions of *Endozoicomonas* and Chlamydiae in Microbial Aggregates of the Coral *Pocillopora Acuta*.” *Science Advances* 9 (20): eadg0773. https://doi.org/10.1126/sciadv.adg0773.

Manasrah, Riyad, Ahmad Abu-Hilal, and Mohammad Rasheed. 2019. “Physical and Chemical Properties of Seawater in the Gulf of Aqaba and Red Sea.” In *Oceanographic and Biological Aspects of the Red Sea*, edited by Najeeb M.A. Rasul and Ian C.F. Stewart. Springer International Publishing. https://doi.org/10.1007/978-3-319-99417-8_3.

Manasrah, Riyad, Lojen Alsaad, Khalid Trabeen, et al. 2020. “Physical and Chemical Properties of Seawater during 2013–2015 in the 400 m Water Column in the Northern Gulf of Aqaba, Red Sea.” *Environmental Monitoring and Assessment* 192 (3): 188. https://doi.org/10.1007/s10661-020-8134-4.

Mandal, Fatik Baran. 2024. “The Impact of Ciliate Nutrition on Aquatic Ecosystems.” *Israel Journal of Ecology and Evolution*, May 16, 1–11. https://doi.org/10.1163/22244662-bja10081.

Marangon, Emma, Nils Rädecker, Joan Y. Q. Li, et al. 2025. “Destabilization of Mutualistic Interactions Shapes the Early Heat Stress Response of the Coral Holobiont.” *Microbiome* 13 (1): 31. https://doi.org/10.1186/s40168-024-02006-5.

Marcelino, Vanessa Rossetto, and Heroen Verbruggen. 2016. “Multi-Marker Metabarcoding of Coral Skeletons Reveals a Rich Microbiome and Diverse Evolutionary Origins of Endolithic Algae.” *Scientific Reports* 6 (1): 31508. https://doi.org/10.1038/srep31508.

Marchese, Pietro, Laura Garzoli, Ryan Young, et al. 2021. “Fungi Populate Deep-sea Coral Gardens as Well as Marine Sediments in the Irish Atlantic Ocean.” *Environmental Microbiology* 23 (8): 4168–84. https://doi.org/10.1111/1462-2920.15560.

Margulis, Lynn, and René Fester. 1991. “Symbiosis as a Source of Evolutionary Innovation: Speciation and Morphogenesis.” *MIT Press*.

Marhaver, Kristen L., Robert A. Edwards, and Forest Rohwer. 2008. “Viral Communities Associated with Healthy and Bleaching Corals.” *Environmental Microbiology* 10 (9): 2277–86. https://doi.org/10.1111/j.1462-2920.2008.01652.x.

Martin, Marcel. 2011. “Cutadapt Removes Adapter Sequences from High-Throughput Sequencing Reads.” *EMBnet.Journal* 17 (1): 10. https://doi.org/10.14806/ej.17.1.200.

Martin, Y., J.L. Bonnefont, and L. Chancerelle. 2002. “Gorgonians Mass Mortality during the 1999 Late Summer in French Mediterranean Coastal Waters: The Bacterial Hypothesis.” *Water Research* 36 (3): 779–82. https://doi.org/10.1016/S0043-1354(01)00251-2.

Martin-Cuadrado, Ana-Belen, Esther Rubio-Portillo, Francesc Rosselló, and Josefa Antón. 2024. “The Coral Oculina Patagonica Holobiont and Its Response to Confinement, Temperature, and Vibrio Infections.” *Microbiome* 12 (1): 222. https://doi.org/10.1186/s40168-024-01921-x.

Martinez, Edwin A. 1980. “Sensitivity of Marine Ciliates (Protozoa, Ciliophora) to High Thermal Stress.” *Estuarine and Coastal Marine Science* 10 (4): 369-IN1. https://doi.org/10.1016/S0302-3524(80)80117-4.

Masigol, Hossein, Seyed Akbar Khodaparast, Jason Nicholas Woodhouse, et al. 2019. “The Contrasting Roles of Aquatic Fungi and Oomycetes in the Degradation and Transformation of Polymeric Organic Matter.” *Limnology and Oceanography* 64 (6): 2662–78. https://doi.org/10.1002/lno.11242.

Massé, A., I. Domart-Coulon, S. Golubic, D. Duché, and A. Tribollet. 2018. “Early Skeletal Colonization of the Coral Holobiont by the Microboring Ulvophyceae Ostreobium Sp.” *Scientific Reports* 8 (1): 2293. https://doi.org/10.1038/s41598-018-20196-5.

Materna, Arne C, Jonathan Friedman, Claudia Bauer, et al. 2012. “Shape and Evolution of the Fundamental Niche in Marine *Vibrio*.” *The ISME Journal* 6 (12): 2168–77. https://doi.org/10.1038/ismej.2012.65.

Matthews, Jennifer L., Jean-Baptiste Raina, Tim Kahlke, Justin R. Seymour, Madeleine J. H. Oppen, and David J. Suggett. 2020. “Symbiodiniaceae-bacteria Interactions: Rethinking Metabolite Exchange in Reef-building Corals as Multi-partner Metabolic Networks.” *Environmental Microbiology* 22 (5): 5. https://doi.org/10.1111/1462-2920.14918.

Mayasich, Sally A., and Richard A. Smucker. 1987. “Role ofCristispira Sp. and Other Bacteria in the Chitinase and Chitobiase Activities of the Crystalline Style of Crassostrea Virginica (Gmelin).” *Microbial Ecology* 14 (2): 157–66. https://doi.org/10.1007/BF02013020.

McCauley, Erin P., Brad Haltli, Hebelin Correa, and Russell G. Kerr. 2016. “Spatial and Temporal Investigation of the Microbiome of the Caribbean Octocoral *Erythropodium Caribaeorum*.” *FEMS Microbiology Ecology* 92 (9): fiw147. https://doi.org/10.1093/femsec/fiw147.

McCauley, M., T. L. Goulet, C. R. Jackson, and S. Loesgen. 2023. “Systematic Review of Cnidarian Microbiomes Reveals Insights into the Structure, Specificity, and Fidelity of

Marine Associations." *Nature Communications* 14 (1): 4899. https://doi.org/10.1038/s41467-023-39876-6.

McDevitt-Irwin, Jamie M., Julia K. Baum, Melissa Garren, and Rebecca L. Vega Thurber. 2017. "Responses of Coral-Associated Bacterial Communities to Local and Global Stressors." *Frontiers in Marine Science* 4 (August): 262. https://doi.org/10.3389/fmars.2017.00262.

McFadden, C. S. 1999a. "Genetic and Taxonomic Relationships among Northeastern Atlantic and Mediterranean Populations of the Soft Coral Alcyonium Coralloides." *Marine Biology* 133 (2): 171–84. https://doi.org/10.1007/s002270050456.

McFadden, C. S. 1999b. "Genetic and Taxonomic Relationships among Northeastern Atlantic and Mediterranean Populations of the Soft Coral Alcyonium Coralloides." *Marine Biology* 133 (2): 171–84. https://doi.org/10.1007/s002270050456.

McFadden, Catherine S., Yehuda Benayahu, Eric Pante, Jana N. Thoma, P. Andrew Nevarez, and Scott C. France. 2011. "Limitations of Mitochondrial Gene Barcoding in Octocorallia." *Molecular Ecology Resources* 11 (1): 19–31. https://doi.org/10.1111/j.1755-0998.2010.02875.x.

McFadden, Catherine S., Leen P. Van Ofwegen, and Andrea M. Quattrini. 2022. "Revisionary Systematics of Octocorallia (Cnidaria: Anthozoa) Guided by Phylogenomics." *Bulletin of the Society of Systematic Biologists* 1 (3). https://doi.org/10.18061/bssb.v1i3.8735.

McLean, Norman, and David Porter. 1982. "The Yellow-Spot Disease of Tritonia Diomedea Bergh, 1894 (Mollusca: Gastropoda: Nudibranchia): Encapsulation of the Thraustochytriaceous Parasite by Host Amoebocytes." *The Journal of Parasitology* 68 (2): 243. https://doi.org/10.2307/3281182.

McMurdie, Paul J., and Susan Holmes. 2013. "Phyloseq: An R Package for Reproducible Interactive Analysis and Graphics of Microbiome Census Data." *PLoS ONE* 8 (4): 61217. https://doi.org/10.1371/journal.pone.0061217.

McMurdie, Paul J., and Susan Holmes. 2014. "Waste Not, Want Not: Why Rarefying Microbiome Data Is Inadmissible." *PLoS Computational Biology* 10 (4): 1003531. https://doi.org/10.1371/journal.pcbi.1003531.

MedECC. 2020. *Climate and Environmental Change in the Mediterranean Basin – Current Situation and Risks for the Future. First Mediterranean Assessment Report*. Version 1. With Wolfgang Cramer, Joël Guiot, Katarzyna Marini, and MedECC. Zenodo. https://doi.org/10.5281/ZENODO.7224821.

Meyer, Julie L., Jessy Castellanos-Gell, Greta S. Aeby, Claudia C. Häse, Blake Ushijima, and Valerie J. Paul. 2019. "Microbial Community Shifts Associated With the Ongoing Stony Coral Tissue Loss Disease Outbreak on the Florida Reef Tract." *Frontiers in Microbiology* 10 (September): 2244. https://doi.org/10.3389/fmicb.2019.02244.

Mezger, E. M., L. J. De Nooijer, W. Boer, G. J. A. Brummer, and G. J. Reichart. 2016. "Salinity Controls on Na Incorporation in Red Sea Planktonic Foraminifera." *Paleoceanography* 31 (12): 1562–82. https://doi.org/10.1002/2016PA003052.

Middlebrook, Rachael, Kenneth R. N. Anthony, Ove Hoegh-Guldberg, and Sophie Dove. 2010. "Heating Rate and Symbiont Productivity Are Key Factors Determining Thermal Stress in

the Reef-Building Coral *Acropora Formosa*." *Journal of Experimental Biology* 213 (7): 1026–34. https://doi.org/10.1242/jeb.031633.

Mikryukov, Vladimir. 2017. *Vmikk/metagMisc: V.0.0.0.9000*. V. v.0.0.0.9000. Zenodo, released May 4. https://doi.org/10.5281/ZENODO.571403.

Millot, Claude. 1979. "Wind Induced Upwellings in the Gulf of Lions." *Oceanologica Acta* 2 (3): 261–74.

Misic, Cristina, Michela Castellano, and Anabella Covazzi Harriague. 2011. "Organic Matter Features, Degradation and Remineralisation at Two Coastal Sites in the Ligurian Sea (NW Mediterranean) Differently Influenced by Anthropogenic Forcing." *Marine Environmental Research* 72 (1–2): 67–74. https://doi.org/10.1016/j.marenvres.2011.05.006.

Mitra, A., K. J. Flynn, J. M. Burkholder, et al. 2014. "The Role of Mixotrophic Protists in the Biological Carbon Pump." *Biogeosciences* 11 (4): 995–1005. https://doi.org/10.5194/bg-11-995-2014.

Moeller, Andrew H., Taichi A. Suzuki, Dana Lin, Eileen A. Lacey, Samuel K. Wasser, and Michael W. Nachman. 2017. "Dispersal Limitation Promotes the Diversification of the Mammalian Gut Microbiota." *Proceedings of the National Academy of Sciences* 114 (52): 13768–73. https://doi.org/10.1073/pnas.1700122114.

Mohamed, Amin R, Michael A Ochsenkühn, Ahmed M Kazlak, Ahmed Moustafa, and Shady A Amin. 2023. "The Coral Microbiome: Towards an Understanding of the Molecular Mechanisms of Coral–Microbiota Interactions." *FEMS Microbiology Reviews* 47 (2): fuad005. https://doi.org/10.1093/femsre/fuad005.

Mokhtar-Jamaï, K., M. Pascual, J.-B. Ledoux, et al. 2011. "From Global to Local Genetic Structuring in the Red Gorgonian *Paramuricea Clavata* : The Interplay between Oceanographic Conditions and Limited Larval Dispersal." *Molecular Ecology* 20 (16): 3291–305. https://doi.org/10.1111/j.1365-294X.2011.05176.x.

Montalbetti, Enrico, Sofia Cavallo, Annalisa Azzola, et al. 2023. "Mucilage-Induced Necrosis Reveals Cellular Oxidative Stress in the Mediterranean Gorgonian Paramuricea Clavata." *Journal of Experimental Marine Biology and Ecology* 559 (February): 151839. https://doi.org/10.1016/j.jembe.2022.151839.

Montano, Simone, Davide Maggioni, Giulia Liguori, et al. 2020. "Morpho-Molecular Traits of Indo-Pacific and Caribbean Halofolliculina Ciliate Infections." *Coral Reefs* 39 (2): 375–86. https://doi.org/10.1007/s00338-020-01899-6.

Montaño-Salazar, Sandra, Elena Quintanilla, and Juan A. Sánchez. 2023a. "Microbial Shifts Associated to ENSO-Derived Thermal Anomalies Reveal Coral Acclimation at Holobiont Level." *Scientific Reports* 13 (1): 22049. https://doi.org/10.1038/s41598-023-49049-6.

Montaño-Salazar, Sandra, Elena Quintanilla, and Juan A. Sánchez. 2023b. "Microbial Shifts Associated to ENSO-Derived Thermal Anomalies Reveal Coral Acclimation at Holobiont Level." *Scientific Reports* 13 (1): 22049. https://doi.org/10.1038/s41598-023-49049-6.

Montero-Serra, Ignasi, Joaquim Garrabou, Daniel F. Doak, Jean-Baptiste Ledoux, and Cristina Linares. 2019. "Marine Protected Areas Enhance Structural Complexity but Do Not

Buffer the Consequences of Ocean Warming for an Overexploited Precious Coral." *Journal of Applied Ecology* 56 (5): 1063–74. https://doi.org/10.1111/1365-2664.13321.

Montero-Serra, Ignasi, Cristina Linares, Marina García, et al. 2015. "Harvesting Effects, Recovery Mechanisms, and Management Strategies for a Long-Lived and Structural Precious Coral." *PLOS ONE* 10 (2): e0117250. https://doi.org/10.1371/journal.pone.0117250.

Moore, R. B. 2003. "Highly Organized Structure in the Non-Coding Region of the psbA Minicircle from Clade C Symbiodinium." *INTERNATIONAL JOURNAL OF SYSTEMATIC AND EVOLUTIONARY MICROBIOLOGY* 53 (6): 1725–34. https://doi.org/10.1099/ijs.0.02594-0.

Moran, Mary Ann. 2015. "The Global Ocean Microbiome." *Science* 350 (6266): aac8455. https://doi.org/10.1126/science.aac8455.

Morrow, Kathleen M, David G Bourne, Craig Humphrey, et al. 2015. "Natural Volcanic CO2 Seeps Reveal Future Trajectories for Host–Microbial Associations in Corals and Sponges." *The ISME Journal* 9 (4): 894–908. https://doi.org/10.1038/ismej.2014.188.

Morrow, Kathleen M., Anthony G. Moss, Nanette E. Chadwick, and Mark R. Liles. 2012. "Bacterial Associates of Two Caribbean Coral Species Reveal Species-Specific Distribution and Geographic Variability." *Applied and Environmental Microbiology* 78 (18): 6438–49. https://doi.org/10.1128/AEM.01162-12.

Mouchka, Morgan E., Ian Hewson, and C. Drew Harvell. 2010. "Coral-Associated Bacterial Assemblages: Current Knowledge and the Potential for Climate-Driven Impacts." *Integrative and Comparative Biology* 50 (4): 662–74. https://doi.org/10.1093/icb/icq061.

Muehlstein, Lisa K., David Porter, and Frederick T. Short. 1991. "*Labyrinthula Zosterae Sp. Nov.* , The Causative Agent of Wasting Disease of Eelgrass, *Zostera Marina*." *Mycologia* 83 (2): 180–91. https://doi.org/10.1080/00275514.1991.12025994.

Munn, Colin B. 2015. "The Role of Vibrios in Diseases of Corals." *Microbiology Spectrum* 3 (4): 3.4.25. https://doi.org/10.1128/microbiolspec.VE-0006-2014.

Muscatine, L., C. Ferrier-Pagès, A. Blackburn, R. D. Gates, G. Baghdasarian, and D. Allemand. 1998. "Cell-Specific Density of Symbiotic Dinoflagellates in Tropical Anthozoans." *Coral Reefs* 17 (4): 329–37. https://doi.org/10.1007/s003380050133.

Muscatine, L., and James W. Porter. 1977. "Reef Corals: Mutualistic Symbioses Adapted to Nutrient-Poor Environments." *BioScience* 27 (7): 454–60. https://doi.org/10.2307/1297526.

Muscatine, L., L. R. McCloskey, and R. E. Marian. 1981. "Estimating the Daily Contribution of Carbon from Zooxanthellae to Coral Animal Respiration." *Limnology and Oceanography* 26 (4): 4. https://doi.org/10.4319/lo.1981.26.4.0601.

Nagano, Naoki, Shou Matsui, Tomoyo Kuramura, Yousuke Taoka, Daiske Honda, and Masahiro Hayashi. 2011. "The Distribution of Extracellular Cellulase Activity in Marine Eukaryotes, Thraustochytrids." *Marine Biotechnology* 13 (2): 133–36. https://doi.org/10.1007/s10126-010-9297-8.

Nagelkerken, I, K Buchan, Gw Smith, et al. 1997. “Widespread Disease in Caribbean Sea Fans:II. Patterns of Infection and Tissue Loss.” *Marine Ecology Progress Series* 160: 255–63. https://doi.org/10.3354/meps160255.

Neave, Matthew J., Amy Apprill, Christine Ferrier-Pagès, and Christian R. Voolstra. 2016. “Diversity and Function of Prevalent Symbiotic Marine Bacteria in the Genus Endozoicomonas.” *Applied Microbiology and Biotechnology* 100 (19): 8315–24. https://doi.org/10.1007/s00253-016-7777-0.

Neave, Matthew J., Craig T. Michell, Amy Apprill, and Christian R. Voolstra. 2017. “Endozoicomonas Genomes Reveal Functional Adaptation and Plasticity in Bacterial Strains Symbiotically Associated with Diverse Marine Hosts.” *Scientific Reports* 7 (1): 40579. https://doi.org/10.1038/srep40579.

Nelson, Craig E., Linda Wegley Kelly, and Andreas F. Haas. 2023. “Microbial Interactions with Dissolved Organic Matter Are Central to Coral Reef Ecosystem Function and Resilience.” *Annual Review of Marine Science* 15 (1): 431–60. https://doi.org/10.1146/annurev-marine-042121-080917.

Neulinger, Sven C., Andrea Gärtner, Johanna Järnegren, Martin Ludvigsen, Karin Lochte, and Wolf-Christian Dullo. 2009. “Tissue-Associated ‘ *Candidatus* Mycoplasma Corallicola’ and Filamentous Bacteria on the Cold-Water Coral *Lophelia Pertusa* (Scleractinia).” *Applied and Environmental Microbiology* 75 (5): 1437–44. https://doi.org/10.1128/AEM.01781-08.

Ng, Jenny C. Y., Yuki Chan, Hein M. Tun, Frederick C. C. Leung, Paul K. S. Shin, and Jill M. Y. Chiu. 2015. “Pyrosequencing of the Bacteria Associated with Platygyra Carnosus Corals with Skeletal Growth Anomalies Reveals Differences in Bacterial Community Composition in Apparently Healthy and Diseased Tissues.” *Frontiers in Microbiology* 6 (October). https://doi.org/10.3389/fmicb.2015.01142.

Nissimov, Jozef, Eugene Rosenberg, and Colin B. Munn. 2009. “Antimicrobial Properties of Resident Coral Mucus Bacteria of Oculina Patagonica.” *FEMS Microbiology Letters* 292 (2): 2. https://doi.org/10.1111/j.1574-6968.2009.01490.x.

Nocker, Andreas, Mark Burr, and Anne K. Camper. 2007. “Genotypic Microbial Community Profiling: A Critical Technical Review.” *Microbial Ecology* 54 (2): 276–89. https://doi.org/10.1007/s00248-006-9199-5.

O’Brien, Paul A., Nikos Andreakis, Shangjin Tan, et al. 2021. “Testing Cophylogeny between Coral Reef Invertebrates and Their Bacterial and Archaeal Symbionts.” *Molecular Ecology* 30 (15): 3768–82. https://doi.org/10.1111/mec.16006.

O’Brien, Paul A., Shangjin Tan, Chentao Yang, et al. 2020. “Diverse Coral Reef Invertebrates Exhibit Patterns of Phylosymbiosis.” *The ISME Journal* 14 (9): 2211–22. https://doi.org/10.1038/s41396-020-0671-x.

Odic, Roxane, Nathaniel Bensoussan, Christel Pinazo, Isabelle Taupier-Letage, and Vincent Rossi. 2022. “Sporadic Wind-Driven Upwelling/Downwelling and Associated Cooling/Warming along Northwestern Mediterranean Coastlines.” *Continental Shelf Research* 250 (November): 104843. https://doi.org/10.1016/j.csr.2022.104843.

Ogaki, Mayara B., Maria T. De Paula, Daniele Ruas, Franciane M. Pellizzari, César X. García-Laviña, and Luiz H. Rosa. 2019. “Marine Fungi Associated with Antarctic Macroalgae.” In *The Ecological Role of Micro-Organisms in the Antarctic Environment*, edited by Susana Castro-Sowinski. Springer Polar Sciences. Springer International Publishing. https://doi.org/10.1007/978-3-030-02786-5_11.

Oksanen, J, FG Blanchet, R Kindt, et al. 2022. *Vegan: Community Ecology Package. R Package Version 22-1 2:1-2*. https://cran.r-project.org/web/packages/vegan/index.html.

Oksanen, J, FG Blanchet, R Kindt, et al. n.d. *Vegan: Community Ecology Package. R Package Version 22-1 2:1-2*. https://cran.r-project.org/web/packages/vegan/index.html.

Oksanen, Jari, F. Guillaume Blanchet, Roeland Kindt, et al. 2012. *Vegan: Community Ecology Package. R Package Version 2.0-2*. January 1.

Oliver, Eric C. J., Markus G. Donat, Michael T. Burrows, et al. 2018. “Longer and More Frequent Marine Heatwaves over the Past Century.” *Nature Communications* 9 (1): 1324. https://doi.org/10.1038/s41467-018-03732-9.

Omneya, Ibrahim, Mohamed Bayoumy, and Nagy Hazem. 2021. “Spatial Variability and Trends of Marine Heat Waves in the Eastern Mediterranean Sea over 39 Years.” *Journal of Marine Science and Engineering* 9 (6): 643. https://doi.org/10.3390/jmse9060643.

Oppen, Madeleine J. H. van, and Linda L. Blackall. 2019. “Coral Microbiome Dynamics, Functions and Design in a Changing World.” *Nature Reviews Microbiology* 17 (9): 557–67. https://doi.org/10.1038/s41579-019-0223-4.

Orejas, Covadonga, Marina Carreiro-Silva, Christian Mohn, et al. 2022. “Marine Animal Forests of the World: Definition and Characteristics.” *Research Ideas and Outcomes* 8 (November): 96274. https://doi.org/10.3897/rio.8.e96274.

Orenes-Salazar, Víctor, Pedro Clemente Navarro-Martínez, Juan Manuel Ruíz, and José Antonio García-Charton. 2023. “Recurrent Marine Heatwaves Threaten the Resilience and Viability of a Key Mediterranean Octocoral Species.” *Aquatic Conservation: Marine and Freshwater Ecosystems* 33 (11): 1161–74. https://doi.org/10.1002/aqc.3997.

Osman, Eslam O., David J. Suggett, Christian R. Voolstra, et al. 2020. “Coral Microbiome Composition along the Northern Red Sea Suggests High Plasticity of Bacterial and Specificity of Endosymbiotic Dinoflagellate Communities.” *Microbiome* 8 (1): 8. https://doi.org/10.1186/s40168-019-0776-5.

Otero Del Mar, Maria, Covadonga Orejas, Joaquim Garrabou, et al. 2017. *Overview of the Conservation Status of Mediterranean Anthozoa*. With Marzia Bo and Catherine Numa. IUCN International Union for Conservation of Nature. https://doi.org/10.2305/IUCN.CH.2017.RA.2.en.

Page, R. M. 2003. *Tangled Trees: Phylogeny, Cospeciation, and Coevolution*. Ed R.M. Page. University of Chicago Press.

Palacio-Castro, Ana M., Stephanie M. Rosales, Caroline E. Dennison, and Andrew C. Baker. 2022. “Microbiome Signatures in Acropora Cervicornis Are Associated with Genotypic Resistance to Elevated Nutrients and Heat Stress.” *Coral Reefs* 41 (5): 1389–403. https://doi.org/10.1007/s00338-022-02289-w.

Palarea-Albaladejo, Javier, and Josep Antoni Martín-Fernández. 2015. “zCompositions — R Package for Multivariate Imputation of Left-Censored Data under a Compositional Approach.” *Chemometrics and Intelligent Laboratory Systems* 143 (April): 85–96. https://doi.org/10.1016/j.chemolab.2015.02.019.

Paletta, Maria Grazia, Jordi Grinyó, Josep-Maria Gili, et al. 2019. “Exploring the Genetic Diversity and the Population Structure of the Mesophotic Paramuricea Macrospina in the Menorca Channel.” *Estuarine, Coastal and Shelf Science* 219 (April): 444–52. https://doi.org/10.1016/j.ecss.2019.02.024.

Paliaga, Guido, Fabio Luino, Laura Turconi, Jerome V. De Graff, and Francesco Faccini. 2020. “Terraced Landscapes on Portofino Promontory (Italy): Identification, Geo-Hydrological Hazard and Management.” *Water* 12 (2): 435. https://doi.org/10.3390/w12020435.

Palleroni, Norberto J. 1997. “Prokaryotic Diversity and the Importance of Culturing.” *Antonie van Leeuwenhoek* 72 (1): 3–19. https://doi.org/10.1023/A:1000394109961.

Palutikof, J. 2003. “Analysis of Mediterranean Climate Data: Measured and Modelled.” In *Mediterranean Climate*, edited by Hans-Jürgen Bolle. Springer Berlin Heidelberg. https://doi.org/10.1007/978-3-642-55657-9_6.

Pan, Jingwen, Javier Del Campo, and Patrick J. Keeling. 2017. “Reference Tree and Environmental Sequence Diversity of Labyrinthulomycetes.” *Journal of Eukaryotic Microbiology* 64 (1): 88–96. https://doi.org/10.1111/jeu.12342.

Panno, Luigi, Maurizio Bruno, Samuele Voyron, et al. 2013. “Diversity, Ecological Role and Potential Biotechnological Applications of Marine Fungi Associated to the Seagrass Posidonia Oceanica.” *New Biotechnology* 30 (6): 685–94. https://doi.org/10.1016/j.nbt.2013.01.010.

Pantos, Olga, Pim Bongaerts, Paul G Dennis, Gene W Tyson, and Ove Hoegh-Guldberg. 2015. “Habitat-Specific Environmental Conditions Primarily Control the Microbiomes of the Coral Seriatopora Hystrix.” *The ISME Journal* 9 (9): 1916–27. https://doi.org/10.1038/ismej.2015.3.

Paoli, Chiara, Monica Montefalcone, Carla Morri, Paolo Vassallo, and Carlo Nike Bianchi. 2017. “Ecosystem Functions and Services of the Marine Animal Forests.” In *Marine Animal Forests*, edited by Sergio Rossi, Lorenzo Bramanti, Andrea Gori, and Covadonga Orejas. Springer International Publishing. https://doi.org/10.1007/978-3-319-21012-4_38.

Parfrey, Laura Wegener, William A. Walters, Christian L. Lauber, et al. 2014. “Communities of Microbial Eukaryotes in the Mammalian Gut within the Context of Environmental Eukaryotic Diversity.” *Frontiers in Microbiology* 5 (June). https://doi.org/10.3389/fmicb.2014.00298.

Park, Joon Sang, Jeonghoon Han, Sung-Suk Suh, Hyun-Jung Kim, Taek-Kyun Lee, and Seung Won Jung. 2022. “Characterization of Bacterial Community Structure in Two Alcyonacean Soft Corals (Litophyton Sp. and Sinularia Sp.) from Chuuk, Micronesia.” *Coral Reefs* 41 (3): 563–74. https://doi.org/10.1007/s00338-021-02176-w.

Parker, Katherine E., Jeremy O. Ward, Erin M. Eggleston, et al. 2020. “Characterization of a Thermally Tolerant Orbicella Faveolata Reef in Abaco, The Bahamas.” *Coral Reefs* 39 (3): 675–85. https://doi.org/10.1007/s00338-020-01948-0.

Pastor, Francisco, Laura Paredes-Fortuny, and Samira Khodayar. 2024. “Mediterranean Marine Heatwaves Intensify in the Presence of Concurrent Atmospheric Heatwaves.” *Communications Earth & Environment* 5 (1): 797. https://doi.org/10.1038/s43247-024-01982-8.

Pastor, Francisco, Jose Antonio Valiente, and Samiro Khodayar. 2020. “A Warming Mediterranean: 38 Years of Increasing Sea Surface Temperature.” *Remote Sensing* 12 (17): 2687. https://doi.org/10.3390/rs12172687.

Peixoto, Raquel S., Phillipe M. Rosado, Deborah Catharine de Assis Leite, Alexandre S. Rosado, and David G. Bourne. 2017. “Beneficial Microorganisms for Corals (BMC): Proposed Mechanisms for Coral Health and Resilience.” *Frontiers in Microbiology* 8 (March). https://doi.org/10.3389/fmicb.2017.00341.

Peixoto, Raquel S., Michael Sweet, Helena D.M. Villela, et al. 2021. “Coral Probiotics: Premise, Promise, Prospects.” *Annual Review of Animal Biosciences* 9 (1): 265–88. https://doi.org/10.1146/annurev-animal-090120-115444.

Peixoto, Raquel S., Christian R. Voolstra, Michael Sweet, et al. 2022. “Harnessing the Microbiome to Prevent Global Biodiversity Loss.” *Nature Microbiology* 7 (11): 1726–35. https://doi.org/10.1038/s41564-022-01173-1.

Peng, Xiao-Yue, Jin-Tao Wu, Chang-Lun Shao, Zhi-Yong Li, Min Chen, and Chang-Yun Wang. 2021. “Co-Culture: Stimulate the Metabolic Potential and Explore the Molecular Diversity of Natural Products from Microorganisms.” *Marine Life Science & Technology* 3 (3): 363–74. https://doi.org/10.1007/s42995-020-00077-5.

Pernice, Massimo C., Ramiro Logares, Laure Guillou, and Ramon Massana. 2013. “General Patterns of Diversity in Major Marine Microeukaryote Lineages.” *PLoS ONE* 8 (2): e57170. https://doi.org/10.1371/journal.pone.0057170.

Peterson, Ch, Jh Grabowski, and Sp Powers. 2003. “Estimated Enhancement of Fish Production Resulting from Restoring Oyster Reef Habitat: Quantitative Valuation.” *Marine Ecology Progress Series* 264: 249–64. https://doi.org/10.3354/meps264249.

Pfaffl, M. W. 2001. “A New Mathematical Model for Relative Quantification in Real-Time RT-PCR.” *Nucleic Acids Research* 29 (9): 45e–445. https://doi.org/10.1093/nar/29.9.e45.

Pfeifer, Eugen, Slawomir Michniewski, Cornelia Gätgens, et al. 2019. “Generation of a Prophage-Free Variant of the Fast-Growing Bacterium Vibrio Natriegens.” *Applied and Environmental Microbiology* 85 (17): e00853-19. https://doi.org/10.1128/AEM.00853-19.

Piazzi, L., E. Cecchi, M.F. Cinti, and G. Ceccherelli. 2021. “Extreme Events and Conservation of Subtidal Habitats: Effects of a Rainfall Flood on Coralligenous Reefs.” *Marine Pollution Bulletin* 165 (April): 112106. https://doi.org/10.1016/j.marpolbul.2021.112106.

Piazzi, Luigi, Fabrizio Atzori, Nicoletta Cadoni, et al. 2021a. “Animal Forest Mortality: Following the Consequences of a Gorgonian Coral Loss on a Mediterranean Coralligenous Assemblage.” *Diversity* 13 (3): 3. https://doi.org/10.3390/d13030133.

Piazzi, Luigi, Fabrizio Atzori, Nicoletta Cadoni, et al. 2021b. “Animal Forest Mortality: Following the Consequences of a Gorgonian Coral Loss on a Mediterranean Coralligenous Assemblage.” *Diversity* 13 (3): 133. https://doi.org/10.3390/d13030133.

Piazzi, Luigi, Fabrizio Atzori, Nicoletta Cadoni, et al. 2021c. “Animal Forest Mortality: Following the Consequences of a Gorgonian Coral Loss on a Mediterranean Coralligenous Assemblage.” *Diversity* 13 (3): 133. https://doi.org/10.3390/d13030133.

Pica, D., B. Calcinai, A. Poliseno, E. Trainito, and C. Cerrano. 2018. “Distribution and Phenotypic Variability of the Mediterranean Gorgonian *Paramuricea Macrospina* (Cnidaria: Octocorallia).” *The European Zoological Journal* 85 (1): 392–408. https://doi.org/10.1080/24750263.2018.1529202.

Pike, Rebecca E., Brad Haltli, and Russell G. Kerr. 2013. “Description of Endozoicomonas Euniceicola Sp. Nov. and Endozoicomonas Gorgoniicola Sp. Nov., Bacteria Isolated from the Octocorals Eunicea Fusca and Plexaura Sp., and an Emended Description of the Genus Endozoicomonas.” *International Journal of Systematic and Evolutionary Microbiology* 63 (Pt_11): 4294–302. https://doi.org/10.1099/ijs.0.051490-0.

Pilczynska, Joanna, Silvia Cocito, Joana Boavida, et al. 2019. “Genetic Diversity Increases with Depth in Red Gorgonian Populations of the Mediterranean Sea and the Atlantic Ocean.” *PeerJ* 7 (May): e6794. https://doi.org/10.7717/peerj.6794.

Pinzón, Jorge H., Bishoy Kamel, Colleen A. Burge, et al. 2015. “Whole Transcriptome Analysis Reveals Changes in Expression of Immune-Related Genes during and after Bleaching in a Reef-Building Coral.” *Royal Society Open Science* 2 (4): 140214. https://doi.org/10.1098/rsos.140214.

Pisano, Andrea, Salvatore Marullo, Vincenzo Artale, et al. 2020. “New Evidence of Mediterranean Climate Change and Variability from Sea Surface Temperature Observations.” *Remote Sensing* 12 (1): 1. https://doi.org/10.3390/rs12010132.

Pivotto, I. D., D. Nerini, M. Masmoudi, H. Kara, L. Chaoui, and D. Aurelle. 2015. “Highly Contrasted Responses of Mediterranean Octocorals to Climate Change along a Depth Gradient.” *Royal Society Open Science* 2 (5): 140493. https://doi.org/10.1098/rsos.140493.

Pogoreutz, Claudia, Clinton A. Oakley, Nils Rädecker, et al. 2022. “Coral Holobiont Cues Prime Endozoicomonas for a Symbiotic Lifestyle.” *The ISME Journal* 16 (8): 1883–95. https://doi.org/10.1038/s41396-022-01226-7.

Pogoreutz, Claudia, and Maren Ziegler. 2024. “Frenemies on the Reef? Resolving the Coral–Endozoicomonas Association.” *Trends in Microbiology* 32 (5): 422–34. https://doi.org/10.1016/j.tim.2023.11.006.

Pollock, F. Joseph, Ryan McMinds, Styles Smith, et al. 2018. “Coral-Associated Bacteria Demonstrate Phylosymbiosis and Cophylogeny.” *Nature Communications* 9 (1): 4921. https://doi.org/10.1038/s41467-018-07275-x.

Ponti, M, E Turicchia, F Costantini, et al. 2019. *Mediterranean Gorgonian Forests: Distribution Patterns and Ecological Roles*. https://www.researchgate.net/publication/332344511.

Pootakham, Wirulda, Wuttichai Mhuantong, Thippawan Yoocha, et al. 2019a. “Heat-induced Shift in Coral Microbiome Reveals Several Members of the Rhodobacteraceae Family as Indicator Species for Thermal Stress in *Porites Lutea*.” *MicrobiologyOpen* 8 (12). https://doi.org/10.1002/mbo3.935.

Pootakham, Wirulda, Wuttichai Mhuantong, Thippawan Yoocha, et al. 2019b. “Heat-induced Shift in Coral Microbiome Reveals Several Members of the Rhodobacteraceae Family as Indicator Species for Thermal Stress in *Porites Lutea*.” *MicrobiologyOpen* 8 (12). https://doi.org/10.1002/mbo3.935.

Porporato, E. M. D., A. Lo Giudice, L. Michaud, E. De Domenico, and N. Spanò. 2013. “Diversity and Antibacterial Activity of the Bacterial Communities Associated with Two Mediterranean Sea Pens, Pennatula Phosphorea and Pteroeides Spinosum (Anthozoa: Octocorallia).” *Microbial Ecology* 66 (3): 3. https://doi.org/10.1007/s00248-013-0260-x.

Poynton, Sl, Br Whitaker, and Ab Heinrich. 2001. “A Novel Trypanoplasm-like Flagellate Jarrellia Atramenti n. g., n. Sp. (Kinetoplastida: Bodonidae) and Ciliates from the Blowhole of a Stranded Pygmy Sperm Whale Kogia Breviceps (Physeteridae): Morphology, Life Cycle and Potential Pathogenicity.” *Diseases of Aquatic Organisms* 44: 191–201. https://doi.org/10.3354/dao044191.

Prada, C., E. Weil, and P. M. Yoshioka. 2010. “Octocoral Bleaching during Unusual Thermal Stress.” *Coral Reefs* 29 (1): 41–45. https://doi.org/10.1007/s00338-009-0547-z.

Pratlong, M., A. Haguenauer, K. Brener, et al. 2021. “Separate the Wheat from the Chaff: Genomic Scan for Local Adaptation in the Red Coral Corallium Rubrum.” *Peer Community Journal* 1 (November): e31. https://doi.org/10.24072/pcjournal.12.

Previati, Monica, Alice Scinto, Carlo Cerrano, and Ronald Osinga. 2010. “Oxygen Consumption in Mediterranean Octocorals under Different Temperatures.” *Journal of Experimental Marine Biology and Ecology* 390 (1): 39–48. https://doi.org/10.1016/j.jembe.2010.04.025.

Priori, Cristina, Vincenza Mastascusa, Fabrizio Erra, Michela Angiolillo, Simonpietro Canese, and Giovanni Santangelo. 2013. “Demography of Deep-Dwelling Red Coral Populations: Age and Reproductive Structure of a Highly Valued Marine Species.” *Estuarine, Coastal and Shelf Science* 118 (February): 43–49. https://doi.org/10.1016/j.ecss.2012.12.011.

Prioux, C., C. Ferrier-Pages, J. Deter, et al. 2024. “Insights into the Occurrence of Phylosymbiosis and Co-Phylogeny in the Holobionts of Octocorals from the Mediterranean Sea and Red Sea.” *Animal Microbiome* 6 (1): 62. https://doi.org/10.1186/s42523-024-00351-2.

Prioux, Camille, Christine Ferrier-Pagès, Javier Del Campo, et al. 2025. “Unraveling the Impact of Marine Heatwaves on the Eukaryome of the Emblematic Mediterranean Red Coral *Corallium Rubrum*.” *ISME Communications*, February 21, ycaf035. https://doi.org/10.1093/ismeco/ycaf035.

Prioux, Camille, Christine Ferrier-Pagès, Thibaut Lamarca, Denis Allemand, and Romie Tignat-Perrier. 2025. “Heatwave-Driven Persistent Microbes Threaten the Resilience of Mediterranean Coral Holobionts.” *Environmental Microbiome* 20 (1): 107. https://doi.org/10.1186/s40793-025-00765-8.

Prioux, Camille, Romie Tignat-Perrier, Ophélie Gervais, et al. 2023. “Unveiling Microbiome Changes in Mediterranean Octocorals during the 2022 Marine Heatwaves: Quantifying Key Bacterial Symbionts and Potential Pathogens.” *Microbiome* 11 (1): 271. https://doi.org/10.1186/s40168-023-01711-x.

Pupier, Chloé A., Renaud Grover, Cécile Rottier, and Christine Ferrier-Pagès. 2024. “Impact of Seawater Warming and Nutrient Deprivation on the Physiology and Energy Metabolism of Corals.” *Frontiers in Marine Science* 11 (October): 1423034. https://doi.org/10.3389/fmars.2024.1423034.

Qiu, Dajun, Liangmin Huang, Yunyun Zhuang, et al. 2021. “Dinoflagellate-Targeted PCR Reveals Highly Abundant and Diverse Communities of Parasitic Dinoflagellates in and near Zhubi Reef, South China Sea.” *Coral Reefs* 40 (6): 1931–39. https://doi.org/10.1007/s00338-021-02168-w.

Quade, Gratianne. 2022. “Record-High Marine Heatwaves in the Mediterranean Sea, Summer 2022.” *Mercator Ocean*, September 26. https://www.mercator-ocean.eu/en/news/marine-heatwaves-mediterranean-summer-2022/.

Quinn, Thomas P, Ionas Erb, Mark F Richardson, and Tamsyn M Crowley. 2018. “Understanding Sequencing Data as Compositions: An Outlook and Review.” *Bioinformatics* 34 (16): 2870–78. https://doi.org/10.1093/bioinformatics/bty175.

Quintanilla, E, Jm Gili, Pj López-González, et al. 2013. “Sexual Reproductive Cycle of the Epibiotic Soft Coral Alcyonium Coralloides (Octocorallia, Alcyonacea).” *Aquatic Biology* 18 (2): 113–24. https://doi.org/10.3354/ab00493.

Quintanilla, Elena, Clara F. Rodrigues, Isabel Henriques, and Ana Hilário. 2022. “Microbial Associations of Abyssal Gorgonians and Anemones (>4,000 m Depth) at the Clarion-Clipperton Fracture Zone.” *Frontiers in Microbiology* 13 (March): 828469. https://doi.org/10.3389/fmicb.2022.828469.

Quistad, Steven D., Aleksandr Stotland, Katie L. Barott, et al. 2014. “Evolution of TNF-Induced Apoptosis Reveals 550 My of Functional Conservation.” *Proceedings of the National Academy of Sciences* 111 (26): 9567–72. https://doi.org/10.1073/pnas.1405912111.

Rabbani, Golam, Danwei Huang, and Benjamin J. Wainwright. 2021. “The Mycobiome of Pocillopora Acuta in Singapore.” *Coral Reefs* 40 (5): 1419–27. https://doi.org/10.1007/s00338-021-02152-4.

Rädecker, Nils, Claudia Pogoreutz, Hagen M. Gegner, et al. 2021. “Heat Stress Destabilizes Symbiotic Nutrient Cycling in Corals.” *Proceedings of the National Academy of Sciences* 118 (5): e2022653118. https://doi.org/10.1073/pnas.2022653118.

Ragan, Ma, Gs MacCallum, Ca Murphy, Jj Cannone, Rr Gutell, and Se McGladdery. 2000. “Protistan Parasite QPX of Hard-Shell Clam Mercenaria Mercenaria Is a Member of Labyrinthulomycota.” *Diseases of Aquatic Organisms* 42: 185–90. https://doi.org/10.3354/dao042185.

Raghukumar, Chandralata, and S. Raghukumar. 1991. “Fungal Invasion of Massive Corals.” *Marine Ecology* 12 (3): 251–60. https://doi.org/10.1111/j.1439-0485.1991.tb00257.x.

Raghukumar, Chandralata, and J. Ravindran. 2012. “Fungi and Their Role in Corals and Coral Reef Ecosystems.” In *Biology of Marine Fungi*, edited by Chandralata Raghukumar. Springer. https://doi.org/10.1007/978-3-642-23342-5_5.

Raghukumar, Seshagiri. 2017. “The Marine Environment and the Role of Fungi.” In *Fungi in Coastal and Oceanic Marine Ecosystems*, by Seshagiri Raghukumar. Springer International Publishing. https://doi.org/10.1007/978-3-319-54304-8_2.

Raghukumar, Seshagiri, and Varada S. Damare. 2011. “Increasing Evidence for the Important Role of Labyrinthulomycetes in Marine Ecosystems.” *Botanica Marina* 54 (1). https://doi.org/10.1515/bot.2011.008.

Ragone Calvo, Lm, Jg Walker, and E Burreson. 1998. “Prevalence and Distribution of QPX, Quahog Parasite Unknown, in Hard Clams Mercenaria Mercenaria in Virginia, USA.” *Diseases of Aquatic Organisms* 33: 209–19. https://doi.org/10.3354/dao033209.

Rahav, O, Zvy Dubinsky, Y Achituv, and Paul G. Falkowski. 1989. “Ammonium Metabolism in the Zooxanthellate Coral, *Stylophora Pistillata*.” *Proceedings of the Royal Society of London. B. Biological Sciences* 236 (1284): 325–37. https://doi.org/10.1098/rspb.1989.0026.

Raina, Jean-Baptiste, Elizabeth A. Dinsdale, Bette L. Willis, and David G. Bourne. 2010. “Do the Organic Sulfur Compounds DMSP and DMS Drive Coral Microbial Associations?” *Trends in Microbiology* 18 (3): 101–8. https://doi.org/10.1016/j.tim.2009.12.002.

Raina, Jean-Baptiste, Dianne Tapiolas, Cherie A. Motti, et al. 2016. “Isolation of an Antimicrobial Compound Produced by Bacteria Associated with Reef-Building Corals.” *PeerJ* 4 (August): e2275. https://doi.org/10.7717/peerj.2275.

Raina, Jean-Baptiste, Dianne Tapiolas, Bette L. Willis, and David G. Bourne. 2009a. “Coral-Associated Bacteria and Their Role in the Biogeochemical Cycling of Sulfur.” *Applied and Environmental Microbiology* 75 (11): 11. https://doi.org/10.1128/AEM.02567-08.

Raina, Jean-Baptiste, Dianne Tapiolas, Bette L. Willis, and David G. Bourne. 2009b. “Coral-Associated Bacteria and Their Role in the Biogeochemical Cycling of Sulfur.” *Applied and Environmental Microbiology* 75 (11): 3492–501. https://doi.org/10.1128/AEM.02567-08.

Ramirez-Calero, S., J. Garrabou, S. Suresh, et al. 2025. “Does Local Adaptation Influence Thermal Responses in Red Coral Populations across Depth Gradients? Transcriptomic Insights for Effective Conservation.” Preprint, May 15. https://doi.org/10.1101/2025.05.12.653513.

Ramirez-Calero, Sandra, D Gómez-Gras, A Barreiro, et al. 2024. “Recurrent Extreme Climatic Events Are Driving Gorgonian Populations to Local Extinction: Low Adaptive Potential to Marine Heatwaves.” Preprint, May 14. https://doi.org/10.1101/2024.05.13.593802.

Randall, Carly J., Adán G. Jordán-Garza, and Robert Van Woesik. 2015. “Ciliates Associated with Signs of Disease on Two Caribbean Corals.” *Coral Reefs* 34 (1): 243–47. https://doi.org/10.1007/s00338-014-1212-8.

Randone, Mauro, Giuseppe Di Carlo, and Marco Costantini. 2017. *Reviving the Economy of the Mediterranean Sea: Actions for a Sustainable Future*. WWF Mediteranean Marine Initiative. https://www.wwf.fr/sites/default/files/doc-2017-09/170927_rapport_reviving_mediterranean_sea_economy.pdf.

Ransome, Emma, Sonia J. Rowley, Simon Thomas, Karen Tait, and Colin B. Munn. 2014. “Disturbance to Conserved Bacterial Communities in the Cold-Water Gorgonian Coral

Eunicella Verrucosa." *FEMS Microbiology Ecology*, August, n/a-n/a. https://doi.org/10.1111/1574-6941.12398.

Rappé, Michael S., and Stephen J. Giovannoni. 2003. "The Uncultured Microbial Majority." *Annual Review of Microbiology* 57 (1): 369–94. https://doi.org/10.1146/annurev.micro.57.030502.090759.

Rasmussen, Jacob A, Pia Kiilerich, Abdullah S Madhun, et al. 2023. "Co-Diversification of an Intestinal *Mycoplasma* and Its Salmonid Host." *The ISME Journal* 17 (5): 682–92. https://doi.org/10.1038/s41396-023-01379-z.

Ravindran, Chinnarajan, Haritha P. Raveendran, and Lawrance Irudayarajan. 2022. "Ciliated Protozoan Occurrence and Association in the Pathogenesis of Coral Disease." *Microbial Pathogenesis* 162 (January): 105211. https://doi.org/10.1016/j.micpath.2021.105211.

Ravindran, J, C Raghukumar, and S Raghukumar. 2001. "Fungi in Porites Lutea: Association with Healthy and Diseased Corals." *Diseases of Aquatic Organisms* 47: 219–28. https://doi.org/10.3354/dao047219.

Ricolleau, Angèle, Nicole Floquet, Jean-Luc Devidal, et al. 2019. "Lead (Pb) Profiles in Red Coral Skeletons as High Resolution Records of Pollution in the Mediterranean Sea." *Chemical Geology* 525 (October): 112–24. https://doi.org/10.1016/j.chemgeo.2019.07.005.

Ritchie, Kb. 2006. "Regulation of Microbial Populations by Coral Surface Mucus and Mucus-Associated Bacteria." *Marine Ecology Progress Series* 322 (September): 1–14. https://doi.org/10.3354/meps322001.

Roach, Ty N. F., Jenna Dilworth, Christian Martin H., A. Daniel Jones, Robert A. Quinn, and Crawford Drury. 2021. "Metabolomic Signatures of Coral Bleaching History." *Nature Ecology & Evolution* 5 (4): 495–503. https://doi.org/10.1038/s41559-020-01388-7.

Robbins, Steven J., Caitlin M. Singleton, Cheong Xin Chan, et al. 2019. "A Genomic View of the Reef-Building Coral Porites Lutea and Its Microbial Symbionts." *Nature Microbiology* 4 (12): 2090–100. https://doi.org/10.1038/s41564-019-0532-4.

Roberts, Callum M., Colin J. McClean, John E. N. Veron, et al. 2002. "Marine Biodiversity Hotspots and Conservation Priorities for Tropical Reefs." *Science* 295 (5558): 5558. https://doi.org/10.1126/science.1067728.

Robertson, Veronica, Brad Haltli, Erin McCauley, David Overy, and Russell Kerr. 2016. "Highly Variable Bacterial Communities Associated with the Octocoral Antillogorgia Elisabethae." *Microorganisms* 4 (3): 23. https://doi.org/10.3390/microorganisms4030023.

Robinson, D.F., and L.R. Foulds. 1981. "Comparison of Phylogenetic Trees." *Mathematical Biosciences* 53 (1–2): 131–47. https://doi.org/10.1016/0025-5564(81)90043-2.

Roder, Cornelia, Till Bayer, Manuel Aranda, Maren Kruse, and Christian R. Voolstra. 2015. "Microbiome Structure of the Fungid Coral C Tenactis Echinata Aligns with Environmental Differences." *Molecular Ecology* 24 (13): 3501–11. https://doi.org/10.1111/mec.13251.

Roik, Anna, Miriam Reverter, and Claudia Pogoreutz. 2022. “A Roadmap to Understanding Diversity and Function of Coral Reef-Associated Fungi.” *FEMS Microbiology Reviews* 46 (6): fuac028. https://doi.org/10.1093/femsre/fuac028.

Rosado, Phillipe M, Deborah C A Leite, Gustavo A S Duarte, et al. 2019. “Marine Probiotics: Increasing Coral Resistance to Bleaching through Microbiome Manipulation.” *The ISME Journal* 13 (4): 921–36. https://doi.org/10.1038/s41396-018-0323-6.

Rosales, Stephanie M., Abigail S. Clark, Lindsay K. Huebner, Rob R. Ruzicka, and Erinn M. Muller. 2020. “Rhodobacterales and Rhizobiales Are Associated With Stony Coral Tissue Loss Disease and Its Suspected Sources of Transmission.” *Frontiers in Microbiology* 11 (April): 681. https://doi.org/10.3389/fmicb.2020.00681.

Rosales, Stephanie M., Lindsay K. Huebner, James S. Evans, et al. 2023. “A Meta-Analysis of the Stony Coral Tissue Loss Disease Microbiome Finds Key Bacteria in Unaffected and Lesion Tissue in Diseased Colonies.” *ISME Communications* 3 (1): 19. https://doi.org/10.1038/s43705-023-00220-0.

Rossi, Sergio, Lorenzo Bramanti, Andrea Gori, and Covadonga Orejas. 2017a. “An Overview of the Animal Forests of the World.” In *Marine Animal Forests*, edited by Sergio Rossi, Lorenzo Bramanti, Andrea Gori, and Covadonga Orejas. Springer International Publishing. https://doi.org/10.1007/978-3-319-17001-5_1-1.

Rossi, Sergio, Lorenzo Bramanti, Andrea Gori, and Covadonga Orejas, eds. 2017b. *Marine Animal Forests: The Ecology of Benthic Biodiversity Hotspots*. Springer International Publishing. https://doi.org/10.1007/978-3-319-21012-4.

Rossi, Sergio, Lorenzo Bramanti, Andrea Gori, and Covadonga Orejas, eds. 2017c. *Marine Animal Forests: The Ecology of Benthic Biodiversity Hotspots*. Springer International Publishing. https://doi.org/10.1007/978-3-319-21012-4.

Röthig, Till, Michael A. Ochsenkühn, Anna Roik, Riaan Van Der Merwe, and Christian R. Voolstra. 2016. “Long-term Salinity Tolerance Is Accompanied by Major Restructuring of the Coral Bacterial Microbiome.” *Molecular Ecology* 25 (6): 1308–23. https://doi.org/10.1111/mec.13567.

Rubio-Portillo, Esther, Juan F. Gago, Manuel Martínez-García, et al. 2018. “Vibrio Communities in Scleractinian Corals Differ According to Health Status and Geographic Location in the Mediterranean Sea.” *Systematic and Applied Microbiology* 41 (2): 131–38. https://doi.org/10.1016/j.syapm.2017.11.007.

Rubio-Portillo, Esther, Alfonso A. Ramos-Esplá, and Josefa Antón. 2021a. “Shifts in Marine Invertebrate Bacterial Assemblages Associated with Tissue Necrosis during a Heat Wave.” *Coral Reefs* 40 (2): 395–404. https://doi.org/10.1007/s00338-021-02075-0.

Rubio-Portillo, Esther, Alfonso A. Ramos-Esplá, and Josefa Antón. 2021b. “Shifts in Marine Invertebrate Bacterial Assemblages Associated with Tissue Necrosis during a Heat Wave.” *Coral Reefs* 40 (2): 395–404. https://doi.org/10.1007/s00338-021-02075-0.

Rubio-Portillo, Esther, Pablo Yarza, Cindy Peñalver, Alfonso A Ramos-Esplá, and Josefa Antón. 2014. “New Insights into *Oculina Patagonica* Coral Diseases and Their Associated *Vibrio* Spp. Communities.” *The ISME Journal* 8 (9): 1794–807. https://doi.org/10.1038/ismej.2014.33.

Ruehland, Caroline, Anna Blazejak, Christian Lott, Alexander Loy, Christer Erséus, and Nicole Dubilier. 2008. “Multiple Bacterial Symbionts in Two Species of Co-occurring Gutless Oligochaete Worms from Mediterranean Sea Grass Sediments.” *Environmental Microbiology* 10 (12): 3404–16. https://doi.org/10.1111/j.1462-2920.2008.01728.x.

Said, Gulab, Xiao-Feng Mou, Yao-Wei Fang, et al. 2018. “Secondary Metabolites Isolated from the Soft Coral-Derived Fungus Aspergillus Sp. from the South China Sea.” *Chemistry of Natural Compounds* 54 (3): 547–49. https://doi.org/10.1007/s10600-018-2402-3.

Sakalli, A. 2017. “Sea Surface Temperature Change in the Mediterranean Sea under Climate Change: A Linear Model for Simulation of the Sea Surface Temperature up to 2100.” *Applied Ecology and Environmental Research* 15 (1): 707–16. https://doi.org/10.15666/aeer/1501_707716.

Sala, Maria Montserrat, Vanessa BalaguÃ©, Carlos PedrÃ³s-AliÃ³, et al. 2005. “Phylogenetic and Functional Diversity of Bacterioplankton during Alexandrium Spp. Blooms.” *FEMS Microbiology Ecology* 54 (2): 257–67. https://doi.org/10.1016/j.femsec.2005.04.005.

Sampaio, Ana, Vanessa Silva, Patrícia Poeta, and Florin Aonofriesei. 2022. “Vibrio Spp.: Life Strategies, Ecology, and Risks in a Changing Environment.” *Diversity* 14 (2): 97. https://doi.org/10.3390/d14020097.

Sánchez, J. A., C. S. McFadden, S. C. France, and H. R. Lasker. 2003. “Molecular Phylogenetic Analyses of Shallow-Water Caribbean Octocorals.” *Marine Biology* 142 (5): 975–87. https://doi.org/10.1007/s00227-003-1018-7.

Santangelo, G, and L Bramanti. 2010. “Quantifying the Decline in Corallium Rubrum Populations.” *Marine Ecology Progress Series* 418 (November): 295–97. https://doi.org/10.3354/meps08897.

Santangelo, Giovanni, and Marco Abbiati. 2001a. “Red Coral: Conservation and Management of an Over-exploited Mediterranean Species.” *Aquatic Conservation: Marine and Freshwater Ecosystems* 11 (4): 253–59. https://doi.org/10.1002/aqc.451.

Santangelo, Giovanni, and Marco Abbiati. 2001b. “Red Coral: Conservation and Management of an Over-exploited Mediterranean Species.” *Aquatic Conservation: Marine and Freshwater Ecosystems* 11 (4): 253–59. https://doi.org/10.1002/aqc.451.

Santín, Andreu, Jordi Grinyó, Maria Jesús Uriz, Claudio Lo Iacono, Josep Maria Gili, and Pere Puig. 2021. “Mediterranean Coral Provinces as a Sponge Diversity Reservoir: Is There a Mediterranean Cold-Water Coral Sponge Fauna?” *Frontiers in Marine Science* 8 (June): 662899. https://doi.org/10.3389/fmars.2021.662899.

Santoferrara, Luciana, Fabien Burki, Sabine Filker, Ramiro Logares, Micah Dunthorn, and George B. McManus. 2020. “Perspectives from Ten Years of Protist Studies by High-Throughput Metabarcoding.” *Journal of Eukaryotic Microbiology* 67 (5): 612–22. https://doi.org/10.1111/jeu.12813.

Sarda, Julia, Andrea Gori, Ruth Doñate-Ordóñez, et al. 2024. “Recurrent Marine Heatwaves Compromise the Reproduction Success and Long-Term Viability of Shallow Populations of the Mediterranean Gorgonian Eunicella Singularis.” *Marine Environmental Research*, October, 106822. https://doi.org/10.1016/j.marenvres.2024.106822.

Savary, Romain, Daniel J. Barshis, Christian R. Voolstra, et al. 2021. “Fast and Pervasive Transcriptomic Resilience and Acclimation of Extremely Heat-Tolerant Coral Holobionts from the Northern Red Sea.” *Proceedings of the National Academy of Sciences* 118 (19): e2023298118. https://doi.org/10.1073/pnas.2023298118.

Schleifer, Karl-Heinz. 2004. “Microbial Diversity: Facts, Problems and Prospects.” *Systematic and Applied Microbiology* 27 (1): 3–9. https://doi.org/10.1078/0723-2020-00245.

Schoch, Conrad L., Keith A. Seifert, Sabine Huhndorf, et al. 2012. “Nuclear Ribosomal Internal Transcribed Spacer (ITS) Region as a Universal DNA Barcode Marker for *Fungi*.” *Proceedings of the National Academy of Sciences* 109 (16): 6241–46. https://doi.org/10.1073/pnas.1117018109.

Schubert, Nadine, Darren Brown, and Sergio Rossi. 2016. “Symbiotic Versus Non-Symbiotic Octocorals: Physiological and Ecological Implications.” In *Marine Animal Forests*, edited by Sergio Rossi, Lorenzo Bramanti, Andrea Gori, and Covadonga Orejas Saco Del Valle. Springer International Publishing. https://doi.org/10.1007/978-3-319-17001-5_54-1.

Seeber, Frank, and Svenja Steinfelder. 2016. “Recent Advances in Understanding Apicomplexan Parasites.” *F1000Research* 5 (June): 1369. https://doi.org/10.12688/f1000research.7924.1.

Sekar, R, Lt Kaczmarsky, and Ll Richardson. 2008. “Microbial Community Composition of Black Band Disease on the Coral Host Siderastrea Siderea from Three Regions of the Wider Caribbean.” *Marine Ecology Progress Series* 362 (June): 85–98. https://doi.org/10.3354/meps07496.

Seneca, Francois O., and Stephen R. Palumbi. 2015. “The Role of Transcriptome Resilience in Resistance of Corals to Bleaching.” *Molecular Ecology* 24 (7): 1467–84. https://doi.org/10.1111/mec.13125.

Setyati, Wilis Ari, Sri Sedjati, Alun Samudra, and Dafit Ariyanto. 2023. “Investigation of Seagrass-Associated Fungi as Antifouling Candidates with Anti-Bacterial Properties.” *Jordan Journal of Biological Sciences* 16 (June): 323–27. https://doi.org/10.54319/jjbs/160216.

Shaltout, Mohamed, and Anders Omstedt. 2014. “Recent sea surface temperature trends and future scenarios for the Mediterranean Sea.” *Oceanologia* 56 (3): 411–43. https://doi.org/10.5697/oc.56-3.411.

Sharon, Gil, and Eugene Rosenberg. 2010. “Healthy Corals Maintain *Vibrio* in the VBNC State.” *Environmental Microbiology Reports* 2 (1): 116–19. https://doi.org/10.1111/j.1758-2229.2009.00113.x.

Shimpi, Gaurav G., Sergio Vargas, and Gert Wörheide. 2016. “Evaluation and Validation of Reference Genes for qPCR Analysis to Study Climate Change-Induced Stresses in Sinularia Cf. Cruciata (Octocorallia: Alcyonidae).” *Journal of Experimental Marine Biology and Ecology* 483 (October): 42–52. https://doi.org/10.1016/j.jembe.2016.06.001.

Shiu, Jia-Ho, Sheng-Ping Yu, Chia-Ling Fong, et al. 2020. “Shifting in the Dominant Bacterial Group Endozoicomonas Is Independent of the Dissociation With Coral Symbiont Algae.” *Frontiers in Microbiology* 11 (July): 1791. https://doi.org/10.3389/fmicb.2020.01791.

Shnit-Orland, Maya, Alex Sivan, and Ariel Kushmaro. 2012. “Antibacterial Activity of Pseudoalteromonas in the Coral Holobiont.” *Microbial Ecology* 64 (4): 851–59. https://doi.org/10.1007/s00248-012-0086-y.

Siboni, Nachshon, Eitan Ben-Dov, Alex Sivan, and Ariel Kushmaro. 2008. “Global Distribution and Diversity of Coral-associated *Archaea* and Their Possible Role in the Coral Holobiont Nitrogen Cycle.” *Environmental Microbiology* 10 (11): 2979–90. https://doi.org/10.1111/j.1462-2920.2008.01718.x.

Siboni, Nachshon, Eitan Ben-Dov, Alex Sivan, and Ariel Kushmaro. 2012. “Geographic Specific Coral-Associated Ammonia-Oxidizing Archaea in the Northern Gulf of Eilat (Red Sea).” *Microbial Ecology* 64 (1): 18–24. https://doi.org/10.1007/s00248-011-0006-6.

Siboni, Nachshon, Diana Rasoulouniriana, Eitan Ben-Dov, et al. 2010. “Stramenopile Microorganisms Associated with the Massive Coral *Favia* Sp.” *Journal of Eukaryotic Microbiology* 57 (3): 236–44. https://doi.org/10.1111/j.1550-7408.2010.00469.x.

Sievers, Fabian, Andreas Wilm, David Dineen, et al. 2011. “Fast, Scalable Generation of High-quality Protein Multiple Sequence Alignments Using Clustal Omega.” *Molecular Systems Biology* 7 (1): 539. https://doi.org/10.1038/msb.2011.75.

Simon, Jean-Christophe, Julian R. Marchesi, Christophe Mougel, and Marc-André Selosse. 2019a. “Host-Microbiota Interactions: From Holobiont Theory to Analysis.” *Microbiome* 7 (1): 5. https://doi.org/10.1186/s40168-019-0619-4.

Simon, Jean-Christophe, Julian R. Marchesi, Christophe Mougel, and Marc-André Selosse. 2019b. “Host-Microbiota Interactions: From Holobiont Theory to Analysis.” *Microbiome* 7 (1): 5. https://doi.org/10.1186/s40168-019-0619-4.

Singer, David, Christophe V.W. Seppey, Guillaume Lentendu, et al. 2021. “Protist Taxonomic and Functional Diversity in Soil, Freshwater and Marine Ecosystems.” *Environment International* 146 (January): 106262. https://doi.org/10.1016/j.envint.2020.106262.

Šlapeta, Jan, and Marjorie C. Linares. 2013. “Combined Amplicon Pyrosequencing Assays Reveal Presence of the Apicomplexan ‘Type-N’ (Cf. Gemmocystis Cylindrus) and Chromera Velia on the Great Barrier Reef, Australia.” *PLoS ONE* 8 (9): e76095. https://doi.org/10.1371/journal.pone.0076095.

Smale, Dan A., Thomas Wernberg, Eric C. J. Oliver, et al. 2019. “Marine Heatwaves Threaten Global Biodiversity and the Provision of Ecosystem Services.” *Nature Climate Change* 9 (4): 306–12. https://doi.org/10.1038/s41558-019-0412-1.

Smith, Christopher Irwin, William K. W. Godsoe, Shantel Tank, Jeremy B. Yoder, and Olle Pellmyr. 2008. “Distinguishing Coevolution from Covicariance in an Obligate Pollination Mutualism: Asynchronous Divergence in Joshua Tree and Its Pollinators.” *Evolution* 62 (10): 2676–87. https://doi.org/10.1111/j.1558-5646.2008.00500.x.

Smith, Edward G, Remi N Ketchum, and John A Burt. 2017. “Host Specificity of *Symbiodinium* Variants Revealed by an ITS2 Metahaplotype Approach.” *The ISME Journal* 11 (6): 1500–1503. https://doi.org/10.1038/ismej.2016.206.

Smith, Garriet W., Lisa D. Ives, Ivan A. Nagelkerken, and Kim B. Ritchie. 1996. “Caribbean Sea-Fan Mortalities.” *Nature* 383 (6600): 487–487. https://doi.org/10.1038/383487a0.

Smith, Rob. 2021. *Ecole: School of Ecology Package*. V. R package version 0.9. Released. https://github.com/phytomosaic/ecole.

Sniezek, James H., D. Wayne Coats, and Eugene B. Small. 1995. "*Kyaroikeus Cetarius* N. G., N. Sp.: A Parasitic Ciliate from the Respiratory Tract of Odonticete Cetacea." *Journal of Eukaryotic Microbiology* 42 (3): 260–68. https://doi.org/10.1111/j.1550-7408.1995.tb01577.x.

Soares, Marcelo de Oliveira, Jorge Thé de Araújo, Sarah Maria Cavalcante Ferreira, et al. 2020. "Why Do Mesophotic Coral Ecosystems Have to Be Protected?" *Science of The Total Environment* 726 (July): 138456. https://doi.org/10.1016/j.scitotenv.2020.138456.

Soler-Hurtado, M. Mar, José Vladimir Sandoval-Sierra, Annie Machordom, and Javier Diéguez-Uribeondo. 2016. "Aspergillus Sydowii and Other Potential Fungal Pathogens in Gorgonian Octocorals of the Ecuadorian Pacific." *PLOS ONE* 11 (11): e0165992. https://doi.org/10.1371/journal.pone.0165992.

Song, Jy, Si Kitamura, Mj Oh, et al. 2009. "Pathogenicity of Miamiensis Avidus (Syn. Philasterides Dicentrarchi), Pseudocohnilembus Persalinus, Pseudocohnilembus Hargisi and Uronema Marinum (Ciliophora, Scuticociliatida)." *Diseases of Aquatic Organisms* 83 (February): 133–43. https://doi.org/10.3354/dao02017.

Spalding, Mark, Lauretta Burke, Spencer A. Wood, Joscelyne Ashpole, James Hutchison, and Philine Zu Ermgassen. 2017. "Mapping the Global Value and Distribution of Coral Reef Tourism." *Marine Policy* 82 (August): 104–13. https://doi.org/10.1016/j.marpol.2017.05.014.

Speck, Mark D., and Stuart P. Donachie. 2012. "Widespread Oceanospirillaceae Bacteria in *Porites* Spp." *Journal of Marine Biology* 2012: 1–7. https://doi.org/10.1155/2012/746720.

Steininger, Fritz F., and Fred Rögl. 1984. "Paleogeography and Palinspastic Reconstruction of the Neogene of the Mediterranean and Paratethys." *Geological Society, London, Special Publications* 17 (1): 659–68. https://doi.org/10.1144/GSL.SP.1984.017.01.52.

Stévenne, Chloé, Maud Micha, Jean-Christophe Plumier, and Stéphane Roberty. 2021. "Corals and Sponges Under the Light of the Holobiont Concept: How Microbiomes Underpin Our Understanding of Marine Ecosystems." *Frontiers in Marine Science* 8 (August): 698853. https://doi.org/10.3389/fmars.2021.698853.

Stoddard, Steven F., Byron J. Smith, Robert Hein, Benjamin R.K. Roller, and Thomas M. Schmidt. 2015. "rrnDB: Improved Tools for Interpreting rRNA Gene Abundance in Bacteria and Archaea and a New Foundation for Future Development." *Nucleic Acids Research* 43 (D1): D593–98. https://doi.org/10.1093/nar/gku1201.

Stoeck, Thorsten, David Bass, Markus Nebel, et al. 2010. "Multiple Marker Parallel Tag Environmental DNA Sequencing Reveals a Highly Complex Eukaryotic Community in Marine Anoxic Water." *Molecular Ecology* 19 (s1): 21–31. https://doi.org/10.1111/j.1365-294X.2009.04480.x.

Strano, Francesca, Valerio Micaroni, Torsten Thomas, Lisa Woods, Simon K. Davy, and James J. Bell. 2023. "Marine Heatwave Conditions Drive Carryover Effects in a Temperate Sponge Microbiome and Developmental Performance." *Proceedings of the Royal Society B: Biological Sciences* 290 (2000): 20222539. https://doi.org/10.1098/rspb.2022.2539.

Sully, S., D. E. Burkepile, M. K. Donovan, G. Hodgson, and R. Van Woesik. 2019. “A Global Analysis of Coral Bleaching over the Past Two Decades.” *Nature Communications* 10 (1): 1264. https://doi.org/10.1038/s41467-019-09238-2.

Sun, Xiaohui, Yan Li, Qian Yang, et al. 2023. “Identification of Quorum Sensing-Regulated Vibrio Fortis as Potential Pathogenic Bacteria for Coral Bleaching and the Effects on the Microbial Shift.” *Frontiers in Microbiology* 14 (February): 1116737. https://doi.org/10.3389/fmicb.2023.1116737.

Sunagawa, Shinichi, Todd Z DeSantis, Yvette M Piceno, et al. 2009. “Bacterial Diversity and White Plague Disease-Associated Community Changes in the Caribbean Coral *Montastraea Faveolata*.” *The ISME Journal* 3 (5): 512–21. https://doi.org/10.1038/ismej.2008.131.

Sunagawa, Shinichi, Cheryl M. Woodley, and Mónica Medina. 2010. “Threatened Corals Provide Underexplored Microbial Habitats.” *PLoS ONE* 5 (3): e9554. https://doi.org/10.1371/journal.pone.0009554.

Sunda, W., D. J. Kieber, R. P. Kiene, and S. Huntsman. 2002. “An Antioxidant Function for DMSP and DMS in Marine Algae.” *Nature* 418 (6895): 317–20. https://doi.org/10.1038/nature00851.

Suzuki, Ryota, and Hidetoshi Shimodaira. 2006. “Pvclust: An R Package for Assessing the Uncertainty in Hierarchical Clustering.” *Bioinformatics* 22 (12): 1540–42. https://doi.org/10.1093/bioinformatics/btl117.

Sweet, M. J., A. Croquer, and J. C. Bythell. 2014. “Experimental Antibiotic Treatment Identifies Potential Pathogens of White Band Disease in the Endangered Caribbean Coral *Acropora Cervicornis*.” *Proceedings of the Royal Society B: Biological Sciences* 281 (1788): 20140094. https://doi.org/10.1098/rspb.2014.0094.

Sweet, Michael, Alfred Burian, James Fifer, Mark Bulling, David Elliott, and Laurie Raymundo. 2019. “Compositional Homogeneity in the Pathobiome of a New, Slow-Spreading Coral Disease.” *Microbiome* 7 (1): 139. https://doi.org/10.1186/s40168-019-0759-6.

Sweet, Michael, and John Bythell. 2012. “Ciliate and Bacterial Communities Associated with White Syndrome and Brown Band Disease in Reef-building Corals.” *Environmental Microbiology* 14 (8): 2184–99. https://doi.org/10.1111/j.1462-2920.2012.02746.x.

Sweet, Michael, and John Bythell. 2015. “White Syndrome in *Acropora Muricata:* Nonspecific Bacterial Infection and Ciliate Histophagy.” *Molecular Ecology* 24 (5): 1150–59. https://doi.org/10.1111/mec.13097.

Sweet, Michael, Rachel Jones, and John Bythell. 2012. “Coral Diseases in Aquaria and in Nature.” *Journal of the Marine Biological Association of the United Kingdom* 92 (4): 791–801. https://doi.org/10.1017/S0025315411001688.

Sweet, M.J., and M.G. Séré. 2016. “Ciliate Communities Consistently Associated with Coral Diseases.” *Journal of Sea Research* 113 (July): 119–31. https://doi.org/10.1016/j.seares.2015.06.008.

Taberlet, Pierre, Eric Coissac, François Pompanon, Christian Brochmann, and Eske Willerslev. 2012. “Towards Next-generation Biodiversity Assessment Using DNA Metabarcoding.” *Molecular Ecology* 21 (8): 2045–50. https://doi.org/10.1111/j.1365-294X.2012.05470.x.

Takemura, Alison F., Diana M. Chien, and Martin F. Polz. 2014. “Associations and Dynamics of Vibrionaceae in the Environment, from the Genus to the Population Level.” *Frontiers in Microbiology* 5. https://doi.org/10.3389/fmicb.2014.00038.

Tandon, Kshitij, Yu-Jing Chiou, Sheng-Ping Yu, et al. 2022. “Microbiome Restructuring: Dominant Coral Bacterium *Endozoicomonas* Species Respond Differentially to Environmental Changes.” *mSystems* 7 (4): e00359-22. https://doi.org/10.1128/msystems.00359-22.

Tanhua, T., D. Hainbucher, K. Schroeder, V. Cardin, M. Álvarez, and G. Civitarese. 2013. “The Mediterranean Sea System: A Review and an Introduction to the Special Issue.” *Ocean Science* 9 (5): 789–803. https://doi.org/10.5194/os-9-789-2013.

Tant, Cynthia J., Amy D. Rosemond, Andrew S. Mehring, Kevin A. Kuehn, and John M. Davis. 2015. “The Role of Aquatic Fungi in Transformations of Organic Matter Mediated by Nutrients.” *Freshwater Biology* 60 (7): 1354–63. https://doi.org/10.1111/fwb.12573.

Taoka, Yousuke, Naoki Nagano, Yuji Okita, Hitoshi Izumida, Shinichi Sugimoto, and Masahiro Hayashi. 2009. “Extracellular Enzymes Produced by Marine Eukaryotes, Thraustochytrids.” *Bioscience, Biotechnology, and Biochemistry* 73 (1): 180–82. https://doi.org/10.1271/bbb.80416.

Taylor, D Lee, William A Walters, Niall J Lennon, et al. 2016. “Accurate Estimation of Fungal Diversity and Abundance through Improved Lineage-Specific Primers Optimized for Illumina Amplicon Sequencing.” *Applied and Environmental Microbiology* 82 (24).

Temperini, Carolina Virginia, Alejandro Guillermo Pardo, and Graciela Noemí Pose. 2018. “Diversity of Airborne Cladosporium Species Isolated from Agricultural Environments of Northern Argentinean Patagonia: Molecular Characterization and Plant Pathogenicity.” *Aerobiologia* 34 (2): 227–39. https://doi.org/10.1007/s10453-018-9509-7.

Thompson, Janelle R., Mark A. Randa, Luisa A. Marcelino, Aoy Tomita-Mitchell, Eelin Lim, and Martin F. Polz. 2004. “Diversity and Dynamics of a North Atlantic Coastal *Vibrio* Community.” *Applied and Environmental Microbiology* 70 (7): 4103–10. https://doi.org/10.1128/AEM.70.7.4103-4110.2004.

Thompson, Janelle R., Hanny E. Rivera, Collin J. Closek, and MÃ³nica Medina. 2015. “Microbes in the Coral Holobiont: Partners through Evolution, Development, and Ecological Interactions.” *Frontiers in Cellular and Infection Microbiology* 4 (January). https://doi.org/10.3389/fcimb.2014.00176.

Thurber, Rebecca Vega, Jérôme P. Payet, Andrew R. Thurber, and Adrienne M. S. Correa. 2017. “Virus–Host Interactions and Their Roles in Coral Reef Health and Disease.” *Nature Reviews Microbiology* 15 (4): 205–16. https://doi.org/10.1038/nrmicro.2016.176.

Thurber, Rebecca Vega, Dana Willner-Hall, Beltran Rodriguez-Mueller, et al. 2009. “Metagenomic Analysis of Stressed Coral Holobionts.” *Environmental Microbiology* 11 (8): 2148–63. https://doi.org/10.1111/j.1462-2920.2009.01935.x.

Tignat-Perrier, R., L. Bramanti, B. Giordano, et al. 2025. “Microbiome Dynamics in Early Life Stages of the Precious Mediterranean Red Coral *CORALLIUM RUBRUM*.” *Environmental Microbiology Reports* 17 (3): e70127. https://doi.org/10.1111/1758-2229.70127.

Tignat-Perrier, Romie, Jeroen A. J. M. van de Water, Denis Allemand, and Christine Ferrier-Pagès. 2023. “Holobiont Responses of Mesophotic Precious Red Coral Corallium Rubrum to Thermal Anomalies.” *Environmental Microbiome* 18 (1): 70. https://doi.org/10.1186/s40793-023-00525-6.

Tignat-Perrier, Romie, Jeroen A.J.M. van de Water, Dorian Guillemain, Didier Aurelle, Denis Allemand, and Christine Ferrier-Pagès. 2022. “The Effect of Thermal Stress on the Physiology and Bacterial Communities of Two Key Mediterranean Gorgonians.” *Applied and Environmental Microbiology*, February 2, aem.02340-21. https://doi.org/10.1128/aem.02340-21.

T-MEDNet. 2023. “Marine Heatwaves.” https://t-mednet.org/visualize-data/marine-heatwaves.

Todaro, F., A. Berdar, A. Cavaliere, G. Criseo, and L. Pernice. 1983. “Gasophthalmus in Black Sea Bream (Spondyliosoma Cantharus) Caused by Sarcinomyces Crustaceus Lindner.” *Mycopathologia* 81 (2): 95–97. https://doi.org/10.1007/bf00436985.

Toledo-Hernández, C., A. Zuluaga-Montero, A. Bones-González, J. A. Rodríguez, A. M. Sabat, and P. Bayman. 2008. “Fungi in Healthy and Diseased Sea Fans (Gorgonia Ventalina): Is Aspergillus Sydowii Always the Pathogen?” *Coral Reefs* 27 (3): 707–14. https://doi.org/10.1007/s00338-008-0387-2.

Tonin, Stefania. 2018. “Economic Value of Marine Biodiversity Improvement in Coralligenous Habitats.” *Ecological Indicators* 85 (February): 1121–32. https://doi.org/10.1016/j.ecolind.2017.11.017.

Torrents, O., J. Garrabou, C. Marschal, and J.G. Harmelin. 2005. “Age and Size at First Reproduction in the Commercially Exploited Red Coral Corallium Rubrum (L.) in the Marseilles Area (France, NW Mediterranean).” *Biological Conservation* 121 (3): 391–97. https://doi.org/10.1016/j.biocon.2004.05.010.

Torrents, O., E. Tambutté, N. Caminiti, and J. Garrabou. 2008. “Upper Thermal Thresholds of Shallow vs. Deep Populations of the Precious Mediterranean Red Coral Corallium Rubrum (L.): Assessing the Potential Effects of Warming in the NW Mediterranean.” *Journal of Experimental Marine Biology and Ecology* 357 (1): 7–19. https://doi.org/10.1016/j.jembe.2007.12.006.

Tout, Jessica, Nachshon Siboni, Lauren F. Messer, et al. 2015. “Increased Seawater Temperature Increases the Abundance and Alters the Structure of Natural Vibrio Populations Associated with the Coral Pocillopora Damicornis.” *Frontiers in Microbiology* 6 (May). https://doi.org/10.3389/fmicb.2015.00432.

Treignier, C., R. Grover, C. Ferrier-Pagés, and I. Tolosa. 2008. “Effect of Light and Feeding on the Fatty Acid and Sterol Composition of Zooxanthellae and Host Tissue Isolated from the Scleractinian Coral Turbinaria Reniformis.” *Limnology and Oceanography* 53 (6): 2702–10. https://doi.org/10.4319/lo.2008.53.6.2702.

Tremblay, P., R. Grover, J. F. Maguer, M. Hoogenboom, and C. Ferrier-Pagès. 2014. “Carbon Translocation from Symbiont to Host Depends on Irradiance and Food Availability in the

Tropical Coral Stylophora Pistillata." *Coral Reefs* 33 (1): 1–13. https://doi.org/10.1007/s00338-013-1100-7.

Tremblay, Pascale, Renaud Grover, Jean François Maguer, Louis Legendre, and Christine Ferrier-Pagès. 2012. "Autotrophic Carbon Budget in Coral Tissue: A New 13C-Based Model of Photosynthate Translocation." *Journal of Experimental Biology* 215 (8): 1384–93. https://doi.org/10.1242/jeb.065201.

Tribollet, Aline, and Claude Payri. 2001. "Bioerosion of the Coralline Alga Hydrolithon Onkodes by Microborers in the Coral Reefs of Moorea, French Polynesia." *Oceanologica Acta* 24 (4): 329–42. https://doi.org/10.1016/S0399-1784(01)01150-1.

Tsounis, Georgios, Sergio Rossi, Lorenzo Bramanti, and Giovanni Santangelo. 2013. "Management Hurdles for Sustainable Harvesting of Corallium Rubrum." *Marine Policy* 39 (May): 361–64. https://doi.org/10.1016/j.marpol.2012.12.010.

Tsounis, Georgios, Sergio Rossi, Josep-Maria Gili, and Wolf Arntz. 2006. "Population Structure of an Exploited Benthic Cnidarian: The Case Study of Red Coral (Corallium Rubrum L.)." *Marine Biology* 149 (5): 1059–70. https://doi.org/10.1007/s00227-006-0302-8.

Tsounis, Georgios, Sergio Rossi, Richard Grigg, Giovanni Santangelo, Lorenzo Bramanti, and Josep-Maria Gili. 2010. *The Exploitation and Conservation of Precious Corals*.

Tuel, A., and E. A. B. Eltahir. 2020. "Why Is the Mediterranean a Climate Change Hot Spot?" *Journal of Climate* 33 (14): 5829–43. https://doi.org/10.1175/JCLI-D-19-0910.1.

Underwood, Graham J. C., Alex J. Dumbrell, Terry J. McGenity, Boyd A. McKew, and Corinne Whitby. 2022. "The Microbiome of Coastal Sediments." In *The Marine Microbiome*, edited by Lucas J. Stal and Mariana Silvia Cretoiu, vol. 3. The Microbiomes of Humans, Animals, Plants, and the Environment. Springer International Publishing. https://doi.org/10.1007/978-3-030-90383-1_12.

Ushijima, Blake, Sarath P. Gunasekera, Julie L. Meyer, et al. 2023. "Chemical and Genomic Characterization of a Potential Probiotic Treatment for Stony Coral Tissue Loss Disease." *Communications Biology* 6 (1): 248. https://doi.org/10.1038/s42003-023-04590-y.

Van Bel, Mikayla, Amanda E. Fisher, Laymon Ball, J. Travis Columbus, and Renaud Berlemont. 2021. "Phylosymbiosis in the Rhizosphere Microbiome Extends to Nitrogen Cycle Functional Potential." *Microorganisms* 9 (12): 2476. https://doi.org/10.3390/microorganisms9122476.

Van De Water, Jeroen A. J. M., Maryam Chaib De Mares, Groves B. Dixon, et al. 2018. "Antimicrobial and Stress Responses to Increased Temperature and Bacterial Pathogen Challenge in the Holobiont of a Reef-building Coral." *Molecular Ecology* 27 (4): 1065–80. https://doi.org/10.1111/mec.14489.

Van Woesik, Robert, Tom Shlesinger, Andréa G. Grottoli, et al. 2022. "Coral-bleaching Responses to Climate Change across Biological Scales." *Global Change Biology* 28 (14): 4229–50. https://doi.org/10.1111/gcb.16192.

Vargas-Yáñez, M., F. Moya, M.C. García-Martínez, et al. 2010. “Climate Change in the Western Mediterranean Sea 1900–2008.” *Journal of Marine Systems* 82 (3): 171–76. https://doi.org/10.1016/j.jmarsys.2010.04.013.

Verbruggen, Heroen, and Aline Tribollet. 2011. “Boring Algae.” *Current Biology* 21 (21): R876–77. https://doi.org/10.1016/j.cub.2011.09.014.

Verdura, Jana, Cristina Linares, Enric Ballesteros, et al. 2019a. “Biodiversity Loss in a Mediterranean Ecosystem Due to an Extreme Warming Event Unveils the Role of an Engineering Gorgonian Species.” *Scientific Reports* 9 (1): 1. https://doi.org/10.1038/s41598-019-41929-0.

Verdura, Jana, Cristina Linares, Enric Ballesteros, et al. 2019b. “Biodiversity Loss in a Mediterranean Ecosystem Due to an Extreme Warming Event Unveils the Role of an Engineering Gorgonian Species.” *Scientific Reports* 9 (1): 5911. https://doi.org/10.1038/s41598-019-41929-0.

Vezzulli, Luigi, Ingrid Brettar, Elisabetta Pezzati, et al. 2012. “Long-Term Effects of Ocean Warming on the Prokaryotic Community: Evidence from the Vibrios.” *The ISME Journal* 6 (1): 21–30. https://doi.org/10.1038/ismej.2011.89.

Vezzulli, Luigi, Rita R. Colwell, and Carla Pruzzo. 2013. “Ocean Warming and Spread of Pathogenic Vibrios in the Aquatic Environment.” *Microbial Ecology* 65 (4): 817–25. https://doi.org/10.1007/s00248-012-0163-2.

Vezzulli, Luigi, Monica Previati, Carla Pruzzo, et al. 2010a. “Vibrio Infections Triggering Mass Mortality Events in a Warming Mediterranean Sea: Vibrio Infections Triggering Sea-Fan Mass Mortality.” *Environmental Microbiology* 12 (7): 2007–19. https://doi.org/10.1111/j.1462-2920.2010.02209.x.

Vezzulli, Luigi, Monica Previati, Carla Pruzzo, et al. 2010b. “Vibrio Infections Triggering Mass Mortality Events in a Warming Mediterranean Sea: Vibrio Infections Triggering Sea-Fan Mass Mortality.” *Environmental Microbiology* 12 (7): 2007–19. https://doi.org/10.1111/j.1462-2920.2010.02209.x.

Vidal-Dupiol, Jeremie, Ophélie Ladrière, Delphine Destoumieux-Garzón, et al. 2011. “Innate Immune Responses of a Scleractinian Coral to Vibriosis.” *Journal of Biological Chemistry* 286 (25): 22688–98. https://doi.org/10.1074/jbc.M110.216358.

Vieira, Christophe, Aschwin H. Engelen, Linda Guentas, et al. 2016. “Species Specificity of Bacteria Associated to the Brown Seaweeds Lobophora (Dictyotales, Phaeophyceae) and Their Potential for Induction of Rapid Coral Bleaching in Acropora Muricata.” *Frontiers in Microbiology* 7 (March). https://doi.org/10.3389/fmicb.2016.00316.

Vieira, Christophe, Olivier P. Thomas, Gérald Culioli, et al. 2016. “Allelopathic Interactions between the Brown Algal Genus Lobophora (Dictyotales, Phaeophyceae) and Scleractinian Corals.” *Scientific Reports* 6 (1): 18637. https://doi.org/10.1038/srep18637.

Vila-Costa, Maria, Elena Cerro-Gálvez, Alicia Martínez-Varela, Gemma Casas, and Jordi Dachs. 2020. “Anthropogenic Dissolved Organic Carbon and Marine Microbiomes.” *The ISME Journal* 14 (10): 2646–48. https://doi.org/10.1038/s41396-020-0712-5.

Virgen-Urcelay, Alejandra, and Simon D. Donner. 2023. “Increase in the Extent of Mass Coral Bleaching over the Past Half-Century, Based on an Updated Global Database.” *PLOS ONE* 18 (2): e0281719. https://doi.org/10.1371/journal.pone.0281719.

Vohsen, Samuel A., Kaitlin E. Anderson, Andrea M. Gade, et al. 2020. “Deep-Sea Corals Provide New Insight into the Ecology, Evolution, and the Role of Plastids in Widespread Apicomplexan Symbionts of Anthozoans.” *Microbiome* 8 (1): 34. https://doi.org/10.1186/s40168-020-00798-w.

Vohsen, Samuel A., and Santiago Herrera. 2023. *A Seascape Approach to the Microbial Biogeography of Mesophotic and Deep-Sea Octocorals*. Preprint. Microbiology. https://doi.org/10.1101/2023.07.05.547877.

Volkmann, Marc, Kenia Whitehead, Heike Rütters, Jürgen Rullkötter, and Anna A. Gorbushina. 2003. “Mycosporine-glutamicol-glucoside: A Natural UV-absorbing Secondary Metabolite of Rock-inhabiting Microcolonial Fungi.” *Rapid Communications in Mass Spectrometry* 17 (9): 897–902. https://doi.org/10.1002/rcm.997.

Vompe, Alex D., Hannah E. Epstein, Kelly E. Speare, et al. 2024. “Microbiome Ecological Memory and Responses to Repeated Marine Heatwaves Clarify Variation in Coral Bleaching and Mortality.” *Global Change Biology* 30 (1): e17088. https://doi.org/10.1111/gcb.17088.

Von Scheibner, Markus, Ulrich Sommer, and Klaus Jürgens. 2017. “Tight Coupling of Glaciecola Spp. and Diatoms during Cold-Water Phytoplankton Spring Blooms.” *Frontiers in Microbiology* 8 (January). https://doi.org/10.3389/fmicb.2017.00027.

Voolstra, Christian R., Carol Buitrago-López, Gabriela Perna, et al. 2020. “Standardized Short-term Acute Heat Stress Assays Resolve Historical Differences in Coral Thermotolerance across Microhabitat Reef Sites.” *Global Change Biology* 26 (8): 4328–43. https://doi.org/10.1111/gcb.15148.

Voolstra, Christian R., Jean-Baptiste Raina, Melanie Dörr, et al. 2024a. “The Coral Microbiome in Sickness, in Health and in a Changing World.” *Nature Reviews Microbiology* 22 (8): 460–75. https://doi.org/10.1038/s41579-024-01015-3.

Voolstra, Christian R., Jean-Baptiste Raina, Melanie Dörr, et al. 2024b. “The Coral Microbiome in Sickness, in Health and in a Changing World.” *Nature Reviews Microbiology* 22 (8): 460–75. https://doi.org/10.1038/s41579-024-01015-3.

Voolstra, Christian R., Jean-Baptiste Raina, Melanie Dörr, et al. 2024c. “The Coral Microbiome in Sickness, in Health and in a Changing World.” *Nature Reviews Microbiology*, ahead of print, March 4. https://doi.org/10.1038/s41579-024-01015-3.

Voolstra, Christian R., Jacob J. Valenzuela, Serdar Turkarslan, et al. 2021. “Contrasting Heat Stress Response Patterns of Coral Holobionts across the Red Sea Suggest Distinct Mechanisms of Thermal Tolerance.” *Molecular Ecology* 30 (18): 4466–80. https://doi.org/10.1111/mec.16064.

Wahid, M Iftekharul, Takeshi Yoshikawa, and Taizo Sakata. 2007. “Bacteriolytic Activity and Growth of Marine Isolates of Labyrinthulids on Dead Bacterial Cells.” *Fisheries Science* 73 (6): 1286–94. https://doi.org/10.1111/j.1444-2906.2007.01467.x.

Wallace, Bailey, Natascha Varona, and Cynthia Silveira. 2025. “Viruses.” In *Coral Reef Microbiome*, edited by Raquel S. Peixoto and Christian R. Voolstra, vol. 20. Coral Reefs of the World. Springer Nature Switzerland. https://doi.org/10.1007/978-3-031-76692-3_5.

Wan, Yuanyuan, Feng Zhao, Sabine Filker, Ariani Hatmanti, Rongjie Zhao, and Kuidong Xu. 2024. “Parasitic Taxa Are Key to the Vertical Stratification and Community Variation of Pelagic Ciliates from the Surface to the Abyssopelagic Zone.” *Environmental Microbiome* 19 (1): 85. https://doi.org/10.1186/s40793-024-00630-0.

Wang, Chao-Nan, Hu-Mu Lu, Cheng-Hai Gao, et al. 2021. “Cytotoxic Benzopyranone and Xanthone Derivatives from a Coral Symbiotic Fungus *Cladosporium Halotolerans* GXIMD 02502.” *Natural Product Research* 35 (24): 5596–603. https://doi.org/10.1080/14786419.2020.1799363.

Wang, Chenying, Xinqing Zheng, Hagit Kvitt, et al. 2023. “Lineage-Specific Symbionts Mediate Differential Coral Responses to Thermal Stress.” *Microbiome* 11 (1): 211. https://doi.org/10.1186/s40168-023-01653-4.

Wang, Junfeng, Peipei Liu, Yi Wang, et al. 2012. “Antimicrobial Aromatic Polyketides from Gorgonian-Associated Fungus, *Penicillium Commune* 518.” *Chinese Journal of Chemistry* 30 (6): 1236–42. https://doi.org/10.1002/cjoc.201100640.

Wang, Lu, Andrew A. Shantz, Jérôme P. Payet, et al. 2018. “Corals and Their Microbiomes Are Differentially Affected by Exposure to Elevated Nutrients and a Natural Thermal Anomaly.” *Frontiers in Marine Science* 5 (March): 101. https://doi.org/10.3389/fmars.2018.00101.

Water, Jeroen A. J. M. van de, Denis Allemand, and Christine Ferrier-Pagès. 2018. “Host-Microbe Interactions in Octocoral Holobionts - Recent Advances and Perspectives.” *Microbiome* 6 (1): 64. https://doi.org/10.1186/s40168-018-0431-6.

Water, Jeroen A. J. M. van de, Denis Allemand, and Christine Ferrier-Pagès. 2024. “Bacterial Symbionts of the Precious Coral *Corallium Rubrum* Are Differentially Distributed across Colony-specific Compartments and Differ among Colormorphs.” *Environmental Microbiology Reports* 16 (2): e13236. https://doi.org/10.1111/1758-2229.13236.

Water, Jeroen A. J. M. van de, Rémy Melkonian, Howard Junca, et al. 2016a. “Spirochaetes Dominate the Microbial Community Associated with the Red Coral Corallium Rubrum on a Broad Geographic Scale.” *Scientific Reports* 6 (1): 1. https://doi.org/10.1038/srep27277.

Water, Jeroen A. J. M. van de, Rémy Melkonian, Howard Junca, et al. 2016b. “Spirochaetes Dominate the Microbial Community Associated with the Red Coral Corallium Rubrum on a Broad Geographic Scale.” *Scientific Reports* 6 (1): 1. https://doi.org/10.1038/srep27277.

Water, Jeroen A. J. M. van de, Rémy Melkonian, Howard Junca, et al. 2016c. “Spirochaetes Dominate the Microbial Community Associated with the Red Coral Corallium Rubrum on a Broad Geographic Scale.” *Scientific Reports* 6 (1): 27277. https://doi.org/10.1038/srep27277.

Water, Jeroen A. J. M. van de, Rémy Melkonian, Christian R. Voolstra, et al. 2017a. “Comparative Assessment of Mediterranean Gorgonian-Associated Microbial Communities Reveals Conserved Core and Locally Variant Bacteria.” *Microbial Ecology* 73 (2): 2. https://doi.org/10.1007/s00248-016-0858-x.

Water, Jeroen A. J. M. van de, Rémy Melkonian, Christian R. Voolstra, et al. 2017b. “Comparative Assessment of Mediterranean Gorgonian-Associated Microbial Communities Reveals Conserved Core and Locally Variant Bacteria.” *Microbial Ecology* 73 (2): 466–78. https://doi.org/10.1007/s00248-016-0858-x.

Water, Jeroen A. J. M. van de, Rémy Melkonian, Christian R. Voolstra, et al. 2017c. “Comparative Assessment of Mediterranean Gorgonian-Associated Microbial Communities Reveals Conserved Core and Locally Variant Bacteria.” *Microbial Ecology* 73 (2): 466–78. https://doi.org/10.1007/s00248-016-0858-x.

Water, Jeroen A. J. M. van de, Christian R. Voolstra, Cecile Rottier, et al. 2018a. “Seasonal Stability in the Microbiomes of Temperate Gorgonians and the Red Coral Corallium Rubrum Across the Mediterranean Sea.” *Microbial Ecology* 75 (1): 1. https://doi.org/10.1007/s00248-017-1006-y.

Water, Jeroen A. J. M. van de, Christian R. Voolstra, Cecile Rottier, et al. 2018b. “Seasonal Stability in the Microbiomes of Temperate Gorgonians and the Red Coral Corallium Rubrum Across the Mediterranean Sea.” *Microbial Ecology* 75 (1): 274–88. https://doi.org/10.1007/s00248-017-1006-y.

Waters, John P, Jordan S Pober, and John R Bradley. 2013. “Tumour Necrosis Factor in Infectious Disease.” *The Journal of Pathology* 230 (2): 132–47. https://doi.org/10.1002/path.4187.

Waterworth, Samantha C., Shirley Parker-Nance, Jason C. Kwan, and Rosemary A. Dorrington. 2021. “Comparative Genomics Provides Insight into the Function of Broad-Host Range Sponge Symbionts.” *mBio* 12 (5): e01577-21. https://doi.org/10.1128/mBio.01577-21.

Weatherup, Elizabeth F., Patrick Videau, and Blake Ushijima. 2024. “Genome Sequence of *Alteromonas Macleodii* Strain OCN004 Isolated from the Extracellular Mucus of an Apparently Healthy Rice Coral (*Montipora Capitata*).” *Microbiology Resource Announcements* 13 (4): e00079-24. https://doi.org/10.1128/mra.00079-24.

Weckstein, Jason D. 2004. “Biogeography Explains Cophylogenetic Patterns in Toucan Chewing Lice.” *Systematic Biology* 53 (1): 154–64. https://doi.org/10.1080/10635150490265085.

Wegley, Linda, Robert Edwards, Beltran Rodriguez-Brito, Hong Liu, and Forest Rohwer. 2007. “Metagenomic Analysis of the Microbial Community Associated with the Coral *Porites Astreoides*.” *Environmental Microbiology* 9 (11): 2707–19. https://doi.org/10.1111/j.1462-2920.2007.01383.x.

Wegner, K. Mathias, Benjamin Morga, Laure Guillou, et al. 2025. “Prokaryotic Microbiota Outperform Eukaryotic Microbiota in Differentiating between Infection States of Iconic Diseases of Two Commercial Oyster Species.” *Aquaculture* 594 (January): 741363. https://doi.org/10.1016/j.aquaculture.2024.741363.

Weil, E, and A Cróquer. 2009. “Spatial Variability in Distribution and Prevalence of Caribbean Scleractinian Coral and Octocoral Diseases. I. Community-Level Analysis.” *Diseases of Aquatic Organisms* 83 (February): 195–208. https://doi.org/10.3354/dao02011.

Weil, Ernesto, Caroline S. Rogers, and Aldo Croquer. 2016. “Octocoral Diseases in a Changing Ocean.” In *Marine Animal Forests*, edited by Sergio Rossi, Lorenzo Bramanti, Andrea Gori, and Covadonga Orejas Saco Del Valle. Springer International Publishing. https://doi.org/10.1007/978-3-319-17001-5_43-1.

Weiler, Bradley A., Joost T. P. Verhoeven, and Suzanne C. Dufour. 2018. “Bacterial Communities in Tissues and Surficial Mucus of the Cold-Water Coral Paragorgia Arborea.” *Frontiers in Marine Science* 5 (October): 378. https://doi.org/10.3389/fmars.2018.00378.

Weisburg, W G, S M Barns, D A Pelletier, and D J Lane. 1991. “16S Ribosomal DNA Amplification for Phylogenetic Study.” *Journal of Bacteriology* 173 (2): 2. https://doi.org/10.1128/jb.173.2.697-703.1991.

Wessels, Wiebke, Susanne Sprungala, Sue-Ann Watson, David J. Miller, and David G. Bourne. 2017. “The Microbiome of the Octocoral Lobophytum Pauciflorum: Minor Differences between Sexes and Resilience to Short-Term Stress.” *FEMS Microbiology Ecology* 93 (5). https://doi.org/10.1093/femsec/fix013.

Weynberg, Karen D., Elisha M. Wood-Charlson, Curtis A. Suttle, and Madeleine J. H. Van Oppen. 2014. “Generating Viral Metagenomes from the Coral Holobiont.” *Frontiers in Microbiology* 5 (May). https://doi.org/10.3389/fmicb.2014.00206.

White, Alan T, Helge P Vogt, and Tijen Arin. 2000. “Philippine Coral Reefs Under Threat: The Economic Losses Caused by Reef Destruction.” *Marine Pollution Bulletin* 40 (7): 598–605. https://doi.org/10.1016/S0025-326X(00)00022-9.

Wickham, H, and R Francois. 2015. *Dplyr: A Grammar of Data Manipulation*. V. R Package Version 0.4.3. Released. http://CRAN.R-project.org/package=dplyr.

Wickham, Hadley. 2016. *Ggplot2: Elegant Graphics for Data Analysis*. Springer-Verlag New York. https://ggplot2.tidyverse.or.

Wiens, Matthias, Mohammed S.A Ammar, Ahmed H Nawar, et al. 2000. “Induction of Heat-Shock (Stress) Protein Gene Expression by Selected Natural and Anthropogenic Disturbances in the Octocoral Dendronephthya Klunzingeri.” *Journal of Experimental Marine Biology and Ecology* 245 (2): 265–76. https://doi.org/10.1016/S0022-0981(99)00167-7.

Wigley, T. M. L., and P. D. Jones. 1981. “Detecting CO2-Induced Climatic Change.” *Nature* 292 (5820): 205–8. https://doi.org/10.1038/292205a0.

Wilcox, Justin J.S., and Hope Hollocher. 2018. “Unprecedented Symbiont Eukaryote Diversity Is Governed by Internal Trophic Webs in a Wild Non-Human Primate.” *Protist* 169 (3): 307–20. https://doi.org/10.1016/j.protis.2018.03.001.

Wilcox, Taylor M., Michael K. Schwartz, Kevin S. McKelvey, Michael K. Young, and Winsor H. Lowe. 2014. “A Blocking Primer Increases Specificity in Environmental DNA Detection of Bull Trout (Salvelinus Confluentus).” *Conservation Genetics Resources* 6 (2): 283–84. https://doi.org/10.1007/s12686-013-0113-4.

Wilkinson, Clive. 2008. “Status of Coral Reefs of the World :2008.” *Global Coral Reef Monitoring Network and Reef and Rainforest Research Centre, Townsville, Australia*, 296.

Willis, Amy D. 2019. “Rarefaction, Alpha Diversity, and Statistics.” *Frontiers in Microbiology* 10 (October): 2407. https://doi.org/10.3389/fmicb.2019.02407.

Wong, Hao Jie, Nuradilla Mohamad-Fauzi, Mohammed Rizman-Idid, Peter Convey, and Siti Aisyah Alias. 2019. “Protective Mechanisms and Responses of Micro-Fungi towards Ultraviolet-Induced Cellular Damage.” *Polar Science* 20 (June): 19–34. https://doi.org/10.1016/j.polar.2018.10.001.

Woo, Seonock. 2021. “Bacterial Community Composition Change in Temperate Octocoral, Scleronephthya Gracillimum Responding to Season and Heat Stress.” *KMB 2021 48th Annual Meeting & International Symposium*, June 24, 105–105.

Wood-Charlson, Elisha M., Karen D. Weynberg, Curtis A. Suttle, Simon Roux, and Madeleine J. H. Van Oppen. 2015. “Metagenomic Characterization of Viral Communities in Corals: Mining Biological Signal from Methodological Noise.” *Environmental Microbiology* 17 (10): 3440–49. https://doi.org/10.1111/1462-2920.12803.

Worm, Boris, Edward B. Barbier, Nicola Beaumont, et al. 2006. “Impacts of Biodiversity Loss on Ocean Ecosystem Services.” *Science* 314 (5800): 5800. https://doi.org/10.1126/science.1132294.

Wright, Rachel M., Carly D. Kenkel, Carly E. Dunn, Erin N. Shilling, Line K. Bay, and Mikhail V. Matz. 2017. “Intraspecific Differences in Molecular Stress Responses and Coral Pathobiome Contribute to Mortality under Bacterial Challenge in Acropora Millepora.” *Scientific Reports* 7 (1): 2609. https://doi.org/10.1038/s41598-017-02685-1.

Xu, Meiting, Zhonghua Cai, Keke Cheng, Guofu Chen, and Jin Zhou. 2024. “Mitigation of *Vibrio Coralliilyticus* -Induced Coral Bleaching through Bacterial Dysbiosis Prevention by *Ruegeria Profundi*.” *Applied and Environmental Microbiology* 90 (4): e02274-23. https://doi.org/10.1128/aem.02274-23.

Xu, Wei, Shuangshuang Guo, Linfeng Gong, Siti Aisyah Alias, Ka-Lai Pang, and Zhu-Hua Luo. 2018. “Phylogenetic Survey and Antimicrobial Activity of Cultivable Fungi Associated with Five Scleractinian Coral Species in the South China Sea.” *Botanica Marina* 61 (1): 75–84. https://doi.org/10.1515/bot-2017-0005.

Yarden, Oded. 2014. “Fungal Association with Sessile Marine Invertebrates.” *Frontiers in Microbiology* 5 (May). https://doi.org/10.3389/fmicb.2014.00228.

Yeoh, Yun Kit, Paul G. Dennis, Chanyarat Paungfoo-Lonhienne, et al. 2017. “Evolutionary Conservation of a Core Root Microbiome across Plant Phyla along a Tropical Soil Chronosequence.” *Nature Communications* 8 (1): 215. https://doi.org/10.1038/s41467-017-00262-8.

Yerlikaya, Bayram Ali, Seher Ömezli, and Nazlıcan Aydoğan. 2020. “Climate Change Forecasting and Modeling for the Year of 2050.” In *Environment, Climate, Plant and Vegetation Growth*, edited by Shah Fahad, Mirza Hasanuzzaman, Mukhtar Alam, et al. Springer International Publishing. https://doi.org/10.1007/978-3-030-49732-3_5.

Ying, Zhen, Xiao-Ming Li, Bin-Gui Wang, Hong-Lei Li, and Ling-Hong Meng. 2023. “Rubensteroid A, a New Steroid with Antibacterial Activity from Penicillium Rubens AS-130.” *The Journal of Antibiotics* 76 (9): 563–66. https://doi.org/10.1038/s41429-023-00634-x.

Ying, Zhen, Xiao-Ming Li, Sui-Qun Yang, Bin-Gui Wang, Hong-Lei Li, and Ling-Hong Meng. 2023. “New Polyketide and Sesquiterpenoid Derivatives from the Magellan Seamount-Derived Fungus *Penicillium Rubens* AS-130.” *Chemistry & Biodiversity* 20 (4): e202300229. https://doi.org/10.1002/cbdv.202300229.

Youngblut, Nicholas D., Georg H. Reischer, William Walters, et al. 2019. “Host Diet and Evolutionary History Explain Different Aspects of Gut Microbiome Diversity among Vertebrate Clades.” *Nature Communications* 10 (1): 2200. https://doi.org/10.1038/s41467-019-10191-3.

Yu, Guangchuang, David K. Smith, Huachen Zhu, Yi Guan, and Tommy Tsan-Yuk Lam. 2017. “GGTREE : An R Package for Visualization and Annotation of Phylogenetic Trees with Their Covariates and Other Associated Data.” *Methods in Ecology and Evolution* 8 (1): 28–36. https://doi.org/10.1111/2041-210X.12628.

Zaneveld, Jesse R., Deron E. Burkepile, Andrew A. Shantz, et al. 2016. “Overfishing and Nutrient Pollution Interact with Temperature to Disrupt Coral Reefs down to Microbial Scales.” *Nature Communications* 7 (1): 11833. https://doi.org/10.1038/ncomms11833.

Zaneveld, Jesse R., Ryan McMinds, and Rebecca Vega Thurber. 2017. “Stress and Stability: Applying the Anna Karenina Principle to Animal Microbiomes.” *Nature Microbiology* 2 (9): 17121. https://doi.org/10.1038/nmicrobiol.2017.121.

Zhang, Wenjing, Yongbo Pan, Jun Yang, et al. 2018. “The Diversity and Biogeography of Abundant and Rare Intertidal Marine Microeukaryotes Explained by Environment and Dispersal Limitation.” *Environmental Microbiology* 20 (2): 462–76. https://doi.org/10.1111/1462-2920.13916.

Zhang, Xiaohua, Heyu Lin, Xiaolei Wang, and Brian Austin. 2018. “Significance of Vibrio Species in the Marine Organic Carbon Cycle—A Review.” *Science China Earth Sciences* 61 (10): 1357–68. https://doi.org/10.1007/s11430-017-9229-x.

Zhang, Xiao-Yong, Hui-Li Hao, Stanley Chun Kwan Lau, et al. 2019. “Biodiversity and Antifouling Activity of Fungi Associated with Two Soft Corals from the South China Sea.” *Archives of Microbiology* 201 (6): 757–67. https://doi.org/10.1007/s00203-019-01639-7.

Zhang, Xiaoyong, Yiyang Li, Zonghe Yu, Xiao Liang, and Shuhua Qi. 2021. “Phylogenetic Diversity and Bioactivity of Culturable Deep-Sea-Derived Fungi from Okinawa Trough.” *Journal of Oceanology and Limnology* 39 (3): 892–902. https://doi.org/10.1007/s00343-020-0003-z.

Zhang, Yanting, Zhichao Li, Bingyao Huang, et al. 2022. “Anti-Osteoclastogenic and Antibacterial Effects of Chlorinated Polyketides from the Beibu Gulf Coral-Derived Fungus Aspergillus Unguis GXIMD 02505.” *Marine Drugs* 20 (3): 3. https://doi.org/10.3390/md20030178.

Zhuang, Yibin, Xiancun Teng, Yi Wang, Peipei Liu, Hui Wang, et al. 2011. “Cyclopeptides and Polyketides from Coral-Associated Fungus, *Aspergillus Versicolor* LCJ-5-4.” *Tetrahedron* 67 (37): 7085–89. https://doi.org/10.1016/j.tet.2011.07.003.

Zhuang, Yibin, Xiancun Teng, Yi Wang, Peipei Liu, Guoqiang Li, and Weiming Zhu. 2011. “New Quinazolinone Alkaloids within Rare Amino Acid Residue from Coral-Associated Fungus, Aspergillus Versicolor LCJ-5-4.” *Organic Letters* 13 (5): 1130–33. https://doi.org/10.1021/ol103164n.

Zibrowius, Helmut, Vasco MONTEIRO Marques, and Manfred Grasshoff. 1984. *LA RÉPARTITION DU CORALLIUM RUBRUMDANS l’ATLANTIQUE (CNIDARIA : ANTHOZOA : GORGONARIA)*.

Ziegler, Maren, Carsten G. B. Grupstra, Marcelle M. Barreto, et al. 2019. “Coral Bacterial Community Structure Responds to Environmental Change in a Host-Specific Manner.” *Nature Communications* 10 (1): 3092. https://doi.org/10.1038/s41467-019-10969-5.

Ziegler, Maren, Francois O. Seneca, Lauren K. Yum, Stephen R. Palumbi, and Christian R. Voolstra. 2017. “Bacterial Community Dynamics Are Linked to Patterns of Coral Heat Tolerance.” *Nature Communications* 8 (1): 14213. https://doi.org/10.1038/ncomms14213.